

CPDI  
red for  
Kodak

# Outer Continental Shelf Environmental Assessment Program

**Final Reports of Principal Investigators**

**Volume 65**

**January 1990**



**U.S. DEPARTMENT OF COMMERCE**  
National Oceanic and Atmospheric Administration  
National Ocean Service  
Office of Oceanography and Marine Assessment  
Ocean Assessments Division  
Alaska Office



**U.S. DEPARTMENT OF THE INTERIOR**  
Minerals Management Service  
Alaska OCS Region  
OCS Study, MMS 90-0002

“Outer Continental Shelf Environmental Assessment Program Final Reports of Principal Investigators” (“OCSEAP Final Reports”) continues the series entitled “Environmental Assessment of the Alaskan Continental Shelf Final Reports of Principal Investigators.”

OCSEAP Final Reports are published by the U.S. Department of Commerce, National Oceanic and Atmospheric Administration, National Ocean Service, Ocean Assessments Division, Alaska Office, Anchorage, and primarily funded by the Minerals Management Service, U.S. Department of the Interior, through interagency agreement.

Requests for receipt of OCSEAP Final Reports on a continuing basis should be addressed to:

NOAA-OMA-OAD  
Alaska Office  
Federal Bldg., U.S. Courthouse Room A13  
222 West Eighth Ave., #56  
Anchorage, AK 99513-7543

OUTER CONTINENTAL SHELF  
ENVIRONMENTAL ASSESSMENT PROGRAM

Final Reports of Principal Investigators

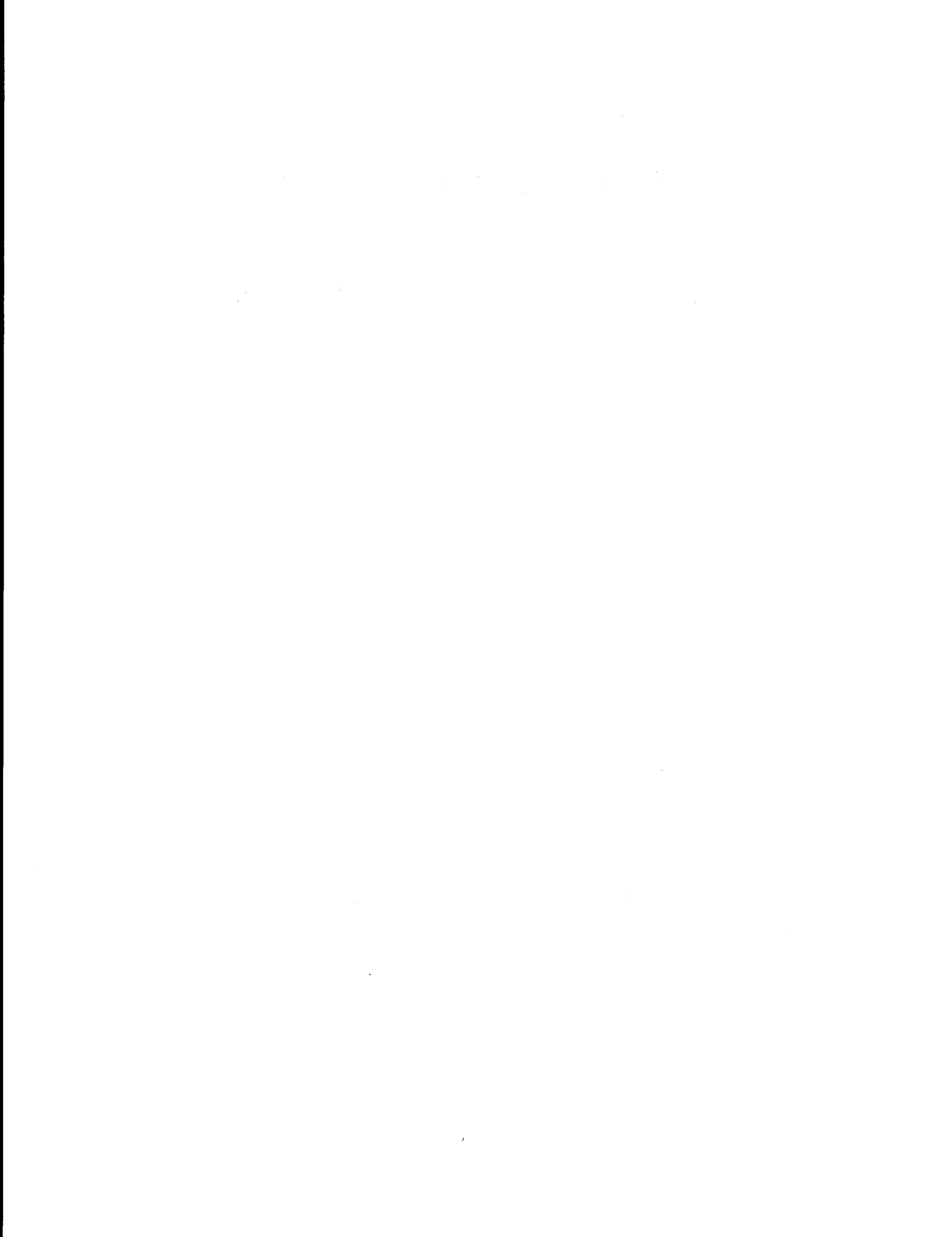
Volume 65

January 1990

U.S. DEPARTMENT OF COMMERCE  
National Oceanic and Atmospheric Administration  
National Ocean Service  
Office of Oceanography and Marine Assessment  
Ocean Assessments Division  
Alaska Office

U.S. DEPARTMENT OF THE INTERIOR  
Minerals Management Service  
Alaska OCS Region  
OCS Study, MMS 90-0002

Anchorage, Alaska



The facts, conclusions, and issues appearing in these reports are based on research results of the Outer Continental Shelf Environmental Assessment Program (OCSEAP), which is managed by the National Oceanic and Atmospheric Administration, U.S. Department of Commerce, and funded (wholly or in part) by the Minerals Management Service, U.S. Department of the Interior, through an Interagency Agreement.

---

Mention of a commercial company or product does not constitute endorsement by the National Oceanic and Atmospheric Administration. Use for publicity or advertising purposes of information from this publication concerning proprietary products or the tests of such products is not authorized.

---

The content of these reports has not been altered from that submitted by the Principal Investigators. In some instances, grammatical, spelling, and punctuation errors have been corrected to improve readability; some figures and tables have been enhanced to improve clarity in reproduction.

The first part of the document discusses the importance of maintaining accurate records of all transactions. This includes not only sales and purchases but also the various expenses incurred in the course of the business. It is essential to ensure that every receipt is properly filed and that the books are kept up to date.

In addition, it is necessary to keep track of the inventory of goods on hand. This will help to determine the cost of goods sold and the gross profit of the business. Regular physical counts should be taken to verify the accuracy of the inventory records.

Another key aspect of bookkeeping is the timely payment of bills and the collection of receivables. This helps to maintain a healthy cash flow and avoid any penalties for late payments. It is also important to review the financial statements regularly to identify any areas where the business may be over-investing or under-performing.

Finally, it is crucial to seek professional advice from an accountant or tax advisor. They can provide valuable insights into the most effective ways to structure the business's finances and minimize its tax liability. This is especially important for businesses that are growing or operating in complex markets.

By following these guidelines, business owners can ensure that their financial records are accurate and complete. This will enable them to make informed decisions about the future of their business and to maximize their profitability.

Outer Continental Shelf Environmental Assessment Program  
Final Reports of Principal Investigators

---

VOLUME 65

JANUARY 1990

---

C O N T E N T S

K. AAGAARD, C. H. PEASE, A. T. ROACH, AND S. A. SALO  
Beaufort Sea mesoscale circulation study ..... 1

# **BEAUFORT SEA MESOSCALE CIRCULATION STUDY**

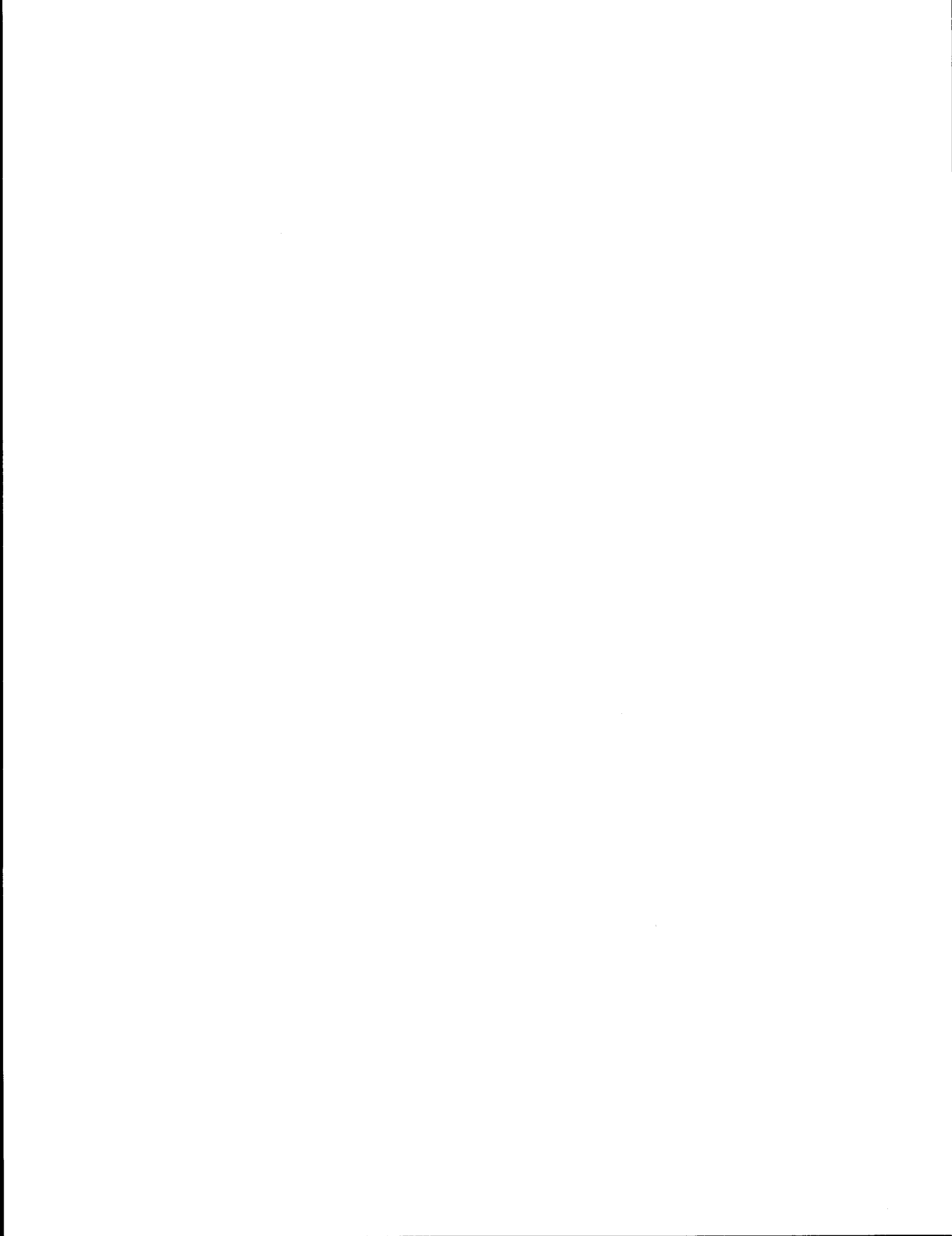
by

**K. Aagaard, C. H. Pease, A. T. Roach, and S. A. Salo**

**U.S. Department of Commerce  
National Oceanic and Atmospheric Administration  
Environmental Research Laboratories  
Pacific Marine Environmental Laboratory  
7600 Sand Point Way, N.E.  
Seattle, Washington 98115-0070**

**Final Report  
Outer Continental Shelf Environmental Assessment Program  
Research Unit 686**

**September 1989**



## ACKNOWLEDGMENTS

The Beaufort Sea Mesoscale Circulation Study is a contribution to the Marine Services Project of the Pacific Marine Environmental Laboratory. This study was funded in part by the Minerals Management Service, Department of the Interior, through an Interagency Agreement with the National Oceanic and Atmospheric Administration, Department of Commerce, as part of the Alaska Outer Continental Shelf Environmental Assessment Program. A portion of the meteorological measurements were funded by the Office of Naval Research, Arctic Programs. The Barrow Canyon moorings were funded by the National Science Foundation, Division of Polar Programs.

C. H. Darnall was chief engineer for the project. G. A. Galasso and W. J. Blake were engineers for the meteorological portion. K. Kroglund of the University of Washington completed the oceanic chemical analyses for the Beaufort Sea. V. L. Long, N. Jenkins, and P. Turet contributed to the data analyses. We also acknowledge the numerous other NOAA, Coast Guard, and civilian personnel who contributed to the successful completion of the experiment in a hostile physical environment.

R. Colony from the Polar Science Center, Applied Physics Laboratory, University of Washington, Seattle, WA, provided all the buoy records as listed in Table 7 and cooperated in the buoy deployments. J. H. Swift, Scripps Institute of Oceanography, LaJolla, CA, supplied data from the AIWEX (Arctic Internal Wave Experiment). L. K. Coachman and R. B. Tripp, School of Oceanography, University of Washington, contributed hydrographic data from ISHTAR (Inner Shelf Transport and Resources).



## ABSTRACT

The Beaufort Sea Mesoscale Project was undertaken to provide a quantitative understanding of the circulation over the Beaufort Sea shelf and its atmospheric and oceanic forcing. Major emphasis has been placed on providing extensive synoptic oceanographic and meteorological coverage of the Alaskan Beaufort Sea during 1986–88. In addition, supplementary measurements have been made in the southern upstream waters of Bering Strait and the Chukchi Sea. The work has resulted in an unprecedented regional data set for both the ocean and the atmosphere. The principal conclusions are as follows:

1) Below the upper 40–50 m of the ocean, the major circulation feature of the outer shelf and slope is the Beaufort Undercurrent, a strong flow which is directed eastward in the mean, but which is subject to frequent reversals toward the west. The reversals are normally associated with upwelling onto the outer shelf. The undercurrent is very likely part of a basin-scale circulation within the Arctic Ocean.

2) While we find statistically significant wind influence on the subsurface flow in the southern Beaufort Sea, it is generally of secondary importance, accounting for less than 25% of the flow variance below 60 m. An important implication is that at least below the mixed layer, the circulation on the relatively narrow Beaufort shelf is primarily forced by the ocean rather than by the local wind. This oceanic forcing includes shelf waves and eddies. Therefore, to the extent that a localized problem or process study requires consideration of the shelf circulation, such as would be the case for oil-spill trajectory modeling, a larger-scale framework must be provided, within which the more local problem may be nested.

3) There were large changes in wind variance with season, with the largest variances occurring in the late summer–early autumn and again in January because of blocking ridges in the North Pacific shifting the storm track westward over the west coast of Alaska and across the North Slope.

4) Despite the seasonally varying wind field, as well as the large seasonal differences in the upper-ocean temperature and salinity fields, we find no evidence for a seasonal variability in the subsurface circulation in the Beaufort Sea. This situation contrasts with that in Bering Strait and probably in the Chukchi Sea, where a seasonal cycle in the transport is apparent. Therefore, while the northward flow of water from the Pacific is of major significance to the structure and chemistry of the upper ocean in the Arctic (including the Beaufort Sea), as well as its ice cover and biota, the dynamic significance of that flow to the Beaufort Sea appears small.

5) In contrast to the lack of a seasonal oceanographic signal at depth, the inter-annual variability in the flow characteristics can be considerable. For example, during the period fall 1986–spring 1987, the Beaufort Undercurrent appears to have been deeper by 30–40 m compared with both earlier and ensuing measurements. The consequences of such anomalies for the upper-ocean velocity structure and transport are likely significant.

6) During much of the experiment, the meteorological conditions were milder than normal, consistent with less coastal ice in the summer and autumn, the passage of more storms up the west coast of Alaska and across the North Slope, and generally higher air temperatures along the North Slope. These climatological near-minimum ice years were followed in 1988 by the heaviest summer ice along the Chukchi coast since 1975.

7) The atmospheric sea-level pressure field was well represented by the METLIB products from the FNOC surface analysis if the 12-hour lag of the FNOC pressures was taken into account. However, the FNOC surface air temperature field does not accurately represent either the land-based stations or the drifting ice buoys. The errors in the FNOC temperature field showed a systematic over-prediction during winter and spring of 10–20°C, leading to an annual over-prediction of air temperature by 3–13°C at all sites. Gradient winds from FNOC are therefore well suited for modeling purposes if they are calculated from the time-shifted surface analysis, but the FNOC surface temperature analysis should not be used for any model calculations, except perhaps as an upper boundary condition for a rather complete planetary boundary layer model.

## TABLE OF CONTENTS

	<i>Page</i>
Acknowledgments .....	3
List of Figures .....	9
List of Tables .....	11
 INTRODUCTION .....	 13
Flow Through Bering Strait .....	15
Flow Through the Chukchi Sea .....	15
Deep Exchange Through Barrow Canyon .....	16
Flow In the Beaufort Sea .....	17
Nutrient Sources .....	17
Meteorology .....	18
 METHODS .....	 20
Chukchi Sea .....	20
Barrow Canyon .....	20
Beaufort Sea .....	25
Meteorological Stations .....	28
 RESULTS AND DISCUSSION .....	 34
Chukchi Sea .....	34
Barrow Canyon .....	42
Beaufort Sea Hydrography .....	54
Beaufort Sea General Flow Characteristics .....	56
Beaufort Sea Variability at Very Low Frequencies .....	66
Beaufort Sea Correlation Analysis .....	70
Beaufort Sea Tidal Characteristics .....	74
Meteorological Results and Correlations .....	77
 SYNOPSIS OF THE REGIONAL CIRCULATION .....	 122
 SUMMARY OF THE PRINCIPAL CONCLUSIONS .....	 128
 REFERENCES CITED .....	 130
 APPENDIX A. Aagaard, K., C. H. Pease, and S. A. Salo, <i>Beaufort Sea Mesoscale Circulation Study—Preliminary Results</i> , NOAA Technical Memorandum ERL PMEL-82 .....	   137
 APPENDIX B. Aagaard, K., S. Salo, and K. Kroglund, <i>Beaufort Sea Mesoscale Circulation Study: Hydrography, USCGC Polar Star Cruise, October, 1986</i> , NOAA Data Report ERL PMEL-19 .....	   313

APPENDIX C. Aagaard, K., S. Salo, and K. Kroglund, *Beaufort Sea Mesoscale  
Circulation Study: Hydrography, Helicopter Operations,  
April, 1987*, NOAA Data Report ERL PMEL-22 . . . . . 401

## LIST OF FIGURES

<i>Figure</i>		<i>Page</i>
1	Regional map . . . . .	14
2	Barrow Canyon location and mooring placement . . . . .	21
3	Barrow Canyon array design . . . . .	22
4	Beaufort Sea array locations . . . . .	26
5	Weekly average current vectors at Cape Thompson . . . . .	35
6	Temperature, salinity, and nutrient structure in the upper 500 m of the Arctic Ocean (from observations by J. J. Swift) . . . . .	38
7	Near-bottom distributions of salinity and nitrate in the Chukchi, East Siberian and Laptev seas . . . . .	39
8	Nutrient profiles from ISHTAR . . . . .	40
9	Nutrient profiles from ISHTAR . . . . .	41
10	Time series of currents from Barrow Canyon . . . . .	43
11	Time series of salinity from Barrow Canyon . . . . .	45
12	Time series of temperature from Barrow Canyon . . . . .	46
13	Volumetric temperature-salinity and mean velocity plots for Barrow Canyon mooring BC1 . . . . .	47
14	Volumetric temperature-salinity and mean velocity plots for Barrow Canyon mooring BC2 . . . . .	48
15	Profile of light attenuation at Section C near 144°W . . . . .	55
16	Low-pass filtered current vectors from Beaufort Sea moorings . . . . .	59
17	Low-pass filtered current vectors from Beaufort Sea moorings . . . . .	60
18	Energy-preserving rotary coherence spectra for Beaufort Sea records . . . . .	61
19	Same as Figure 18 . . . . .	62
20	Same as Figure 18 . . . . .	63
21	Same as Figure 18 . . . . .	64
22	Same as Figure 18 . . . . .	65
23	Monthly mean velocity from outer shelf moorings . . . . .	68
24	Monthly mean variance from outer shelf moorings . . . . .	69
25	Tidal elevation characteristics from mooring MB2B . . . . .	75
26	Tidal currents from mooring MB2B . . . . .	76
27	Plots of all parameters from land-based weather stations . . . . .	80

<i>Figure</i>	<i>Page</i>
28	Same as Figure 27 ..... 81
29	Same as Figure 27 ..... 82
30	Same as Figure 27 ..... 83
31	Same as Figure 27 ..... 84
32	Same as Figure 27 ..... 85
33	Same as Figure 27 ..... 86
34	Same as Figure 27 ..... 87
35	Ice drifts for the ARGOS buoys ..... 88
36	Same as Figure 35 ..... 89
37	Time series of ARGOS buoy and METLIB data ..... 90
38	Same as Figure 37 ..... 91
39	Same as Figure 37 ..... 92
40	Same as Figure 37 ..... 93
41	Same as Figure 37 ..... 94
42	Same as Figure 37 ..... 95
43	Same as Figure 37 ..... 96
44	Same as Figure 37 ..... 97
45	Seasonally averaged values for temperature, pressure and wind ..... 108
46	Same as Figure 46 ..... 109
47	Same as Figure 46 ..... 110
48	Same as Figure 46 ..... 111
49	Monthly mean values for land-based stations ..... 112
50	Same as Figure 49 ..... 113
51	Same as Figure 49 ..... 114
52	Same as Figure 49 ..... 115
53	Monthly mean wind variance for land-based stations ..... 116
54	Weather map for selected times and areas ..... 117
55	Same as Figure 54 ..... 118
56	Same as Figure 54 ..... 119
57	Same as Figure 54 ..... 120
58	Same as Figure 54 ..... 121
59	Annual Bering Strait transport signal ..... 126
60	Forty years of annual transport estimates through Bering Strait ..... 127

## LIST OF TABLES

<i>Table</i>		<i>Page</i>
1	Location, instrumentation, and duration of the Barrow Canyon current meters .....	23
2	Pressure gauge statistics for Barrow Canyon moorings .....	25
3	Surface wind statistics for Barrow Canyon analysis .....	25
4	Location, instrumentation, and duration for Beaufort Sea moorings ...	27
5	GOES station deployment information .....	31
6	ARGOS buoy deployment information .....	32
7	APL buoy deployment information .....	33
8	Record-length current statistics for one year moorings in the Chukchi Sea .....	34
9	Current meter statistics for Barrow Canyon .....	42
10	Record-length statistics for the SeaCat temperature-salinity loggers from Barrow Canyon .....	50
11	Record-length correlations of Barrow Canyon currents with regional winds and surface gradients .....	50
12	Turbulent heat and salt flux estimates for Barrow Canyon .....	53
13	Record-length statistics for Beaufort Sea current meters .....	57
14	Beaufort Sea mean velocity comparison .....	66
15	Linear correlations of Beaufort Sea current meters .....	71
16	Linear correlations of Beaufort Sea currents with regional winds .....	73
17	Record-length statistics for ARGOS, GOES, climate, and METLIB data .....	78
18	Sea-level pressure correlations for ARGOS, GOES, climate, and METLIB data .....	98
19	Air temperature correlations for ARGOS, GOES, climate, and METLIB data .....	99

<i>Table</i>		<i>Page</i>
20	Wind speed correlations for ARGOS, GOES, climate, and METLIB data .....	104
21	Correlations among climate stations .....	105
22	Correlations among METLIB records at climate stations .....	106
23	Correlations among GOES stations .....	107
24	Correlations among METLIB records at GOES stations .....	107

## INTRODUCTION

The Beaufort Sea Mesoscale Circulation Study was initiated in 1986 to develop a quantitative and dynamically founded understanding of the circulation over the Beaufort Sea shelf (Figure 1) and its atmospheric and oceanic forcing. The study was conducted within the overall context of a regional environmental assessment related to petroleum exploration and development.

Earlier work in the Beaufort Sea either concentrated on limited near-shore areas, or did not provide a sufficiently broad spatial and temporal coverage to define the shelf circulation on appropriately large scales. A further serious limitation of previous work was the inadequate determination of the atmospheric forcing on a regional scale. These deficiencies are particularly troublesome when constructing and validating numerical models of the shelf circulation. Finally, the earlier hydrographic sampling on the shelf (which included nutrients and dissolved oxygen) was restricted to a brief period during the summer, yielding no information on conditions during other seasons. To substantially remedy these shortcomings, the present study was designed to provide broad spatial and temporal coverage of the circulation, hydrography and synoptic winds over the continental shelf. The field work began in autumn 1986 and continued through spring 1988, resulting in an unprecedented regional data set for both the ocean and the atmosphere.

This report is divided into five major sections: Introduction (including a brief background), Methods, Results and Discussion, Synopsis of the Regional Circulation, and Summary of the Principal Conclusions. In addition, there is a secondary organization on the basis of geography and discipline: the southern upstream sources for shelf waters in the Beaufort Sea, specifically the flow through Bering Strait and in the Chukchi Sea; the circulation in the Beaufort Sea itself, primarily seaward of the 50-m isobath; and the meteorology and climatology of the Beaufort Sea, including pertinent aspects of sea ice kinematics and dynamics in the region.

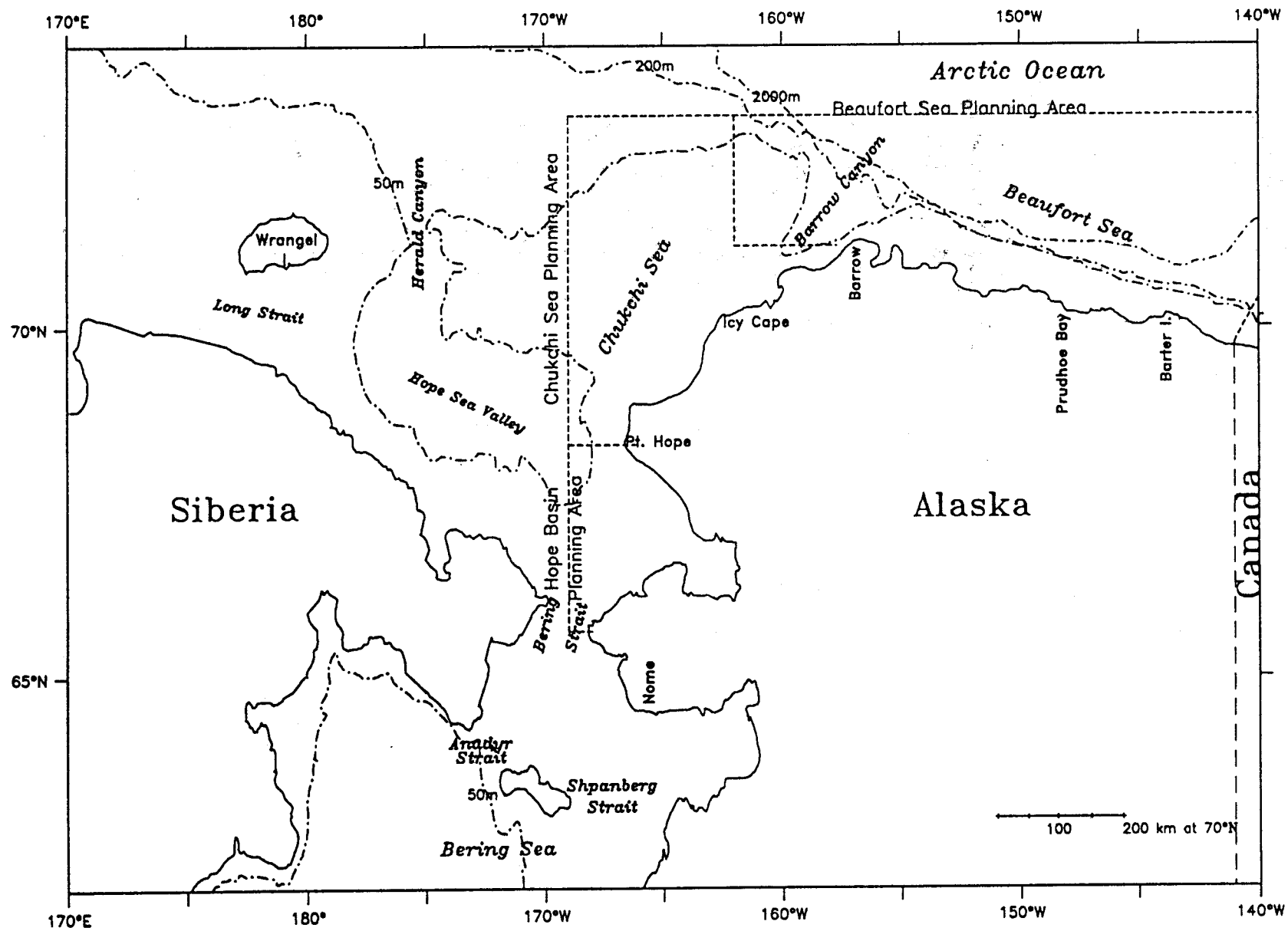


Figure 1. Location figure showing study areas and place names.

## **Flow Through Bering Strait**

The strong northward flow through Bering Strait, which connects the Pacific and Arctic oceans, has major consequences for much of the Arctic Ocean (see Coachman and Barnes, 1961; Codispoti, 1979; Killworth and Smith, 1984; Yeats, 1988; and Walsh et al., in press, for examples). The flow also has a major impact on conditions in the Beaufort Sea, as was first pointed out by Johnson (1956) and has since been elaborated by a number of investigators (see Aagaard, 1984, for a review). Conditions in the strait have been the subject of numerous investigations (see Coachman et al., 1975, and Aagaard et al., 1985b for reviews), but it is only relatively recently that the very large variability of the flow through the strait has become evident (Coachman and Aagaard, 1981). Much of this variability appears to be wind-driven and has been the subject of several recent investigations, both experimental and theoretical (Aagaard et al., 1985b; Overland and Roach, 1987; and Spaulding et al., 1987). We have reassessed this situation in light of the recent study of transport by Coachman and Aagaard (1988).

## **Flow Through the Chukchi Sea**

The generally northward movement of water through the Chukchi Sea represents the flow of Pacific water from the Bering Sea towards the Arctic Ocean; it has considerable spatial and temporal structure (Coachman et al., 1975; Coachman and Aagaard, 1981). From the earlier work of Coachman et al. (1975), we know that in the vicinity of Bering Strait, the relatively saline water which flows northward across the western Bering shelf (termed Anadyr Water) mixes with the central water mass of the Bering Sea and enters the Chukchi Sea, where it is referred to as Bering Sea Water. This water mass remains distinct from the Alaskan Coastal Water to the east, which is characterized by lower salinity. The latter water follows the Alaskan coast northward and enters the Arctic Ocean and the Beaufort Sea immediately west of Pt. Barrow.

The course of the Bering Sea Water, on the other hand, is not well documented, but appears to occupy most of the western Chukchi Sea, and likely follows the Hope Sea Valley northwestward before entering the Arctic Ocean east of Wrangel Island. In addition to the inflow through Bering Strait, there is exchange with the East Siberian Sea through Long Strait (Coachman and Rankin, 1968) and with the Arctic Ocean across the northern shelf break (see Mountain et al., 1976, for an example). There

is also large temporal variability, including prolonged flow reversals, much of which appears to be wind-driven (Aagaard, 1988).

### Deep Exchange Through Barrow Canyon

The most immediate connection between the Beaufort and the Chukchi seas is via Barrow Canyon. During 1986-87 we deployed two densely instrumented arrays in the canyon, primarily under NSF sponsorship. The measurements are of major interest to issues of Beaufort Sea circulation and we have therefore included their analysis in the present study.

Barrow Canyon is a 250-km long depression crossing the northeastern-most Chukchi Sea. It runs parallel to the coast and comes within 10 km of it off Point Barrow (Figure 2). The canyon steepens both at its shelf and its mid-slope terminations, but over its intermediate course, where the depth is between 100-200 m, the along-canyon gradient is small, about  $10^{-3}$ . The characteristic width is about 30 km. Earlier flow measurements in the canyon by Mountain et al. (1976) and Aagaard (1988) have shown a long-term mean velocity directed down-canyon at 15-20  $\text{cm s}^{-1}$  or more, but with instantaneous speeds frequently attaining 100  $\text{cm s}^{-1}$ . Flow reversals are common and may last up to several weeks, during which the daily mean up-canyon speeds commonly reach 40  $\text{cm s}^{-1}$ . Much of the variability has appeared to be atmospherically driven, either by the longshore pressure gradient (Mountain et al., 1976) or by the wind (Aagaard, 1988).

The interaction between the Arctic Ocean and its adjacent shelf seas is of considerable current interest because much of both the hydrographic structure (Aagaard et al., 1981; Melling and Lewis, 1982; Moore et al., 1983; Aagaard et al., 1985a; Jones and Anderson, 1986; Wallace et al., 1987) and the velocity field (Hart and Killworth, 1976; Manley and Hunkins, 1985; D'Asaro, 1988) of the interior ocean appears to originate over certain of the shelves. In the western Arctic, the Chukchi Sea is probably the most important region in this regard (Aagaard et al., 1981), and in particular Barrow Canyon has been suggested by a number of investigators (Coachman et al., 1975; Garrison and Becker, 1976; Mountain et al., 1976; Garrison and Paquette, 1982; Aagaard et al., 1985a; D'Asaro, 1988) as a likely avenue of exchange between the shelf and the deep ocean.

## Flow in the Beaufort Sea

The relatively narrow (50-100 km) Alaskan Beaufort Sea shelf extends about 600 km from Point Barrow to the Canadian border. Aagaard (1984) has pointed out that there are two substantially different circulation regimes on this shelf. Landward of about the 50 m isobath (the inner shelf), the circulation has a large wind-driven component, particularly in summer. In winter, the flow over the inner shelf is much less energetic, but still shows a wind influence. Farther seaward (the outer shelf), the dominant subsurface circulation feature is the Beaufort Undercurrent, which in the mean state is directed eastward along the entire outer shelf and slope. It underlies a very shallow flow regime in which the ice and uppermost ocean in the mean moves westward, representing the southern limb of the clockwise Beaufort gyre. The Beaufort Undercurrent is characterized by large low-frequency variability, including frequent current reversals toward the west. It is probably a part of the large-scale circulation of the Arctic Ocean, which appears to be characterized by relatively strong topographically trapped boundary currents (Aagaard, 1989). While the Beaufort shelf is strongly influenced by the Arctic Ocean, it also shows a clear connection with the Pacific via the flow through Bering Strait and the Chukchi Sea, which results not only in seasonally distinctive water properties, but also in the introduction of Pacific life forms (cf. Johnson, 1956 for a seminal example).

## Nutrient Sources

Almost 30 years ago, Coachman and Barnes (1961) pointed out that the temperature structure of the sub-surface layer of much of the Arctic Ocean originates in the flow of water from the south through Bering Strait, which has mixed with resident shelf waters in the Chukchi Sea before moving into the Arctic Ocean. In particular, they argued that the temperature maximum near 75 m represents summer flow through the strait, and that the temperature minimum between 150-200 m represents winter inflow. The argument was reconsidered by Coachman et al. (1975), who concluded that the subsurface temperature maximum in the Arctic Ocean in fact is contributed entirely by the northeast branch (Alaskan Coastal Water) of the Bering Strait inflow and its mixtures. They looked in vain for an Arctic Ocean temperature maximum originating in the northwest branch (Bering Sea Water).

Detailed vertical profiles of nutrient distributions in the Arctic Ocean were obtained by Kinney et al. (1970), who showed the

pronounced nutrient maximum between 150-200 m. Their analysis supported a Bering Sea origin of the temperature-minimum water, as well as of the temperature-maximum water (which had much lower nutrient concentrations). Moore (1981) and Yeats (1988) found trace metal maxima coincident with the nutrient maximum, and they argued that the data were consistent with a Bering Sea origin. However, Moore et al. (1983), Jones and Anderson (1986), and Moore and Smith (1986) have stressed that the various geochemical profiles in the Arctic Ocean, including those of nutrients, reflect the importance of modification on the shelf, particularly due to sediment interaction.

A new perspective on these issues is provided by recent observations from the Bering and Chukchi seas under the ISHTAR program, which show that nutrient-rich water carried northwestward in the Bering Sea with the Bering Slope Current moves onto the southwestern Bering shelf and thence northward through Anadyr Strait into the northern Bering and southern Chukchi seas, where it supports one of the world's most productive marine ecosystems (Walsh, et al., 1989).

## Meteorology

The topography of the land adjacent to the Beaufort and Chukchi seas can be described as low plains, except for three important features: the Brooks Range which foots at the Chukchi coast near Cape Lisburne and at the Beaufort coast from between Barter and Herschel Islands, Cape Mountain and associated high bluffs near Cape Prince of Wales at the tip of the Seward Peninsula, and several similar low mountains and bluffs along the Siberian Peninsula. These topographic features have localized effects on wind speed and direction for some orientations of atmospheric pressure gradient (Dickey, 1961; Kozo, 1980), especially considering the strong capping inversion present in the atmosphere much of the year (Sverdrup, 1933; Overland, 1985).

The Chukchi and northern Bering seas span the transition between polar oceanic climate typical of the central Bering Sea and high-contrast polar climate typical of the Beaufort Sea. A polar region is a geographic region with a mean monthly air temperature for the warmest month of less than 10°C (Overland, 1981). The polar oceanic climate has the additional constraint of high annual precipitation (> 0.3 m) that is fairly uniformly distributed through the seasons. A high-contrast polar climate like the Beaufort Sea region, has lower total precipitation and larger seasonal variability in temperature and precipitation (Overland, 1981).

A major influence on the general circulation in the area is a region of high pressure normally located over the Beaufort Sea. The region is centered at about 79° N, 170° W in winter and drives easterly winds across the North Slope and northeasterly winds offshore at Icy Cape (Pease, 1987; Aagaard et al., 1988). At Cape Lisburne there are mountain effects, and the vector mean winter wind is southeasterly. The Siberian high pressure system is southwest of the Beaufort high; the two occasionally form a saddle over the central and western Chukchi Sea in winter, resulting in light winds. In summer there is often a low pressure system occupying the same spot over the Beaufort or shifted more symmetrically over the pole. There is considerably more variability in the monthly synoptic conditions than in the interannual pattern (Pease, 1987).

In autumn, as the solar input wanes, the Beaufort and Chukchi seas are cooled by net upward longwave radiation, turbulent (sensible) heat flux to the atmosphere, and melting sea ice advected from the north. Coastally ice-free waters typically reach their freezing point in late September or early October along the North Slope and by early December in Bering Strait. There is enormous interannual variability in the timing of the onset of freezing, especially southwest of Barrow (Campbell et al., 1976; 1980; Carsey and Holt, 1987; Mysak and Manak, 1989). This variability depends on the regional atmospheric temperature anomalies (Rogers, 1978), the transport of heat by the barotropic currents through Bering Strait (Hufford, 1973; Paquette and Bourke, 1974; Aagaard et al., 1985b; Coachman and Aagaard, 1988), and the variability in occurrence of northwesterly winds which push the high-Arctic pack ice against the North Slope and enhance the oceanic cooling in the coastal zone by melting ice (Aagaard et al., 1988; Mysak and Manak, 1989). The latter occurred rather dramatically in the late summer and autumn of 1988, following the completion of this study.

## METHODS

### Chukchi Sea

During 1986-87, we had a mooring deployed in the eastern Chukchi Sea south of Cape Thompson at  $67^{\circ} 39'N$ ,  $165^{\circ} 39'W$  in water 43 m deep. The site lies within the Alaskan Coastal Current, which carries water northward through the eastern Bering and Chukchi seas. A current meter was located at 33 m, and the year-long record extended from 25 August 1986 to 25 August 1987.

### Barrow Canyon

We moored two 14-m long arrays in Barrow Canyon from October 1986 to August 1987 (Figure 3). The array BC1 was near the axis of the canyon at a depth of 145 m, while array BC2 was on the shoreward wall of the canyon at about 90 m (Figure 2, Table 1). These taut-wire moorings were each instrumented with three Aanderaa RCM-4 current meters, four Sea-Bird SeaCat conductivity-temperature data loggers, and one Aanderaa TG-3A pressure gauge. All instruments, except the top current meter on each array and the pressure gauge on the shallower mooring, recorded data of good quality throughout the deployment period. (Table 1). The pressure gauges monitored the vertical motion of the moorings, so that pressure variations could be accounted for in the salinity calculations (tidal heights are of order 10 cm and can be ignored for these purposes). The maximum mooring excursions proved to be only 225 and 175 mb at BC1 and BC2, respectively, corresponding to maximum salinity errors of 0.011 and 0.008 psu, which are well within the salinity error bands due to conductivity uncertainties. The standard deviation of the pressure was considerably less, about 35-40 mb (Table 2), with a corresponding reduction of the standard error in salinity associated with pressure variations. We have therefore ignored the effects of mooring motion in calculating salinity.

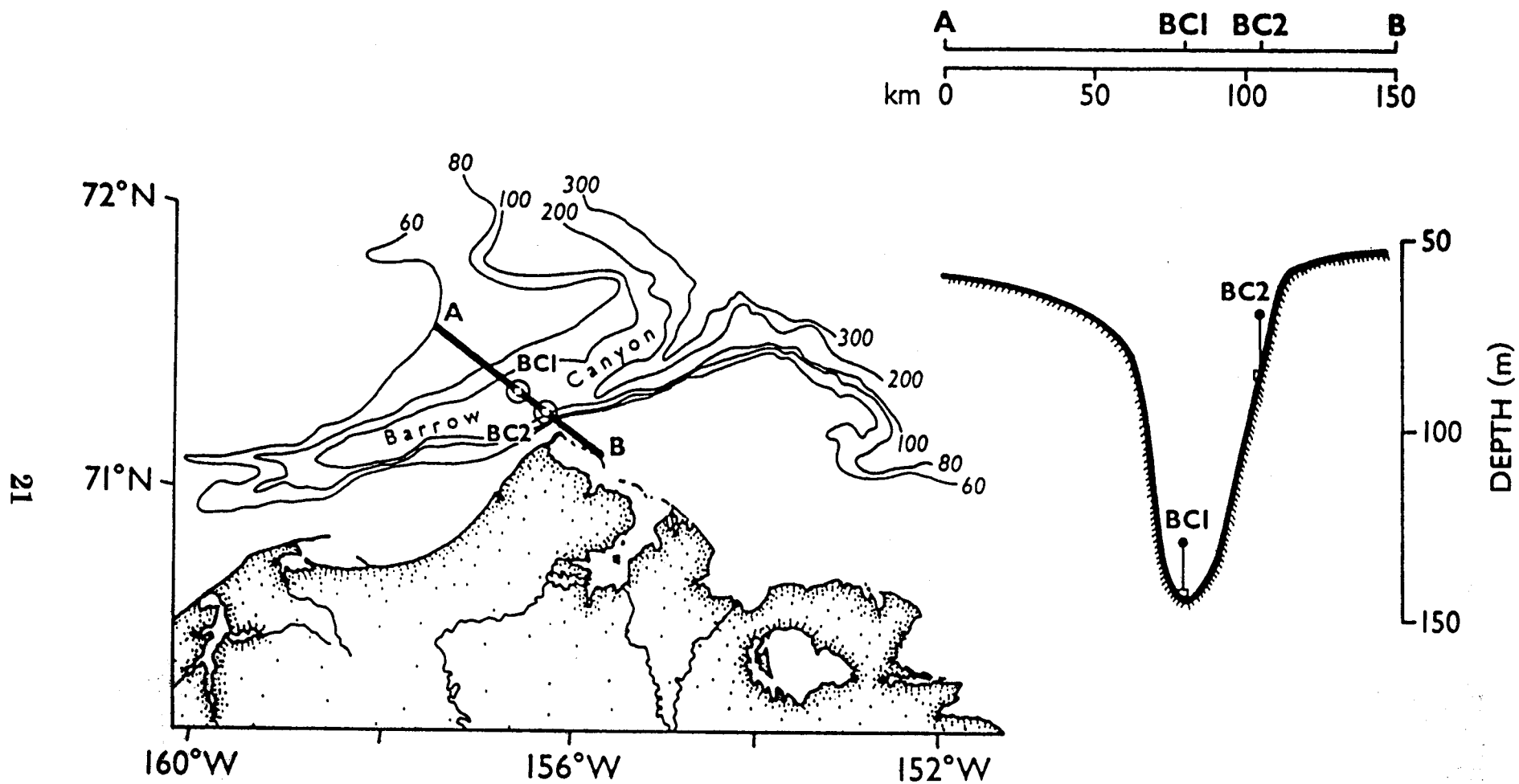


Figure 2. Location and local bathymetry of Barrow Canyon, indicating placement of moorings BC1 and BC2. A plan view along the transect labelled AB showing placement of moorings within the canyon is to the right of the figure.

### Barrow Canyon Moorings

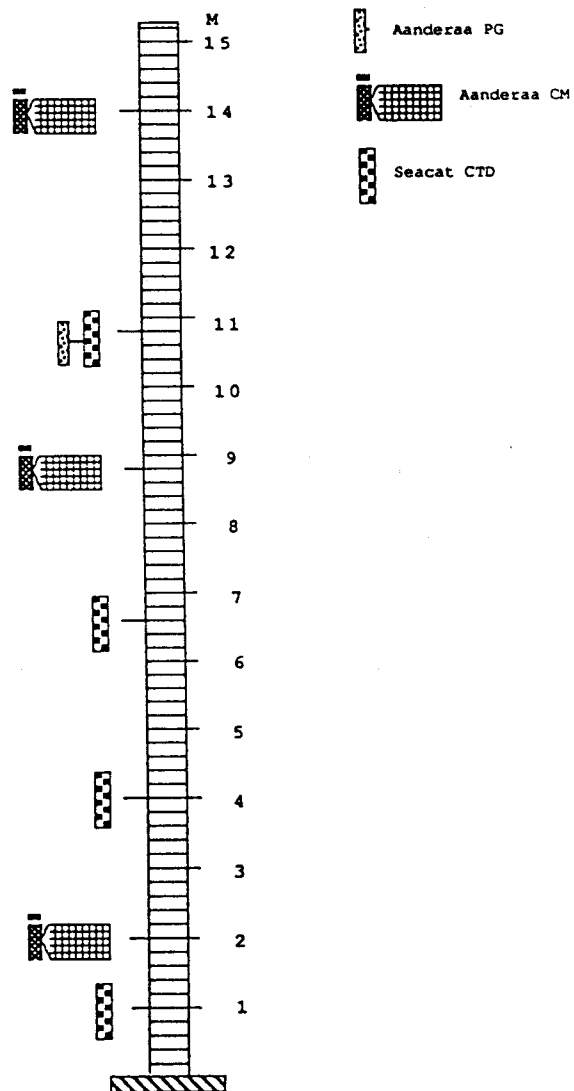


Figure 3. Vertical arrangement of instruments on each Barrow Canyon mooring. Each mooring had three Aanderaa RCM-4 current meters interspersed with four SeaBird SeaCat data loggers with one Aanderaa TG3A pressure gauge attached to the topmost SeaCat.

**Table 1.** Location, instrumentation and duration of the Barrow Canyon current meter moorings and sites for regional wind calculations. The instrument types are :

C M = Aanderaa current meter, S C = Sea-Bird SeaCat temperature-salinity data logger and P G = Aanderaa pressure gauge.

Series	Latitude N	Longitude W
Oceanographic moorings :		
BC1	71° 27.48'	156° 52.87'
BC2	71° 26.16'	156° 40.10'
Winds :		
Barrow	71° 24.00'	157° 00.00'
Shelf break	74° 00.00'	156° 00.00'
Pt. Lay	70° 24.00'	165° 00.00'
Kuparuk R.	70° 48.00'	149° 00.00'

Mooring	Depth m	Inst. type	Height m	Record start GMT	Record end GMT
BC1	129.0	CM	14.0	0000 05 Oct 86	0000 11 Dec 86
	132.2	SC	10.8	0000 05 Oct 86	2100 08 Aug 87
	132.2	PG	10.8	0000 05 Oct 86	2100 08 Aug 87
	134.0	CM	9.0	0000 05 Oct 86	2100 08 Aug 87
	136.4	SC	6.6	0000 05 Oct 86	2100 08 Aug 87
	139.0	SC	4.0	0000 05 Oct 86	2100 08 Aug 87
	141.0	CM	2.0	0000 05 Oct 86	2100 08 Aug 87
	142.0	SC	1.0	0000 05 Oct 86	2100 08 Aug 87
BC2	76.0	CM	14.0	0000 05 Oct 86	0000 15 Nov 86
	79.2	SC	10.8	0000 05 Oct 86	2100 08 Aug 87
	79.2	PG	10.8	0000 05 Oct 86	0200 27 Nov 86
	81.0	CM	9.0	0000 05 Oct 86	2100 08 Aug 87
	82.4	SC	6.6	0000 05 Oct 86	2100 08 Aug 87
	86.0	SC	4.0	0000 05 Oct 86	2100 08 Aug 87
	88.0	CM	2.0	0000 05 Oct 86	2100 08 Aug 87
	89.0	SC	1.0	0000 05 Oct 86	2100 08 Aug 87

Comparison of the pre- and post-deployment calibrations for the SeaCats suggests that the temperatures were stable over the year to within 0.005 °C. Unfortunately, the pre-deployment calibration of conductivity was invalidated by a glycol leak into the calibration tank. An accumulation of silt in the conductivity cell apparently degraded the signal further during the course of the deployment. The silting of the cell occurred because we had mounted it horizontally in an effort to improve flushing. However, the combination of this particular cell geometry and a heavy suspended load in the boundary layer made this an unfortunate choice. Nonetheless, we were able to calibrate the conductivity cells *in situ* by comparing the observed temperature-salinity (T-S) correlations during periods of upwelling of warm intermediate waters into the canyon with a canonical T-S correlation derived from a large number of regional CTD casts. The latter correlation is quite tight, so that in effect an *in situ* calibration bath was advected past the instruments during each upwelling episode. Assuming an accurate temperature measurement, the offset in salinity between the SeaCats and the canonical correlation provided a time history of the conductivity degradation by month. A linear least squares fit to these offsets was computed for each instrument over the deployment period to provide a time-dependent salinity correction. The offsets were largest for the instruments nearest the bottom, where the suspended load presumably was greatest, and they increased with time at all instruments. We estimate that the final salinities are accurate to within 0.06 psu.

The current data were low-pass filtered using a cosine-squared Lanczos filter with a half-power point of 35 hr. We also calculated year-long time series of 6-hr surface winds by reducing (by 36%) and rotating (27° CCW) the geostrophic wind at selected locations. The reduction and rotation were derived by a comparison with measured winds (Table 3). Finally, a surface pressure difference series was created by subtracting the demeaned and detrended surface atmospheric pressure series at Nome from that at Barrow. In the correlation analysis between these various data series, a positive lag indicates that the column data lead the row data, while a negative lag implies the row leads the column. A positive correlation coefficient means that as one parameter increases, so does the other, while a negative coefficient implies that as one parameter increases, the other decreases. If two data sets are related by a correlation coefficient  $r$ , the amount of variance that can be explained in one data set by the variance in the other is  $r^2$ .

**Table 2.** Pressure gauge statistics for Barrow Canyon.

Mooring	Depth (m)	Mean Pressure (mb)	Standard Deviation (mb)
BC1	132.2	13901.0	34.7
BC2	79.2	8755.4	39.7

**Table 3.** Surface wind statistics.

Site	Mean velocity (m/s)	Direction (°T)	Standard Deviation (m/s)
Barrow	3.2	242.0	5.8
Shelf Break	1.8	246.4	5.5
Pt. Lay	3.8	218.9	6.2
Kuparuk R.	2.7	255.5	5.6

## Beaufort Sea

The 1986-87 hydrography and moored measurements, together with the concurrent meteorological and sea-ice investigations, are described in NOAA Technical Memorandum ERL-PMEL 82 and in NOAA Data Reports ERL PMEL-19 and ERL PMEL-22. These are presented in Appendices A, B, and C.

During 1987-88 we had six moored instrument arrays deployed in the Beaufort Sea between Pt. Barrow and Barter Island. Two of the arrays were sited in the mid-shelf region, near the 50 m isobath; three were close to the shelf break, near the 200 m isobath; and one was located over the slope, at about 1000 m depth. The locations are shown in Figure 4, and the mooring particulars are given in Table 4.

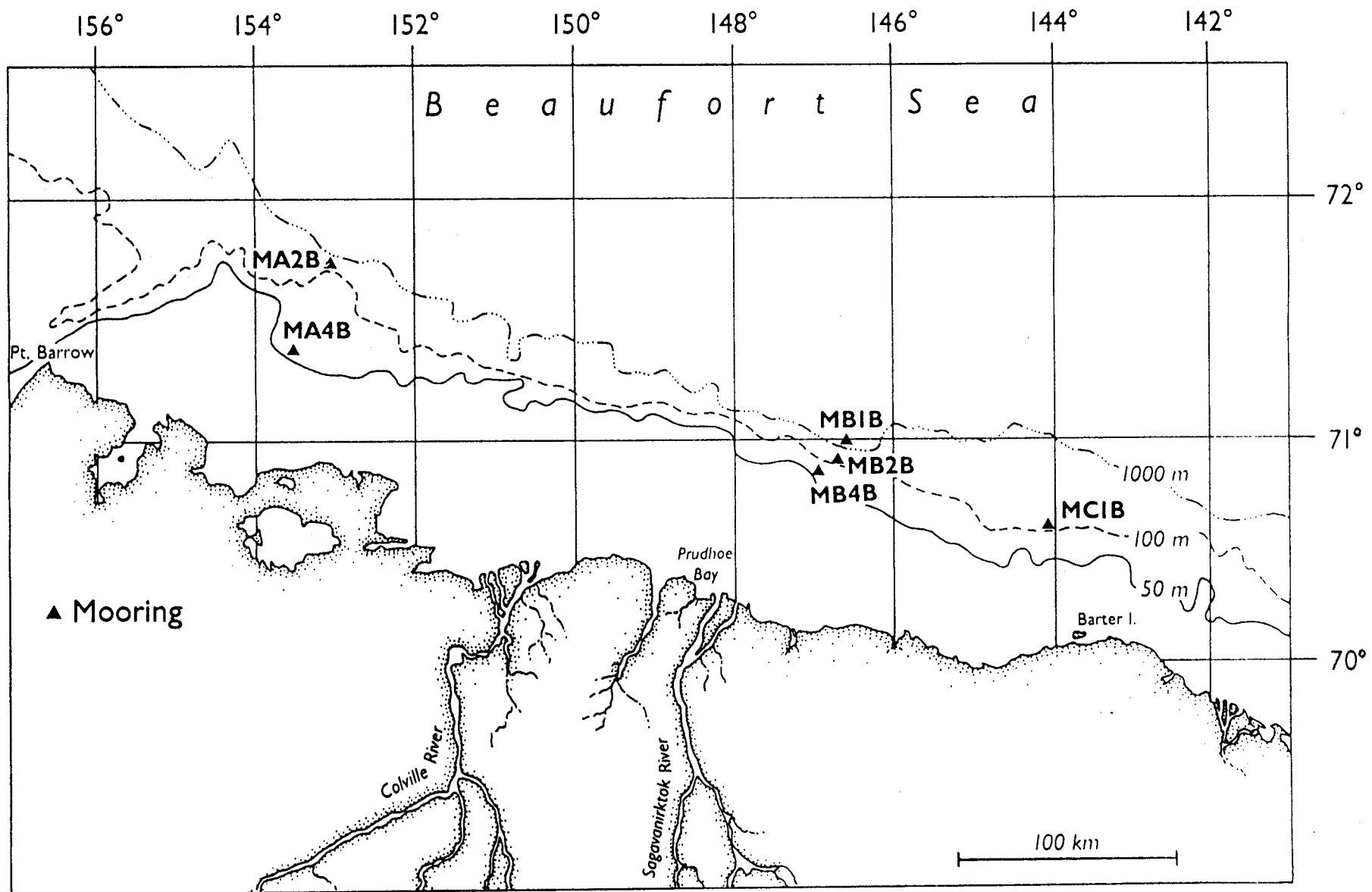


Figure 4. Beaufort Sea mooring locations, 1987-88.

**Table 4. Beaufort Sea Moored Instruments, 1987-88. \*Note that record MA2B, 112 m, lasted only 39 days.**

Mooring	Latitude N	Longitude W	Depth m	Instrument depths, m	Dates GMT
MA2B	71°43.5'	153°04.4'	187	CM: 79 112* 162 PG: 185	18-Apr-87 to 17-Apr-88
MA4B	71°22.6'	153°28.7'	53	CM: 45	28-Mar-87 to 27-Apr-88
MB1B	70°59.4'	146°38.2'	1022	CM: 64 97 162 994	26-Apr-87 to 6-Apr-88
MB2B	70°55.1'	146°45.8'	185	CM: 72 105 155 PG: 183	5-Apr-87 to 4-Apr-88
MB4B	70°52.6'	146°57.3'	60	CM: 52 PG: 58	3-Apr-87 to 30-Mar-88
MC1B	70°36.9'	144°08.1'	216	CM: 108 141 191 PG: 214	11-Apr-87 to 9-Apr-88

## Meteorological Stations

Extensive meteorological and ice drift data were obtained throughout the experiment, using a combination of drifting and land-based stations transmitting through the ARGOS and GOES satellite telemetry systems. Three GOES stations were installed in September 1986 to fill gaps in the primary National Weather Service (NWS) coastal observing network. Stations were established at Resolution Island in Prudhoe Bay, at the Lonely Dewline site near Pitt Point east of Barrow, and at Icy Cape southwest of Barrow. A fourth GOES station, funded by the Office of Naval Research (ONR), was placed at the Cape Prince of Wales navigation daymarker along Bering Strait in September 1987. Each station in the GOES network measured air pressure, ventilated air temperature, and wind components hourly, and transmitted the meteorological observations every three hours to the GOES-West satellite. These data were then rebroadcast to the GOES receiving station at Wallops Island, VA, which maintains a computer database which our laboratory computer interrogated daily. Data gaps shorter than a day were linearly interpolated. Gaps longer than a day, but less than a week were bridged using Joseph's scheme (Anderson, 1974). One gap in the temperature data at Resolution Island lasted from 6 October to 18 November 1987, and was not satisfactorily bridged. Deployment information is given in Table 5. The GOES stations at Lonely and Resolution Island were recovered in April 1988.

Further climate data were obtained for the primary NWS stations at Barter Island, Barrow, Kotzebue, and Nome from the National Climatic Data Center, Asheville, NC. These data included hourly sea-level pressure, air temperature, and wind components for the entire experiment period at standard levels for each station. The use of climate and GOES stations gave a nominal 150 km spacing for the land-based meteorological network.

Pressure and temperature fields at 6- and 12-hour intervals, respectively, were obtained from the Fleet Numerical Oceanography Center (FNOC), Monterey, CA. From these fields, we generated time series of sea-level pressure, surface air temperature, and winds at each of the above stations, at each current meter mooring site, and along the track of each ARGOS buoy, using the METLIB programs (Overland et al., 1980; Macklin et al., 1984). Temperature time series were resampled with a cubic spline to give 6-hourly data.

Time series of the surface winds were first obtained by rotating the gradient wind  $30^\circ$  toward low pressure and reducing the magnitude by a factor of 0.8. To verify this turning angle and reduction factor, we calculated the coherence of the northward component of the Climate or GOES winds with the component of the METLIB wind ranging from  $350^\circ$  to  $010^\circ$  T. We also calculated the complex correlation coefficient between these two types of winds at each meteorological station. The direction comparisons were hindered by the fact that NWS wind directions are reported only to the nearest  $10^\circ$ . However, results from the two most stable stations, Barrow and Resolution Island, suggested that appropriate rotation and reduction for the recalculation of the METLIB winds were  $23^\circ$  and 0.64, respectively. These turning and reduction values are consistent with the seasonal mean wind statistics from the 1975-76 AIDJEX Experiment, which found a range of reduction ratios of 0.55 to 0.60 and turning angles of  $24^\circ$  to  $30^\circ$  (Albright, 1980). Ratios of surface to geostrophic wind seem to vary from 0.75 - 0.80 in the subarctic Bering Sea to 0.55 - 0.60 in the high Arctic, with the North Slope values lying between these estimates.

Additional meteorological coverage was provided by deployments of ARGOS buoys and land stations by helicopter onto sea ice floes along the Beaufort and Chukchi coasts. Eleven ARGOS buoys and three ARGOS stations were deployed over 18 months in support of this study. In addition, four ARGOS buoys were deployed for the ONR Freeze experiment in the Chukchi Sea. Deployment information for the above buoys is summarized in Table 6. An example of one of the drifting meteorological stations is given in Figure 97 of Appendix A. ARGOS buoys were not recovered from the ice, but were left to drift until failure, which was typically caused by the buoys melting out of the ice and sinking.

Three additional ARGOS buoys were deployed from Prudhoe Bay in cooperation with the Polar Science Center, Applied Physics Laboratory (APL) at the University of Washington. They shared the data from 16 additional buoys, which were part of the Arctic Buoy Program. The APL buoy deployments are summarized in Table 7.

ARGOS buoys transmit surface pressure and ventilated air temperature data to the NOAA polar-orbiting satellites when the satellite is overhead and the satellites later rebroadcast to the Service ARGOS receiving stations in Toulouse, France, and/or Suitland, MD. Positions are calculated by Service ARGOS from the Doppler shift of the

transmissions, and the calculated positions and the sensor data are then available in preliminary form for daily computer interrogation and through fortnightly distribution by magnetic tape. Because the satellite passes were irregularly distributed in time, positions and data points were irregularly spaced. Therefore, we resampled the time series with a cubic spline to obtain data with a spacing of 60 minutes. The resampled position data was used to calculate the velocity and acceleration of the ice by central differencing.

**Table 5. Coastal Meteorological Station Summary Information** See Table 4 of Aagaard, Pease and Salo (1988) for information on gaps in the GOES data.

	<u>Type</u>	<u>Start time</u>			<u>End Time</u>			<u>Position</u>	
Barter I.	NWS-10	0000	1 Sep	1986	2300	31 Jul	1988	70.125°N	143.667°W
Resolution I	GOES-6	1800	26 Sep	1986	1200	29 Mar	1988	70.370°N	148.047°W
Lonely	GOES-6	2300	25 Sep	1986	1800	29 Mar	1988	70.917°N	153.253°W
Barrow	NWS-10	0000	1 Sep	1986	2300	31 Jul	1988	71.300°N	156.733°W
Icy Cape	GOES-3	2100	22 Mar	1987	1800	31 Dec	1988	70.325°N	161.867°W
Kotzebue	NWS-10	0000	1 Sep	1986	2300	31 Jul	1988	66.883°N	162.625°W
Wales	GOES-10	1300	14 Sep	1987	1800	31 Dec	1988	65.633°N	168.117°W
Nome	NWS-10	0000	1 Sep	1986	2300	31 Jul	1988	64.517°N	165.433°W

Table 6. ARGOS Buoy Deployment Information. All ARGOS buoys had ventilated air temperature and surface air pressure sensors. In addition, buoys 7420a, 7420b, and 7429 had 3-m vector-averaged anemometers and 6-m vector-averaged current meters. All times are GMT.

<u>Buoy</u>	<u>Start time</u>			<u>Deployment Position</u>		<u>End Time</u>			<u>Last Position</u>		<u>Hours</u>	<u>Type</u> <sup>1</sup>
7424 <sup>3</sup>	1855	9 Oct	1986	71.528°N	145.239°W	0213	18 Dec	1986	71.034°N	164.889°W	1662	EB
7420a	1707	14 Oct	1986	70.660°N	141.282°W	0252	26 Oct	1986	70.526°N	144.314°W	268	CS
7428a	1730	17 Oct	1986	71.919°N	152.146°W	0314	4 Nov	1986	72.136°N	154.557°W	416	EB
7421 <sup>2</sup>	0214	2 Mar	1987	65.899°N	168.469°W	0719	20 Mar	1987	66.886°N	167.909°W	436	PB
7422 <sup>2,3</sup>	2121	1 Mar	1987	64.737°N	167.570°W	1545	12 Jun	1987	63.312°N	165.720°W	2464	PB
7423 <sup>2</sup>	0500	8 Mar	1987	71.843°N	151.910°W	1958	12 Apr	1987	71.078°N	160.621°W	854	EB
7425 <sup>2</sup>	1105	8 Mar	1987	72.018°N	154.984°W	2232	16 Mar	1987	72.025°N	154.860°W	205	EB
7426 <sup>2</sup>	0313	13 Mar	1987	71.338°N	149.020°W	1731	2 Jun	1987	71.961°N	160.118°W	1956	EB
7427 <sup>2</sup>	2017	13 Mar	1987	71.041°N	145.915°W	0709	30 Mar	1987	71.236°N	147.738°W	394	EB
7420b	1332	29 Apr	1987	71.336°N	144.554°W	0253	14 Jun	1987	71.644°N	159.344°W	1092	CS
7013 <sup>2,7,9</sup>	2218	3 Sep	1987	71.936°N	158.086°W	8			73.951°N	178.440°E	9429	CT
7429 <sup>2,5,9</sup>	2213	5 Sep	1987	72.001°N	160.765°W	0849	21 Sep	1987	71.637°N	156.134°W	369	CS
7014 <sup>2,7,9</sup>	0653	8 Sep	1987	72.359°N	164.810°W	8			71.244°N	178.066°E	9325	CT
7015 <sup>2,9</sup>	2308	9 Sep	1987	72.810°N	168.930°W	0236	7 Dec	1987	71.694°N	177.297°W	2114	CT
7430 <sup>7</sup>	1900	17 Nov	1987	71.662°N	148.643°W	0751	30 Jun	1988	71.879°N	177.028°W	5408	CT
7432 <sup>7</sup>	2100	17 Nov	1987	71.454°N	145.466°W	0912	24 Jul	1988	73.095°N	175.412°W	5971	CT
7431	0000	18 Nov	1987	71.893°N	151.744°W	8			71.317°N	150.983°W	7627	CT
7428b	2342	16 Apr	1988	71.594°N	159.043°W	1915	27 May	1988	71.721°N	165.534°W	955	EB

1. Buoy types are: EB=ESI box, CS=Coastal Climate Company Station, PB=PMEL/Synergetics box, CT=Coastal Climate Company short tube 2. Time of first transmission 3. Buoy 7424 had poor transmissions; stable positions were rare. 4. Buoy 7422 had a data gap 21-25 May, 1987. 5. Buoy 7429 had a data gap 1-5 Sept., 1987. 6. Buoy 7428 had a data gap 5-13 April, 1988. 7. Buoys 7013, 7014, 7428, 7430, and 7432 had a data gap 29-31 Apr, 1988. 8. Buoy was still transmitting on 1 Oct 1988. Last transmission processed was 30 Sept 1988. 9. ONR funded deployment

TABLE 7. APL Buoy Deployment Information. Data for the following buoys, from the Applied Physics Laboratory of the University of Washington were used to fill in gaps in our ARGOS buoy array. All start times are times of the first ARGOS transmissions. All times are GMT.

<u>Buoy</u>	<u>Start time</u>			<u>Deployment Position</u>		<u>End Time</u>			<u>Last Position</u>		<u>Hours</u>
3161	0304	1 Aug	1986	70.281°N	145.458°W	2114	20 Sep	1986	70.646°N	145.610°W	1217
3164 <sup>6,7</sup>	0304	1 Aug	1986	75.892°N	157.802°W	0439	22 Nov	1987	80.243°N	150.224°W	11472
3165	0122	1 Aug	1986	72.447°N	173.619°W	1825	12 Sep	1986	72.744°N	168.297°W	1024
3848 <sup>5</sup>	0140	1 Aug	1986	76.724°N	163.814°E	0855	18 Aug	1986	74.349°N	165.704°E	3342
3849 <sup>3,4</sup>	0123	1 Aug	1986	76.578°N	134.065°W	0120	3 Nov	1986	76.517°N	128.183°W	2255
3880	0122	1 Aug	1986	73.332°N	157.428°W	0736	1 Jun	1987	73.027°N	174.152°W	7301
7012	0122	1 Aug	1986	76.975°N	172.230°W	0305	8 Sep	1986	77.538°N	174.109°W	913
7021 <sup>6</sup>	0317	1 Aug	1986	74.361°N	142.797°W	0317	9 Aug	1987	75.776°N	166.470°W	8951
7022 <sup>6</sup>	0307	1 Aug	1986	77.165°N	154.610°W	1700	15 Oct	1987	81.234°N	144.497°W	10573
7002 <sup>6,9</sup>	1125	12 Aug	1986	79.998°N	165.542°E	2222	19 Mar	1988	85.656°N	176.578°E	15802
7011	2259	19 Mar	1987	71.796°N	145.459°W	1658	10 Apr	1987	72.001°N	148.432°W	521
7047 <sup>6</sup>	0535	3 Apr	1987	72.005°N	148.360°W	1441	23 Nov	1987	73.106°N	179.630°W	5624
2380	0050	12 Apr	1987	71.288°N	161.371°W	0215	20 Jul	1988	71.660°N	156.454°W	457
3160 <sup>6,8</sup>	0040	12 Apr	1987	70.200°N	148.468°W	0142	29 Jan	1988	72.704°N	175.199°E	7008
7024	2351	27 Apr	1987	70.198°N	148.466°W	0043	20 Jun	1987	71.767°N	158.176°W	1272
7027 <sup>6</sup>	0112	14 Jun	1987	73.992°N	130.137°W	2114	31 Dec	1987	72.220°N	165.180°W	4819
3831 <sup>9</sup>	2114	31 Oct	1987	73.352°N	131.028°W	2227	31 May	1988	72.340°N	166.261°W	(1*)
7026 <sup>6,9</sup>	1837	1 Nov	1987	74.016°N	130.776°W	2232	31 Dec	1987	72.272°N	141.321°W	(2*)
7054	1147	15 Aug	1988	70.260°N	141.545°W	2009	31 Oct	1988	69.400°N	137.115°W	1856

1\*. Buoy 3831 was missing data from 1-31 July, 1988. Its record was divided into two sections, one spanning 5112 hrs, the other 2954 hrs. 2\*. Buoy 7026 lacked data from 1-31 Jan, 1988. Its file was divided into records 1443 hrs and 2903 hrs long. Other data gaps were: 3. 21-27 Oct., 1986 4. 31 Oct-2 Nov 1986 5. 4-17 Dec, 1986 6. 25-27 July, 1987 7. 18-20 Nov, 1987 8. 18-23 Jan, 1988 and 9. 28 Apr-1 May 1988.

## RESULTS AND DISCUSSION

### Chukchi Sea

The current meter array deployed in the Chukchi Sea during 1986-87 is at essentially the same location as one deployed from 6 September 1981 to 17 August 1982 (Aagaard, 1988). The statistics of the two records are compared in Table 8.

Table 8. Record-length current statistics for one-year moorings in the Chukchi Sea near 67° 39'N, 165° 38'W.

Year	Max. speed	Mean velocity	Principal axis		
	cm s <sup>-1</sup>	cm s <sup>-1</sup>	°T	°T	Variance %
1981-82	74	5.9	345	318	85
1986-87	57	5.6	336	325	87

We see that, on an annual mean basis, the flow was essentially identical in the two years, but that the extreme speed recorded was 30% greater during 1981-82. Figure 5, comparing the weekly mean currents, shows that although the annual mean statistics were very similar for the two years, there are important differences in the low-frequency flow. Compared to 1986-87, the 1981-82 record shows: 1) more extreme currents both northward and southward, 2) flow reversals extending much longer into the spring, and 3) stronger flow during most of the summer. On the other hand, there are points of similarity, with a highly variable flow (including reversals) occurring during the fall and early winter of both years and a period of weaker currents followed by an increasing flow in the spring which reaches a maximum in mid-summer. This sequence is consonant with the normal seasonal cycle in the inflow through Bering Strait (Coachman and Aagaard, 1988).

Our numerous nutrient sections in the Beaufort Sea show the Arctic Ocean nutrient maximum to be present above the continental slope and at times to extend onto the shelf (see Appendix A). The origin and maintenance of the nutrient-rich layer in the Arctic Ocean is therefore of considerable importance to conditions on and adjacent to the Beaufort shelf (see also Aagaard, 1984, and Hufford, 1974).

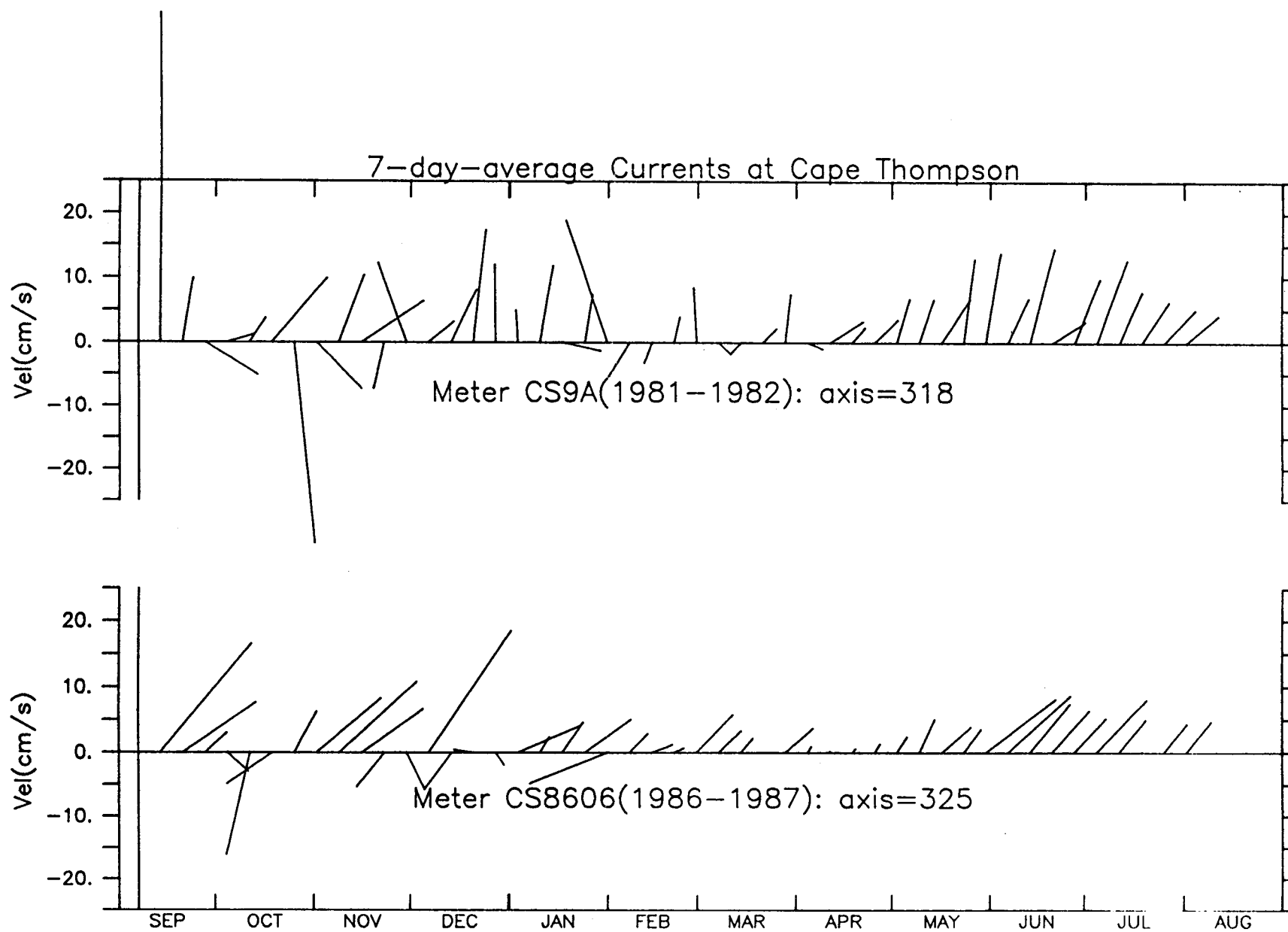


Figure 5. Weekly averaged current vectors at Cape Thompson for years 1981-82 (top) and 1986-87 (bottom) resolved on their respective axes of greatest variance.

Figure 6 shows the temperature, salinity, and nutrient structure in the upper 500 m of the Arctic Ocean about 400 km north of the Alaskan coast; the data were made available by J.H. Swift. The temperature maximum at 75 m occurs near the salinity 32.0 and is associated with relatively low nutrient values. In contrast, the temperature minimum centered near 180 m and corresponding to a salinity near 33.1, coincides with the nutrient maximum. Values for the latter exceed 15 for nitrate and 1.8 for phosphate, and are near 40 for silicate (all values in micromoles per liter). The various distributions are fully consistent with earlier Arctic Ocean profiles and can therefore be considered typical of at least the Canadian Basin.

To address the origin of these waters, consider the near-bottom distributions of salinity and nitrate in the Chukchi, East Siberian and Laptev seas (Figure 7) depicted by Codispoti and Richards (1968). Note that only in the western Chukchi Sea, are waters both saline enough and have sufficiently high nitrate concentrations to account for the properties of the nutrient-maximum layer in the Arctic Ocean. The same conclusion can be drawn from the near-bottom phosphate and silicate distributions (not shown). Now, from where does this water derive?

The essential element in this portrayal is the coincidence of high salinities (~33) and high nutrient levels in the western water mass and the contrasting lower salinities and nutrient levels of the Alaskan Coastal Water. This situation is seen in the recent sections by Tripp (1987) which spanned across Shpanberg and Anadyr straits in the northern Bering Sea and extended west from Point Hope into the central Chukchi Sea. In Anadyr Strait, the deep shelf waters at the time of the 1987 cruise were near 33 in salinity and had a nutrient content even higher than the maximum Arctic Ocean values, while in Shpanberg Strait the salinity was close to 32 and the nutrient values were very low (Figure 8). A similar situation occurred in the Chukchi Sea (Figure 9), where saline high-nutrient water was found at the western stations (although apparently the section did not extend far enough west to observe the water with the highest nutrient values), while the deep water in the eastern part of the section was similar to that observed in Shpanberg Strait.

The implication of these various data is that it is the nutrient-rich Anadyr Water which ultimately is responsible for the high subsurface nutrient levels in the Arctic Ocean. The corresponding Arctic Ocean temperature minimum is therefore not a temporal signal (from a

winter shelf source), but a spatial one (from a western shelf source with a lower mean annual temperature than the eastern source) (Coachman et al., 1975). This saline high-nutrient western source water moves onto the shelf in the southwestern Bering Sea and then northward via the westward-intensified Bering Sea circulation (Kinder et al., 1986) and into the western Chukchi Sea, eventually to supply the Arctic Ocean from east of Wrangel Island.

The salinity and nutrient distributions observed northwest of Pt. Barrow in October 1986 (Appendix A, Figures 8 and 11-15) are consistent with such a scheme. The saline, high-nutrient water was found over the slope (with some suggestion of upwelling at the time of the observations), where it participated in the net eastward flow of the Beaufort Undercurrent, and apparently followed the isobaths to enter Barrow Canyon from the northeast. In contrast, the water in the canyon immediately adjacent to the Alaskan coast was of lower salinity and greatly reduced nutrient content. Note particularly the high ammonia content (Appendix A, Figure 14) of the water with Bering Sea characteristics below 140 m at station W3. Although the applicable nitrogen regeneration rate is uncertain, it's unlikely that significant ammonia concentrations would persist over more than a few months. These concentrations therefore suggest a relatively recent shelf origin for the high-nutrient water, such as Herald Canyon, immediately east of Wrangel Island.

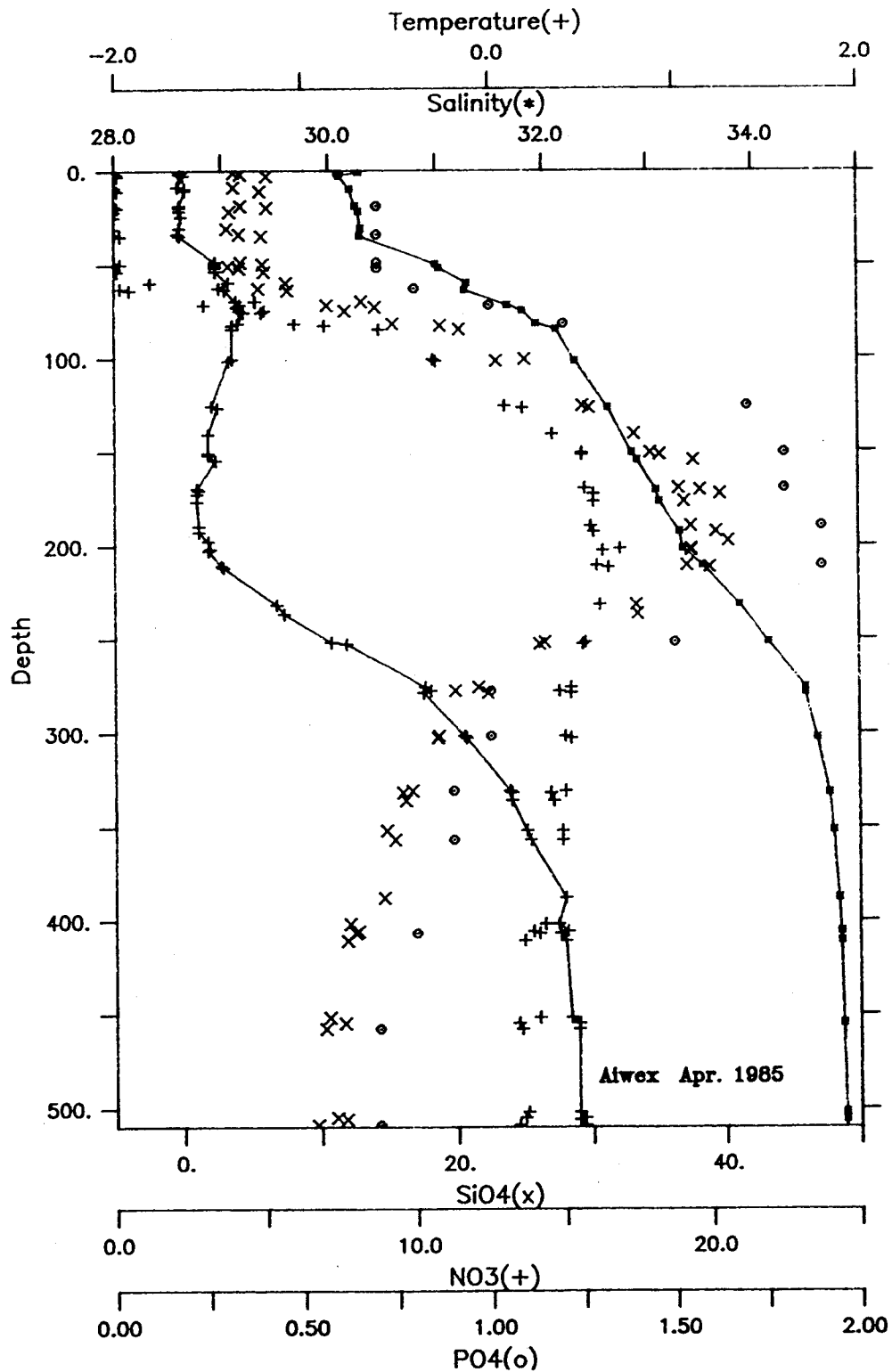


Figure 6. Profiles of temperature and salinity (symbols connected by solid lines) with scatter plots of nutrients composited from AIWEX (Arctic Internal Wave Experiment) conducted in April 1985 near 74 °N and 144 °W.

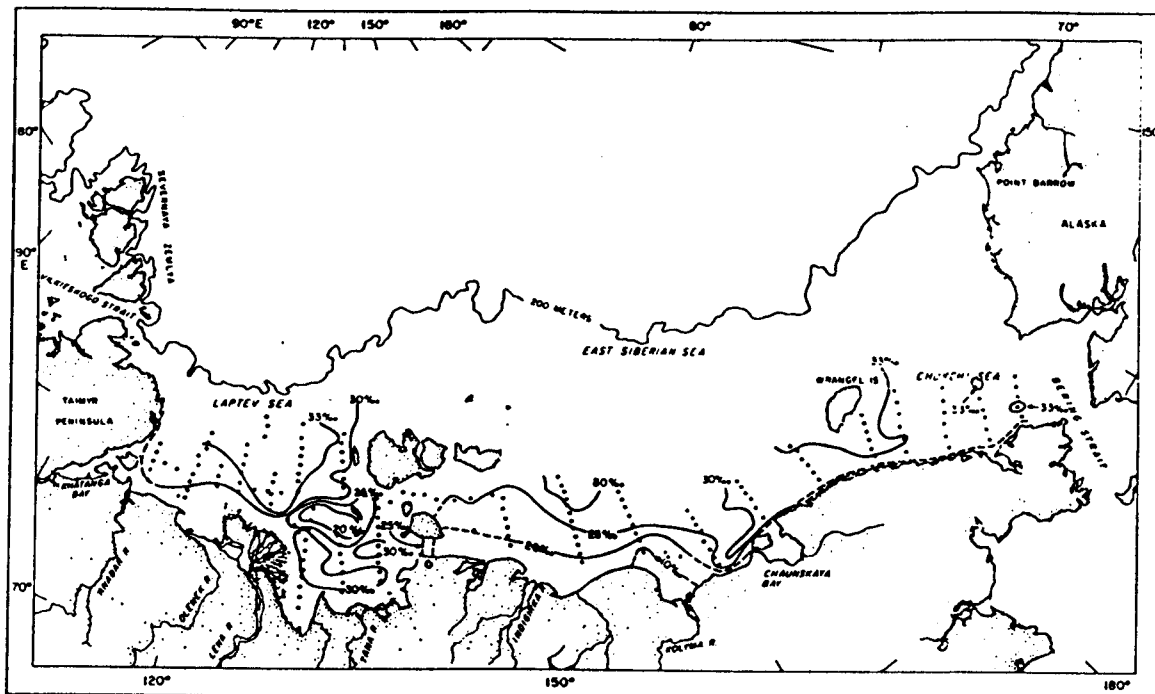


Figure 7a. Horizontal distribution of salinity, in psu, in the bottom waters (from Codispoti, et al, 1969).

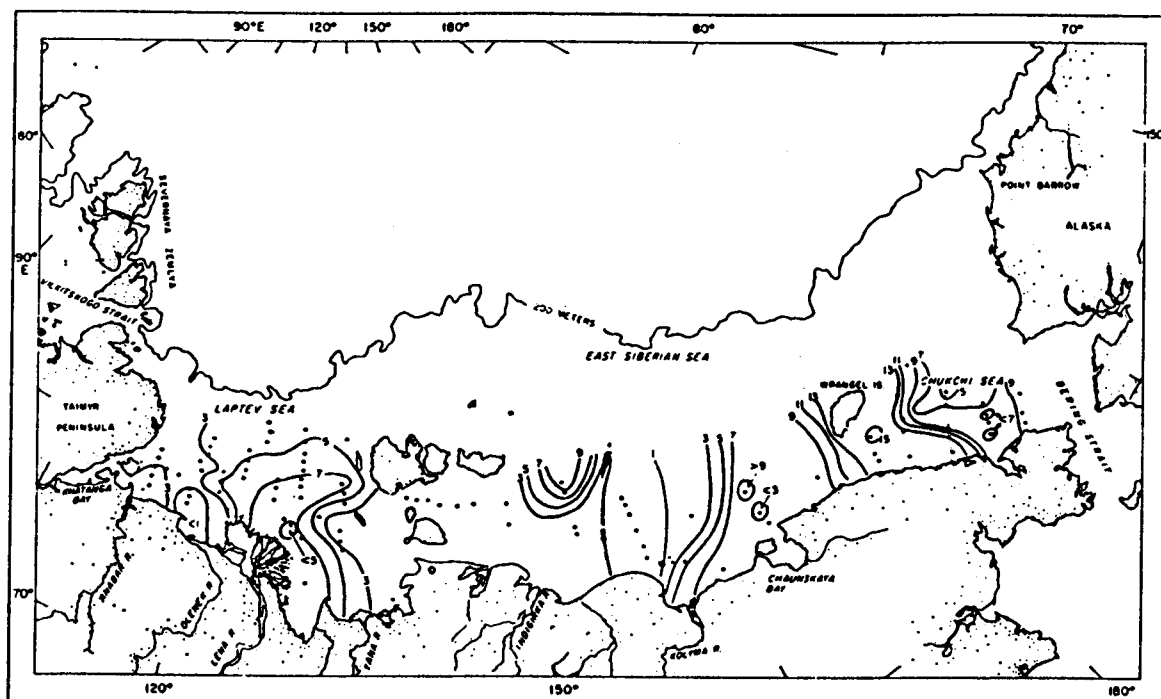


Figure 7b. Horizontal distribution of nitrate, in micro-grams-at/liter, in the bottom waters (from Codispoti, et al, 1969).

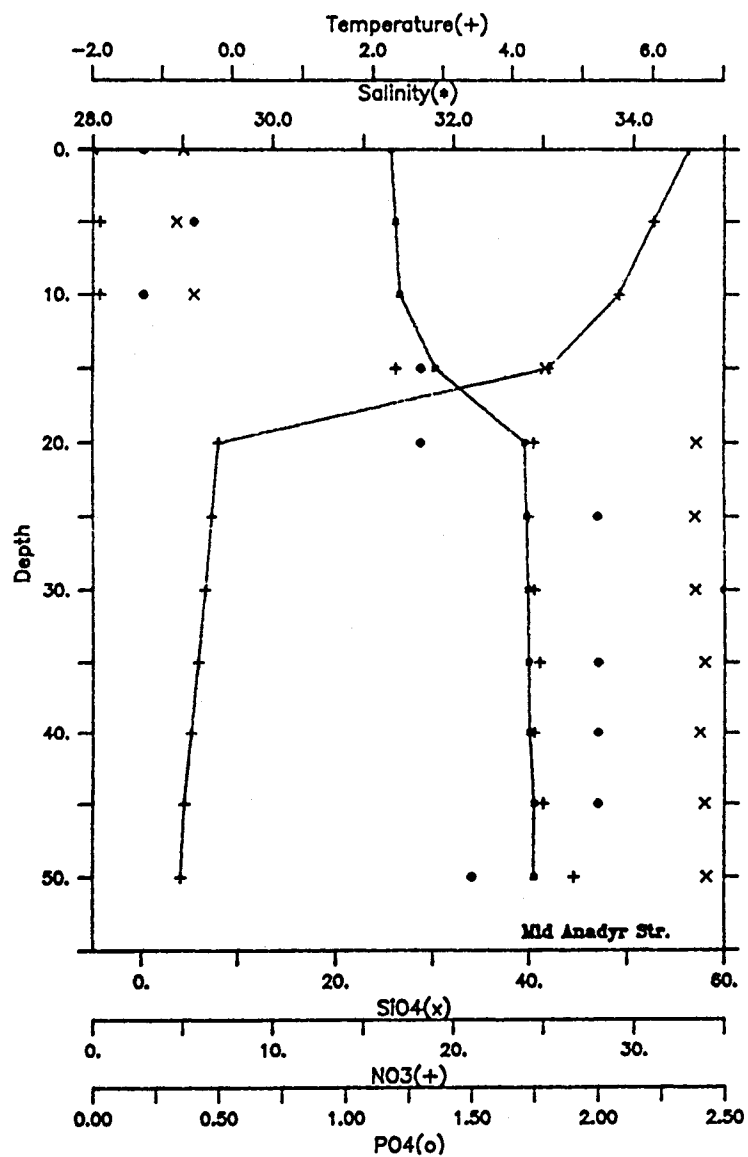


Figure 8a. As in Figure 6, at Anadyr Strait ISHTAR (Inner Shelf Transport and Resources) station.

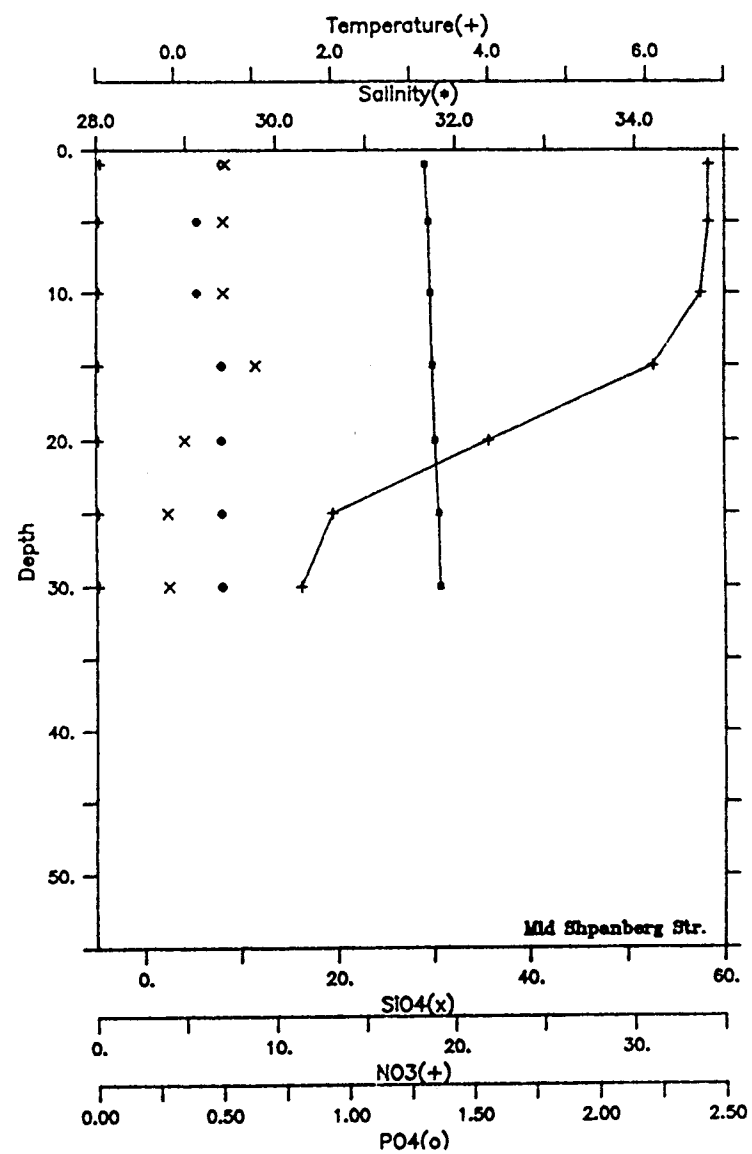


Figure 8b. As in Figure 6, at Shpanberg Strait ISHTAR station.

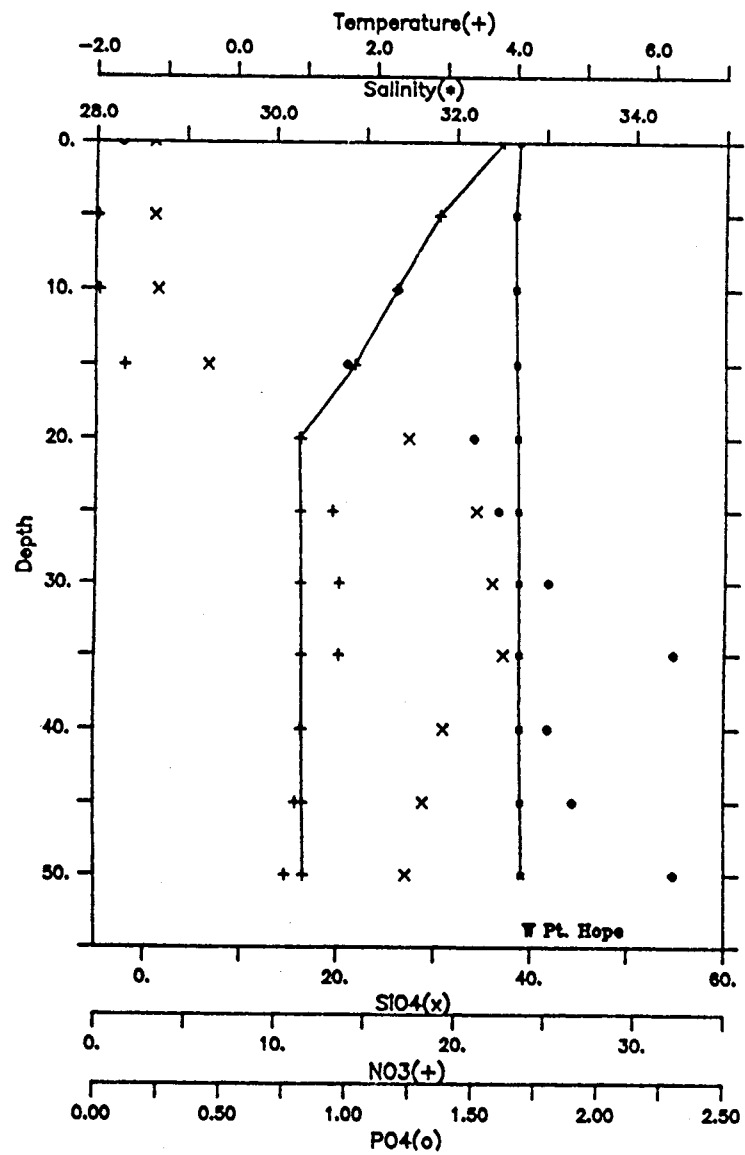


Figure 9a. As in Figure 6, at an ISHTAR station approximately 120 km off of Pt. Hope.

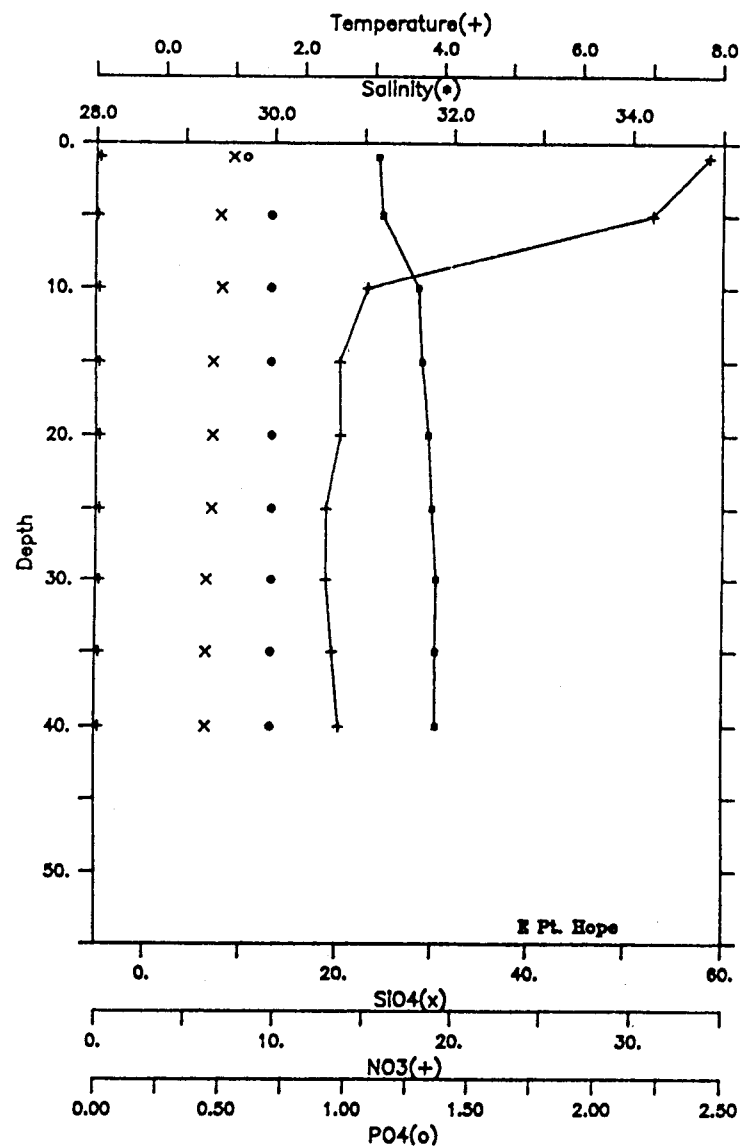


Figure 9b. As in figure 6, at an ISHTAR station approximately 20 km off of Pt. Hope.

## Barrow Canyon

The record-length mean flow through Barrow Canyon was directed northeast throughout the bottom layer (Table 9). Mean speeds were 13-16 cm s<sup>-1</sup> near the axis of the canyon, with somewhat stronger flow of 17-23 cm s<sup>-1</sup> on the shoreward wall of the canyon at BC2. The mean shear between the bottom two instruments, which were in each case separated by 5 m, was 1-3 cm s<sup>-1</sup>. Both moorings measured peak outflow speeds in excess of 90 cm s<sup>-1</sup> and the flow was generally closely aligned with the canyon axis: nearly 98% of the current variance was contained within the sector 45-60°T. The direction of the axis of greatest variance was slightly more variable vertically at BC2 than at BC1, but even the former record contains no significant rotational energy. The flow through the canyon is therefore essentially rectilinear.

**Table 9.** Current meter statistics for Barrow Canyon. Instrument designated by mooring and elevation above sea floor (m).

Instrument	Mean velocity		Principal axis	
	cm s <sup>-1</sup>	°T	°T	% of variance
BC1/14.0	14.8	54.4	225	97.5
/ 9.0	15.9	59.8	226	97.2
/ 2.0	12.8	59.7	223	97.7
BC2/14.0	22.7	53.4	229	98.0
/ 9.0	18.0	45.8	223	94.0
/ 2.0	16.9	48.0	222	97.8

There is, however, a suggestion of eastward rotation of the velocity component at BC1 following flow reversals. The latter are a prominent feature of the records and represent water being moved up-canyon toward the southwest (Figure 10). Each flow reversal typically lasted from two to six days, with southwestward flow as rapid as 60 cm s<sup>-1</sup>. Mooring BC1 generally showed reversals first, leading by 12-13 hr, whereas BC2 reverted to normal down-canyon outflow first, leading by 1-2 hr. While a clear seasonal signal is not evident in the current speeds, the number and intensity of reversal events declined throughout the winter and into the spring. The SeaCat records show that during the reversals, warm and saline water from the Atlantic

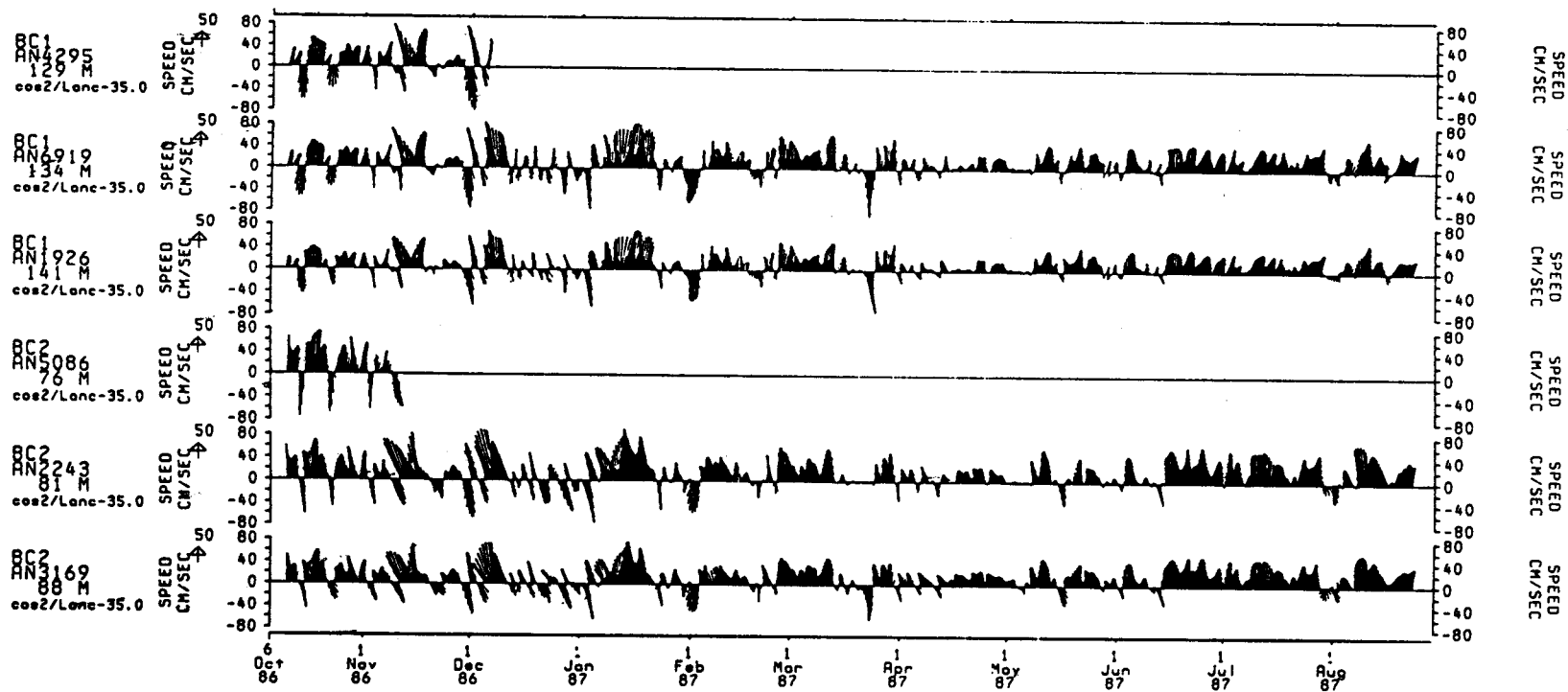


Figure 10. Six hourly, low pass filtered current velocity records from the Barrow Canyon current meters. All records were resolved on 50 °T; the canyon's major axis. The topmost current meters at each location failed in the early winter.

layer (Arctic Intermediate Water [AIW]) in water mass terminology [cf. Aagaard et al., 1985]) moved up-canyon into the Chukchi Sea (compare Figures 10-12), although in a number of instances the clear presence of upwelled water could only be detected at BC1, where the water was about 50 m deeper than at BC2. Such upwelling events in the canyon have previously been described by Mountain et al. (1976), and they have also been inferred by Garrison and Paquette (1982) who hypothesized mixing of upwelled water with ambient shelf waters. While our records do not contain obvious evidence of extensive mixing, the advection of AIW onto the shelf was frequent and often vigorous.

Overall, the temperature-salinity structure observed at the two moorings exhibited two volumetric modes; the largest being of low temperature and salinity and denoting the resident winter water of the Chukchi Sea, while the secondary mode represents upwelled AIW (Figure 13). There were differences between the two moorings, however, both in the mean state and the property range (Table 10, Figure 13). The water passing BC2 was in the mean fresher (by about 0.4) and warmer (by about 0.2°C) than at BC1; and the salinity and temperature over the canyon wall at BC2 varied by 3.8 and 5.5°C, respectively, while at BC1 they varied by only 2.4 and 3.1°C. Another point of difference was the seasonal temperature cycle. Neglecting upwelling events (shown by the elevated salinities in Figure 11), Figure 12 points to a fall cooling at BC2 from 2-3°C in early October to near-freezing temperatures by mid-November. The latter persisted until early July, when a rapid increase temporarily elevated temperatures back to near 3°C, announcing the arrival of summer water from the Bering Sea. Overall, the temperature record from BC1 shows a seasonal response about three weeks delayed and a magnitude perhaps one-third as great as that at BC2. All these differences are consonant with the two moorings being sited at different depths near the interface between the strongly stratified Arctic Ocean and the highly variable and shallow Chukchi Sea.

Note in Figure 13 that no water was seen corresponding to the cold and saline corner of the T-S plane, i.e., that there were no plumes carrying cold brines down the canyon. The search for such outflow had provided the original motivation for the study, and their absence from this data set will be considered below.

For periods exceeding three days, comparable velocity records from each mooring were well correlated ( $r=0.85$ , which is significant at the 95% confidence level). For example, during the first four inflow

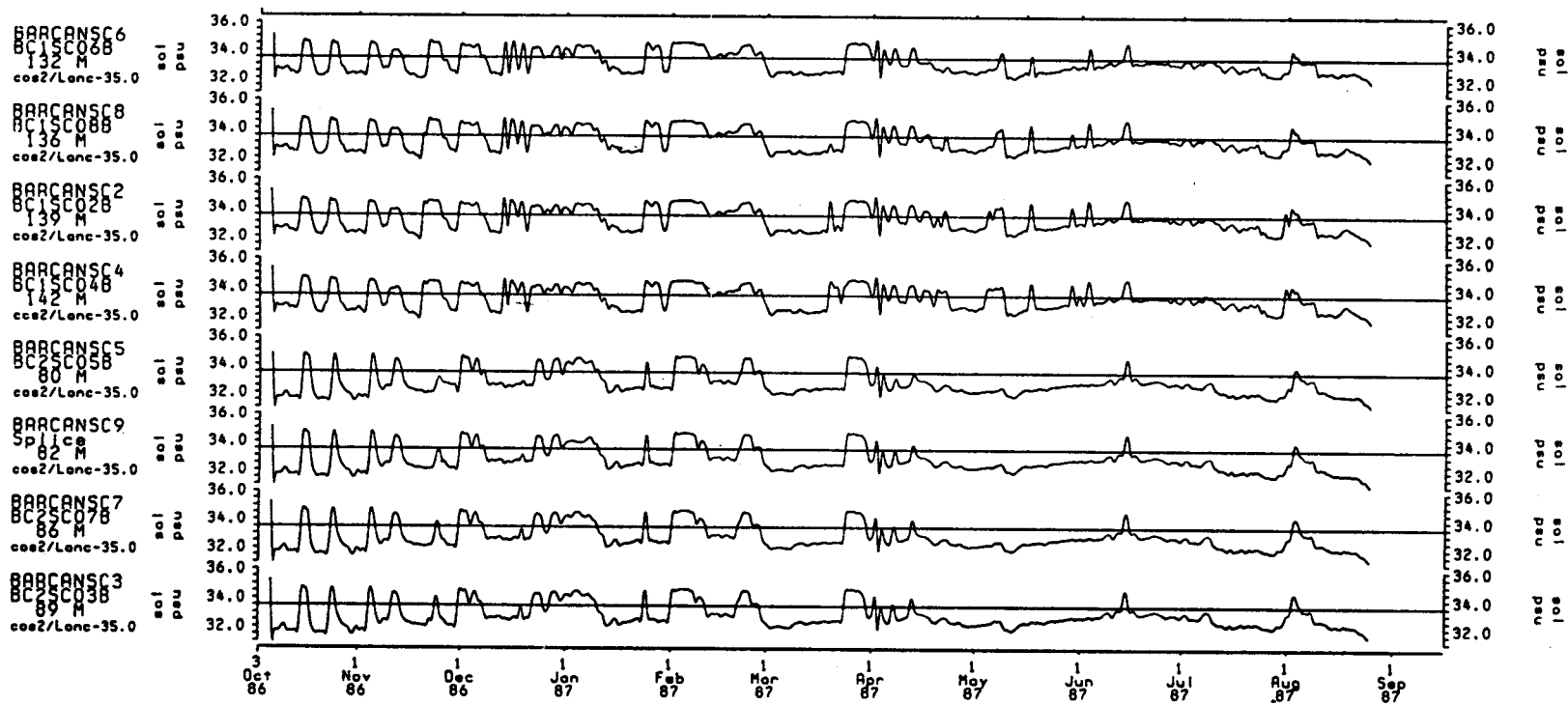


Figure 11. Six hourly, low pass filtered salinity records from the eight Seacats deployed. They are presented BC1, top instrument to bottom; BC2 top to bottom. The vertical scale is 31.0 to 36.0 psu.

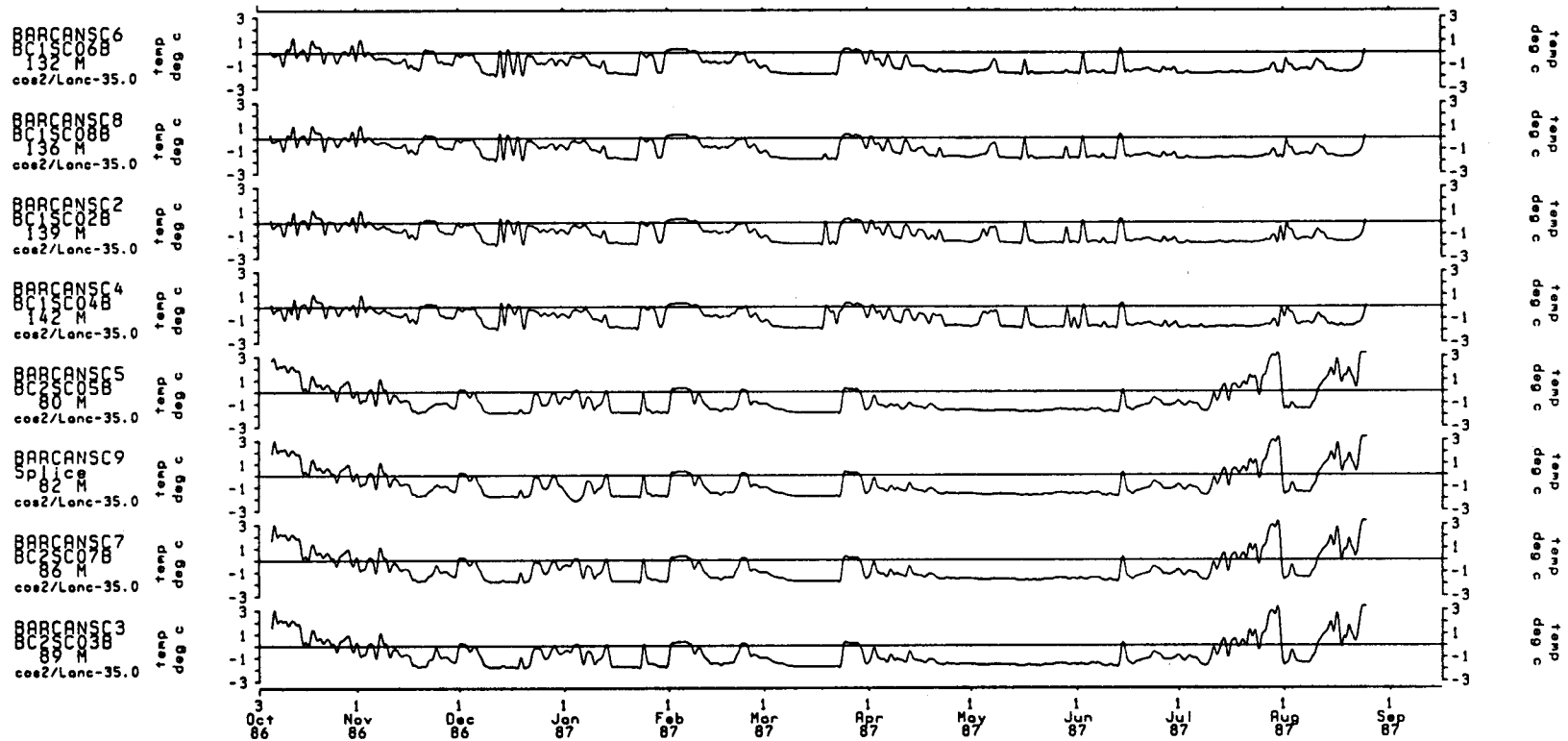


Figure 12. As in Figure 11, except for temperature from -3.0 °C to +3.0 °C.

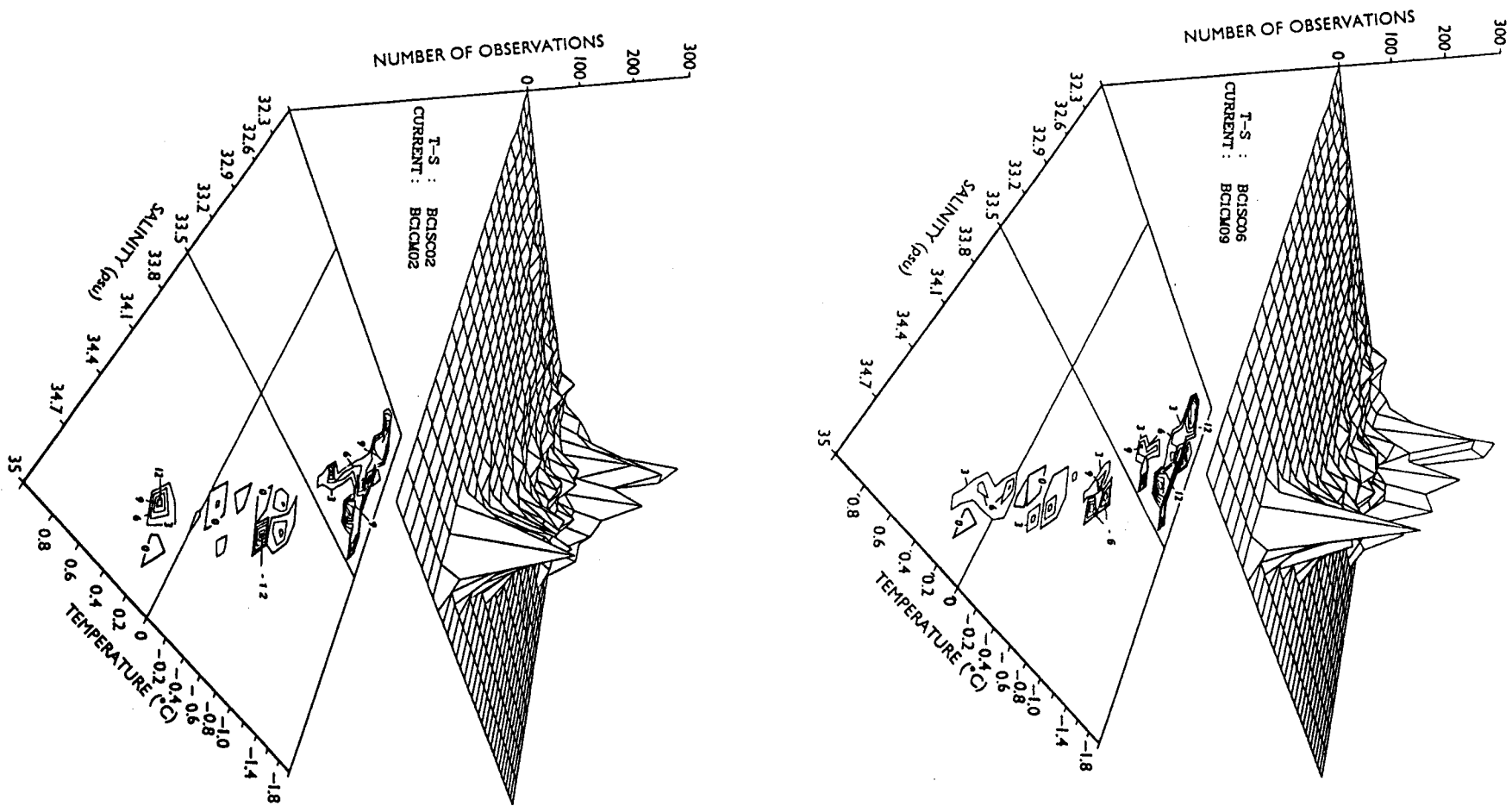


Figure 13. Frequency - mean velocity plot for Seacat and current meter pairs from BC1. The upper mesh plot represents the number of hourly observations of a particular temperature-salinity envelope, while the lower contour plot shows the corresponding net velocity along  $50^\circ T$  in contours of  $3 \text{ cm s}^{-1}$ . The pairs chosen are the uppermost Seacat with the current meter directly below it and the lowest current meter with the Seacat directly above it.

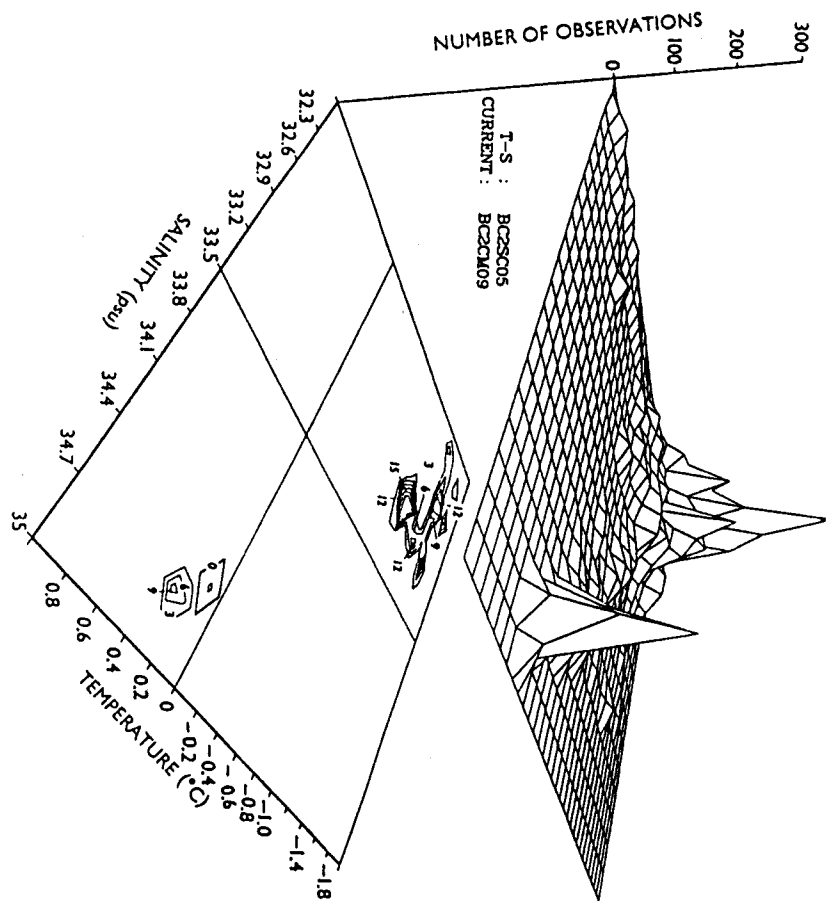
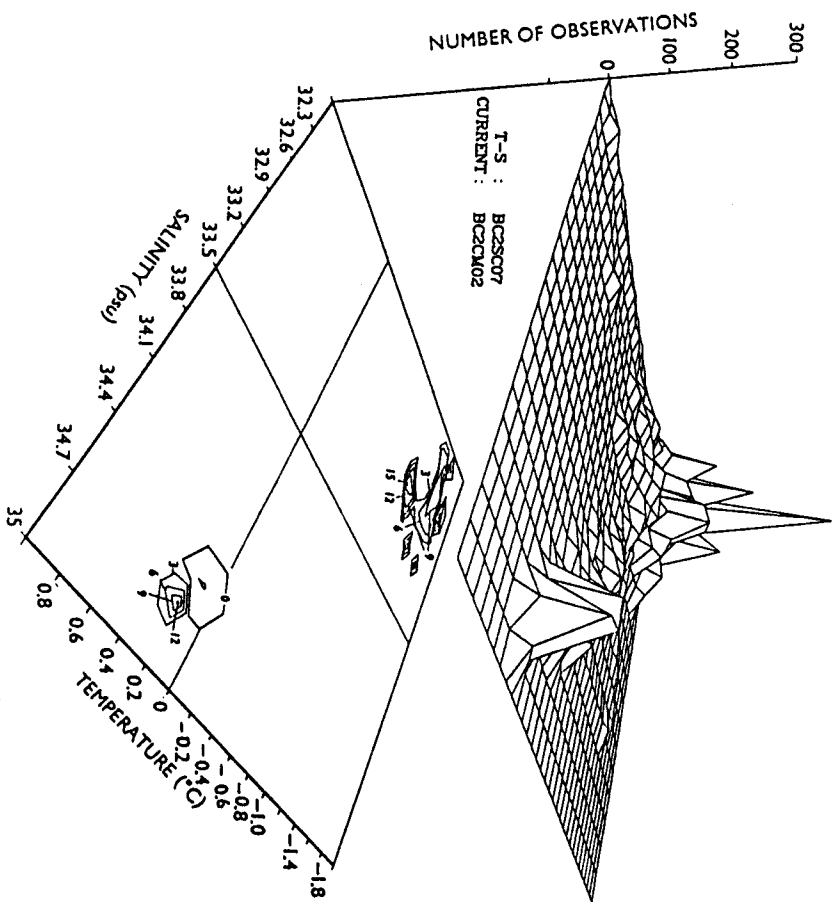


Figure 14. As in Figure 13, but for BC2.

events in October-November 1986 (Figure 10), the moorings showed a nearly uniform behavior, with the current recorded by each instrument leading the one above it by 2-3 hr (presumably a frictional effect) and maintaining a vertical velocity shear of 3-9 cm s<sup>-1</sup> over the instrument separation. On the other hand, because of the depth differences between the two moorings, the temperature and salinity records were only sporadically similar (Figures 11,12). For example, during the same first four inflow events, the variation in water properties recorded by the eight SeaCats was nearly identical. In contrast, during the weaker inflow events in May and early June, only the BC1 instruments showed significantly elevated temperature and salinity. There were also intermediate cases, e.g., in late January, in which the duration of elevated properties was much shorter along the canyon wall than near the floor. These observations are of course consistent with an inflow of AIW into the canyon, which only on occasion introduced a sufficiently thick layer to allow its observation at mid-depth. The frequently very limited thickness of the warm and saline intrusions was perhaps most obvious at the individual moorings. For example, during the mid-December property elevation at BC2 (Figures 11,12), the temperature and salinity 1 m above the bottom increased by nearly 1°C and 1psu, respectively, but the increases were less than one-half that only 10 m higher in the water column.

About 25% of the total low-frequency current variance can be accounted for by estimates of the wind variability near the north coast of Alaska ( $r \sim 0.5$ , significant at the 95% level), with the wind leading by 6-12 hr (Table 11). The Nome wind was equally well correlated with the flow, but with a greater lead, showing the regional coherence of the wind field. (The latter is also seen in the direct comparison between the Nome and Barrow winds, with a correlation exceeding 0.6 and the former series leading by about a day.) We also found about the same correlation between the surface atmospheric pressure difference between Barrow and Nome and the along-channel flow as with the wind and the flow. Note, however, that the portion of the current variance which can be accounted for by this pressure difference (29%) is significantly less than the 55% found by Mountain et al. (1976). We do not know the reason for this. We have checked the possible effect of seasonality by calculating the correlation between the flow and the Barrow-Nome pressure difference for 1987 during the same four-month period used by Mountain et al. (1976) for 1973, but we find that this correlation does not differ significantly from that for the full year 1986-87. The difference between our results and the earlier ones therefore remain unexplained, although we should expect the earlier

**Table 10.** Seacat statistics.

Mooring	Depth m	Mean Sal.	Sal. RMS	Max. Sal.	Min.Sal.
BC1					
SC 6	132.2	33.199	0.093	34.849	31.839
SC 8	136.4	33.244	0.091	34.848	31.843
SC 2	139.0	33.260	0.093	34.848	31.689
SC 4	142.0	33.300	0.093	34.850	31.649
BC2					
SC 5	79.2	32.754	0.106	34.803	31.161
SC 9	82.4	32.789	0.110	34.831	30.997
SC 7	86.0	32.828	0.110	34.844	31.247
SC 3	89.0	32.869	0.105	34.785	31.357
Mooring	Depth m	Mean Temp. Deg C	RMS	Max. Temp. Deg C	Min. Temp. Deg C
BC1					
SC 6	132.2	-1.012	0.182	1.287	-1.940
SC 8	136.4	-0.985	0.180	1.105	-1.942
SC 2	139.0	-0.952	0.179	1.070	-1.944
SC 4	142.0	-0.920	0.178	1.076	-1.940
BC2					
SC 5	79.2	-0.762	0.230	3.587	-1.904
SC 9	82.4	-0.791	0.203	3.512	-1.915
SC 7	86.0	-0.759	0.237	3.334	-1.919
SC 3	89.0	-0.755	0.237	3.230	-1.912

**Table 11.** Record length correlations of Barrow Canyon currents to regional winds and surface pressure gradients using 6 hourly data (lag in hours); positive lag means column leads.

	Barrow	Barter Isl.	Nome	Barrow-Nome Del P
BC1 134m	0.45 (6)	0.49 (6)	0.52 (18)	-0.53 (24)
BC1 141m	0.45 (6)	0.48 (6)	0.52 (24)	-0.51 (24)
BC2 81m	0.46 (6)	0.55 (6)	0.50 (24)	-0.55 (24)
BC2 88m	0.46 (6)	0.53 (12)	0.50 (24)	-0.57 (24)

results to be less representative because of the much shorter period of measurements.

Finally, we have calculated the turbulent fluxes of salt and heat from the combined current and SeaCat records (Table 12). The estimates are for two levels, approximately 2 and 7.5 m above the bottom, and the fluxes are referenced to the principal-axis coordinate system. Note that whereas the salt fluxes at BC2 are of various sign and the heat fluxes are directed down-canyon (because of the surge of warm outflow from the shelf in summer), the salt and heat fluxes at BC1 are all directed up-canyon. These fluxes represent the effect of upwelling events in driving a net onshore turbulent transport of salt and sensible heat near the bottom of the canyon. If we assume a layer 20 m thick and 25 km wide, the up-canyon heat flux will be about  $3 \times 10^{10}$  W and that of salt  $6 \times 10^6$  g s<sup>-1</sup>; the latter corresponds to an annual flux of  $1.9 \times 10^{14}$  g. The surface area over the canyon deeper than 100 m and lying inshore of the measurements is about 1200 km<sup>2</sup>. If the deep heat flux were all discharged through this surface area, it would represent an annual average flux of 26 W m<sup>-2</sup>, which is capable of melting about 3.5 m ice over the year. Intermittent upwelling into the canyon could therefore conceivably be locally significant in instances of efficient vertical mixing. A similar calculation for the turbulent up-canyon salt flux yields an annual value of  $1.9 \times 10^{14}$  g in the near-bottom layer, which is equivalent to a surface salt flux over the same 1200 km<sup>2</sup> of 16 g cm<sup>-2</sup> yr<sup>-1</sup>. This is about the amount of salt which would be expelled during the freezing of 6.5 m of ice. On the other hand, using the 1985 estimate by Aagaard et al. of brine discharge through Barrow Canyon during the winter of 1982, and referencing it to the annual mean salinity observed at the BC1 instruments, shows that the same excess salt ( $1.9 \times 10^{14}$  g) was discharged down the canyon during the last week of February 1982 alone. Our conclusion is therefore that the turbulent up-canyon salt flux may be locally significant, but is probably small (perhaps by one order of magnitude) compared to the collective discharge through Barrow Canyon of brine from the eastern Chukchi Sea during years of active brine build-up. Since the winter 1986-87 was one of no measurable brine discharge, the onshore flux driven by upwelling looms relatively large in these records.

Also shown in Table 12 are the turbulent fluxes calculated for 1986-87 at the two moorings MA2 and MB2, located near the shelf break farther east at 153°W and 147°W respectively. The temperature and salinity series were derived from Aanderaa sensors mounted on

the current meters. Particularly notable is the absence of indications of net onshore sensible heat and salt fluxes associated with the frequent upwelling which has been observed along this shelf. The potential for at least locally significant fluxes of heat and salt onto the shelf through upwelling therefore appears to be restricted to major topographic breaks in the shelf, such as Barrow Canyon.

Our original interest in making these measurements was directed toward the outflow of cold brines from the shelf, such as we had found earlier both in Barrow Canyon [Aagaard et al., 1985] and farther south in the Chukchi Sea [Aagaard et al., 1981]. The year 1986-87, however, proved to be one which either had insufficient brine production to give measurable signals in the canyon or the brine produced was not exported through the canyon. We do not know the reason for this failure to observe brines, for while the autumn of 1986 was abnormally warm, with an unusually large number of lows propagating northward along the Chukchi coast, the ensuing winter was markedly abnormal in neither air temperature nor wind regime. Furthermore, inspection of the AVHRR imagery for January and February shows the frequent and prolonged occurrence of open water or thin ice along the coast, as much as in any other year. Nevertheless, it is clear that whatever the long-term contribution to the Arctic Ocean of saline outflows from the Chukchi Sea proves to be, there are years in which at least the outflow through Barrow Canyon makes no contribution whatsoever to the shelf-derived brine flux which on longer time scales appears so important to the structure of the Arctic Ocean.

Table 12. Estimates of salt and heat flux. Instruments from Barrow Canyon are referred by depth above the bottom for the current meters and by the SeaCat number using principal axes of 50°T (U) and 140°T (V). The Beaufort Sea current meters are referred to by their depth in meters with 300°T (U) and 30°T (V).

Instrument	Salt Flux (cm psu s <sup>-1</sup> )				Temperature Flux (cm °C s <sup>-1</sup> )			
	U'S'	V'S'	R	Theta	U'T'	V'T'	R	Theta
<b>BC1</b>								
CM9 SC6	-0.62	-0.77	0.99	281	-1.17	-0.56	1.30	256
CM2 SC2	-1.75	-1.06	2.05	261	-1.78	-0.87	1.98	256
<b>BC2</b>								
CM9 SC5	-0.53	-1.11	0.95	295	6.23	0.53	6.26	055
CM2 SC7	-0.79	1.44	1.64	169	4.89	0.10	4.89	051
<b>MA2</b>								
CM 60	-1.06	0.11	1.06	114	1.48	-0.48	1.56	282
CM 93	-0.37	0.05	0.38	112	0.35	0.29	0.46	260
CM 143	1.80	0.38	1.84	312	1.08	0.32	1.13	317
<b>MB2</b>								
CM 62	-0.31	0.12	0.33	099	-1.45	-0.32	1.49	132
CM 95	-0.32	-0.03	0.32	125	0.49	0.00	0.49	300
CM 145	1.07	-0.40	1.14	279	0.22	-0.01	-0.22	298

## Beaufort Sea Hydrography

The hydrography of the Beaufort Sea is discussed and portrayed in detail in **Appendix A**. Note that the hydrographic data of **Appendix B** also includes profiles of light attenuation during the October 1986 cruise. These profiles were measured to complement the listed discrete measurements of suspended particulate matter (SPM). **Figure 15** shows the light attenuation in Section C, near 144°W; it can be considered characteristic of the fall sections. Section C contains an attenuation maximum over the inner shelf and extending seaward over the middle shelf in the lower half of the water column. The maximum measured attenuation exceeded  $3 \text{ m}^{-1}$ . There is a strong optical front at the surface seaward of the 25 m isobath. Farther offshore, attenuation was quite low, generally less than  $0.8 \text{ m}^{-1}$ , even over the shelf break. Within the region of maximum attenuation, SPM values exceeded  $6 \text{ mg l}^{-1}$ . Comparison with **Figures 43-51 in Appendix A** shows no coincidence of attenuation with other properties, other than some correlation with the density structure over the shallower portions of the shelf. The implication of these various observations is that the increased water turbidity over the shallower portions of the shelf is primarily due to resuspension of fine sediment. It therefore depends both on water velocity and on the sedimentary nature of the bottom. We note that in general there is little, if any, connection between light attenuation and the principal water masses.

**Appendices B and C** also show that discrete sampling was done for several transient tracers, including tritium, carbon-14, freons, and radioactive isotopes of cesium, radium, and strontium. These were all add-on measurements, with analysis being done by other investigators and laboratories. The analytical procedures and schedules are such that to date, only the tritium and carbon-14 analyses have been completed. These have been released by Prof. Ostlund of the University of Miami as Tritium Laboratory Data Release #88-01. They demonstrate that all the water above 1600 m shows some degree of ventilation within the past 30 years, with values above 1 tritium unit (normalized to 1981).

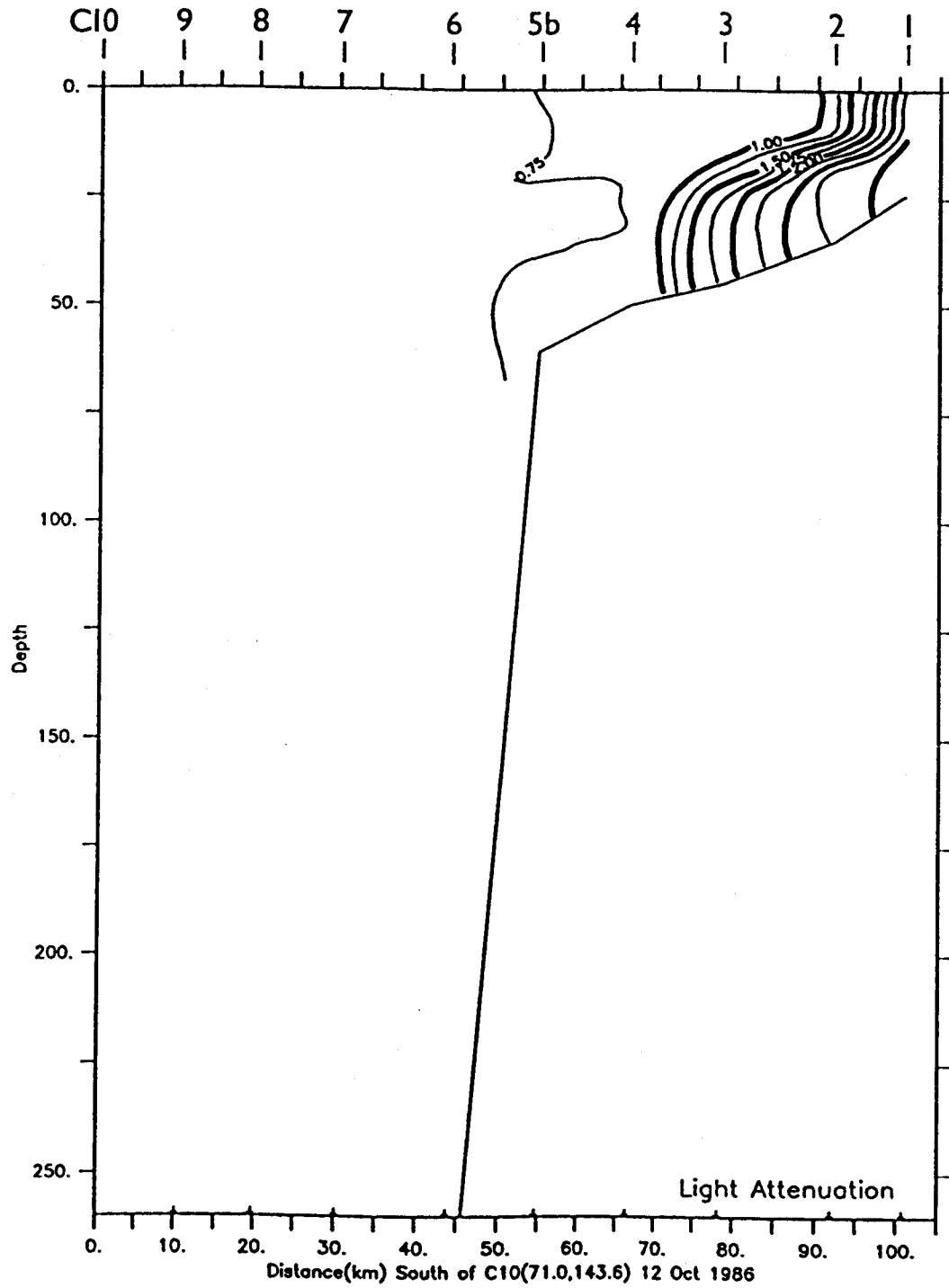


Figure 15. Profile of light attenuation ( $m^{-1}$ ) at Section C near  $114^{\circ}W$ .

## Beaufort Sea General Flow Characteristics

Table 13 shows the record-length current statistics for the various instruments at the six moorings deployed during 1987-88. Maximum low-pass filtered speeds in the upper 200 m generally ranged from 30-100 cm s<sup>-1</sup>, with the most rapid flow occurring in the upper part of the water column near the shelf break and over the slope. The mean velocity was also greater in this outer region than over the middle shelf. In contrast to the high-speed flow events, however, the mean motion registered by the uppermost instruments was generally less than at intermediate depths, although the variance was sufficiently large that the error bars at the various levels overlap. At two locations (MA2B, 79 m; and MA4B, 45 m) the mean flow was statistically indistinguishable from zero. Note that the former instrument recorded the fastest short-duration flow of any during the year. Except for the very deep instrument at MB1B (994 m), all statistically significant mean flow was nominally towards the east, manifesting the Beaufort Undercurrent, which sets eastward following the outer shelf and slope over the entire Alaskan and Canadian Beaufort Sea (Aagaard, 1984).

There was considerable low-frequency variation in this flow, but this variability was largely restricted to the mean flow axis, and comparison with local isobath trends suggests strong topographic steering of the flow (compare Aagaard, 1984). Table 13 shows the principal axis (the axis of greatest variance) for each current record, as well as the fraction of the total variance occurring along that axis, and it is clear that at least below the upper 40-50 m the flow is highly two-dimensional, with the principal axis nearly coincident with the mean flow and containing the vast majority of the variance. Interestingly, it is over the continental slope, where the bottom slope is the largest and one might expect the strongest topographic steering, that the variance along the principal axis is the least, indicating the greater relative importance of cross-isobath flow there (although the principal-axis variance is still 86% or more of the total).

**Table 13.** Beaufort Sea Record-Length Current Statistics, 1987-88. Maximum speed calculated from 35-hour low-passed velocity. The rms error along the principal axis is given in parentheses. Record MA2B, 112 m, lasted only 39 days.

Mooring	Depth m	Maximum speed cm s <sup>-1</sup>	Mean velocity cm s <sup>-1</sup>	°T	Principal axis °T	%Variance
MA2B	79	99.4	1.6 (3.8)	102	120	96
	112	38.8	3.3 (5.0)	130	124	97
	162	78.0	5.6 (2.0)	113	117	96
MA4B	45	39.2	1.1 (1.1)	321	125	91
MB1B	64	67.2	3.8 (2.3)	107	095	87
	97	47.7	3.7 (2.2)	106	100	86
	162	31.2	1.1 (0.5)	097	098	92
	994	13.6	0.8 (0.2)	023	082	86
MB2B	72	57.1	5.9 (1.7)	113	106	95
	105	48.5	7.6 (1.2)	110	105	96
	155	51.1	6.6 (1.1)	109	108	99
MB4B	52	30.9	1.4 (0.8)	118	100	94
MC1B	108	72.7	5.1 (2.5)	111	105	93
	141	63.6	5.7 (2.2)	105	103	96
	191	45.0	3.6 (1.1)	103	099	97

Figures 16 and 17 show the 35-hr low-passed velocity vectors recorded at the 15 current meters. Each record has been resampled at 12 hr intervals, and the vertical direction in each display represents the principal axis for that record (see Table 13). Note the differences in the speed scales on the vertical axes. The prevailing downward orientation of the vectors represents the nominally eastward Beaufort Undercurrent. The considerable coherence between many of the records, both vertically and horizontally, is obvious in the figures; we return to this issue later.

In addition to the largely reciprocating motion, in which the velocity switches along the principal axis, corresponding to a local

reversal of the undercurrent, there are instances in which the current vector appears to rotate, yielding either an open or a closed pattern. For example, at the two upper current meters at MC1B (Figure 16), early July shows an open vector pattern, and early November a closed one. Comparison with Figure 6 in Foldvik et al. (1988), suggests that these represent the passage of clockwise (anticyclonic) and counterclockwise (cyclonic) eddies, respectively. Figures 16 and 17 suggest the clockwise eddies to be the more common. We note that the predominance of clockwise eddies is also a feature of the deep Canadian Basin, where baroclinic eddies embedded in the pycnocline are an extremely important feature of the circulation (Manley and Hunkins, 1985). For a typical rotation time scale of 3 days and an advection velocity of the eddies past the current meter of 10-20 cm s<sup>-1</sup>, the eddy diameter would be in the range 25-50 km. Such a reconstruction corresponds rather well with the warm eddies suggested in Figure 2 of Aagaard (1984).

Figures 18-22 show the energy-preserving rotary coherence spectra for the various Beaufort Sea current meter records. Note that the spectral shapes and amplitudes vary considerably. The lack of a low-frequency roll-off at the uppermost instrument on MA2B is particularly noticeable. This is probably due to the relatively brief period of high speeds (particularly toward the west) during late summer and early fall of 1987 (Figure 16), which contrasts with the more uniform distribution of current speeds recorded by the other instruments. Such non-steady statistics alias the spectral estimates, folding the energy into lower frequencies. Among the other spectral peaks in Figures 18-22, a consistent peak corresponding to about a 4.5 day period is found at the shelf break moorings, i.e., at MA2B, MB2b, and MC1B, particularly at the deepest meters. This may represent the frequent eastward propagation of a shelf wave, as also suggested by the coherent phased upwelling events extending along the entire Alaskan Beaufort Sea shelf (see Section III.C4). In the suggested eddy frequency band, the spectra generally show more energy in the clockwise mode (e.g., Figure 18, record MA4B), in agreement with the visual impression from Figures 16 and 17.

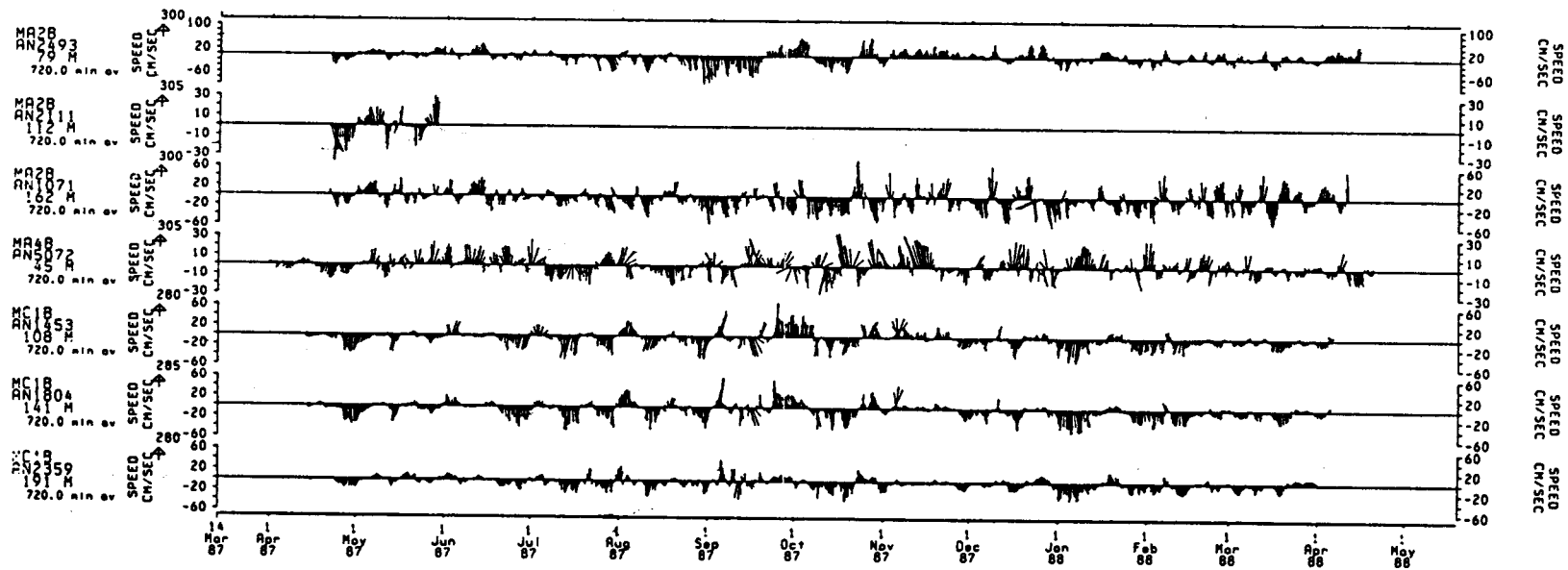


Figure 16. Low-passed velocity records at MA2B, MA4B, and MC1B. The vertical axis is parallel with the principal axis for each record; up is nominally westward.

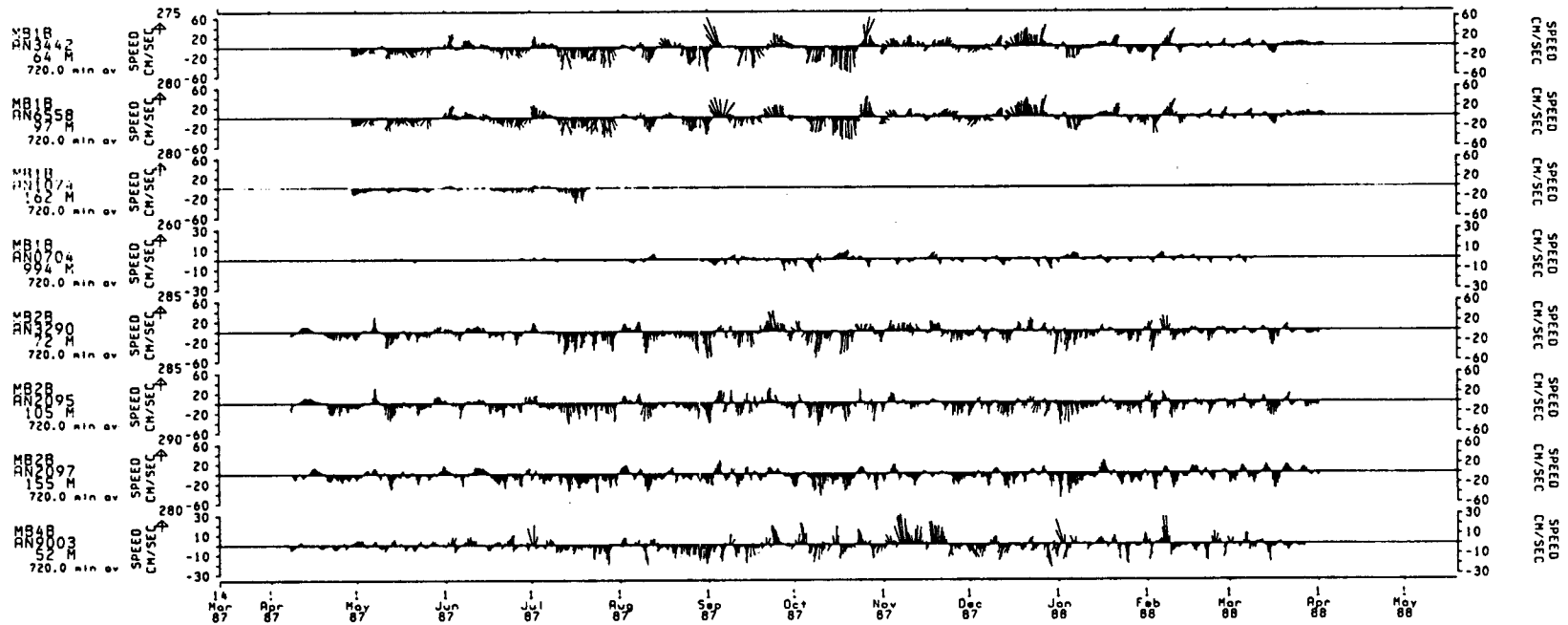


Figure 17. As in Figure 16 for low-passed currents from MB1B, MB2B, and MB4B.

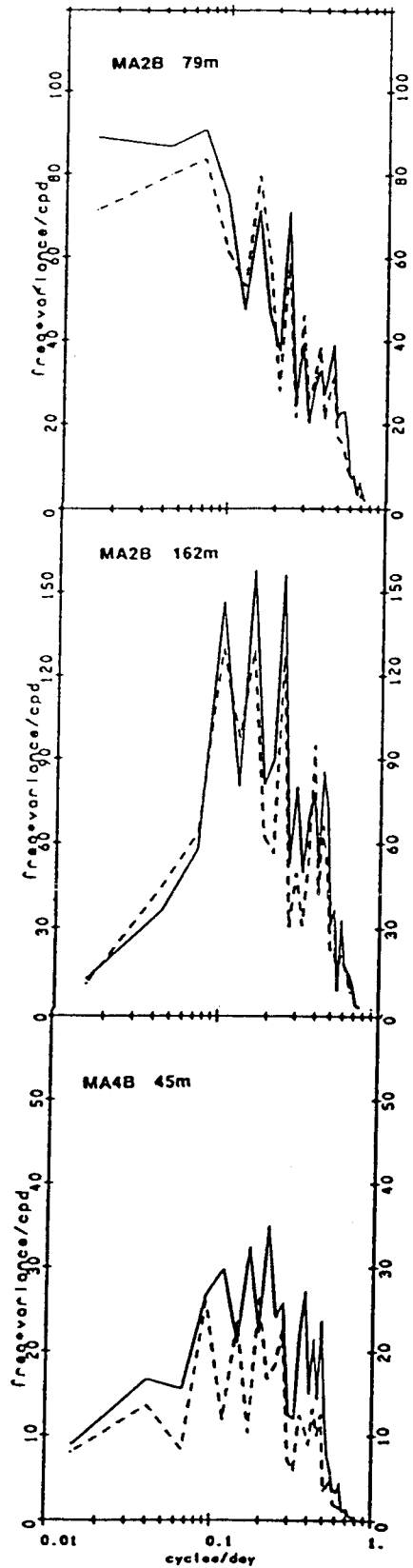


Figure 18. Energy-preserving rotary spectra for moorings MA2B and MA4B. The solid lines represent clockwise rotation and the dashed lines counterclockwise.

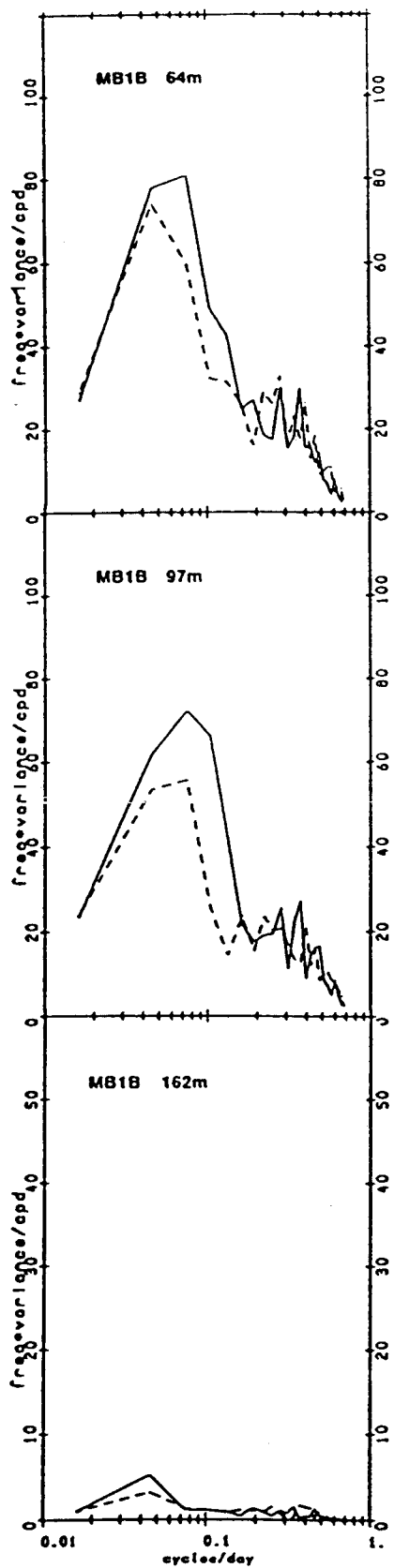


Figure 19. As in Figure 18, for mooring MB1B.

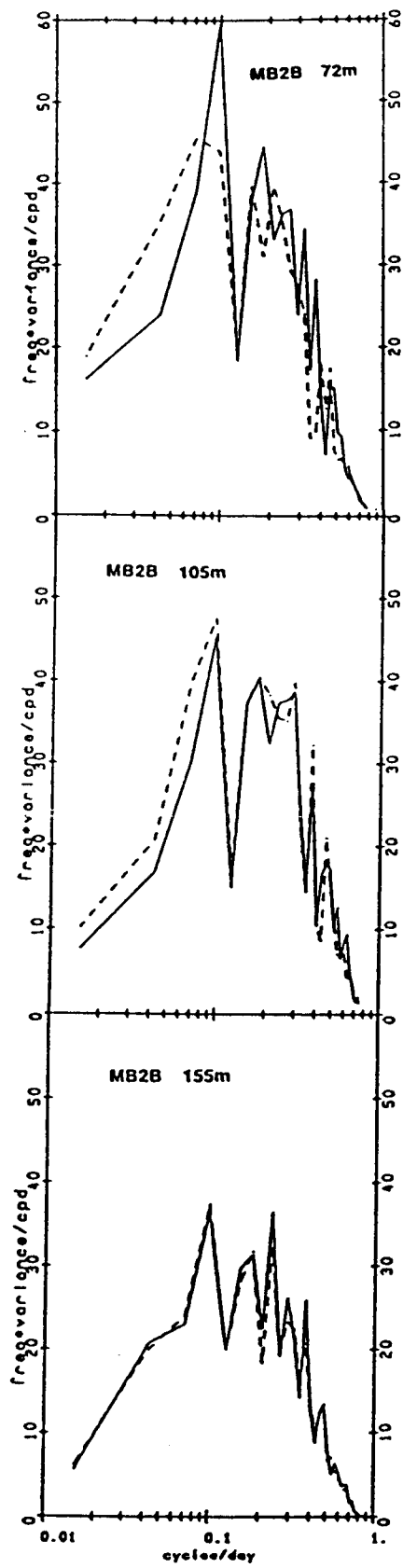


Figure 20. As in Figure 18, for mooring MB2B.

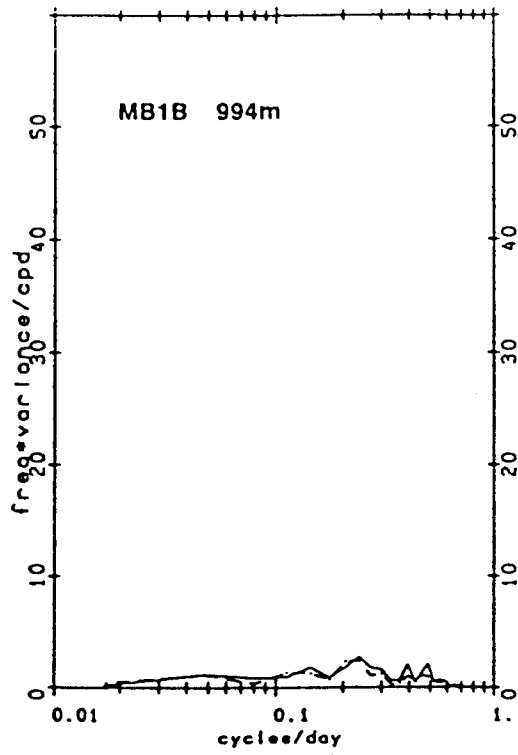
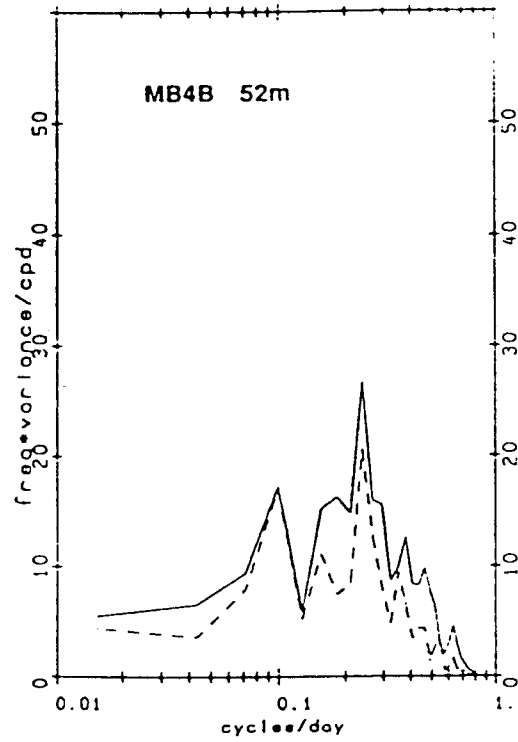


Figure 21. As in Figure 18, for moorings MB4B and MB1B (994m)

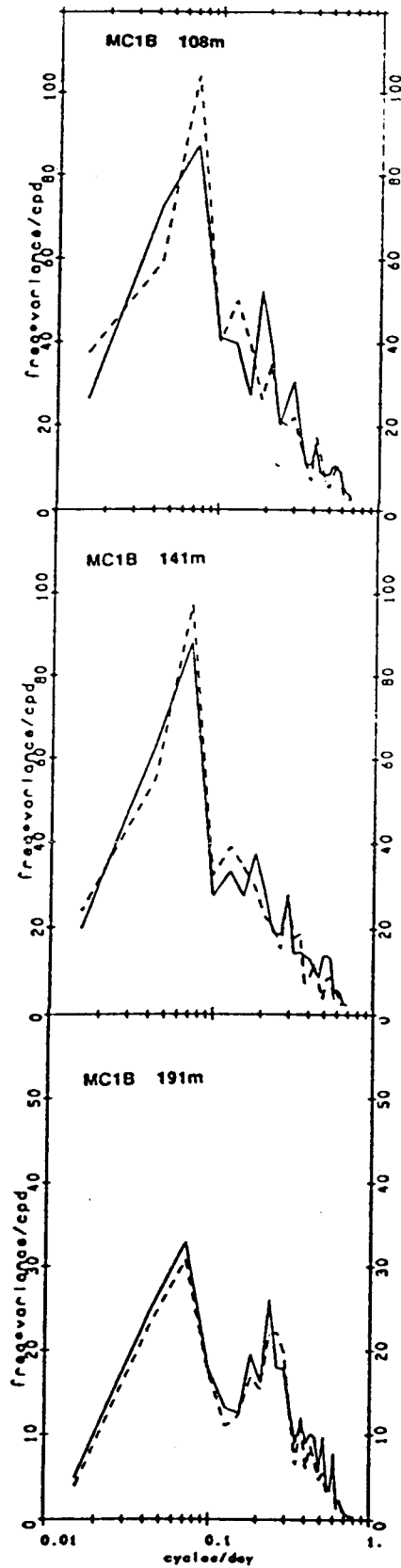


Figure 22. As in Figure 18, for moorings MC1B.

## Beaufort Sea Variability at Very Low Frequencies

At mooring sites MA2, MB1, and MB2 the current meter records were essentially continuous for 18 months and thereby provide evidence of variability on at least seasonal time scales. Table 14 shows the record-length mean currents at comparable locations for nominally the first six and the last twelve months of the joint records. Perhaps the most striking difference between the record segments is in the upper ocean, where during the first period the uppermost current meters recorded either westerly flow (albeit with large rms error estimates) or very weak flow. During the final period the motion was easterly and slower at the two shelf-edge moorings than deeper in the water column. The suggestion is that during the first period the Beaufort Undercurrent did not extend as close to the surface, in the mean, as it did during the second period. This is in agreement with our conclusion in Appendix A, pp.3-4 that compared to earlier measurements, the undercurrent was anomalously deep during the October 1986 - March 1987 period.

Table 14. Beaufort Sea Mean Velocity Comparison: October 1986 - March 1987 and April 1987 - April 1988. \*Record MA2B at 112 m lasted only 39 days.

Mooring site	Approximate depth m	Mean velocity	
		1986-87 cm s <sup>-1</sup> (RMS) °T	1987-88 cm s <sup>-1</sup> (RMS) °T
MA2	70	3.5 (4.1), 291	1.6 (3.8), 102
	100	0.1 (0.5), 219	3.3*(5.0), 130
	150	7.8 (4.7), 119	5.6 (2.0), 113
MB1	80	1.5 (1.4), 168	3.8 (2.0), 106
	155	6.9 (3.0), 097	1.1 (0.5), 097
	985	0.0 (0.0)	0.8 (0.2), 023
MB2	65	0.3 (0.5), 181	5.9 (1.6), 113
	100	5.0 (2.0), 112	7.6 (1.2), 110
	150	8.0 (1.8), 103	6.6 (1.1), 109

**Figure 23** shows the monthly mean velocity recorded at the upper- and lowermost current meters at the outer shelf moorings (MA2 and MB2), together with the corresponding estimated wind vector at Barrow. The seasonal cycle in the wind, with maxima in the fall and spring has no obvious reflection in the current records. (On the other hand, the difference in the mean depth of the undercurrent between the first 6 months and the last 12 is clear in the figure.)

**Figure 24** shows the mean monthly variance in the current at the same sites as in **Figure 23**. The anomalously large variance in the MA2, 150 m record during December 1986 is due to the extremely rapid flow recorded during that period (see **Appendix A, p.3**): up to  $166 \text{ cm s}^{-1}$  in the 35-hour low-passed series, which is well over twice that previously recorded for the Beaufort Undercurrent. Inspection of the filtered time series (**Appendix A, Figure 4**) suggests that the event may represent passage of two intense counterrotating baroclinic eddies, the first one counterclockwise and the second clockwise (compare **Figure 6** in Foldvik et al, 1988). While the variance in the wind portrayed in **Figure 24** has a clear seasonal cycle, with a maximum in mid-winter and a minimum in mid-summer, the current variance shows neither a seasonal cycle, nor is the month-to-month variability in the individual records similar. The lack of a seasonal signal in the flow was pointed out earlier by Aagaard (1984), as were the significant differences in the flow to be expected from year to year.

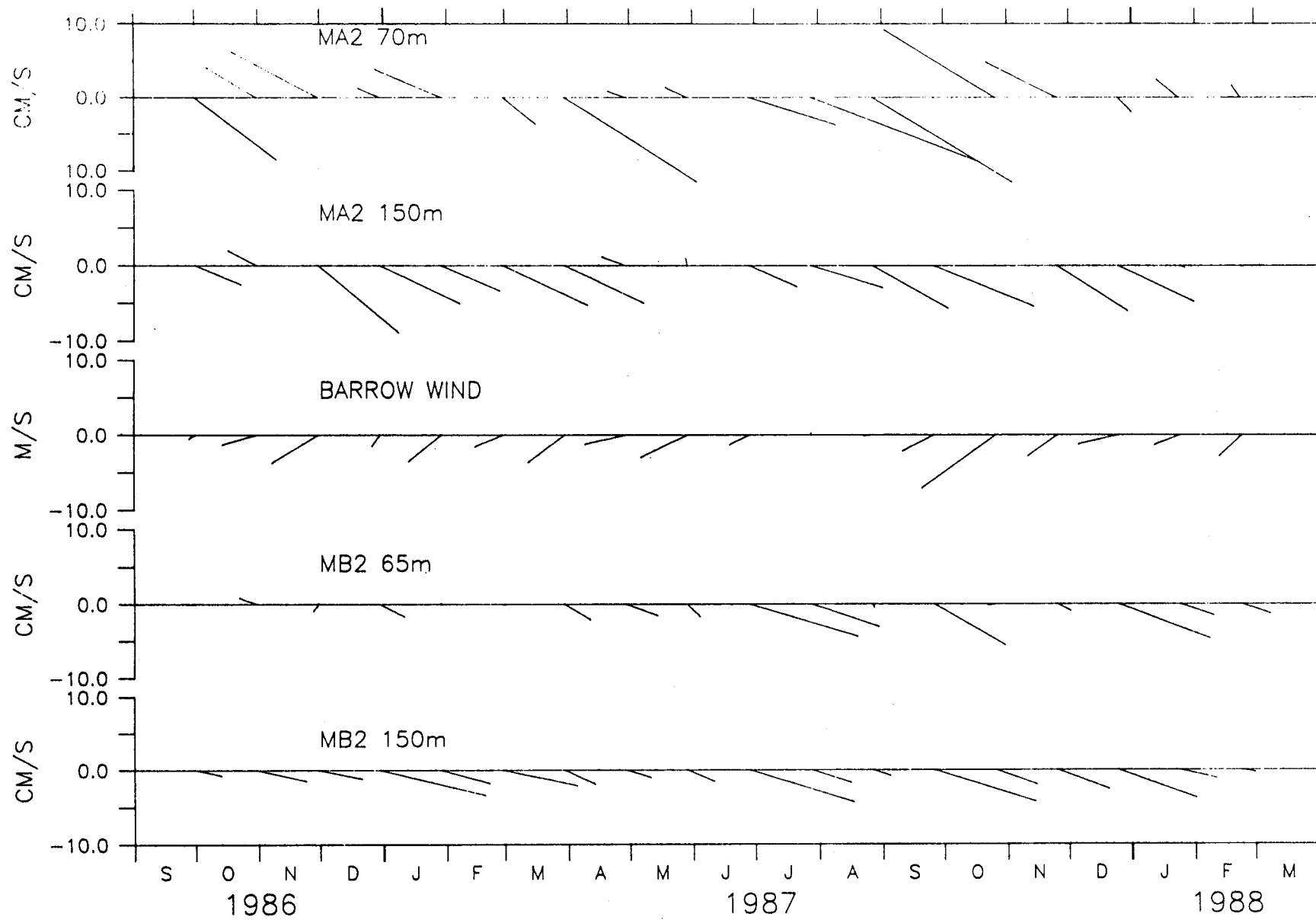


Figure 23. Monthly mean currents at sites MA2 and MB2 during 1986-88, together with the monthly mean wind at Barrow. Up is north.

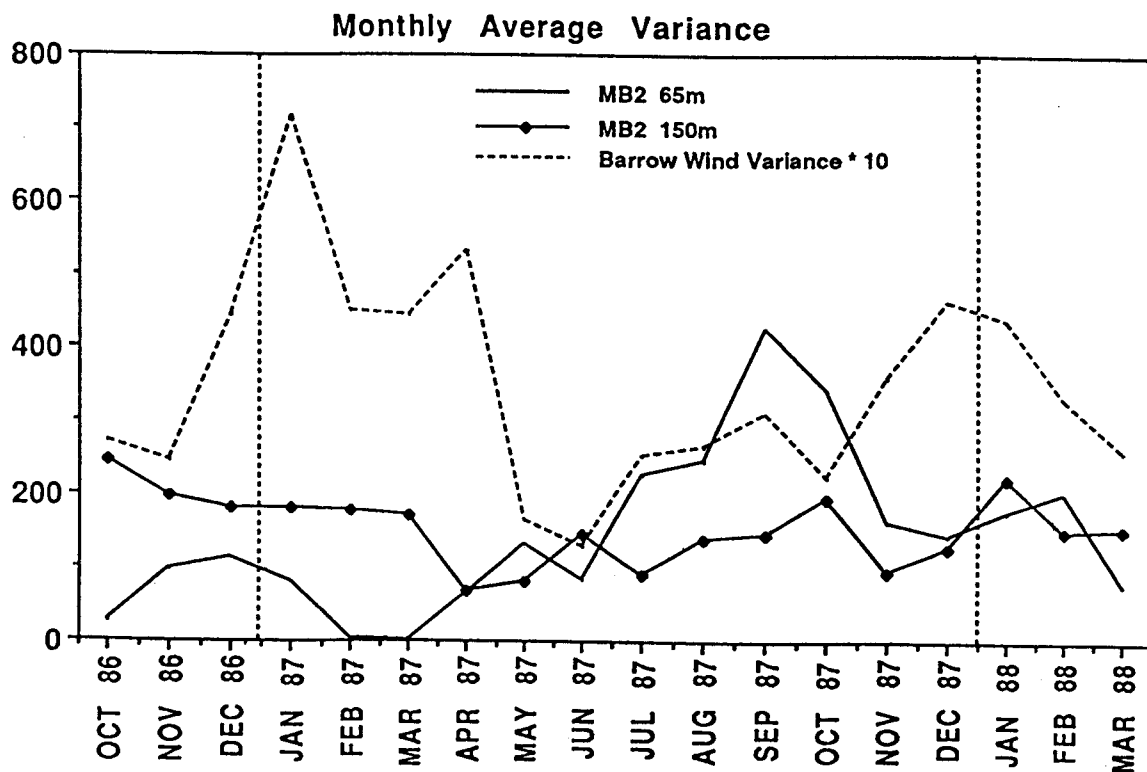
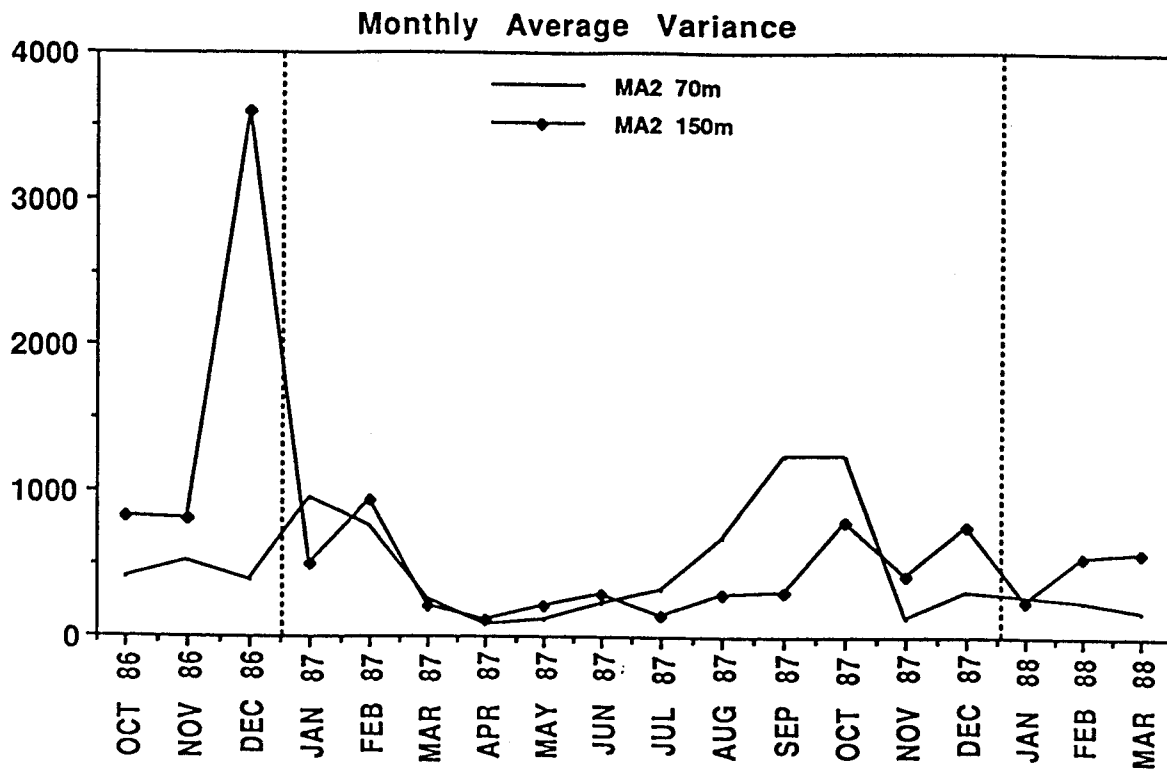


Figure 24. Monthly mean variance in the current at sites MA2 and MB2 during 1986-88. Note the difference in scale (vertical axis) between the two sites.

## Beaufort Sea Correlation Analysis

Table 15 shows the correlation matrix for the 1987-88 current records. The lag in hours for maximum correlation is in parentheses; where no lag is shown, it is zero. A positive lag represents the record listed at the beginning of each row leading the record listed in the corresponding column. All listed correlations are significant at the 95% confidence level.

Vertically the currents were in phase, but the correlation degrades with depth, going from characteristic values near  $r=0.9$  over the upper instrument separations of 33 m to as low as  $r=0.26$  for the 78 m separation between the top and intermediate instruments over the slope at MB1B. For the three moorings over the outer shelf, the degradation of the correlation at intermediate depths was less, ranging from  $r=0.53-0.72$  over 83 m.

Table 15 suggests that the cross-shelf correlation decreases considerably over fairly short distances. At MA2B and MA4B, separated by about 45 km, less than 10% of the variance was linearly related. However, between instrument pairs separated by about 10 km, such as MB1B and MB2B, the related portion was as much as 44% and as much as 34% between MB2B and MB4B.

Along the shelf, a significant fraction of the low-frequency current variance was linearly related over the entire length of the shelf, as much as 28% between MA2B and MC1B. The phase relations were such that the western records consistently led the eastern ones, corresponding to eastward-propagating disturbances, probably shelf waves. From the typical lags of 30 hr between MA2B and MB2B, and 18 hr between MB2B and MC1B, respectively separated by about 250 km and 100 km, the characteristic phase velocity was about  $2 \text{ m s}^{-1}$ . This is only slightly slower than suggested by Aagaard (1984), and it is close to the  $1.1-1.6 \text{ m s}^{-1}$  eastward phase velocity suggested by the 1986-87 upwelling events in Barrow Canyon and at the Beaufort Sea SeaCat sites.

Table 15. Linear Correlations of Beaufort Sea Current Meters. For 87119 to 88072, 1274 points, 6 hourly records(lag in hours), positive lag means column lags row. \* means not significant at the 95% level.

	MA2B 79 m	MA2B 162 m	MB1B 64 m	MB2B 72 m	MC1B 108 m
MA2B					
162 m	0.53 (6)	1.0	0.34 (42)	0.47 (30)	0.26 (60)
MA4B					
45 m	0.31 (96)	0.18 (96)	0.22 (96)	0.22 (96)	0.14*(96)
MB1B					
97 m	0.58 (-48)	0.36 (-48)	0.94	0.66 (-12)	0.62 (6)
MB1B					
162 m	0.10*	-0.13* (42)	0.26	0.23	0.27
MB1B					
994 m	-0.37 (-72)	0.31 (-78)	-0.35 (-36)	-0.31 (-54)	-0.37 (-36)
MB2B					
105 m	0.43 (-24)	0.51 (-30)	0.47 (24)	0.85	0.48 (30)
MB2B					
155 m	0.43 (-24)	0.58 (-36)	0.46 (12)	0.72 (-6)	0.48 (30)
MB4B					
52 m	0.56	0.50 (-6)	0.43 (30)	0.58 (18)	0.39 (42)
MC1B					
141 m	0.47 (-42)	0.29 (-60)	0.61	0.59 (-12)	0.95
MC1B					
191 m	0.45 (-30)	0.42 (-60)	0.54 (-6)	0.59 (-12)	0.69
MA2B					
79 m	1.0	0.53 (6)	0.64 (30)	0.63 (18)	0.53 (42)
MB1B					
64 m	0.64 (-30)	0.34 (42)	1.0	0.64 (18)	0.63 (6)
MB2B					
72 m	0.63 (-18)	0.47 (-30)	0.64 (-18)	1.0	0.61 (18)

We have also correlated the current records with the wind at three locations: Barter Island, Barrow, and Resolution Island. The results are summarized in Table 16. In general, the Barrow wind record was best correlated with the current and the Barter Island wind was the least well correlated. The latter is probably explainable by the proximity of the mountains to the coast in the vicinity of Barter Island, giving rise to both cyclostrophic and baroclinic effects. On the whole, the wind accounted for a relatively small fraction of the current variance, even at the uppermost current meters, ranging from 2-25% of the total variance (calculated as  $r^2$ , which corresponds to correlation coefficients of  $r=0.14-0.50$ ). Indeed, at MA4B, the shallow mooring closest to Barrow, the wind and current were effectively uncoupled. Only at MB4B, where the correlation coefficient is  $r=0.73$ , did the wind account for more than half the current variance ( $r^2=53\%$ ). The wind generally led the current by 1-2 days, and there was some tendency for the lag to increase with increasing depth.

All our instruments were located below the surface mixed layer, which is typically 30-m thick in winter and much less during summer. Table 16 suggests that only about 15-25% of the fluctuating kinetic energy (which is proportional to their variance) in the currents deeper than 60-80 m was wind-driven. Note that Table 16 shows a further systematic decrease of the wind/current correlation with depth below the top current meter. On the average, this represents a decrease in the correlated variance (which we can interpret as a decrease in the wind-driven kinetic energy in the ocean) of  $1.5 \times 10^{-3} \text{ m}^{-1}$ . We should therefore expect that an additional 15% of the wind energy is dissipated for every 100-m increase in depth. Effectively, on the open shelf and slope, the circulation below the mixed layer is primarily ocean-driven rather than wind-driven.

Table 16. Linear Correlations: Regional Winds vs. Beaufort Sea Current. For April 29, 1987 to March 13, 1988, 1274 pts, 6 hourly records (lag in hours), positive lag means current lags wind. \* means not significant at the 95% level.

	Barrow (250T) m s <sup>-1</sup>	Resolution Island (280T) m s <sup>-1</sup>	Barter Island (280T) m s <sup>-1</sup>
MA2B 79m	0.52 (24)	0.35 (42)	0.29 (30)
MA2B 162m	0.39 (24)	0.30 (30)	0.28 (24)
MA4B 45m	0.14*	0.15*(18)	0.13*(12)
MB1B 64m	0.40 (54)	0.32 (48)	0.24 (42)
MB1B 97m	0.35 (54)	0.26 (54)	0.20 (54)
MB1B 162m	-0.10*	-0.09*	-0.11*
MB1B 994m	-0.17 (90)	-0.16 (96)	-0.11*
MB2B 72m	0.48 (42)	0.38 (42)	0.32 (36)
MB2B 105m	0.38 (42)	0.29 (54)	0.27 (42)
MB2B 155m	0.35 (48)	0.25 (54)	0.23 (42)
MB4B 52m	0.73 (24)	0.63 (30)	0.61 (24)
MC1B 108m	0.37 (60)	0.34 (54)	0.26 (42)
MC1B 141m	0.28 (66)	0.25 (48)	0.17 (42)
MC1B 191m	0.26 (78)	0.22 (84)	0.17 (72)

## Beaufort Sea Tidal Characteristics

Tidal effects are small in the Beaufort Sea. Characteristic tidal heights are 10 cm or less, and the variance in the tidal bands of the sea surface elevation is typically less than 1% of total variance. Figure 25 shows the tidal elevation characteristics for the five largest constituents at MB2B near the shelf break at 147°W. The estimates are for consecutive 29-day periods. The largest semidiurnal constituent, M2, was close to 8 cm, and the two largest diurnal constituents, O1 and K1, were each about 3 cm. The amplitude estimates vary by as much as 5 cm over the year, and most of the phase estimates also show large variability.

Tidal currents were also small, typically 5 cm s<sup>-1</sup> or less, and constituted only 1-2% of the total variance in the velocity field. Figure 26 shows the tidal current characteristics for the five largest constituents at 155 m at MB2B. In contrast to the tidal elevation constituents, the largest tidal current constituents were diurnal, and a variance analysis shows that some 80% of the total tidal variance in the current record was in the diurnal band. This was also true at 105 m depth at this mooring, but at the upper instrument at 72 m the variance in the diurnal band was nearly 40% less, suggesting vertical structure in the diurnal current field (but not in the semidiurnal, the variance of which does not decrease at the upper instrument). Note that the estimated characteristics of most of the tidal ellipses vary considerably over the year.

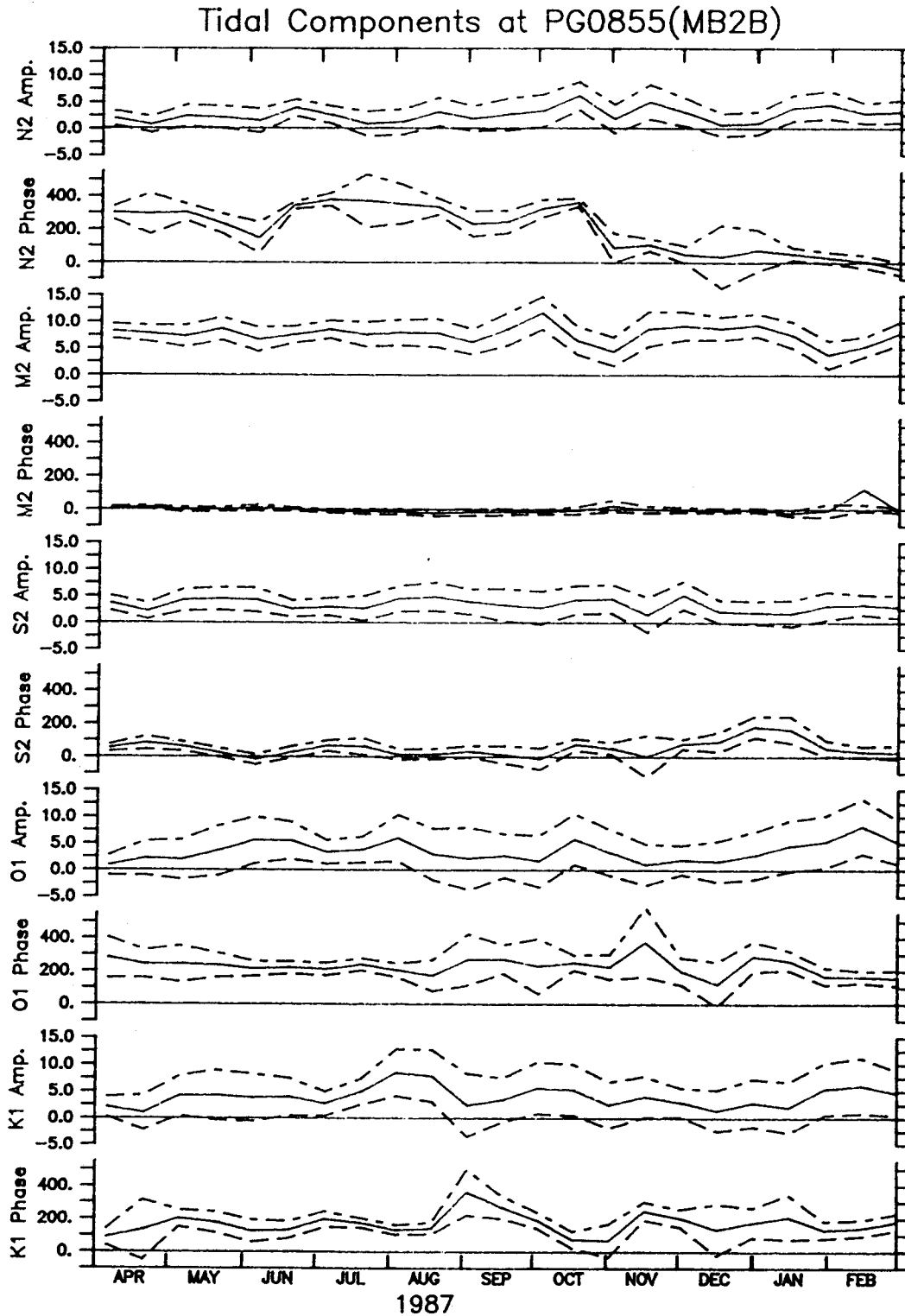


Figure 25. Elevations (cm) and phase (degrees) for the five largest tidal constituents at MB2B. Dashed lines show RMS error. Calculations are for 29-day segments.

# Tidal Components at AN2097(MB2B)

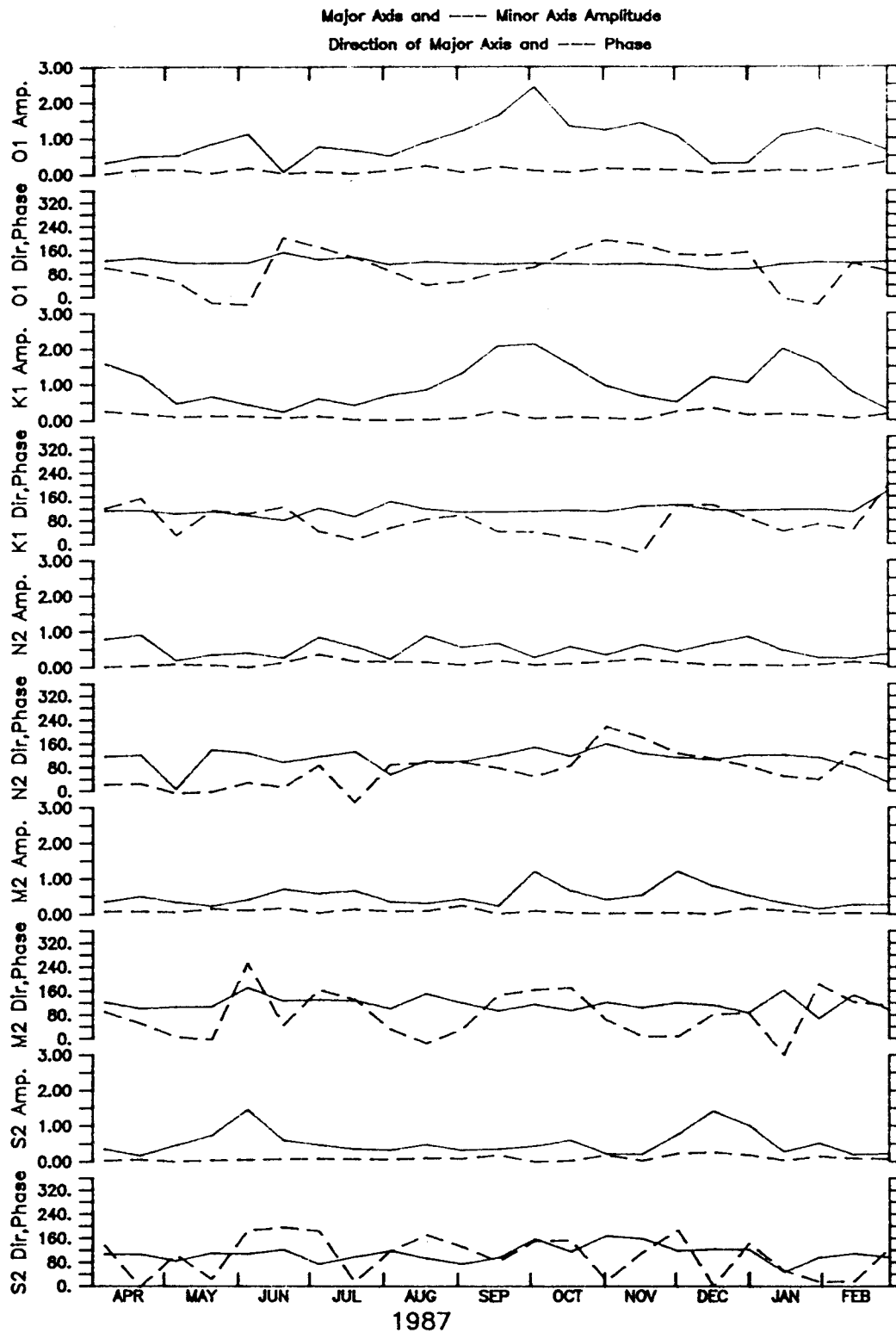


Figure 26. Tidal current characteristics for the five largest constituents at MB2B. Amplitudes are in  $\text{cm s}^{-1}$  and major axis directions and phases are in degrees. Calculations are for 29-day segments.

## Meteorological Results and Correlations

The results from the eight land-based meteorological stations are summarized from southwest to northeast along the coast in **Table 17** and **Figures 27 to 34**. Note that Cape Prince of Wales and Icy Cape stations had a different time base than the other stations, because the Wales station was setup later for an ONR project. The computer module at Icy Cape failed shortly after deployment and was replaced in March 1987. All the other records begin in September 1986. The most obvious results from visual inspection of the records are 1) that in all cases the pressures derived by METLIB from FNOC fields overlay the station pressures with the caveat that METLIB pressures were shifted some hours later in time; 2) that summer temperatures derived from FNOC fields reasonably match the station data, but throughout the winter, temperatures from FNOC were 10 - 20°C too warm during two or three week increments for all stations; 3) that autumn 1987 was even warmer than autumn 1986 (**Appendix A**); and 4) that the winds at a few stations were better modeled than others by the gradient wind generated by METLIB. Nome, Cape Prince of Wales, Icy Cape, and Barrow were fit well, while Kotzebue and Barter Island were not. The winds at Lonely were inaccurate since the anemometer had been nearly covered with snow in the winter of 1986-87 due to snow blower exhaust. Barter Island winds were strongly affected by the presence of the Brooks Range so that mountain barrier effects should be included for the nearshore zone (Kozo 1980, 1984). The most inaccurate winds were at Kotzebue, but the reason has not been isolated.

The ice drifts for all ARGOS buoys are shown in **Figures 35 and 36**. **Table 17c** gives record length statistics and **Figures 39 - 44** give time series results for eight of the longer lived ARGOS buoys. The overwhelming impression from the ice drift study is that 1) under most circumstances the Beaufort gyre extended onto the shelf and 2) there was little shear in the ice field outside the 20-m isobath and little coupling with the ocean below 60 m depth. This result is consistent with the relatively narrow fast ice zones along the Beaufort Shelf and with the general drift pattern seen by other investigators (Barry et al., 1979; Campbell et al., 1976; Campbell et al., 1980; Carsey and Holt, 1987; Marko and Thompson, 1975; Pritchard, 1984; Weeks et al., 1977).

**Table 17. Statistics on Full-Length Records with RMS values.**  
a) Climate and METLIB data (First line climate, second line METLIB).

	<u>Barter I</u>	<u>Barrow</u>	<u>Kotzebue</u>	<u>Nome</u>
Pressure	1015.52(0.95)	1016.10(1.02)	1009.86(0.98)	1007.27(1.12)
	1015.53(1.00)	1015.82(1.00)	1010.27(0.96)	1007.74(1.11)
Temperature	-12.62(6.20)	-13.10(5.96)	-6.44(5.45)	-3.57(4.31)
	-6.29(4.25)	-8.25(4.40)	-2.32(4.34)	-0.92(3.68)
Mean Speed	5.57(0.17)	5.39(0.16)	5.25(0.20)	4.17(0.15)
	4.52(0.20)	5.79(0.33)	6.46(0.77)	6.73(0.81)
Net Wind Speed.	1.36(0.09)	2.70(0.17)	1.28(0.15)	1.64(0.25)
	2.65(0.19)	3.58(0.43)	3.84(0.64)	3.78(0.60)
Net Wind Direction.	276	252	255	230
	250	235	222	223
Principal. Axis (% Variance along that axis)	280(92.9%)	254(76.0%)	284(81.0%)	251(58.8%)
	247(76.8%)	225(83.7%)	196(69.6%)	349(61.0%)

Table 17 (cont.)

b). GOES and METLIB data (First line GOES, second line METLIB)

	<u>Resolution I.</u>	<u>Lonely</u>	<u>Icy Cape</u>	<u>C.P.of Wales</u>
Pressure				
	1013.63(1.15)	1013.48(1.24)	1012.93(1.00)	1008.24(1.14)
	1015.16(1.15)	1015.36(1.17)	1014.33(1.01)	1009.27(1.11)
Temperature				
	-22.13(6.83)	-15.09(6.09)	-8.63(5.67)	-0.89(6.58)
	-8.69(3.95)	-9.79(4.16)	-3.29(3.88)	-2.34(3.66)
Mean Speed				
	4.73(0.22)	2.89(0.60)	5.50(0.27)	6.75(0.29)
	4.88(0.20)	5.67(0.26)	5.96(0.32)	7.31(0.65)
Net Wind Speed				
	1.92(0.43)	1.61(0.36)	3.28(0.55)	2.70(0.62)
	2.98(0.48)	3.48(0.55)	3.66(0.53)	4.59(0.89)
Net Wind Direction.				
	248	249	262	233
	245	240	226	209
Principal. Axis				
	253(90.9%)	253(83.2%)	260(84.8%)	019(82.5%)
	234(83.8%)	226(85.7%)	217(74.6%)	005(68.0%)

c) ARGOS and METLIB pressure and temperature

	<u>Pressure</u>		<u>Temperature</u>	
	<u>ARGOS</u>	<u>METLIB</u>	<u>ARGOS</u>	<u>METLIB</u>
7013	1015.93 (1.92)	1016.32 (0.90)	-14.89 (6.73)	-8.75 (4.75)
7014	1014.97 (1.56)	1015.78 (0.54)	-12.55 (6.21)	-8.64 (4.87)
7015	1014.34 (2.67)	1015.77 (0.03)	-15.81 (4.92)	-13.66 (5.27)
7422	1010.69 (1.75)	1009.39 (0.74)	Bad Thermistor	
7426	1018.83 (2.44)	1018.67 (0.43)	-17.13 (4.55)	-6.70 (3.38)
7430	1016.85 (1.87)	1017.58 (0.87)	Bad Thermistor	
7431	1014.29 (1.60)	1014.91 (0.61)	-12.41 (7.14)	-6.14 (4.78)
7432	1017.28 (1.74)	1017.57 (0.73)	-14.21 (6.07)	-8.57 (3.59)

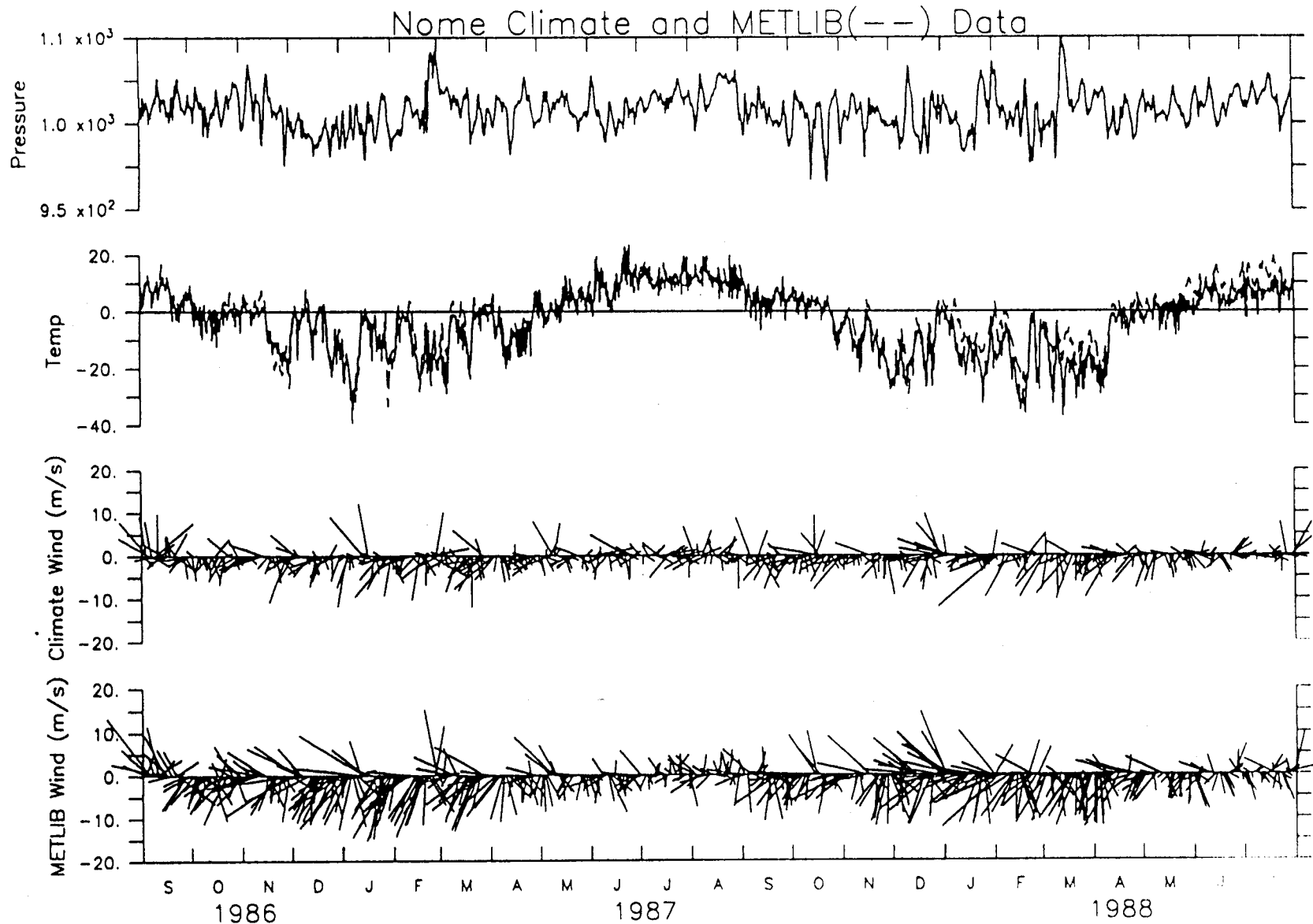


Figure 27. Comparison of National Weather Service and METLIB surface level pressure(mb), temperature(°C), and winds( $m s^{-1}$ ) at Nome. Pressure and temperature data are 6-hourly; one wind vector per day is plotted. In the pressure and temperature plots, METLIB values are plotted with a dashed line. Note that the METLIB pressure is indistinguishable from NWS pressure, and that the high end of the pressure scale (1050 mb) was labeled  $1.1 \times 10^3$  by the plotting package.

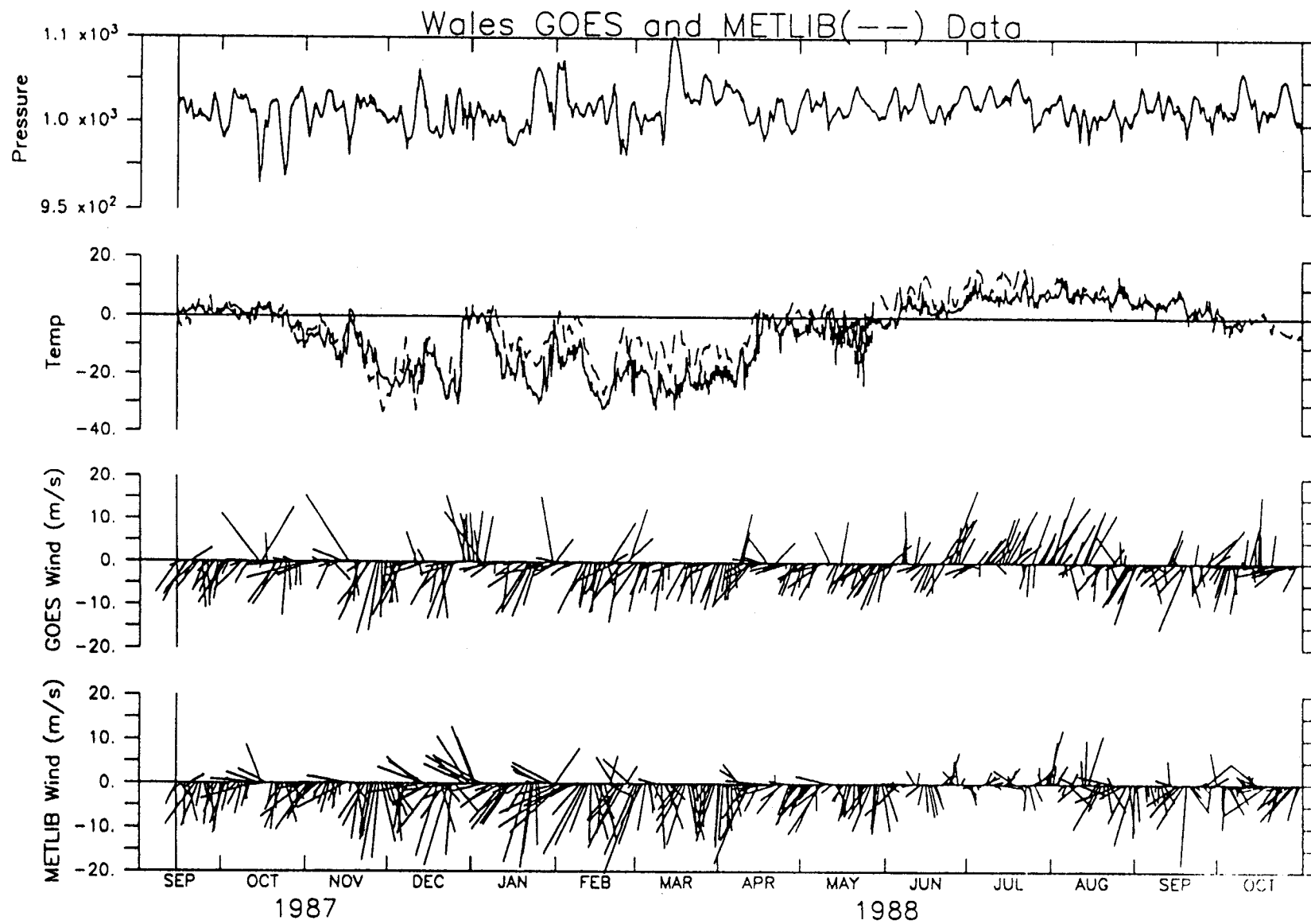


Figure 28. NWS and METLIB pressure, temperature, and winds at Cape Prince of Wales (Bering Strait). See Figure 27.

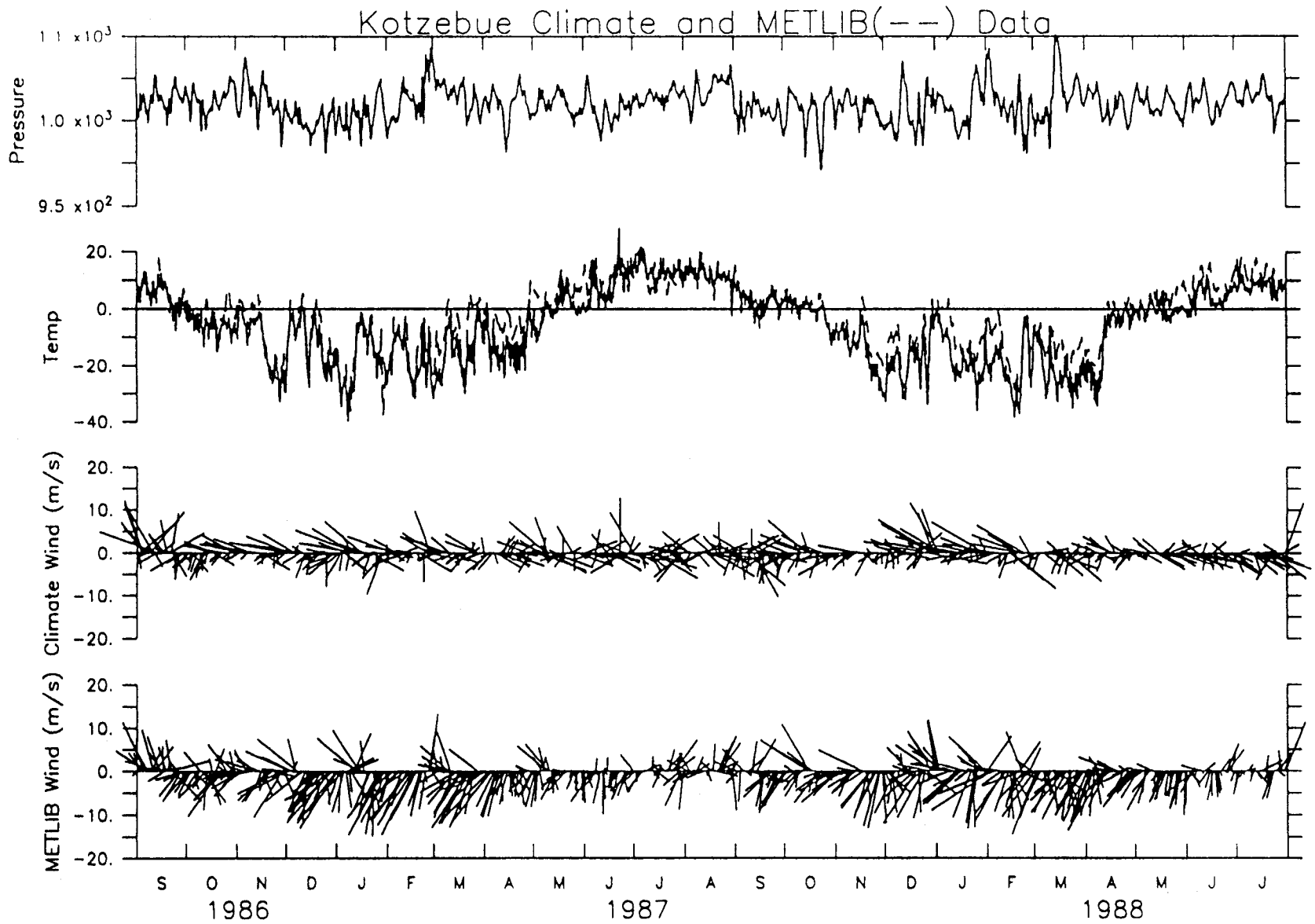


Figure 29. NWS and METLIB pressure, temperature, and winds at Kotzebue. See figure 27.

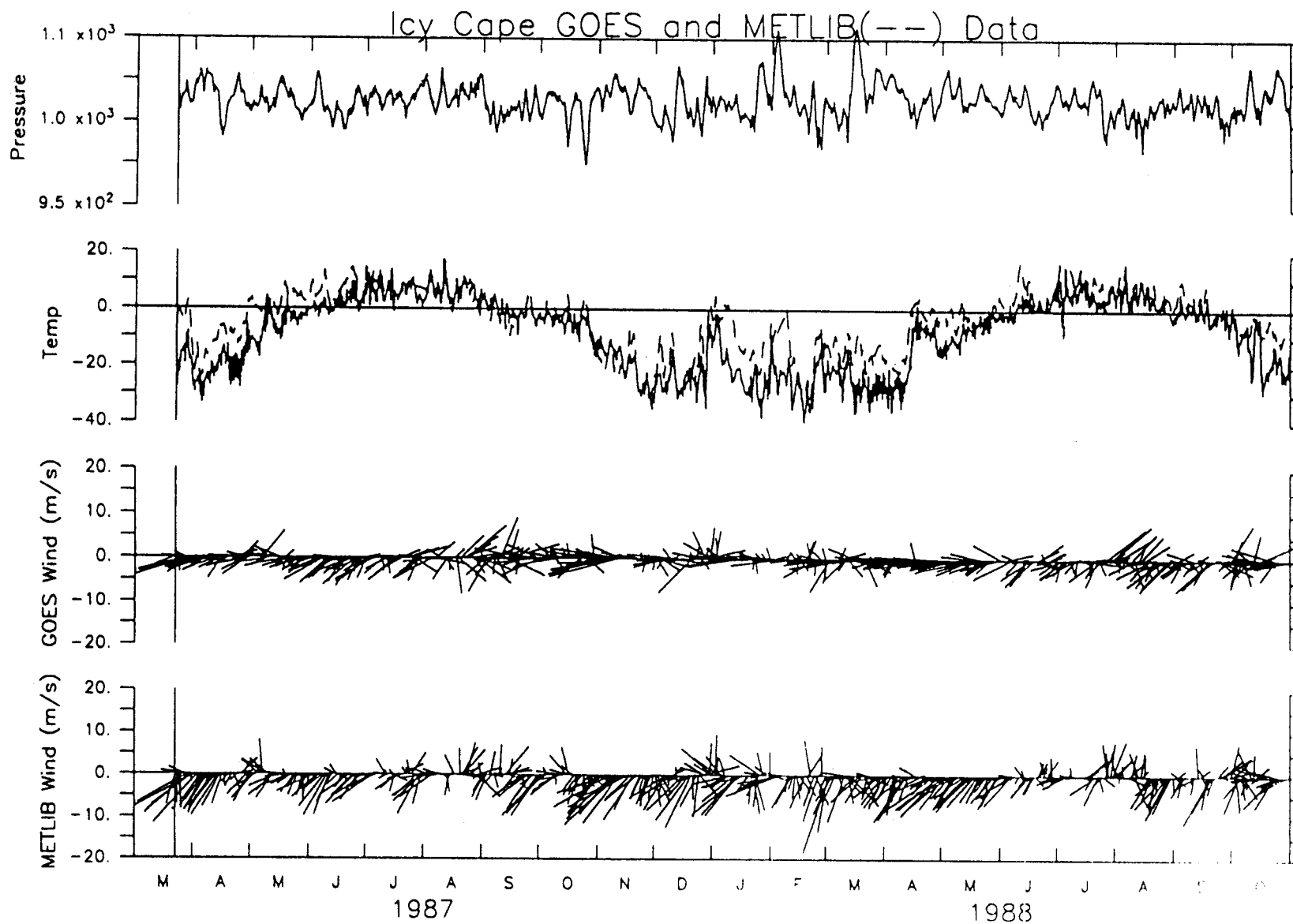


Figure 30. NWS and METLIB pressure, temperature, and winds at Icy Cape. See Figure 27.

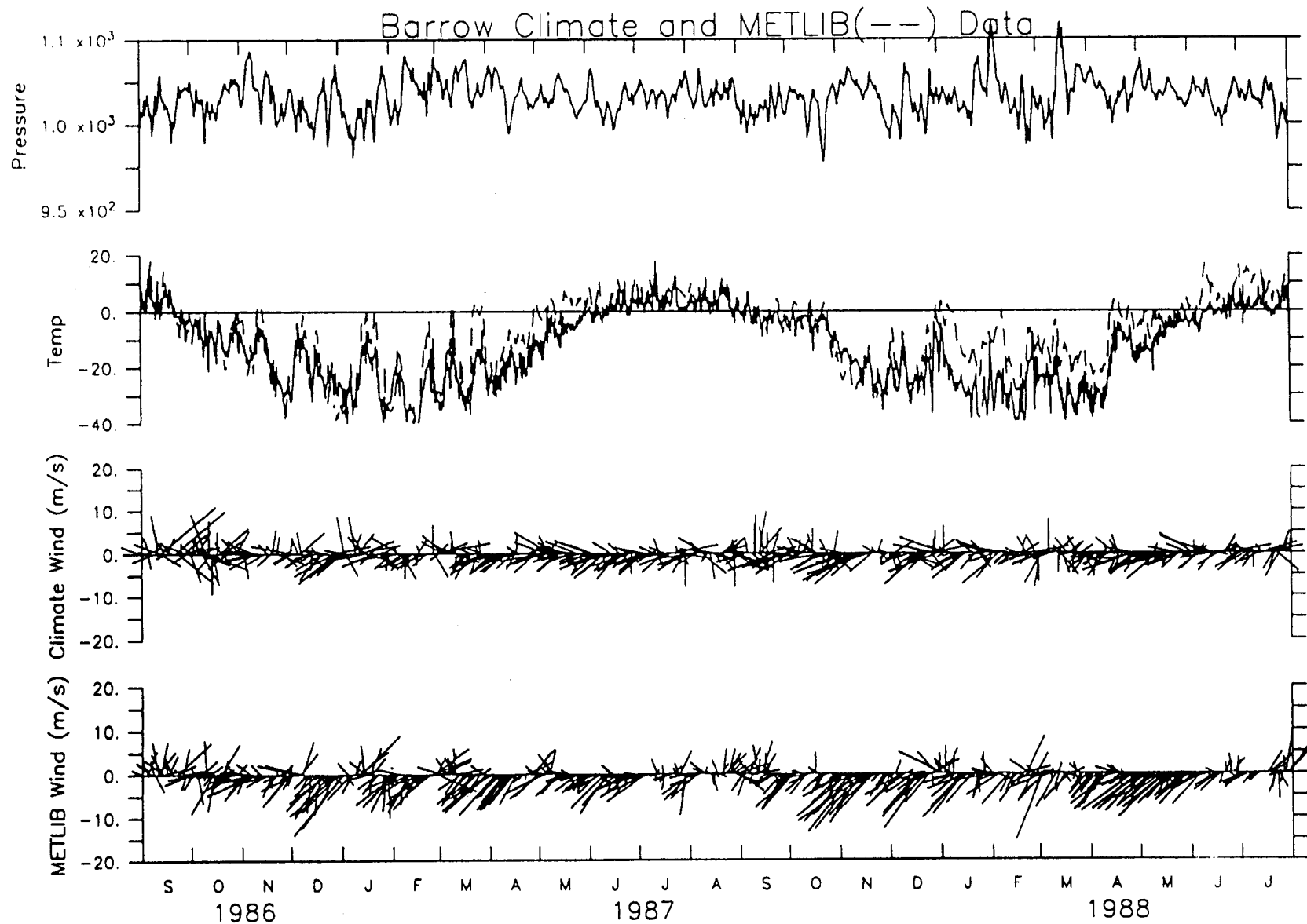


Figure 31. Comparison of surface level pressure (mb), air temperature ( $^{\circ}\text{C}$ ), and winds ( $\text{m s}^{-1}$ ) measured at the shore station at Barrow with METLIB values. See Figure 27.

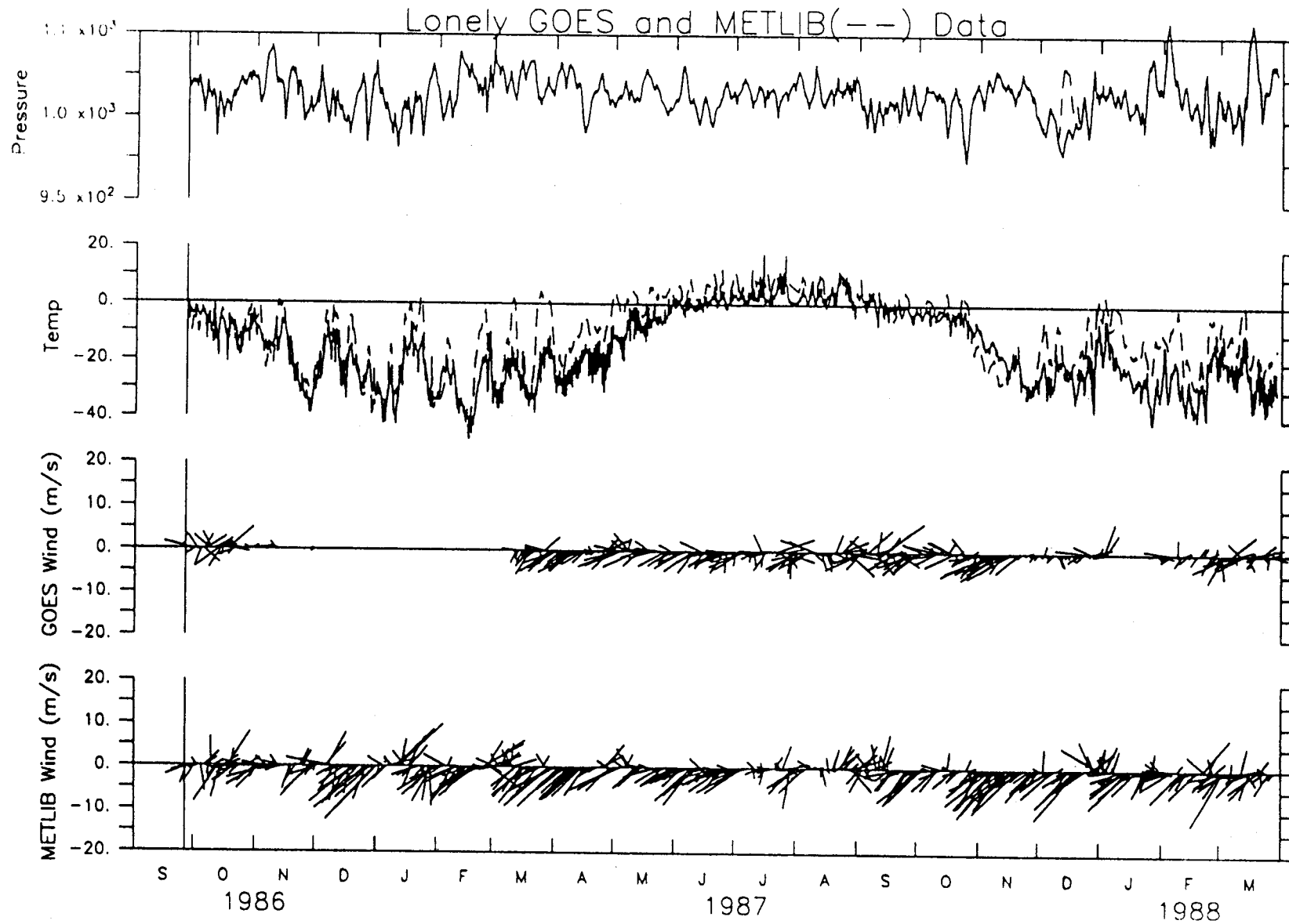


Figure 32. GOES and METLIB pressure, temperature, and winds at Lonely. See Figure 27.

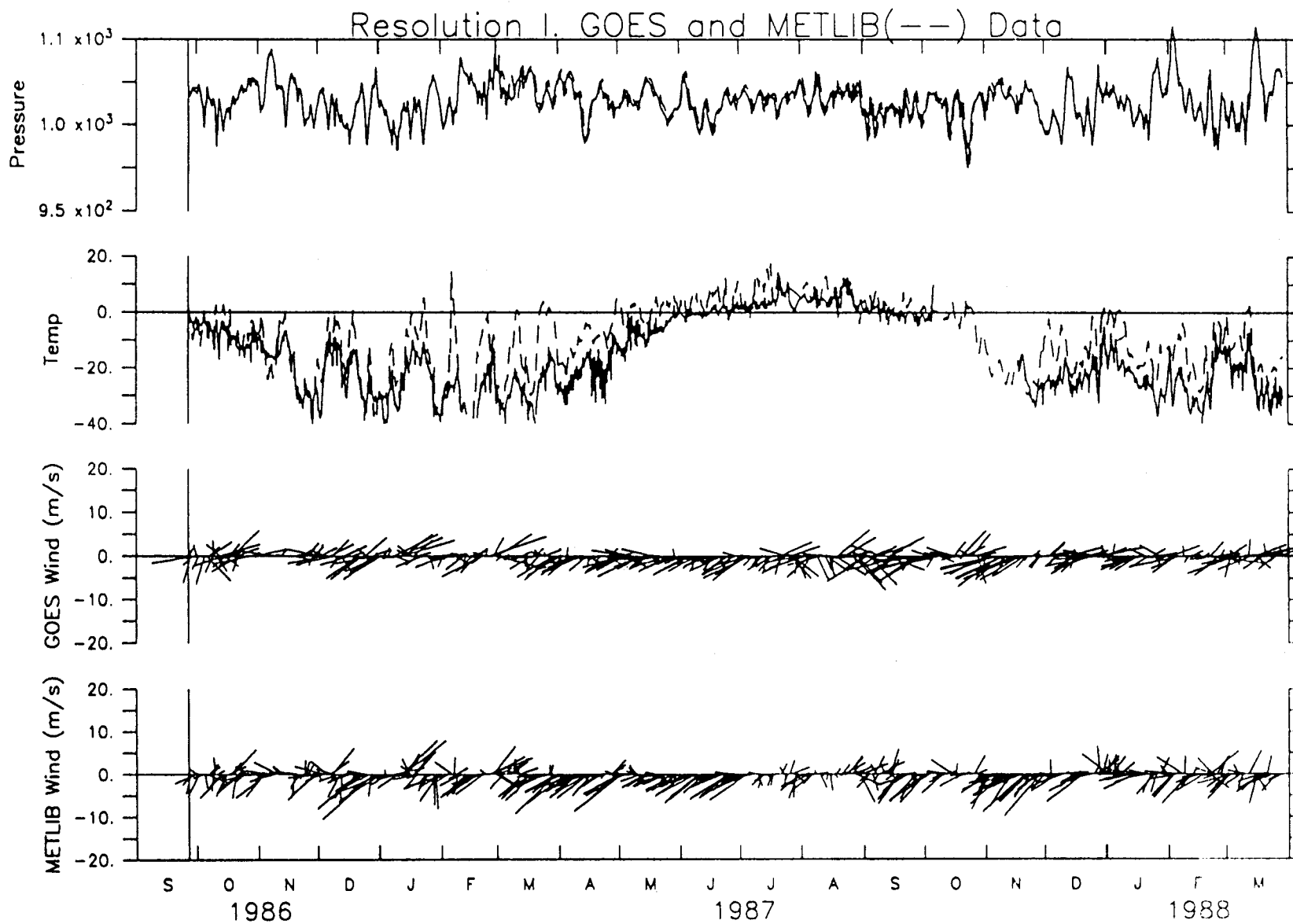


Figure 33. GOES and METLIB pressure, temperature, and winds at Resolution Island (Prudhoe Bay). See Figure 27.

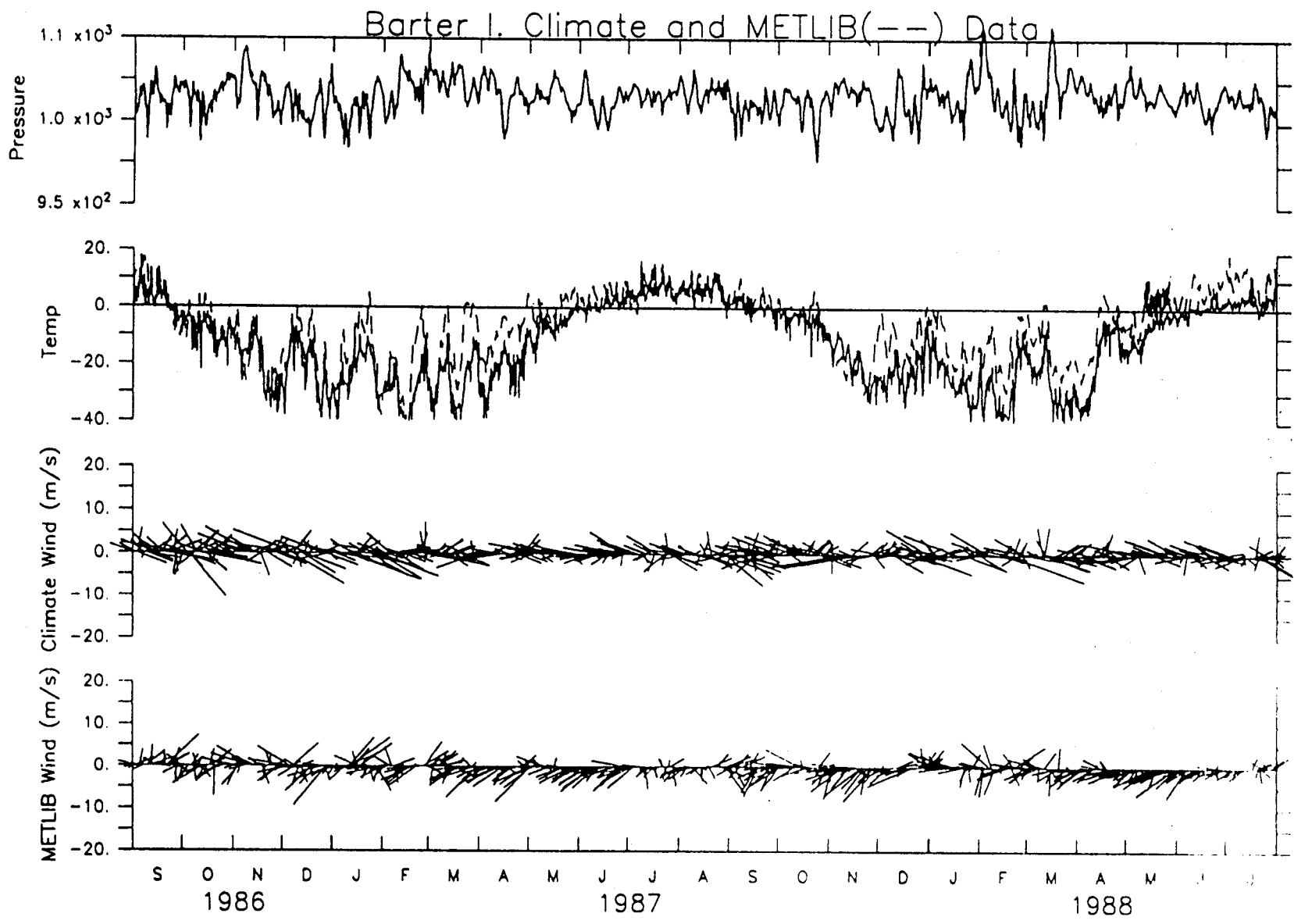
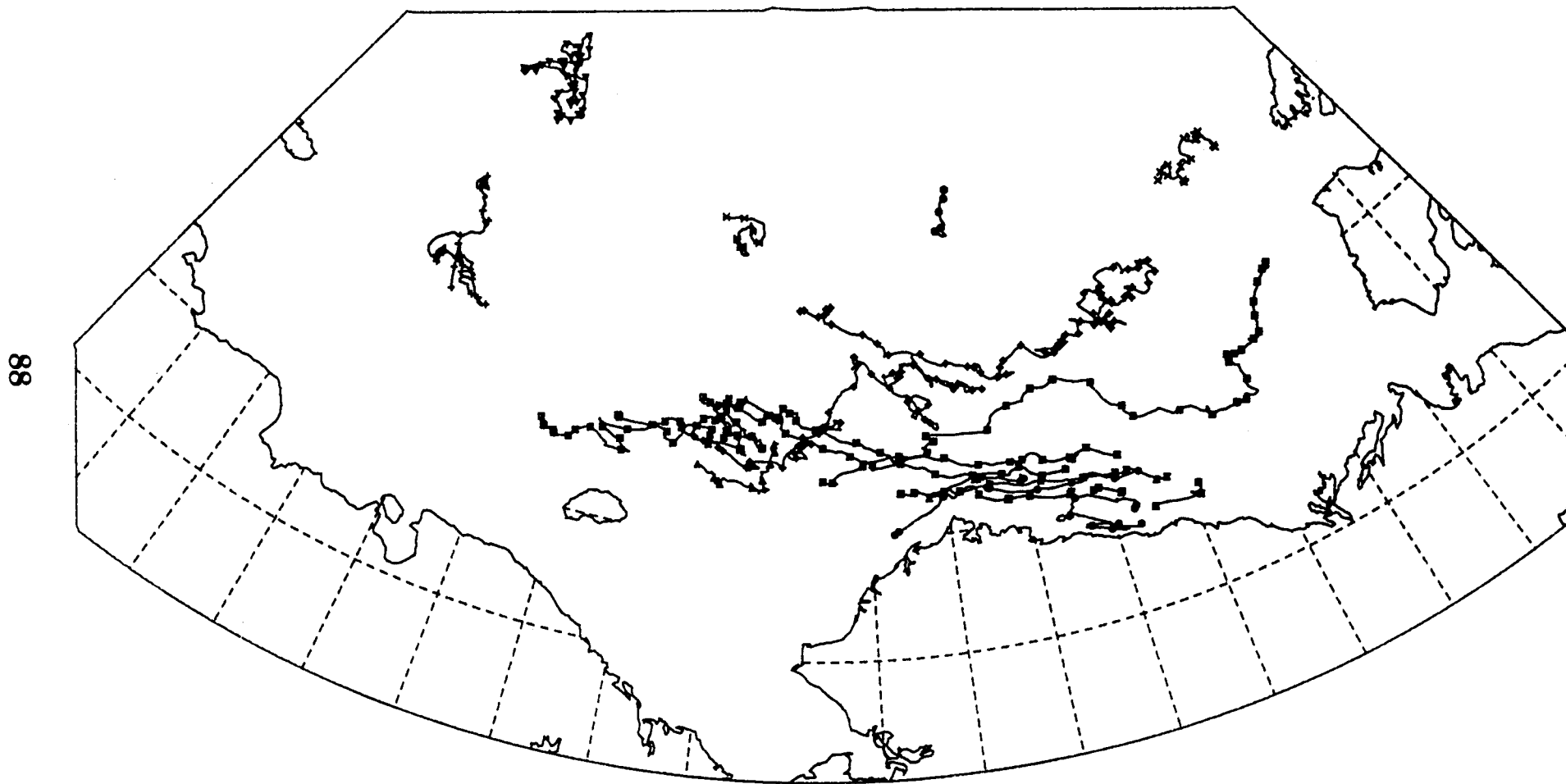


Figure 34. GOES and METLIB pressure, temperature, and winds at Barter Island. See Figure 27.

1986-87



88

Figure 35. Plot of the 1986-1987 ARGOS buoy tracks.

1987-88

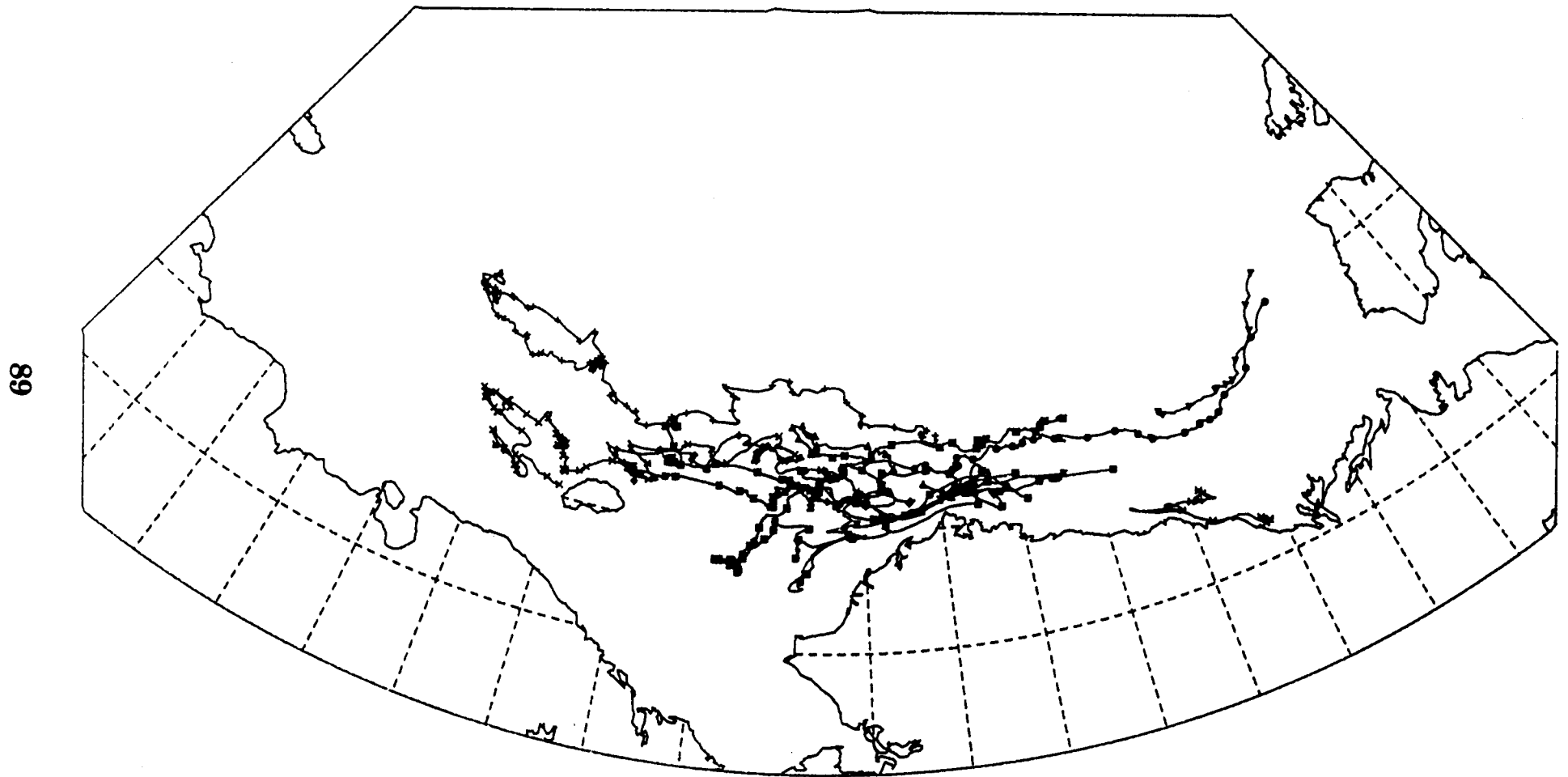


Figure 36. Plot of the 1988 ARGOS buoy tracks.

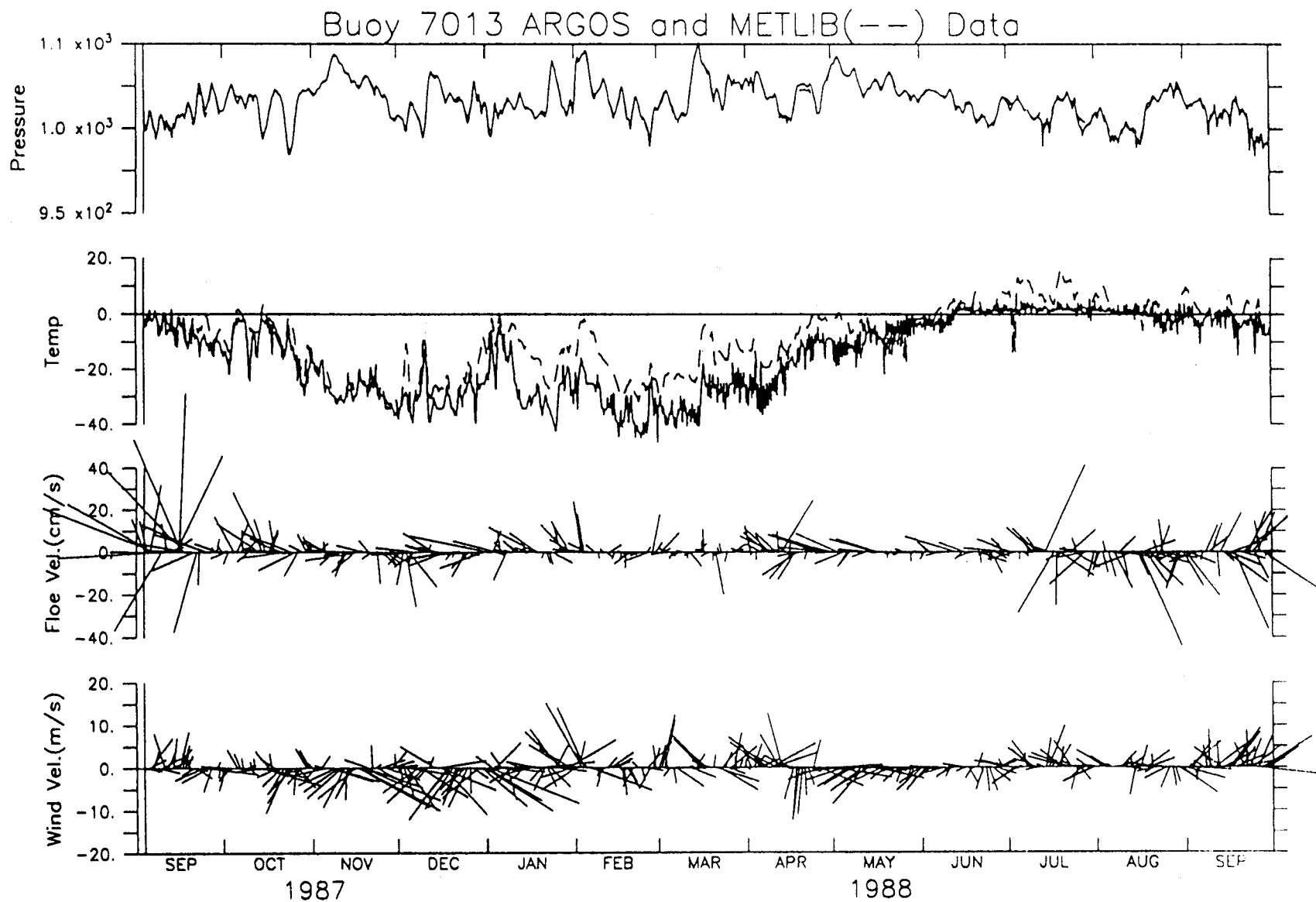


Figure 37. Comparison of surface level pressure (mb) and temperature ( $^{\circ}\text{C}$ ) measured by ARGOS buoy 7013 with METLIB pressure and temperature. METLIB winds and the velocity of the ice floe are also plotted; the buoy did not have an anemometer. See figure 27.

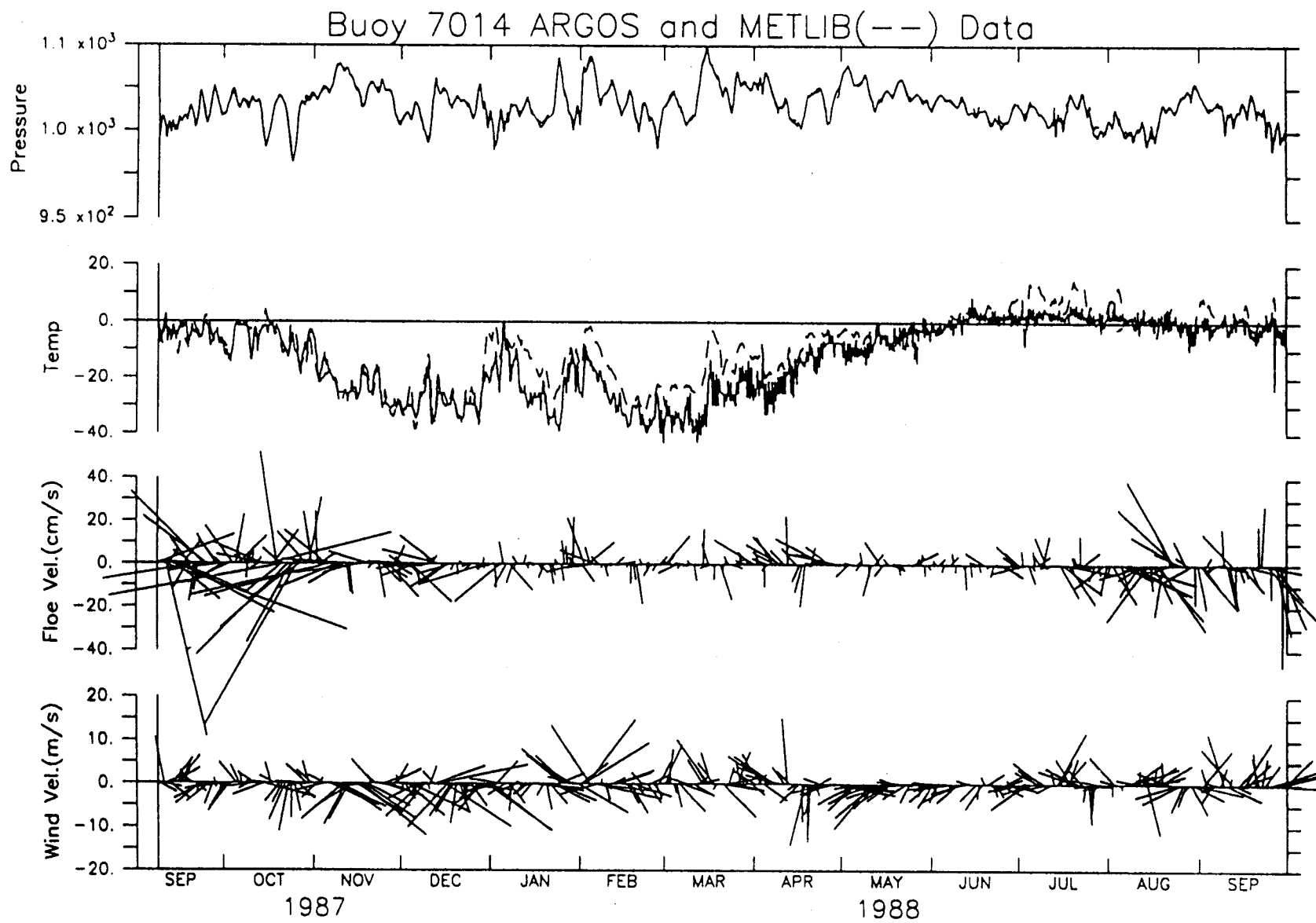


Figure 38. Pressure, temperature, floe velocity, and METLIB winds at ARGOS buoy 7014. See figure 27.

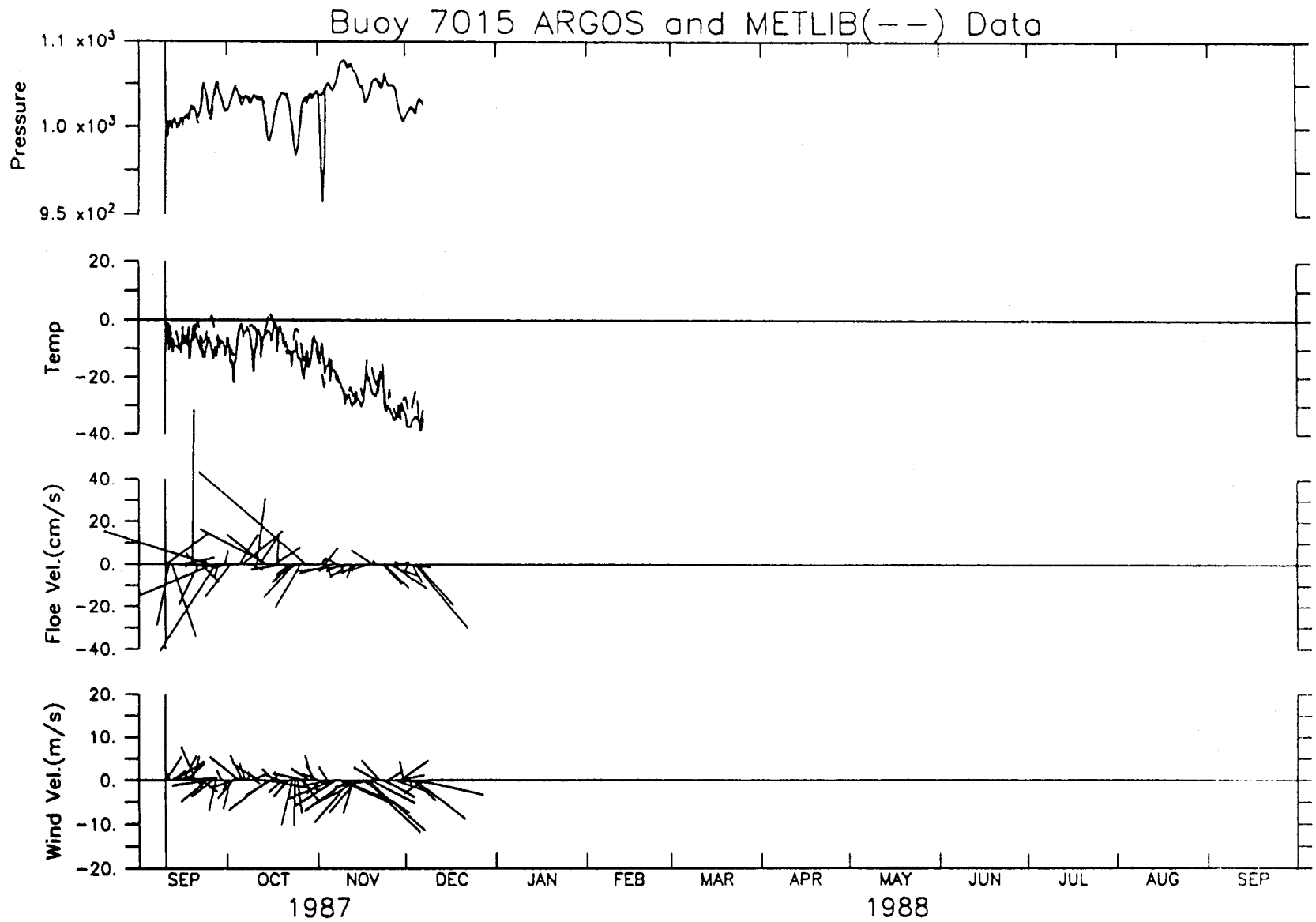


Figure 39. Pressure, temperature, floe velocity, and METLIB winds at ARGOS buoy 7015. See figure 27.

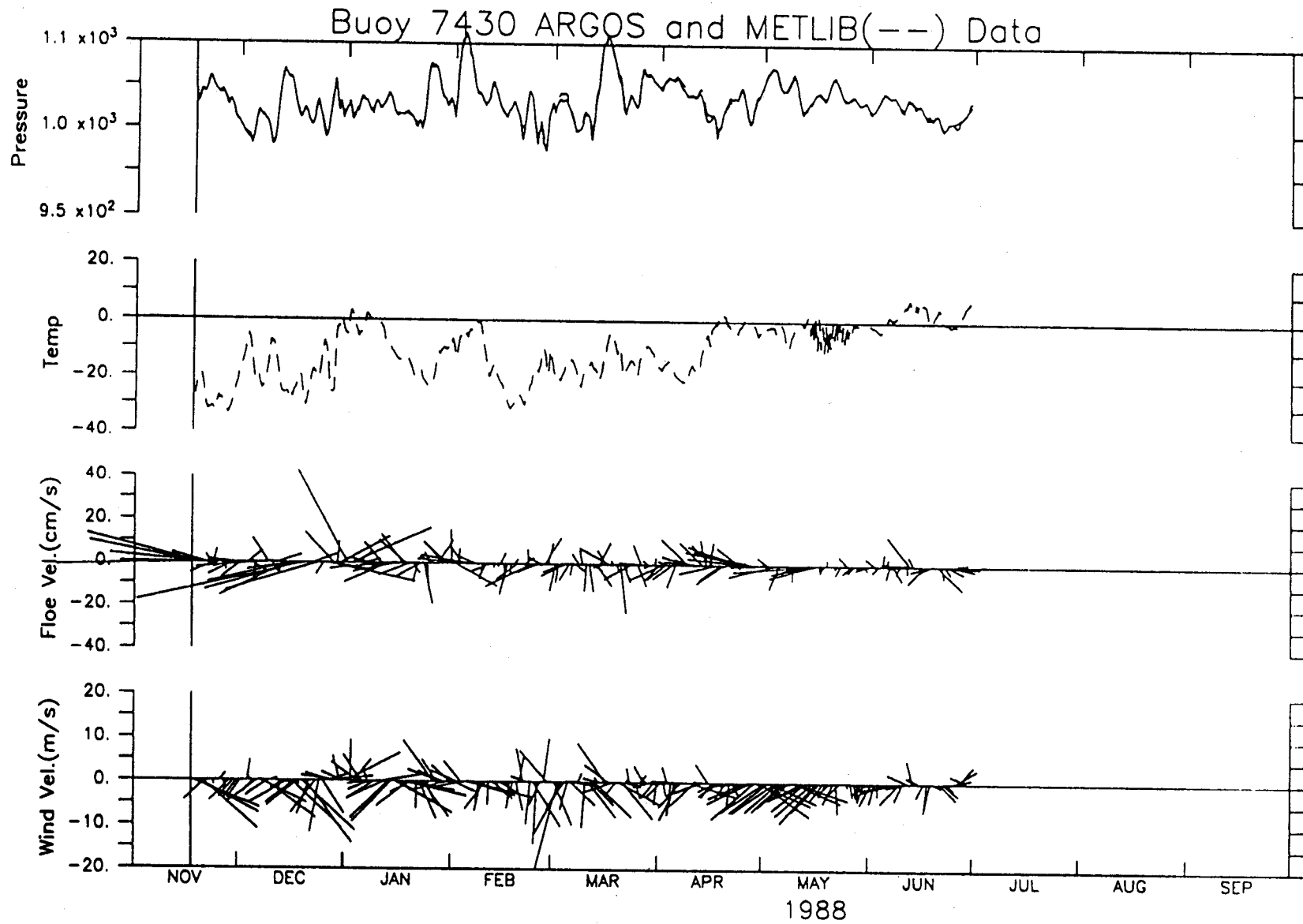


Figure 40. Pressure, temperature, floe velocity, and METLIB winds at ARGOS buoy 7430. See figure 27.

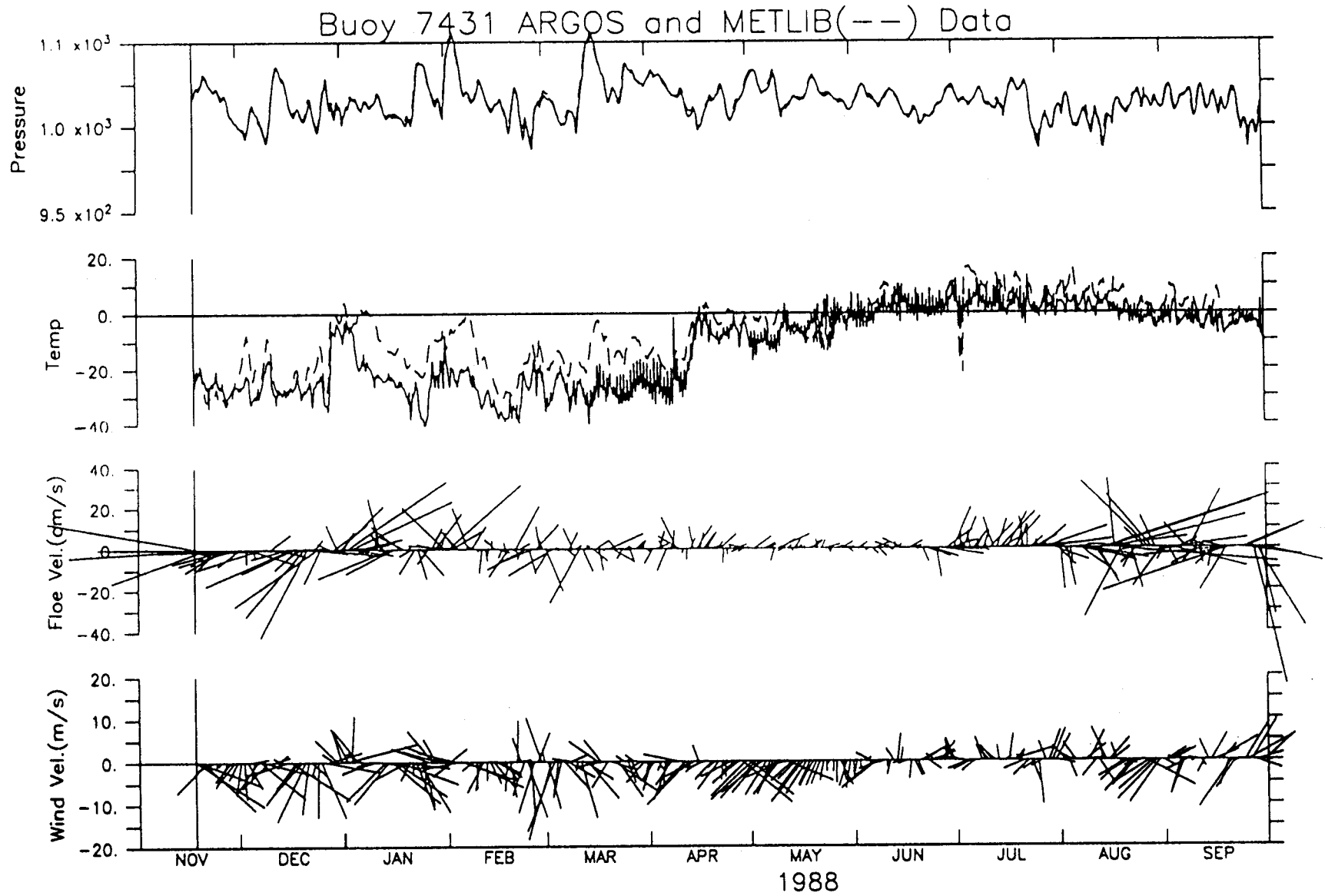


Figure 41. Pressure, temperature, floe velocity, and METLIB winds at ARGOS buoy 7431. See figure 27.

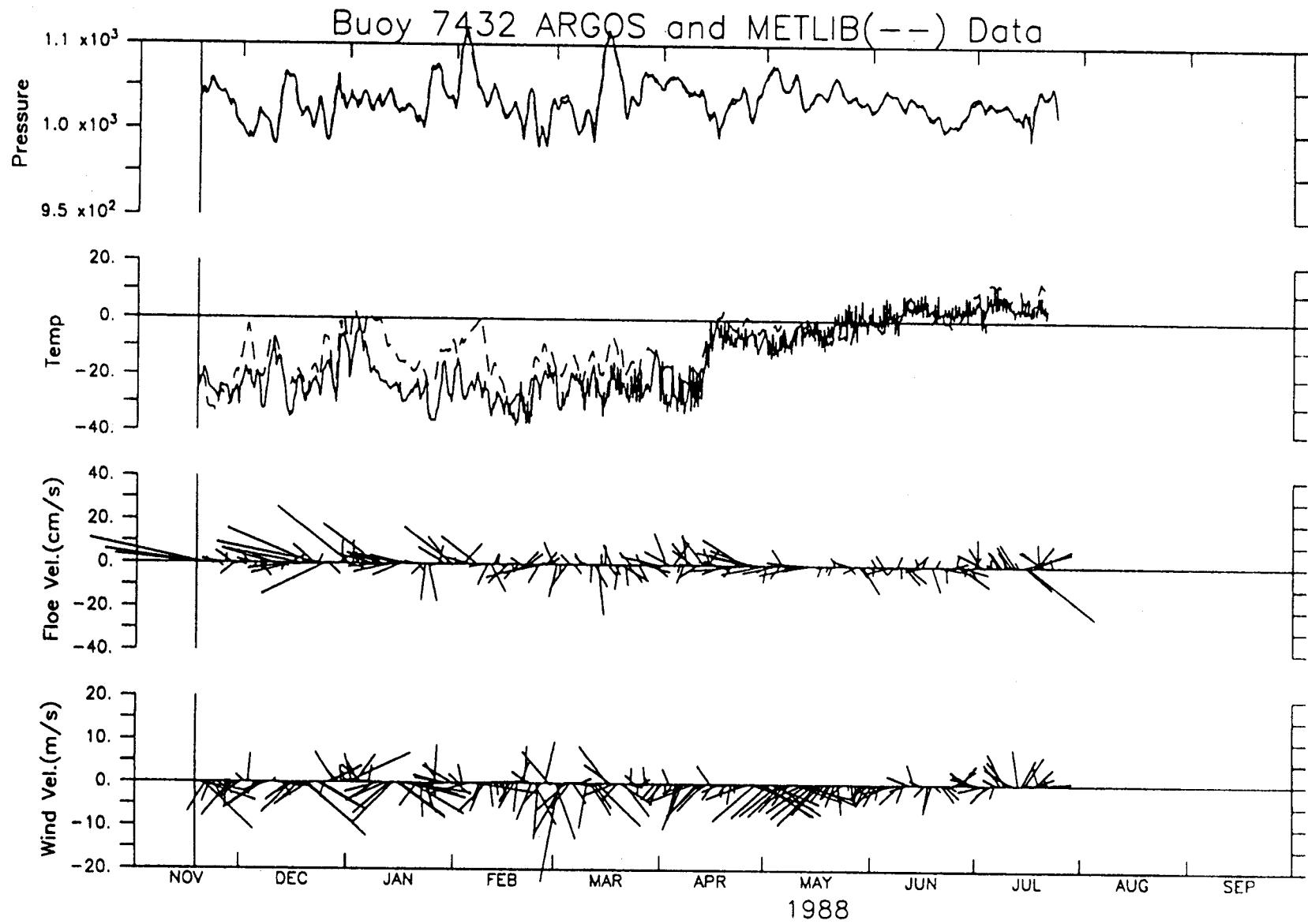


Figure 42. Pressure, temperature, floe velocity, and METLIB winds at ARGOS buoy 7432. See figure 27.

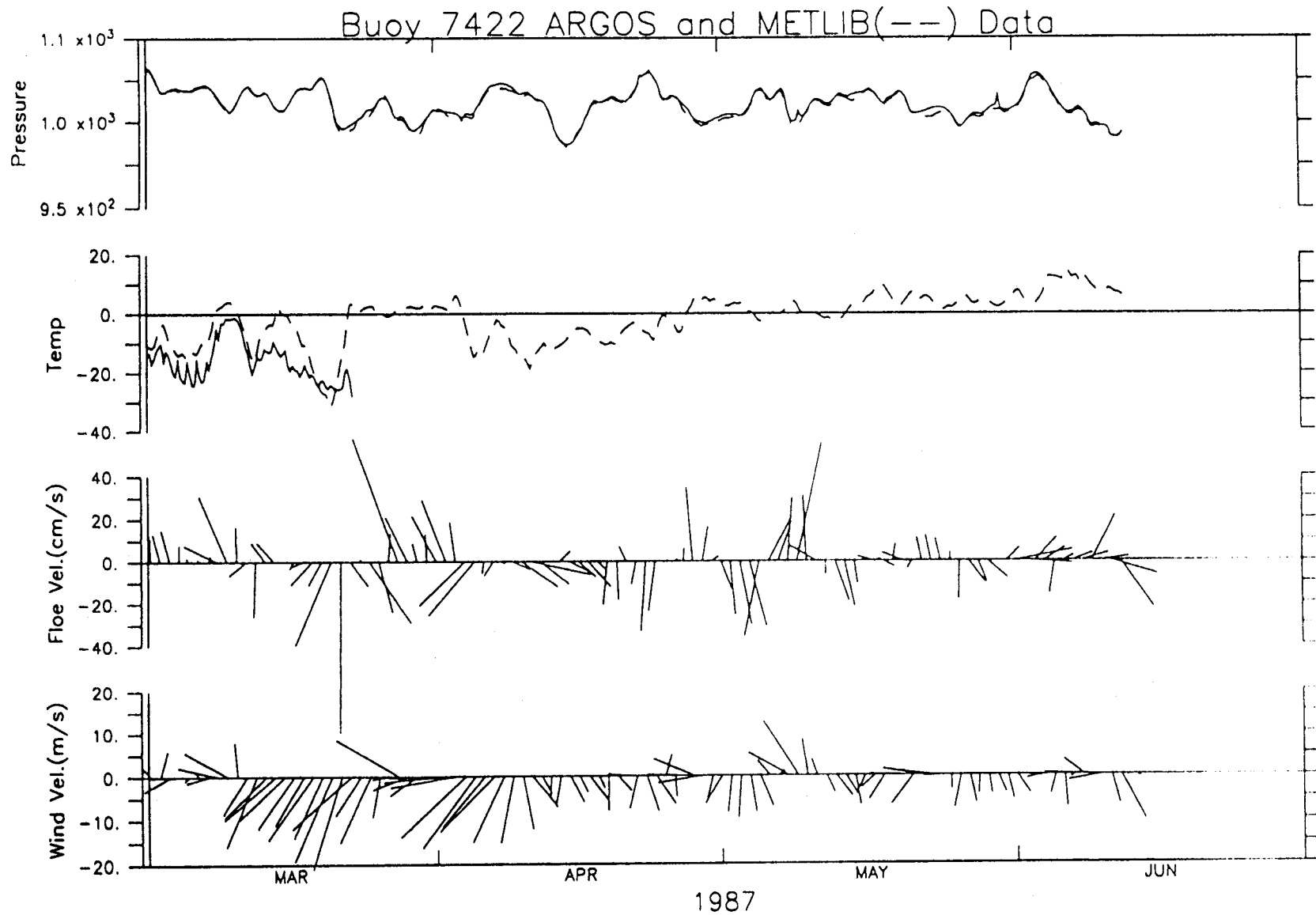


Figure 43. Pressure, temperature, floe velocity, and METLIB winds at ARGOS buoy 7422. See figure 27.

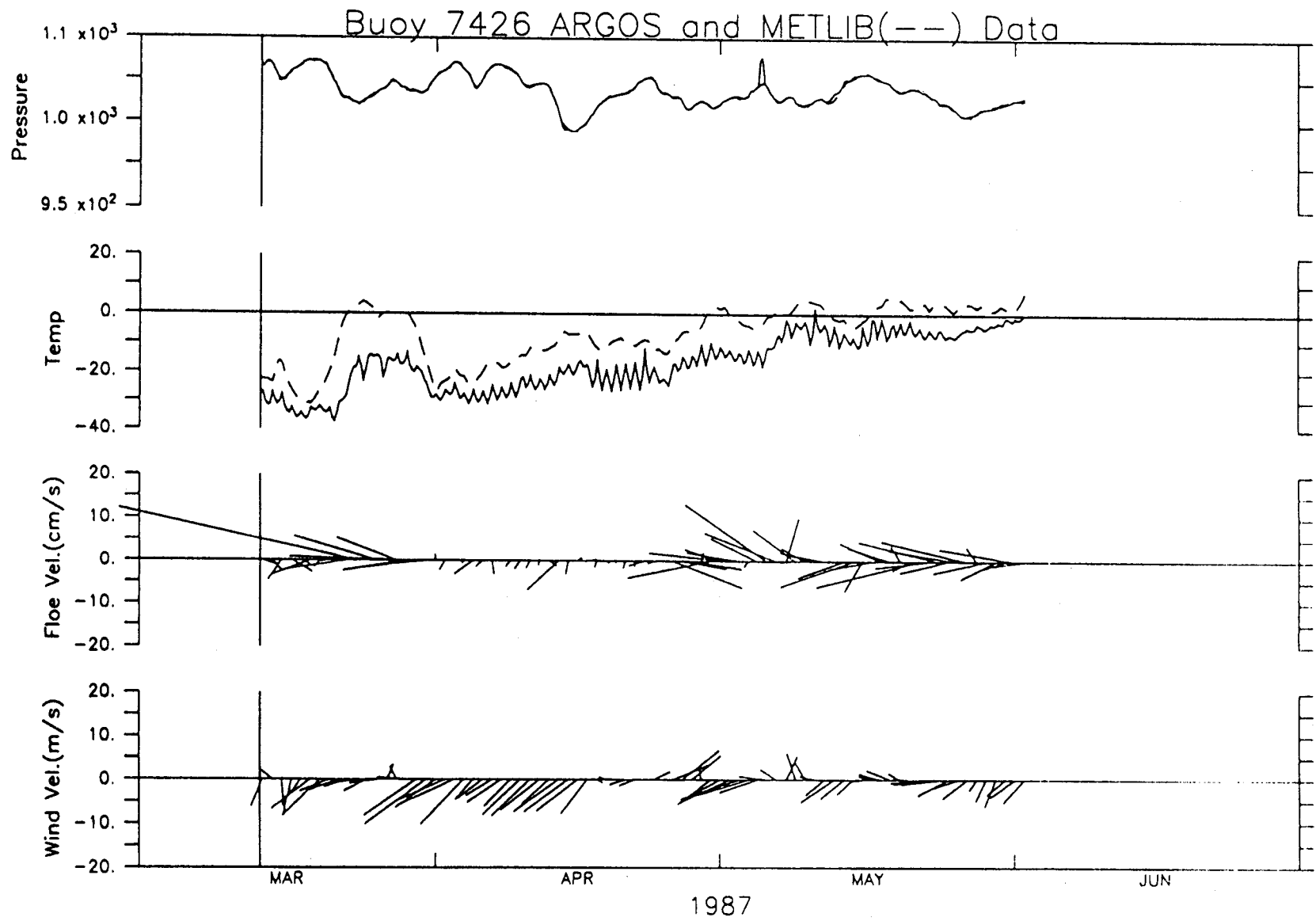


Figure 44. Pressure, temperature, floe velocity, and METLIB winds at ARGOS buoy 7426. See figure 27.

**Table 18. Sea-level Pressure Correlations.** Data were 35-hr filtered and correlated for their full record lengths, as listed in Tables 14-16. Note that the climate data comparisons are made over a common time interval, but that the GOES and ARGOS comparisons are not. METLIB data always lagged Climate, GOES, or ARGOS data.

a) Climate and METLIB

	<u>Barter I.</u>	<u>Barrow</u>	<u>Kotzebue</u>	<u>Nome</u>
0 lag	.93	.94	.94	.94
6 hr lag	.97	.97	.97	.98
12 hr lag	.98	.98	.98	.98
18 hr lag	.95	.95	.94	.95
24 hr lag	.90	.90	.88	.88
30 hr lag	.82	.83	.80	.80
95% level	.18	.18	.18	.19

b) GOES and METLIB

	<u>Resolution I.</u>	<u>Lonely</u>	<u>Icy Cape</u>	<u>C.P.of Wales</u>
0 lag	.93	.94	1.00	1.00
6 hr lag	.94	.93	.98	.98
12 hr lag	.93	.89	.95	.93
18 hr lag	.90	.83	.89	.86
24 hr lag	.85	.75	.82	.78
30 hr lag	.79	.68	.74	.69
95% level	.20	.20	.20	.21

c) ARGOS and METLIB

	<u>7013</u>	<u>7014</u>	<u>7015</u>	<u>7422</u>	<u>7426</u>	<u>7430</u>	<u>7431</u>	<u>7432</u>
0 lag	.99	.99	.80	.99	.99	.99	.99	.99
6 hr lag	.98	.98	.79	.97	.99	.98	.98	.98
12 hr lag	.96	.95	.76	.95	.92	.96	.94	.95
18 hr lag	.92	.91	.72	.84	.92	.90	.89	.89
24 hr lag	.88	.85	.66	.74	.86	.84	.82	.83
30 hr lag	.83	.79	.60	.63	.80	.77	.75	.76
95% level	.32	.29	.45	.40	.53	.32	.29	.30

Table 19. Air Temperature Correlations.

a) Climate and METLIB				
	<u>Barter I.</u>	<u>Barrow</u>	<u>Kotzebue</u>	<u>Nome</u>
0 lag	.89	.86	.92	.92
6 hr lag	.89	.86	.93	.92
12 hr lag	.88	.86	.92	.92
18 hr lag	.87	.85	.91	.92
24 hr lag	.86	.84	.90	.90
30 hr lag	.85	.82	.89	.89
95% level	.78	.77	.78	.73

b) GOES and METLIB				
	<u>Resolution I</u>	<u>.Lonely</u>	<u>Icy Cape</u>	<u>C.P.of Wales</u>
0 lag	.44	.85	.89	.40
6 hr lag	.44	.84	.88	.40
12 hr lag	.44	.83	.87	.40
18 hr lag	.44	.82	.86	.40
24 hr lag	.43	.81	.85	.39
30 hr lag	.43	.79	.84	.39
95% level	.44	.76	.78	.56

c) ARGOS and METLIB ( Buoy 7422 and 7430 had bad thermistors.)								
	<u>7013</u>	<u>7014</u>	<u>7015</u>	<u>7422</u>	<u>7426</u>	<u>7430</u>	<u>7431</u>	<u>7432</u>
0 lag	.90	.91	.93	XX	.90	XX	.89	.88
6 hr lag	.90	.91	.93	XX	.89	XX	.89	.88
12 hr lag	.89	.90	.92	XX	.87	XX	.88	.87
18 hr lag	.89	.90	.90	XX	.85	XX	.88	.86
24 hr lag	.88	.89	.88	XX	.83	XX	.87	.85
30 hr lag	.87	.88	.87	XX	.81	XX	.86	.84
95% level	.86	.86	.96	XX	.87	XX	.91	.76

For every Alaskan coastal station there is a lag of 6 to 12 hours from the observation time until that data is used by FNOC (or any other center) in the surface analysis (Table 18). These delays are usually caused by the time for the physical transmittal of the station data over the data collection network, the extensive error checking done at the NWS central site, and the artifice that a miss of the analysis cut-off time by a few minutes is effectively a miss of 6 hours. The consistent 12-hour lags for sea-level pressure of the METLIB data relative to the climate station data is directly attributable to this process. This lag must be taken into account if gradient or geostrophic winds based on existing NMC or FNOC analyses are to be used to drive numerical models of sea ice drift and surface currents. Although it may seem like a small effect, this bias would introduce errors of about 10% into the estimates of wind stress, which is the same order of magnitude as the internal ice stress, geostrophic sea-surface tilt contribution, and the Coriolis term in the sea ice balance.

It is also important to note that it would be inappropriate to blend mesoscale surface meteorological observations with either the NWS or FNOC surface pressure fields without time-shifting the analysis fields backwards by 12 hours. The hidden time-shift is probably the major reason that the mesoscale network along the Alaska coast gave such an improved forecasting capability over using geostrophic or gradient winds calculated from standard analysis fields (Kozo, 1980, 1982a, 1982b, 1984; Kozo and Robe, 1986). With a continued adequate coverage by the Arctic Buoy Program and the input of those data into the international meteorological network, there is no further improvement to be gained by maintaining a separate sea-level pressure network along the North Slope. Other meteorological measurements, however, including the anemometer records, the drifting buoy positions, and all the mesoscale air temperature measurements were important to the study.

Temperatures at the four NWS coastal stations also seem to be shifted 6 to 12 hours, although the coefficients change little between 0 and 12 hours lag (Table 19). The temperature correlations overall are 10% lower than the pressure correlations. A disturbing aspect of the analyzed temperatures (METLIB from FNOC analyses) is that they are too warm in the winter and spring at all stations by 3° to 13°C (Table 17, Figures 28 - 34, and Figures 37, 38, 41, 42, and 44). Barrow (Climate) and Resolution Island (GOES) were both quite exposed to marine air and should have had minimal local continentality effects (due to the vastly different thermal characteristics of water and

land), yet the FNOC temperatures generated by METLIB were too warm by 13° and 5°C, respectively, with the biggest errors in the coldest months (Table 17). These are huge errors and would be expected to drive an equilibrium thermodynamic ice model to ice-free conditions. Sverdrup (1933) stated that all land stations underpredict the polar marine winter temperatures (give winter air temperatures which are too cold) because of the cumulative effect of leads on the polar marine boundary layer air temperature. However, even the ARGOS buoys, which were riding modest sized floes, showed METLIB temperatures which were 2° to 6°C too warm in their respective record means with the same bias toward errors in winter and spring (Figures 37, 38, 41, and 42).

One interpretation that could be given to the striking air temperature errors from the FNOC analysis fields is that these temperatures are representative of the mean boundary-layer temperature or the temperature near the top of the planetary boundary layer rather than the surface. Since outward long wave radiative cooling (Maykut and Church, 1973) and sensible heat fluxes dominate the surface balance, there is strong cooling at the surface and a general subsidence in winter months (Sverdrup, 1933; Overland, 1985). Thus any thermodynamic sea ice model would need to be driven by a relatively complete boundary-layer model and should not use the FNOC analysis fields in the surface balance, as is typically done for longer model calculations.

The correlations between the gradient winds calculated by METLIB from FNOC fields with the measured winds have the same time delays as sea-level pressure and surface air temperature, but have lower absolute correlations compared to the scalar quantities (Table 20). The somewhat low correlations were caused by several factors: 1) the high-frequency variations had not been removed, so diurnal effects, such as the sea breeze were not deleted (Moritz, 1977; Kozo, 1982a, 1982b); 2) for certain stations, such as Barter Island, mountain barrier effects, especially enhanced in the winter by the stability of the lower boundary layer, were not included in the METLIB wind calculation (Dickey, 1961; Kozo, 1980, 1984; Kozo and Robe, 1986); and 3) seasonal variations in surface drag and radiation effects on boundary layer dynamics were not included in METLIB calculated winds (Banke and Smith, 1971; Banke et al., 1976; Feldman et al., 1979; Langleben, 1971; Maykut and Church, 1973; Smith and Banke, 1971; Wendler et al., 1981).

There appear to be three regimes among the various weather stations. The Bering Strait region (Cape Prince of Wales, Nome and Kotzebue), the North Slope (Barrow, Lonely, Resolution, and Barter), and a transition zone represented by Icy Cape (Tables 21 - 24). More low pressure systems reach the southern stations than the North Slope stations; near the southern stations, the ocean is always ice free in summer, while near the northern stations there may be ice all year or only a short ice-free season. The seasonal air temperature maxima were in August in the south and shifted closer to the summer solstice along the North Slope (Pease, 1987).

Seasonally averaged values for temperature, pressure, and wind are given in Figures 45 - 48; monthly averaged values are in Figures 49 - 52; and monthly averaged wind variances are in Figure 53 for all the land stations. Along the North Slope, there were sea-level pressure maxima in both years in December and February and pressure minima in September-October and January. The January minimum may seem odd because of the generally higher winter pressures than summer; however, this is seen in the Bering and Chukchi seas also, and is driven by blocking ridge activity over the eastern North Pacific each winter (Overland, 1981; Overland and Pease, 1982; Pease, 1987). Generally, Nome, Kotzebue, and Cape Prince of Wales are warmer, windier, and more randomly affected by winds from various directions than the North Slope, where summer mean maximum air temperatures are less than 10°C, winds are persistently

northeasterly to easterly, and wind-direction variances are lower. Maximum wind variances were highest at all stations in the autumn and typically again in January.

A selection of weather maps for 1986-87 are presented in Figures 143 - 150 in Appendix B. An added selection of maps for 1987-88 are given in Figures 54 - 58. The October 1987 maps show weak ridges over the northern areas retrograding to set-up of the Aleutian low - Siberian high with concomitant North Slope easterlies in November and December 1987. Late December and early January storms passed along the Alaskan west coast, driving some periods of southerly and southeasterly winds along the North Slope. Northeasterly to easterly flow resumed in February and March and continued through the end of the experiment.

One aspect of the 1986 - 1988 seasonal conditions which has not been satisfactorily explained by this analysis is whether the extreme minimum ice extents for this period were caused by atmospheric thermodynamic or circulation anomalies or by the advection of warm water from upstream sources, such as the Bering and Chukchi seas (Barry et al., 1979; Bruno and Madsen, 1989; Henry and Heaps, 1976; Hufford, 1973; Mysak and Manak, 1989; Paquette and Bourke, 1974; Parker et al., 1985; Reed and Kunkel, 1960; Rogers, 1978; Short and Wiseman, 1975; Walsh and Sater, 1981). It is thought that the analysis of the Chukchi Sea hydrographic data from the ONR-funded Freeze cruises may help us understand this important point.

**Table 20. Wind Speed Correlations.** Note that the correlations for Icy Cape and Cape Prince of Wales were on significantly shorter time series than for the other stations.

a) Linear Correlations along axes of maximum variance:  
Climate and METLIB

	<u>Barter I.</u>	<u>Barrow</u>	<u>Kotzebue</u>	<u>Nome</u>
0 lag	.40	.57	.17	.55
6 hr lag	.46	.63	.19	.60
12 hr lag	.50	.64	.17	.59
18 hr lag	.48	.59	.11	.52
24 hr lag	.42	.51	.06	.43
30 hr lag	.35	.43	.02	.35
95% level	.09	.11	.11	.15

Complex Correlations (average angle of separation):

0 lags	0.53(-2.8°)	0.72(+1.2°)	0.53(-10.4°)	.64(-10.1°)
--------	-------------	-------------	--------------	-------------

b) Linear Correlations along axes of maximum variance:  
GOES and METLIB

	<u>Resolution I.</u>	<u>Lonely</u>	<u>Icy Cape</u>	<u>C.P.of Wales</u>
0 lags	.35	.30	.74	.64
6 hr lag	.37	.29	.71	.63
12 hr lag	.36	.25	.65	.57
18 hr lag	.35	.20	.57	.48
24 hr lag	.32	.16	.50	.39
30 hr lag	.29	.13	.45	.31
95% level	.11	.16	.15	.16

Complex Correlations (average angle of separation):

0 lags	0.56(-8.5°)	0.59(-7.7°)	0.79(18.3°)	0.81(22.1°)
--------	-------------	-------------	-------------	-------------

**TABLE 21. Correlations among Climate Stations. (Lag which gives the greatest correlation; 0 hours unless explicitly stated otherwise). \*\*\* indicates correlation was not significant at the 95% level. Positive correlation means column lags row.**

**Pressure**

	<u>Barter I.</u>	<u>Barrow</u>	<u>Kotzebue</u>	<u>Nome</u>
Barter I.	1.0	0.96	0.84	0.69
Barrow	0.96	1.0	0.77	0.63
Kotzebue	0.86(6)	0.80(6)	1.0	0.96
Nome	0.75(12)	0.68(12)	0.96(6)	1.0

**Temperature**

	<u>Barter I.</u>	<u>Barrow</u>	<u>Kotzebue</u>	<u>Nome</u>
Barter I.	1.0	0.96	0.90	0.84
Barrow	0.96(6)	1.0	0.91	0.86
Kotzebue	0.90(18)	0.91(12)	1.0	0.95
Nome	0.85(18)	0.86(18)	0.95(6)	1.0

**Wind Speed**

	<u>Barter I.</u>	<u>Barrow</u>	<u>Kotzebue</u>	<u>Nome</u>
Barter I.	1.0	0.53	***	-0.12(6)
Barrow	0.53	1.0	0.15	***
Kotzebue	0.09(24)	0.21(18)	1.0	0.43
Nome	-0.12	0.11(30)	0.44(6)	1.0

**Table 22. Correlations Among METLIB Records at Climate Stations.**

**Pressure**

	<u>Barter I.</u>	<u>Barrow</u>	<u>Kotzebue</u>	<u>Nome</u>
Barter I.	1.0	0.96	0.84	0.68
Barrow	0.96	1.0	0.81	0.65
Kotzebue	0.86(6)	0.82(6)	1.0	0.95
Nome	0.73(12)	0.69(12)	0.96(6)	1.0

**Temperature**

	<u>Barter I.</u>	<u>Barrow</u>	<u>Kotzebue</u>	<u>Nome</u>
Barter I.	1.0	0.93	0.82	0.74
Barrow	0.93(6)	1.0	0.88	0.79
Kotzebue	0.83(12)	0.88(6)	1.0	0.95
Nome	0.73(12)	0.79(6)	0.95	1.0

**Wind Speed**

	<u>Barter I.</u>	<u>Barrow</u>	<u>Kotzebue</u>	<u>Nome</u>
Barter I.	1.0	0.68	0.23	***
Barrow	0.68	1.0	0.34	***
Kotzebue	0.25(6)	0.37(12)	1.0	0.83
Nome	0.14(24)	0.20(24)	0.85(6)	1.0

**Table 23. Correlations Among Goes Stations. Time interval is 28 March 1987 to 29 March 1988.**

<u>Pressure</u>			
	<u>Resolution I.</u>	<u>Lonely</u>	<u>Icy Cape</u>
Resolution I.	1.0	0.87(12)	0.91(6)
Lonely	0.83	1.0	0.88
Icy Cape	0.90	0.88(6)	1.0
<u>Temperature</u>			
	<u>Resolution I.</u>	<u>Lonely</u>	<u>Icy Cape</u>
Resolution I.	1.0	***	***
Lonely	***	1.0	0.96
Icy Cape	***	0.96(6)	1.0
<u>Wind Speed</u>			
	<u>Resolution I</u>	<u>Lonely</u>	<u>Icy Cape</u>
Resolution	1.0	0.68(24)	0.52(12)
Lonely	0.54	1.0	0.52
Icy Cape	0.51	0.54(6)	1.0

**Table 24. Correlations among METLIB Records at GOES Stations.**

<u>Pressure</u>			
	<u>Resolution I.</u>	<u>Lonely</u>	<u>Icy Cape</u>
Resolution I.	1.0	0.99	0.96
Lonely	0.99	1.0	0.98
Icy Cape	0.96	0.98	1.0
<u>Temperature</u>			
	<u>Resolution I.</u>	<u>Lonely</u>	<u>Icy Cape</u>
Resolution I.	1.0	0.98	0.91
Lonely	0.98	1.0	0.96
Icy Cape	0.91(6)	0.96	1.0
<u>Wind Speed</u>			
	<u>Resolution I</u>	<u>Lonely</u>	<u>Icy Cape</u>
Resolution	1.0	0.89	0.63
Lonely	0.89	1.0	0.82
Icy Cape	0.63	0.82	1.0

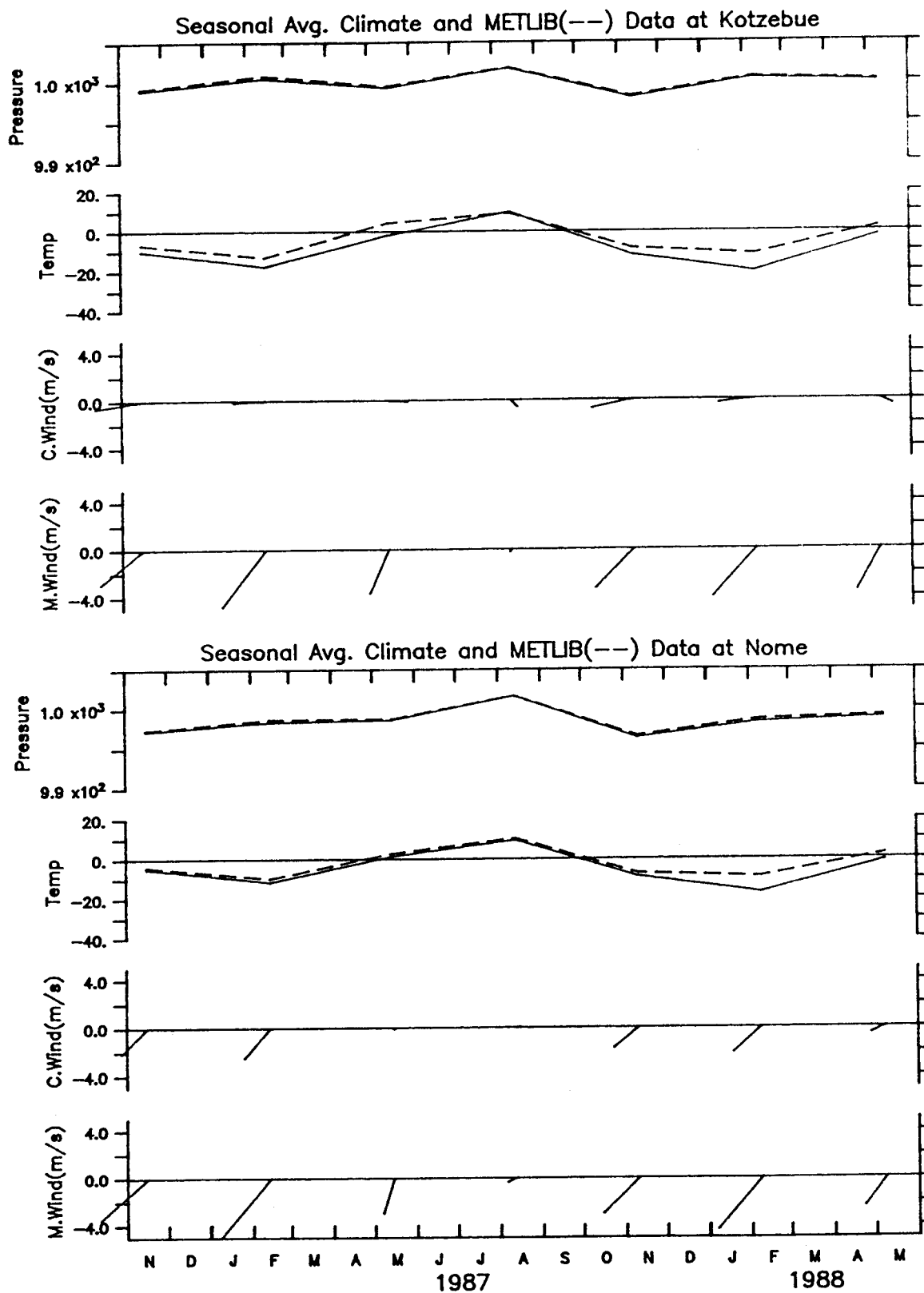


Figure 45. Seasonal average NWS and METLIB pressure (mb), temperature ( $^{\circ}\text{C}$ ), and winds ( $\text{m s}^{-1}$ ) at Kotzebue and Nome. Data were averaged over January-March, April-June, July-September, and October-December and are plotted at the midpoint of the averaging interval.

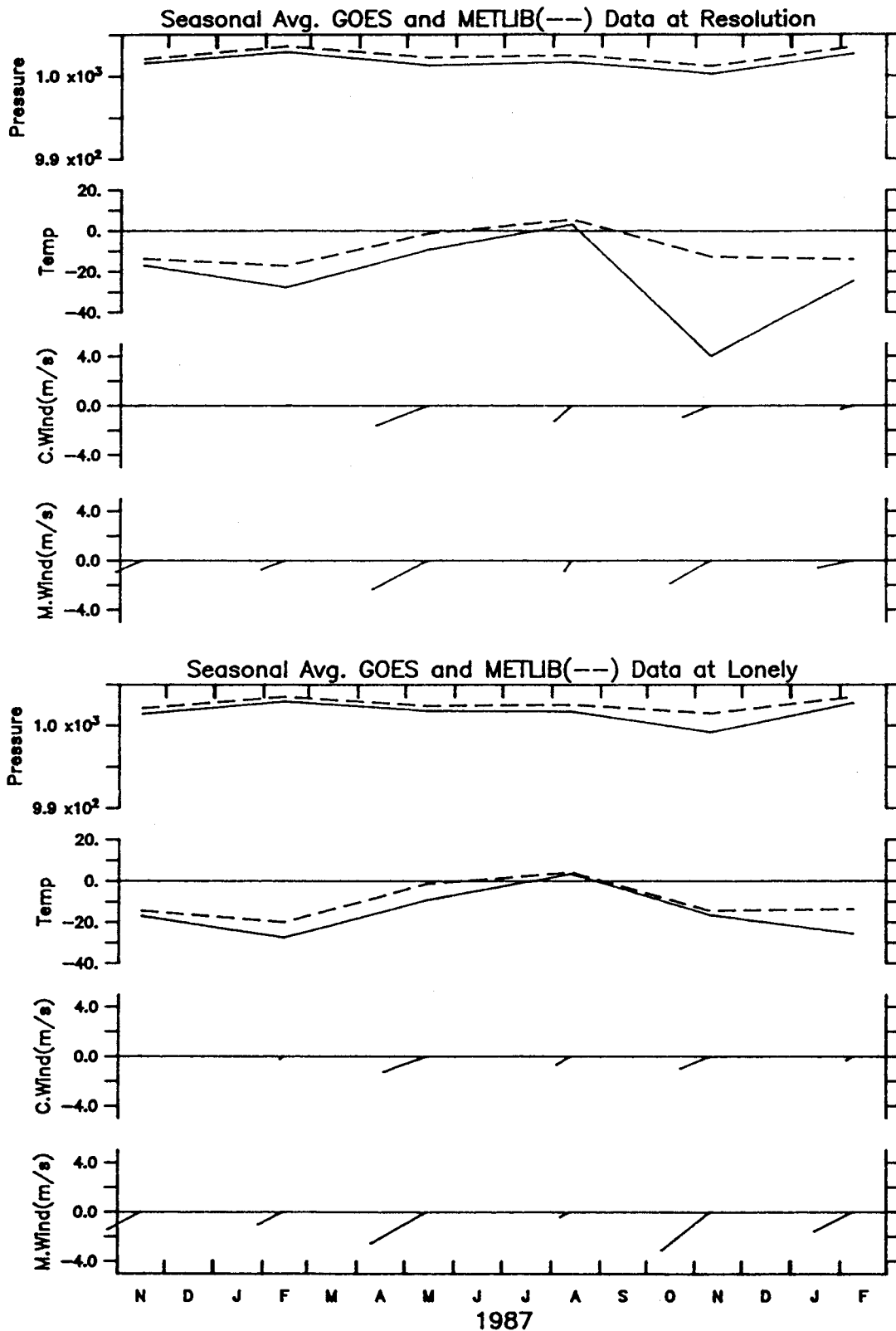


Figure 46. Seasonal average GOES station and METLIB pressure (mb), temperature(°C), and winds ( $\text{m s}^{-1}$ ) at Resolution Island and Lonely. See figure 45.

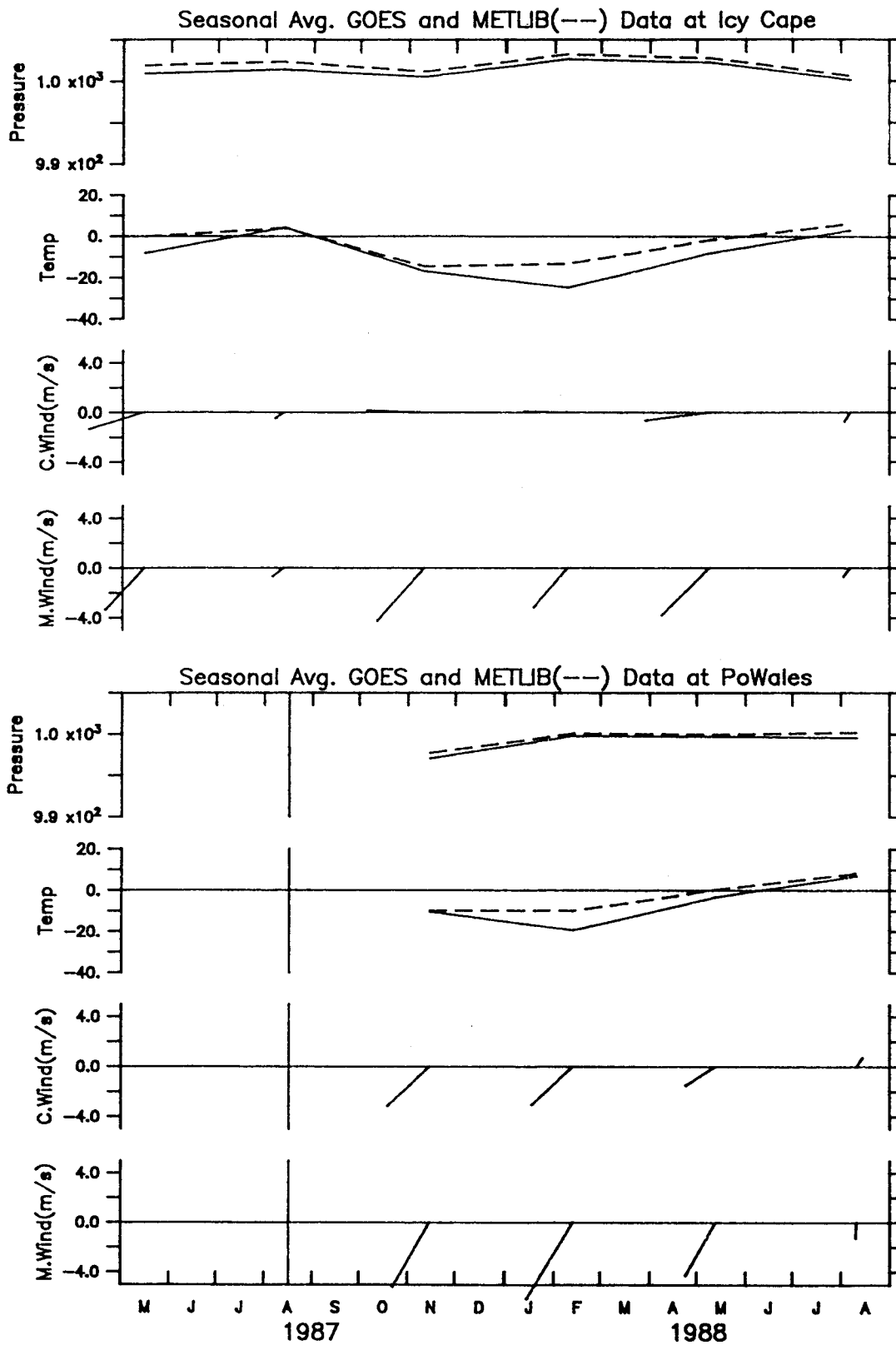


Figure 47. Seasonal average GOES station and METLIB pressure (mb), temperature ( $^{\circ}\text{C}$ ), and winds ( $\text{m s}^{-1}$ ) at Icy Cape and Wales. See figure 45.

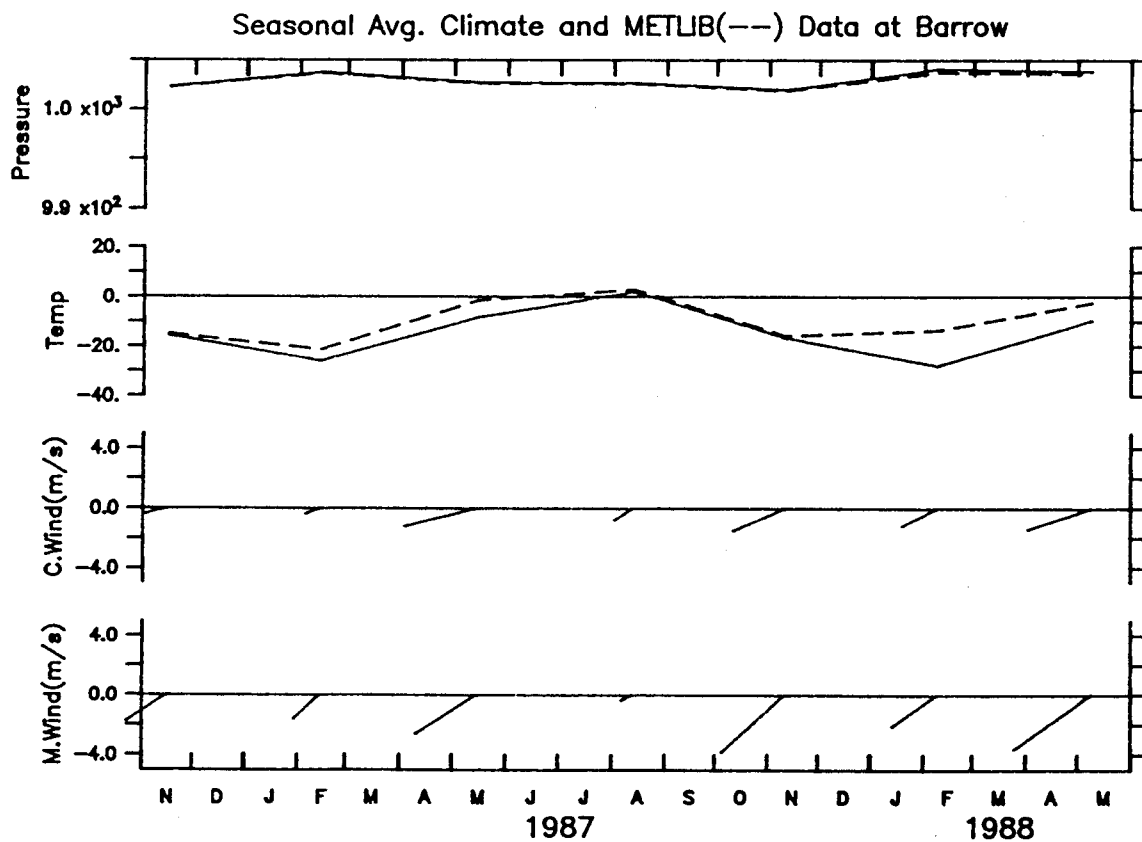
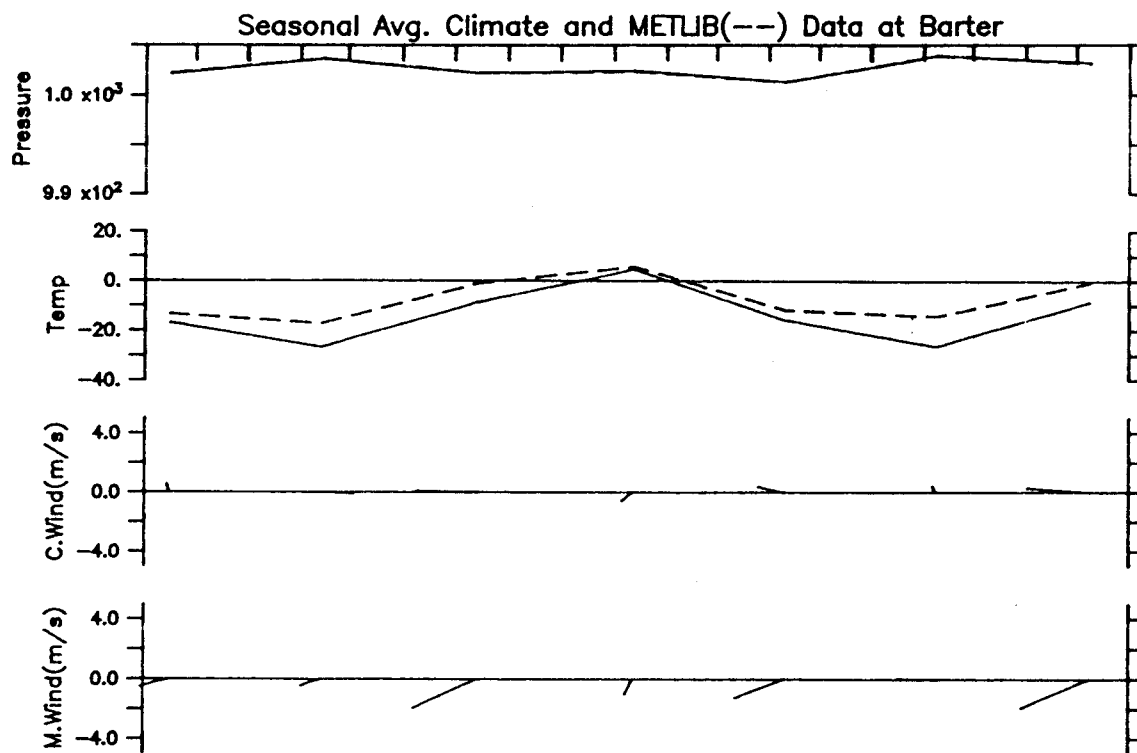


Figure 48. Seasonal average NWS and METLIB pressure (mb), temperature ( $^{\circ}\text{C}$ ), and winds ( $\text{m s}^{-1}$ ) at Barter Island and Barrow.

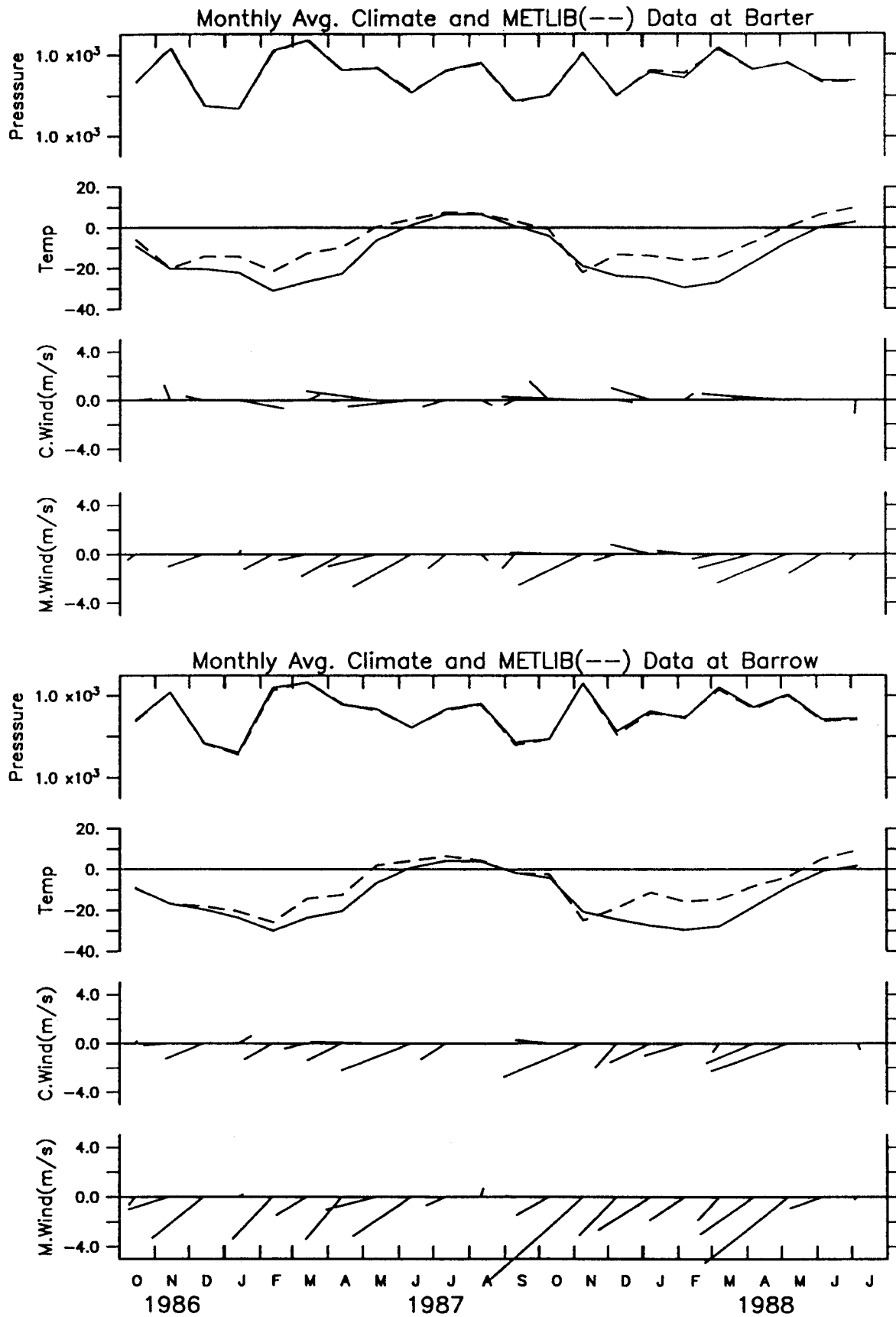


Figure 49. Monthly average NWS and METLIB pressure (mb), temperature ( $^{\circ}\text{C}$ ), and winds ( $\text{m s}^{-1}$ ) at Barter Island and Barrow.

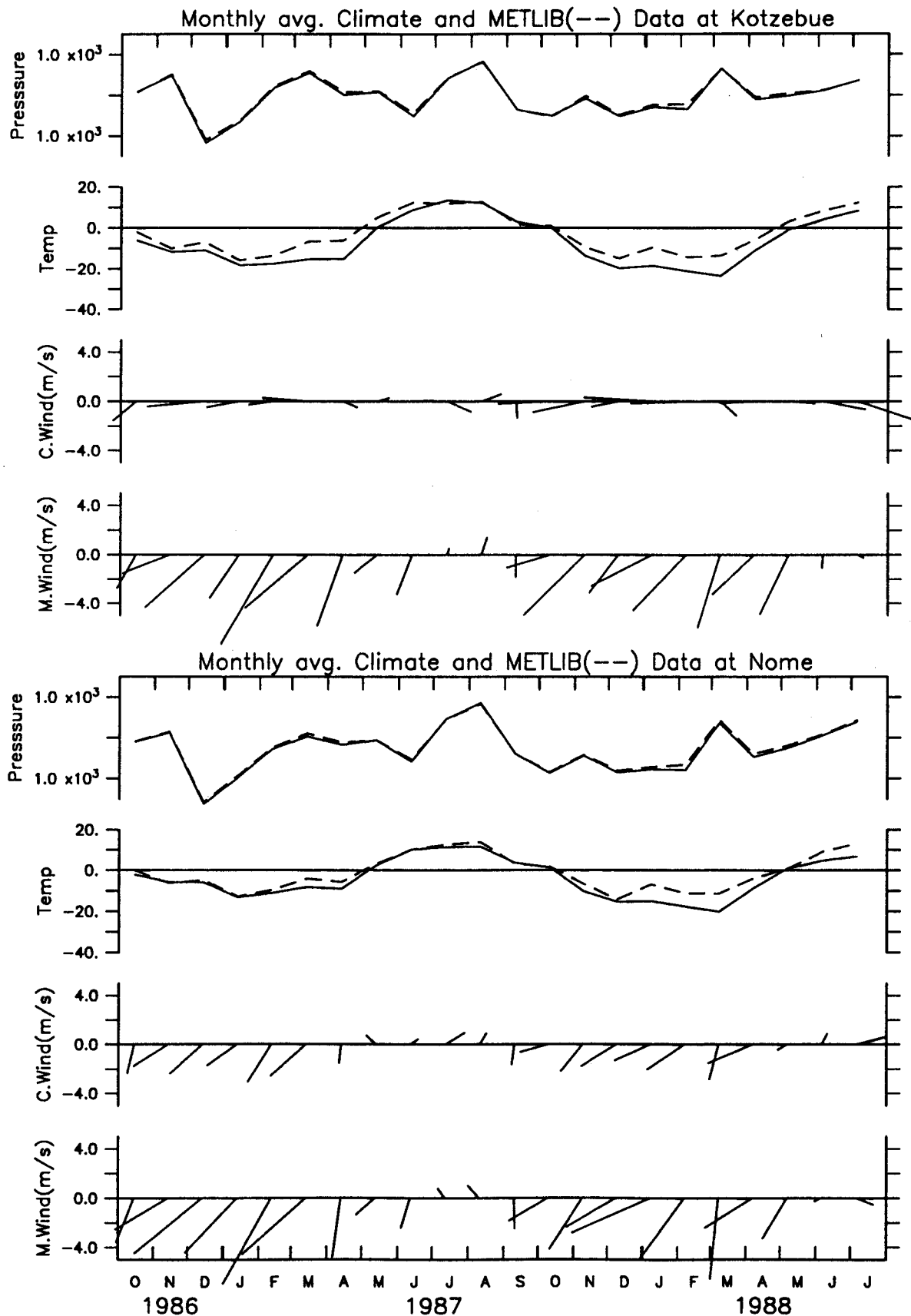


Figure 50. Monthly average NWS and METLIB pressure (mb), temperature ( $^{\circ}\text{C}$ ), and winds ( $\text{m s}^{-1}$ ) at Kotzebue and Nome.

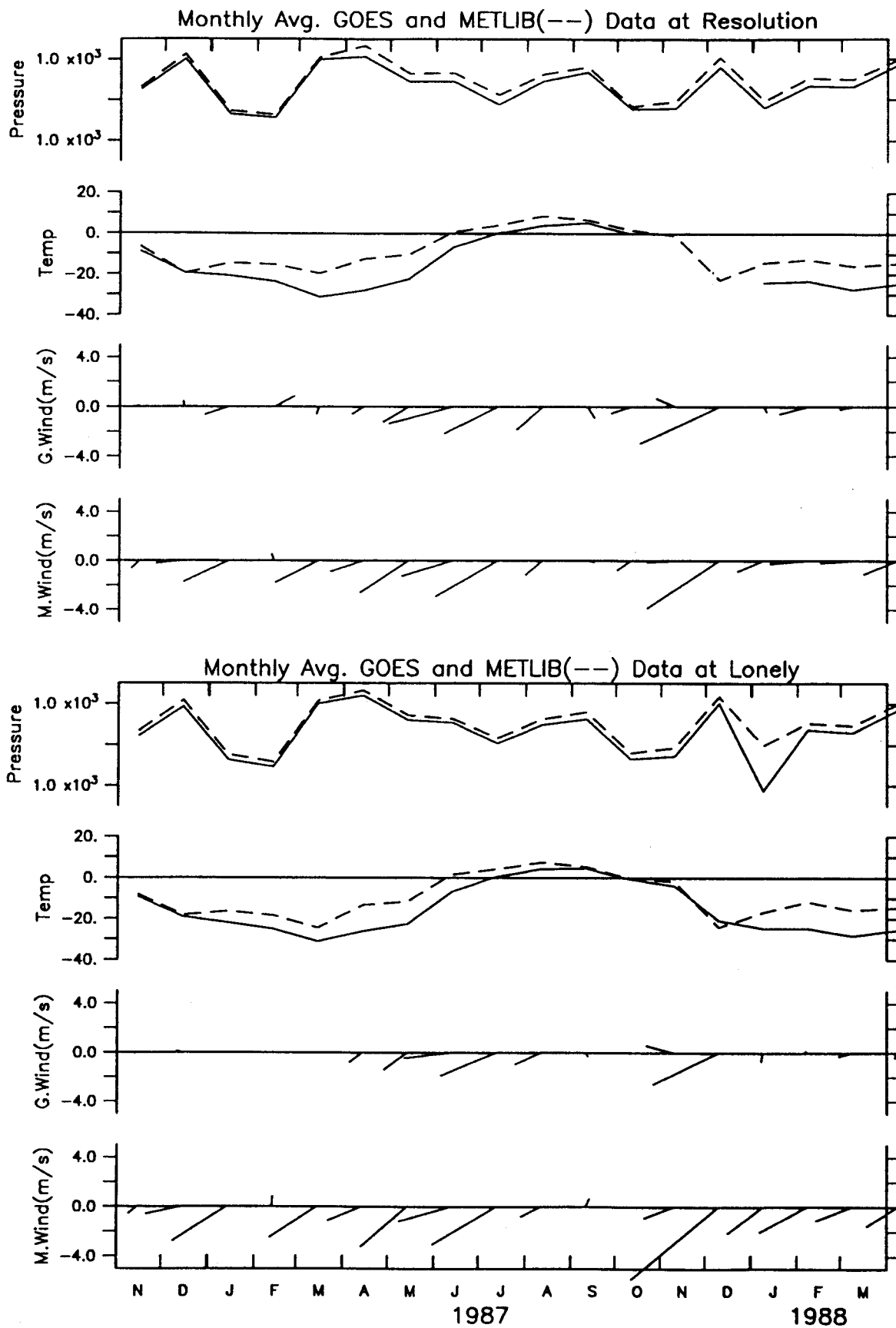


Figure 51. Monthly average GOES-station and METLIB pressure (mb), temperature ( $^{\circ}\text{C}$ ), and winds ( $\text{m s}^{-1}$ ) at Resolution Island and Lonely.

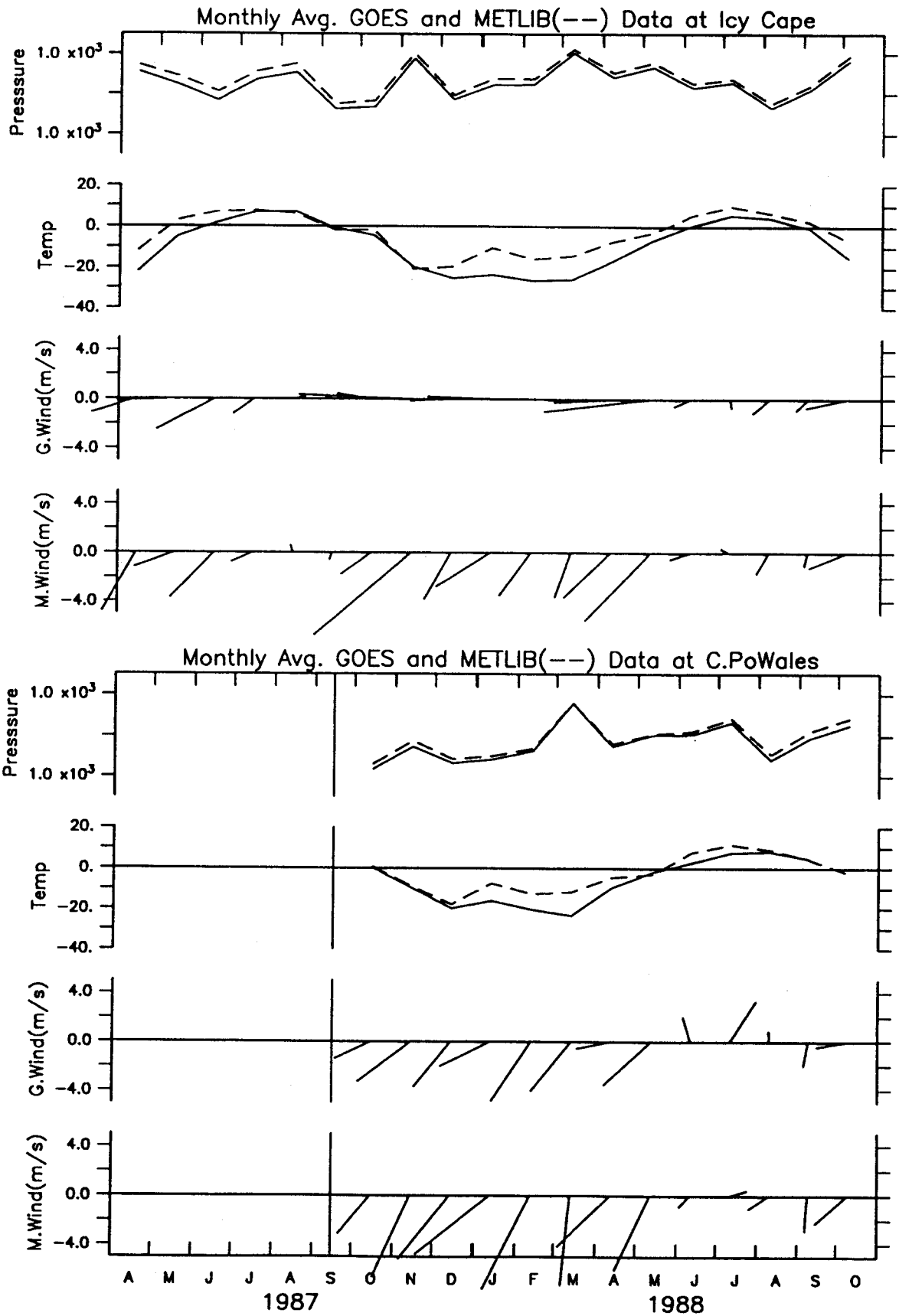


Figure 52. Monthly average GOES-station and METLIB pressure (mb), temperature ( $^{\circ}\text{C}$ ), and winds ( $\text{m s}^{-1}$ ) at Icy Cape and Wales. The vertical bars mark the start of the data.

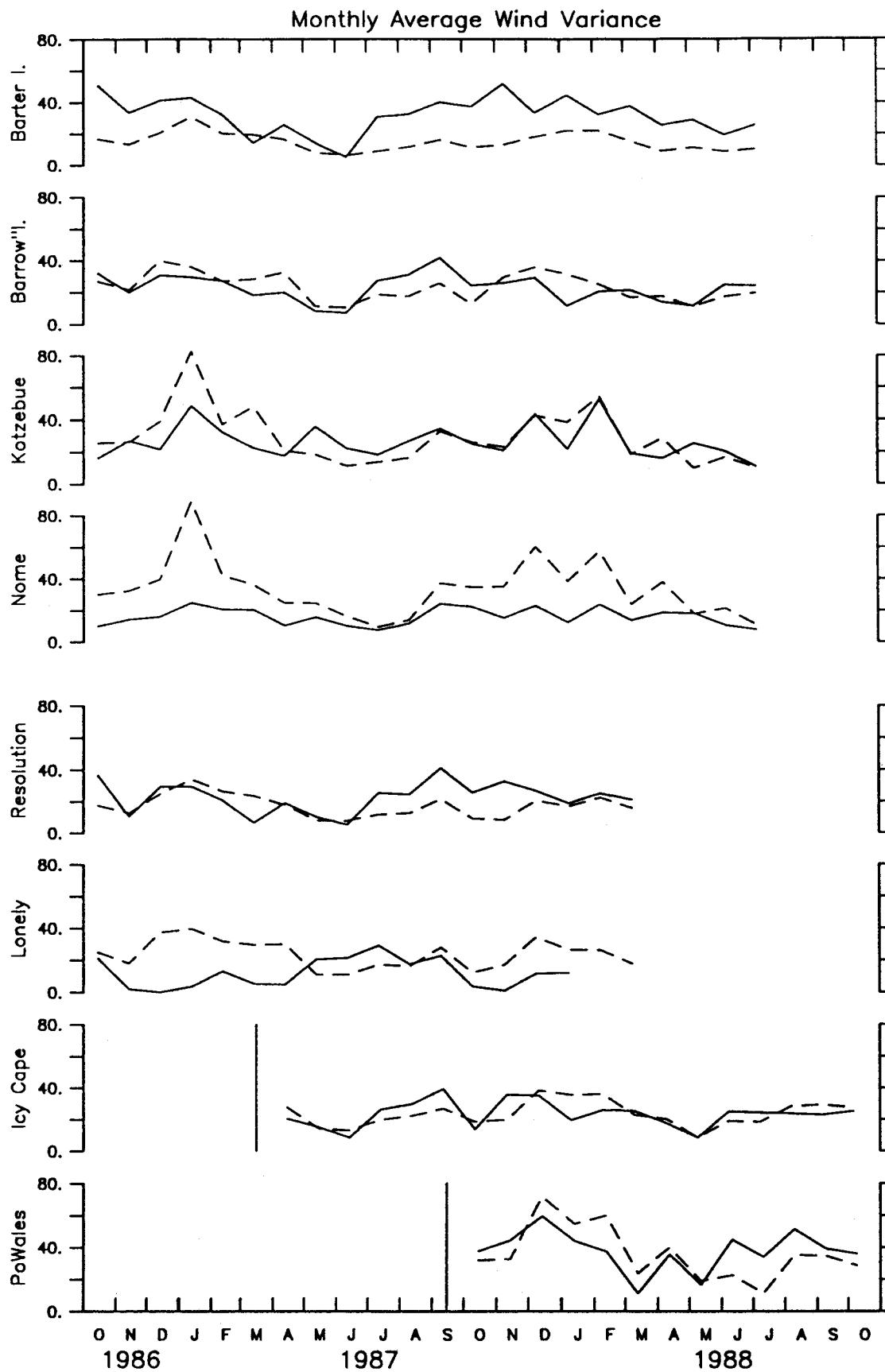


Figure 53. Monthly average wind variance ( $m^2 s^{-2}$ ) at the four National Weather Service Stations and four GOES stations. The vertical bars mark the start of the data.

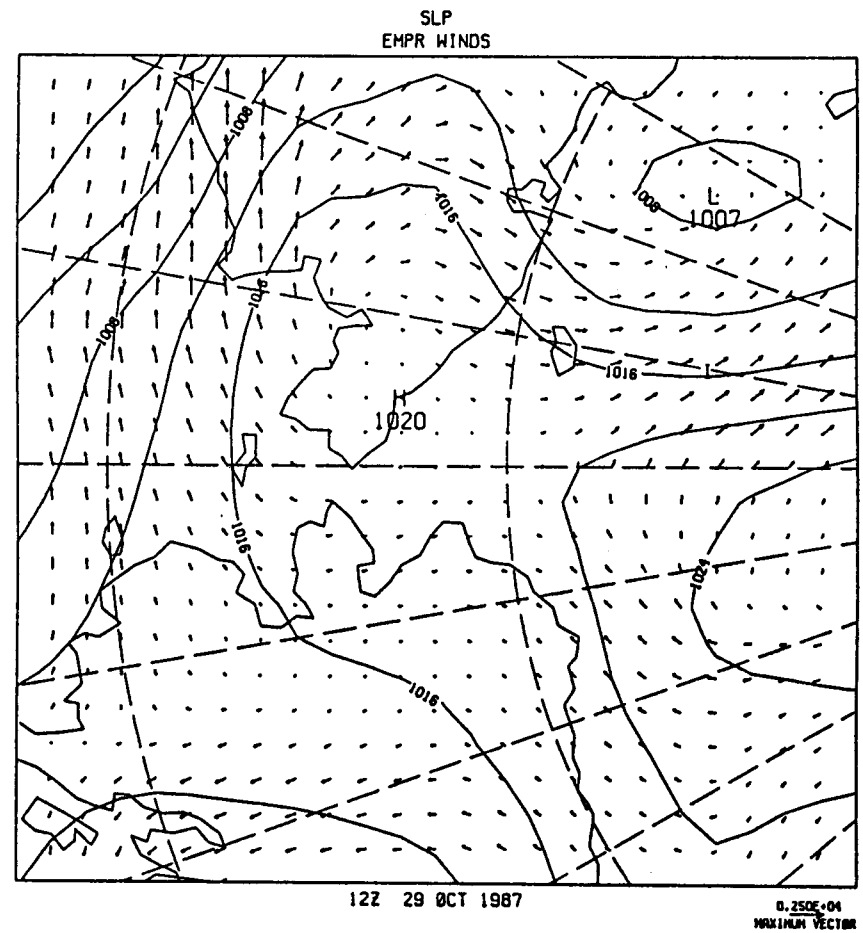
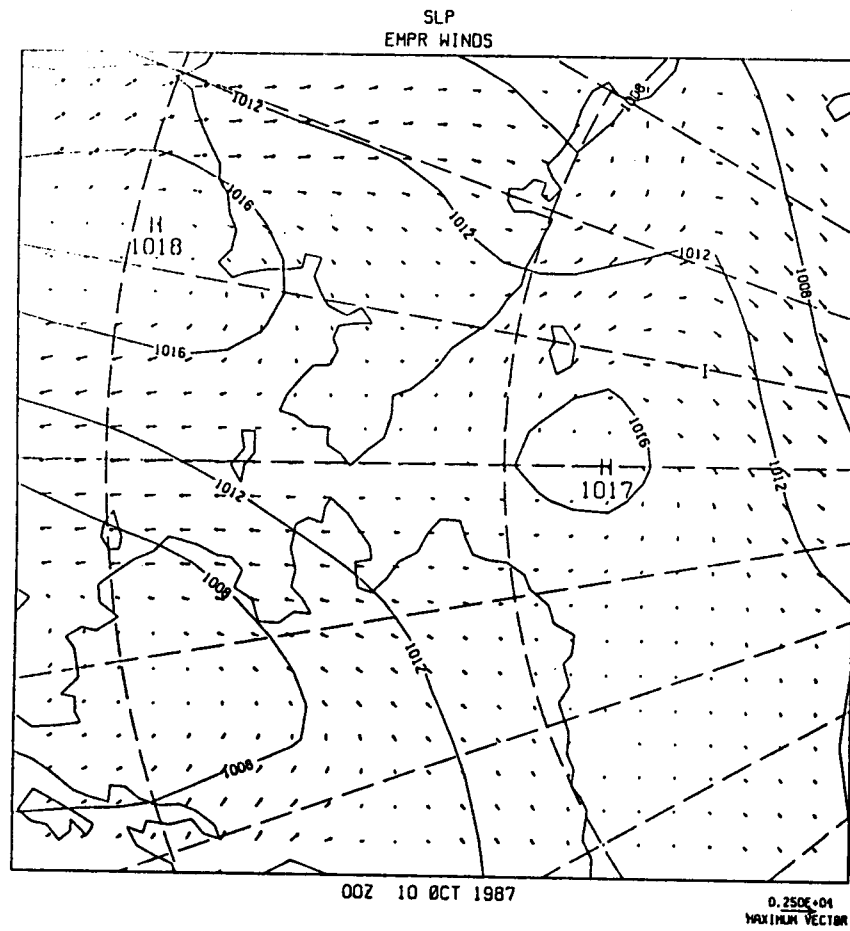


Figure 54. Pressure and wind fields over northern Alaska and eastern Siberia at 00Z 10 October 1987 and 12Z 29 October 1987.

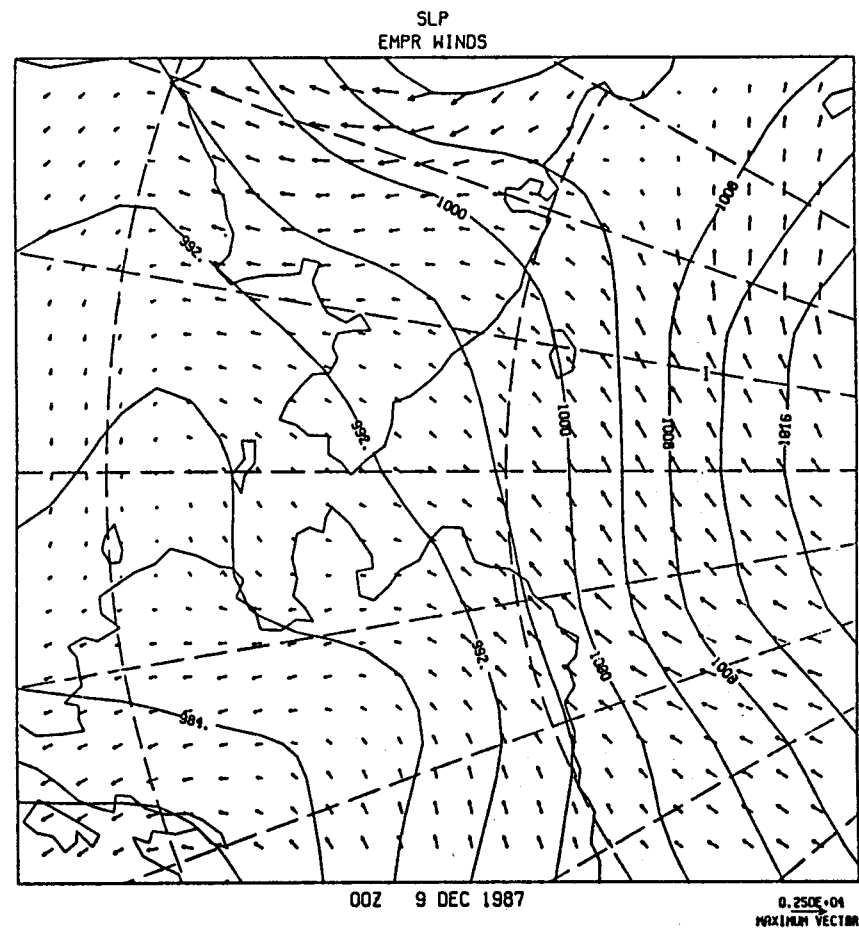
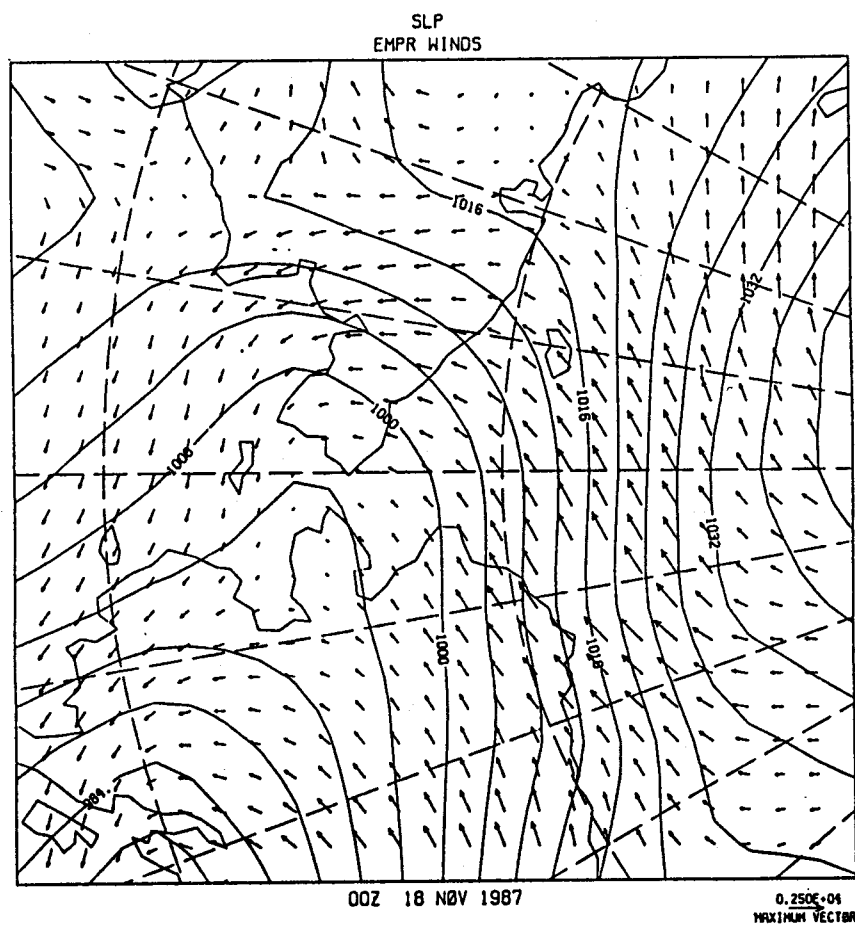


Figure 55. Pressure and wind fields over northern Alaska and eastern Siberia at 00Z 18 November 1987 and 00Z 9 December 1987. The absence of wind vectors northwest of Alaska in the first map indicates that the wind speed was greater than  $25 \text{ m s}^{-1}$ .

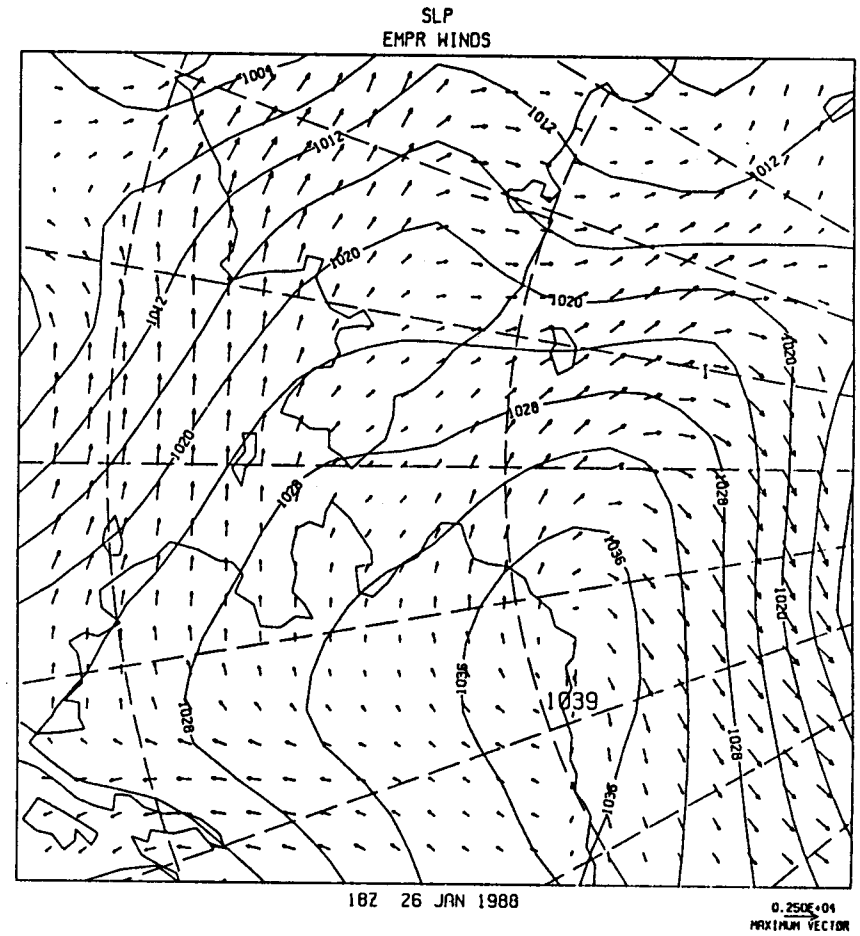
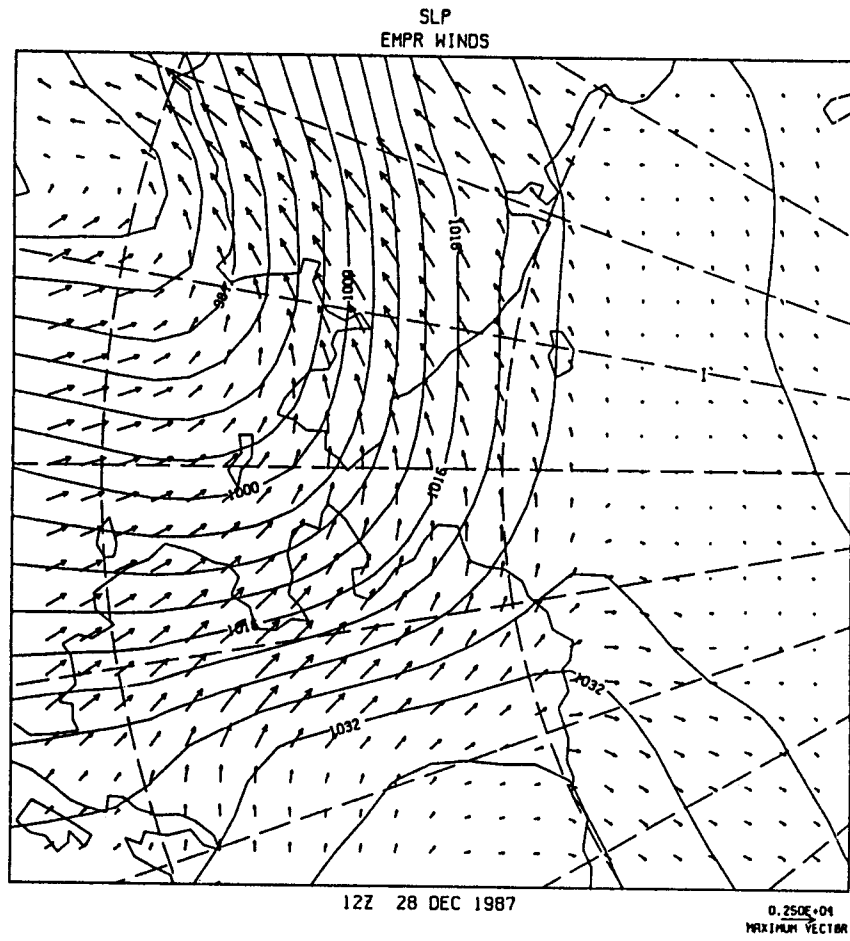


Figure 56. Pressure and wind fields over northern Alaska and eastern Siberia at 12Z 28 December 1987 and 18Z 26 January 1988.

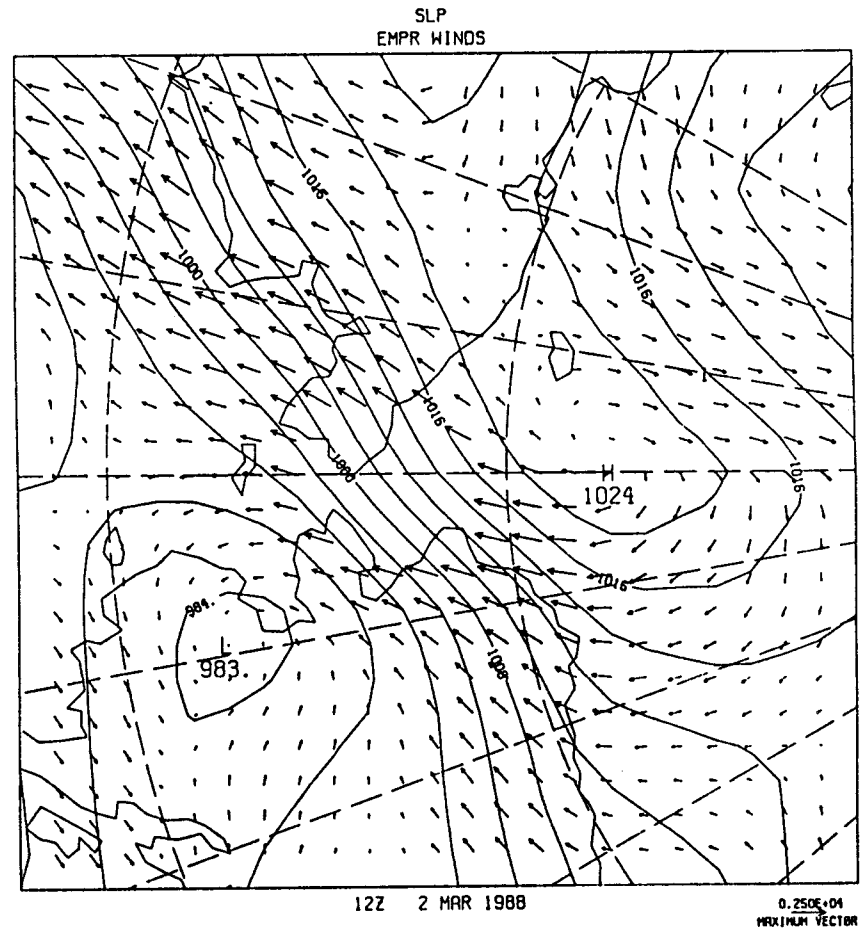
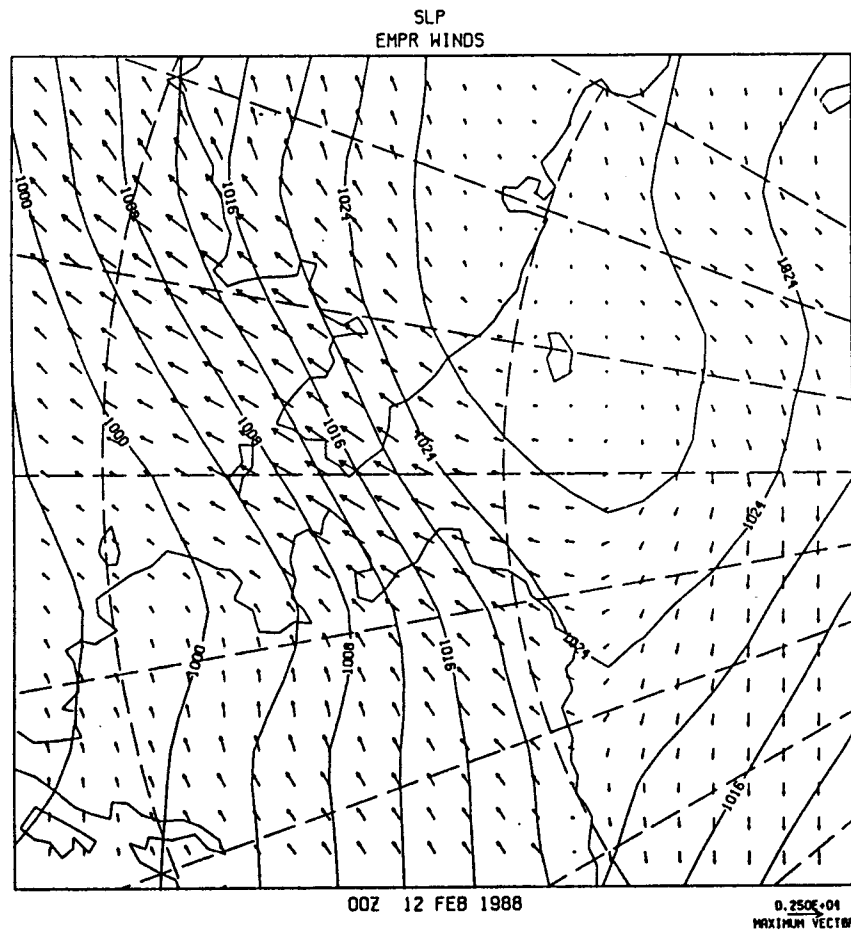


Figure 57. Pressure and wind fields over northern Alaska and eastern Siberia at 00Z 12 February 1988 and 12Z 2 March, 1988. In the latter chart, winds were greater than 25 m s<sup>-1</sup> over much of the Chukchi Sea.

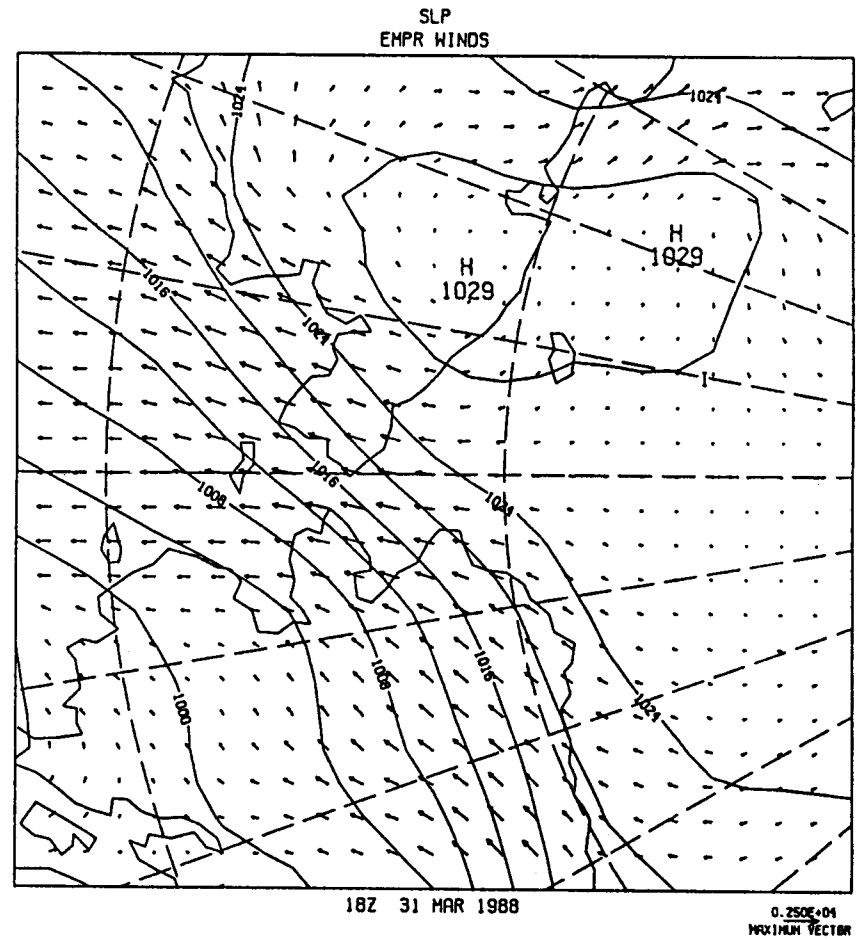
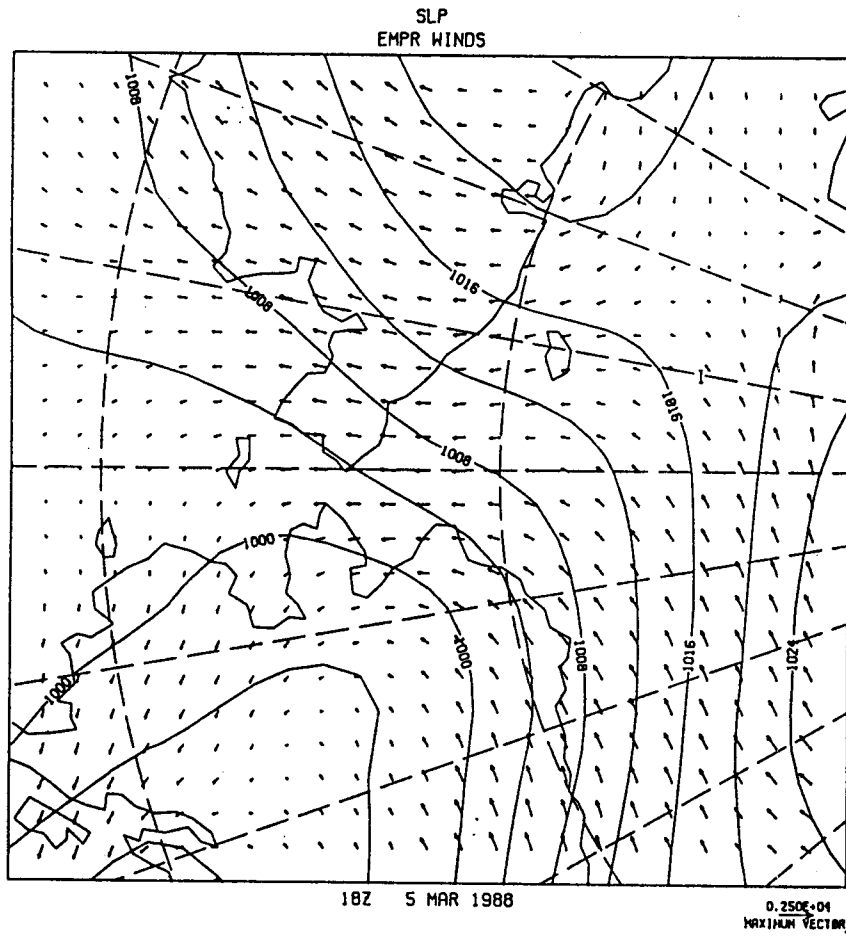


Figure 58. Pressure and wind fields over northern Alaska and eastern Siberia at 18Z 5 March 1988 and 18Z 31 March 1988.

## SYNOPSIS OF THE REGIONAL CIRCULATION

The northern Alaskan shelves, from the northern Bering Sea through the Chukchi and Beaufort seas to the Canadian border, extend over nearly 2000 km and include two substantially different oceanic regimes. The southern regime, covering about 70% of the total extent, is comprised of the northern Bering and Chukchi seas. It consists of a vast shallow shelf dominated by atmospheric forcing and by the great throughflow of Pacific waters into the Arctic Ocean. The circulation in the southern portion of this region, from the straits bordering St. Lawrence Island northward through Bering Strait, shows the effects of the constraining boundaries. On the other hand, the northern regime, comprised of the Alaskan Beaufort shelf, is narrow and is predominantly forced by the adjacent Arctic Ocean, to which it is completely open. It is in many ways simply an edge of the Arctic Ocean.

Bering Strait constitutes a choke point for the regional circulation and provides a convenient monitoring location for the Pacific inflow into the Arctic. That inflow is important not only to the northern Bering and Chukchi seas, but also to conditions in the upper several hundred meters of the Arctic Ocean (e.g., Killworth and Smith, 1984). We find that the transport through Bering Strait is predictable from the reduced geostrophic wind field according to the equation

$$T = 1.06 - 0.112 W,$$

where  $T$  is the transport in sverdrups ( $1 \text{ Sv} = 10^6 \text{ m}^3 \text{ s}^{-1}$ ) and  $W$  is the component of the reduced geostrophic wind along  $192^\circ\text{T}$  in meters per second (cf. Coachman and Aagaard, 1988 for a complete discussion).

The reason for the strong control of the northward transport by the wind is that convergences and divergences are created by the interaction of the wind-driven Ekman layer with the restrictive and complex coastal geometry of the Alaskan and Siberian land masses. Such modifications alter the pressure field associated with the higher steric sea level of the Pacific Ocean relative to the Arctic Ocean. The northward mean flow driven by the latter pressure gradient is thereby considerably modified by the wind field on time scales ranging from the synoptic to the interannual. Our recent measurements suggest, however, that there is an asymmetry in the dynamical response of the Bering Strait flow to major changes in wind direction, with the flow responding readily to the northerly winds typical of winter, but that

the effect of southerly winds is buffered. This differential response is probably associated with the different coastal geometry north and south of the strait.

With respect to the very low-frequency variability of the Bering Strait flow, Figures 59 and 60, from Coachman and Aagaard (1988), show the estimated seasonal and interannual variability of that transport. Note the marked annual cycle, with the maximum northerly flow in summer, but with a brief secondary maximum in January, which corresponds to a statistical decrease in the strength of the northerly winter winds. Note in Figure 60 the large decrease in transport which occurred in the late 1960's. An extended analysis shows that, in fact, three of the four lowest-transport years of the century have occurred since 1969. It is therefore conceivable that significant aspects of the regional oceanography may not have been well sampled by the various observational programs of recent years.

Waters moving through Bering Strait show large temporal variability in their properties on all time scales and, in addition, there are, in general, pronounced property gradients across the strait at any given time. For example, the water passing through the western part of the strait is the most saline. This western water, which, south of the strait, is referred to as the Anadyr water mass, derives from water which has moved onto the shelf from the northwestern part of the deep Bering Sea and flowed northward through the Gulf of Anadyr and Anadyr Strait, west of St. Lawrence Island. The Anadyr Water, and its descendant north of Bering Strait, called the Bering Sea Water, are characterized by very high nutrient concentrations and in the northern Bering and southern Chukchi seas they support one of the world's most productive marine ecosystems. Within the Chukchi Sea, the Bering Sea Water appears to move principally northward following Hope Sea Valley, probably entering the Arctic Ocean east of Herald Island. The nutrient maximum within the Arctic Ocean derives from this inflow, as does the wide-spread secondary temperature minimum which is found at a salinity of about 33.1. The water which moves northward through eastern Bering Strait is marked by both lower salinity and much lower nutrient concentrations than waters to the west. It roughly follows the Alaskan coast line through the Chukchi Sea, primarily entering the Arctic Ocean through Barrow Canyon. Its contribution to the Arctic Ocean is most easily seen in the secondary temperature maximum found at about 75 m depth throughout the Canadian Basin.

Another important contribution to the characteristics of the water on the shelf comes during winter, when both the northern Bering and the Chukchi seas are marked by numerous, large coastal polynyas. These are maintained by the prevailing offshore winds over the south- and west-facing coasts, which transport new ice seaward. Because of the high formation rates of new ice in the polynyas, they salinize the underlying water through brine rejection. The cold and saline waters thus formed over the shelves give rise to much of the density structure of the Arctic Ocean and is therefore of major climatic significance. Cold brines have previously been seen draining from the Chukchi Sea through Barrow Canyon, but during 1986-87 they were absent. While the reason for this absence is unknown, it points toward the need to take interannual variability into account both in observational and modelling efforts.

While most of the Chukchi Sea is characterized by a general northward flow, in the Beaufort Sea the motion of the surface waters as deduced from the ice drift is nominally westward, manifesting the southern limb of the clockwise Beaufort gyre. However, the ice can undergo prolonged periods of eastward drift as well. Deeper in the water column over the inner shelf (landward of about the 40-50 m isobath) there is also a mean westward set, and the circulation appears strongly wind-driven. There is, however, some evidence for mean eastward motion east of 146°W, possibly corresponding to the different wind regime in the eastern Beaufort Sea.

Over the outer shelf and slope, the circulation is characterized by a strong subsurface flow which in the mean is eastward, i.e., contrary to the mean ice motion, but which experiences frequent reversals toward the west. This current dominates the outer Alaskan Beaufort shelf and it appears to be part of the large-scale circulation of the Arctic Ocean, an important component of which is a deep and relatively narrow boundary current circulating in a counterclockwise sense in each of the two major Arctic Ocean basins. In the Beaufort Sea this flow is referred to as the Beaufort Undercurrent, where it has characteristic long-term mean speeds in the neighborhood of 5-10 cm s<sup>-1</sup>, while daily mean values are typically ten times as great. In the mean sense, the undercurrent is probably typically found below about 40 m, but its depth appears to vary markedly. While the undercurrent shows a wind influence, the correlations are small, so that effectively the circulation over the outer shelf and slope is primarily ocean-driven rather than locally wind-driven, both in its mean and variable components. The ocean-driven variability includes both eddies and

shelf waves, the latter commonly having eastward phase velocities of about  $1.5 \text{ m s}^{-1}$ .

Upwelling along the outer shelf of the Beaufort Sea is a frequent occurrence and appears to be connected with the eastward-traveling wave-like disturbances observed in the velocity records. Vertical displacements may be as much as 150 m, but there is no indication of a significant net onshore flux associated with these events, except in Barrow Canyon, where the resultant turbulent salt and heat fluxes are sufficiently large to potentially be of local importance. Temporarily, of course, water with deep offshore properties can be found on the Beaufort shelf, even though it apparently does not remain there in large quantities.

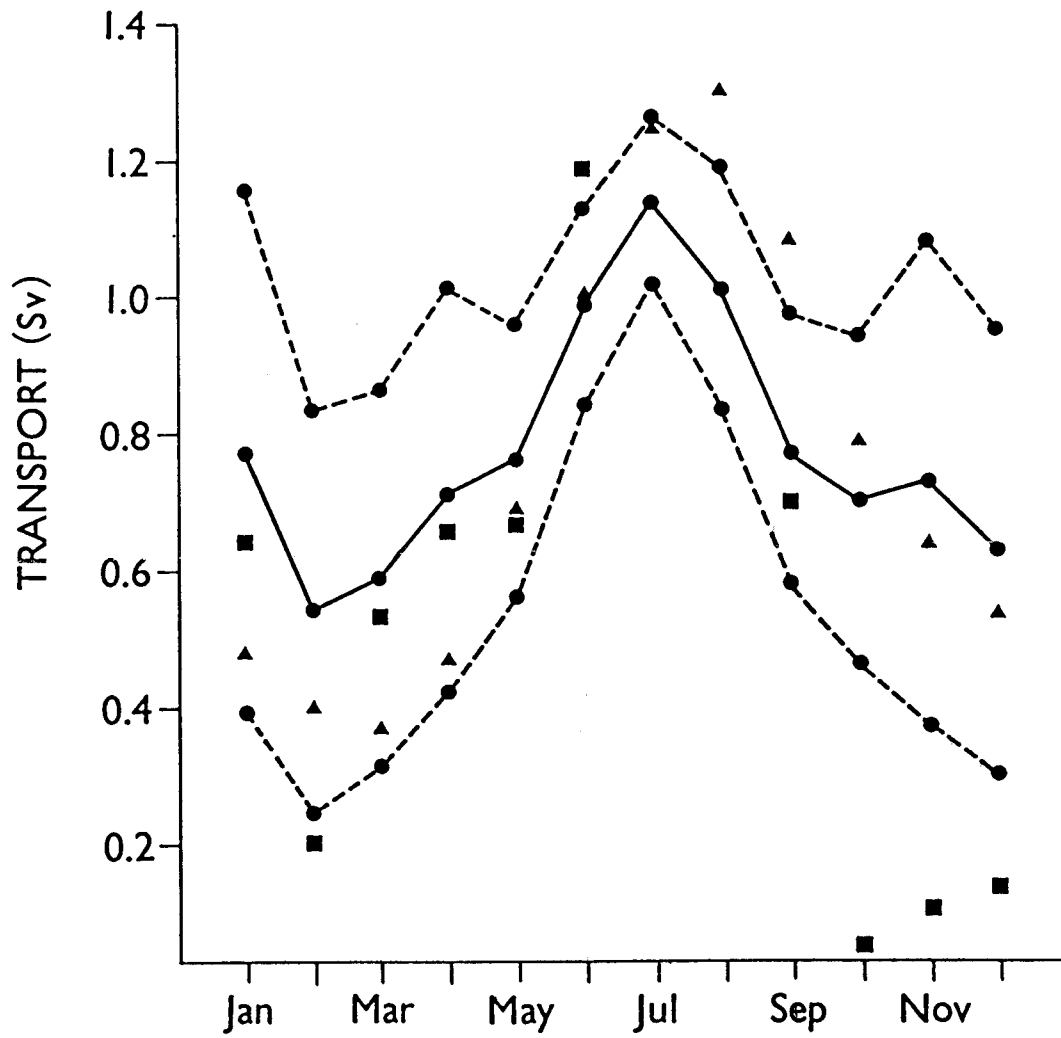


Figure 59. Annual Bering Strait transport signal.

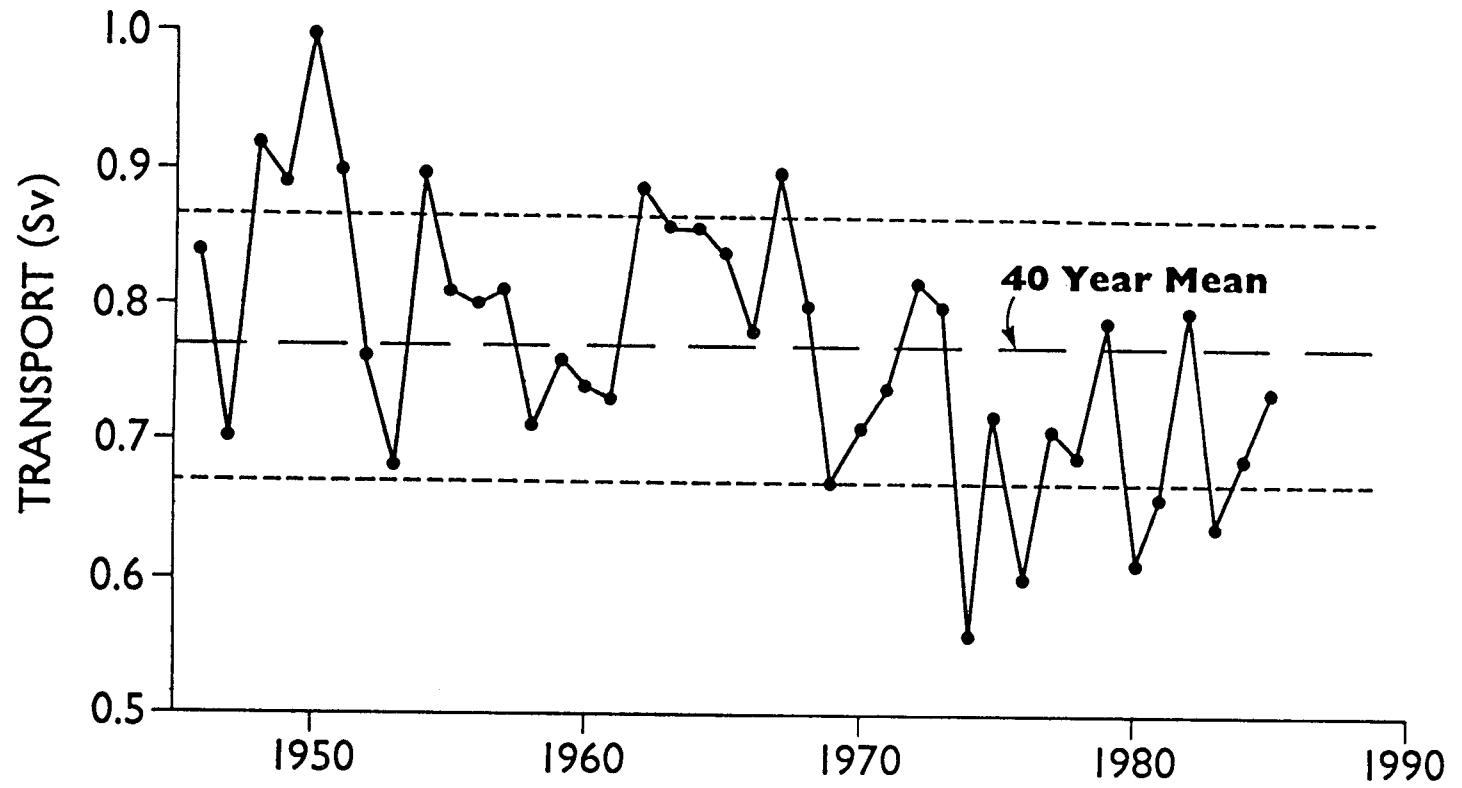


Figure 60. Forty years of annual transport estimates through Bering Strait.

## SUMMARY OF THE PRINCIPAL CONCLUSIONS

1. Below the upper 40-50 m of the ocean, the principal circulation feature of the outer shelf and slope of the Beaufort Sea is the Beaufort Undercurrent, a strong flow which in the mean is directed eastward, but which is subject to frequent reversals toward the west. The reversals are normally associated with upwelling onto the outer shelf. The undercurrent is very likely part of a basin-scale circulation within the Arctic Ocean.
2. While we find statistically significant wind influence on the subsurface flow in the southern Beaufort Sea, it is generally of secondary importance, accounting for less than 25% of the flow variance below 60 m. An important implication is that at least below the mixed layer, the circulation on the narrow Beaufort shelf is primarily forced by the ocean rather than by the local wind. Therefore, to the extent that a localized problem or process study requires consideration of the shelf circulation, such as would be the case for oil-spill trajectory modeling, a larger-scale framework must be provided, within which the more local problem may be nested.
3. There were large changes in wind variance with season, with the largest variances occurring in the late-summer/early autumn and again in January because of blocking ridges in the North Pacific shifting the storm track westward over the west coast of Alaska and across the North Slope.
4. Despite the seasonally varying wind field, as well as the large seasonal differences in the upper-ocean temperature and salinity fields, we find no evidence for a seasonal variability in the subsurface circulation in the Beaufort Sea. This situation contrasts with that in Bering Strait, and probably also in much of the Chukchi Sea, where a seasonal cycle in the transport is apparent. Therefore, while the northward flow of water from the Pacific is of major significance to the structure and chemistry of the upper ocean in the Arctic (including the Beaufort Sea), as well as its ice cover and biota, the dynamic significance of that flow to the Beaufort Sea appears minimal.
5. In contrast to the lack of a seasonal oceanographic signal at depth, the interannual variability in the flow characteristics can be considerable. For example, during the period fall 1986 - spring 1987, the Beaufort Undercurrent appears to have been anomalously deep compared with both earlier and ensuing measurements, perhaps by

30-40 m. The consequences of such anomalies for the upper-ocean velocity structure and transport are likely significant.

6. During much of the experiment the meteorological conditions were milder than normal, consistent with less coastal ice in the summer and autumn, the passage of more storms up the west coast of Alaska and across the North Slope, and generally higher air temperatures along the North Slope. These climatological near-minimum ice years were followed in 1988 by the heaviest summer ice along the Chukchi coast since 1975.

7. The atmospheric sea-level pressure field is well represented at all buoys and stations by the METLIB products from the FNOC surface analysis, if the 12-hour lag of the FNOC pressures is taken into account. Unfortunately the surface air temperature field from FNOC is not representative of the station data from either land-based stations or drifting ice buoys. The errors in the temperature field are characterized by a systematic over-prediction during winter and spring of some 10-20°C, leading to an annual average over-prediction for air temperature of 3-13°C at all measuring sites. Although we recommend that gradient winds be used for modeling purposes and that these be calculated from the time-shifted surface analysis, the surface temperature analysis should not be used for any model calculations, except perhaps as an upper boundary condition for a rather complete planetary boundary layer model.

## REFERENCES CITED

- Aagaard, K., A synthesis of the Arctic Ocean circulation, *Rapp. P.-v. Reun. Cons. Int. Explor. Mer*, 188, 11-22, 1989.
- Aagaard, K., The Beaufort Undercurrent, in *The Alaskan Beaufort Sea: Ecosystems and Environments*, edited by P.W. Barnes, D.M. Schell, and E. Reimnitz, 47-71, Academic Press, Orlando, FL, 1984.
- Aagaard, K., Current, CTD, and pressure measurements in possible dispersal regions of the Chukchi Sea, Outer Continental Shelf Environmental Assessment Program. *Final Reports of the Principal Investigators*, 57, 255-333, Department of Commerce/Department of Interior, Anchorage, 1988.
- Aagaard, K., L.K. Coachman, and E.C. Carmack, On the halocline of the Arctic Ocean, *Deep-Sea Research*, 28, 529-545, 1981.
- Aagaard, K., C.H. Pease, and S.A. Salo, *Beaufort Sea Mesoscale Circulation Study - Preliminary Results*, NOAA Technical Memorandum ERL PMEL-82, 171 pp, 1988a.
- Aagaard, K., S. Salo, and K. Kroglund, *Beaufort Sea Mesoscale Circulation Study: Hydrography, USCGC Polar Star Cruise, October, 1986*, NOAA Data Report ERL PMEL-19, 83 pp, 1987.
- Aagaard, K., S. Salo, and K. Kroglund, *Beaufort Sea Mesoscale Circulation Study: Hydrography, Helicopter Operations, April, 1987*, NOAA Data Report ERL PMEL-22, 25 pp, 1988b.
- Aagaard, K., J.H. Swift, and E.C. Carmack, Thermohaline circulation in the arctic mediterranean seas, *Journal of Geophysical Research*, 90, 4833-4846, 1985a.
- Aagaard, K., A.T. Roach, and J.D. Schumacher, On the wind-driven variability of the flow through Bering Strait, *Journal of Geophysical Research*, 90, 7213-7221, 1985b.
- Albright, M., Geostrophic wind calculations for AIDJEX, *Sea Ice Processes and Models*, edited by R.S. Pritchard, 402-409, University of Washington Press, Seattle, WA, 1980.

- Anderson, N.O., A Short Note on the Calculation of Filter Coefficients, *Geophysics*, 39 (1), 69-72, 1974.
- Banke, E.G., and S.D. Smith, Wind stress over ice and over water in the Beaufort Sea, *Journal of Geophysical Research*, 76, 7368-7374, 1971.
- Banke, E.G., S.D. Smith, and R.J. Anderson, Recent measurements of wind stress on Arctic sea ice, *Journal of the Fisheries Research Board of Canada*, 33, 2307-2317, 1976.
- Barry, R.G., R.E. Moritz, and J.C. Rogers, The fast ice regimes of the Beaufort and Chukchi Sea coasts, Alaska, *Cold Regions Science and Technology*, 1 (2), 129-152, 1979.
- Bruno, M.S., and O.S. Madsen, Coupled circulation and ice floe movement model for partially ice-covered continental shelves, *Journal of Geophysical Research*, 94 (C2), 2065-2077, 1989.
- Campbell, W.J., P. Gloersen, W.J. Webster, T.T. Wilheit, and R.O. Ramseier, Beaufort Sea ice zones as delineated by microwave imagery, *Journal of Geophysical Research*, 81, 1103-1110, 1976.
- Campbell, W.J., P. Gloersen, H.J. Zwally, R.O. Ramseier, and C. Elachi, Simultaneous passive and active microwave observations of near-shore Beaufort Sea ice, *Journal of Petroleum Technology*, 21, 1105-1112, 1980.
- Carsey, F., and B. Holt, Beaufort-Chukchi ice margin data from Seasat: Ice motion, *Journal of Geophysical Research*, 92 (C7), 7163-7172, 1987.
- Coachman, L.K., and K. Aagaard, Re-evaluation of water transports in the vicinity of Bering Strait, in *The Eastern Bering Sea Shelf: Oceanography and Resources*, vol. 1, edited by D.W. Hood and J.A. Calder, 95-110, University of Washington Press, Seattle, WA, 1981.
- Coachman, L.K., and K. Aagaard, Transports through Bering Strait: Annual and interannual variability, *Journal of Geophysical Research*, 93, 15535-15539, 1988.
- Coachman, L.K., and C.A. Barnes, The contribution of Bering Sea water to the Arctic Ocean, *Arctic*, 14, 147-161, 1961.

Coachman, L.K., K. Aagaard, and R.B. Tripp, *Bering Strait: The Regional Physical Oceanography*, 172 pp., University of Washington Press, Seattle, 1975.

Coachman, L.K., and D.A. Rankin, Currents in Long Strait, Arctic Ocean, *Arctic*, 21, 27-38, 1968.

Codispoti, L.A., Arctic Ocean processes in relation to the dissolved silicon content of the Atlantic, *Marine Science Communications*, 5, 361-381, 1979.

Codispoti, L.A., and F.A. Richards, Micronutrient distributions in the East Siberian and Laptev seas during summer 1963, *Arctic*, 21, 67-83, 1968.

D'Asaro, E.A., Generation of sub-mesoscale vortices: A new mechanism, *Journal of Geophysical Research*, 93, 6685-6693, 1988.

Dickey, W.W., A study of a topographic effect on wind in the Arctic, *Journal of Meteorology*, 18, 790-803, 1961.

Feldman, U., P.J. Howarth, and J.A. Davies, Estimating the surface wind speed over drifting pack ice from surface weather charts, *Boundary Layer Meteorology*, 16, 421-429, 1979.

Foldvik, A., K. Aagaard, and T. Torresen, On the velocity field of the East Greenland Current, *Deep-Sea Research*, 35A, 1335-1354, 1988.

Garrison, G.R., and P. Becker, The Barrow Submarine Canyon: A drain for the Chukchi Sea, *Journal of Geophysical Research*, 81, 4445-4453, 1976.

Garrison, G.R., and R.G. Paquette, Warm water interactions in the Barrow Canyon in winter, *Journal of Geophysical Research*, 87, 5853-5859, 1982.

Hart, J.E., and P.D. Killworth, On open ocean baroclinic instability in the Arctic, *Deep-Sea Research*, 23, 637-645, 1976.

Henry, R.F., and N.S. Heaps, Storm surges in the southern Beaufort Sea, *Journal of Fisheries Research Board of Canada*, 33, 2362-2376, 1976.

Hufford, G.L., Warm water advection in the southern Beaufort Sea, August-September 1971, *Journal of Geophysical Research*, 78, 2702-2707, 1973.

- Hufford, G.L., On apparent upwelling in the southern Beaufort Sea, *Journal of Geophysical Research*, 79, 1305-1306, 1974.
- Johnson, M.W., *The plankton of the Beaufort and Chukchi Sea Areas of the Arctic and its Relation to the Hydrography*, Arctic Institute of North America Technical Paper No. 1, Montreal, P.Q., 1956.
- Jones, E.P., and L.G. Anderson, On the origin of the chemical properties of the Arctic Ocean halocline, *Journal of Geophysical Research*, 91, 10759-10767, 1986.
- Killworth, P.D., and J.M. Smith, A one-and-a-half dimensional model for the Arctic halocline, *Deep-Sea Research*, 31A, 271-293, 1984.
- Kinder, T.H., D.C. Chapman, and J.A. Whitehead Jr., Westward intensification of the mean circulation on the Bering Sea shelf, *Journal of Physical Oceanography*, 16 (7), 1217-1229, 1986.
- Kinney, P., M.E. Arhelger, and D.C. Burrell, Chemical characteristics of water masses in the Amerasian Basin of the Arctic Ocean, *Journal of Geophysical Research*, 75, 4097-4104, 1970.
- Kozo, T.L., Mountain barrier baroclinicity effects on surface winds along the Alaskan Arctic coast, *Geophysical Research Letters*, 7, 377-380, 1980.
- Kozo, T.L., An observational study of sea breezes along the Alaskan Beaufort Sea coast: Part I, *Journal of Applied Meteorology*, 21, 891-905, 1982a.
- Kozo, T.L., An observational study of sea breezes along the Alaskan Beaufort Sea coast: Part II, *Journal of Applied Meteorology*, 21, 906-924, 1982b.
- Kozo, T.L., Mesoscale wind phenomena along the Alaskan Beaufort Sea coast, In *The Alaskan Beaufort Sea: Ecosystem and Environment*, edited by P. Barnes, D. Schell, and E. Reimnitz, 23-45, Academic Press, Orlando, FL., 1984.
- Kozo, T.L., and R.Q. Robe, Modeling winds and open water buoy drift along the eastern Beaufort Sea coast, including the effects of the Brooks Range, *Journal of Geophysical Research*, 91, 13011-13032, 1986.

Langleben, M.P., Albedo of melting sea ice in the southern Beaufort Sea, *Journal of Glaciology*, 10 (58), 101-104, 1971.

Macklin, S.A., R.L. Brown, J. Gray, and R.W. Lindsay, *METLIB-II - A Program Library for Calculating and Plotting Atmospheric and Oceanic Fields*, NOAA Technical Memorandum ERL PMEL-54, Pacific Marine Environmental Laboratory, Seattle, WA, 53 pp, 1984.

Manley, T.O., and K. Hunkins, Mesoscale eddies of the Arctic Ocean, *Journal of Geophysical Research*, 90, 4911-4930, 1985.

Marko, J.R. and R.E. Thomson, Spatially periodic lead patterns in the Canadian Basin sea ice: A possible relationship to planetary waves, *Geophysical Research Letters*, 2 (10), 431-434, 1975.

Maykut, G.A., and P.E. Church, Radiation climate of Barrow, Alaska, 1962-1966, *Journal of Applied Meteorology*, 12, 620-628, 1973.

Melling, H., and E.L. Lewis, Shelf drainage flows in the Beaufort Sea and their effect on the Arctic Ocean pycnocline, *Deep-Sea Research*, 29, 967-986, 1982.

Moore, R.M., Oceanographic distributions of zinc, cadmium, copper and aluminum in waters of the central Arctic, *Geochim. Cosmochim. Acta*, 45, 2475-2482, 1981.

Moore, R.M., and J.N. Smith, Disequilibria between  $^{226}\text{Ra}$ ,  $^{210}\text{Pb}$  and  $^{210}\text{Po}$  in the Arctic Ocean and the implications for chemical modification of the Pacific water inflow, *Earth Planetary Science Letters*, 77, 285-292, 1986.

Moore, R.M., M.G. Lowings, and F.C. Tan, Geochemical profiles in the central Arctic Ocean: Their relation to freezing and shallow circulation, *Journal of Geophysical Research*, 88, 2667-2674, 1983.

Moritz, R.E., On a possible sea-breeze circulation near Barrow, Alaska, *Arctic and Alpine Research*, 9 (4), 427-431, 1977.

Mountain, D.G., L.K. Coachman, and K. Aagaard, On the flow through Barrow Canyon, *Journal of Physical Oceanography*, 6, 461-470, 1976.

Mysak, L.A., and D.K. Manak, Arctic sea ice extent and anomalies, 1953-1984, *Atmosphere-Ocean*, in press, 1989.

Overland, J.E., Marine climatology of the Bering Sea, In *The Eastern Bering Sea Shelf: Oceanography and Resources, Vol. 1*, edited by D.W. Hood and J.A. Calder, 15-22, University of Washington Press, Seattle, WA, 1981.

Overland, J.E., Atmospheric boundary layer structure and drag coefficients over sea ice, *Journal of Geophysical Research*, 90, 9029-9049, 1985.

Overland, J.E., R.A. Brown, and C.D. Mobley, *METLIB - A Program Library for Calculating and Plotting Marine Boundary Layer Wind Fields*, NOAA Technical Memorandum ERL PMEL-20, Pacific Marine Environmental Laboratory, Seattle, WA, 53 pp, 1980.

Overland, J.E., and C.H. Pease, Cyclone climatology of the Bering Sea and its relation to sea ice extent, *Monthly Weather Review*, 110, 5-13, 1982.

Overland, J.E., and A.T. Roach, Northward flow in the Bering and Chukchi seas, *Journal of Geophysical Research*, 92, 7097-7105, 1987.

Paquette, R.G. and R.H. Bourke, Observation on the coastal current of Arctic Alaska, *Journal of Marine Research*, 32, 195-207, 1974.

Parker, N., B. Thomson, J. Bullas, and W. Hume, September 1985 Beaufort Sea storm, Report 85-7, 24 pp, Scientific Services, AES Western Region, Edmonton, Alberta, 1985.

Pease, C.H., Meteorology of the Chukchi Sea: An overview, In *Chukchi Sea Information Update*, edited by D.A. Hale, 11-19, NOAA/NOS Ocean Assessments Division - Alaska Office, Anchorage, AK, 1987.

Pritchard, R.S., Beaufort Sea ice motions, *The Alaskan Beaufort Sea Ecosystems and Environments*, 95-113, (P.W. Barnes, D.M. Schell, and E. Reimnitz, eds.) Academic Press, Orlando, FL, 1984.

Reed, R.J. and B.A. Kunkel, The Arctic circulation in summer, *Journal of Meteorology*, 17, 489-506, 1960.

Rogers, J.C., Meteorological factors affecting interannual variability of summertime ice extent in the Beaufort Sea, *Monthly Weather Review*, 106 (6), 890-897, 1978.

Short, A.D. and W.M.J. Wiseman Jr., Coastal breakup in the Alaskan Arctic, *Geological Society of American Bulletin*, 86, 199-202, 1975.

Smith, S.D., and E.G. Banke, Wind stress over ice and over water in the Beaufort Sea, *Journal of Geophysical Research*, 76, 7368-7374, 1971.

Spaulding, M., T. Isaji, D. Mendelsohn, and A.C. Turner, Numerical simulation of wind-driven flow through the Bering Strait, *Journal of Physical Oceanography*, 17, 1799-1816, 1987.

Sverdrup, H.U., Meteorology, Part 1, Discussion, *The Norwegian North Polar Expedition with the "Maud", 1918-1925, Scientific Results*, 2 (1), Geofysik Institut, Bergen, 331 pp, 1933.

Tripp, R.B., ISHTAR cruise report: R/V Thomas G. Thompson Cruise TT-212, 29 June-19 July 1987, School of Oceanography, University of Washington, Seattle, unpublished data report, 1987.

Wallace, D.W.R., R.M. Moore, and E.P. Jones, Ventilation of the Arctic Ocean cold halocline: Rates of diapycnal and isopycnal transport, oxygen utilization and primary production inferred using chlorofluoromethane distributions, *Deep-Sea Research*, 34A, 1957-1979, 1987.

Walsh, J.J., C.P. McRoy, L.K. Coachman, and 18 other authors, Carbon and nitrogen cycling within the Bering/Chukchi seas: Source regions for organic matter affecting AOU demands of the Arctic Ocean, *Progress in Oceanography*, in press, 1989.

Walsh, J.E., and J.E. Sater, Monthly and seasonal variability in the ocean-ice-atmosphere systems of the North Pacific and the North Atlantic, *Journal of Geophysical Research*, 86 (C8), 7425-7445, 1981.

Weatherly, G.L., and P.J. Martin, On the structure and dynamics of the oceanic bottom boundary layer, *Journal of Physical Oceanography*, 8, 557-570, 1978.

Weeks, W.F., A. Kovacs, S.J. Mock, W.B. Tucker, W.D. Hibler III, A.J. Gow, Studies of the movement of coastal sea ice near Prudhoe Bay, Alaska, *Journal of Glaciology*, 19 (81), 533-546, 1977.

Wendler, G., F.D. Eaton, and T. Ohtake, Multiple reflection effects on irradiance in the presence of Arctic stratus clouds, *Journal of Geophysical Research*, 86 (C3), 2049-2057, 1981.

Yeats, P.A., Manganese, nickel, zinc and cadmium distributions at the Fram 3 and Cesar ice camps in the Arctic Ocean, *Oceanolog. Acta*, 11, 383-388, 1988.

**APPENDIX A.  
BEAUFORT SEA MESOSCALE CIRCULATION STUDY—  
PRELIMINARY RESULTS**

**K. Aagaard, C. H. Pease, and S. A. Salo**

**U.S. Department of Commerce  
National Oceanic and Atmospheric Administration  
Environmental Research Laboratories  
Pacific Marine Environmental Laboratory  
Seattle, Washington**

**July 1988**

**Reprint of NOAA Technical Memorandum ERL PMEL-82**

## NOTICE

Mention of a commercial company or product does not constitute an endorsement by NOAA/ERL. Use of information from this publication concerning proprietary products or the tests of such products for publicity or advertising purposes is not authorized.

Contribution No. 1040 from NOAA/Pacific Marine Environmental Laboratory

---

For sale by the National Technical Information Service, 5285 Port Royal Road  
Springfield, VA 22161

## CONTENTS

	PAGE
Abstract .....	143
1. Introduction .....	143
2. Oceanographic time series .....	145
3. Hydrographic measurements .....	149
4. Meteorological time series and ice drift .....	151
5. Summary .....	158
6. Acknowledgments .....	159
7. References .....	160

## TABLES

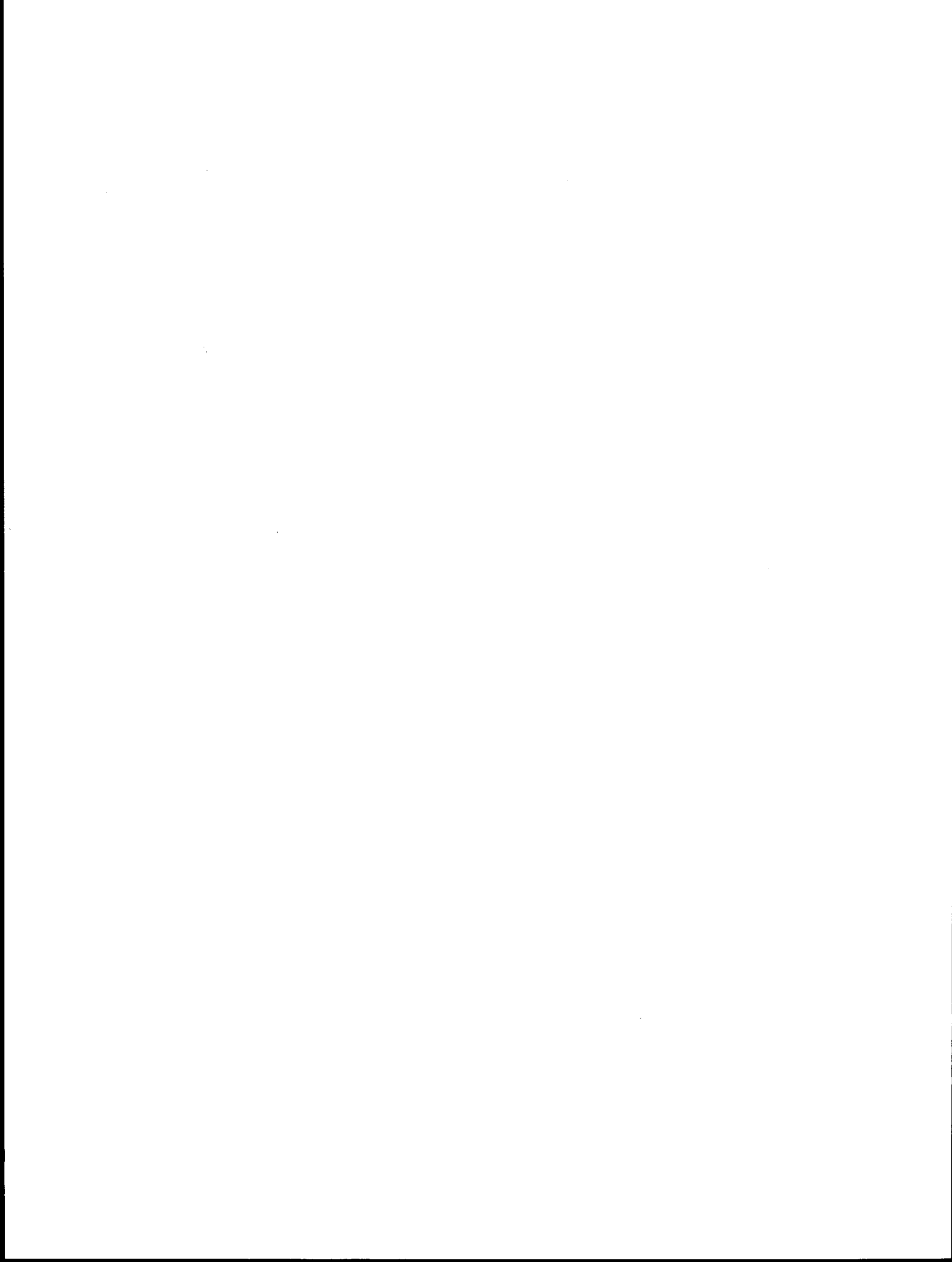
1. Current meter maximum speeds and vector mean velocities, 1986-87 .....	146
2. Selected correlations for current meters, 1986-87 .....	147
3. ARGOS buoy deployment information.....	152
4. Coastal meteorological station summary information .....	153
5. Correlations of hourly data from six coastal meteorological stations .....	155
6. Correlations of six-hourly data from four coastal meteorological stations and equivalent FNOC data .....	157
7. Correlation of pressure between two ARGOS buoys and equivalent FNOC data.....	158

## FIGURES

1. Locations of hydrographic sections occupied in October 1986 and moorings recovered in 1987 .....	162
2. Locations of hydrographic sections occupied in April 1987 .....	163
3. Positions at which ARGOS buoys and stations, and GOES meteorological stations were deployed in 1986-87 .....	164
4. Current vectors from the instruments deployed in October 1986 at the moorings in water 165-170 m deep .....	165
5. Current vectors at the deeper moorings deployed in October 1986 .....	166

6.	SeaCat temperature and salinity at MA2 and MB2 and current vectors at the deepest meter .....	167
7.-15.	Temperature, salinity, density, dissolved oxygen, phosphate, nitrate, nitrite, ammonia, and silicate at section W in October 1986 .....	168
16.-24.	Same for section A in October 1986 .....	177
25.-33.	Same for section E in October 1986 .....	186
34.-42.	Same for section B in October 1986 .....	195
43.-51.	Same for section C in October 1986 .....	204
52.-60.	Same for section D in October 1986 .....	213
61.-69.	Same for section W in April 1987 .....	222
70.-78.	Same for section A in April 1987 .....	231
79.-87.	Same for section B in April 1987 .....	240
88.-96.	Same for section C in April 1987 .....	249
97.	Section view of an ARGOS station .....	258
98.	Air temperature and wind speed and direction from Resolution Island for October-December 1986 .....	259
99.	Sea-level pressure, wind components and vectors from Resolution Island for October-December 1986 .....	260
100.-101.	Same as for 98.-99. for January-March 1987 .....	261
102.-103.	Same as for 98.-99. for April-June 1987 .....	263
104.-105.	Same as for 98.-99. for July-September 1987 .....	265
106.-107.	Same as for 98.-99. for October-December 1987 .....	267
108.	Air temperature wind speed and direction from Lonely for October-December 1986 .....	269
109.	Sea-level pressure, wind components and vectors from Lonely for October-December 1986 .....	270
110.-111.	Same as for 108.-109. for January-March 1987 .....	271
112.-113.	Same as for 108.-109. for April-June 1987 .....	273
114.-115.	Same as for 108.-109. for July-September 1987 .....	275
116.-117.	Same as for 108.-109. for October-December 1987 .....	277

118.	Air temperature and wind speed and direction from Icy Cape for April-June 1987 .....	279
119.	Sea-level pressure, wind components and vectors from Icy Cape for April-June 1987 .....	280
120.-121.	Same as for 118.-119. for July-September 1987 .....	281
122.-123.	Same as for 118.-119. for October-December 1987 .....	283
124.	Air temperature and wind speed and direction from Bering Strait for October-December 1987.....	285
125.	Sea-level pressure, wind components and vectors from Bering Strait for October-December 1987.....	286
126.-142.	Drift tracks for ARGOS buoys .....	287
143.-150.	Examples of sea-level pressure and gradient wind fields over the Beaufort and Chukchi Seas .....	304



# Beaufort Sea Mesoscale Circulation Study - Preliminary Results

K. Aagaard, C.H. Pease, and S.A. Salo

**ABSTRACT.** The Beaufort Sea Mesoscale Circulation Study was initiated in the autumn of 1986 and included measurements of currents, winds, and ice velocities, as well as observations of state variables and nutrient distributions in the ocean and state variables in the polar atmosphere, principally between Barrow and Demarcation Point along the American Beaufort Sea shelf. This report describes the preliminary results from observations made during the first year of the project, including current velocity results from meters recovered through the ice in April 1987, hydrographic and nutrient sections completed in October 1986 and April 1987, wind velocity, air pressure and temperature records recovered continuously through the end of 1987, ARGOS buoy tracks through 1987, and a representative sample of analyzed weather maps during the first year. Data collection continued through April 1988. The total data set is extraordinary in the temporal and spatial extent of its synoptic coverage, and in the variety of its constituent measurements. The data set is also extremely large, and its full reduction and analysis will provide an exceptional opportunity for improving our understanding of the shelf circulation and its forcing, as well as conditions important to the marine ecology of the area.

## 1. INTRODUCTION

The purpose of this study is to gain a quantitative and dynamically founded understanding of the circulation over the Beaufort Sea shelf and its atmospheric and oceanic forcing. The study is within the overall context of a regional environmental assessment related to petroleum exploration and development.

Earlier work under OCSEAP was either concentrated within restricted nearshore areas, or did not provide sufficiently broad spatial and temporal coverage to define the shelf circulation on appropriately large scales. A further serious limitation on earlier work was the grossly inadequate determination of the wind field, so that relatively little could be said about the atmospheric forcing of the ocean. Finally, hydrographic sampling on the shelf including nutrients and dissolved oxygen had earlier been restricted to a brief period during the summer, giving no idea of conditions during other times. To substantially remedy this situation, the present study was designed to provide spatially broad coverage of the circulation and hydrography over the shelf, together with the synoptic wind field; and to do so over a sufficiently long period that the important longer time scales could be defined.

We began by setting up the coastal meteorological stations along the north slope by aircraft, and then proceeded with an October 1986 ice breaker cruise on board the USCGC POLAR STAR during the summer-winter transition. On this cruise we occupied six closely-spaced sections which provided full hydrographic coverage over the entire shelf from Barrow to the U.S.-Canadian border, including five-channel nutrients. The section locations are shown in Figure 1. These data have been published by Aagaard *et al.* (1987). Moored instrument arrays

were deployed on four of the six sections, including current meters and a prototype new instrument, the SeaCat, which is a very stable conductivity/temperature recorder.

The majority of the instruments were recovered during March-April 1987, using helicopter logistics, while three more current meters were picked up in September 1987 from the Canadian research vessel J.P. TULLY (cf. Figure 1 for mooring locations). During April 1987 we also ran four hydrographic sections across the shelf from Barrow to Barter Island. Section locations are shown in Figure 2. These are the first full hydrographic sections done during winter. The data have been published by Aagaard *et al.* (1988).

Additionally, during 1986-87 two moored arrays with a total of 16 instruments were deployed in Barrow Canyon for the purpose of determining the outflow from the shelf of dense winter water and the fluid mechanical structure of the outflow plume. These matters are of major importance in understanding the structure of the Arctic Ocean. The project is sponsored by the National Science Foundation and will provide information complementary to that of the Beaufort Sea study.

Extensive meteorological and ice drift data were obtained throughout this period, using a combination of drifting and land based stations transmitting through the ARGOS and GOES satellite telemetry systems (Figure 3). Three GOES stations were installed to fill gaps in the primary National Weather Service (NWS) coastal observing network. Stations were established at Resolution Island in Prudhoe Bay, at the Lonely Dewline site near Pitt Point east of Barrow, and at Icy Cape southwest of Barrow. Each station in the GOES network transmitted hourly meteorological observations every three hours to the GOES-West satellite. These data are then rebroadcast to the GOES-West receiving station in Wallops Island, VA, which maintains a computer database which our laboratory computer interrogated daily. The GOES stations at Lonely and Resolution were recovered in April 1988. Further data were obtained from the primary NWS stations at Barter Island, Barrow, Kotzebue, and Nome. A fourth GOES station funded by the Office of Naval Research was placed at the Cape Prince of Wales navigation daymarker along Bering Strait. The data from this station will be available for September 1987 through April 1988.

Additional meteorological coverage was provided by deployments of ARGOS buoys and stations by helicopter onto sea ice floes along the Beaufort and Chukchi coasts. Eleven ARGOS buoys and three ARGOS stations were deployed over 18 months in support of this study. ARGOS buoys transmit to the NOAA polar orbiting satellites which rebroadcast to the Service ARGOS receiving station in Toulouse, France or in Suitland, MD. Positions are calculated from the doppler shift of the transmissions, and the calculated positions and the sensor data are then available in preliminary form for daily computer interrogation and through fortnightly distribution by magnetic tape. Buoys and stations were not recovered from the ice, but were left to drift until failure.

While not included in this interim report, a further set of moored oceanographic instruments and meteorological stations were deployed in April and September 1987, and these were retrieved in March and April 1988. In addition, three ARGOS buoys were deployed in cooperation with the Polar Science Center of the University of Washington and three were deployed for the ONR FREEZE program. These data will be included in the final analysis, together with pertinent supporting data from the Chukchi Sea.

## 2. OCEANOGRAPHIC TIME SERIES

Table 1 lists the maximum speed and the vector mean velocity observed at moorings MA1 (in water 1216 m deep), MA2 (168 m), MB1 (1008 m), MB2 (170 m), and MD1 (165 m); and Figures 4-6 show the 35-hr low-passed time series from both the current meters and the SeaCats at these moorings. All the mooring locations are shown in Figure 1. The time series depictions of Figures 4-6 are 12-hr realizations of the low-passed data. Each time tick is 3 days, and the vertical axis units are  $\text{cm s}^{-1}$ ,  $^{\circ}\text{C}$ , and psu, respectively, for velocity, temperature, and salinity. In the figures, each current meter record is identified by the mooring designation, the depth, and in parentheses the direction of the principal axis (the axis of greatest variance). The latter is in degrees true, and in practice it is normally nearly parallel with the vector mean direction of the flow, as can be seen by comparison with Table 1. Note that the SeaCats on MA2 and MB2 were located within 2 m of the bottom.

Consider first Table 1. In the mean, the flow above about 60-90 m, depending on location, is westward; but below this the flow is eastward and generally increases with depth. (Note, however, that the upper westward flow is sufficiently variable that the rms error exceeds the mean.) The subsurface easterly flow apparent in Table 1 is the Beaufort Undercurrent described by Aagaard (1984). While maximum speeds in this current normally appear to be in the range  $30\text{-}70 \text{ cm s}^{-1}$  (compare our Table 1 with Table 2 in Aagaard, 1984), long-term mean flows are much less, typically below  $10 \text{ cm s}^{-1}$ . Note, however, the extremely high maximum speed recorded at 143 m at MA2, well over twice as great as any ever observed. Figure 4 shows that this represents a single event, albeit of over a week's duration, and we speculate that the event may represent an intense baroclinic eddy passing the mooring site. Less extreme examples of such eddies, centered on about the same depth, were first found in the Beaufort Sea in 1972 (Newton *et al.*, 1974). The sequential orientation of the current vectors in Figure 4 suggests that the hypothesized eddy would have had a CW rotation (cf. Foldvik *et al.*, 1988).

Further comparison of our Table 1 with Table 2 of Aagaard (1984) suggests that at least near the shelf break, the Beaufort Undercurrent did not extend as close to the surface during 1986-87 as it did during the earlier observations. Specifically, Table 1 suggests that the zero in the mean velocity profile was at least 60 m deep (MB2) and possibly as deep as 90 m (MA2). In contrast, mean easterly flows of  $3.8 \text{ cm s}^{-1}$  and  $6.4 \text{ cm s}^{-1}$  were observed during 1978 at about

Table 1. Maximum 35-hour low-passed speed and vector mean velocity, 1986-87. The rms velocity error is given in parentheses.

Mooring	Instrument depth, m	Maximum speed cm s <sup>-1</sup>	Mean Velocity cm s <sup>-1</sup>	T
MA1	1188	7.1	0.6(+/-0.2)	353
MA2	60	73.5	3.5(+/-4.1) <sup>1</sup>	291
	93	71.1	0.1(+/-0.5) <sup>1</sup>	219
	143	166.0	7.8(+/-4.7)	119
MB1	83	72.8	1.5(+/-1.4)	168
	148	58.1	6.9(+/-3.0)	097
	980	0.6	0.0(+/-0.0)	
MB2	62	34.4	0.3(+/-0.5) <sup>1</sup>	181
	95	44.2	5.0(+/-2.0)	112
	145	55.3	8.0(+/-1.8)	103
MD1	57	70.3	2.6(+/-2.7) <sup>1</sup>	292
	90	59.5	4.1(+/-2.6)	095
	140	52.0	4.2(+/-2.2)	100

<sup>1</sup> rms error exceeds mean, so that mean not statistically distinguishable from zero.

65 m depth in water respectively near 100 m and 200 m deep. While the data base at this point is certainly not sufficient to sustain firm conclusions in this regard, it does point to possible interannual differences in the velocity structure of the upper ocean.

We turn next to Figure 4, which portrays conditions at the three mooring sites along the 165-170 m isobath, distributed over essentially the entire length of the Alaskan Beaufort Sea. The mooring separation between MA2 and MB2 is ~240 km, and ~210 km between MB2 and MD1. The records point to very large low-frequency variability over a broad range of time scales. It is also clear from an inspection of Figure 4 that not only are there vertically coherent events, but that a large number of events are horizontally coherent over the entire length of the shelf. Table 2 lists selected vertical and horizontal correlations for lags between 0-24 hours. The letter T, M, or B by each mooring designates the top, middle, or bottom instrument at that mooring. For example, A2/T is the instrument at 60 m depth at mooring MA2, A2/M the instrument at 93 m at the same mooring, etc. (cf. Table 1 for instrument depths). The number in parentheses beneath each correlation is the lag, in multiples of six hours, for which the correlation was a maximum. The sense of the lag is such that the row instrument leads the column instrument. For example, A2/M leads D1/M by 24 hours. Several points are noteworthy. First,

Table 2. Selected correlations for 35-hr low-passed current meter data, 1986-87. Lags are given in parentheses.

**A. Vertical correlations.**

	A2/M	A2/B	B2/M	B2/B	D1/M	D1/B
A2/T	0.95 (0)	0.62 (0)				
A2/M	1.00	0.60 (0)				
B2/T			0.50 (1)	0.41 (1)		
B2/M			1.00	0.84 (0)		
D1/T					0.73 (0)	0.31 (0)
D1/M					1.00	0.53 (0)

**B. Horizontal correlations.**

	B2/T	B2/M	B2/B	D1/T	D1/M	D1/B
A2/T	0.35 (4)	0.65 (4)	0.59 (4)	0.32 (4)	0.52 (4)	0.49 (4)
A2/M	0.36 (4)	0.65 (3)	0.60 (4)	0.40 (4)	0.55 (4)	0.47 (4)
A2/B	0.51 (4)	0.61 (4)	0.56 (4)	0.27 (4)	0.38 (4)	0.24 (4)
B2/T	1.00			0.34 (2)	0.40 (2)	ns
B2/M		1.00		0.44 (2)	0.50 (1)	0.38 (4)
B2/B			1.00	0.30 (1)	0.40 (0)	0.41 (4)

ns means not significant at 95% level.

the vertical structure is different at the three moorings, despite their being sited on the same isobath. At MA1, the correlation between the top and middle instruments is very high, but degrades considerably between the middle and bottom instruments. In contrast, at MB2, the primary vertical correlation degradation occurs between the top and middle instruments, with the correlation between the middle and bottom being high. At MD1, the correlation pattern is qualitatively like that at MA1, but overall considerably weaker. The vertical correlations are essentially in phase. The second noteworthy point is that the maximum horizontal correlations occur for the middle instruments; are as high as 0.65, representing 42% of the variance; and that the western moorings lead the eastern ones, progressively more as the distance increases. Much of the low-frequency energy is therefore propagating coherently eastward over long distances along the shelf margin, with suggested phase speeds of order  $5 \text{ m s}^{-1}$ .

Figure 5 shows currents at the two deeper moorings, each sited in water over 1000 m deep. The flow at MB1 resembles that at MB2 in that in the mean it increases downward from near zero at about 80 m to marked easterly flow deeper. The depth at which the mean easterly flow achieves a maximum cannot be determined from the present data, but near bottom it is effectively zero again. In fact, at that depth the flow is essentially negligible throughout the nearly six months of record. Superimposed on the mean flow at the upper instruments is a large low-frequency variability similar to that farther inshore. The top and middle instruments at MB1 are well correlated (0.89), and the onshore correlation with MB2 is moderate, with slightly less than one-half the variance being accounted for by the correlation between the middle instruments. The impression is of a Beaufort Undercurrent which extends out over the slope well beyond the 1000-m isobath, with a mean eastward velocity maximum over the slope at a depth of probably at least 200 m. There appears to be offshore modal structure in this flow. The near-bottom current at MA1 is quite different from that at MB1, in that measurable speeds are found nearly all the time, with a maximum 35-hr low-passed value of over  $7 \text{ cm s}^{-1}$ . The flow alternates between approximately northerly and southerly, but with a significant net northerly set. The MA1 series is incoherent with that from any other instrument.

The SeaCat records are particularly interesting (Figure 6). They are marked by continual large low-frequency oscillations ( $\sim 2^\circ$  and  $\sim 2$  psu, respectively in temperature and salinity) in which warm saline and cold fresher water alternately moves past the sensors. Considering typical ambient gradients, these oscillations must represent large vertical excursions (upwelling and downwelling) of perhaps 100-150 m. Furthermore, Figure 6 shows the oscillations to be reasonably coherent with the current record. The correlations vary considerably with the instruments being compared, but at MA2 over one-half the variance in the current records at the upper and middle instruments is linearly related to the variance of the bottom temperature records. The current leads the temperature by 12-24 hr. Furthermore, the SeaCat records themselves are quite coherent laterally, as can be seen in Figure 6. The correlation proves to be 0.78 between the

SeaCat temperatures for a lag of 24 hours, accounting for 61% of the variance, with the western mooring leading. This again suggests eastward propagation, with a phase speed of the same order as we calculated earlier. The overall impression from these records is therefore of a low-frequency current regime in which flow reversals to the west are followed within a day by geostrophic adjustment, with warm and saline water upwelling along the continental margin as the adjusting isopycnals tilt upward toward the south. The perturbations propagate eastward with the coast on their right-hand flank. Such a conceptualization of the upwelling is consonant with that proposed by Aagaard (1981), but differs from the directly wind-driven coastal upwelling proposed by Hufford (1974).

### 3. HYDROGRAPHIC MEASUREMENTS

Figures 7-60 show the fall distributions of hydrographic properties for sections W, A, E, B, C, and D, and Figures 61-96 the winter distributions for sections W, A, B, and C (locations of all sections shown in Figures 1 and 2). Several features are of immediate importance and interest.

First, consider Figures 16-24 and 70-78, showing Section A during fall and winter, respectively. During October, the shelf is still substantially occupied by the warm summer water which has moved in from the Chukchi Sea, and in fact water warmer than 3R extends seaward beyond the section as a subsurface layer. However, seaward of the shelf break the warm layer is capped by a cold low-salinity layer of ice melt. A prominent front over the shelf break points to an intensified eastward current there at the time of the section (with a shear reversal near 30 m). The oxygen distribution significantly reflects the temperature distribution, with the highest values in the ice melt water. Nutrients are variably reduced in the upper ocean, with nitrate in particular being nearly absent, consonant with a nitrogen-limited system. Note, however, that ammonia has rather large values on the shelf, whereas nitrite concentrations are very low, suggesting that nutrient regeneration has begun to replace the nitrate depleted during the summer, but that the process is still at a relatively early stage. The maxima in phosphate, nitrate, and silicate near 120-150 m represent the general Arctic Ocean nutrient maximum, which has been attributed to shelf sources (Moore *et al.*, 1983; Jones and Anderson, 1986).

During winter (Figures 70-78) Section A still shows a residue of the summer temperature maximum between 30-60 m, while above about 30 m the water is near freezing. The upper thermocline is notably sharp. In the upper layer, salinity gradients have all but disappeared due to convective mixing during freezing. Oxygen concentrations in the upper ocean have increased from the same process. Silicate has not changed significantly from fall, and phosphate has increased only moderately, since neither was apparently seriously depleted the previous October. However, the nitrogen distributions are substantially different, with a large increase in nitrate and significantly high values of nitrite as well. On the other hand, ammonia concentrations are near zero. It is apparent, therefore, that nitrogen regeneration has been substantial, but not complete

by the beginning of the spring production cycle in April. The very high concentrations of nitrate and silicate near the bottom on the middle shelf, with a maximum at station A4, are probably the residue of an earlier upwelling event from below 100 m.

Examples of both active upwelling and downwelling are in fact apparent in the sections themselves. For example, Section C from April (Figures 88-96) shows both the elevated density-related isopleths (temperature, salinity, and sigma-t) which we would expect to follow a current reversal toward the west (cf. the discussion in II. above), and the flooding of the shelf with nutrient-rich waters. Conversely, Section B from October (Figures 34-42) shows a pronounced down-turning toward the shelf of the isopleths of every parameter measured, as we would expect during eastward motion.

A very important matter is illustrated in Section W from October (Figures 7-15). The section runs southwest across the continental slope to its shallowest point on the shelf at station W8 (indicated by the vertical arrow) and then turns more southerly and crosses Barrow Canyon. Note the warm and relatively fresh water flowing eastward through Barrow Canyon and out of the Chukchi Sea onto the Beaufort shelf, and note also that this water is relatively nutrient-depleted, especially in nitrogen. This is the Alaskan coastal water which has moved northward through eastern Bering Strait (cf. Coachman *et al.*, 1974). The critical point, however, is that warm water is also seen over the slope seaward of station W8. It is the origin of this water which is of paramount interest. The most revealing parameter proves to be ammonia (Figure 14), which shows a remarkably strong core centered between about 50-150 m at station W3. An examination of all the nutrients, together with their corresponding density ranges, and a comparison of these values with recent work in the Chukchi and northern Bering seas under the ISHTAR program (Tripp, 1987), points to the relatively warm nutrient-rich water seen over the slope in Section W as having come through western Bering Strait, and then northward through the central Chukchi Sea. This is the Bering Sea water described by Coachman *et al.*, (1974), which the ISHTAR program has identified as being involved in the enormously high production of the northwestern Bering Sea, and more recently has also implicated in similarly high production rates in the central Chukchi Sea. The important point for present purposes is that a major source of water for the Beaufort Undercurrent lies farther west along the northern Chukchi margin than the Barrow Canyon input which has been the focus in earlier work (e.g., contrast Mountain, 1974, or Aagaard, 1981). Most likely, the principal point of exit from the Chukchi for this water is Hope Sea Valley and Herald Canyon, although the depression between Hanna and Herald shoals may also contribute.

Another point of interest in the fall sections is the contrast between conditions on the western and eastern portions of the Beaufort shelf. The transition appears to be located near Section B, which is near where Barnes and Toimil (1979) suggested that there is a change in the direction of the nearshore flow from westerly to easterly, possibly associated with a change in the

mean wind regime. In the fall the eastern shelf is marked by lower upper-layer salinities and considerably greater stratification, i.e., it has more of the Arctic Ocean character than the shelf farther west, where the Chukchi influence is strong. For example, contrast Section A (Figures 16-18) with sections C (Figures 43-45) or D (Figures 52-54). There are also differences in the nutrient distributions, with distinctly lower values of both ammonia and silicate on the eastern shelf, possibly reflecting the reduced connection with the Chukchi, although the relatively small data base doesn't allow firm conclusions in this regard. The following April, the upper-ocean salinities are again lower in the east and the density stratification greater (contrast Figures 71-72, Section A, with Figures 89-90, Section C). At the same time, the nutrients over the shelf show a marked decrease in going eastward from Section A (contrast Figures 75 with 84 or 93, and Figures 78 with 87 or 96). In this case the difference is most obviously a consequence of the recent upwelling at the western site discussed earlier, and it is conceivable that such events are more common there than on the eastern shelf and may therefore be responsible for the fall situation also. In this connection, note in Figure 6 that the temperature and salinity oscillations recorded at the western SeaCat (MA2) were considerably larger than at the eastern one (MB2). The point is that there appear to be significant large-scale longshore differences in the hydrography, reflecting differences in the governing processes.

#### **4. METEOROLOGICAL TIME SERIES AND ICE DRIFT**

We turn next to the meteorology. Table 3 summarizes the deployment positions, times, and data completeness for the ARGOS buoys and stations, and Table 4 summarizes the deployment information for the GOES coastal stations and the data acquisition periods for the NWS coastal stations. All ARGOS buoys were fitted with Y.S.I. thermistors in a gilled vane housing for a fully ventilated air temperature, typically 30 to 50 cm above the floe surface, with a resolution of 0.1°C and zero-point calibration to within 0.3°C. Also, each buoy measured air pressure with an A.I.R. digital barometer with a resolution of 0.1 mb and calibrated to within 0.4 mb. The ARGOS stations had similar temperature and pressure instrumentation; however, the pressure ports and thermistors were 2 m above the floe surface. The stations also had an R.M. Young aerovane-type anemometer at 3 m and an InterOcean S4 current meter at 6 m below the estimated floe bottom. The computer interfaces and tower assemblies were manufactured by Coastal Climate Co. The ESI and PMEL manufactured buoys used Synergetics ARGOS transmitters, while the Coastal Climate buoys and stations used Telonics transmitters. A typical station configuration is given in Figure 97.

Because the GOES satellite is so near the horizon in northern Alaska, slight variations in the geostationary orbit cause the stations to drop below the horizon. In addition, the satellite itself occasionally has transmission failures, resulting in additional data drops. To combat this problem without giving up the immediate knowledge of the condition of the station and

Table 3. ARGOS buoy deployment information. All ARGOS buoys had ventilated air temperature and surface air pressure sensors. In addition, stations 7420a, 7420b, and 7429 had 3-m vector-averaged anemometers and 6-m vector-averaged current meters.

BUOY IDENT	START TIME	DATE	START POSITION	END POSITION	END TIME	DATE	END POSITION	TOTAL HOURS	BUOY TYPE <sup>1</sup>	
7424	<sup>3</sup> 1855	9Oct 1986	71.528	145.239	0213	18Dec 1986	71.034	164.889	1662	EB
7420a	1707	14Oct 1986	70.660	141.282	0252	26Oct 1986	70.526	144.314	268	CS
7428	1730	17Oct 1986	71.919	152.146	0314	4Nov 1986	72.136	154.557	416	EB
7421	<sup>2</sup> 0214	2Mar 1987	65.899	168.469	0719	20Mar 1987	66.886	167.909	436	PB
7422	<sup>4,2</sup> 2121	1Mar 1987	64.737	167.570	1545	12Jun 1987	63.312	165.720	2464	PB
7423	<sup>2</sup> 0500	8Mar 1987	71.843	151.910	1958	12Apr 1987	71.078	160.621	854	EB
7425	<sup>2</sup> 1105	8Mar 1987	72.018	154.984	2232	16Mar 1987	72.025	154.860	205	EB
7426	<sup>2</sup> 0313	13Mar 1987	71.338	149.020	1731	2Jun 1987	71.961	160.118	1956	EB
7427	<sup>2</sup> 2017	13Mar 1987	71.041	145.915	0709	30Mar 1987	71.236	147.738	394	EB
7420b	1332	29Apr 1987	71.336	144.554	0253	14Jun 1987	71.644	159.344	1092	CS
7013	<sup>2,6</sup> 2218	3Sep 1987	71.936	158.086		<sup>5</sup>	72.948	176.917	2855	CT
7429	<sup>2,6</sup> 2213	5Sep 1987	72.001	160.765	0849	21Sep 1987	71.637	156.134	369	CS
7014	<sup>2,6</sup> 0653	8Sep 1987	72.359	164.810		<sup>5</sup>	71.558	181.724	2729	CT
7015	<sup>2,6</sup> 2308	9Sep 1987	72.810	168.930	0236	7Dec 1987	71.694	177.297	2114	CT
7430	1900	17Nov 1987	71.662	148.643		<sup>5</sup>	71.198	163.387	1032	CT
7431	0000	18Nov 1987	71.893	151.744		<sup>5</sup>	70.152	165.829	1029	CT
7432	2100	18Nov 1987	71.454	145.466		<sup>5</sup>	71.686	155.048	1018	CT

- <sup>1</sup> Buoy type codes: EB = ESI box, CS = Coastal Climate Company station, PB = PMEL/Synergetics box, CT = Coastal Climate Company short tube.
- <sup>2</sup> Buoy start time listed is time of first ARGOS transmission.
- <sup>3</sup> Buoy 7424 had low quality transmissions and stable positions were infrequent.
- <sup>4</sup> Buoy 7422 had a four-day data gap between 21 and 25 May 1987.
- <sup>5</sup> Buoy was still transmitting as of 31 December 1987; last transmission processed was 0000 31 December 1987.
- <sup>6</sup> ONR funded deployment.

Table 4. Coastal meteorological station summary information.

	Type	Start Time	End Time	Position			
Barter	NWS-10	0000	1Sep86	2300	31Dec87	70.125N	143.667W
Resolution <sup>1</sup>	GOES-6	1800	26Sep86	2200	31Dec87	70.370N	148.047W
Lonely <sup>2</sup>	GOES-6	2300	25Sep86	2300	31Dec87	70.917N	153.253W
Barrow	NWS-10	0000	1Sep86	2300	31Dec87	71.300N	156.733W
Icy Cape <sup>3</sup>	GOES-3	2100	22Mar87	2200	31Dec87	70.325N	161.867W
Kotzebue	NWS-10	0000	1Sep86	2300	31Dec87	66.883N	162.625W
Wales <sup>4</sup>	GOES-10	1300	14Sep87	2100	31Dec87	65.633N	168.117W
Nome	NWS-10	0000	1Sep86	2300	31Dec87	64.517N	165.433W

<sup>1</sup> Resolution GOES station did not record temperature from 1200 6Oct87 to 1600 18Nov87, and recorded no data from 1100 3Mar87 to 0000 12Mar87, from 1700 to 1900 18Nov87, and from 0200 to 0400 27Dec87. Missing data were linearly filled. The latter two breaks may be filled with data from internally recorded tapes before the final analysis.

<sup>2</sup> Lonely GOES station did not record from 0800 to 1000 28Sep86, sporadically and without wind speed from 2300 31Oct86 to 2200 12Mar87, 0300 to 1000 4Nov87, 1400 to 1600 12Nov87, 0800 to 1000 2Dec87, 0500 to 0700 4Dec87, 1700 9Dec87 to 0700 20Dec87, and from 1100 to 1300 20Dec87. Missing data were linearly filled. The latter five breaks may be filled from internally recorded tapes before the final analysis.

<sup>3</sup> Icy GOES station was first deployed in September 1986 but didn't function. A replacement was installed 22 March 1987. This is an older style station and doesn't record internally, so recovery from GOES transmission drops are not possible. The station did not transmit from 0200 to 0700 28Mar87, 2000 to 2200 31Mar87, 0200 to 0400 4Apr87, 0500 to 0700 7Apr87, 2000 to 2200 30Apr87, 0500 to 0700 17May87, 0200 to 0700 21May87, 0500 to 0700 11Jun87, 0800 to 1300 14Jun87, 0800 to 1000 19Jun87, 2300 29Jun87 to 0100 30Jun87, 2000 to 2200 30Jun87, 1400 to 1600 10Jul87, 2000 to 2200 11Jul87, 0800 14Jul87 to 0700 15Jul87, 0500 20Jul87 to 0400 21Jul87, 0500 22Jul87 to 0100 23Jul87, 2000 to 2200 25Jul87, 0500 29Jul87 to 0700 30Jul87, 0800 22Aug87 to 0400 23Aug87, 1700 to 1900 25Aug87, 2000 31Aug87 to 1600 2Sep87, 1700 to 1900 20Sep87, 0800 to 1000 24Sep87, 1700 26Sep87 to 0400 28Sep87, 1100 to 1300 28Sep87, 1700 28Sep87 to 0100 30 Sep87, 0200 to 0400 2Oct87, 1400 to 1600 3Oct87, 2000 3Oct87 to 0700 4Oct87, 1100 to 2200 5Oct87, 1400 6Oct87 to 1300 7Oct87, 0800 to 1000 8Oct87, 2000 to 2200 31Oct87, 0500 to 0700 and 1100 to 1300 4Nov87, 0200 to 0400 and 0800 to 1000 2Dec87, 1700 to 1900 3Dec87, 0200 to 0400 15Dec87, 0200 to 0400 27Dec87.

<sup>4</sup> Cape Prince of Wales GOES station was deployed as part of ONR-funded FREEZE experiment, but is included here because it contributes to understanding the spatial variability of the region. The station transmitted intermittently from 1300 15Sep87 to 1200 24Sep 87, and did not transmit from 1600 26Sep87 to 0300 28Sep87, 1300 28Sep87 to 0000 1Oct87, 0400 to 0600 2Oct87, 1000 3Oct87 to 0600 4Oct87, 1000 to 2100 5Oct87, 1300 6Oct87 to 1200 7Oct87, 0700 to 1200 8Oct87, 0100 to 0300 25Oct87, 0100 to 1200 4Nov87, 0400 to 1200 2Dec87, 0100 to 0300 15Dec87, and 0100 to 0300 27Dec87. All the breaks may be filled later. Missing data were linearly filled for this analysis.

providing protection against station loss from bears or humans, the Lonely and Resolution stations were also set to internally record. Overall data recovery was therefore quite good. The detailed list of missing and filled data in Table 4 mainly reflects transmission drops from non-recording stations and data missing since the March 1987 servicing visit. Additional problems were encountered with an unreliable batch of ARGOS buoys manufactured by ESI Company, designated as EB in Table 3. As a result, early failures with the first group of buoys deployed on the ice created an offshore data gap of three months. However, after the first week in March 1987, data coverage over the shelf is generally good, including the buoy data presented in this report, as well as those from buoys belonging to the Polar Science Center from which data will be available for our final analysis. Fleet Naval Oceanographic Center surface analyses will be used to interpolate missing station data.

The GOES station plots are presented in Figures 98-125 for Resolution Island, Lonely, Icy Cape and Cape Prince of Wales (Bering Strait) through the end of December 1987. ARGOS drift tracks are plotted in Figures 126-142 through the end of December 1987. Examples of weather affecting the region are presented in Figures 143-150.

The air temperatures over the coastal Beaufort and Chukchi seas did not cool off until the third week in November in 1986, nearly a month later than the climatological average. The September/October cruise of the Coast Guard icebreaker POLAR STAR encountered the least ice in the coastal Beaufort in thirty years this late in the fall. Low pressure centers passed through the area with frequencies and intensities typical of mid-latitude early autumn, and one storm immediately before the cruise caused extensive storm-surge damage in the Barrow area, including road damage, beach erosion, and destruction of archeological sites. This pattern was generally repeated in the autumn of 1987. The August/October 1987 cruise of the NOAA ship SURVEYOR also encountered nearly minimum ice extents. During light-ice summers, the open ocean plays a major role in affecting air temperatures but not necessarily sea-level pressure (Rogers, 1978).

During late winter and spring of 1987, the wind persisted from the east, the climatologically average direction. Approximately by the spring equinox, the solar radiation through relatively clear skies induced strong diurnal variations in air temperature, and the temperatures across the slope increased from  $-30^{\circ}\text{C}$  at the end of the first week in April to around  $0^{\circ}\text{C}$  by the end of May 1987. At that time the temperature stabilized and the diurnal variations were diminished by the onset of persistent Arctic stratus.

Table 5 shows correlations of the unfiltered 1-hr coastal station data for calendar year 1987. This table shows that North Slope stations are substantially more like each other than like Kotzebue or Nome in temperature, pressure, and wind speed. Except for Resolution, the pressure lags are consistent with a picture that, during late summer and autumn, low pressure systems tend to propagate from the northeastern Bering Sea, northward along the Chukchi coast, and eastward

Table 5. Maximum correlations/at lag n at or above 95% confidence level for unfiltered, 1-hr data from six coastal meteorological stations (column lags row). Common time interval is from 0100 1Jan87 to 2200 31Dec87 with 8758 points. Number of lags is 30 (30 hours).

**A. Sea-level pressure (SLP in mb).**

	Barter	Resolution	Lonely	Barrow	Kotzebue	Nome
Barter	1.00/0	0.90/0	0.91/8	0.96/0	0.82/0	0.68/0
Resolutn	0.91/5	1.00/0	0.85/15	0.89/5	0.77/0	0.65/0
Lonely	0.88/0	0.81/0	1.00/0	0.89/0	0.65/0	0.53/0
Barrow	0.96/1	0.89/0	0.92/9	1.00/0	0.75/0	0.61/0
Kotzebue	0.85/8	0.78/5	0.74/17	0.78/8	1.00/0	0.96/0
Nome	0.74/12	0.67/9	0.64/21	0.66/13	0.96/4	1.00/0
Mean SLP	1014.87	1013.57	1013.13	1015.62	1009.43	1007.11

**B. Surface air temperature (SAT in C).**

	Barter	Resolution	Lonely	Barrow	Kotzebue	Nome
Barter	1.00/0	0.96/8	0.96/9	0.95/0	0.89/0	0.82/1
Resolutn	0.96/13	1.00/0	0.96/0	0.94/0	0.87/0	0.81/16
Lonely	0.95/0	0.96/0	1.00/0	0.95/0	0.88/0	0.83/16
Barrow	0.96/21	0.95/9	0.97/9	1.00/0	0.90/0	0.84/0
Kotzebue	0.89/22	0.88/8	0.89/9	0.90/0	1.00/0	0.94/0
Nome	0.83/23	0.82/9	0.83/30	0.84/0	0.94/1	1.00/0
Mean SAT	-11.47	-11.76	-12.26	-12.07	-5.12	-2.15

**C. Station wind speed (SPD in m/s).**

	Barter	Resolution	Lonely	Barrow	Kotzebue	Nome
Barter	1.00/0	0.52/0	0.41/8	0.49/0	0.04/30	-0.07/10
Resolutn	0.59/15	1.00/0	0.60/24	0.56/13	0.11/10	-0.08/28
Lonely	0.37/0	0.40/0	1.00/0	0.54/0	-0.02/30	-0.13/28
Barrow	0.50/2	0.50/0	0.62/8	1.00/0	0.12/0	-0.05/12
Kotzebue	0.10/20	0.13/16	0.08/30	0.21/24	1.00/0	0.42/0
Nome	-0.08/5	-0.05/0	-0.10/0	0.07/25	0.43/4	1.00/0
Mean SPD	6.13	5.40	3.58	5.90	5.68	4.68

along the Beaufort coast (Overland, 1981; Pease, 1987). For example, Barter lags Resolution by five hours, Lonely lags Barrow by nine hours, Barrow lags Kotzebue by eight hours, and Kotzebue lags Nome by four hours. This conclusion is further supported by the observation that all the North Slope stations lag Kotzebue by four hours less than they do Nome.

In a separate correlation (not shown) for a six-month interval including the spring and summer of 1987, a period of sustained easterly winds, pressure at Resolution strongly led all other stations, suggesting the westward propagation of high pressure anomalies. Also, the Brooks Range foofs near Resolution, and there are interactions with the topography during winter and spring because of the strong capping inversions (Kozo, 1980; Overland, 1985). In the summer, sea breezes asymmetrically modify the surface wind along the north slope, as well (Kozo, 1982a,b; Kozo, 1984).

Considering the surface air temperature correlations in Table 5, we see that Resolution and Lonely lag both Barter and Barrow by 8-9 hours, which supports the idea that warm low pressure systems from the southwest and cold high pressure systems from the northeast pass over the area. All the stations have very high temperature correlations at low lags, because the solar diurnal cycle (especially during the spring months before the summer stratus develops) and the annual cycle account for a large portion of the variance of the air temperature in the polar and polar-marine climatic zone (Overland, 1981; Pease, 1987). Due to the prevalence of summer clouds, short wave radiation peaks in early June (Maykut and Church, 1973).

The wind speeds at Nome are essentially uncorrelated with the wind speeds along the North Slope, related to the orientation of the topography relative to the station and to the fact that many low pressure systems felt in the northeastern Bering Sea do not propagate northward into the Chukchi/Beaufort (Overland and Pease, 1982). Kotzebue wind speeds lag Nome by about four hours, but the correlation is modest and accounts for less than 20% of the variance at Kotzebue. Wind speed variance at Kotzebue leads that at all the North Slope stations by 16-30 hours, but only accounts for 4% of the variance at Barrow. In contrast, wind speed variance at Resolution leads variance at all North Slope stations by 13-24 hours and accounts for about 36% of the variance at the other stations. In general, however, the wind speed correlations are relatively low among all the stations because topographical and other local effects reduce the correlations (Kozo, 1980) compared to pressure correlations.

In order to evaluate the quality of the FNOC surface analyses for use in filling missing data and to aid in spatial interpolations, we compared FNOC data with two independent GOES stations and two non-independent NWS stations along the north slope. Table 6 shows the correlations for pressure, wind speed, and temperature for the four coastal meteorological stations compared with point data stripped from the FNOC gridded fields by METLIB and interpolated to each site. Table 7 correlates pressure measured at two of the ARGOS buoys with FNOC pressure. Since FNOC analyses are generated every six hours (twelve hours for

Table 6. Maximum correlations/at lag n at or above 95% confidence level for 6-hr data from four coastal meteorological stations and the equivalent FNOC data for the same sites (column lags row). N stands for NWS station, G stands for GOES station, and F stands for FNOC equivalent. Common time interval is from 0100 26Sep86 to 2200 31Aug87. Number of lags is 5 (30 hours).

**A. Sea-level pressure (SLP in mb) for 6-hr data.**

	BarterN	BarterF	ResoluG	ResoluF	LonelyG	LonelyF	BarrowN	BarrowF
BarterN	1.00/0	0.99/2	0.93/1	0.99/1	0.98/1	0.98/1	0.96/0	0.96/1
BarterF	0.94/0	1.00/0	0.91/0	1.00/0	0.97/0	0.98/0	0.90/0	0.96/0
ResoluG	0.93/0	0.93/1	1.00/0	0.93/1	0.92/1	0.93/1	0.90/0	0.91/1
ResoluF	0.95/0	1.00/0	0.92/0	1.00/0	0.99/0	0.99/0	0.92/0	0.97/0
LonelyG	0.95/0	0.97/0	0.92/0	0.99/0	1.00/0	1.00/0	0.95/0	0.99/0
LonelyF	0.95/0	0.93/0	0.92/0	0.99/0	1.00/0	1.00/0	0.95/0	0.99/0
BarrowN	0.96/0	0.96/2	0.91/1	0.97/2	0.99/2	0.99/2	1.00/0	1.00/2
BarrowF	0.94/0	0.96/0	0.90/0	0.97/0	0.99/0	0.99/0	0.96/0	1.00/0

**B. Station wind speed (SPD in m/s) for 6-hr data.**

	BarterN	BarterF	ResoluG	ResoluF	LonelyG	LonelyF	BarrowN	BarrowF
BarterN	1.00/0	0.35/2	0.52/1	0.28/1	0.25/1	0.27/1	0.42/0	0.28/1
BarterF	0.26/0	1.00/0	0.33/0	0.93/0	0.23/0	0.77/0	0.33/0	0.67/0
ResoluG	0.45/0	0.35/1	1.00/0	0.31/1	0.41/4	0.30/1	0.40/0	0.28/1
ResoluF	0.23/0	0.93/0	0.31/0	1.00/0	0.15/0	0.92/0	0.35/0	0.81/0
LonelyG	0.21/0	0.23/1	0.35/0	0.15/0	1.00/0	0.14/0	0.36/0	0.13/0
LonelyF	0.22/0	0.77/0	0.30/0	0.92/0	0.14/0	1.00/0	0.39/0	0.97/0
BarrowN	0.42/0	0.43/2	0.44/1	0.43/2	0.44/1	0.47/2	1.00/0	0.48/2
BarrowF	0.24/0	0.67/0	0.28/0	0.81/0	0.13/0	0.97/0	0.41/0	1.00/0

**C. Surface air temperature (SAT in C) for 12-hr data.**

	ResoluG	ResoluF	LonelyG	LonelyF
ResoluG	1.00/0	0.97/2	0.96/0	0.96/2
ResoluF	0.37/0	1.00/0	0.35/0	1.00/0
LonelyG	0.96/0	0.95/0	1.00/0	0.96/2
LonelyF	0.36/0	1.00/0	0.36/0	1.00/0

Table 7. Correlation between pressure measured at two of the ARGOS buoys and pressure from the FNOC fields at the position of the buoys. The analysis was carried out for the lifetime of the buoy: from 1 March to 12 June 1987 for buoy 7422 and from 7 March to 11 April, 1987 for buoy 7423.

	7422A	7422M		7423A	7423M
7422A	----	.99(0)	7423A	----	1.0(0)
7422M	.99(0)	----	7423M	1.0(0)	----

temperature fields), we subsampled the hourly station data at the appropriate intervals. In general, temperatures and pressures were well modeled by the FNOC analyses with one caveat: the FNOC analyses were lagged six to twelve hours from the stations data, although they were in phase with the ARGOS data. For example, both Barter and Barrow pressure and wind speed led the FNOC data by 12 hours.

## 5. SUMMARY

During the period from October 1986 to April 1987, near-surface currents over the Beaufort Sea continental shelf and margin were westward, although the vector mean magnitude at many moorings was smaller than the RMS error. The depth at which the mean flow became easterly, i.e., the depth at which the Beaufort Undercurrent began, was between 60-90 m. This depth varied spatially and also appears to change from year to year. Flow reversals in the undercurrent to westerly motion occurred frequently, and these reversals may have driven upwelling of warm, saline water onto the shelf. Vertical excursions were in the range of 100-150 m. Such upwelling events were evident both in the time-series records and in the hydrographic sections.

An important point is evident from the October occupation of section W, viz. that a major source of water for the Beaufort Undercurrent must lie farther west than had previously been considered. Most likely, this other injection occurs in the vicinity of Herald Canyon.

Many low-frequency flow events were coherent vertically and over large horizontal distances. Maximum horizontal correlations over the outer shelf were measured at depths of 90-100 m. Variance at the western moorings led that at the eastern ones, and the phase difference suggests an eastward propagation rate of about  $5 \text{ m s}^{-1}$ .

The hydrographic data provide extensive coverage of both fall and winter conditions. A possibly important feature in the data is the longshore variability in the hydrography of the Beaufort Sea shelf, including possible major hydrographic differences between the western and eastern Beaufort. The latter transition appears to occur in the vicinity of Prudhoe Bay.

With respect to the meteorology, both the autumns of 1986 and 1987 were abnormally warm, and an unusual number of low-pressure centers passed through the Beaufort Sea. The

autumn ice extents were well below average. The late winter and spring of 1987 were more climatically normal.

Pressure and air temperature measured at the GOES stations were generally better spatially correlated than was wind speed, because of topographic and other effects. Pressure and temperature fields were well modeled by the FNOC analyses, which can therefore be used to fill in missing data. Correlation coefficients and lags suggest that warm low-pressure systems propagate up the Chukchi Sea coast and then eastward along the Beaufort Sea coast, while cold high-pressure systems originate farther east and propagate towards the west.

The total data set is extraordinary in the temporal and spatial extent of its synoptic coverage, and in the variety of its constituent measurements. The data set is also extremely large, and its full reduction and analysis will provide an exceptional opportunity for improving our understanding of the shelf circulation and its forcing, as well as conditions important to the marine ecology of the area.

At the same time, the size of the data set provides a genuine challenge in processing and analysis. Major processing tasks remain. For example, the numerous long current and pressure records for April 1987-April 1988, and just now recovered, have not yet been processed and reduced. Likewise, the ARGOS data from 1988 have not been analyzed, and in fact some of the ARGOS buoys are still transmitting. As the various meteorological and oceanographic components of the composite data set become available in a fully processed form, their synthesis promises new insights into the processes governing conditions over the Beaufort Sea shelf.

## 6. ACKNOWLEDGMENTS

The Beaufort Mesoscale Circulation Study is a contribution to the Marine Services Project of the Pacific Marine Environmental Laboratory. It was financed in part by the Minerals Management Service through an interagency agreement with the National Oceanic and Atmospheric Administration (NOAA) under a multiyear program, responding to the needs of petroleum development of the Alaskan continental shelf and managed by the Outer Continental Shelf Environmental Assessment Program Office. A portion of the ARGOS buoy deployments were funded by the Office of Naval Research-Arctic Programs.

C.H. Darnall was chief engineer for the project. K. Kroglund completed the oceanic chemical analyses. Lt(jg) G.A. Galasso was the engineer for the meteorological stations. V.L. Long and N. Jenkins contributed to the data analyses. We also acknowledge the numerous other NOAA, Coast Guard, and civilian personnel who contributed to the successful completion of the experiment in a hostile physical environment.

## 7. REFERENCES

- Aagaard, K., 1981. Current measurements in possible dispersal regions of the Beaufort Sea. In *Final Reports of Principal Investigators*, Volume 3, Physical Science Studies. National Oceanic and Atmospheric Administration, Boulder, CO, 1-74.
- Aagaard, K., 1984. The Beaufort Undercurrent. In *The Alaskan Beaufort Sea: Ecosystems and Environment* (ed. by D. Schell, P. Barnes, and E. Reimnitz), Academic Press, New York, 47-71.
- Aagaard, K., S. Salo, and K. Kroglund, 1987. Beaufort Sea Mesoscale Circulation Study: Hydrography USCGC Polar Star Cruise, October 1986. NOAA Data Report ERL PMEL-19, Seattle, WA, 83 pp.
- Aagaard, K., S. Salo, and K. Kroglund, 1988. Beaufort Sea Mesoscale Circulation Study: Hydrography Helicopter Operations, April 1987. NOAA Data Report ERL PMEL-22, Seattle, WA, 25 pp.
- Barnes, P.W., and L.J. Toimil, 1979. Inner shelf circulation patterns Beaufort Sea, Alaska. U.S.G.S. Miscellaneous Field Studies Map MF-1125, Menlo Park, CA, 1 plate.
- Coachman, L.K., K. Aagaard, and R.B. Tripp, 1974. Bering Strait: The Regional Physical Oceanography. University of Washington Press, Seattle, WA, 172 pp.
- Foldvik, A., K. Aagaard, and T. Torresen, 1988. On the velocity field of the East Greenland Current. *Deep-Sea Research*, 35, in press.
- Hufford, G.L., 1974. On apparent upwelling in the southern Beaufort Sea. *Journal of Geophysical Research*, 79, 1305-1306.
- Jones, E.P., and L.G. Anderson, 1986. On the origin of the chemical properties of the Arctic Ocean halocline. *Journal of Geophysical Research*, 91, 759-10, 767.
- Kozo, T.L., 1980. Mountain barrier baroclinicity effects on surface winds along the Alaskan Arctic coast. *Geophysical Research Letters*, 7, 377-380.
- Kozo, T.L., 1982a. An observational study of sea breezes along the Alaskan Beaufort Sea Coast: Part I. *Journal of Applied Meteorology*, 21, 891-905.
- Kozo, T.L., 1982b. An observational study of sea breezes along the Alaskan Beaufort Sea Coast: Part II. *Journal of Applied Meteorology*, 21, 906-924.
- Kozo, T.L., 1984. Mesoscale wind phenomena along the Alaskan Beaufort Sea coast. In *The Alaskan Beaufort Sea: Ecosystem and Environment* (ed. by P. Barnes, D. Schell, and E. Reimnitz), Academic Press, Orlando, FL, 23-45.
- Kozo, T.L. and R.Q. Robe, 1986. Modeling winds and open-water buoy drift along the eastern Beaufort Sea coast, including the effects of the Brooks Range. *Journal of Geophysical Research*, 91, 13011-13032.
- Maykut, G.A., and P.E. Church, 1973. Radiation climate of Barrow, Alaska, 1962-1966. *Journal of Applied Meteorology*, 12, 620-628.

- Moore, R.M., M.G. Lowings, and F.C. Tan, 1983. Geochemical profiles in the central Arctic Ocean: Their relation to freezing and shallow circulation. *Journal of Geophysical Research*, 88, 2667-2674.
- Mountain, D.G., 1974. Bering Sea Water on the North Alaskan Shelf. Ph.D. dissertation, University of Washington, Seattle, 154 pp.
- Newton, J.L., K. Aagaard, and L.K. Coachman, 1974. Baroclinic eddies in the Arctic Ocean. *Deep-Sea Research*, 21, 707-719.
- Overland, J.E., 1981. Marine climatology of the Bering Sea. In *The Eastern Bering Sea Shelf: Oceanography and Resources*, Volume 1 (ed. by D.W. Hood and J.A. Calder), University of Washington Press, Seattle, WA, 15-22.
- Overland, J.E., 1985. Atmospheric boundary layer structure and drag coefficients over sea ice. *Journal of Geophysical Research*, 90, 9029-9049.
- Overland, J.E. and C.H. Pease, 1982. Cyclone climatology of the Bering Sea and its relation to sea ice extent. *Monthly Weather Review*, 110, 5-13.
- Pease, C.H., 1987. Meteorology of the Chukchi Sea: an overview. In *Chukchi Sea Information Update* (ed. by D.A. Hale), NOAA/NOS Ocean Assessments Division — Alaska Office, Anchorage, AK, 11-19.
- Rogers, J.C., 1978. Meteorological factors affecting interannual variability of summertime ice extent in the Beaufort Sea. *Monthly Weather Review*, 106, 890-897.
- Tripp, R.B., 1987. ISHTAR Cruise Report, R/V *Thomas G. Thompson* Cruise TT-212, 29 June-19 July 1987. University of Washington, School of Oceanography, informal report, 149 pp.

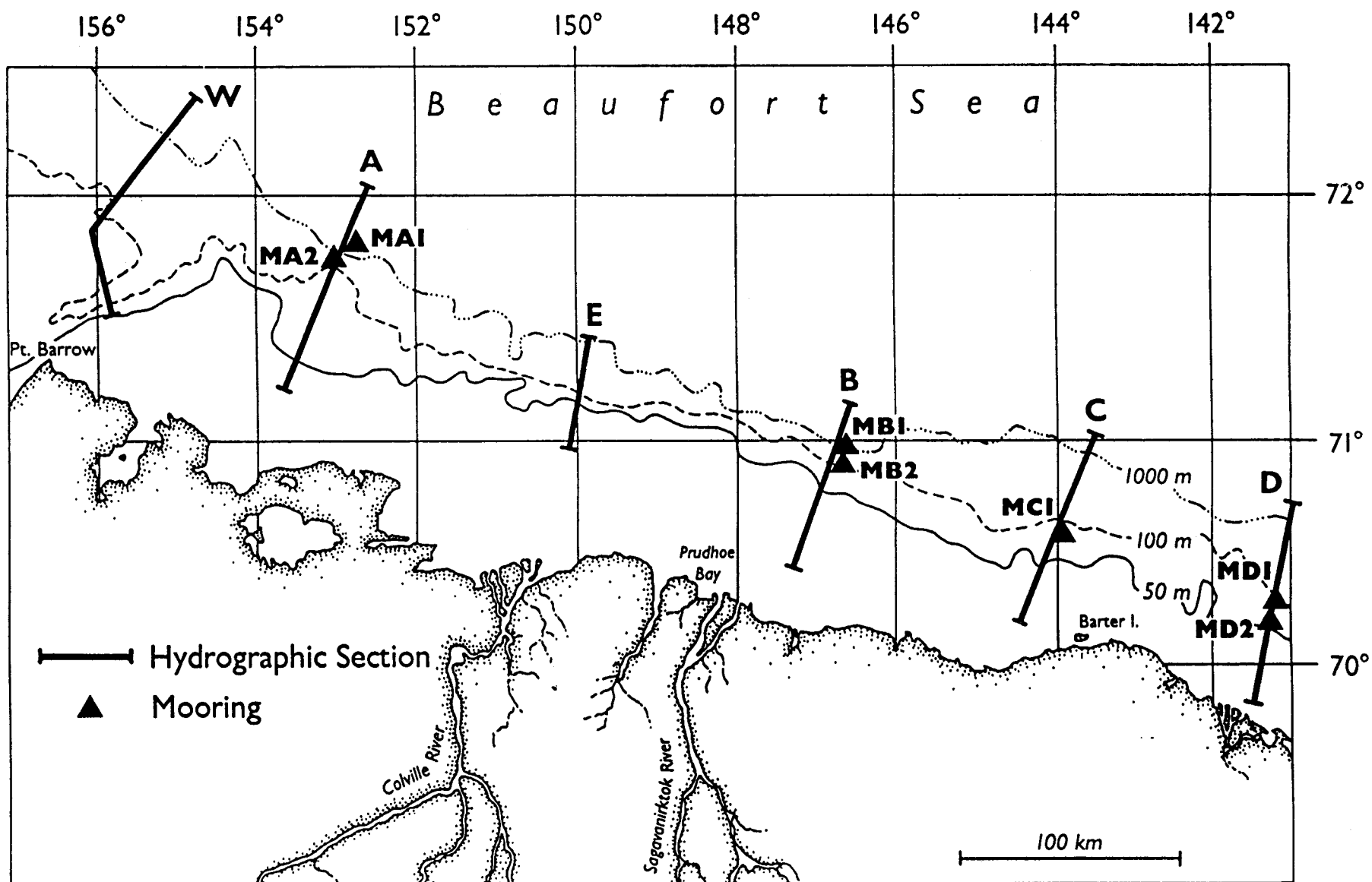


Figure 1. Locations of hydrographic sections occupied in October 1986 and moorings recovered in 1987.

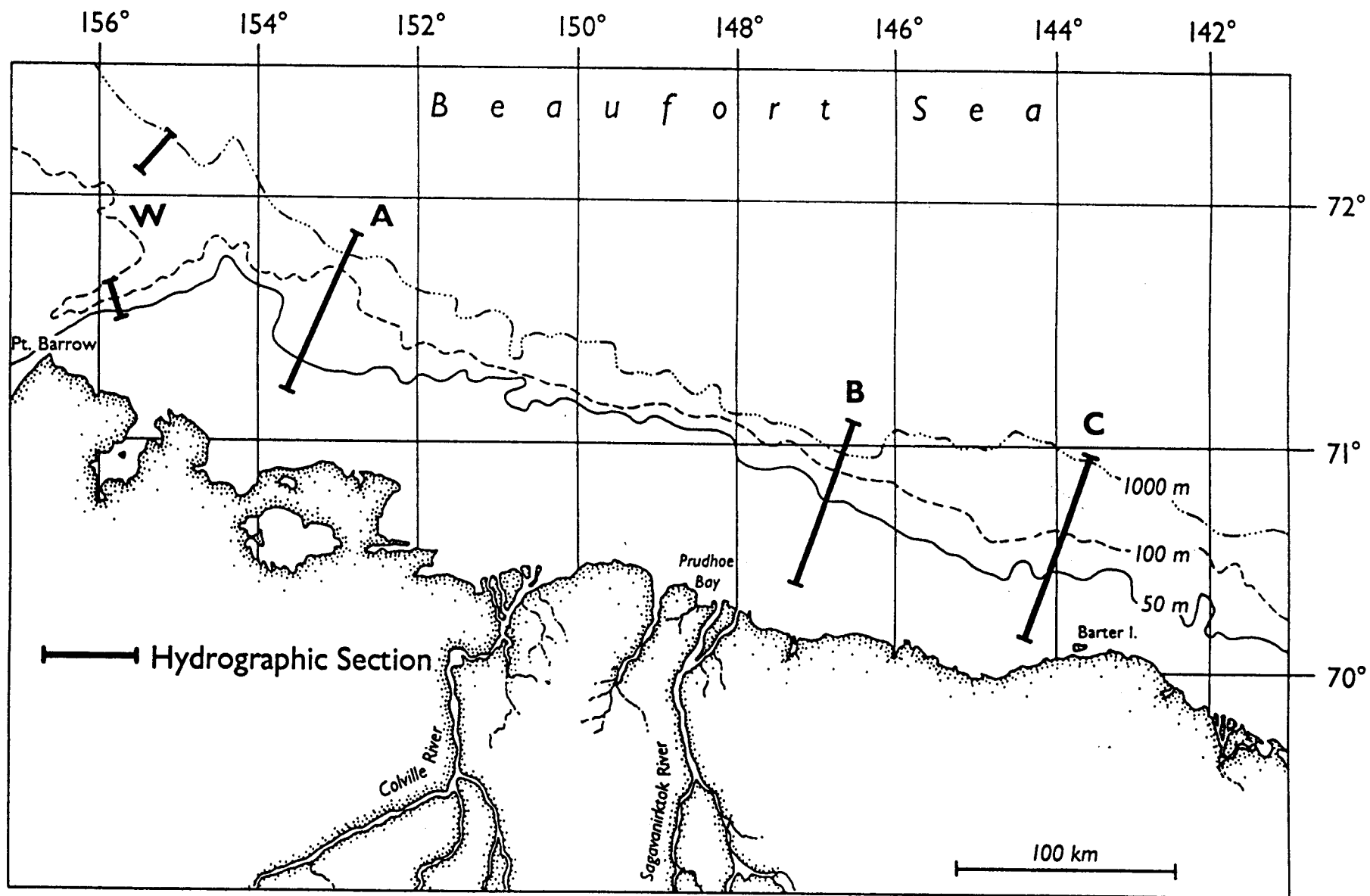


Figure 2. Locations of hydrographic sections occupied in April 1987.

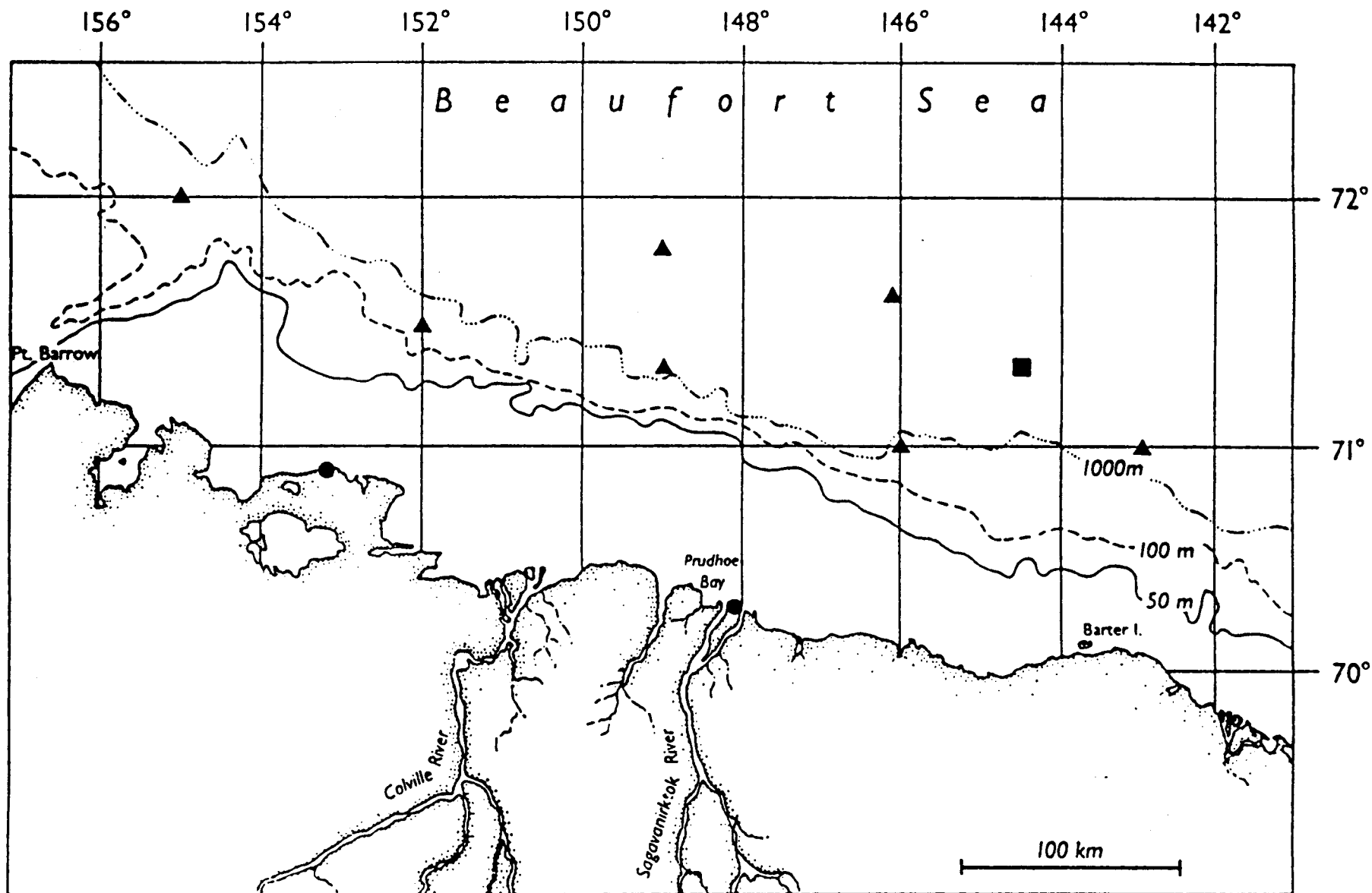


Figure 3. Positions at which ARGOS buoys (▲) and stations (■), and GOES meteorological stations (●) were deployed in 1986-87. Buoys and stations deployed south or west of Barrow are not shown.

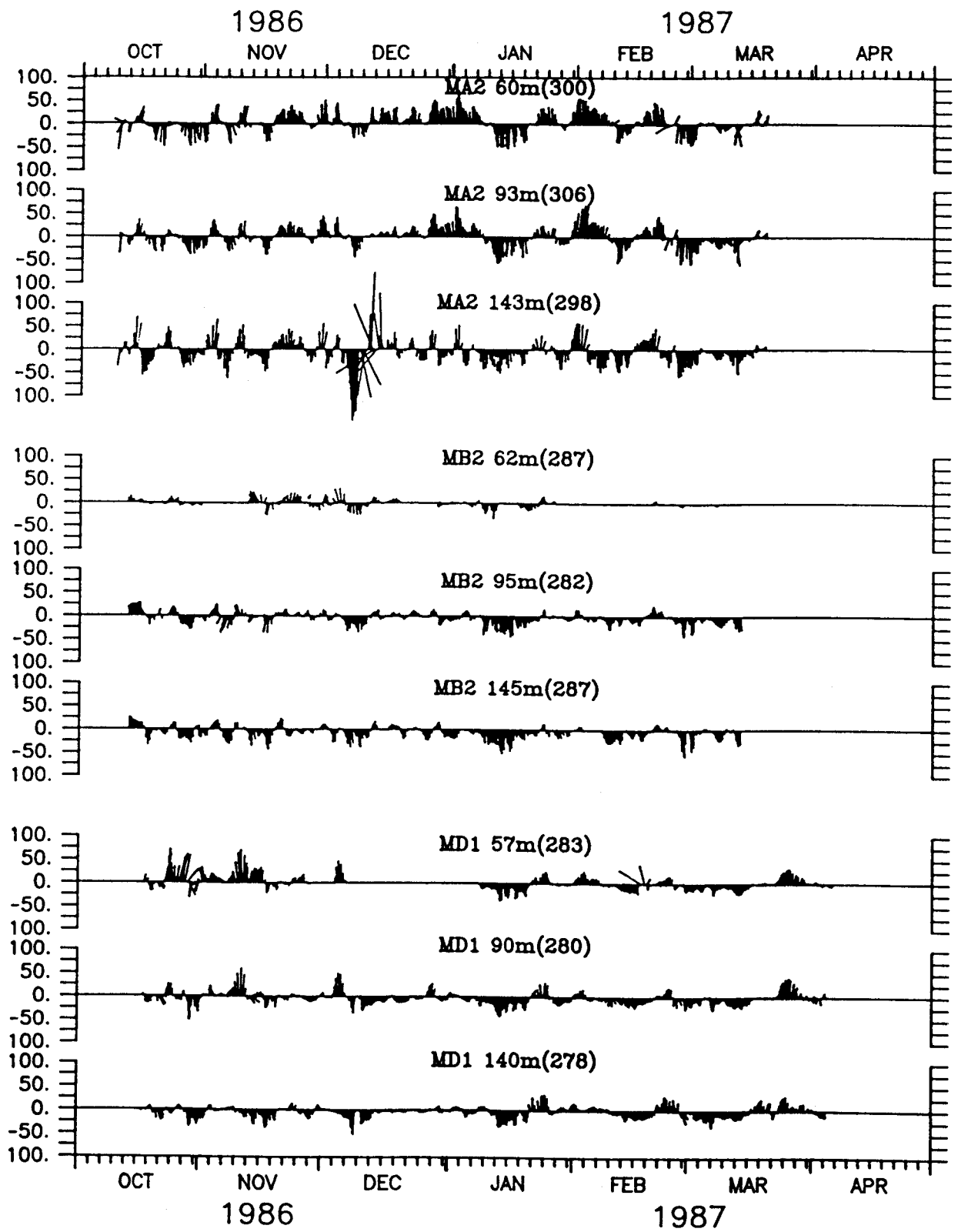


Figure 4. Current vectors from the instruments deployed in October 1986 at the moorings in water 165-170 m deep. Currents were 35-hour filtered.

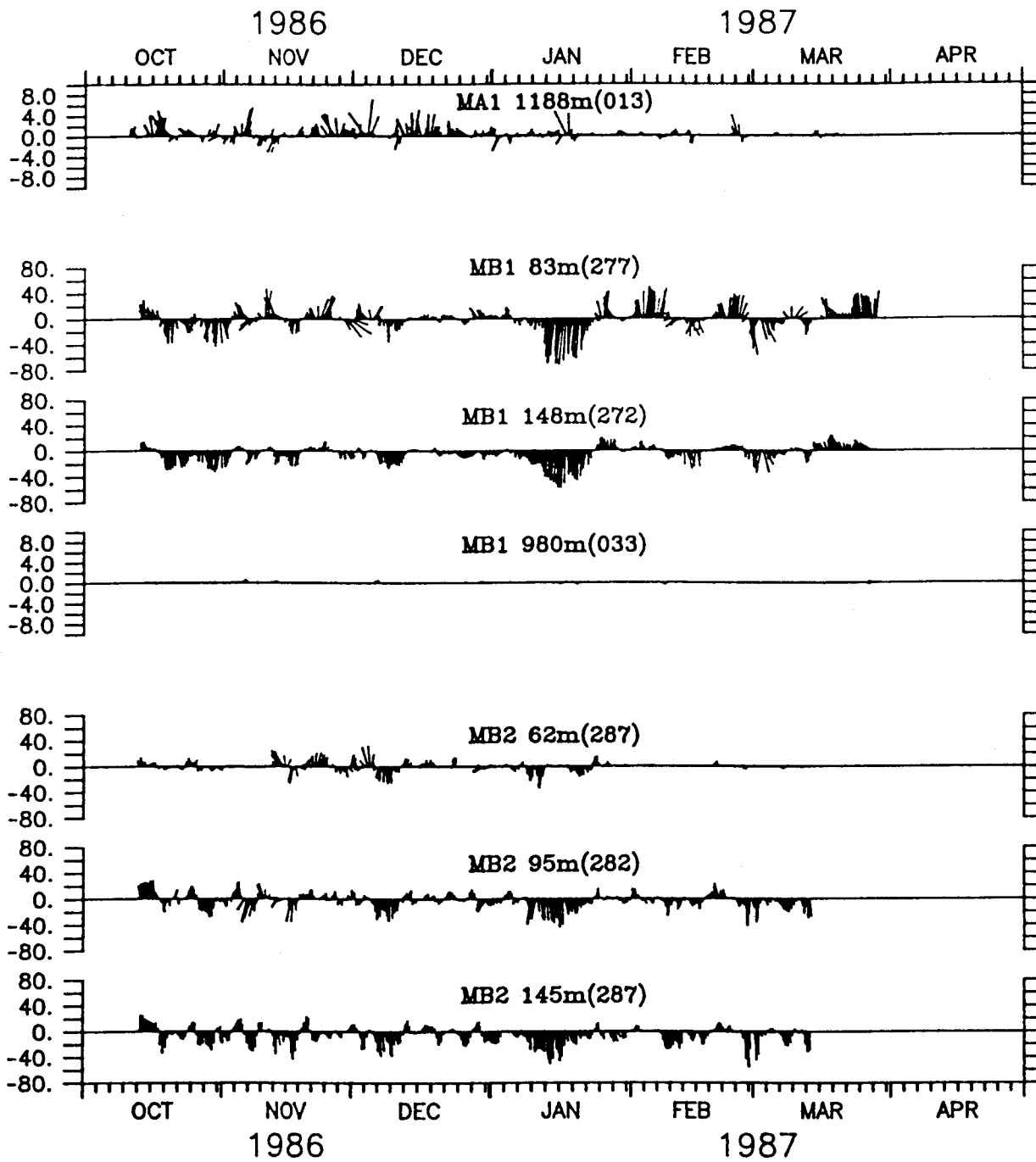


Figure 5. Current vectors at the deeper moorings deployed in October 1986. Mooring MB2 is repeated from Figure 4 for comparison.

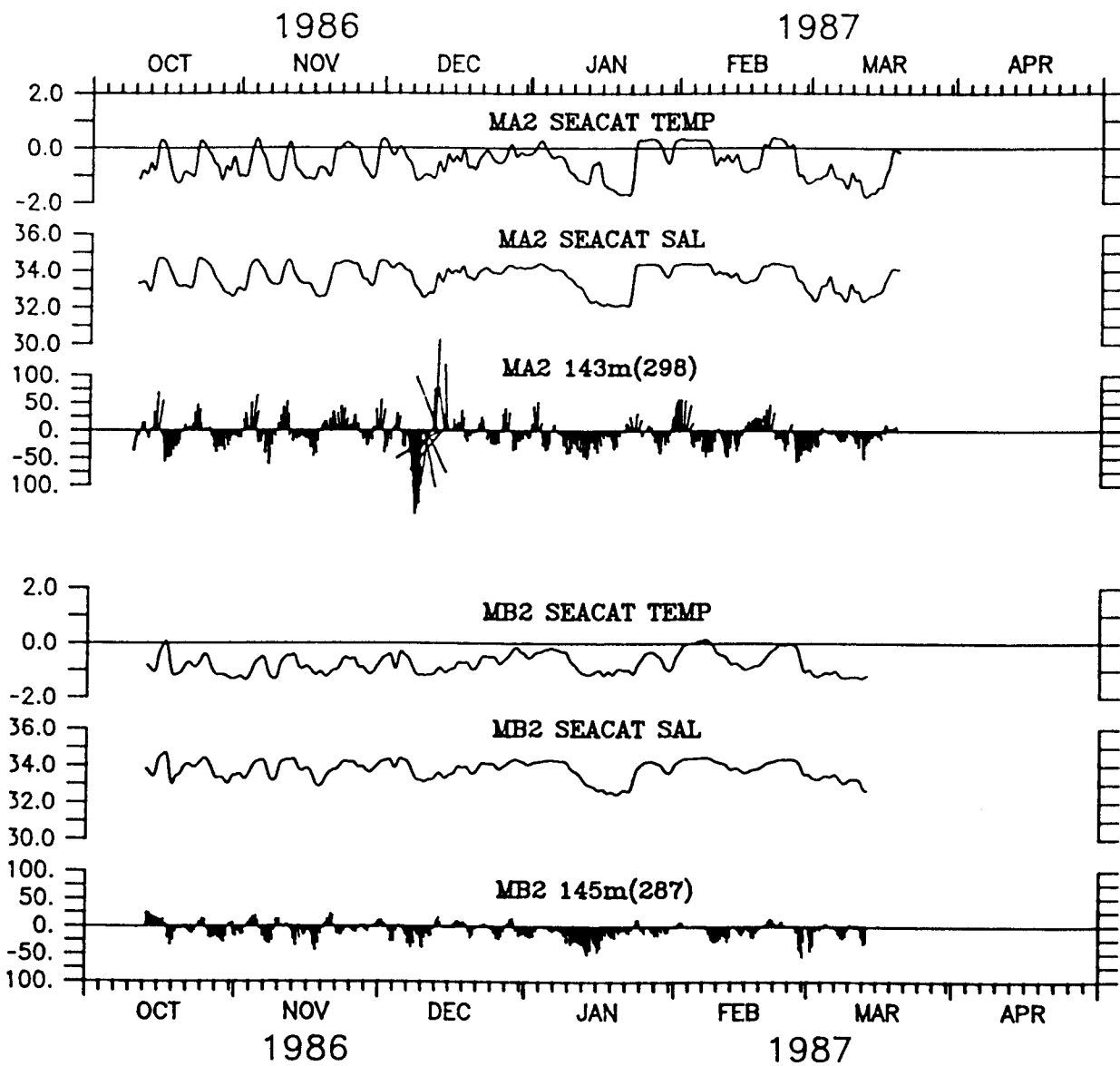


Figure 6. SeaCat temperature and salinity at MA2 and MB2, and current vectors at the deepest meter from these moorings. Data were 35-hour filtered.

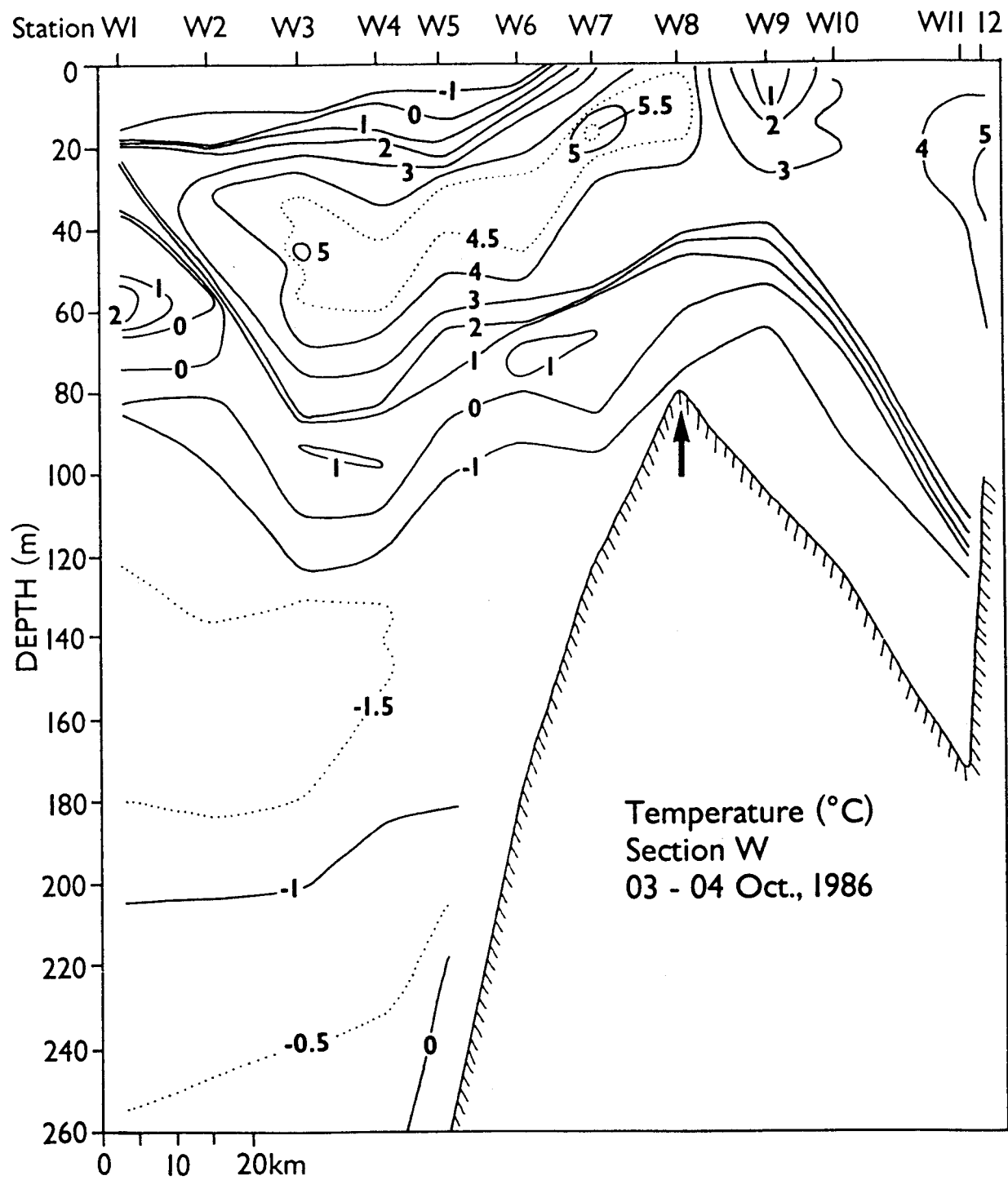


Figure 7. Temperature at section W in October 1986.

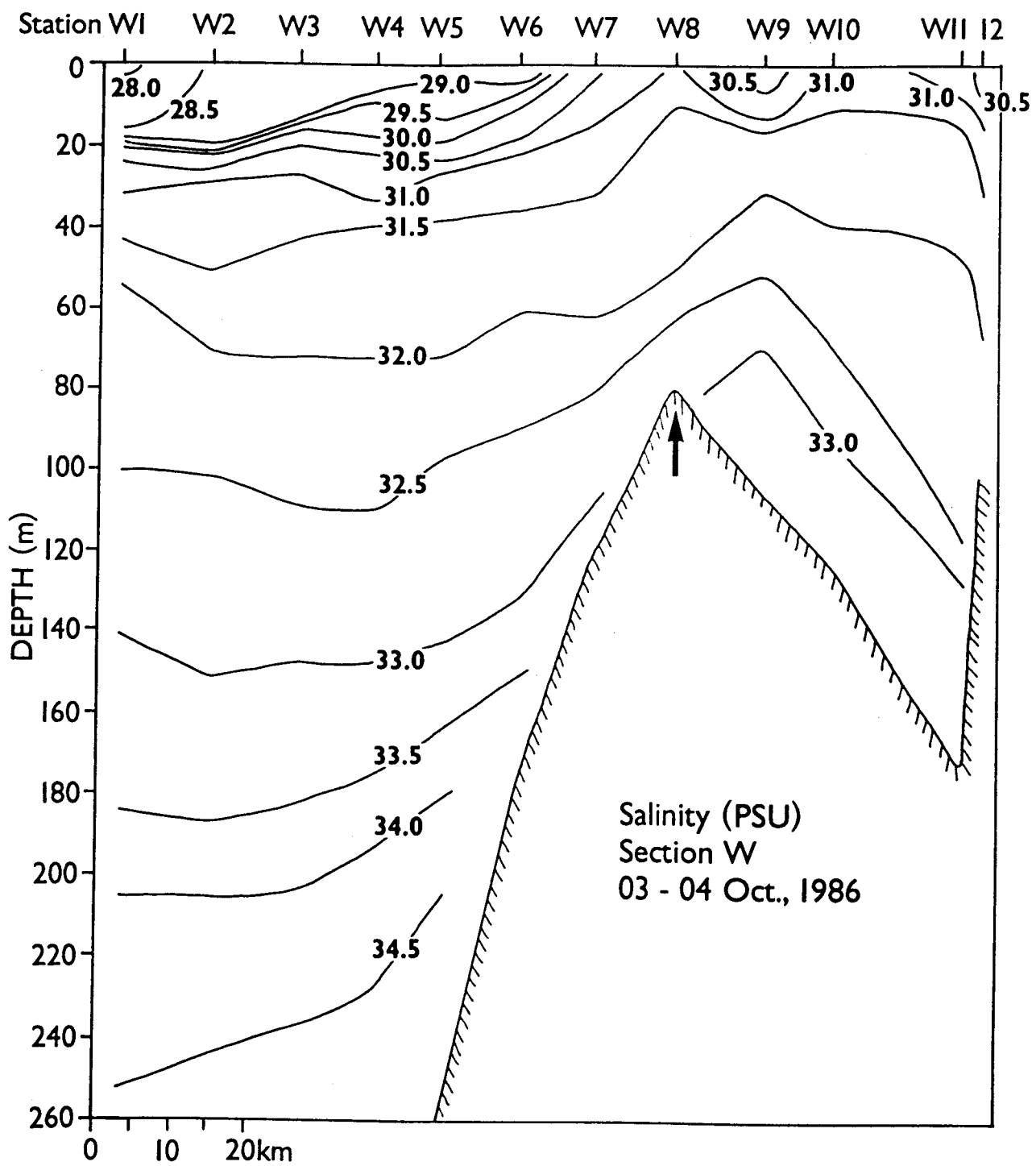


Figure 8. Salinity at section W in October 1986.

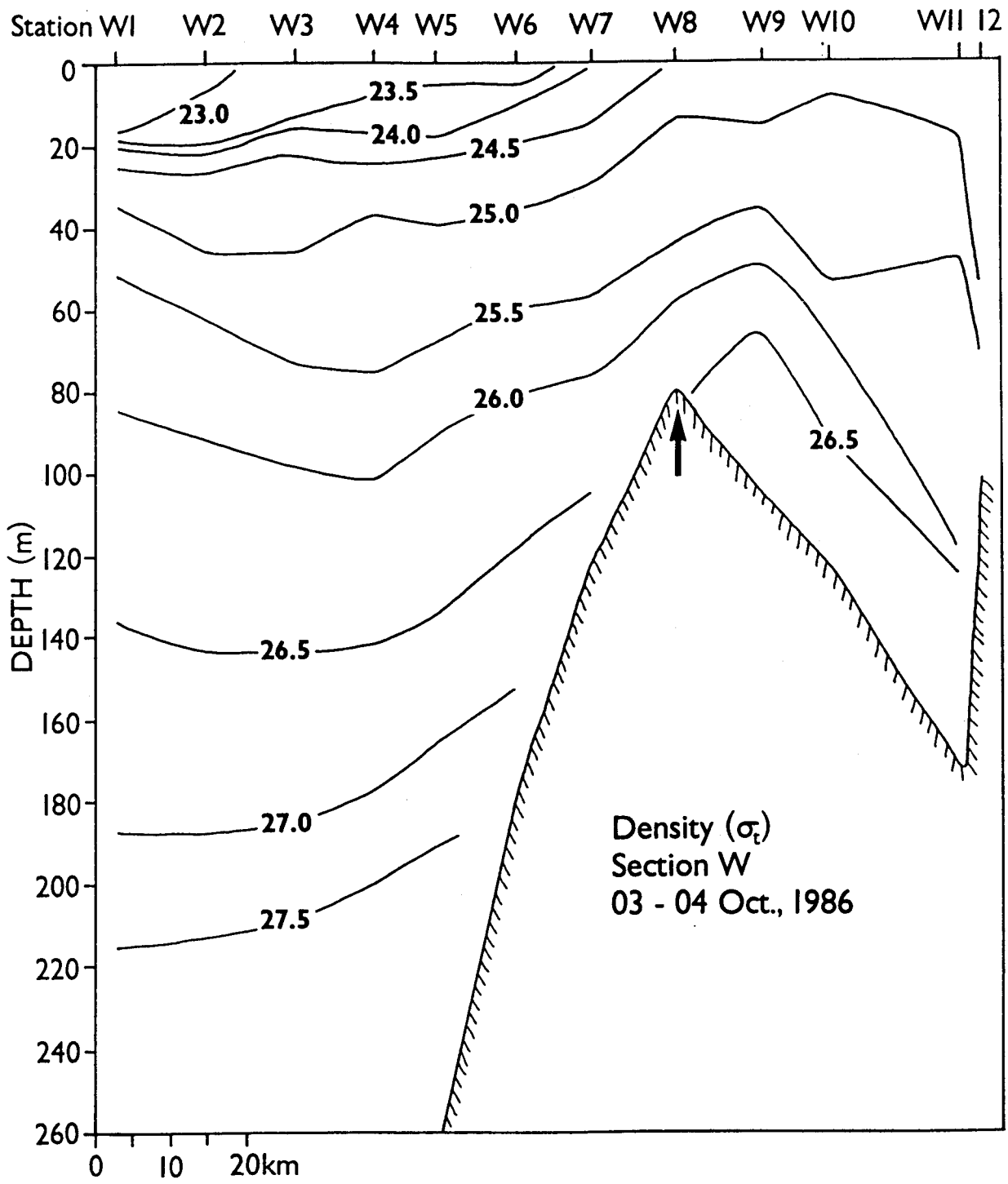


Figure 9. Density at section W in October 1986.

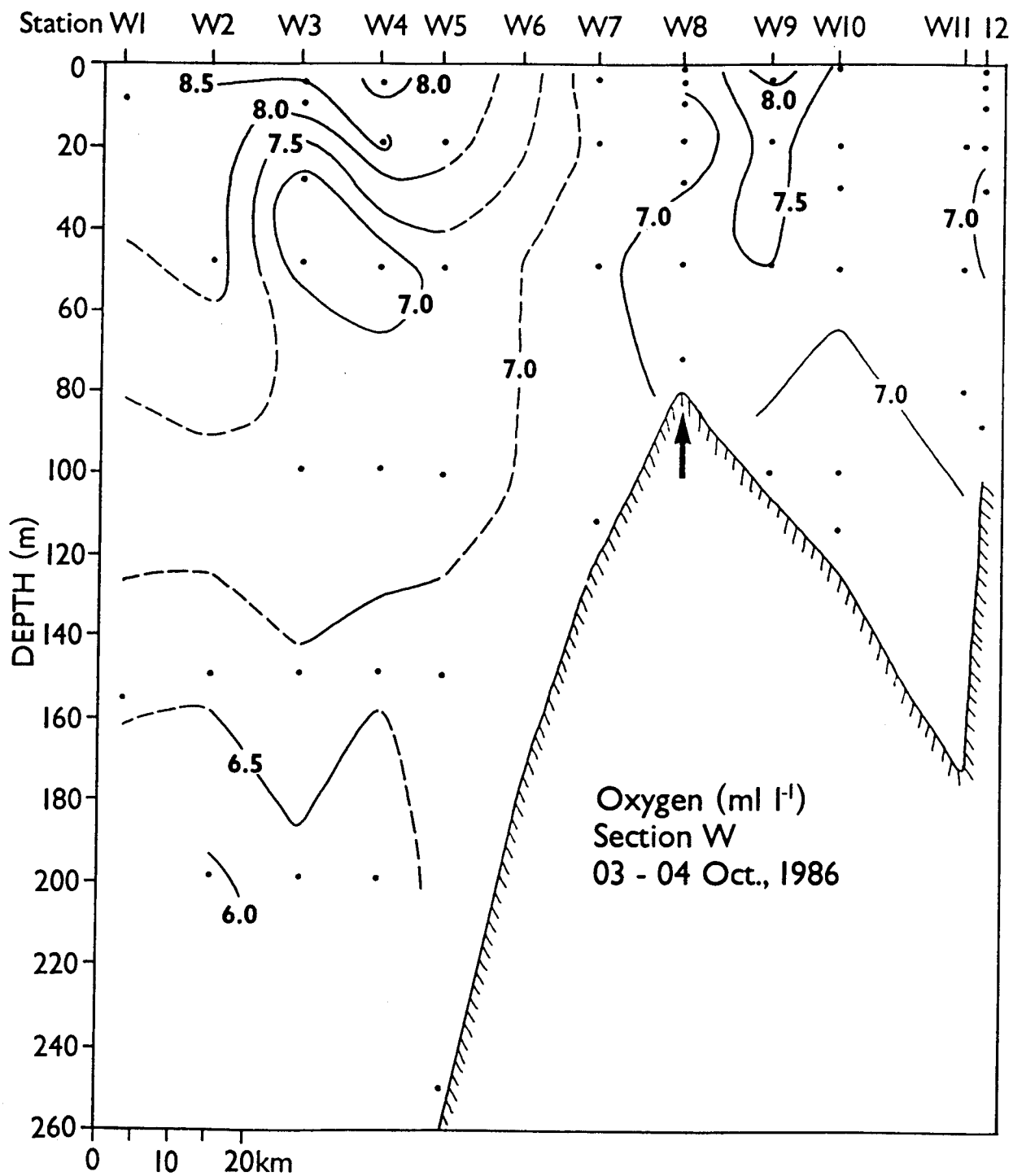


Figure 10. Dissolved oxygen at section W in October 1986.

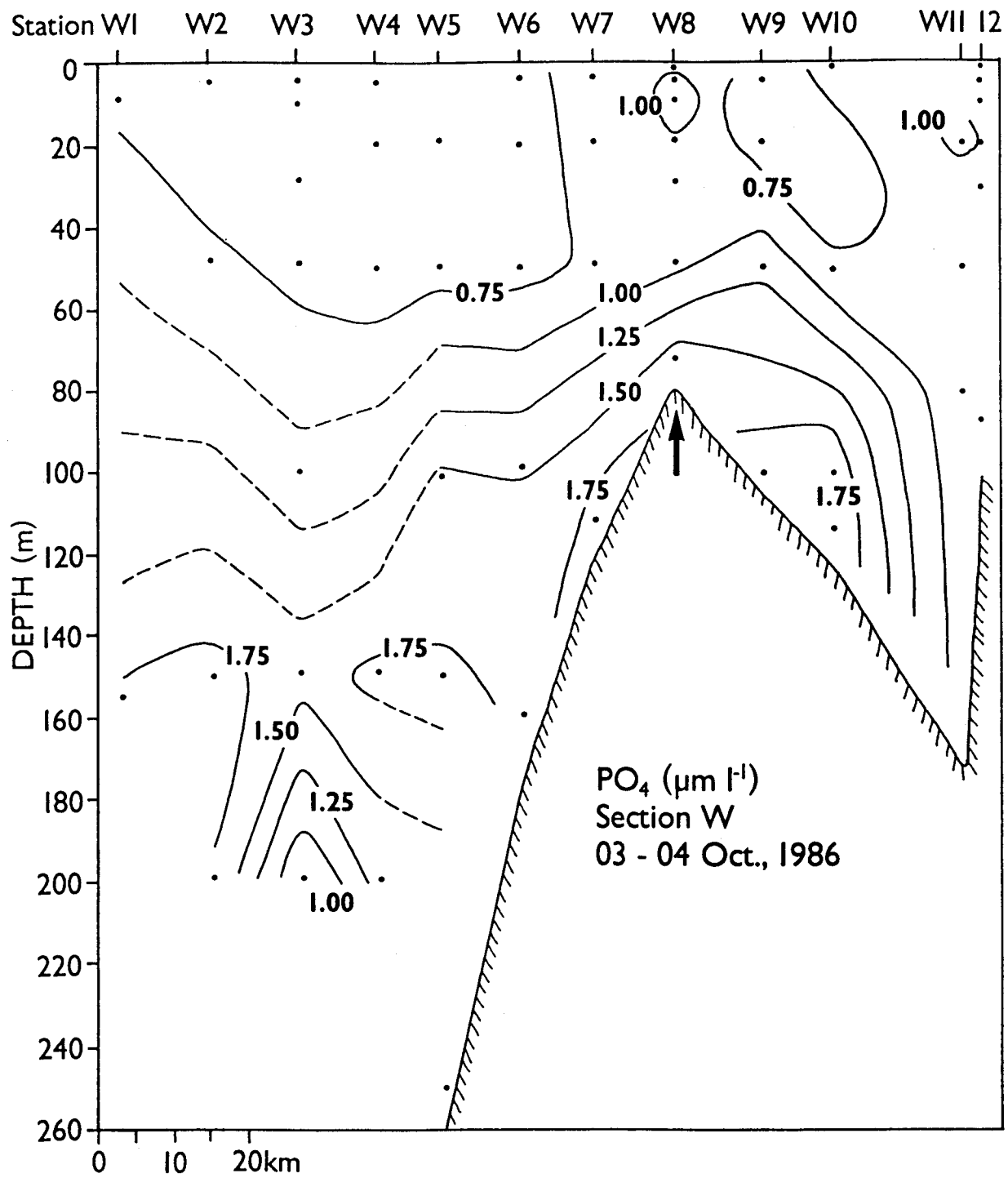


Figure 11. Phosphate at section W in October 1986.

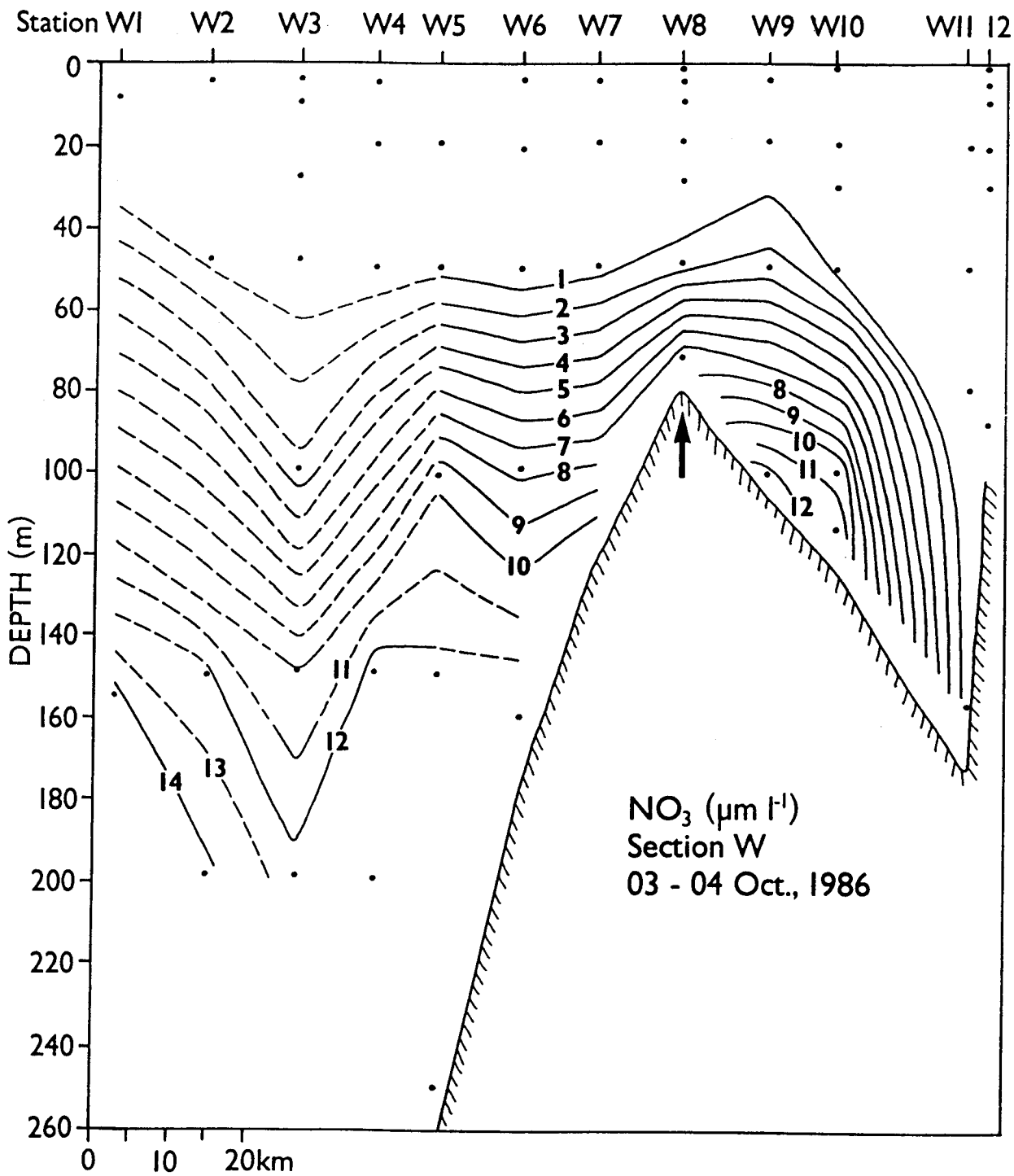


Figure 12. Nitrate at section W in October 1986.

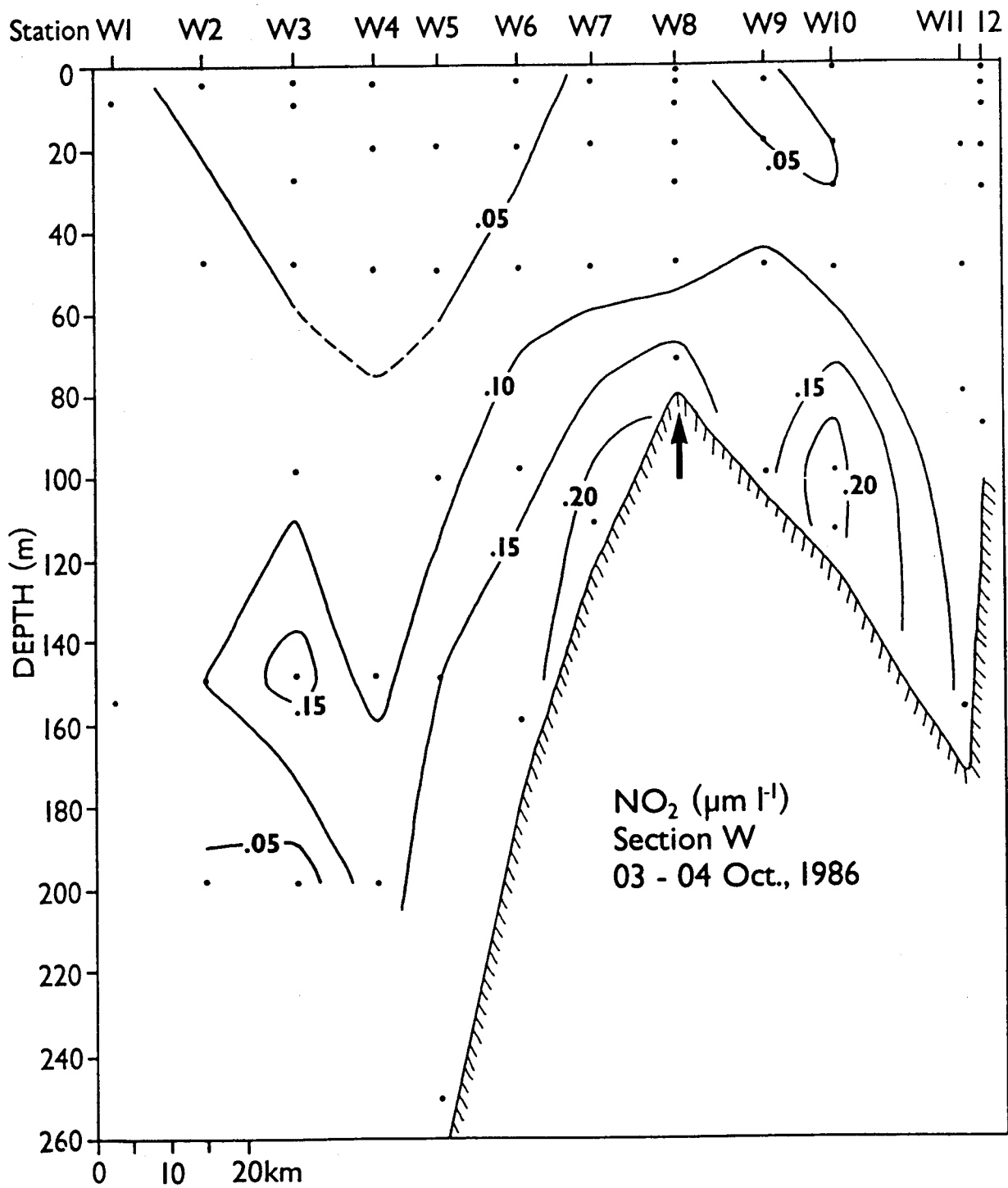


Figure 13. Nitrite at section W in October 1986.

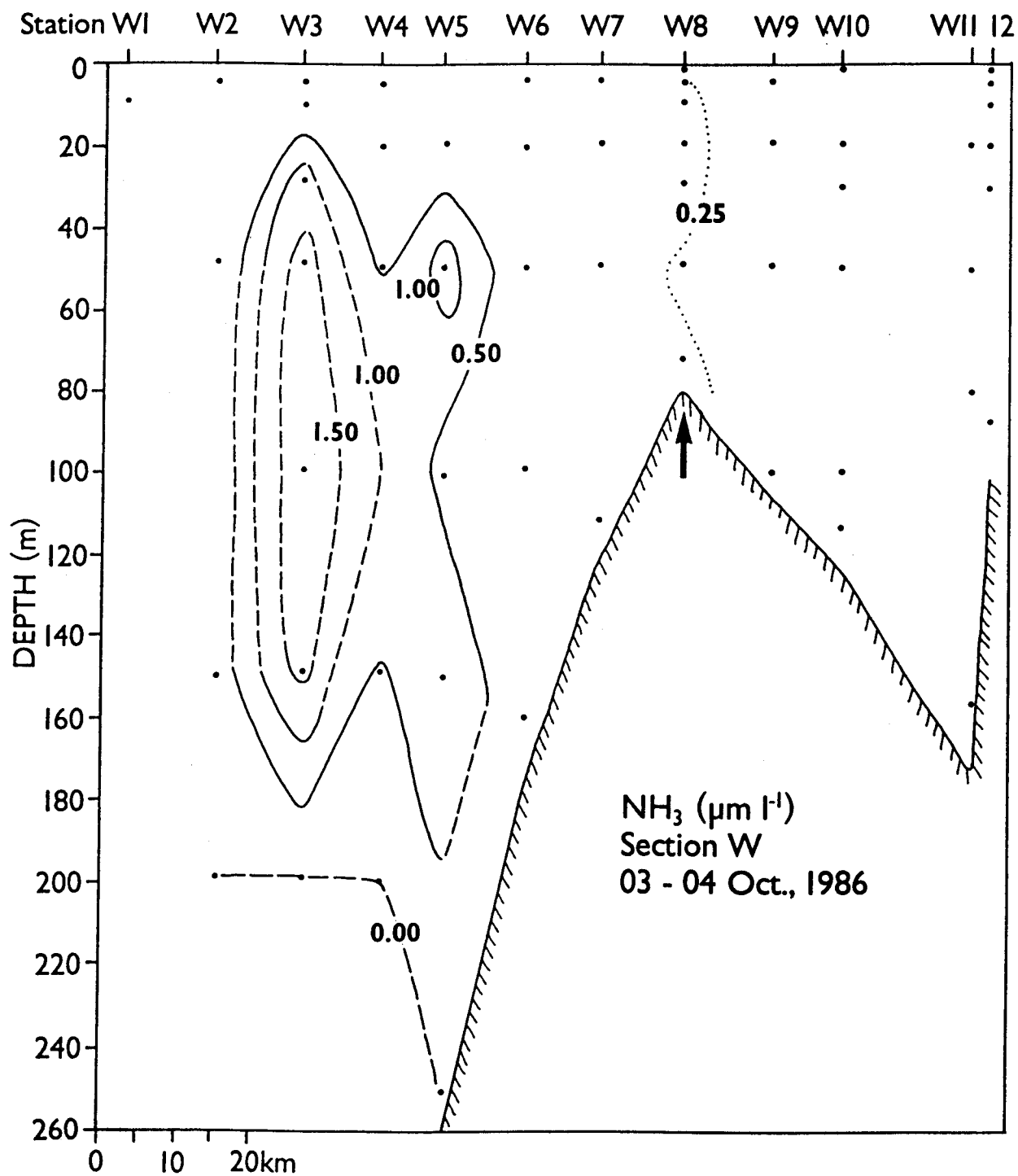


Figure 14. Ammonia at section W in October 1986.

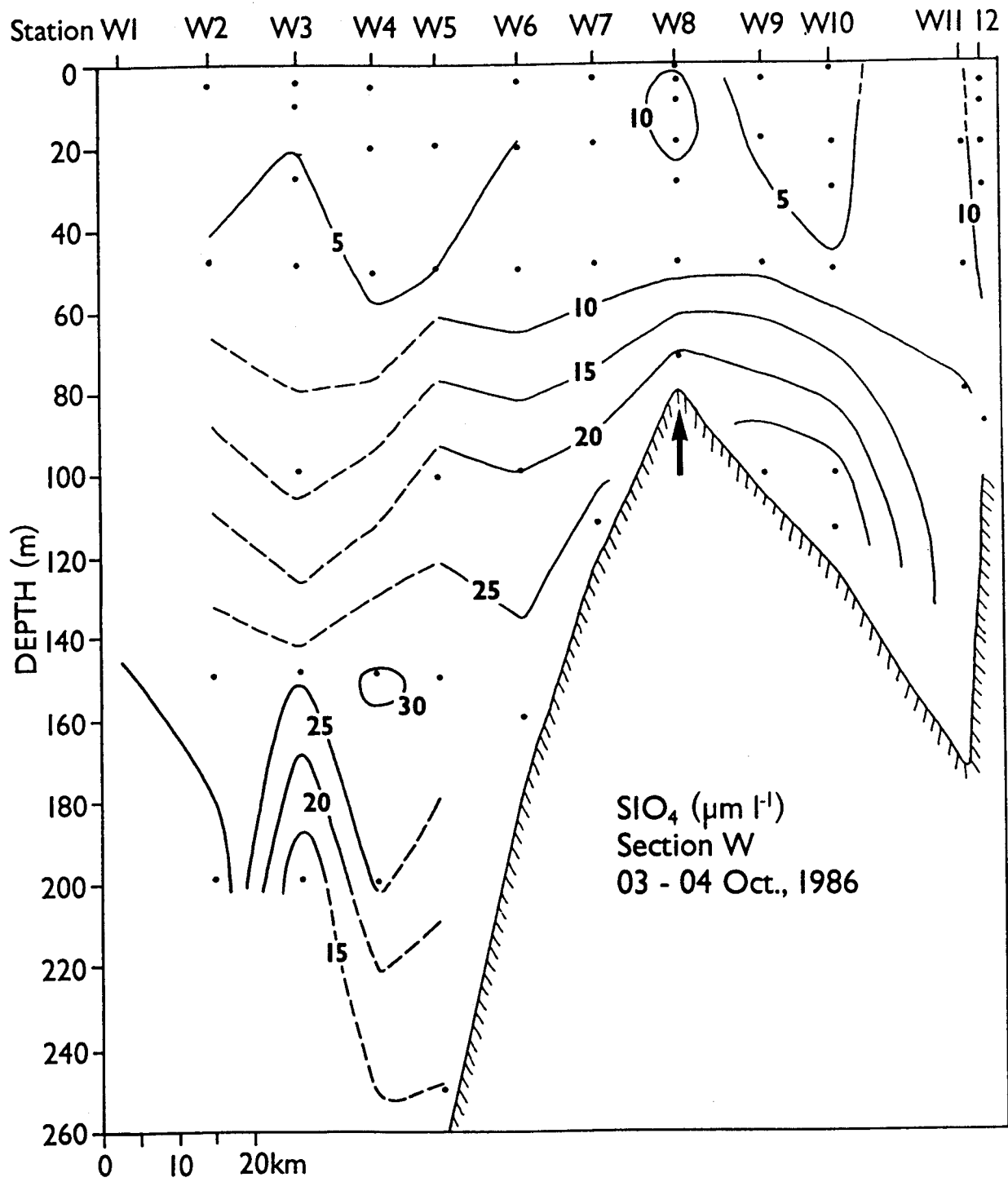


Figure 15. Silicate at section W in October 1986.

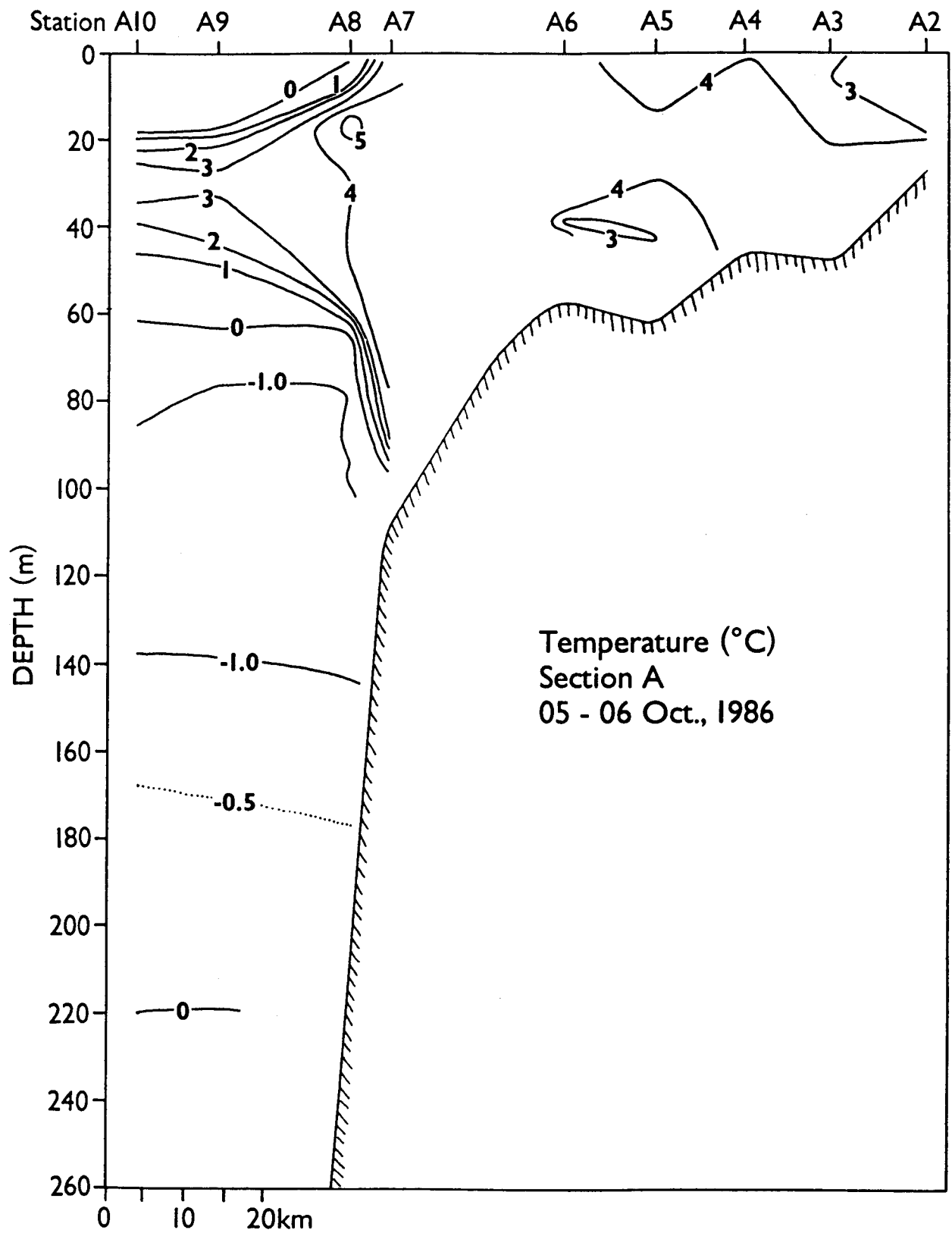


Figure 16. Temperature at section A in October 1986.

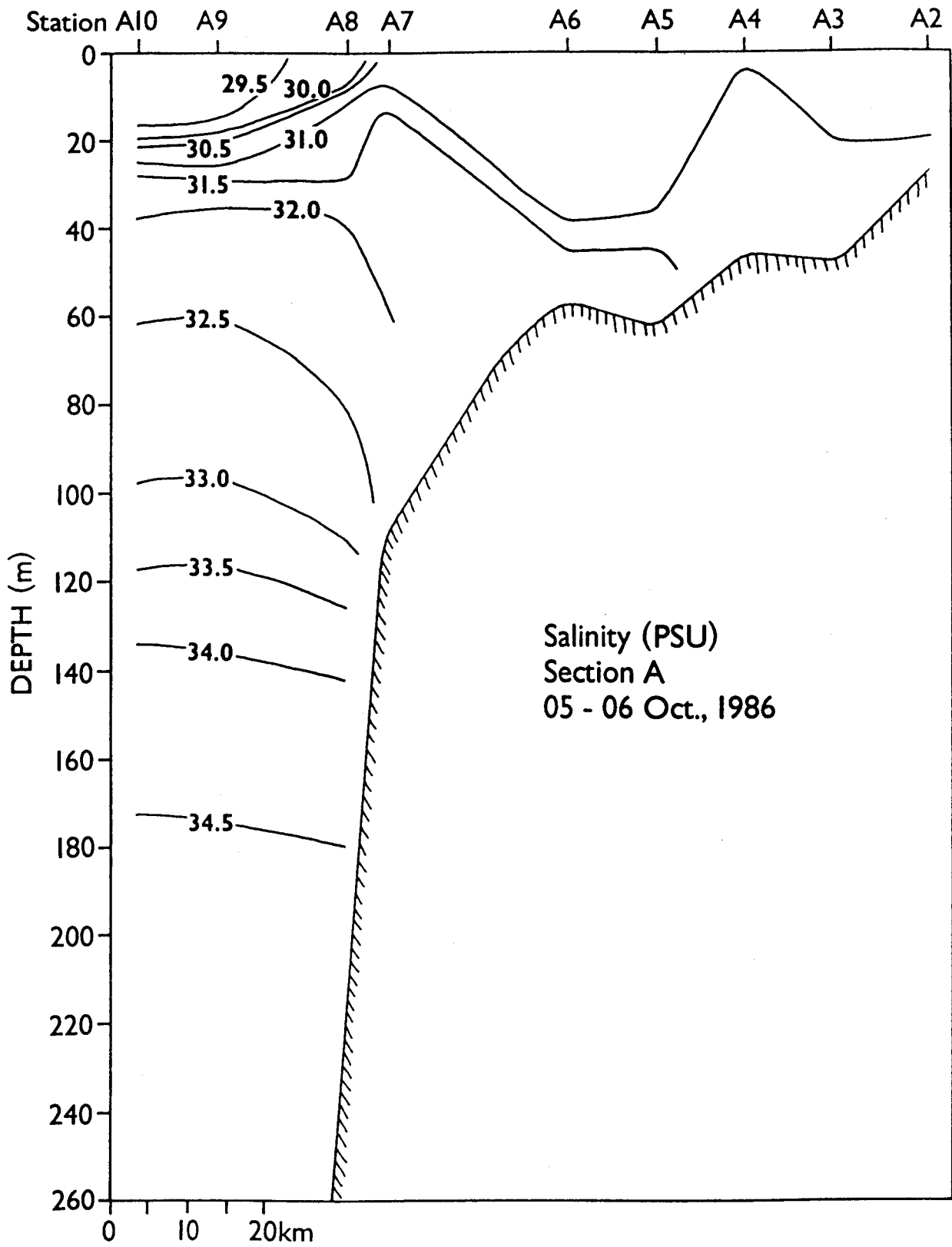


Figure 17. Salinity at section A in October 1986.

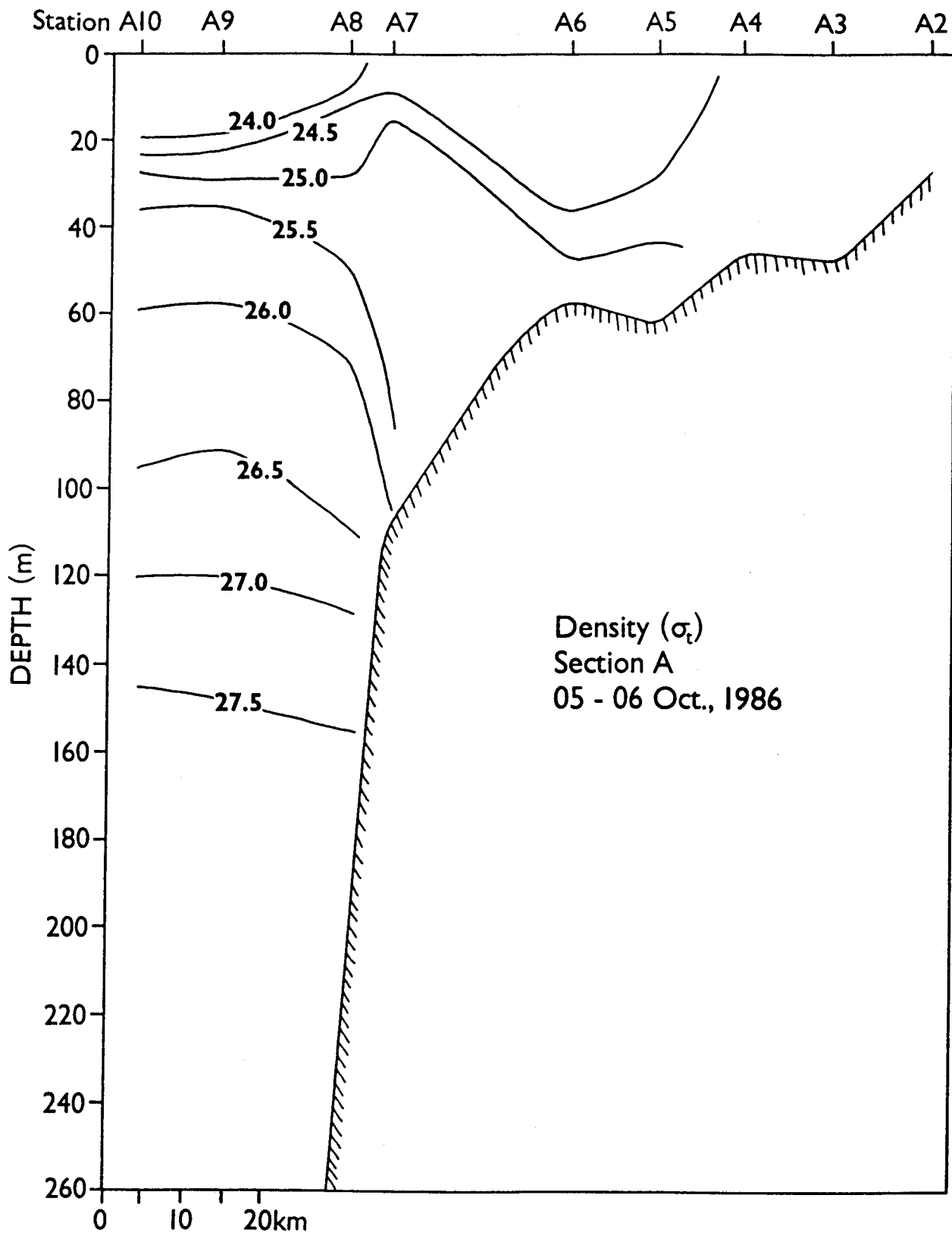


Figure 18. Density at section A in October 1986.

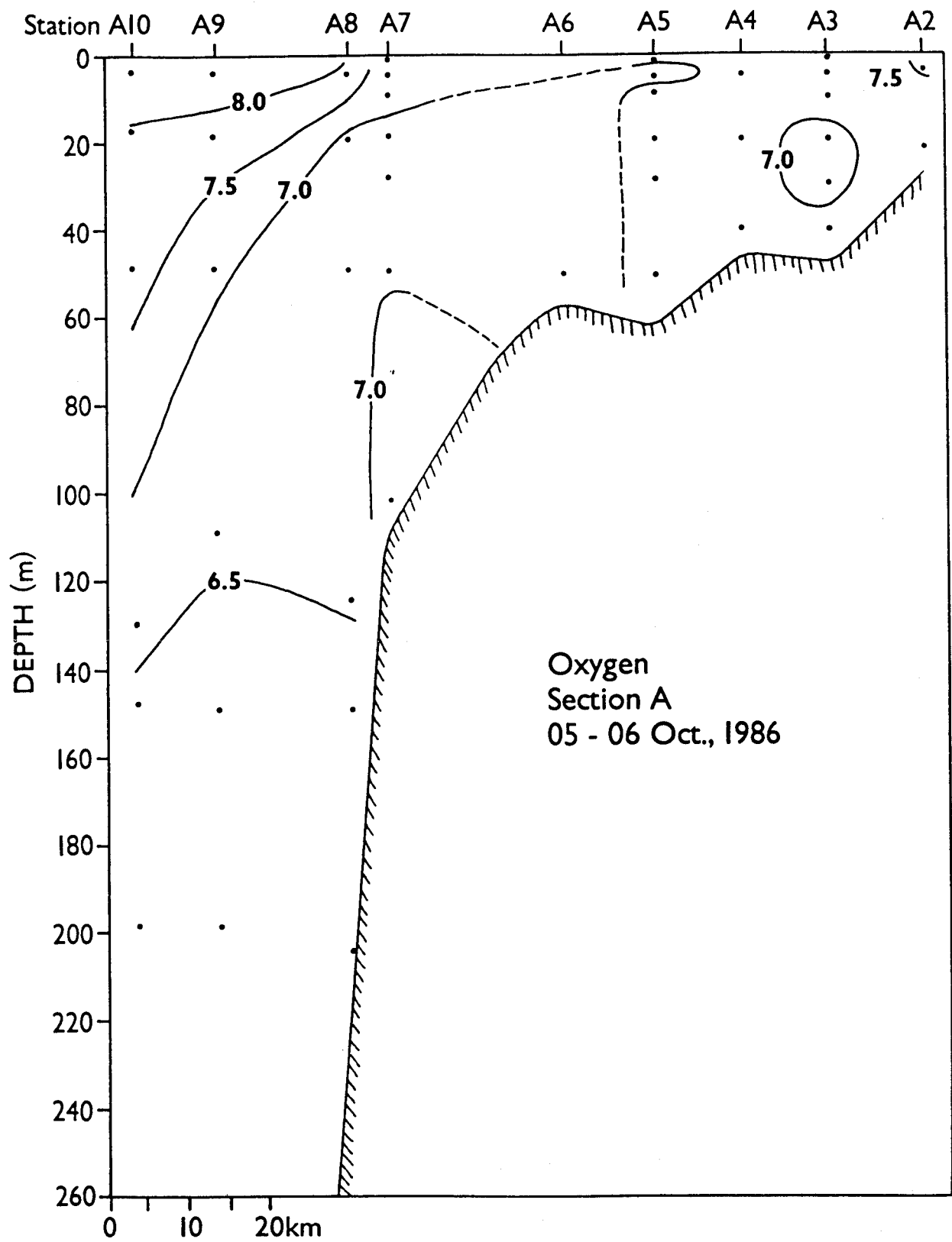


Figure 19. Dissolved oxygen at section A in October 1986.

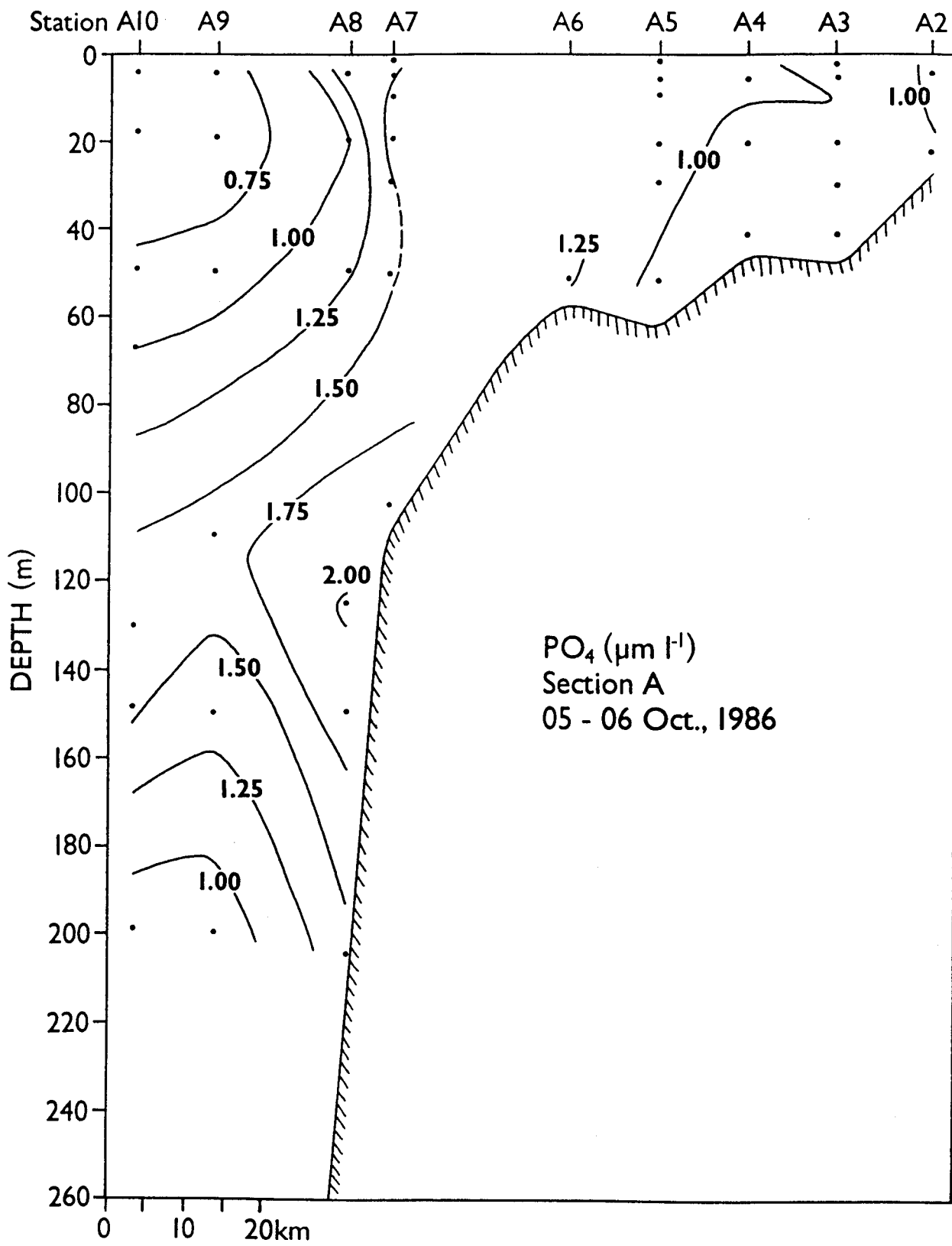


Figure 20. Phosphate at section A in October 1986.

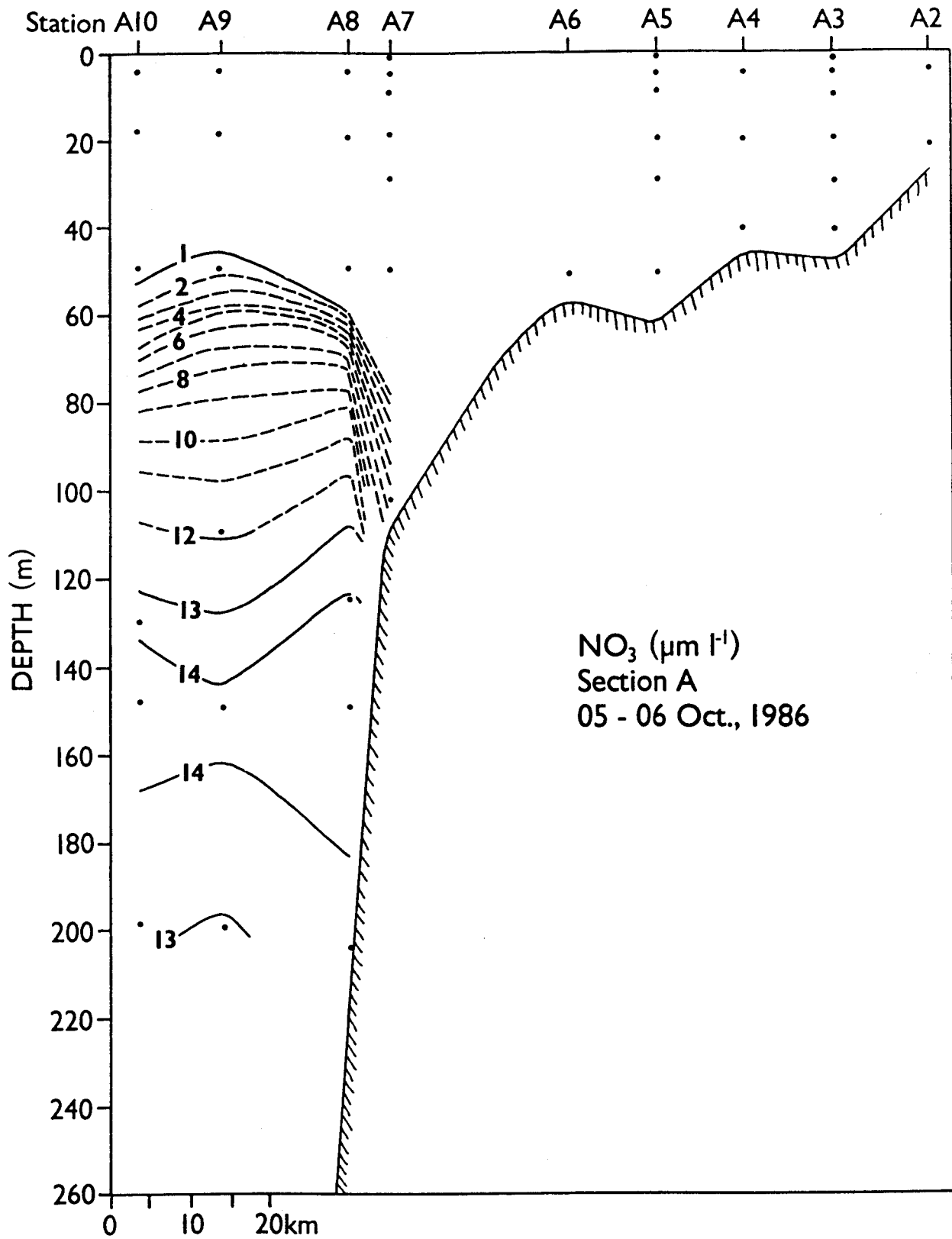


Figure 21. Nitrate at section A in October 1986.

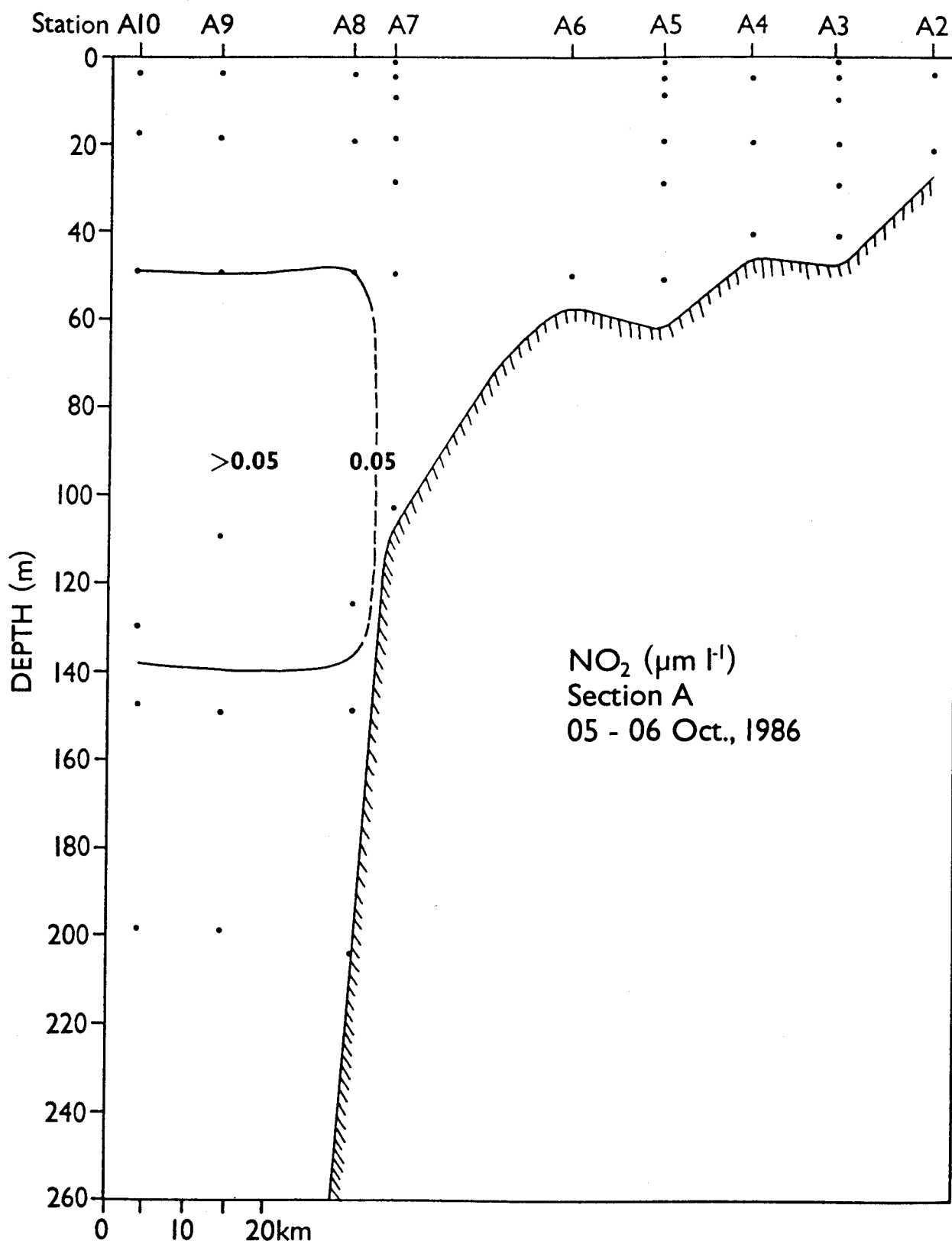


Figure 22. Nitrite at section A in October 1986.

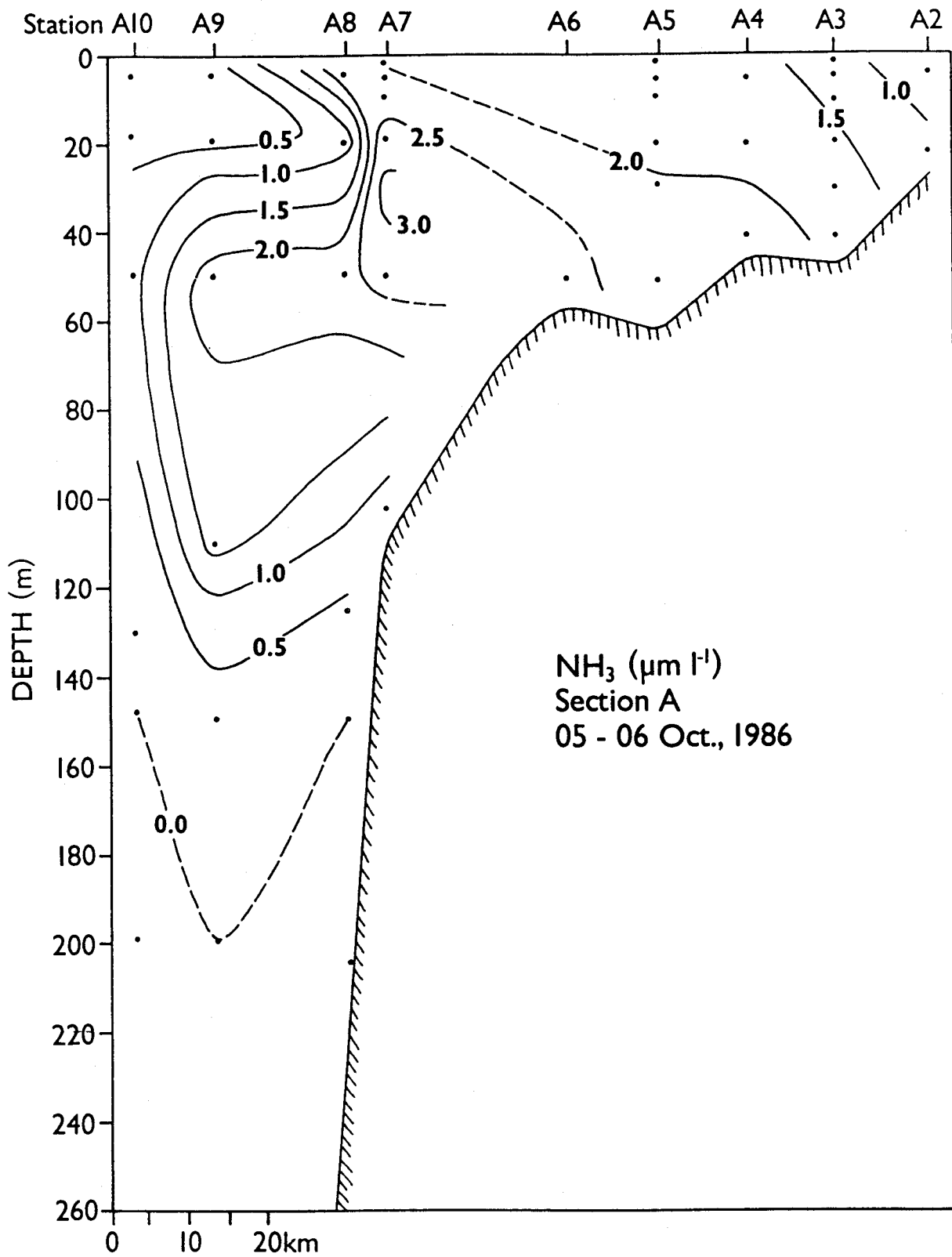


Figure 23. Ammonia at section A in October 1986.

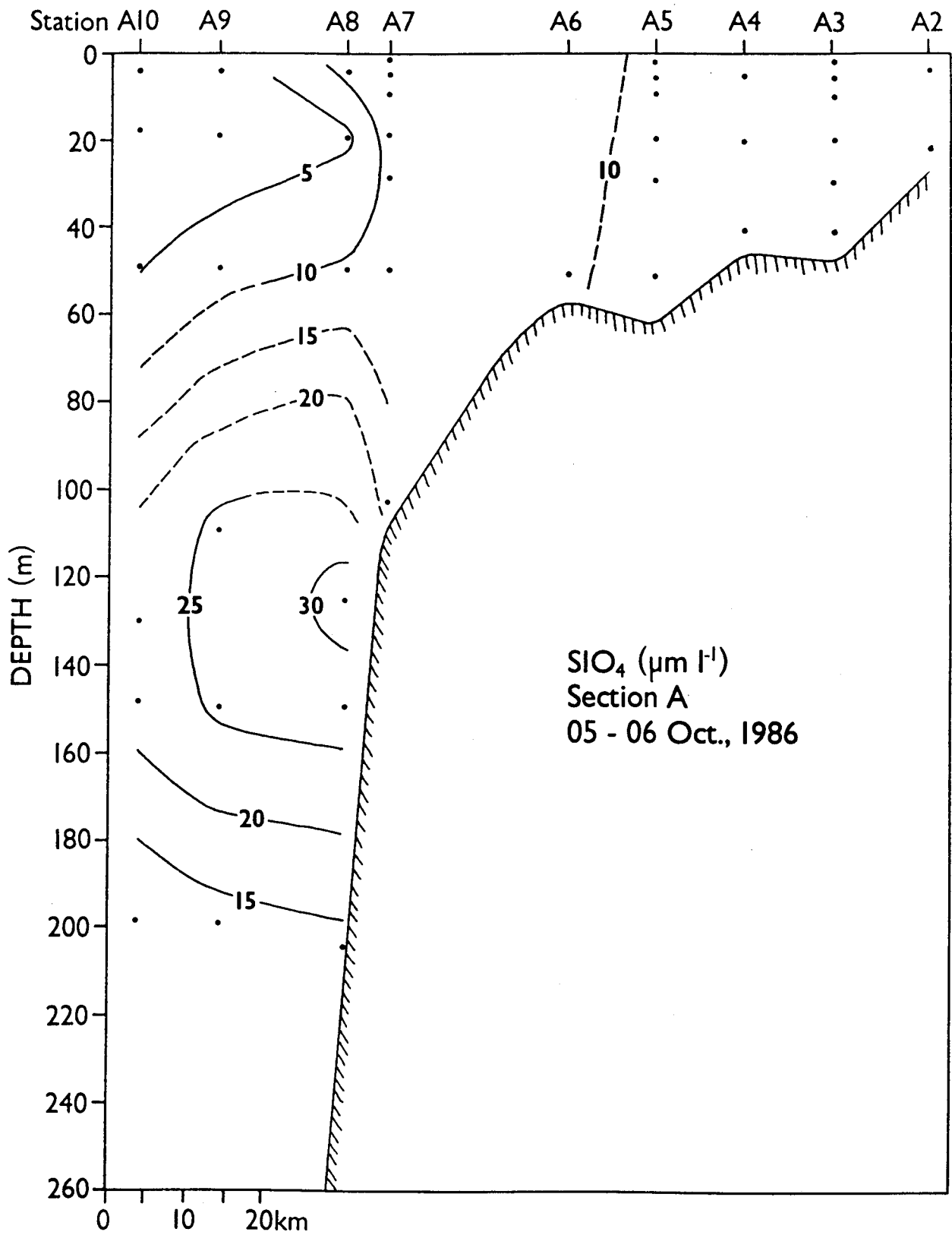


Figure 24. Silicate at section A in October 1986.

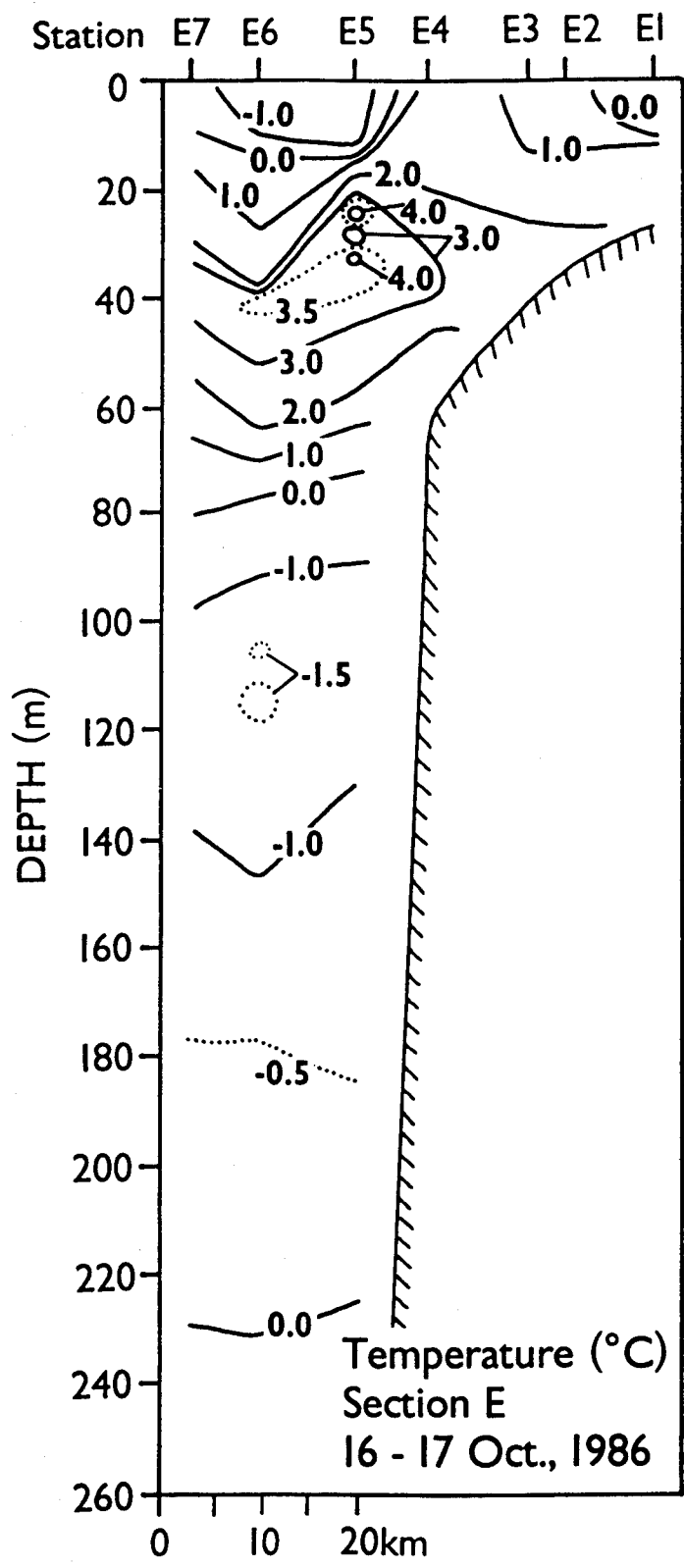


Figure 25. Temperature at section E in October 1986.

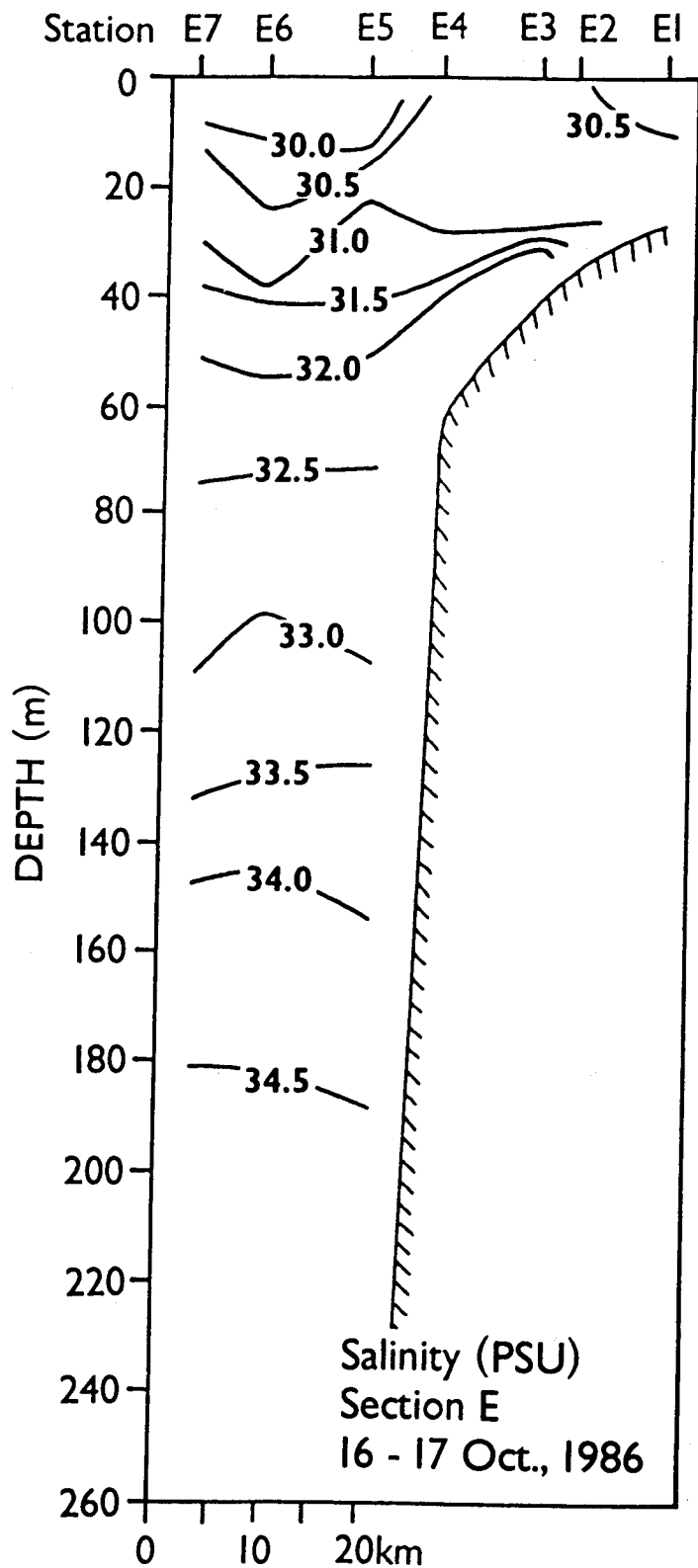


Figure 26. Salinity at section E in October 1986.

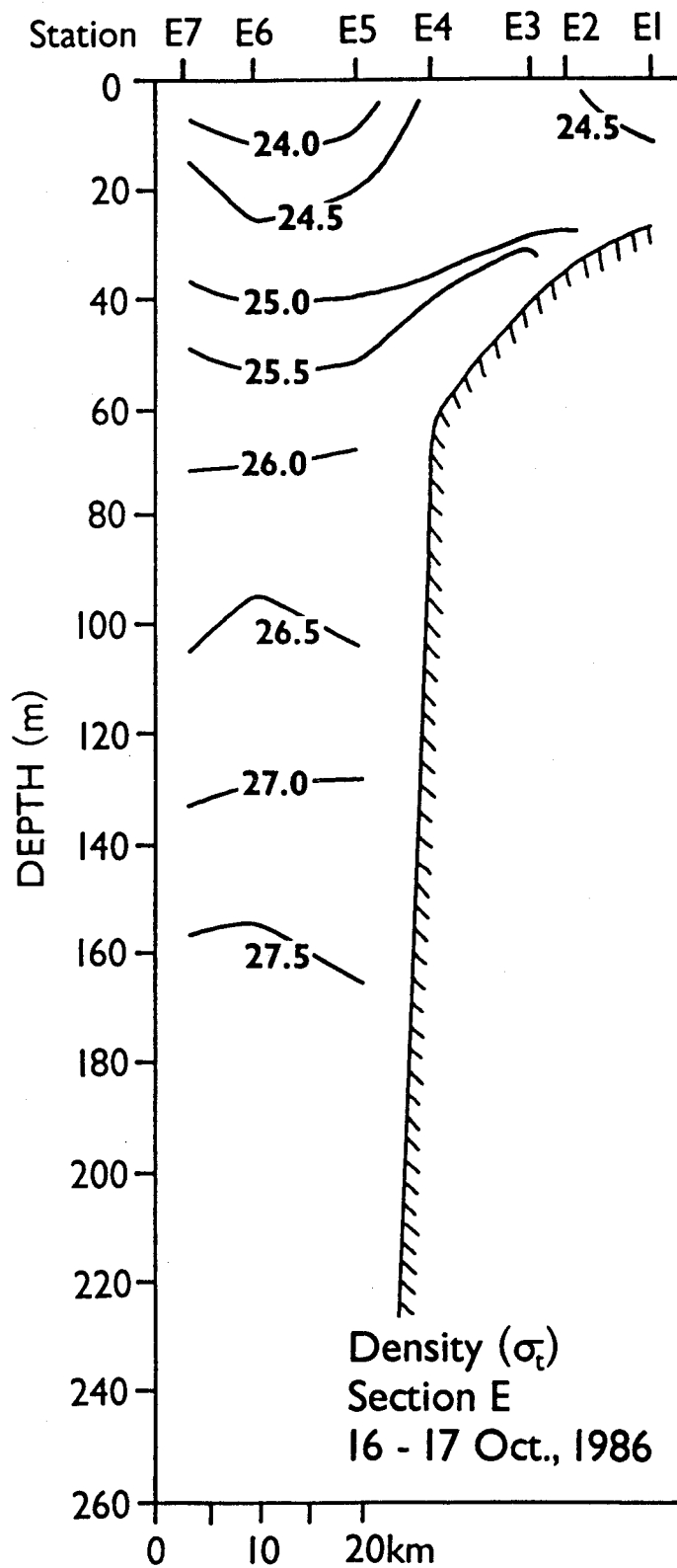


Figure 27. Density at section E in October 1986.

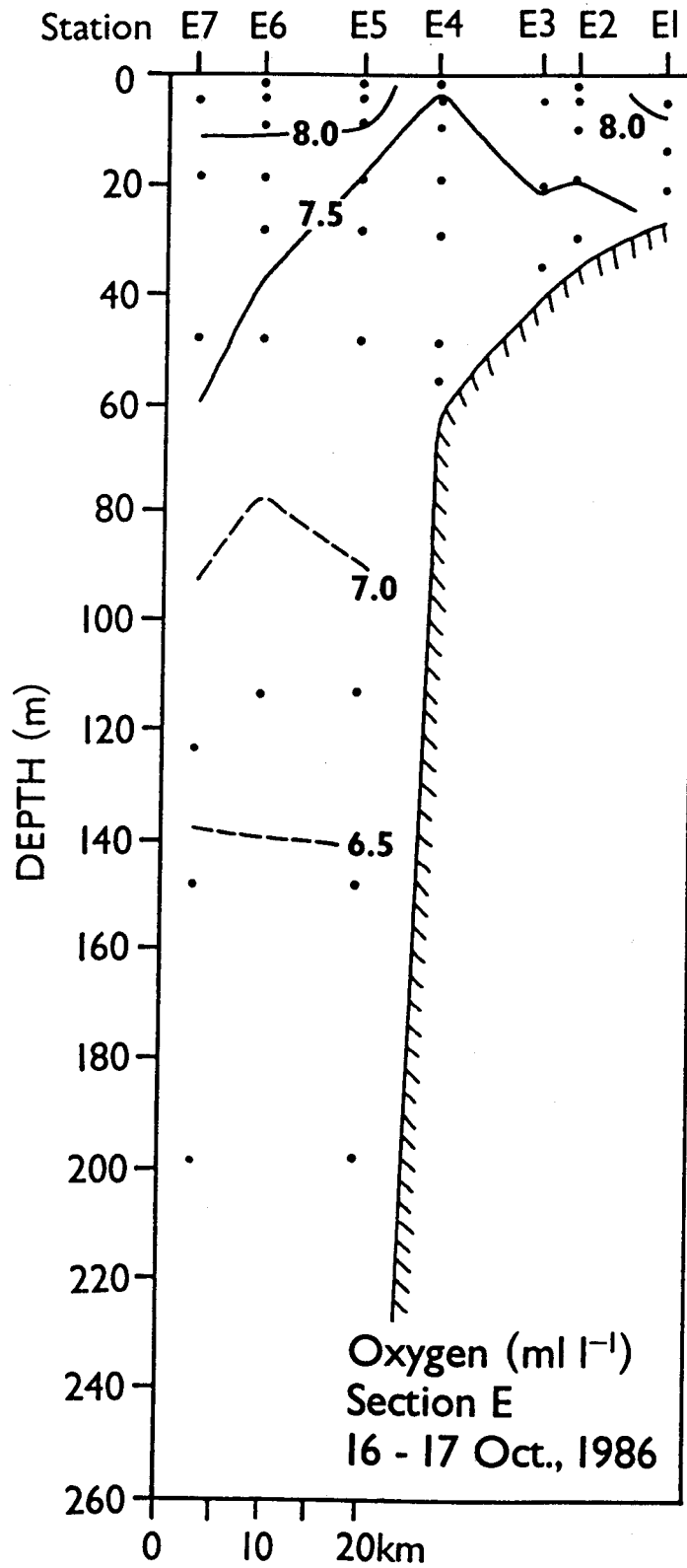


Figure 28. Dissolved oxygen at section E in October 1986.

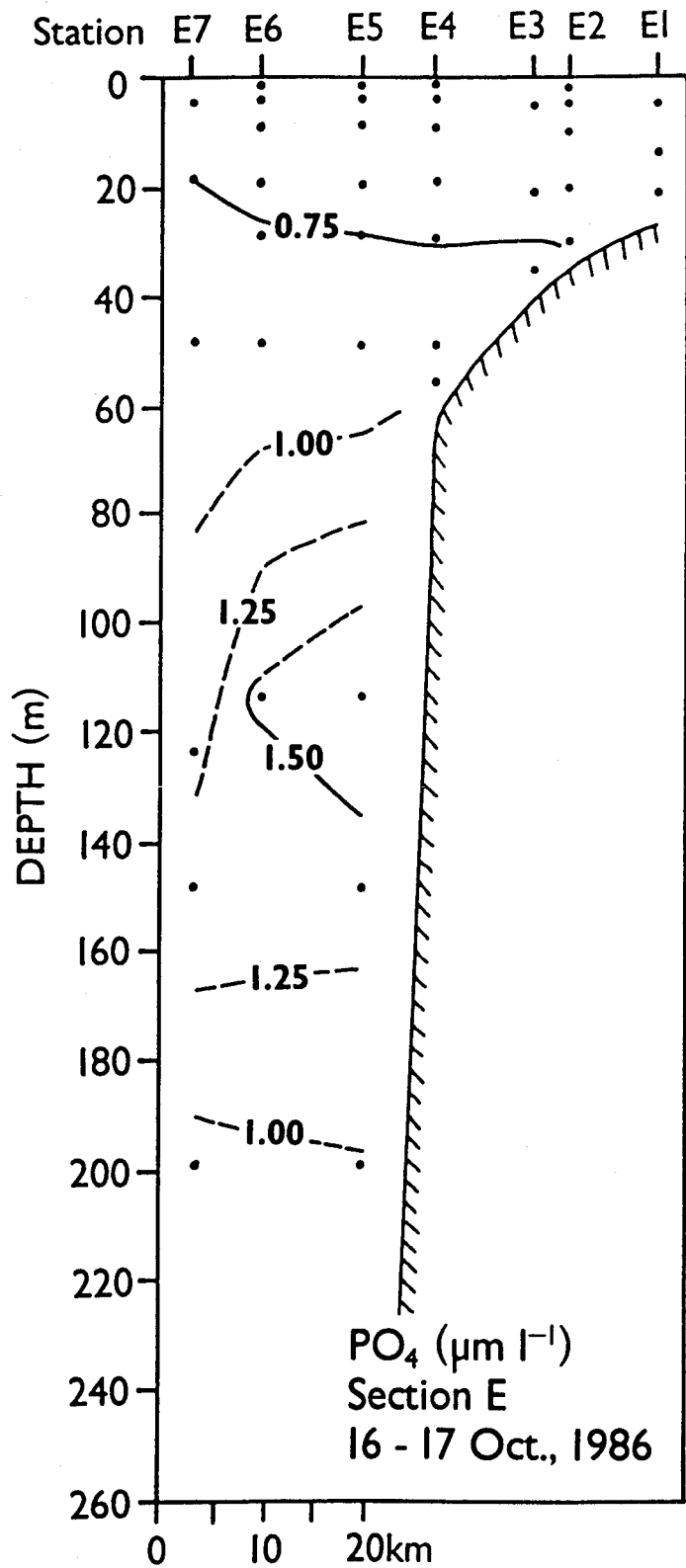


Figure 29. Phosphate at section E in October 1986.

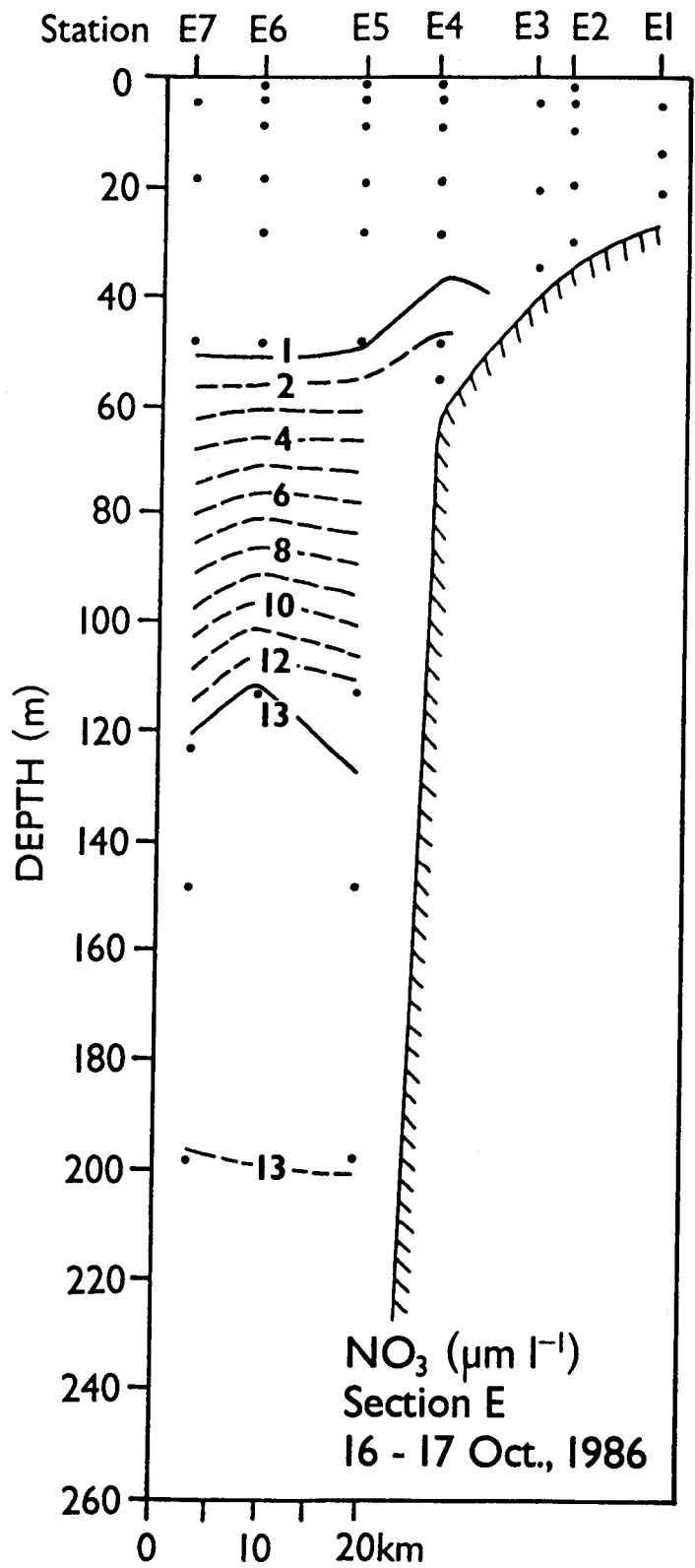


Figure 30. Nitrate at section E in October 1986.

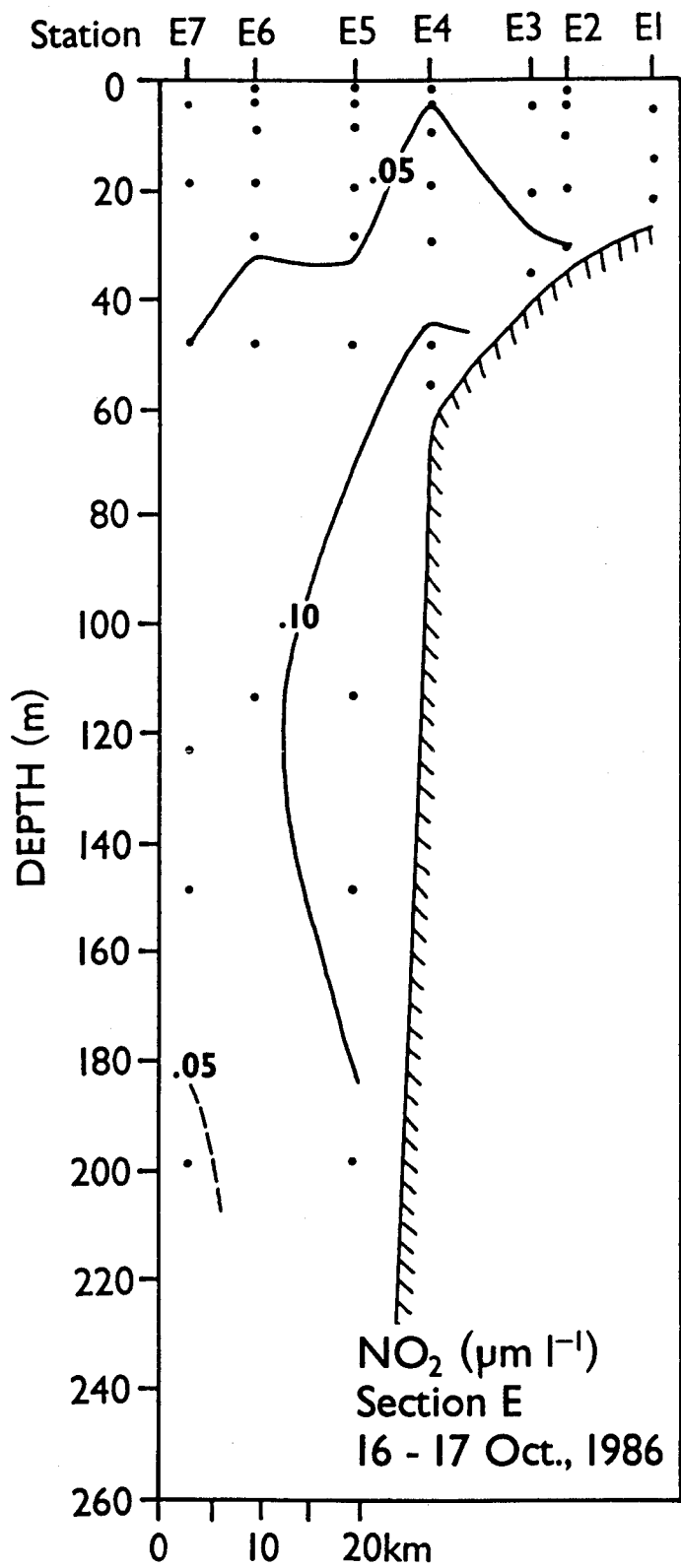


Figure 31. Nitrite at section E in October 1986.

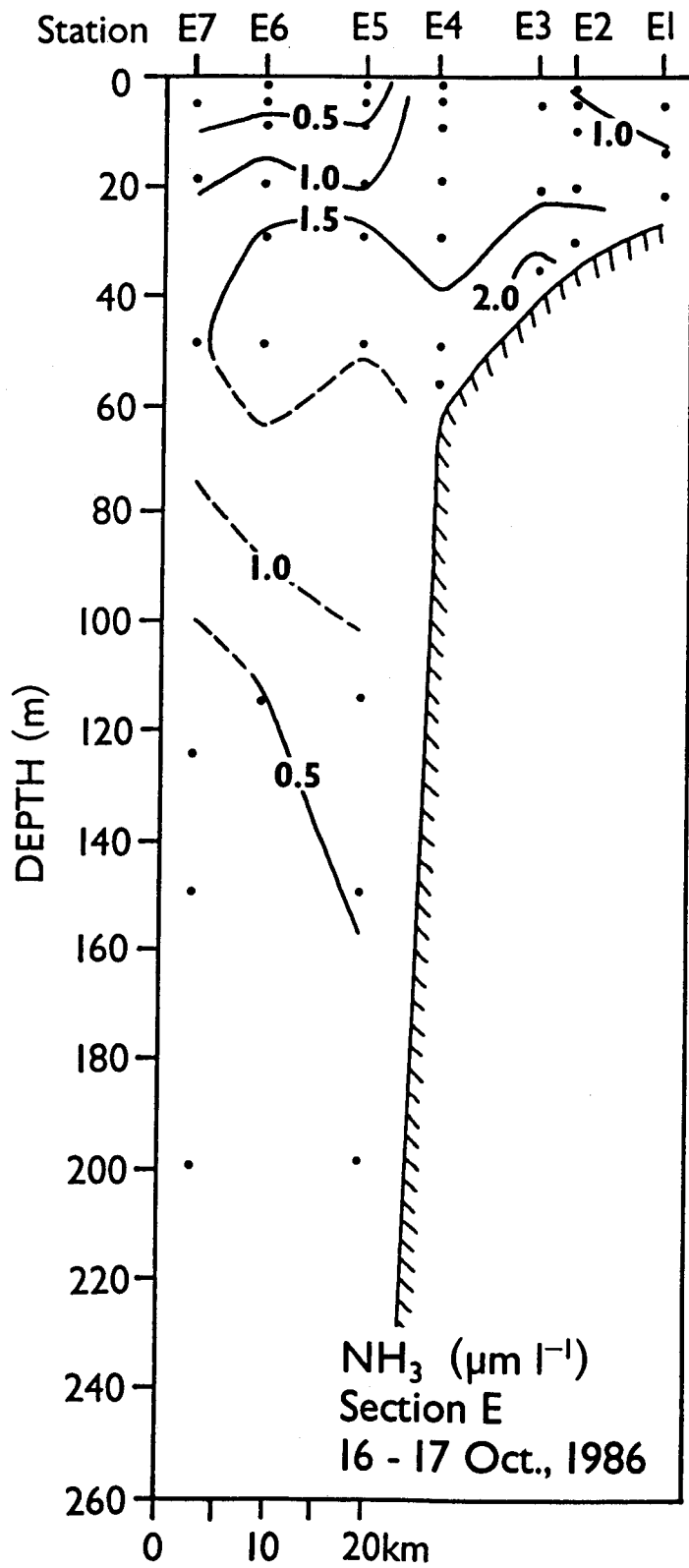


Figure 32. Ammonia at section E in October 1986.

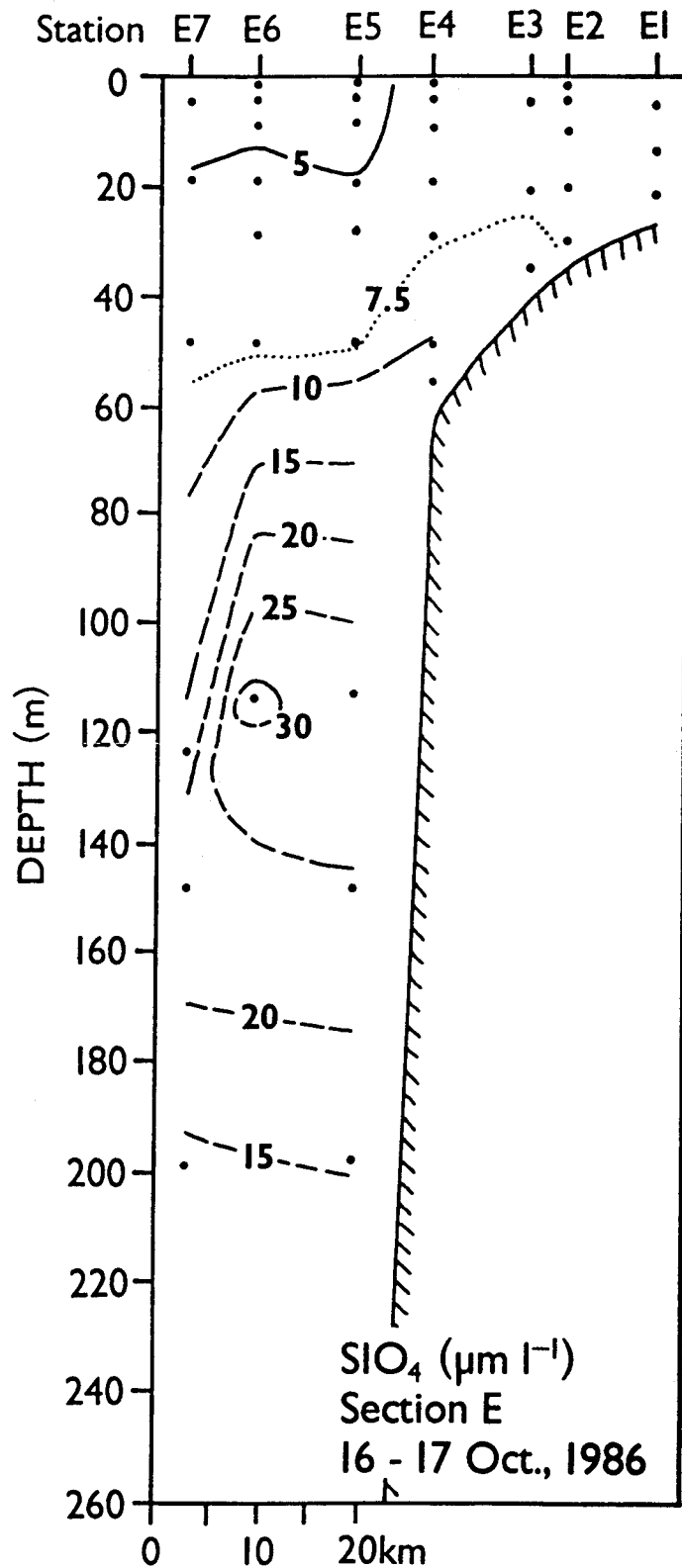


Figure 33. Silicate at section E in October 1986.

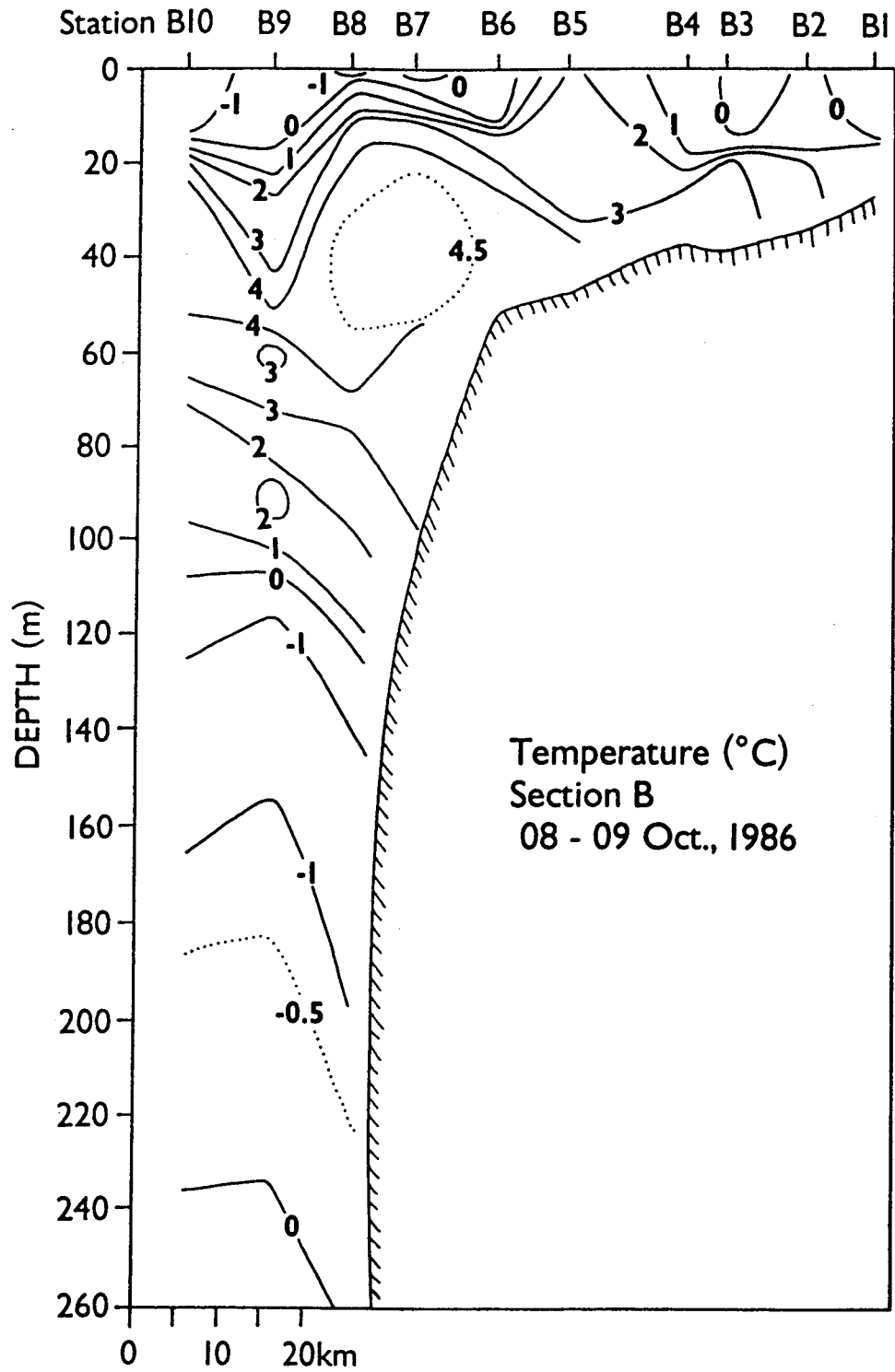


Figure 34. Temperature at section B in October 1986.

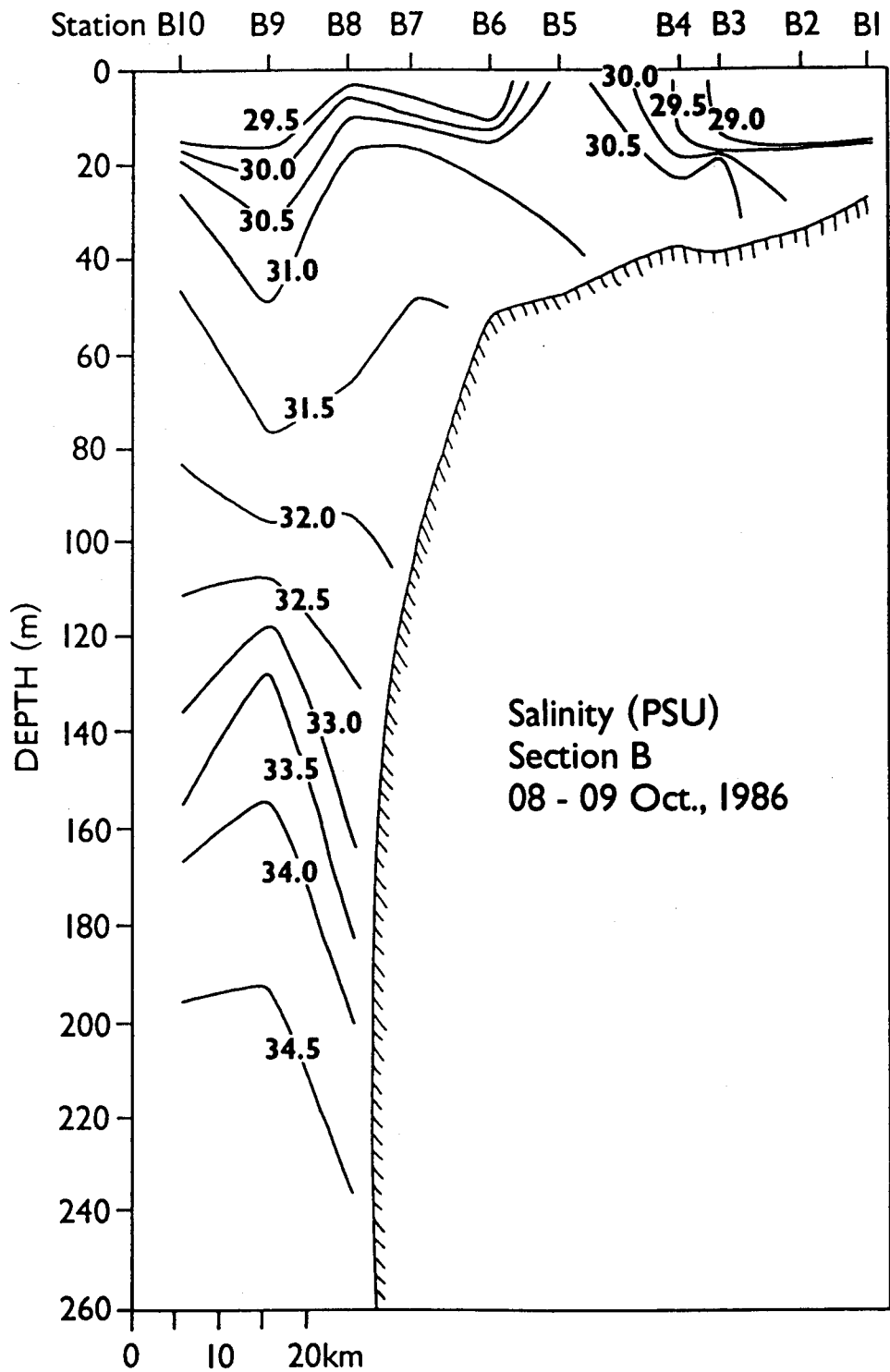


Figure 35. Salinity at section B in October 1986.

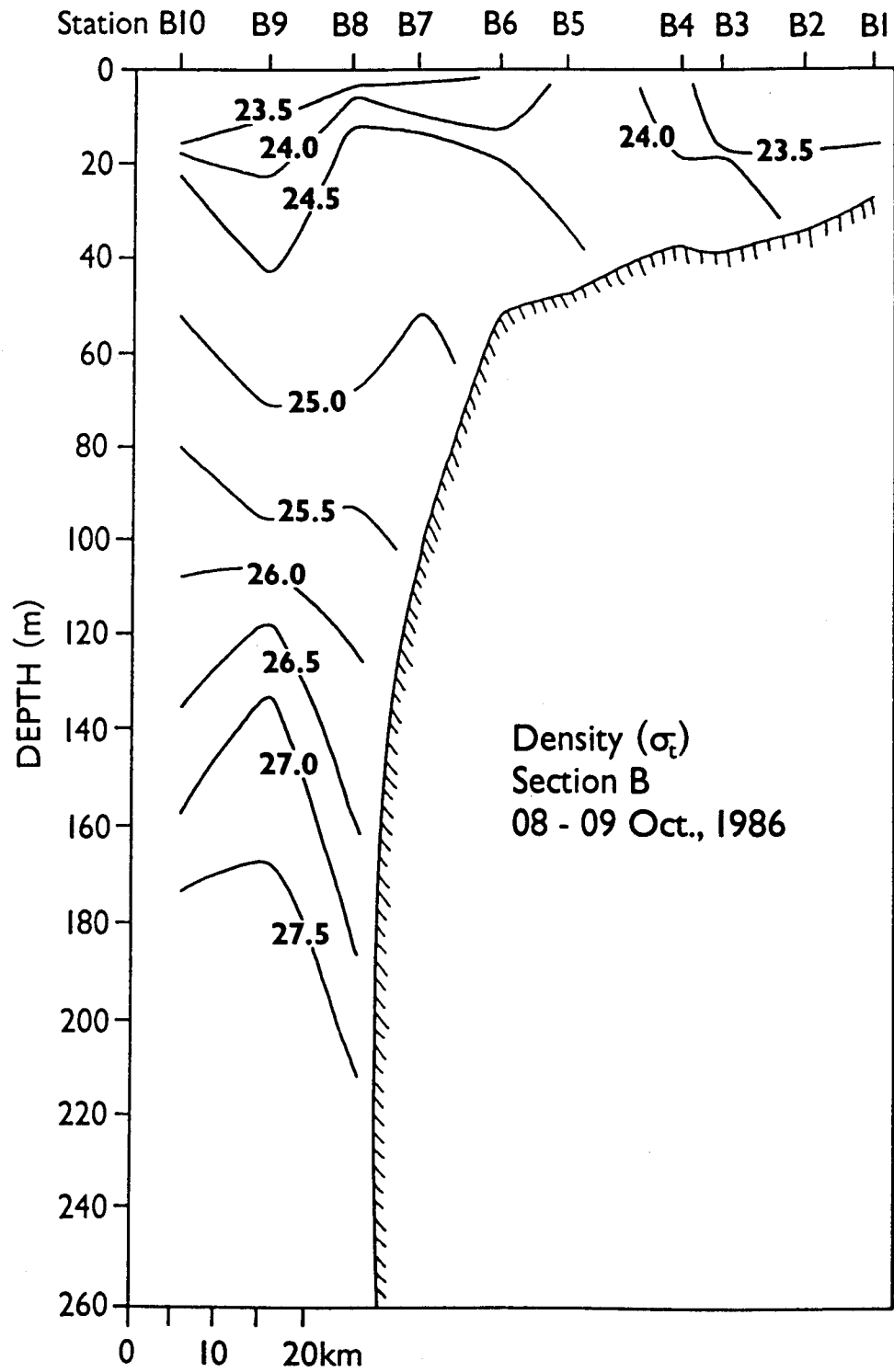


Figure 36. Density at section B in October 1986.

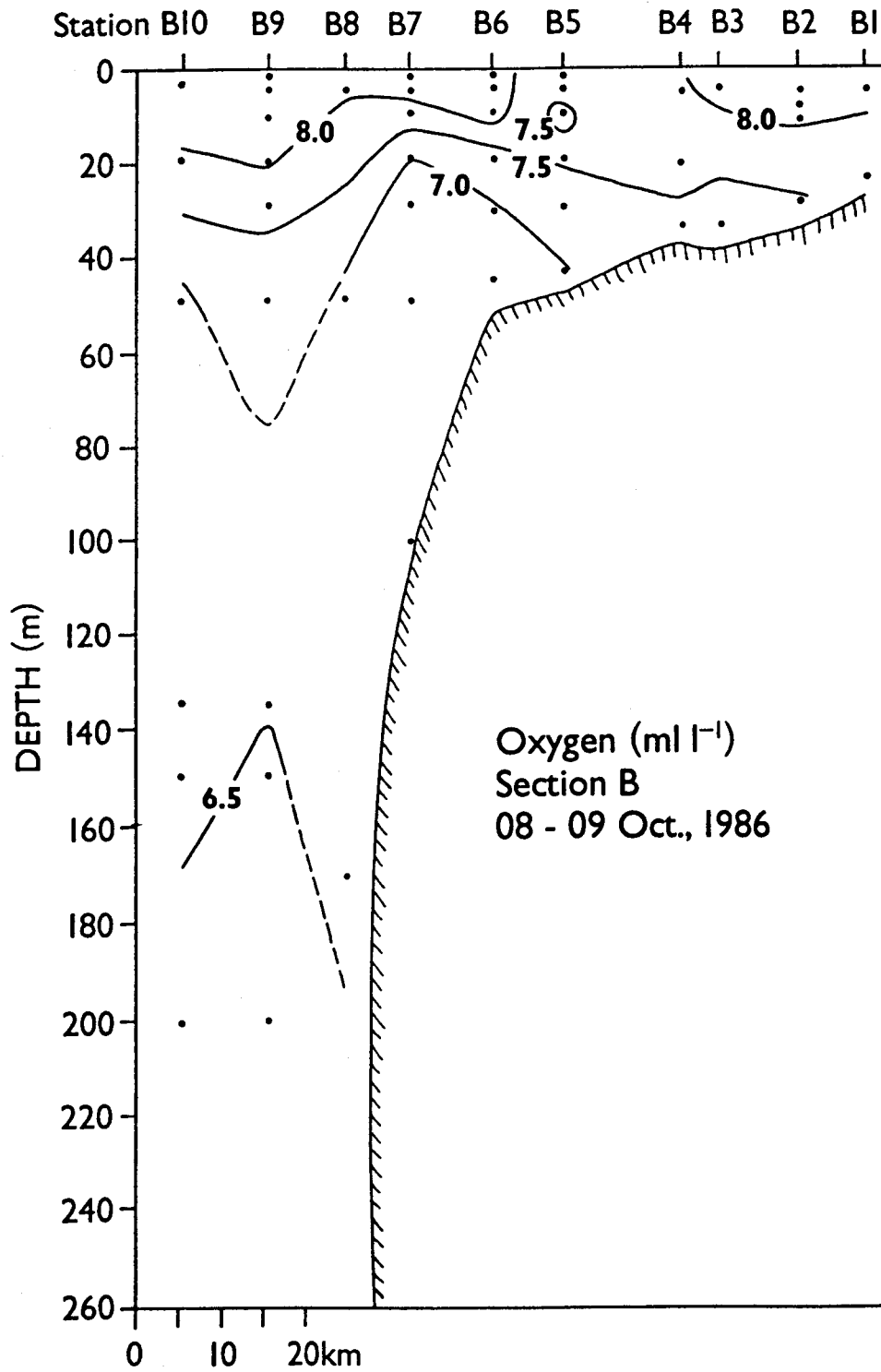


Figure 37. Dissolved oxygen at section B in October 1986.

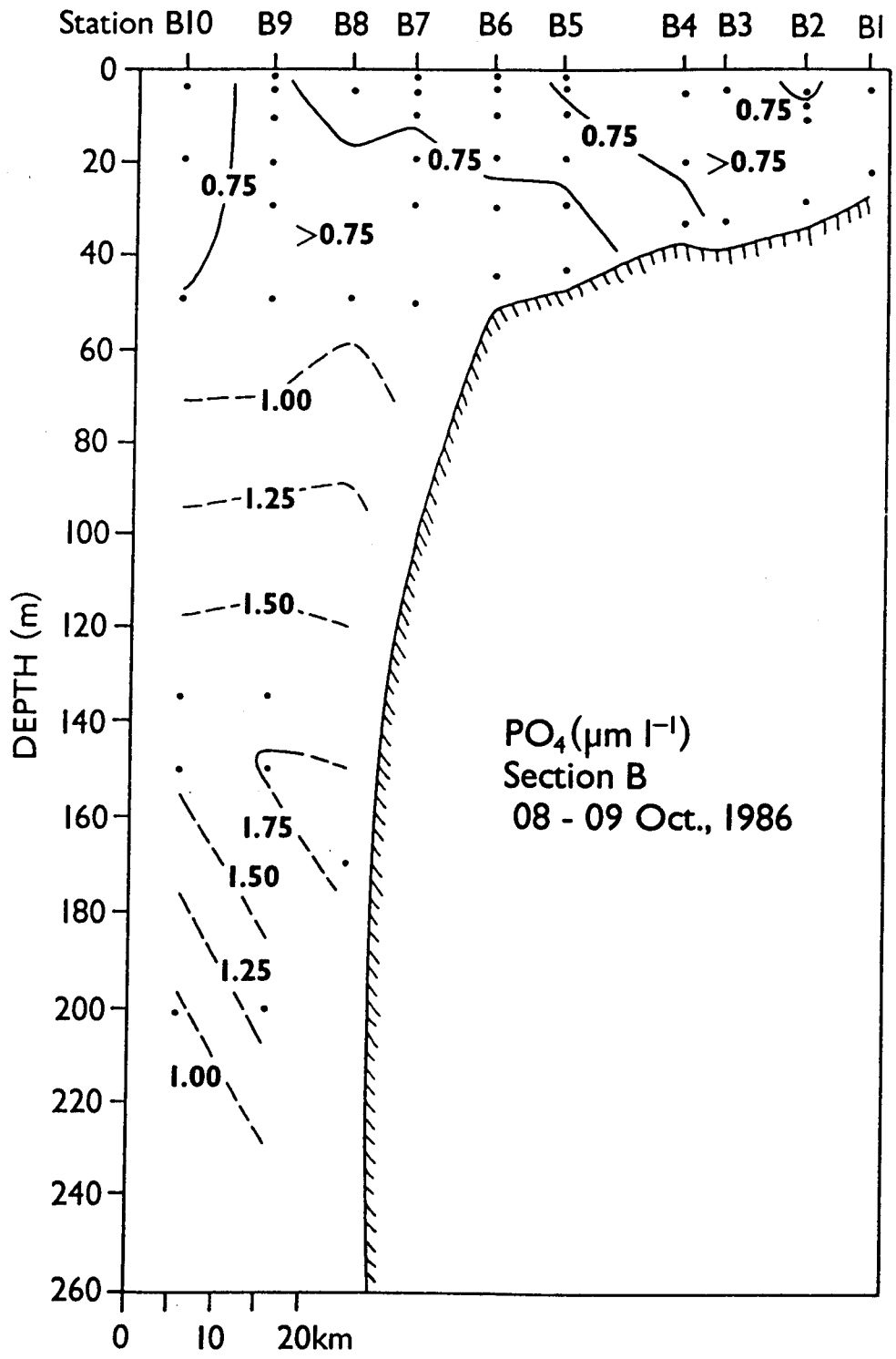


Figure 38. Phosphate at section B in October 1986.

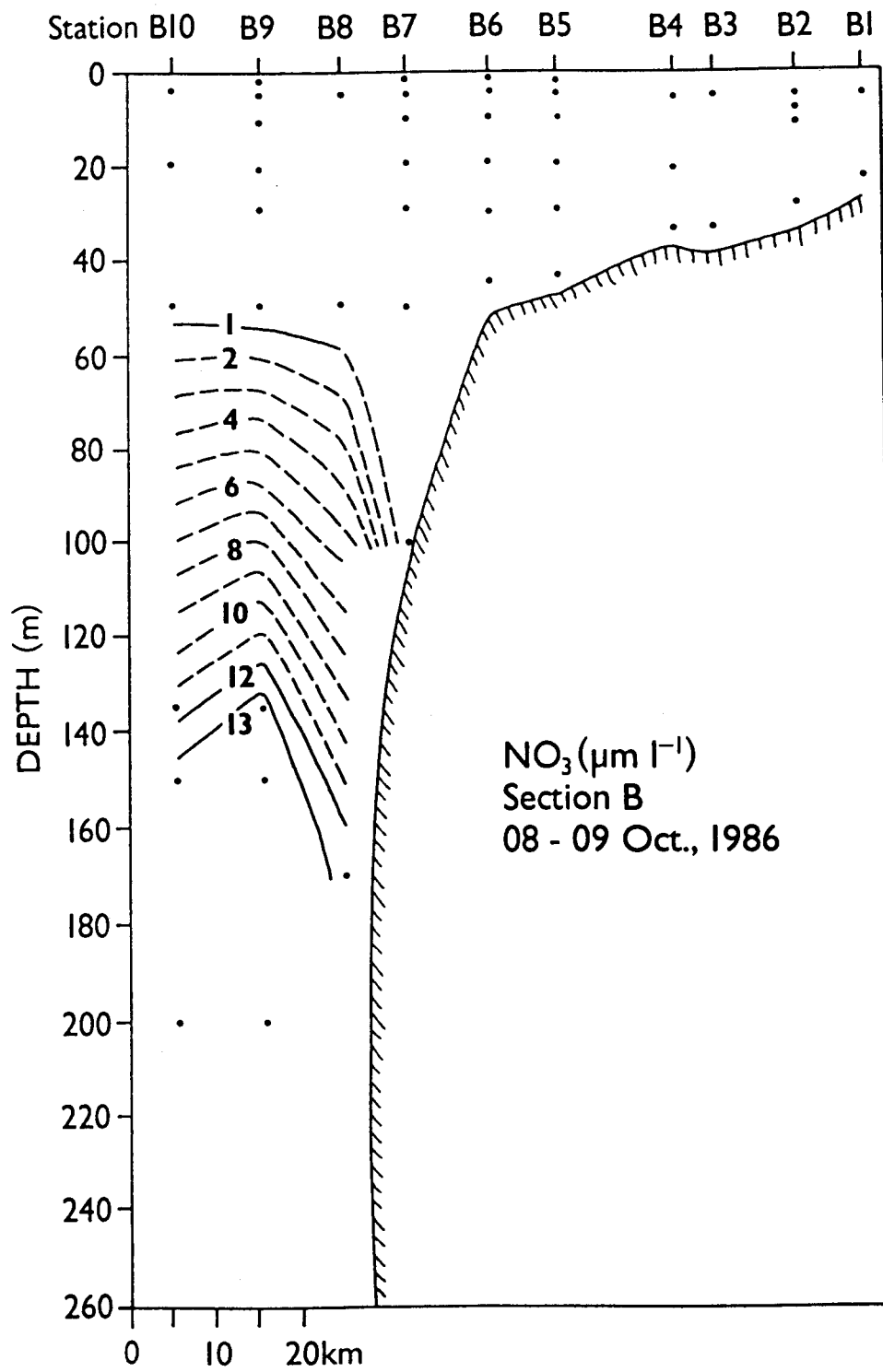


Figure 39. Nitrate at section B in October 1986.

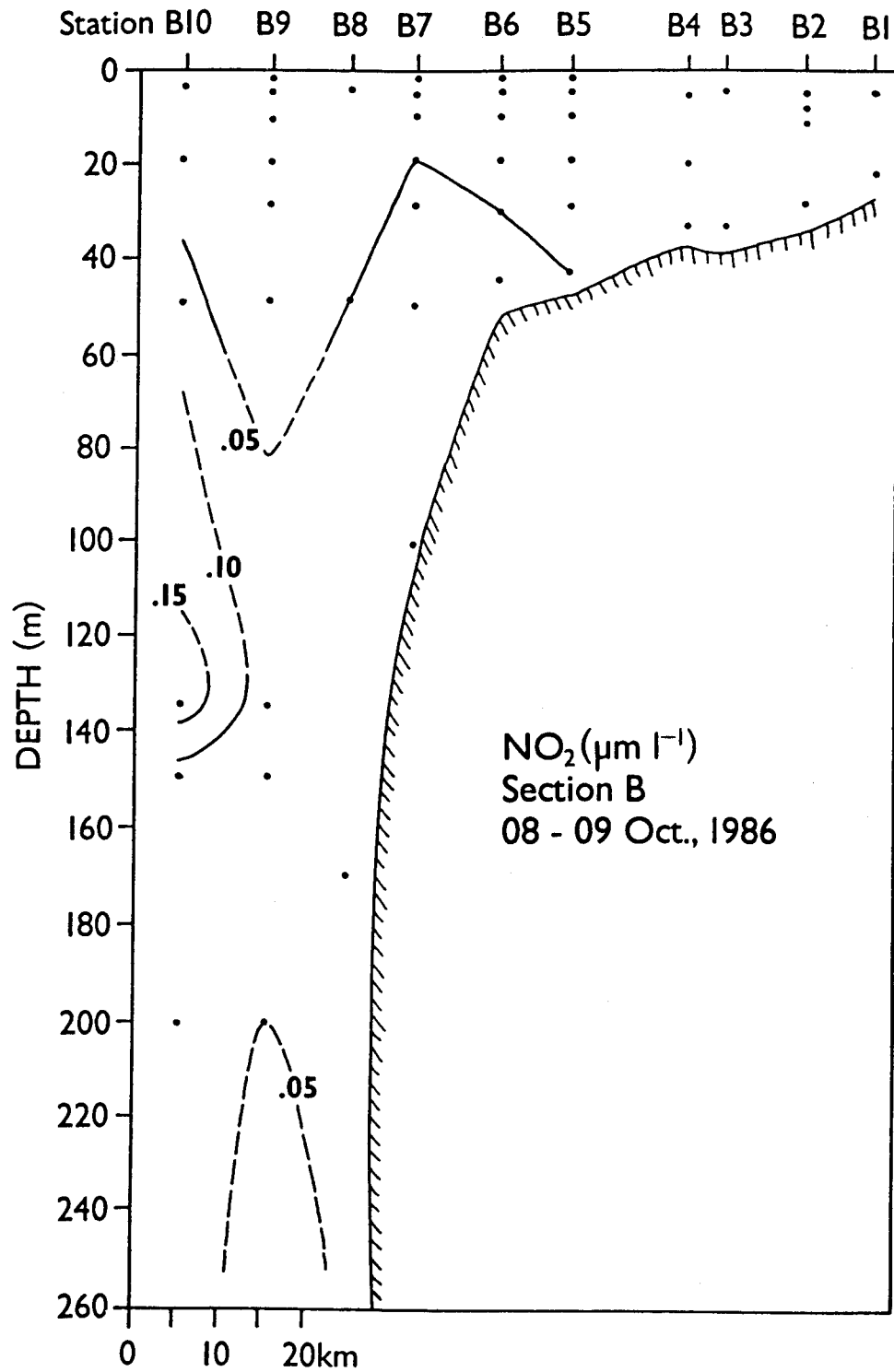


Figure 40. Nitrite at section B in October 1986.

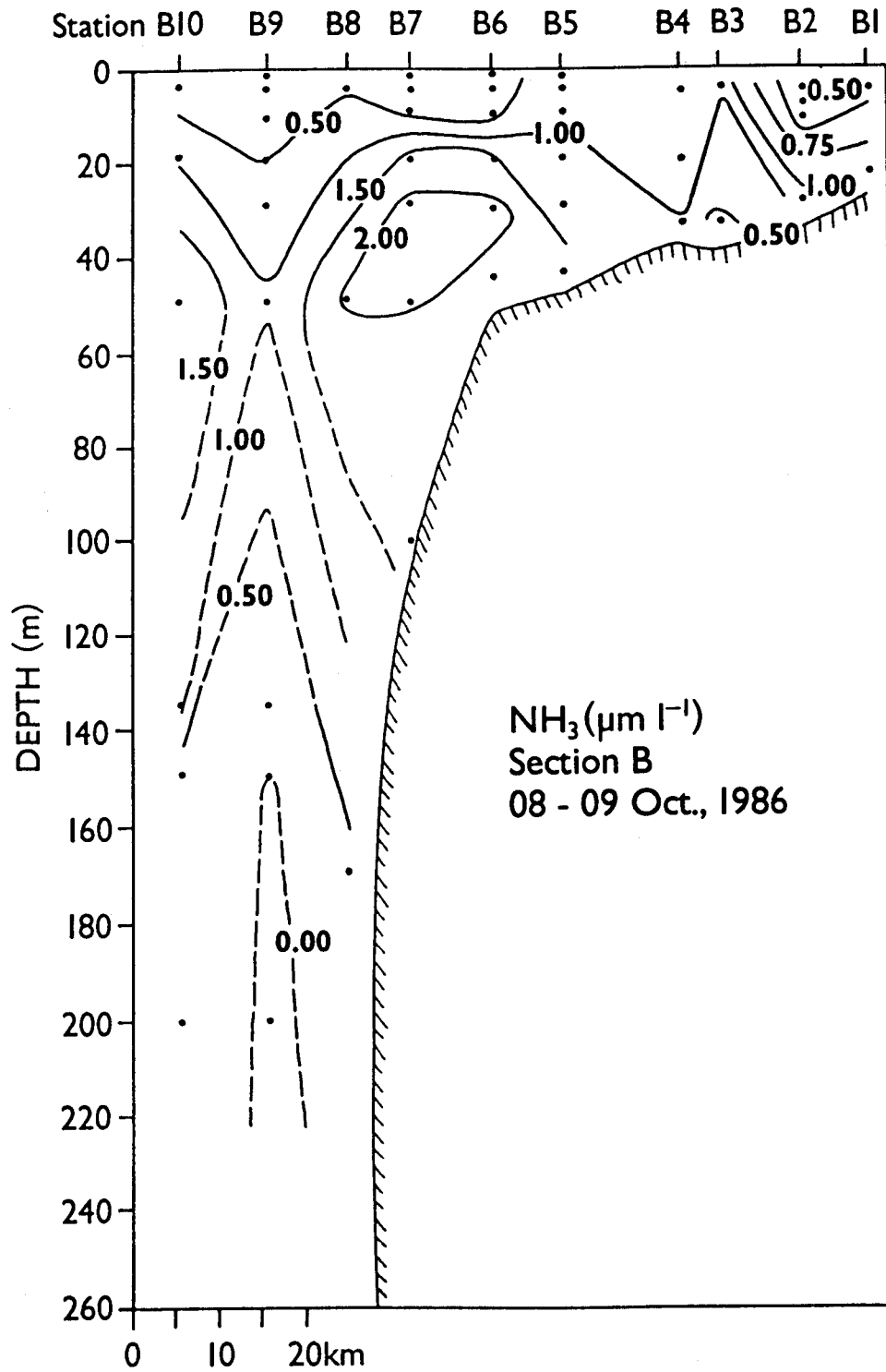


Figure 41. Ammonia at section B in October 1986.

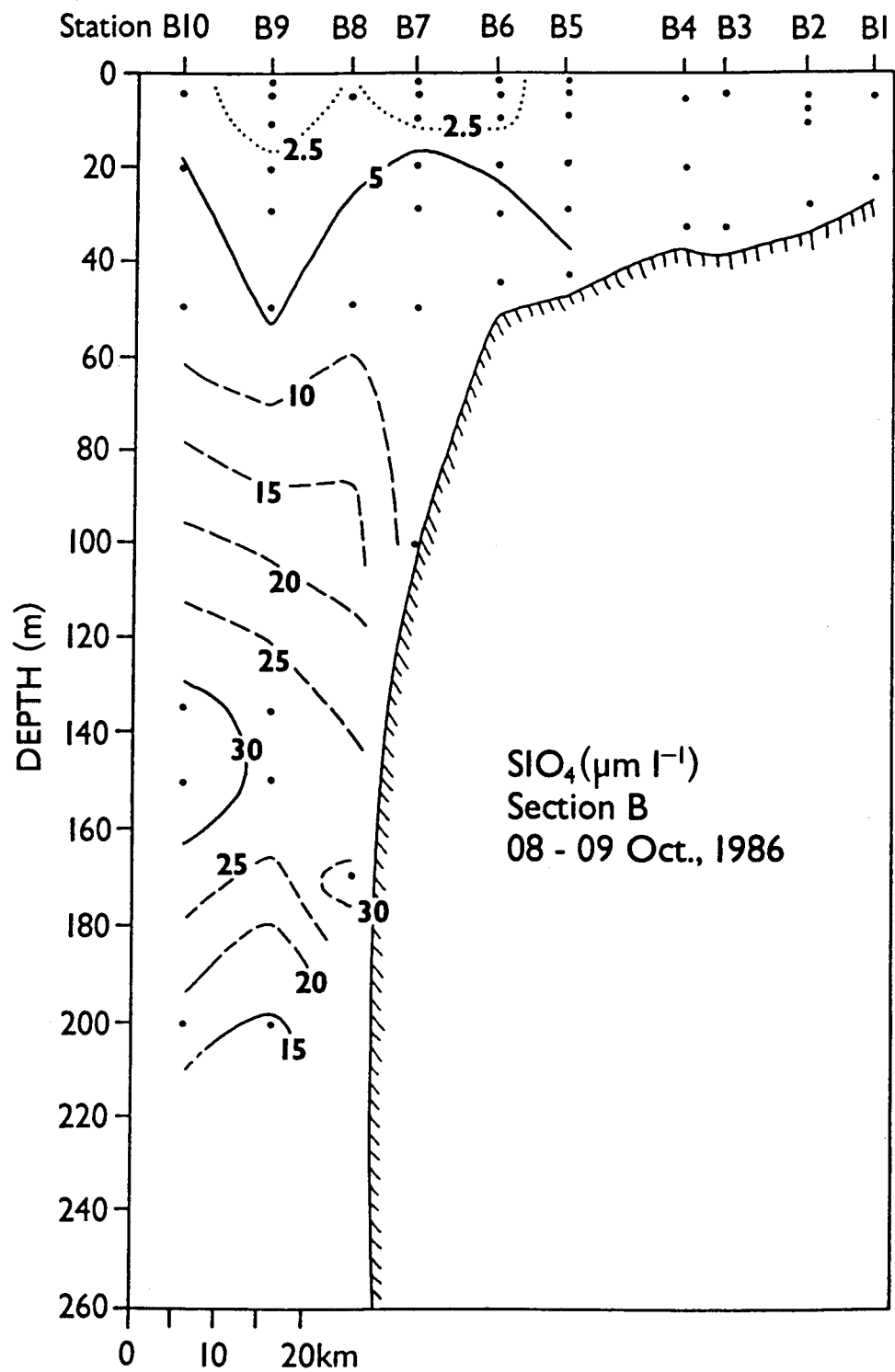


Figure 42. Silicate at section B in October 1986.

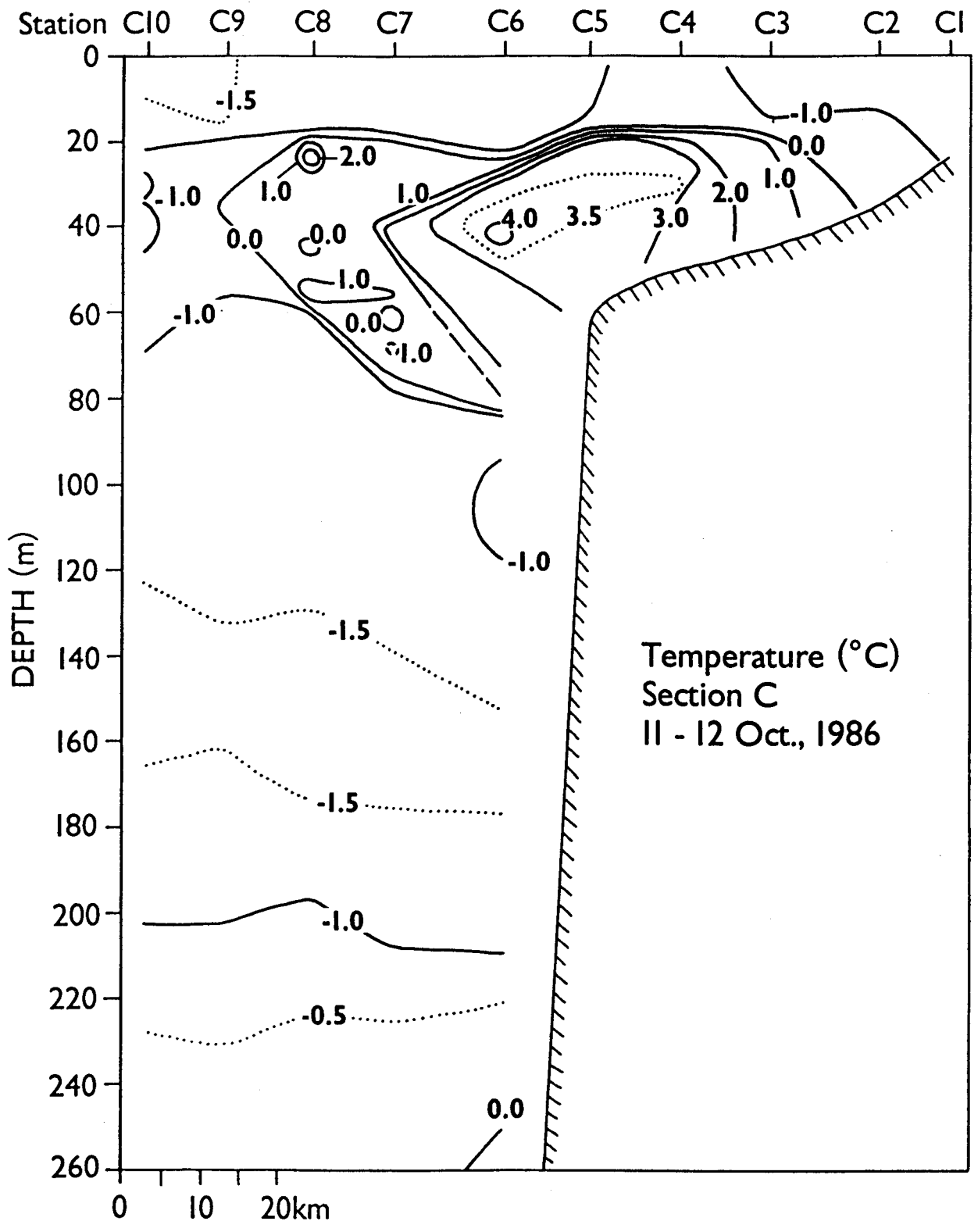


Figure 43. Temperature at section C in October 1986.

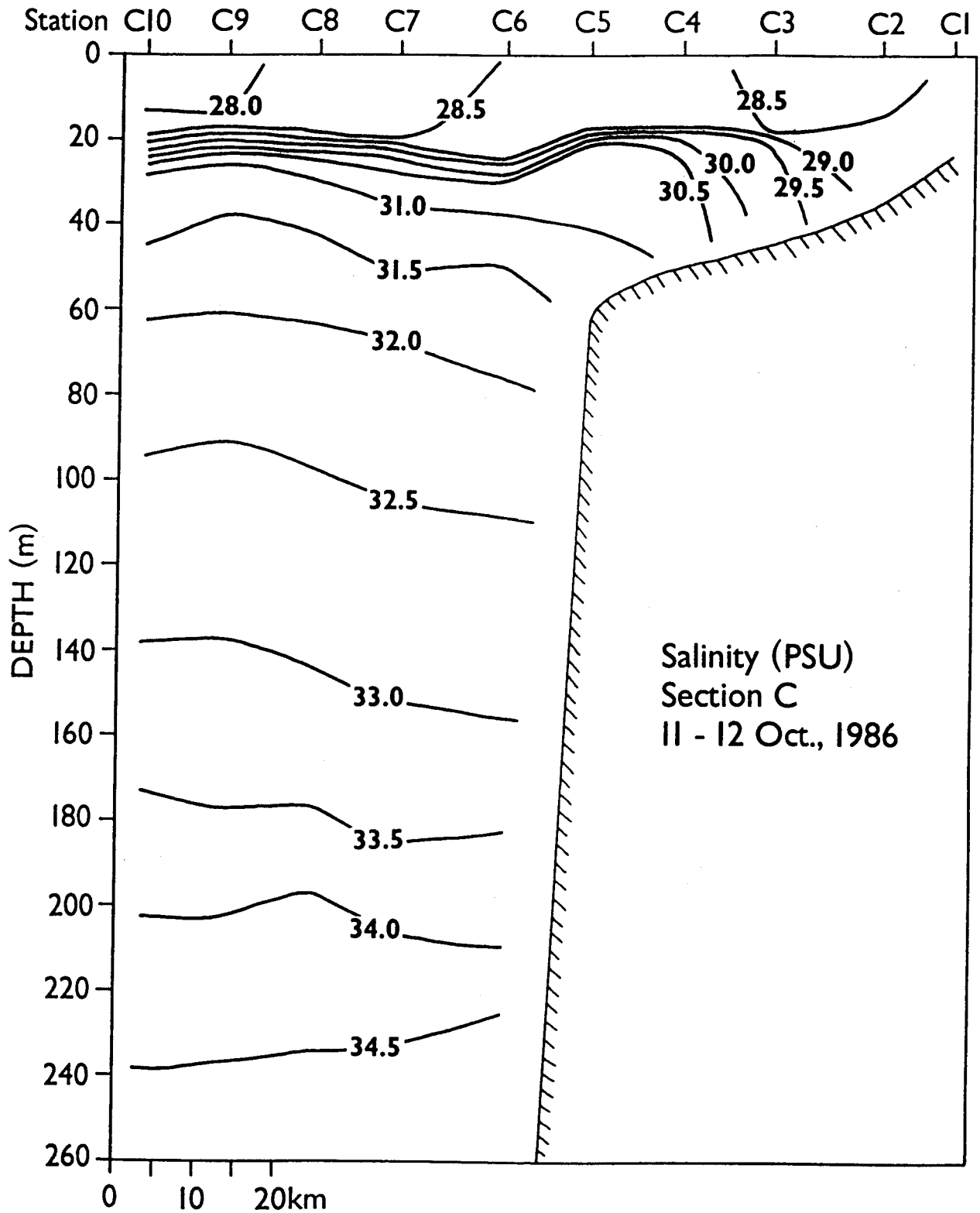


Figure 44. Salinity at section C in October 1986.

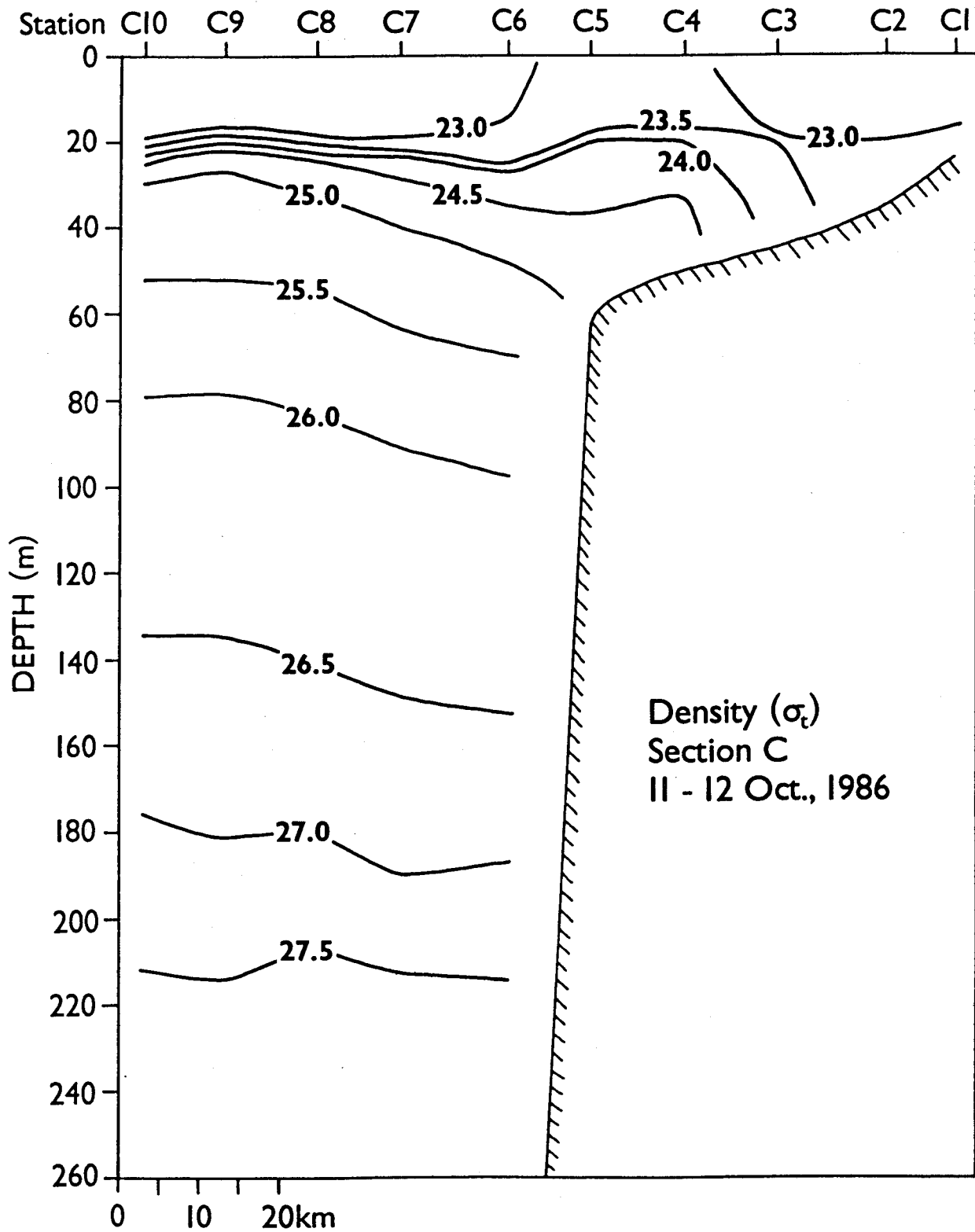


Figure 45. Density at section C in October 1986.

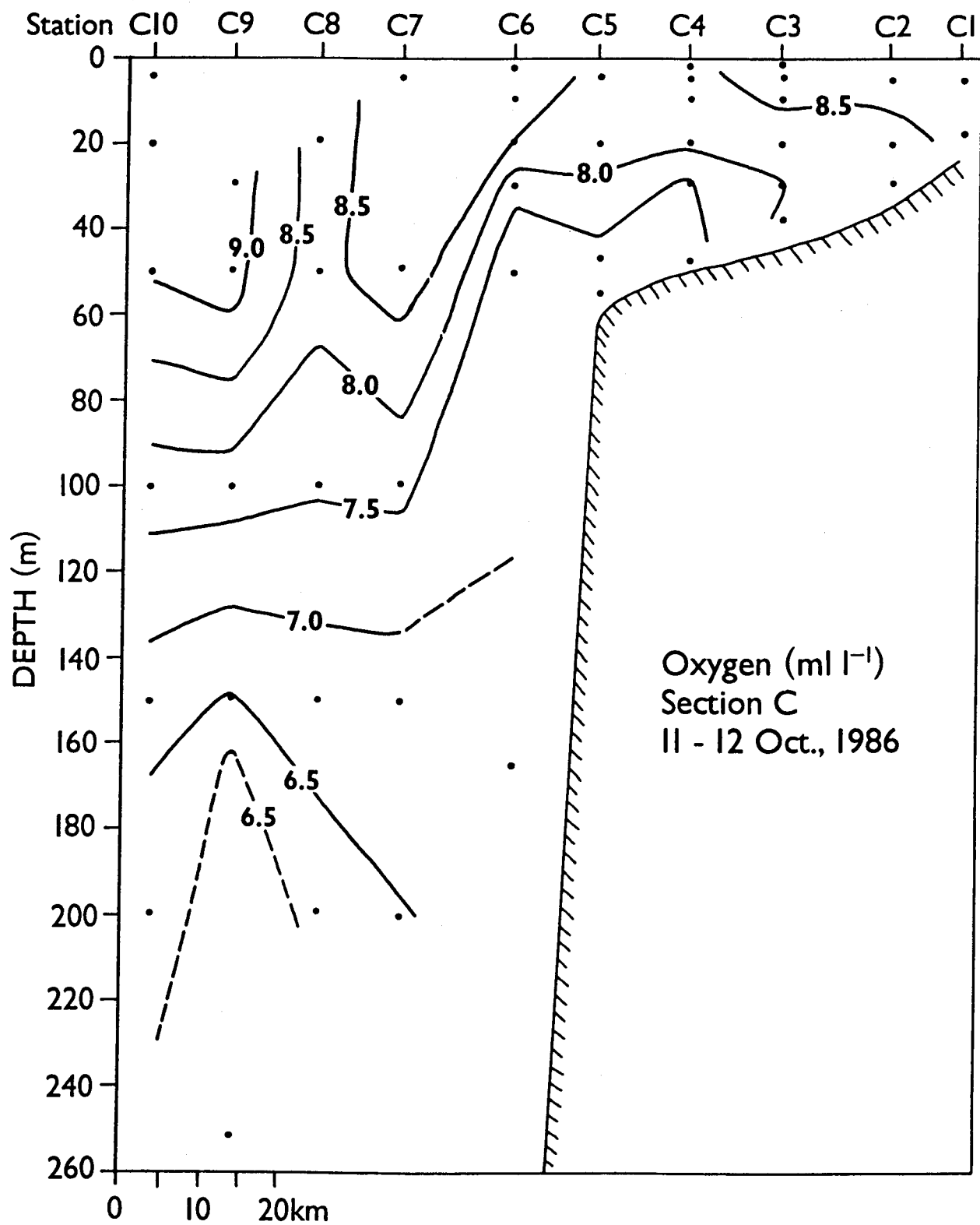


Figure 46. Dissolved oxygen at section C in October 1986.

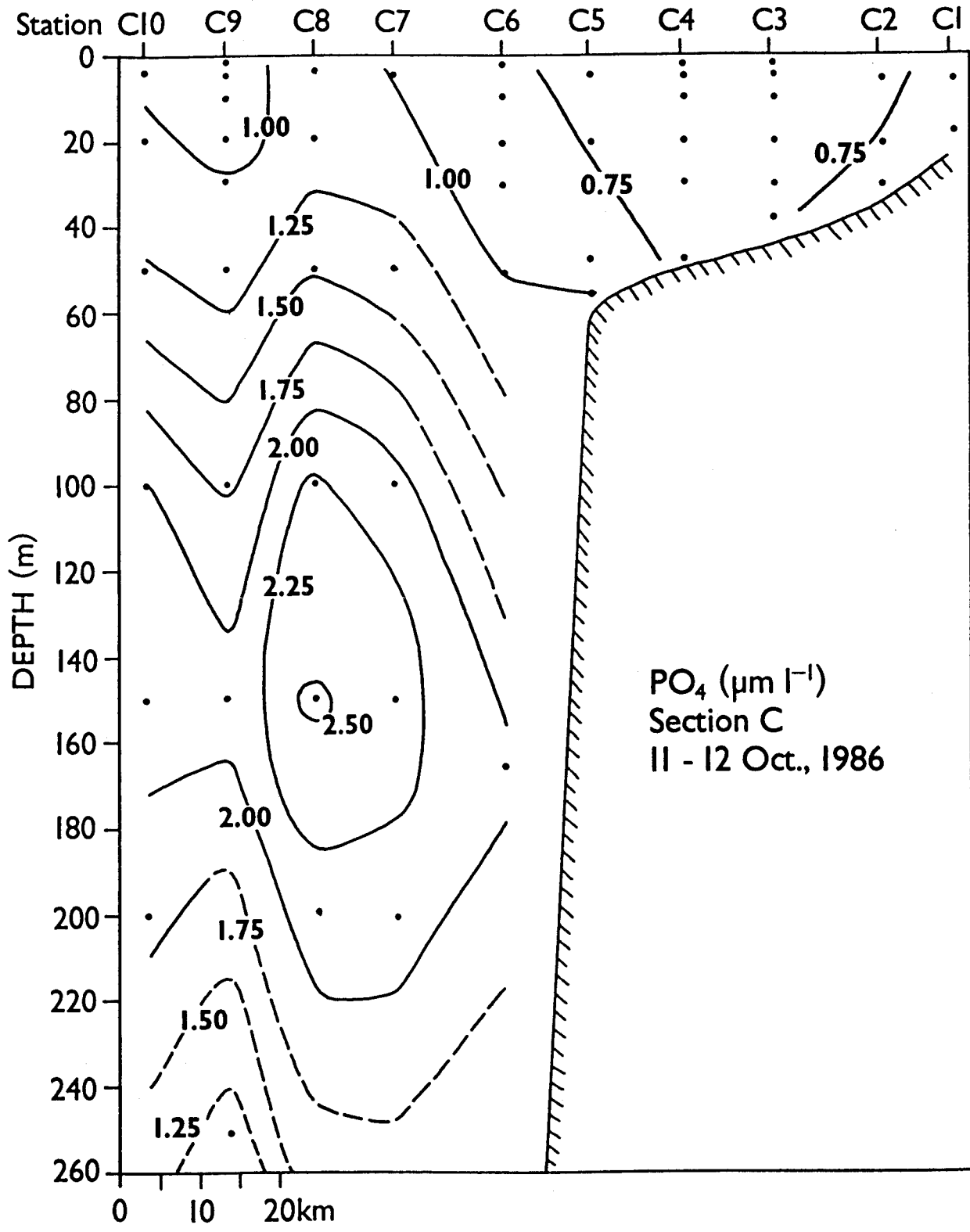


Figure 47. Phosphate at section C in October 1986.

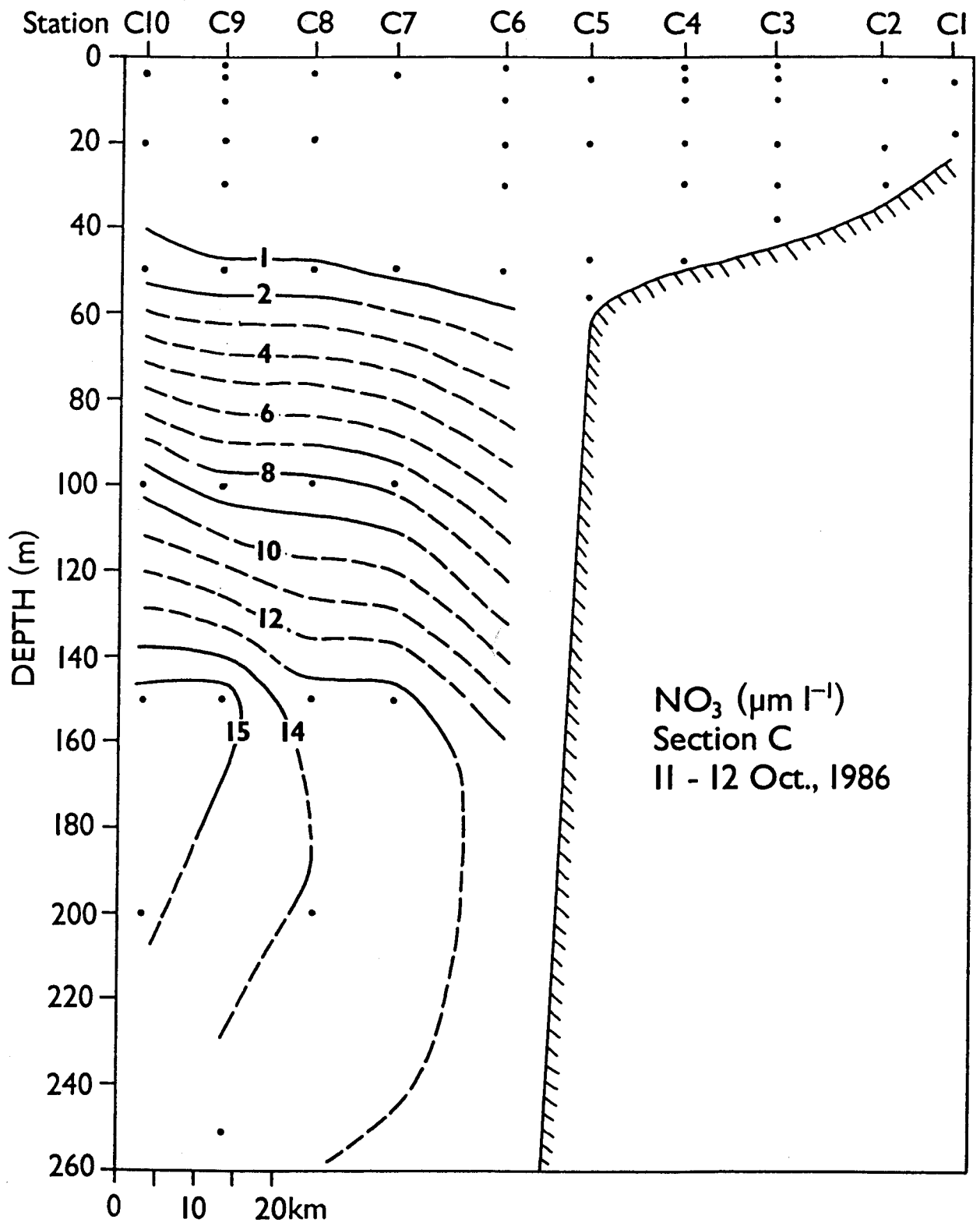


Figure 48. Nitrate at section C in October 1986.

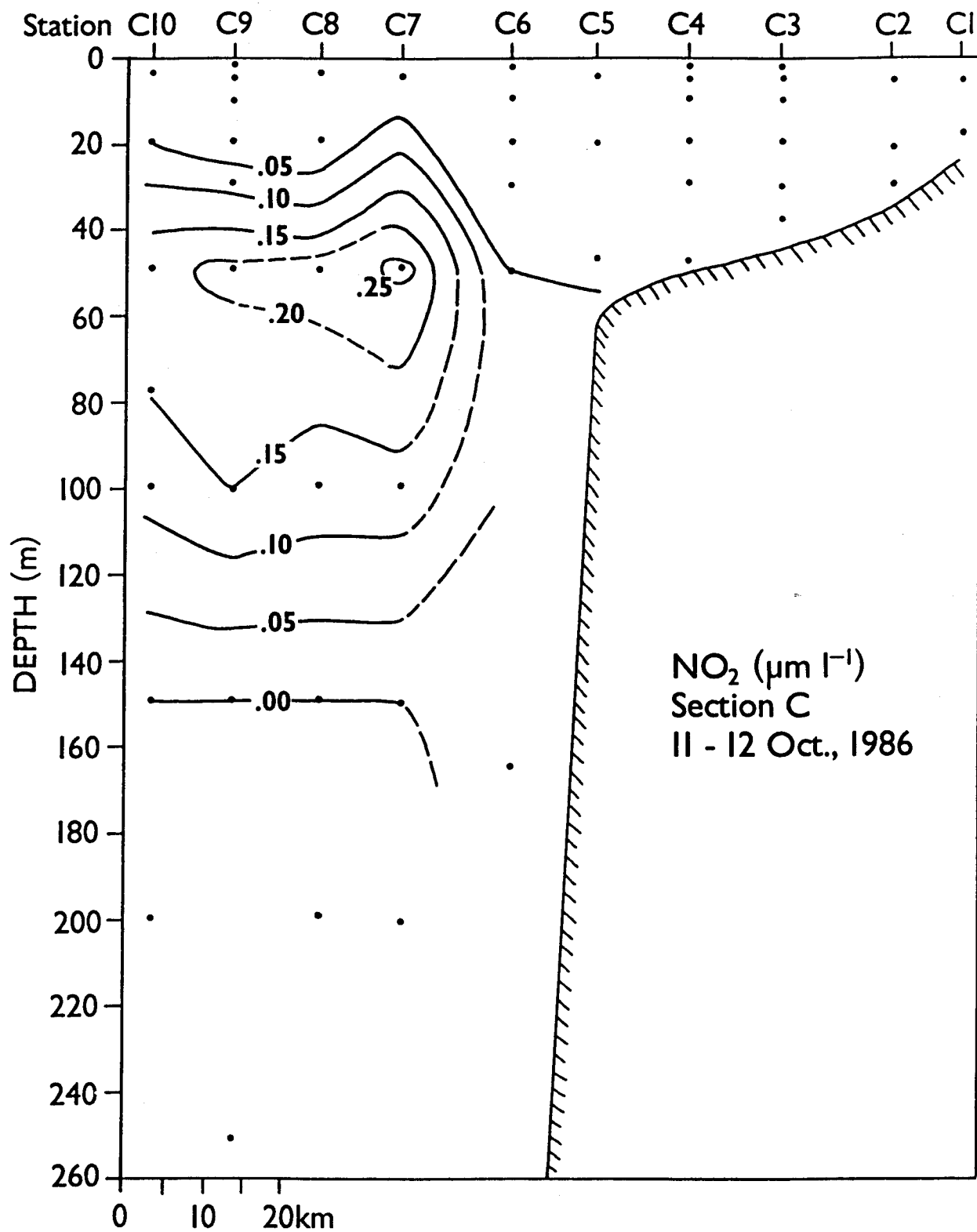


Figure 49. Nitrite at section C in October 1986.

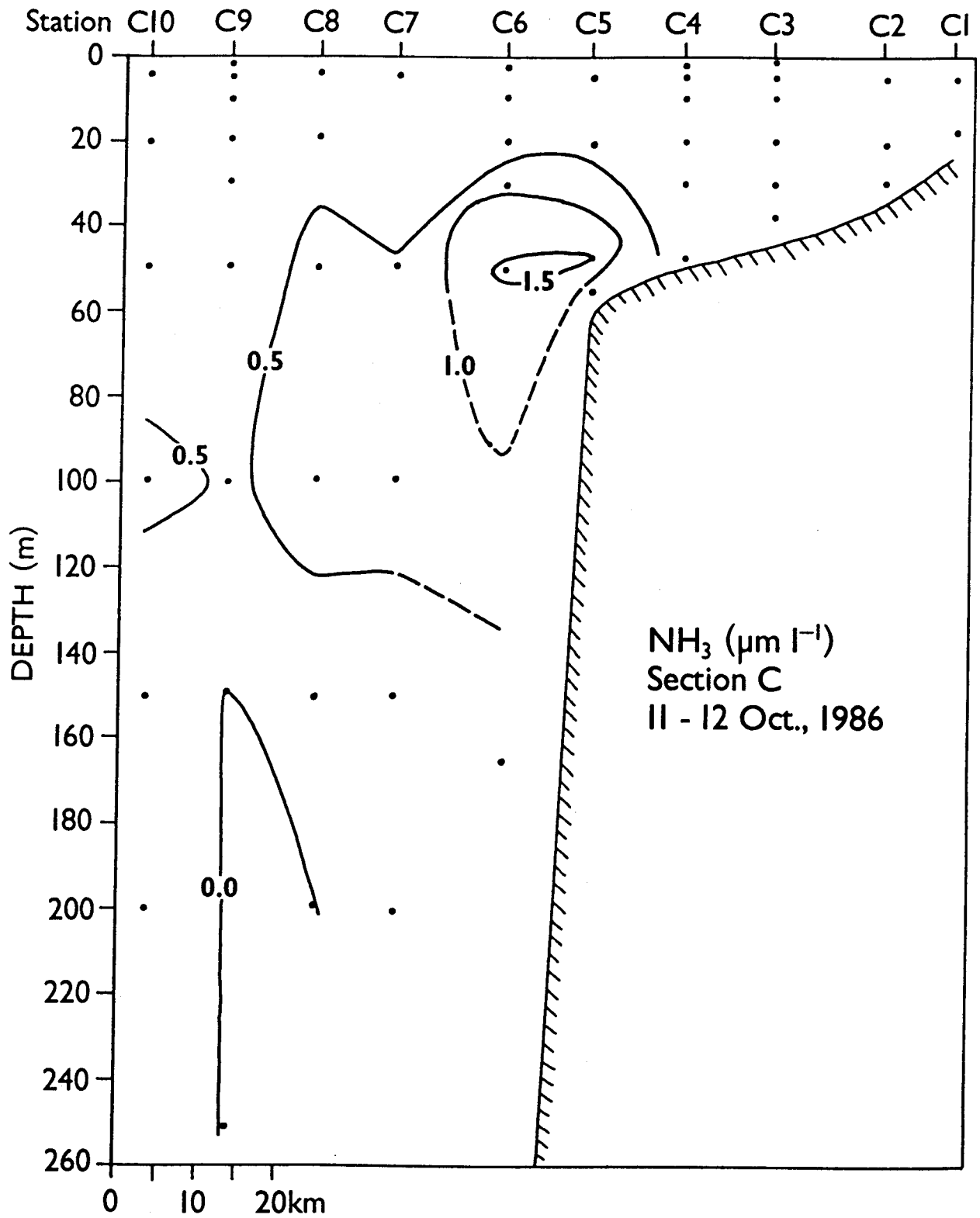


Figure 50. Ammonia at section C in October 1986.

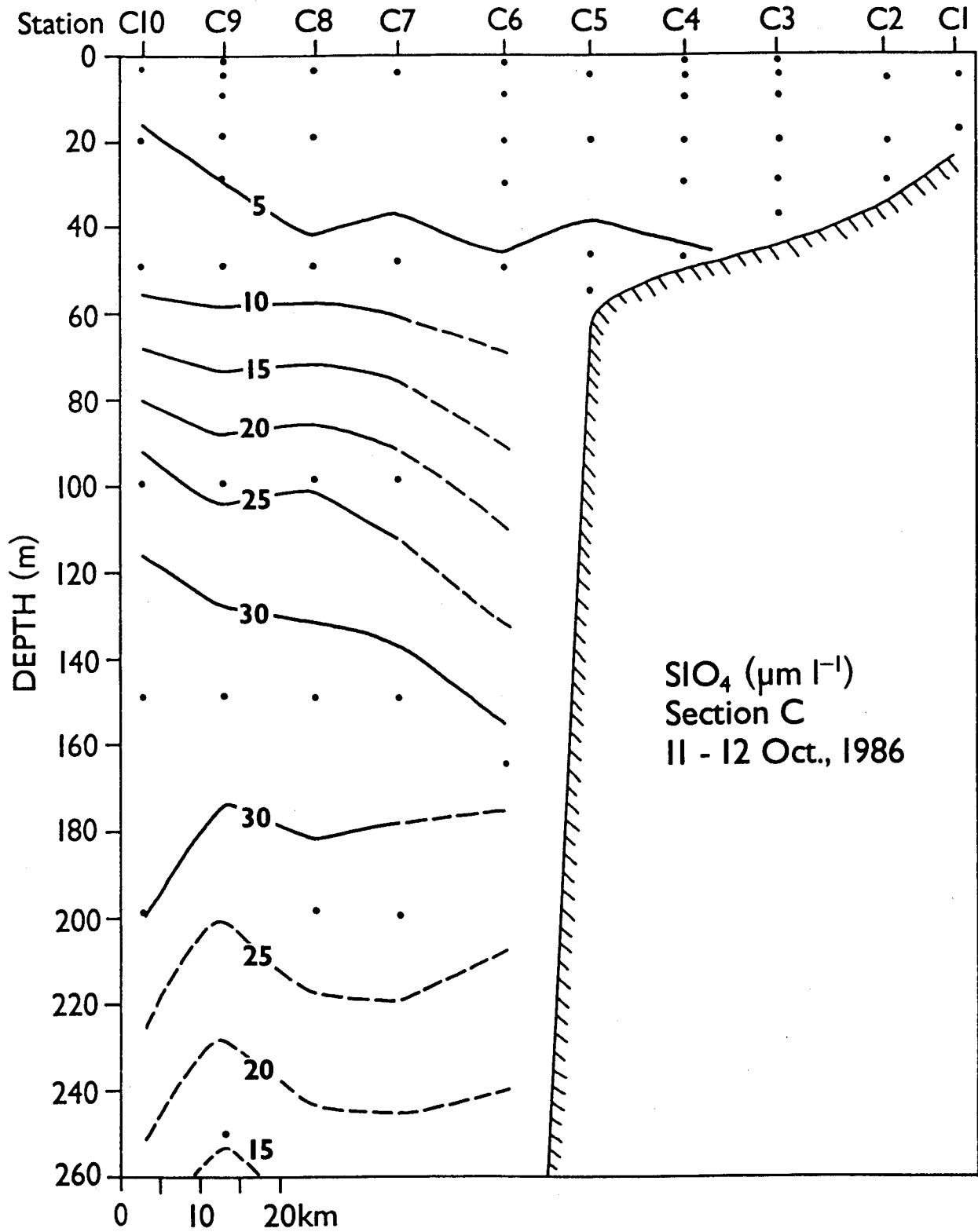


Figure 51. Silicate at section C in October 1986.

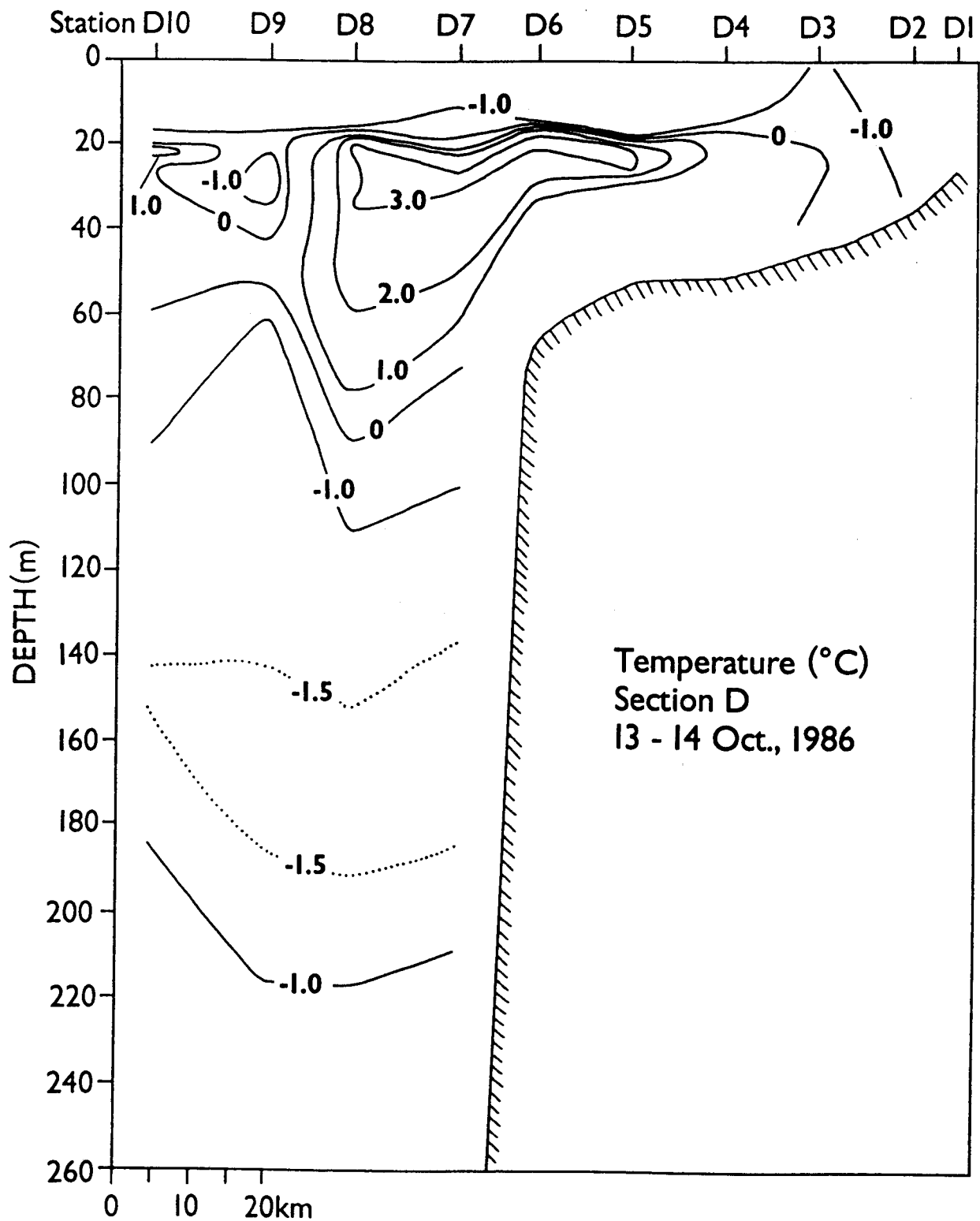


Figure 52. Temperature at section D in October 1986.

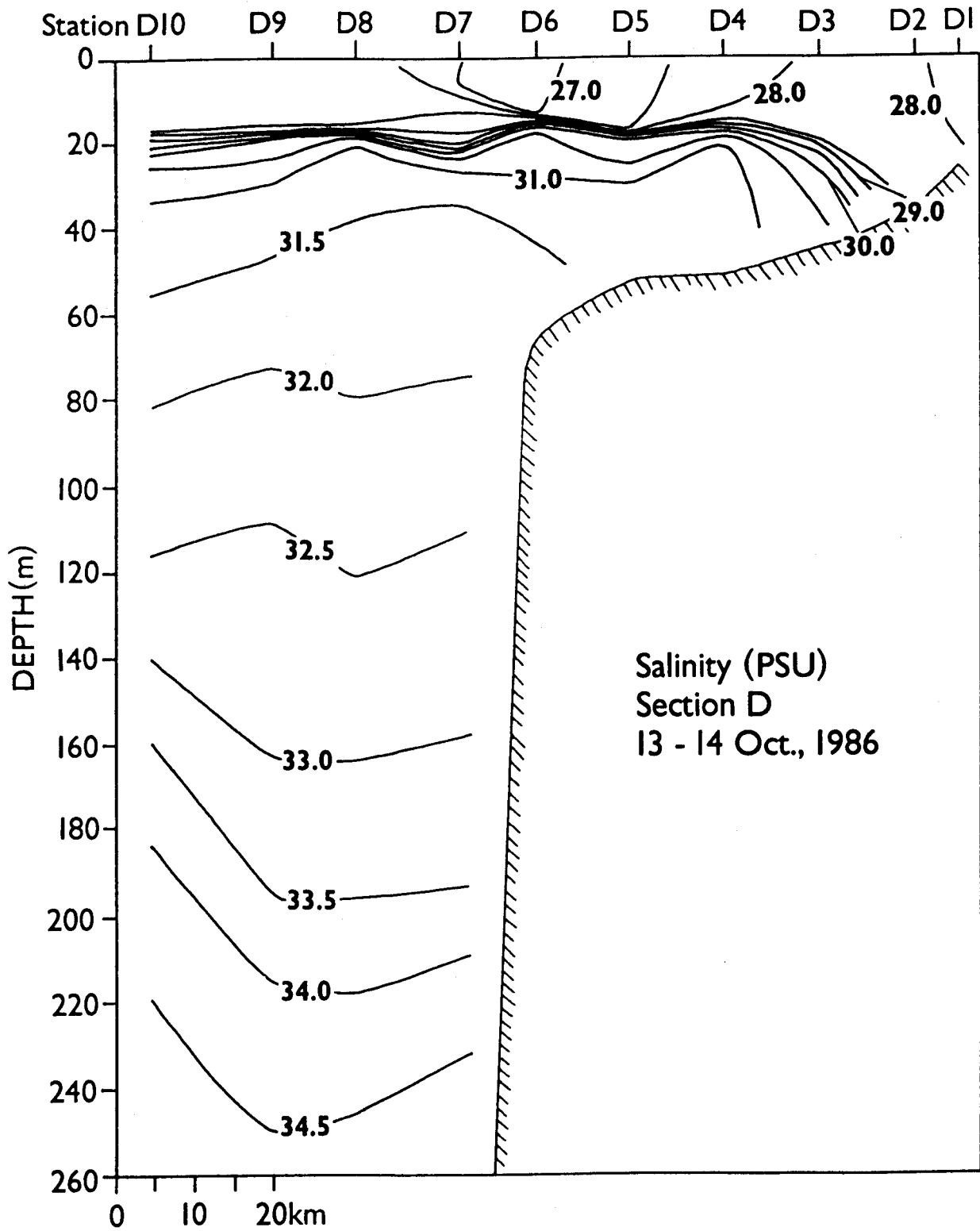


Figure 53. Salinity at section D in October 1986.

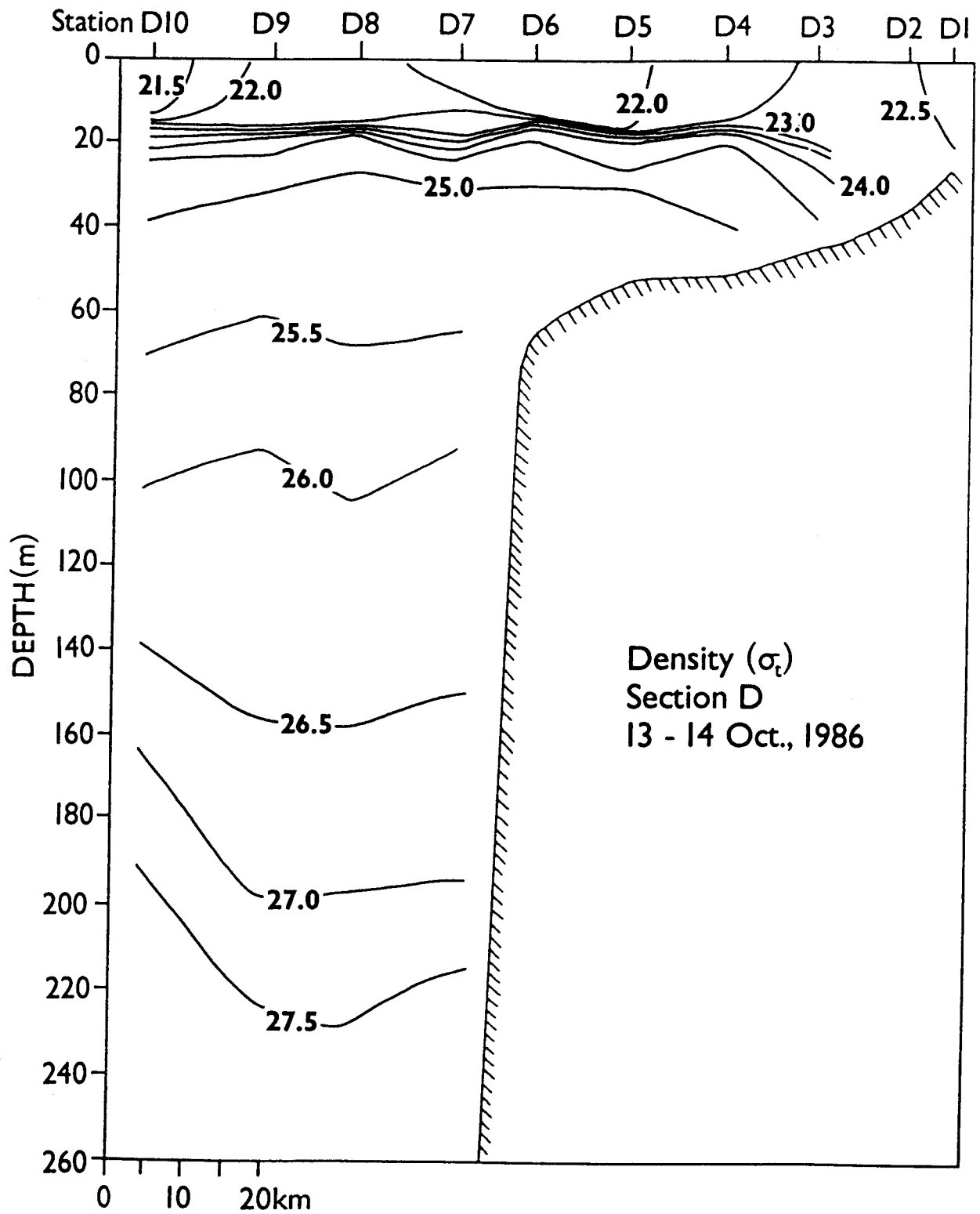


Figure 54. Density at section D in October 1986.

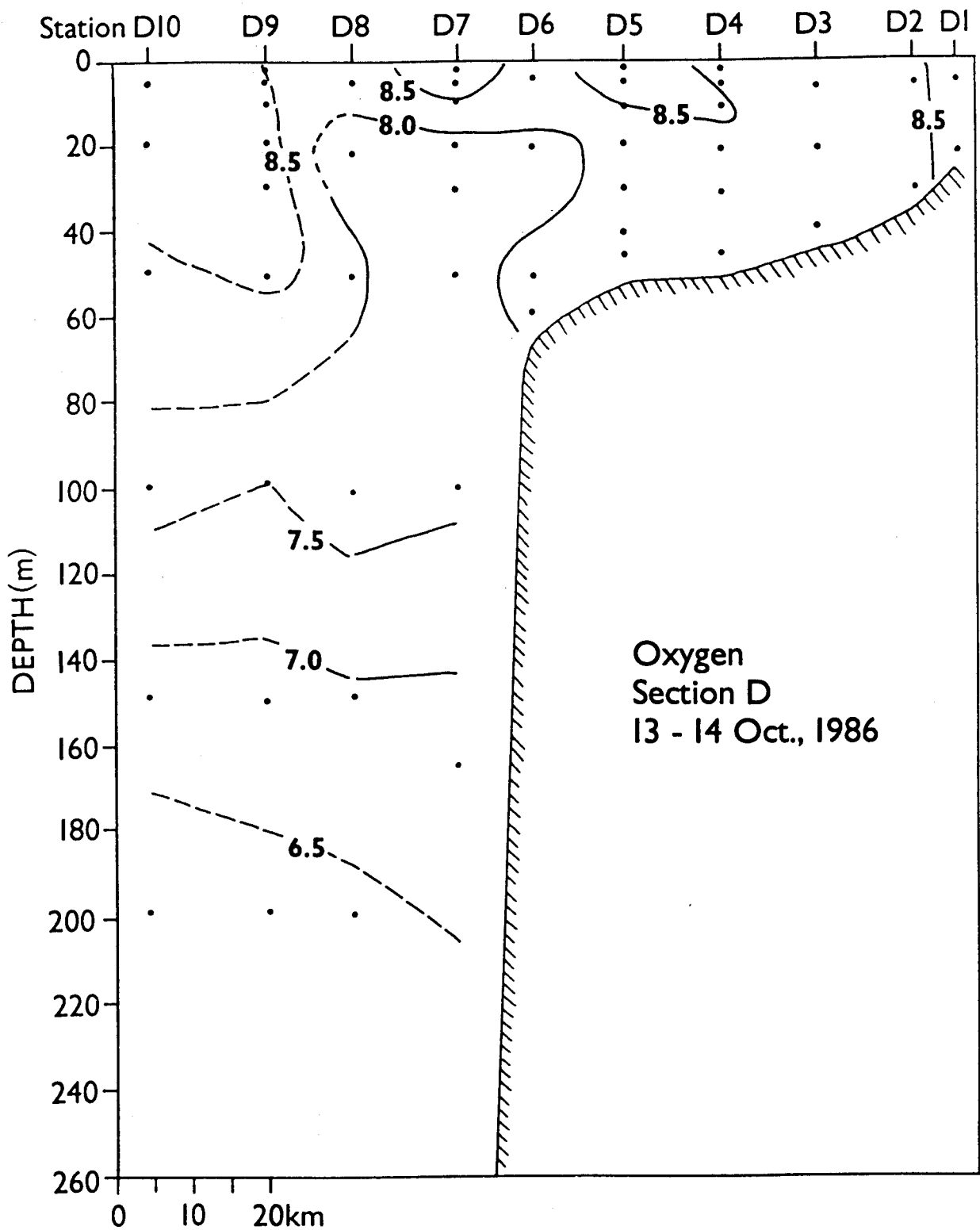


Figure 55. Dissolved oxygen at section D in October 1986.

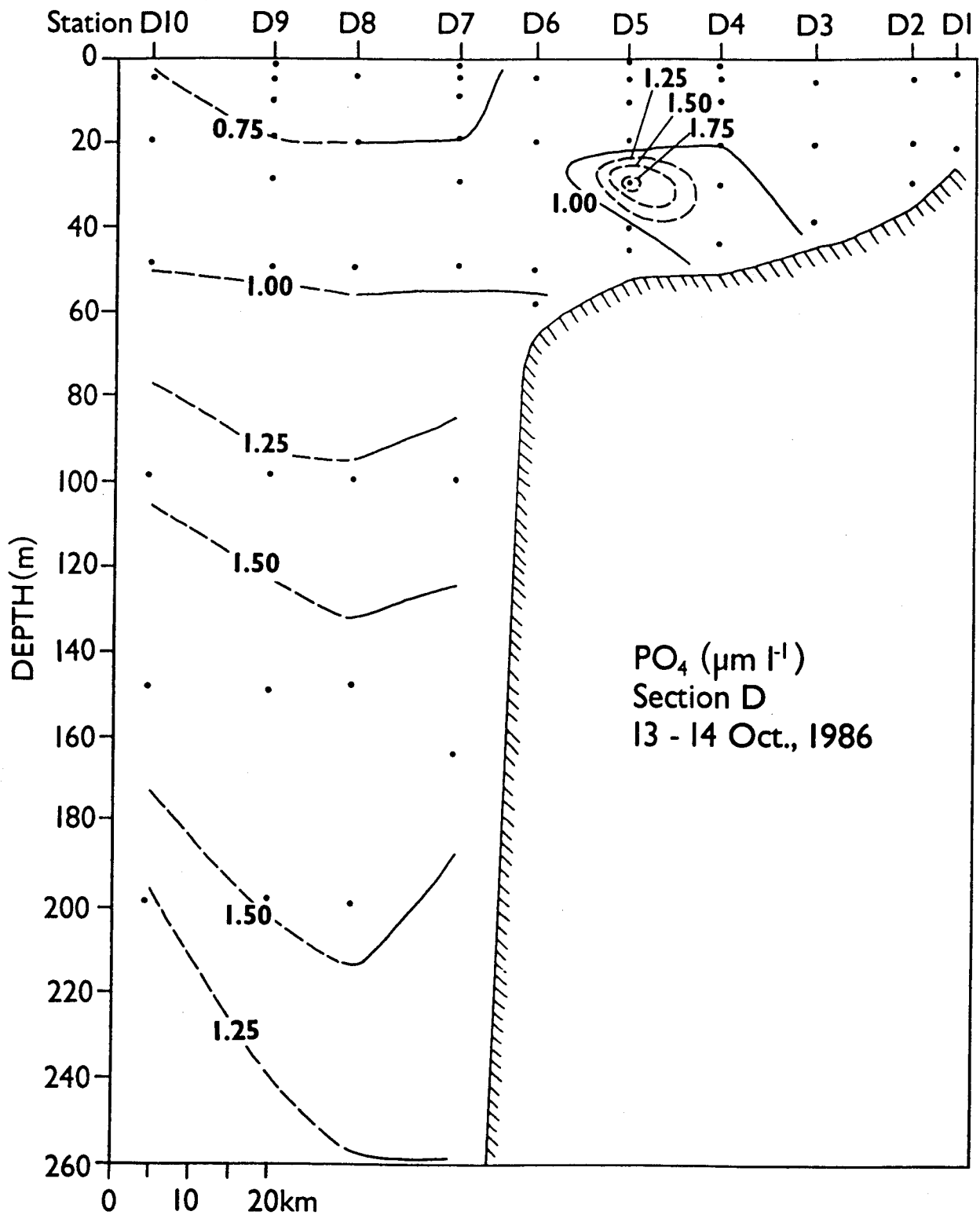


Figure 56. Phosphate at section D in October 1986.

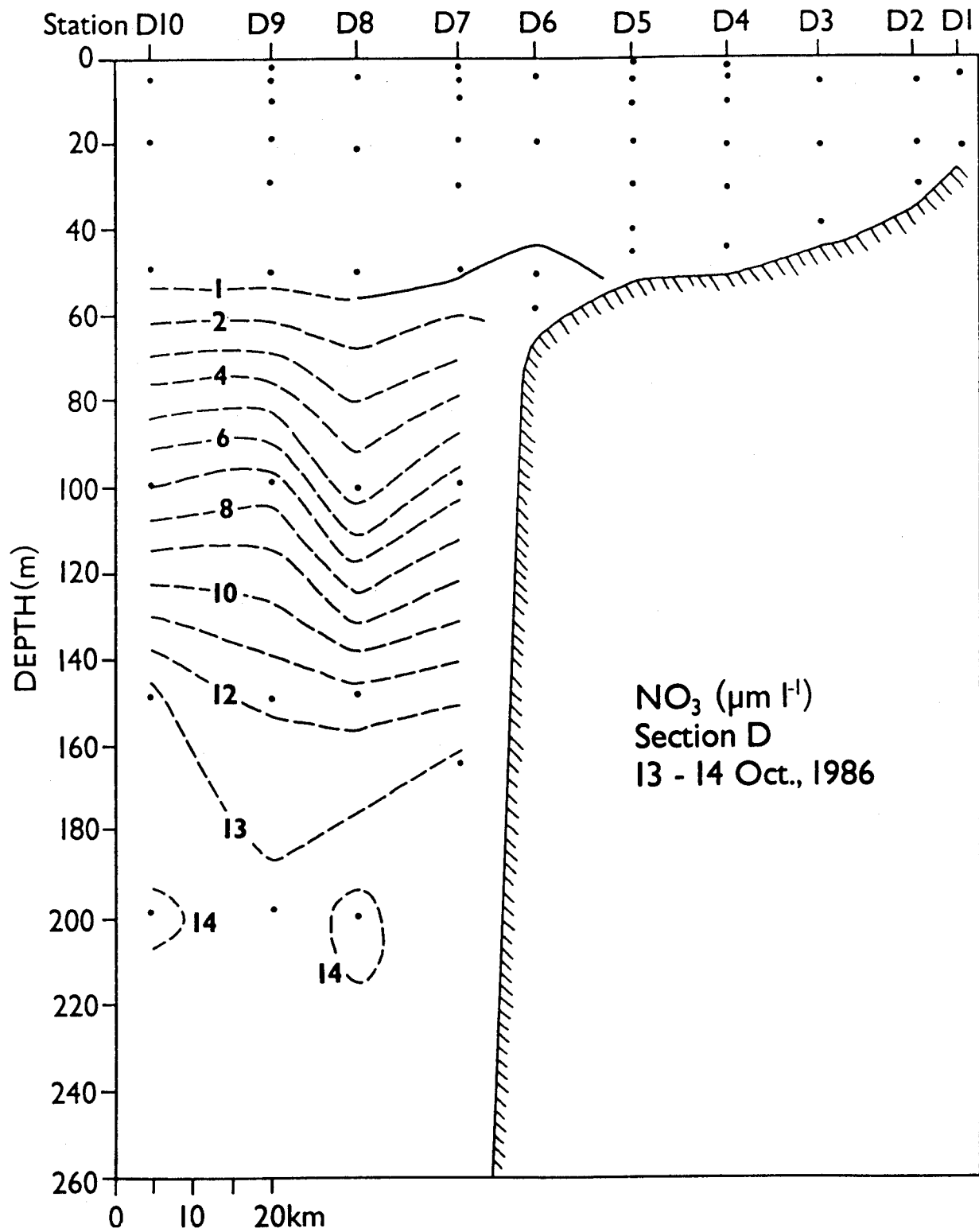


Figure 57. Nitrate at section D in October 1986.

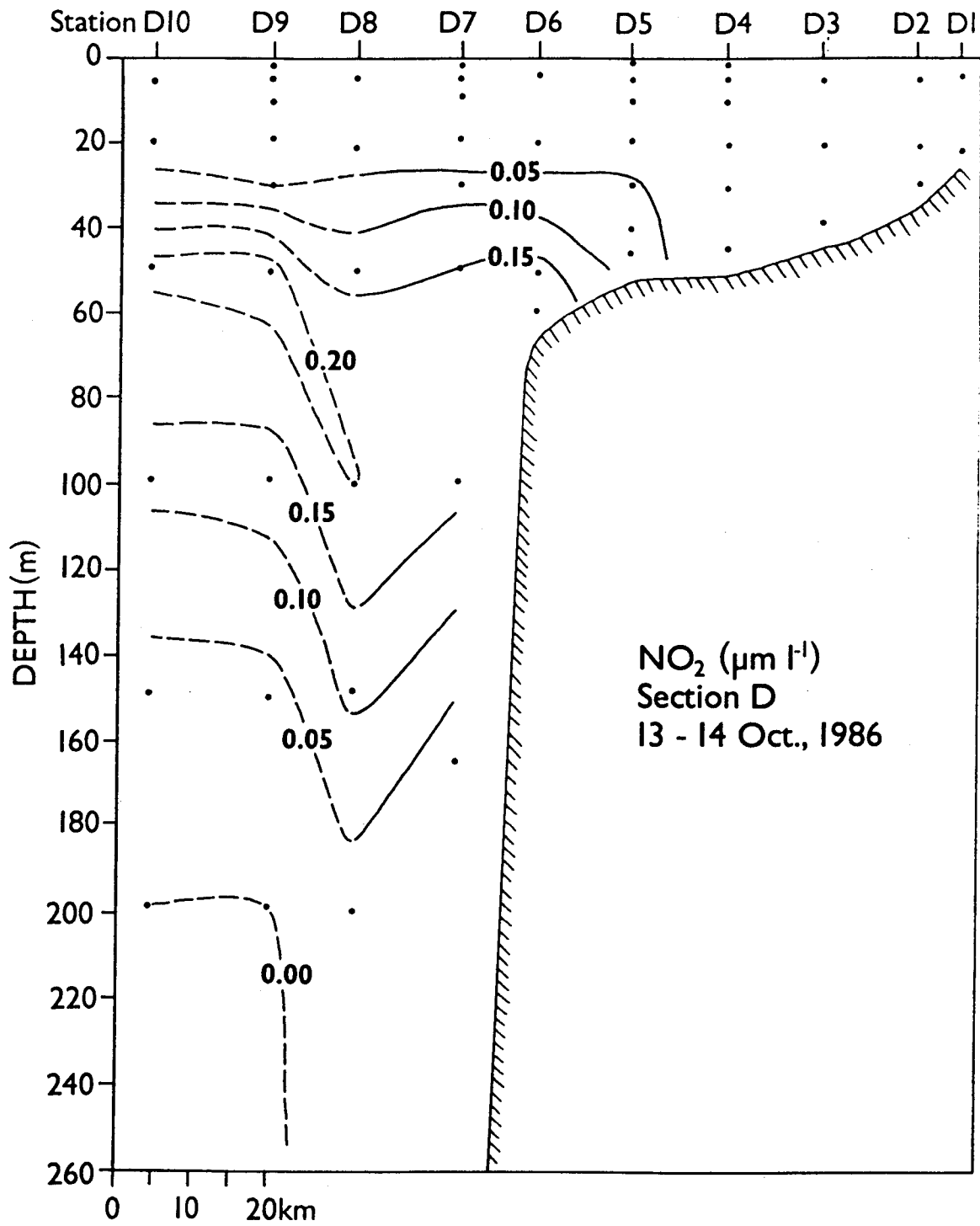


Figure 58. Nitrite at section D in October 1986.

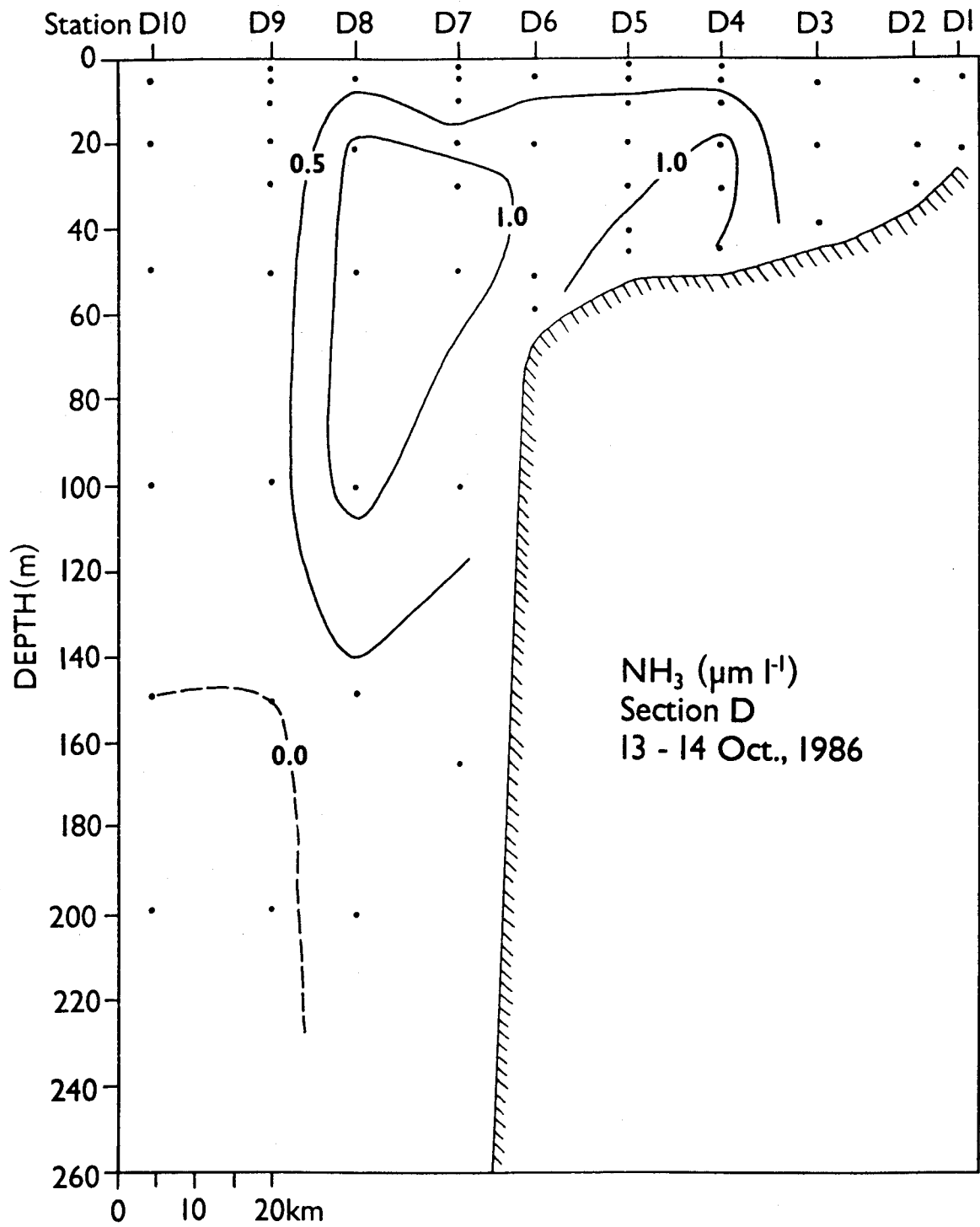


Figure 59. Ammonia at section D in October 1986.

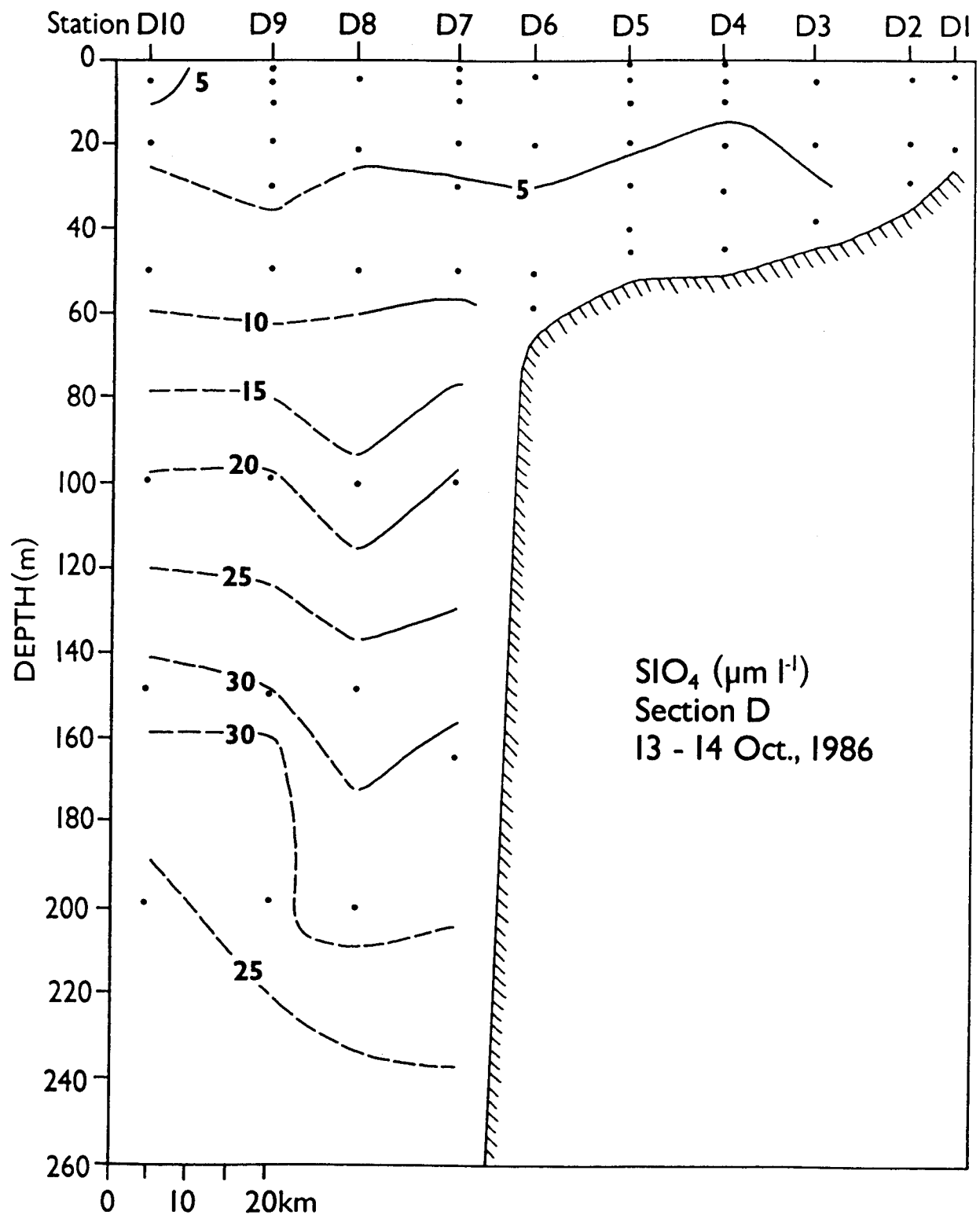


Figure 60. Silicate at section D in October 1986.

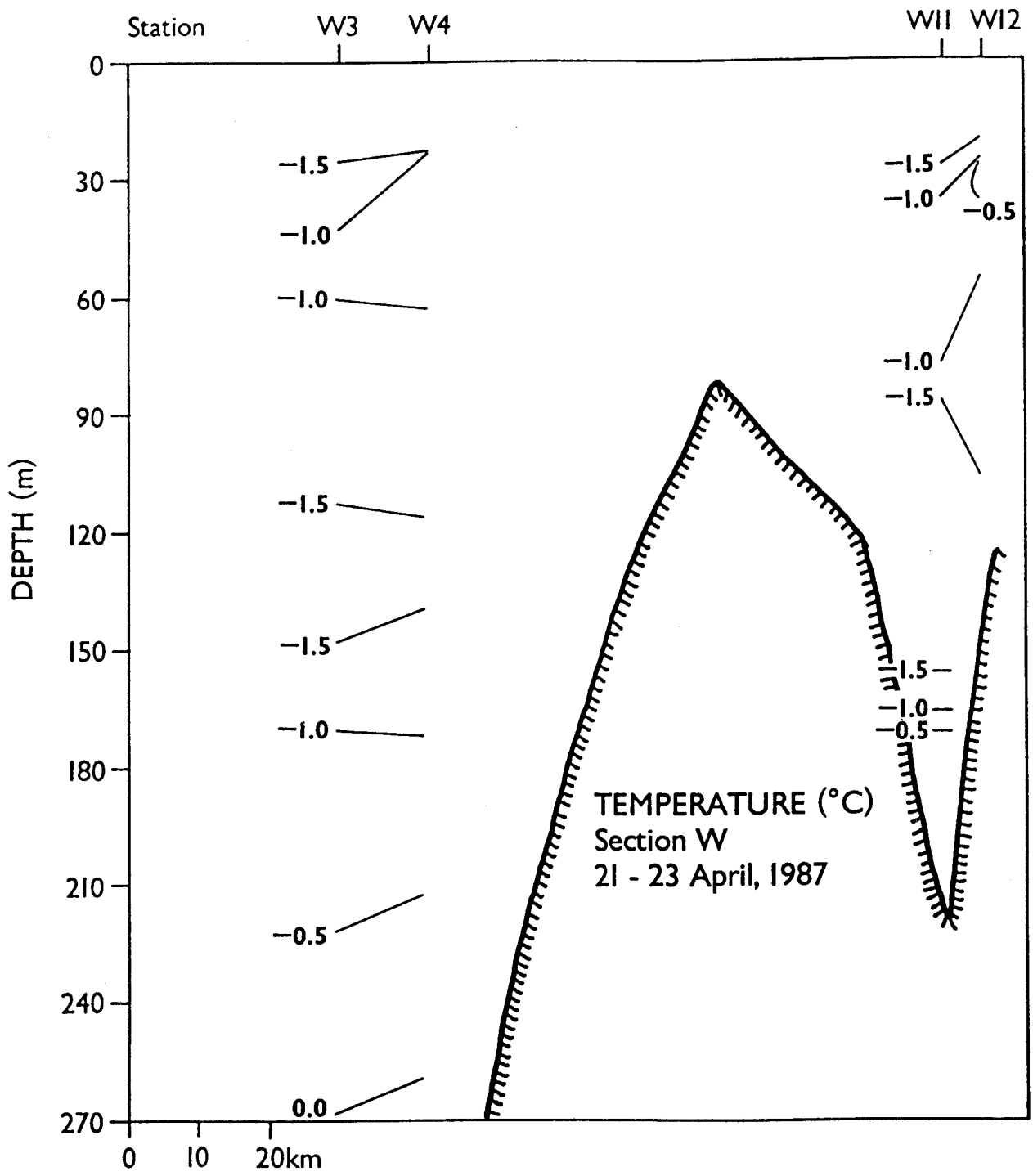


Figure 61. Temperature at section W in April 1987.

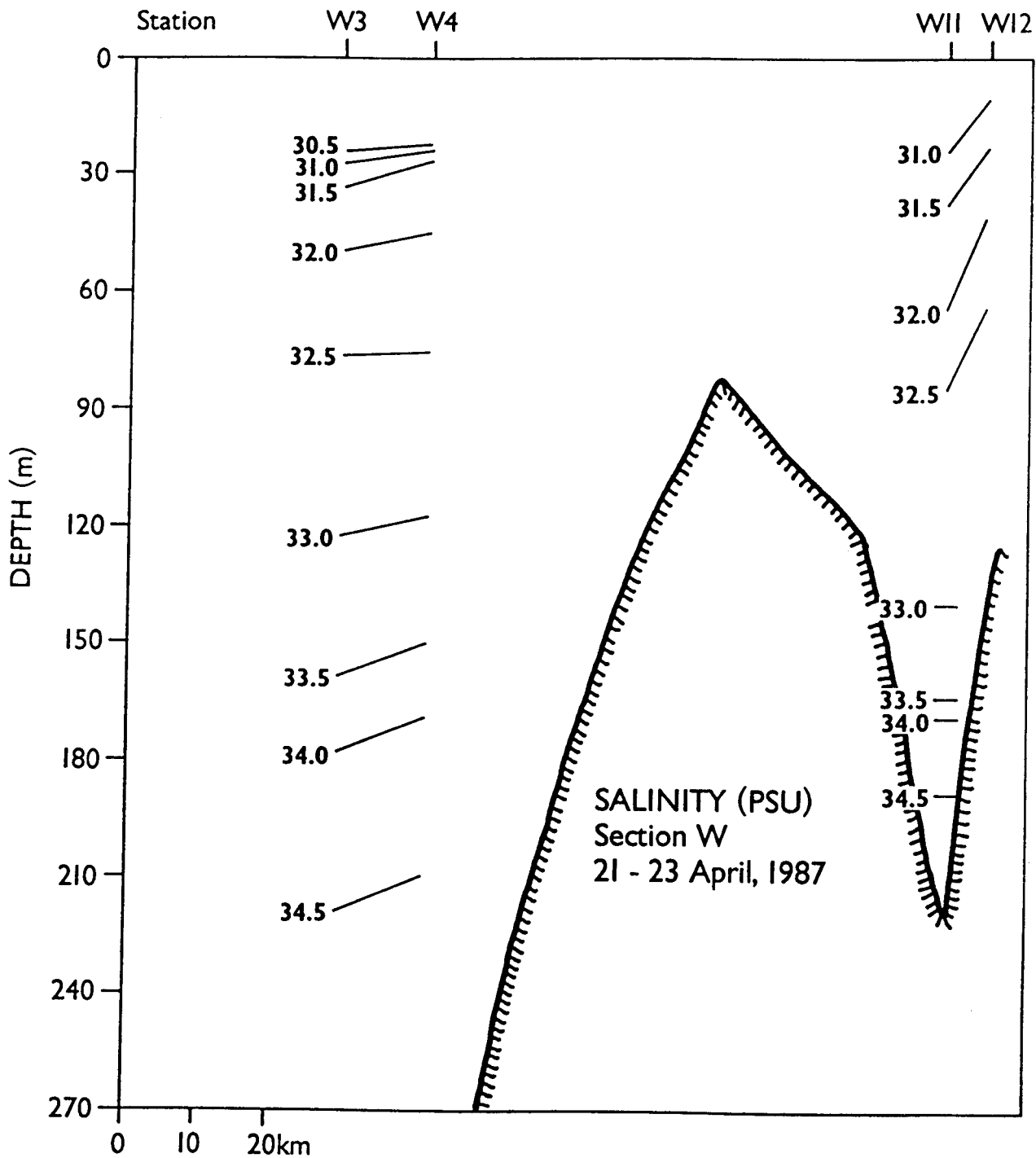


Figure 62. Salinity at section W in April 1987.

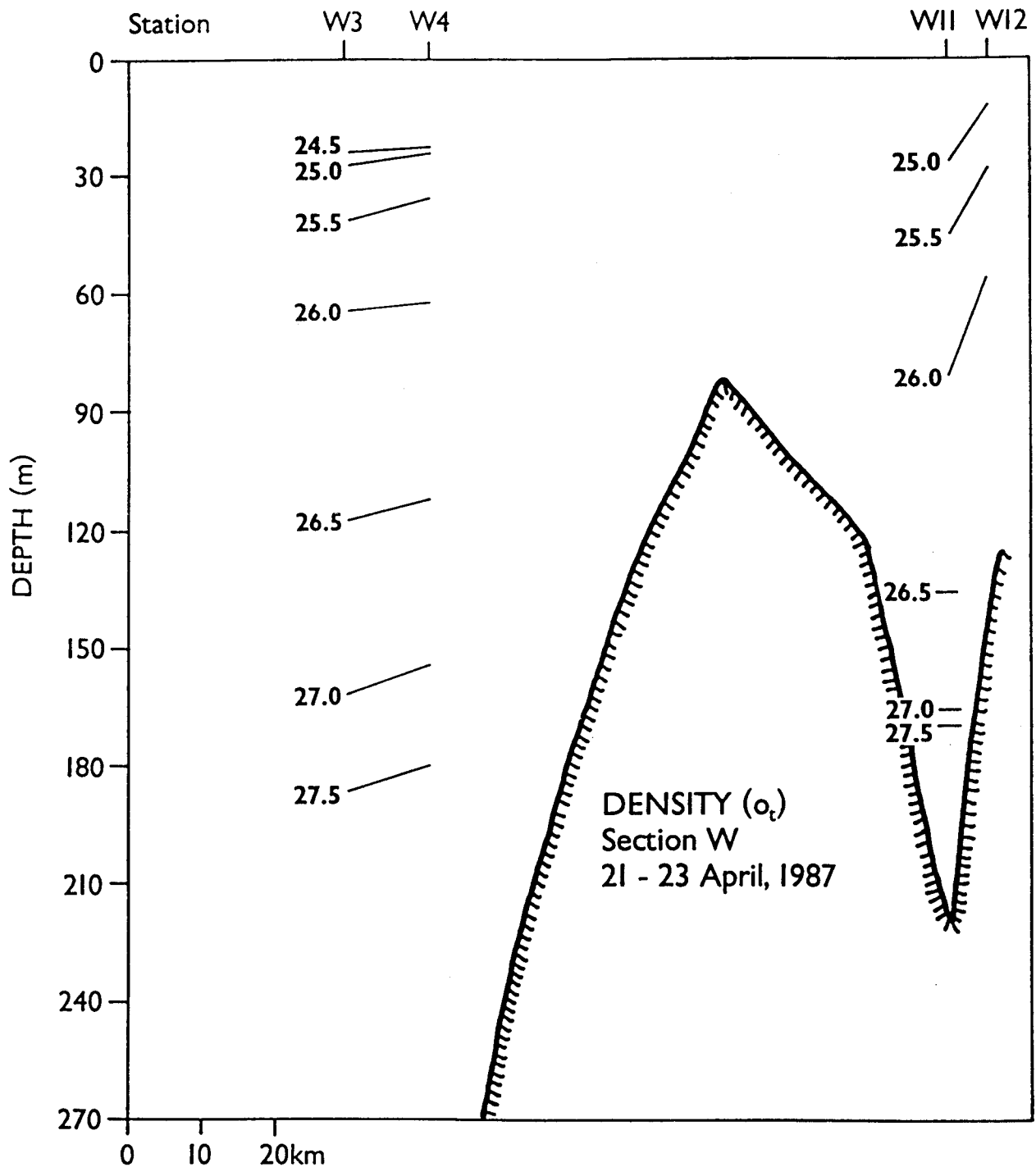


Figure 63. Density at section W in April 1987.

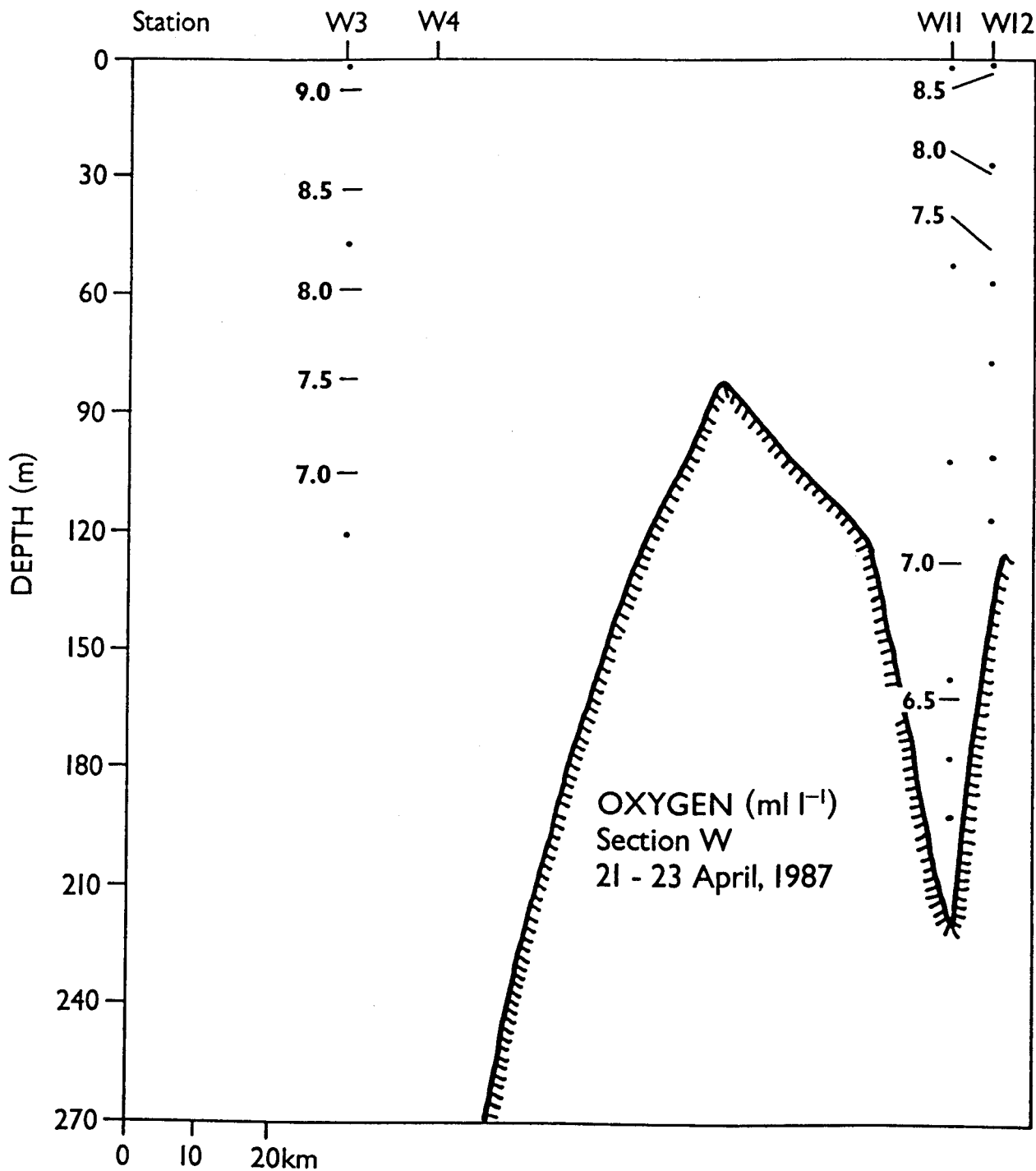


Figure 64. Dissolved oxygen at section W in April 1987.

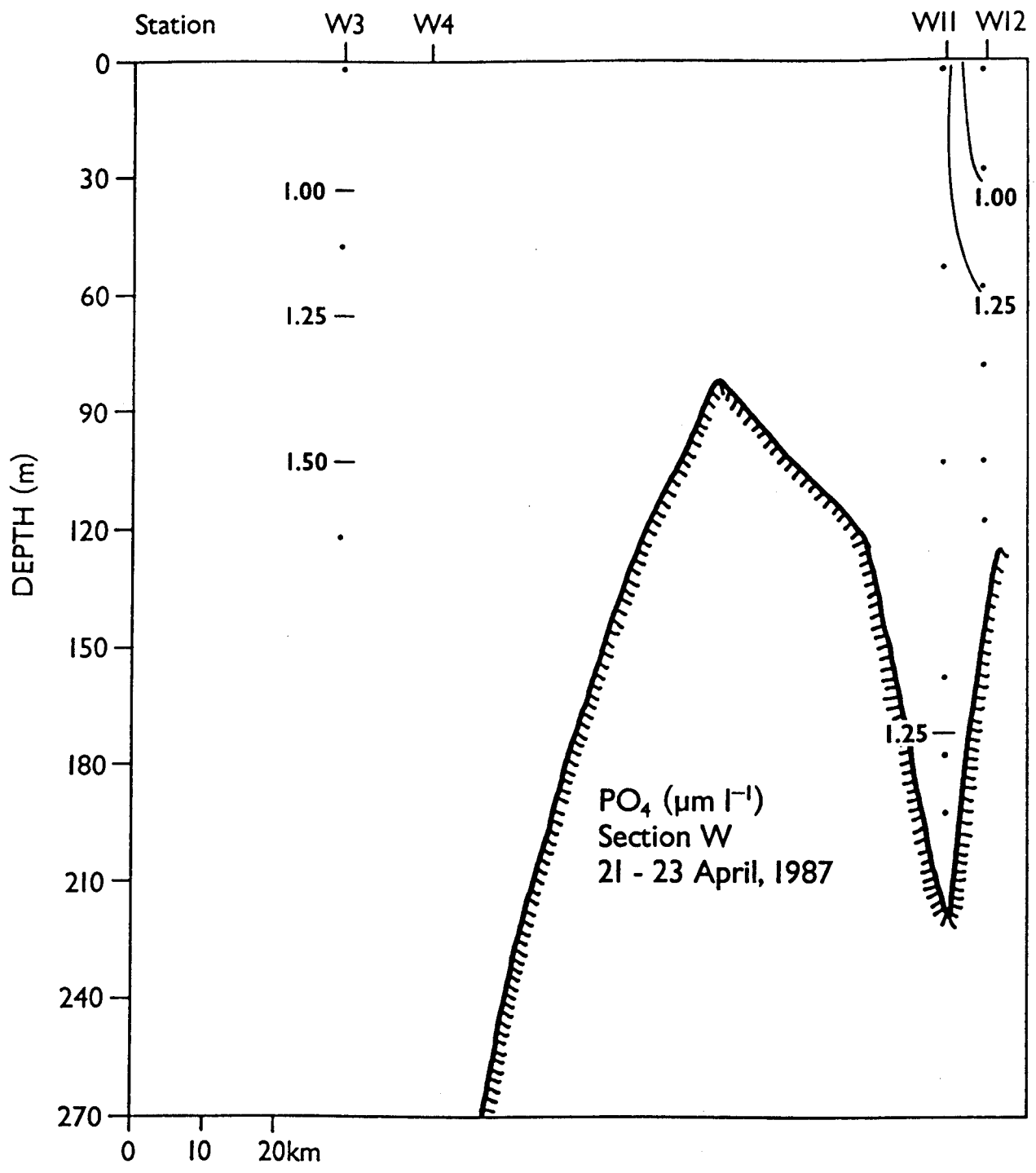


Figure 65. Phosphate at section W in April 1987.

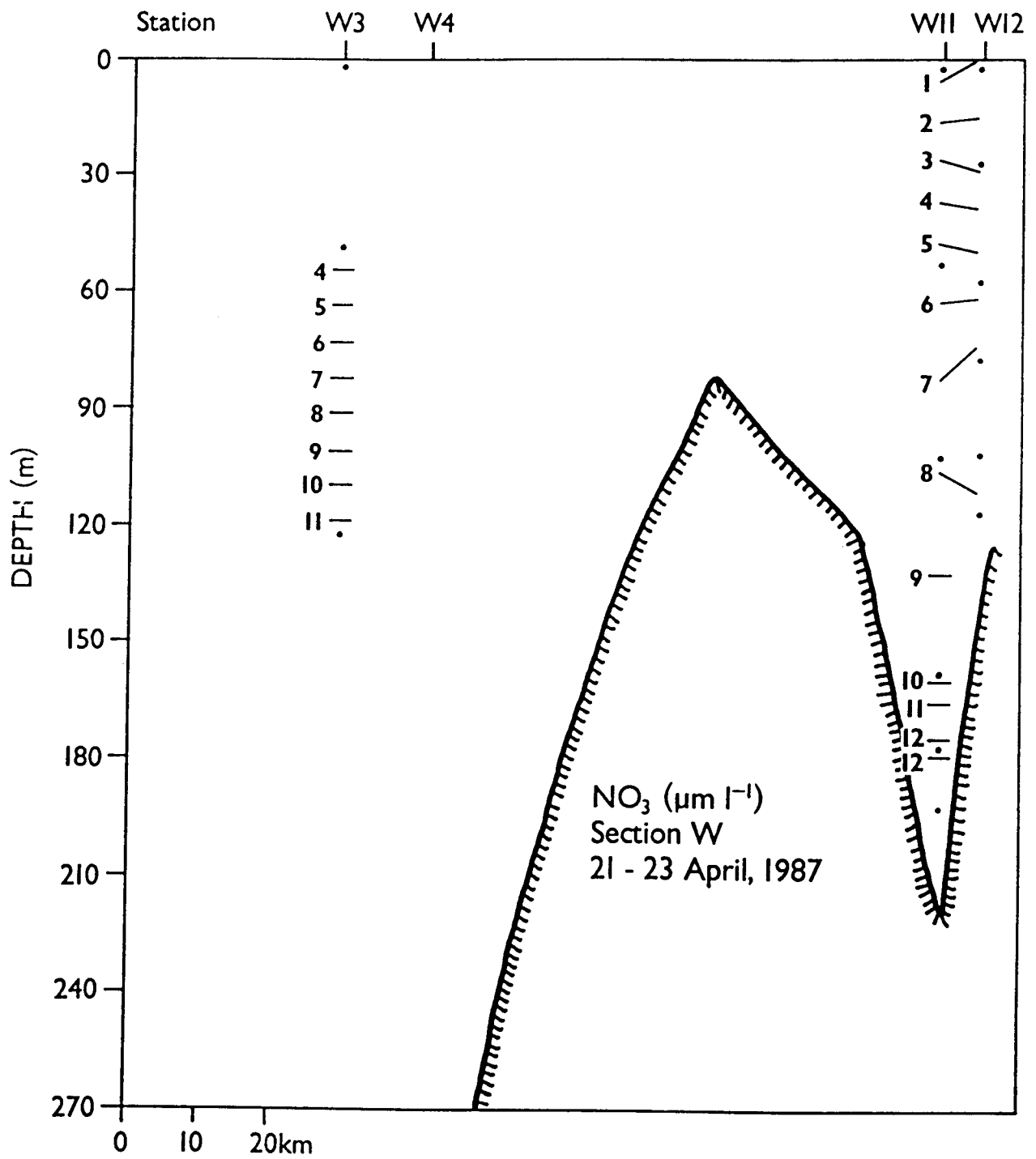


Figure 66. Nitrate at section W in April 1987.

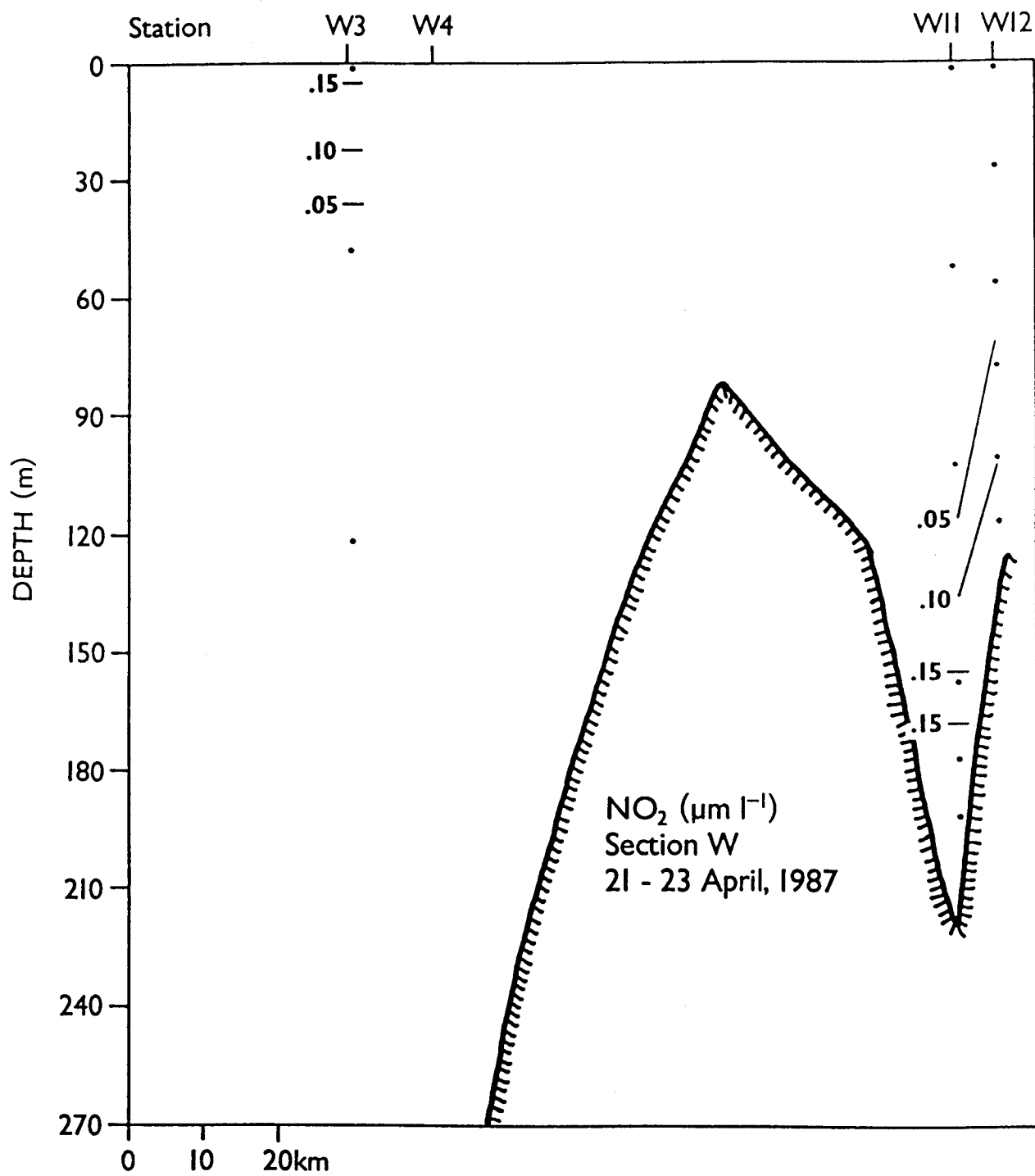


Figure 67. Nitrite at section W in April 1987.

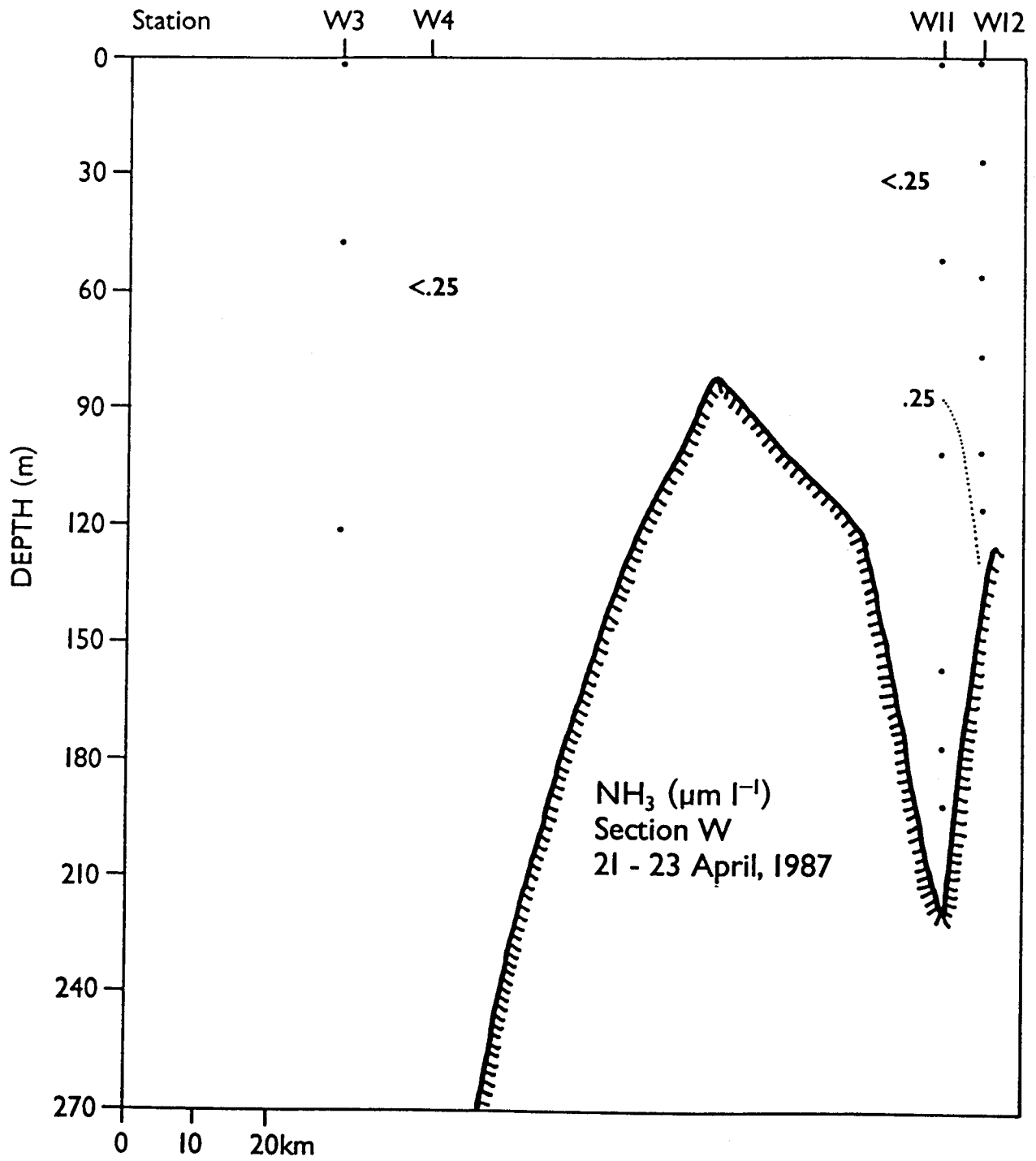


Figure 68. Ammonia at section W in April 1987.

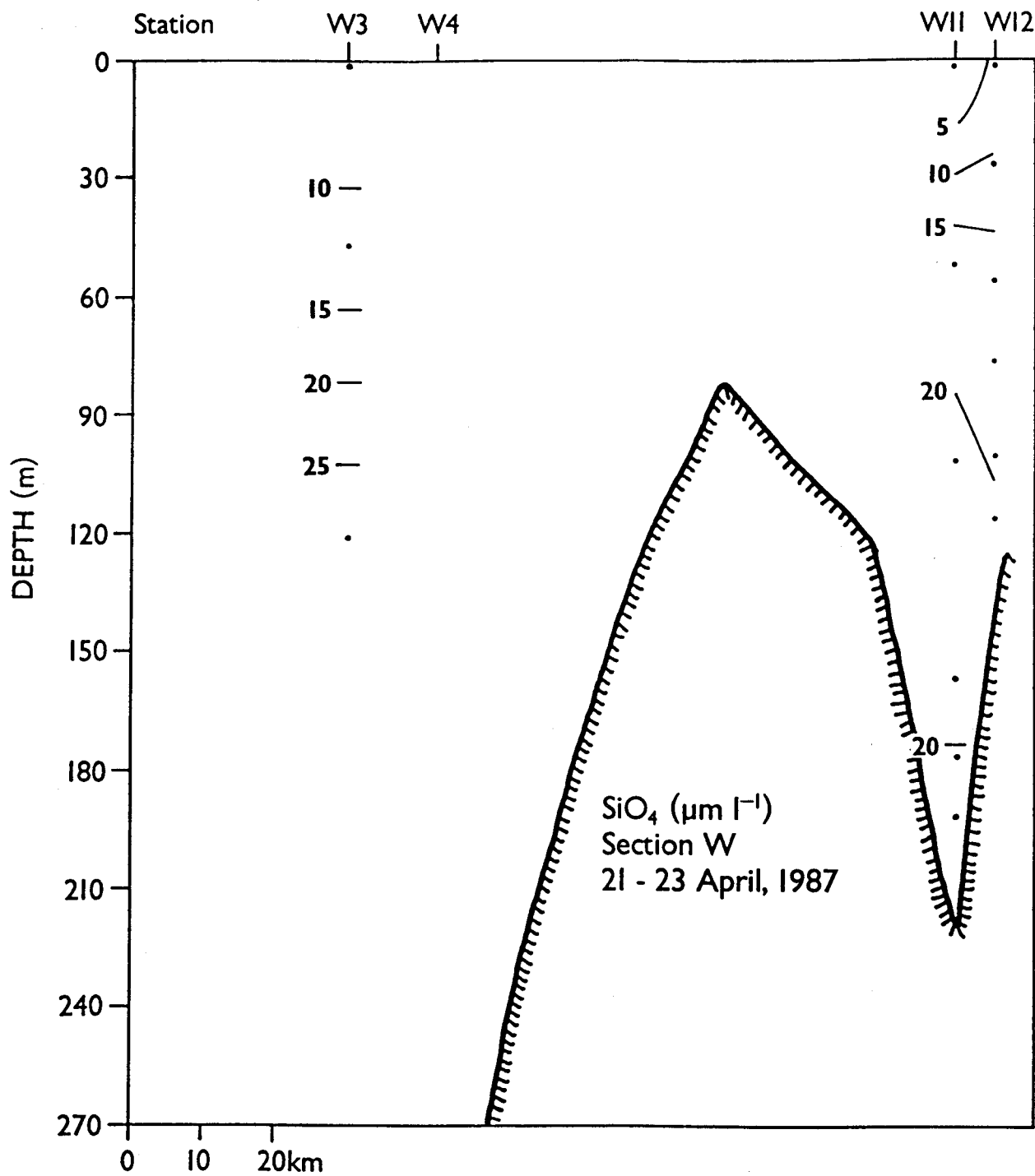


Figure 69. Silicate at section W in April 1987.

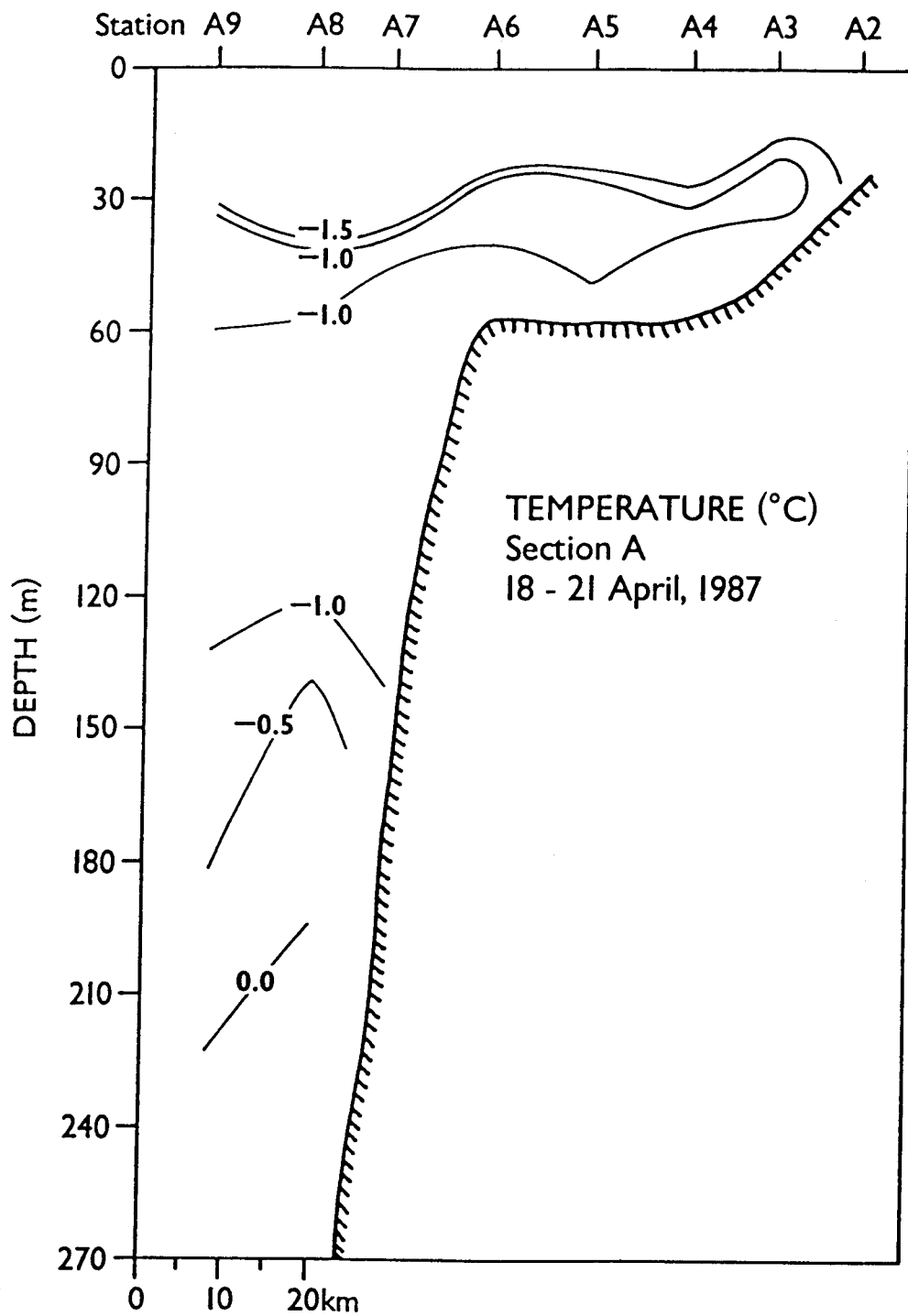


Figure 70. Temperature at section A in April 1987.

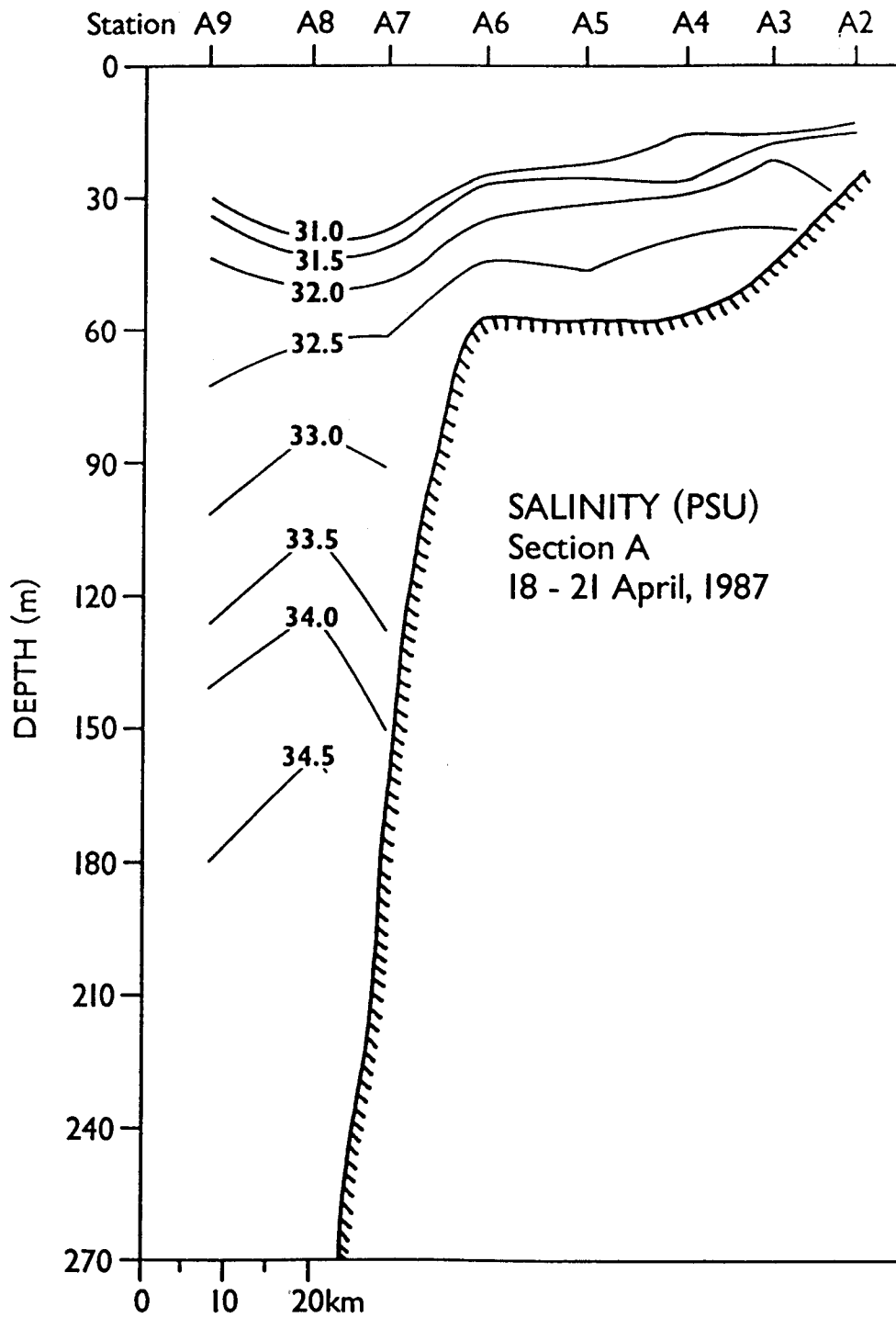


Figure 71. Salinity at section A in April 1987.

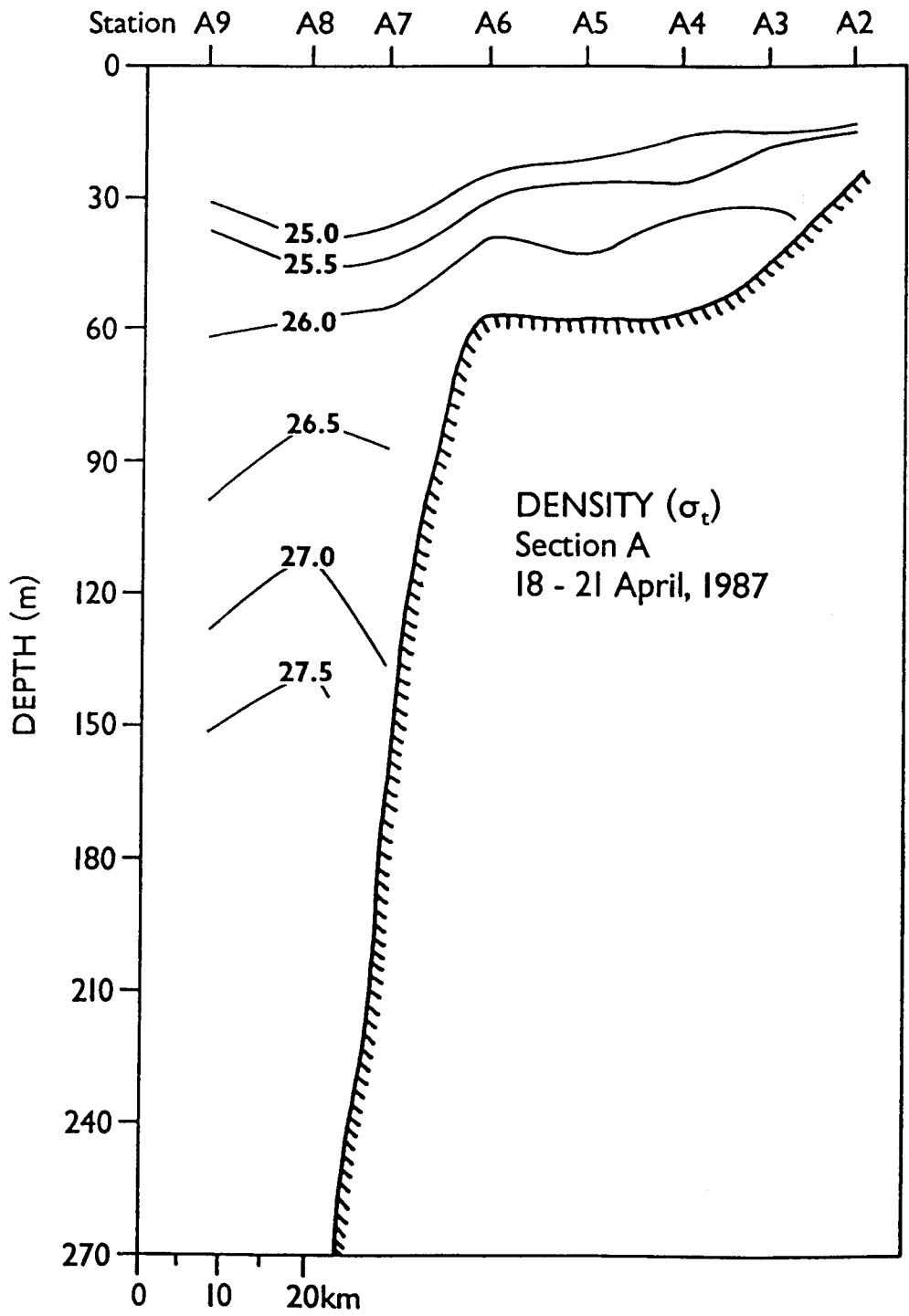


Figure 72. Density at section A in April 1987.

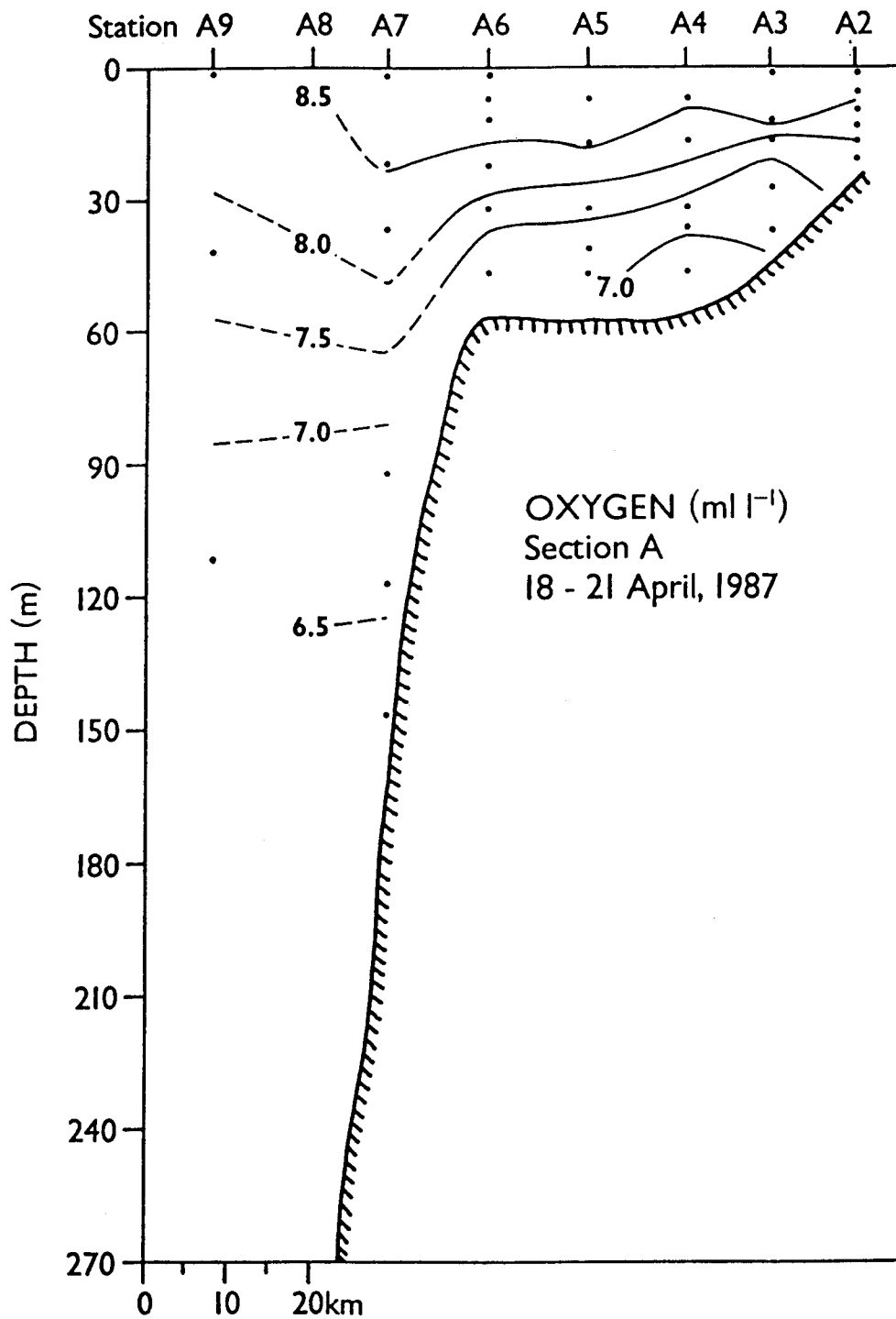


Figure 73. Dissolved oxygen at section A in April 1987.

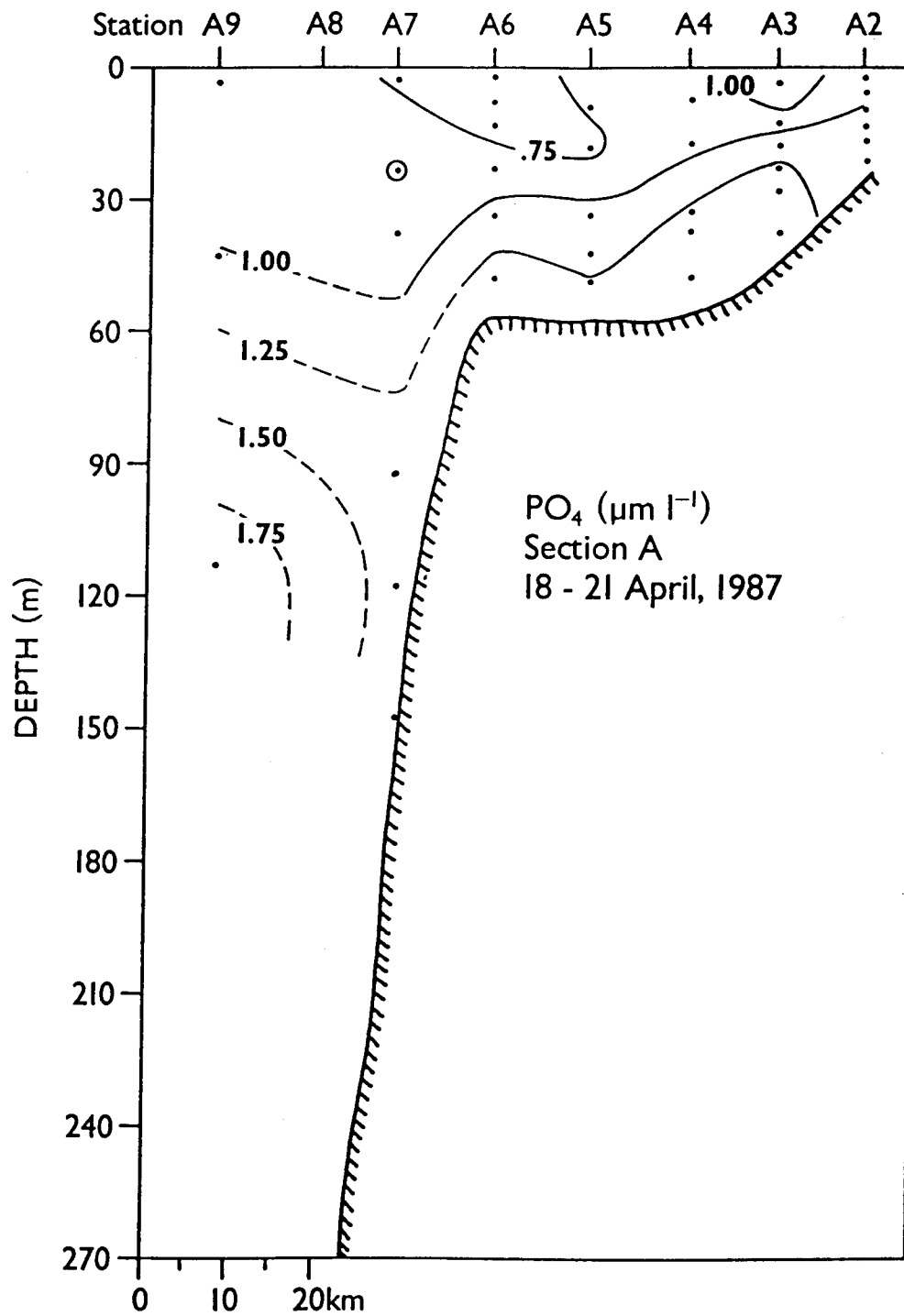


Figure 74. Phosphate at section A in April 1987.

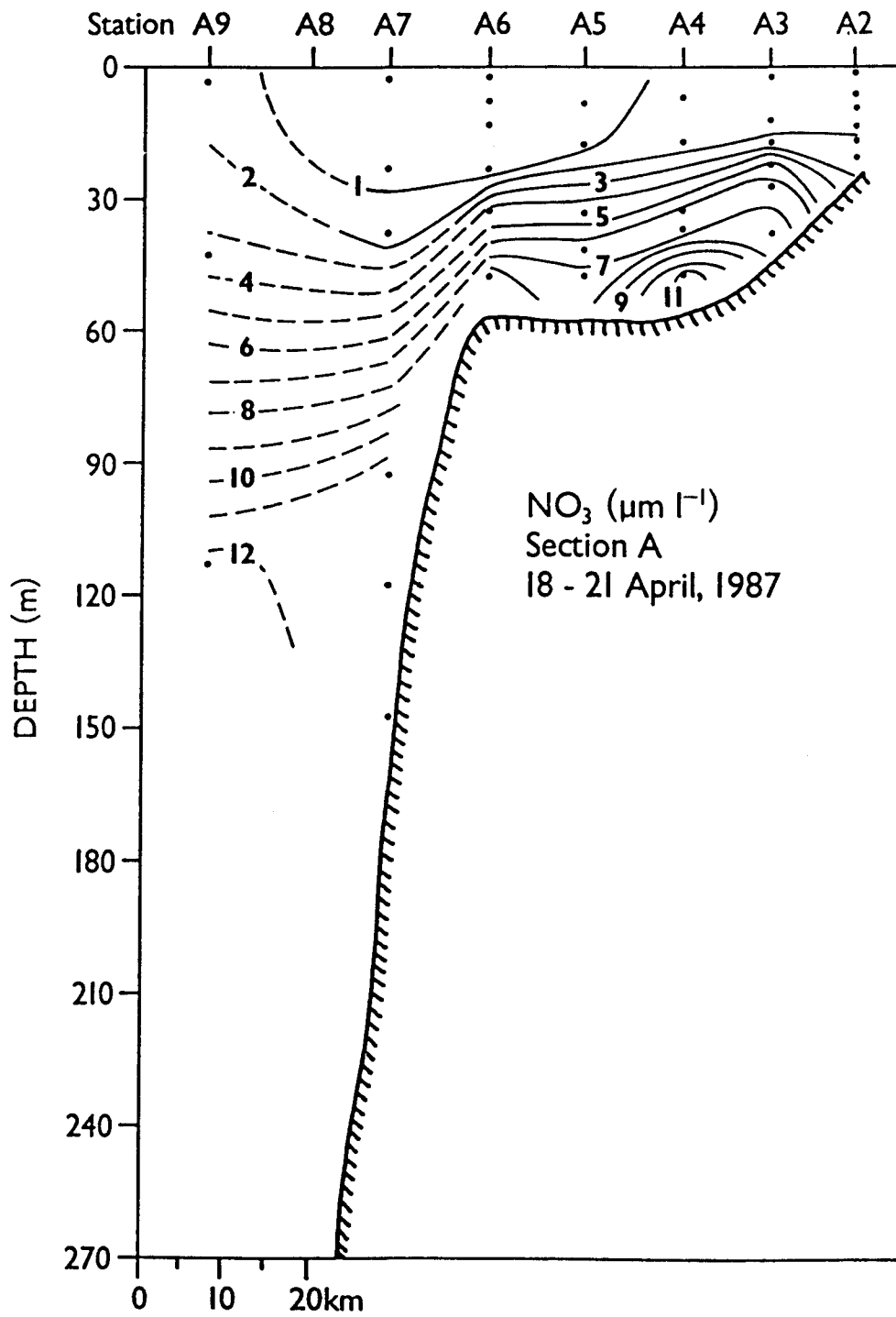


Figure 75. Nitrate at section A in April 1987.

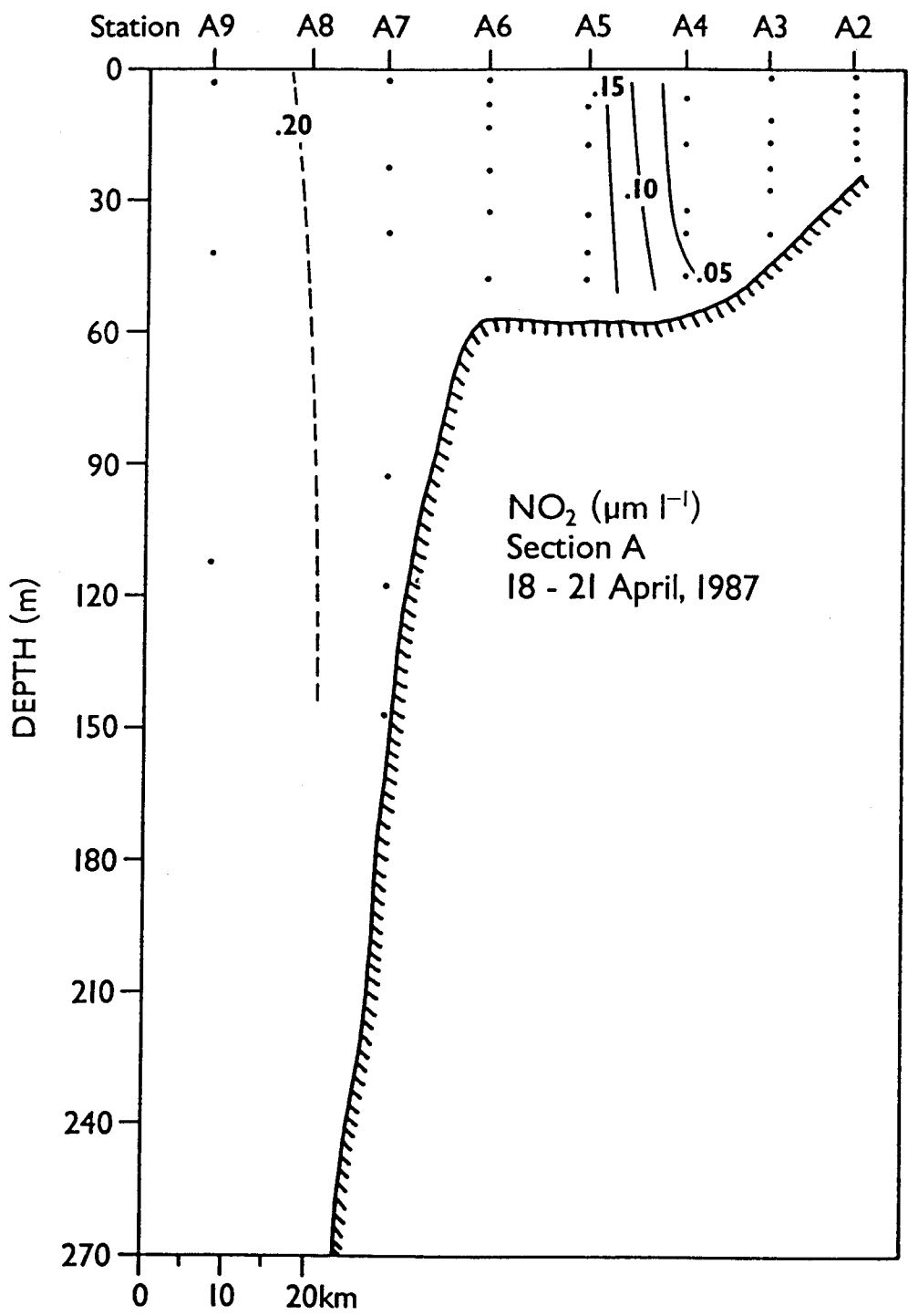


Figure 76. Nitrite at section A in April 1987.

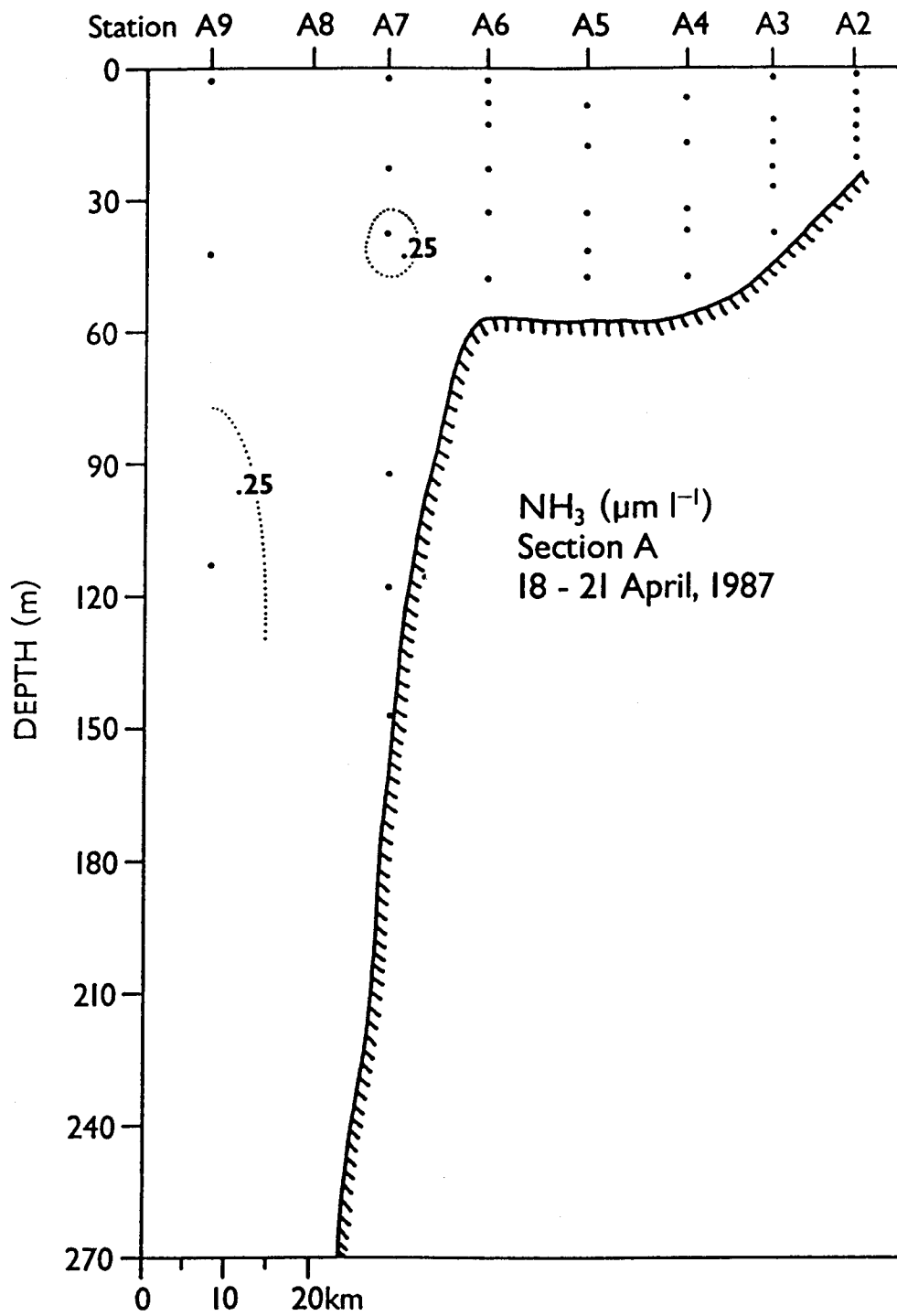


Figure 77. Ammonia at section A in April 1987.

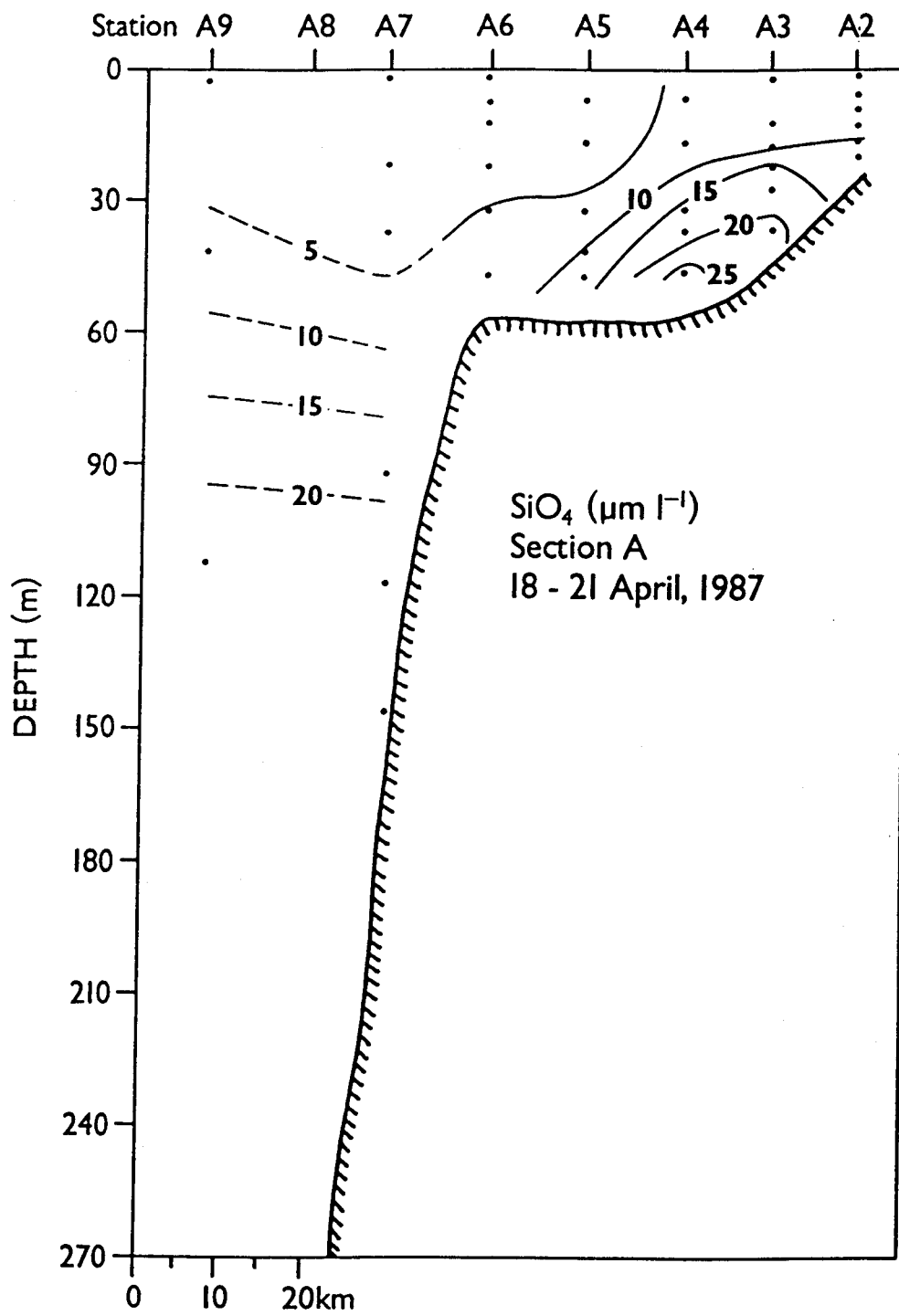


Figure 78. Silicate at section A in April 1987.

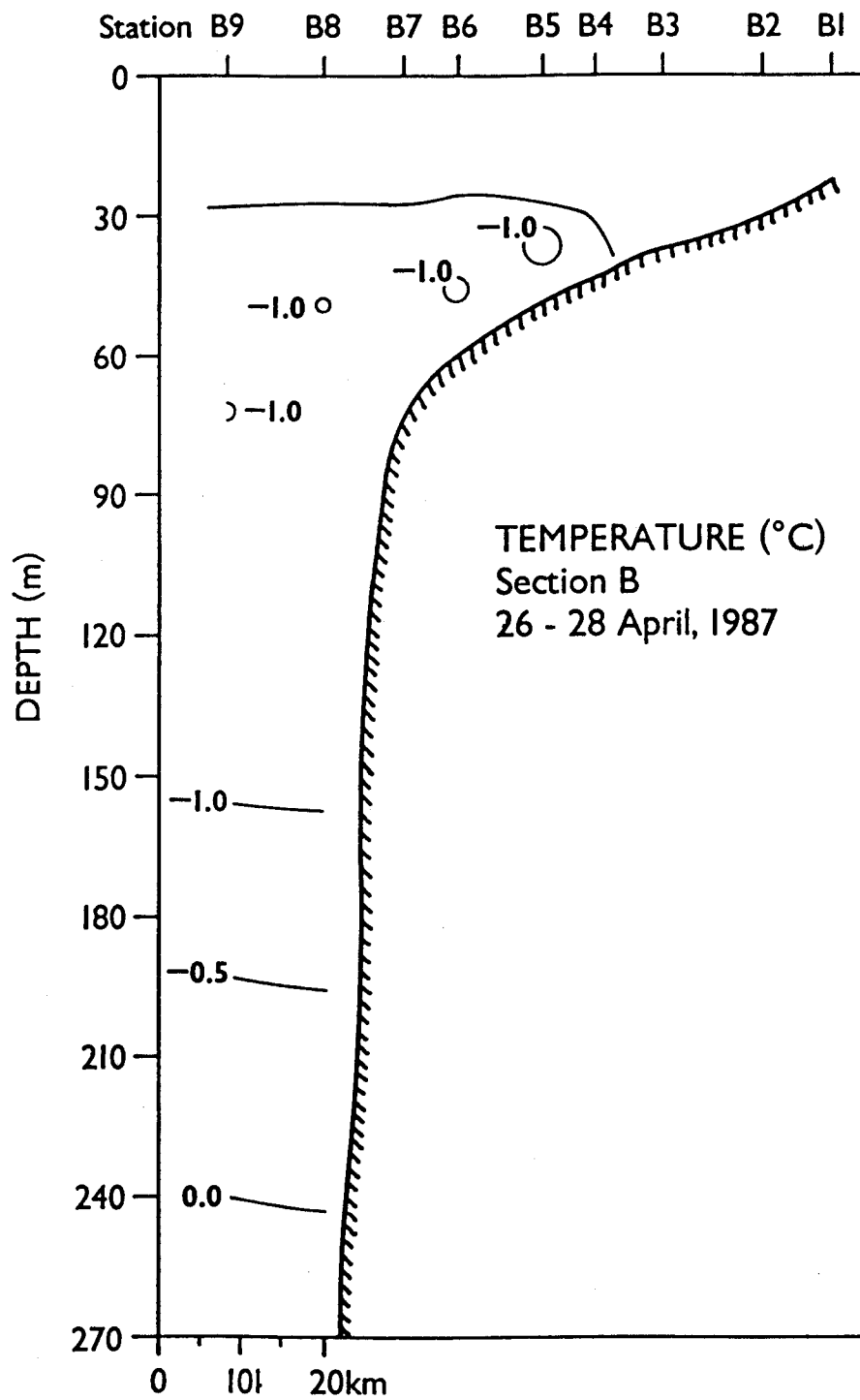


Figure 79. Temperature at section B in April 1987.

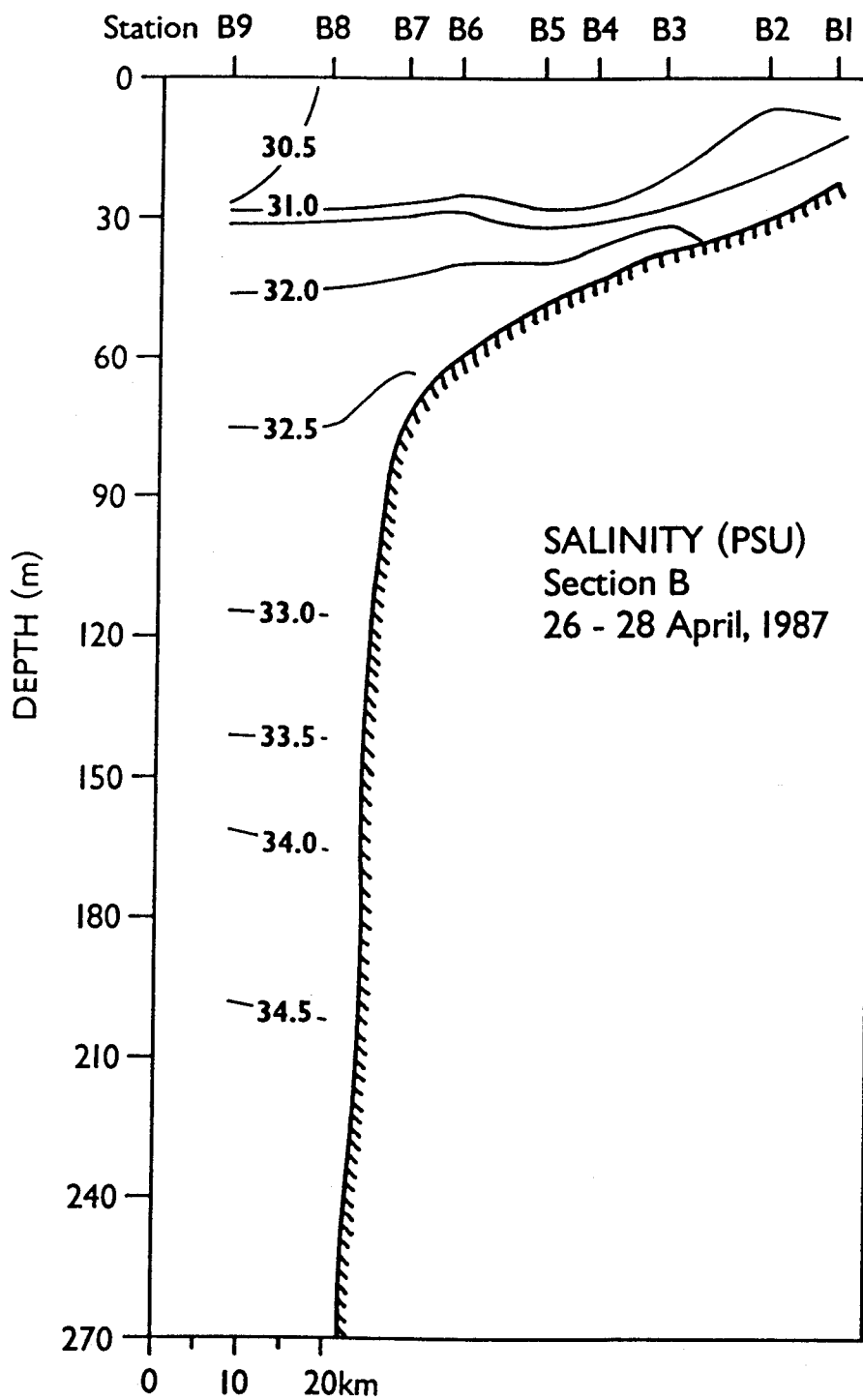


Figure 80. Salinity at section B in April 1987.

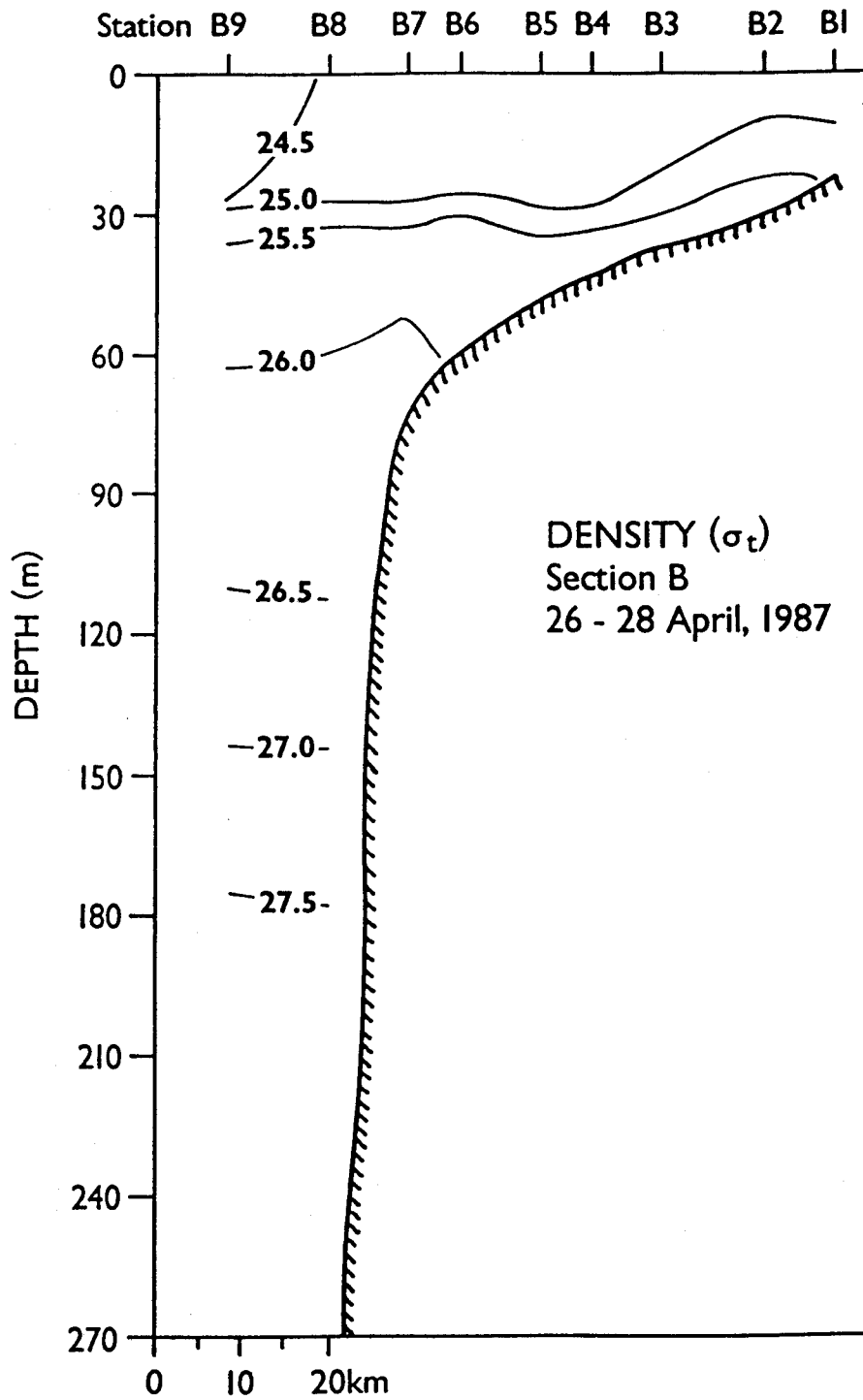


Figure 81. Density at section B in April 1987.

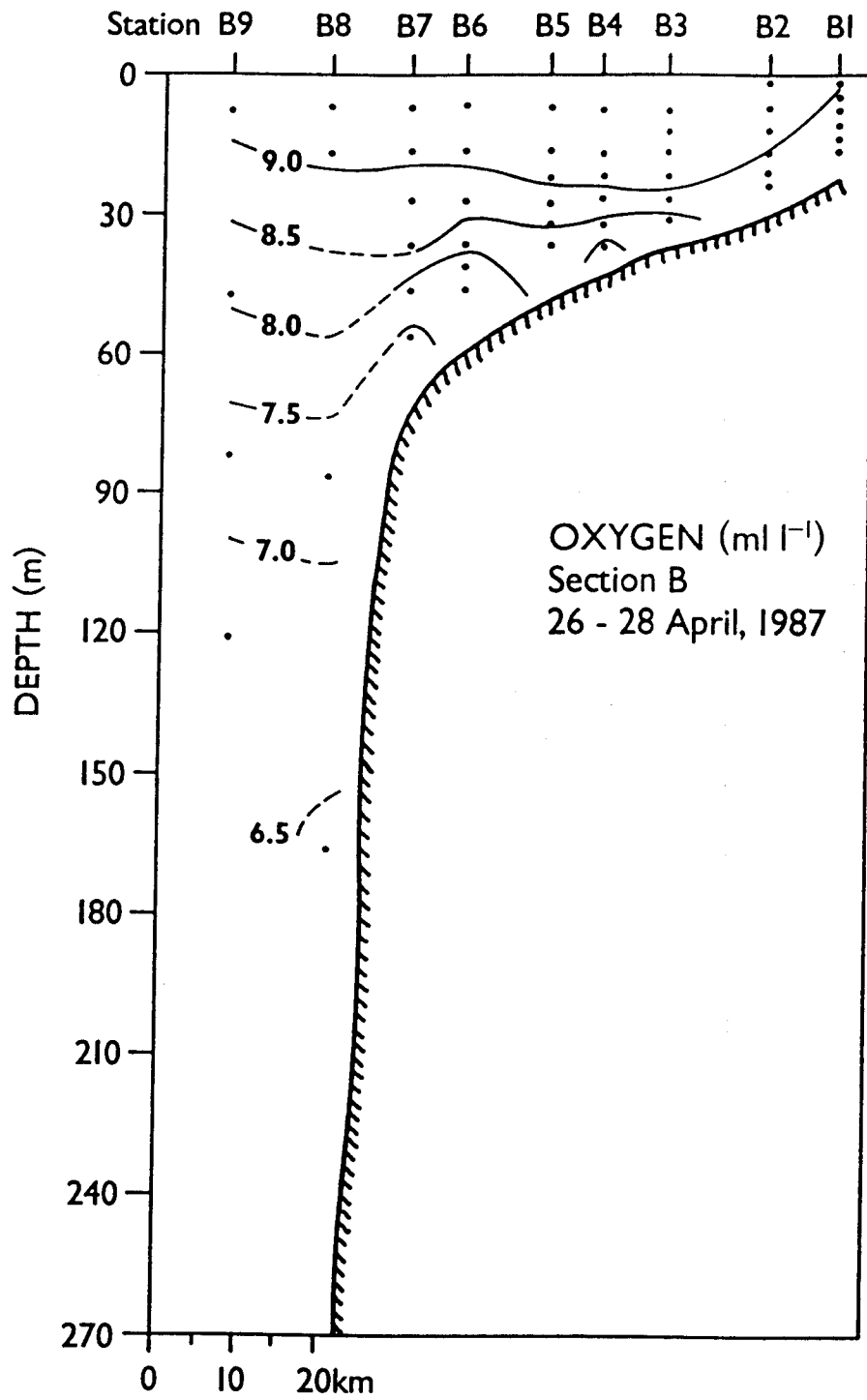


Figure 82. Dissolved oxygen at section B in April 1987.

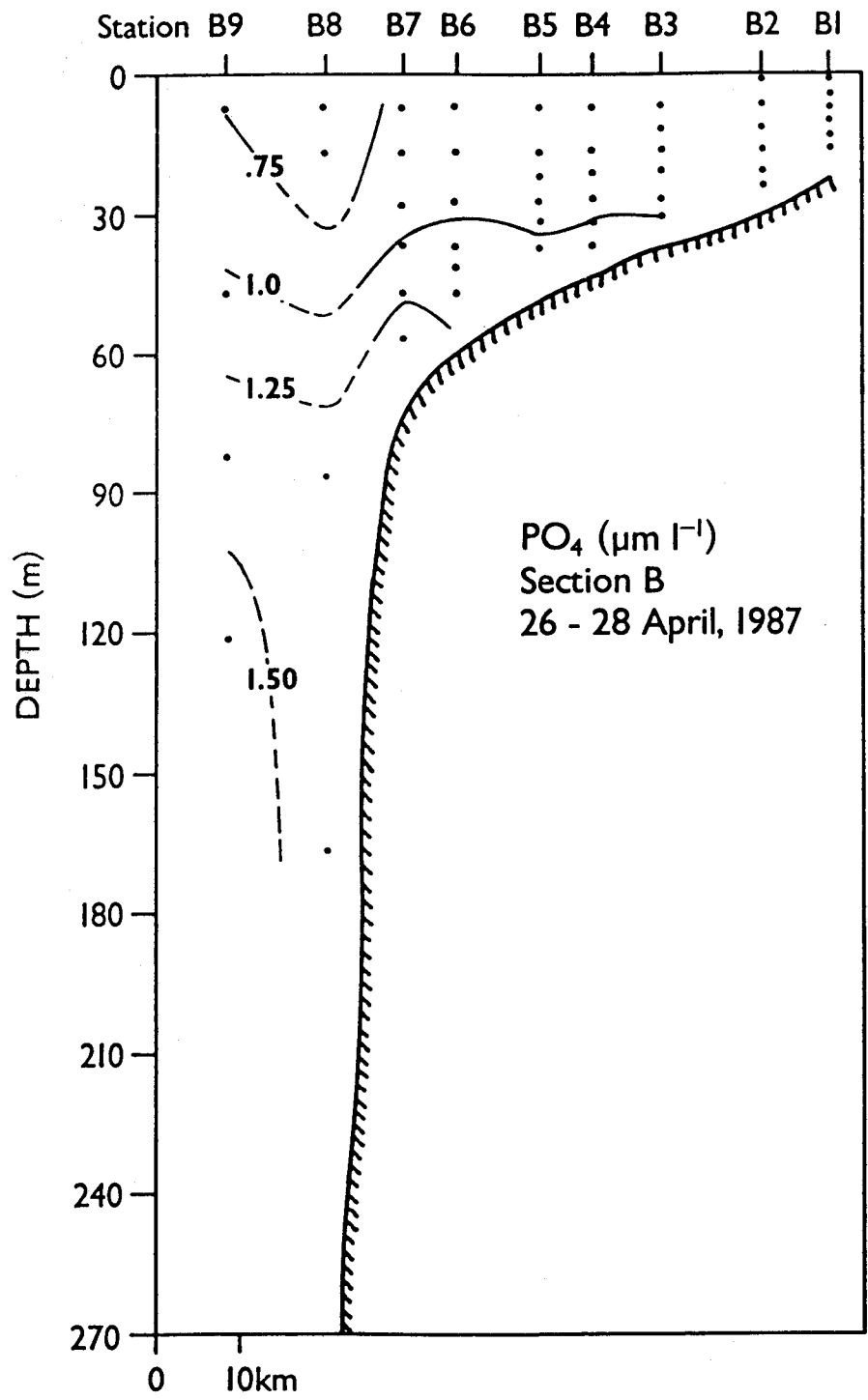


Figure 83. Phosphate at section B in April 1987.

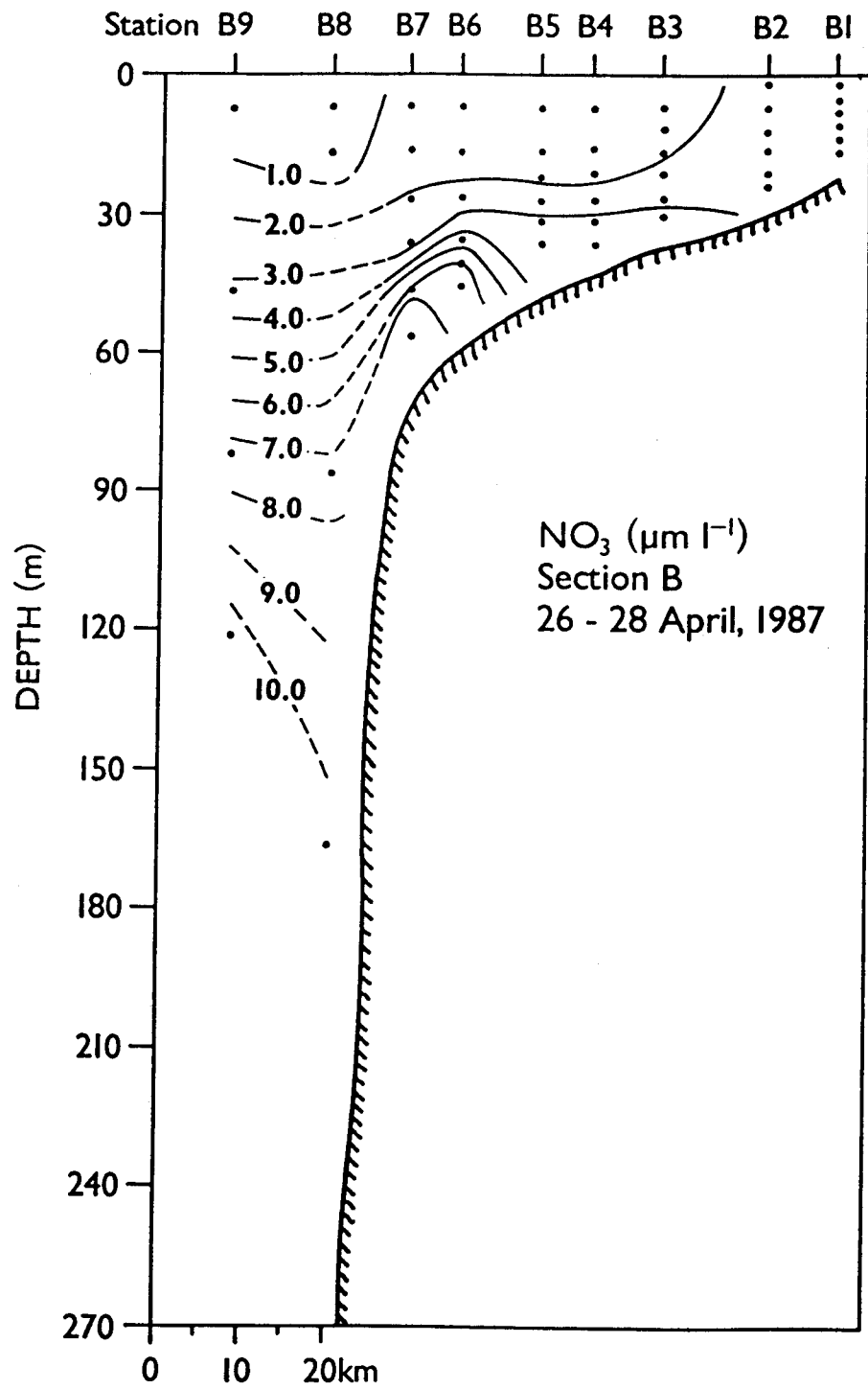


Figure 84. Nitrate at section B in April 1987.

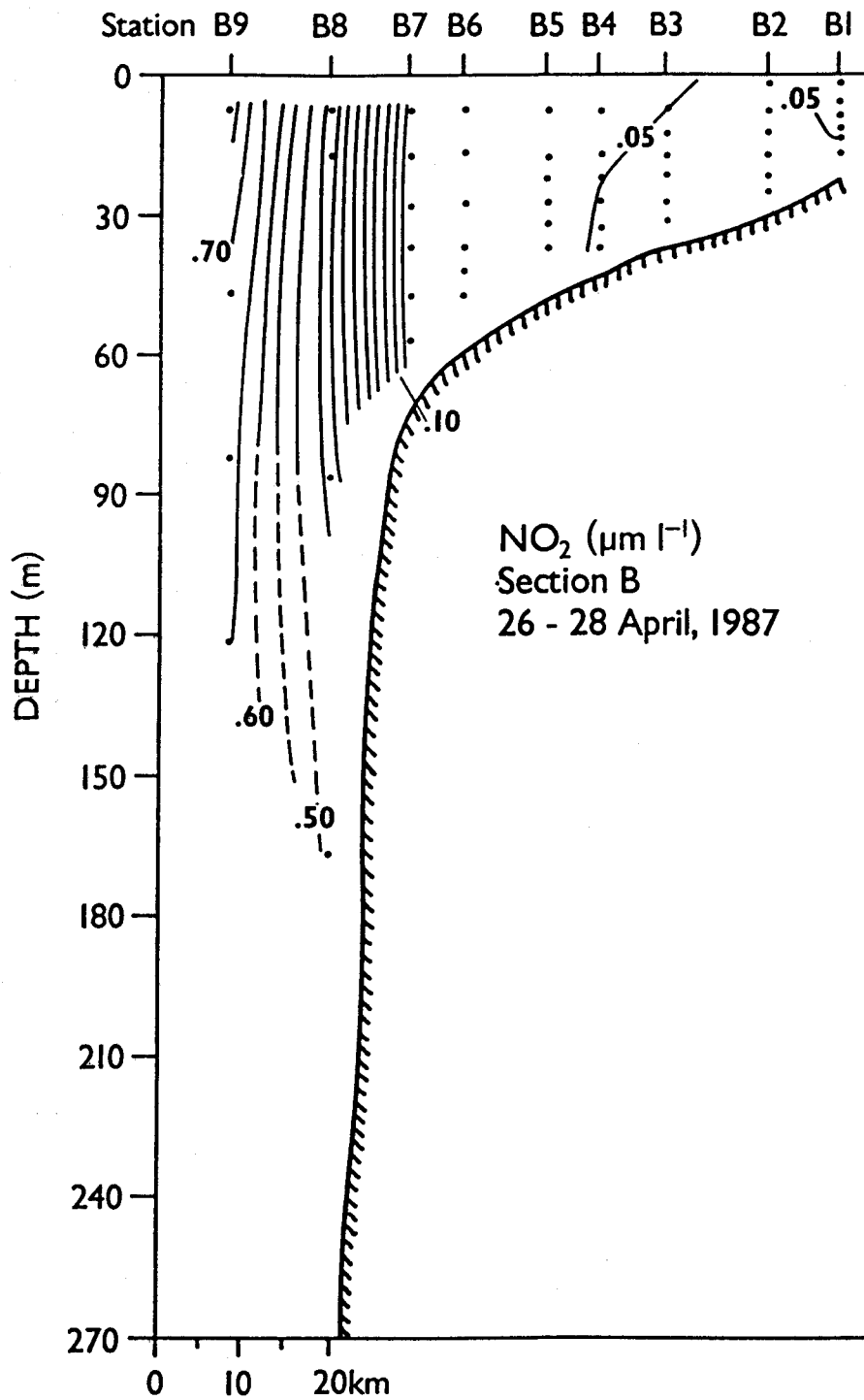


Figure 85. Nitrite at section B in April 1987.

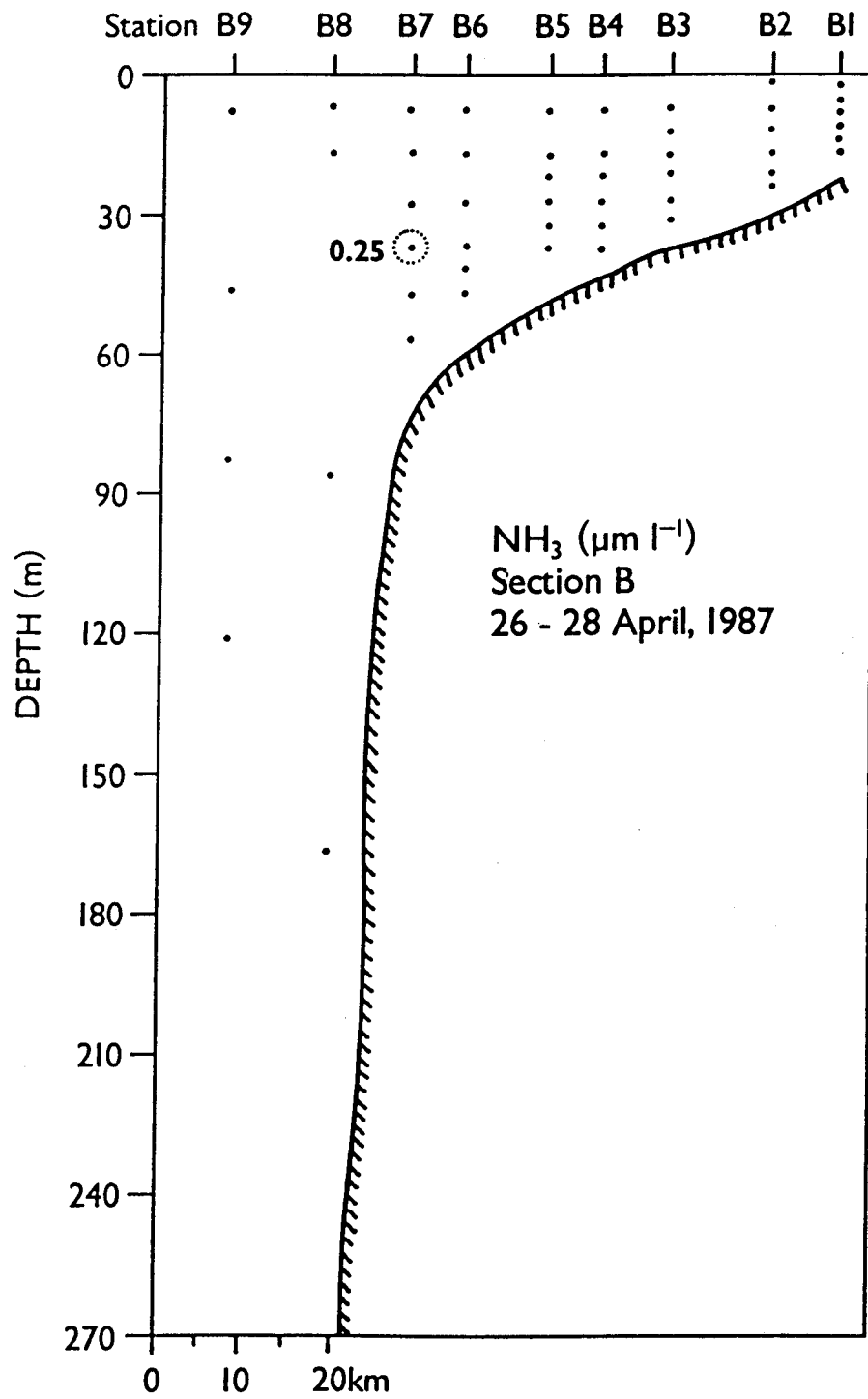


Figure 86. Ammonia at section B in April 1987.

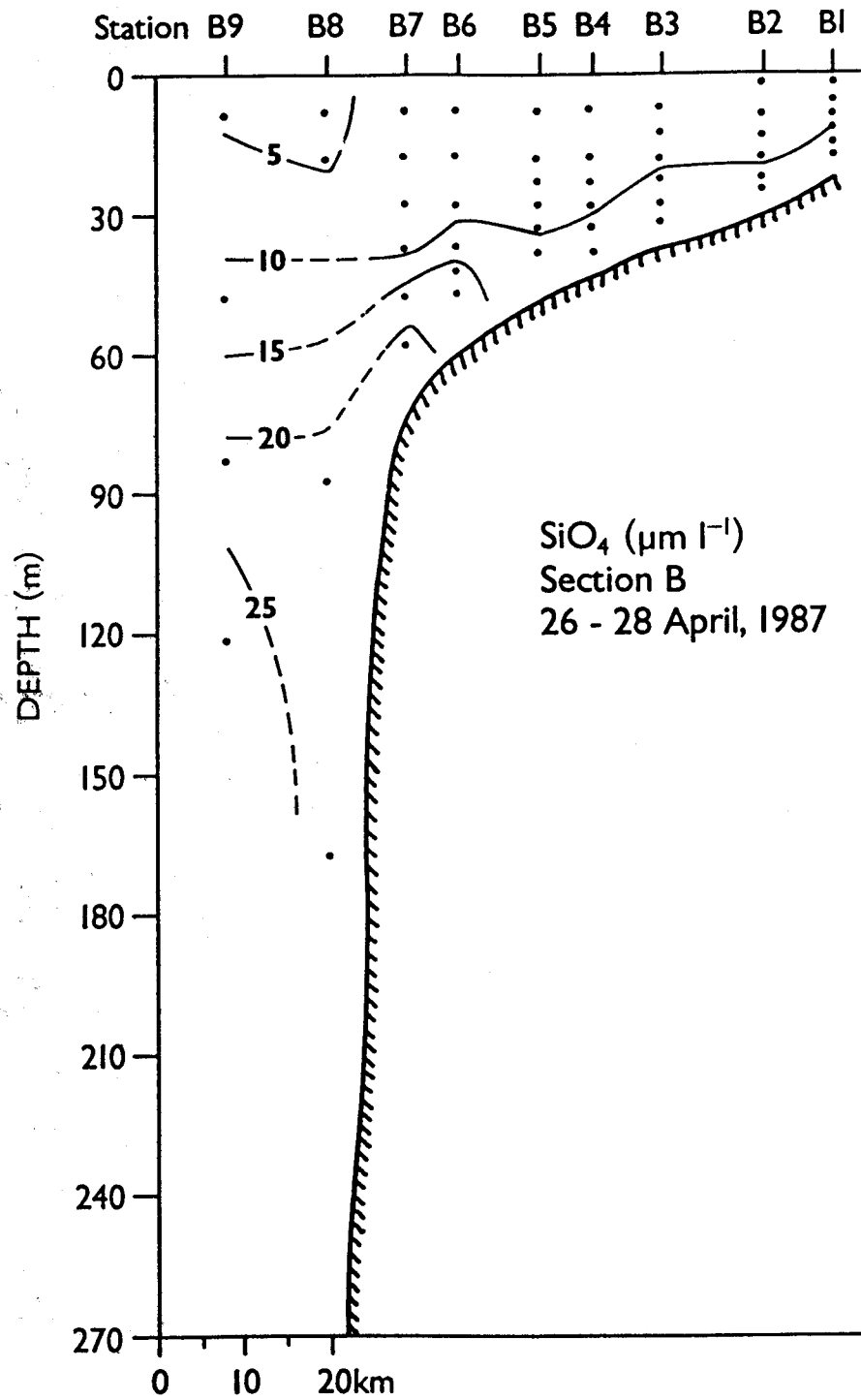


Figure 87. Silicate at section B in April 1987.

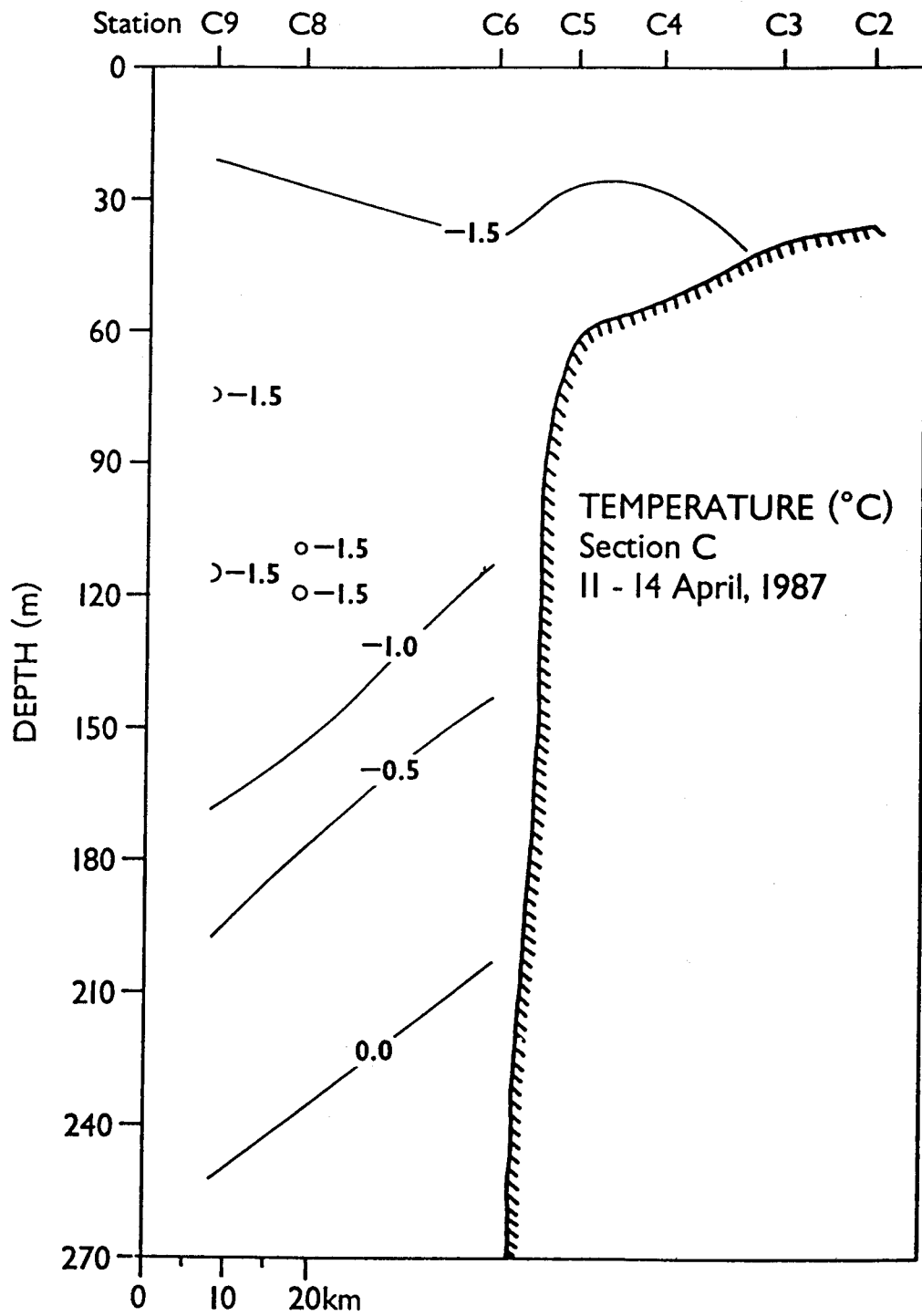


Figure 88. Temperature at section C in April 1987.

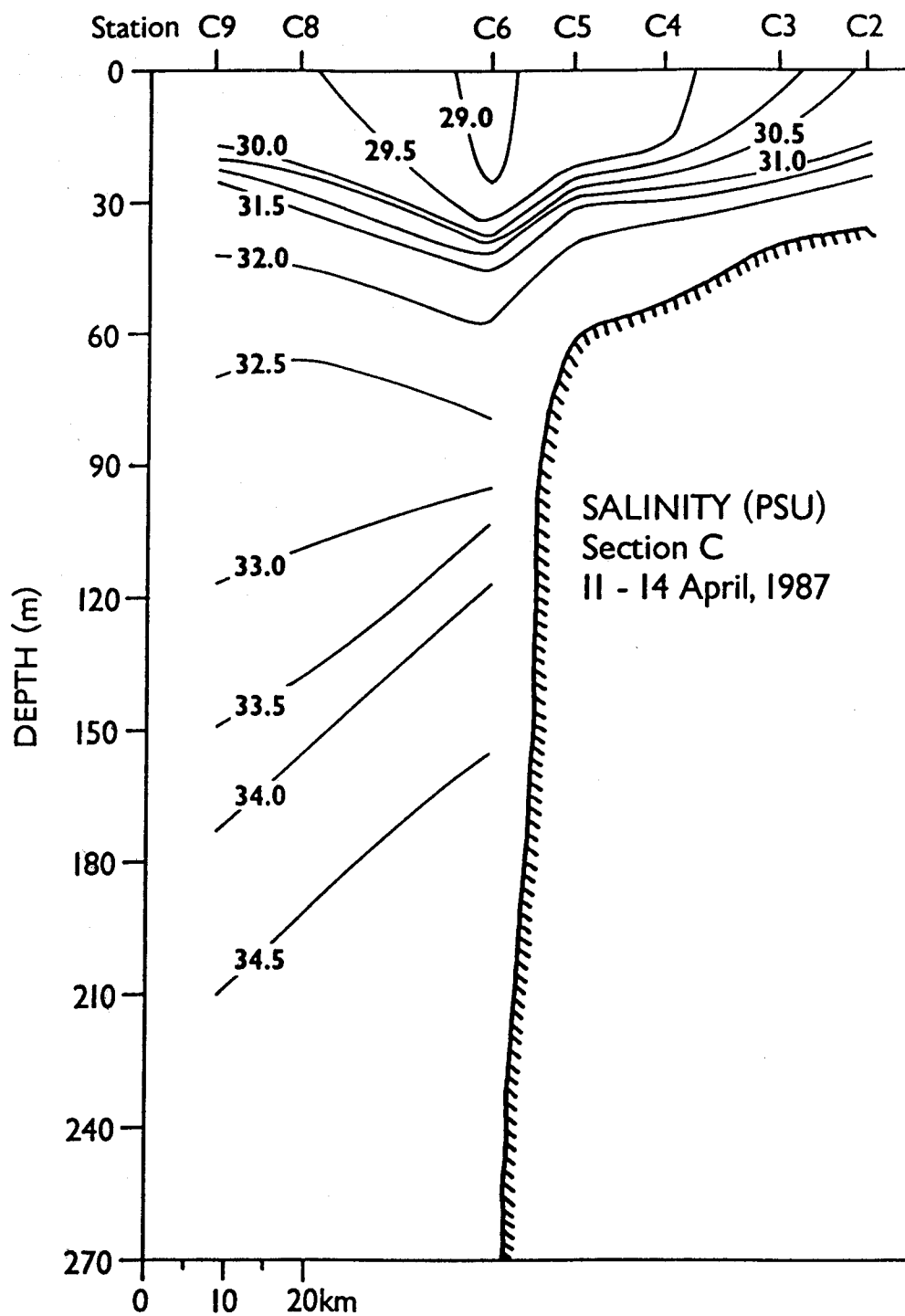


Figure 89. Salinity at section C in April 1987.

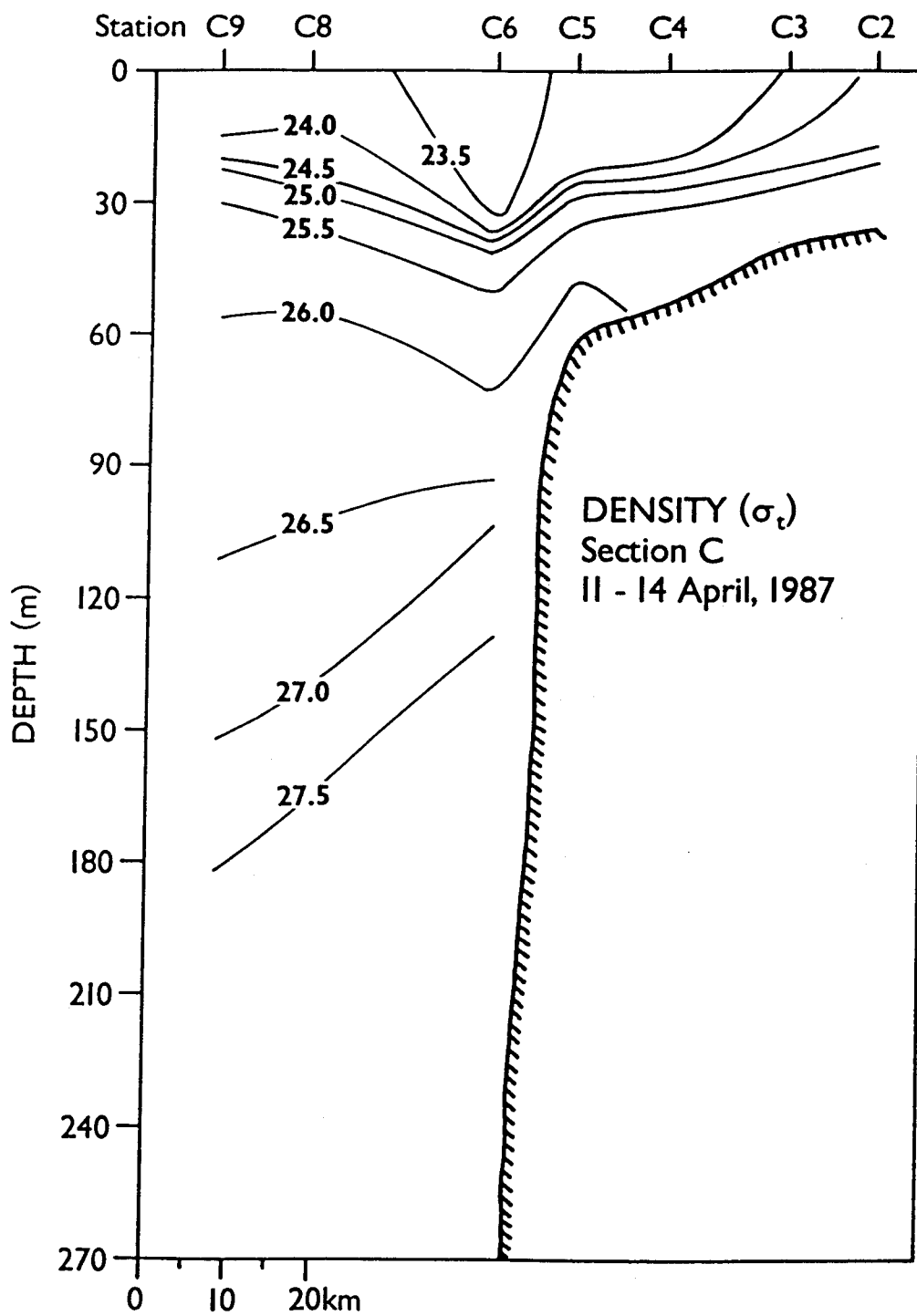


Figure 90. Density at section C in April 1987.

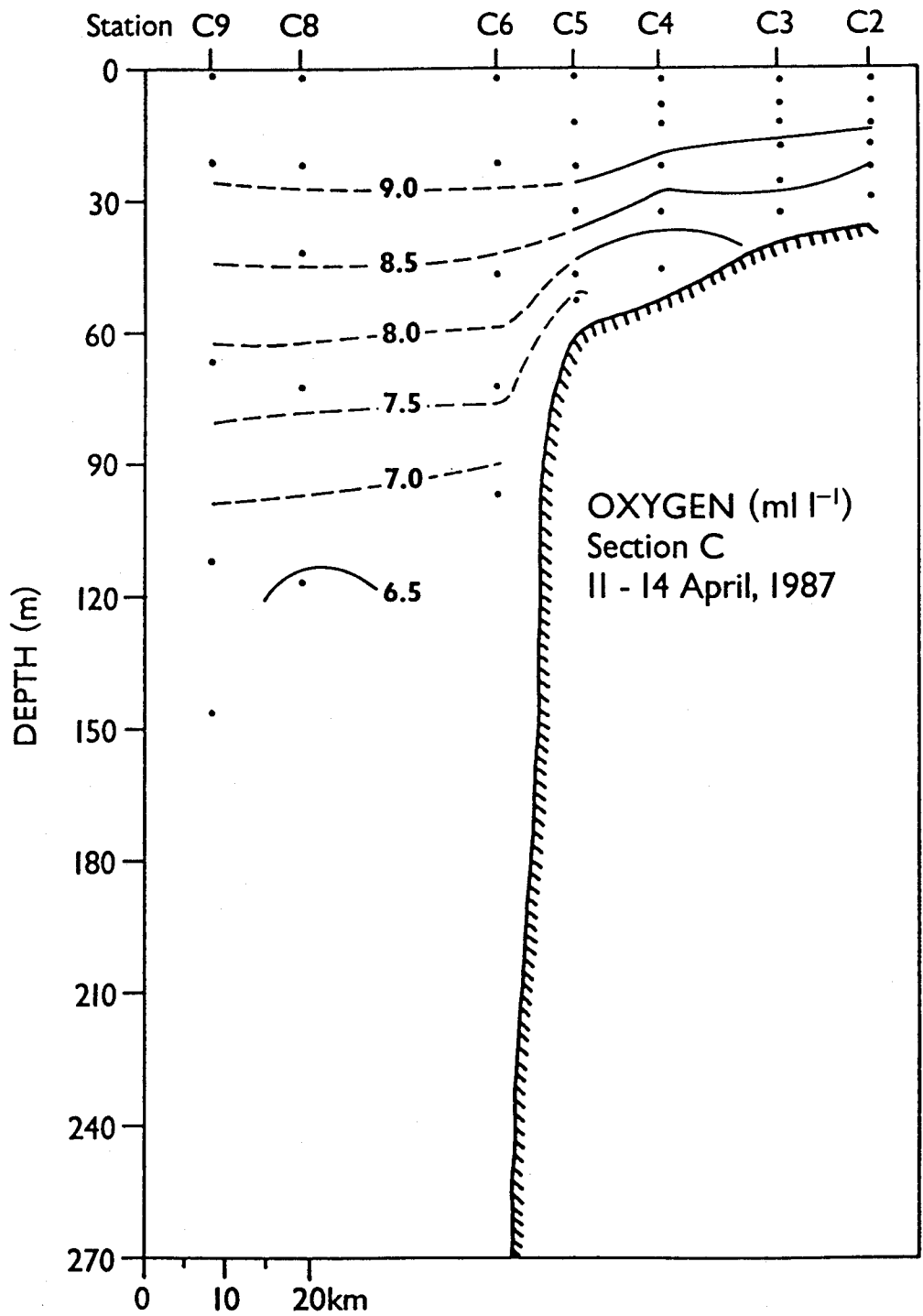


Figure 91. Dissolved oxygen at section C in April 1987.

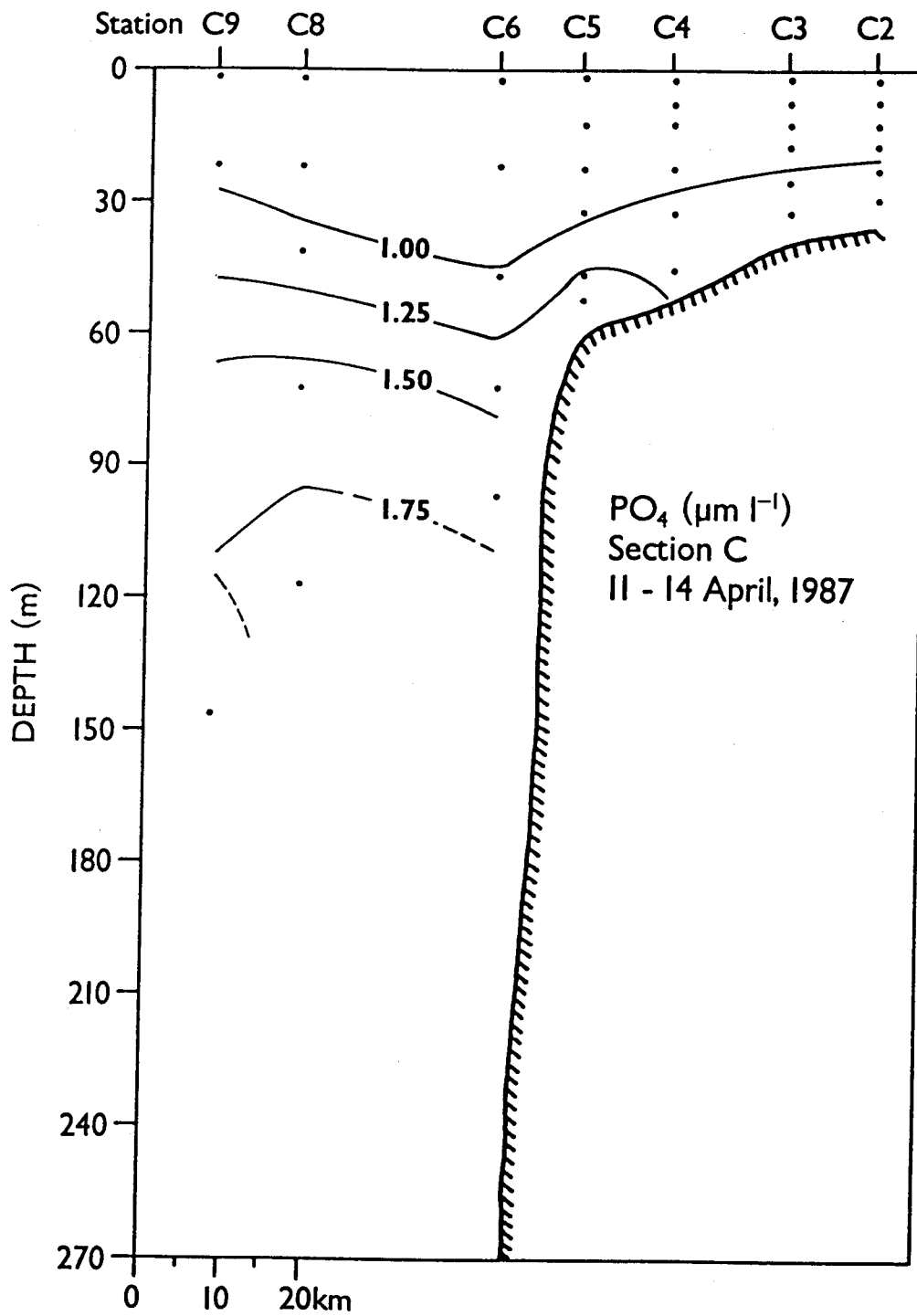


Figure 92. Phosphate at section C in April 1987.

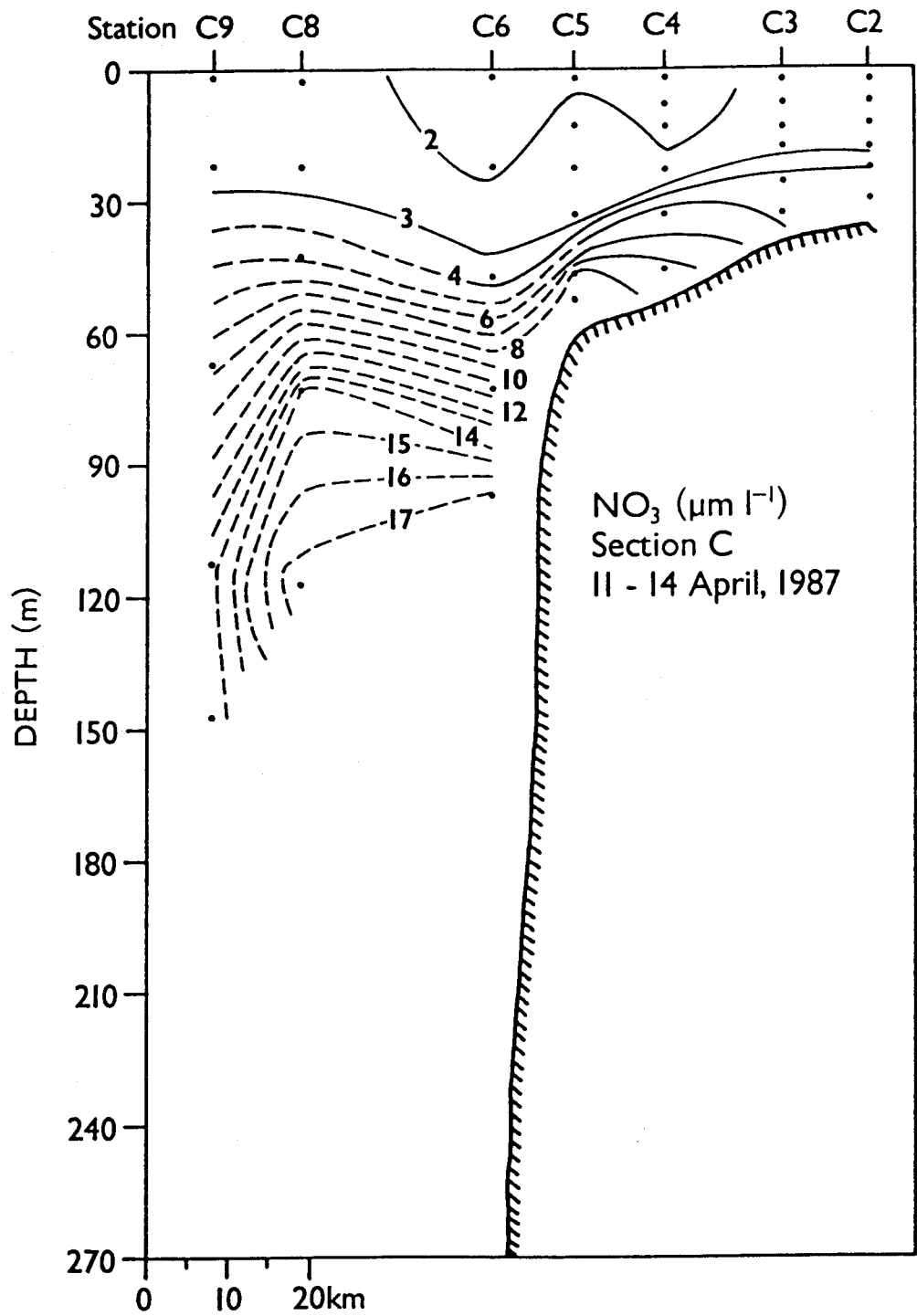


Figure 93. Nitrate at section C in April 1987.

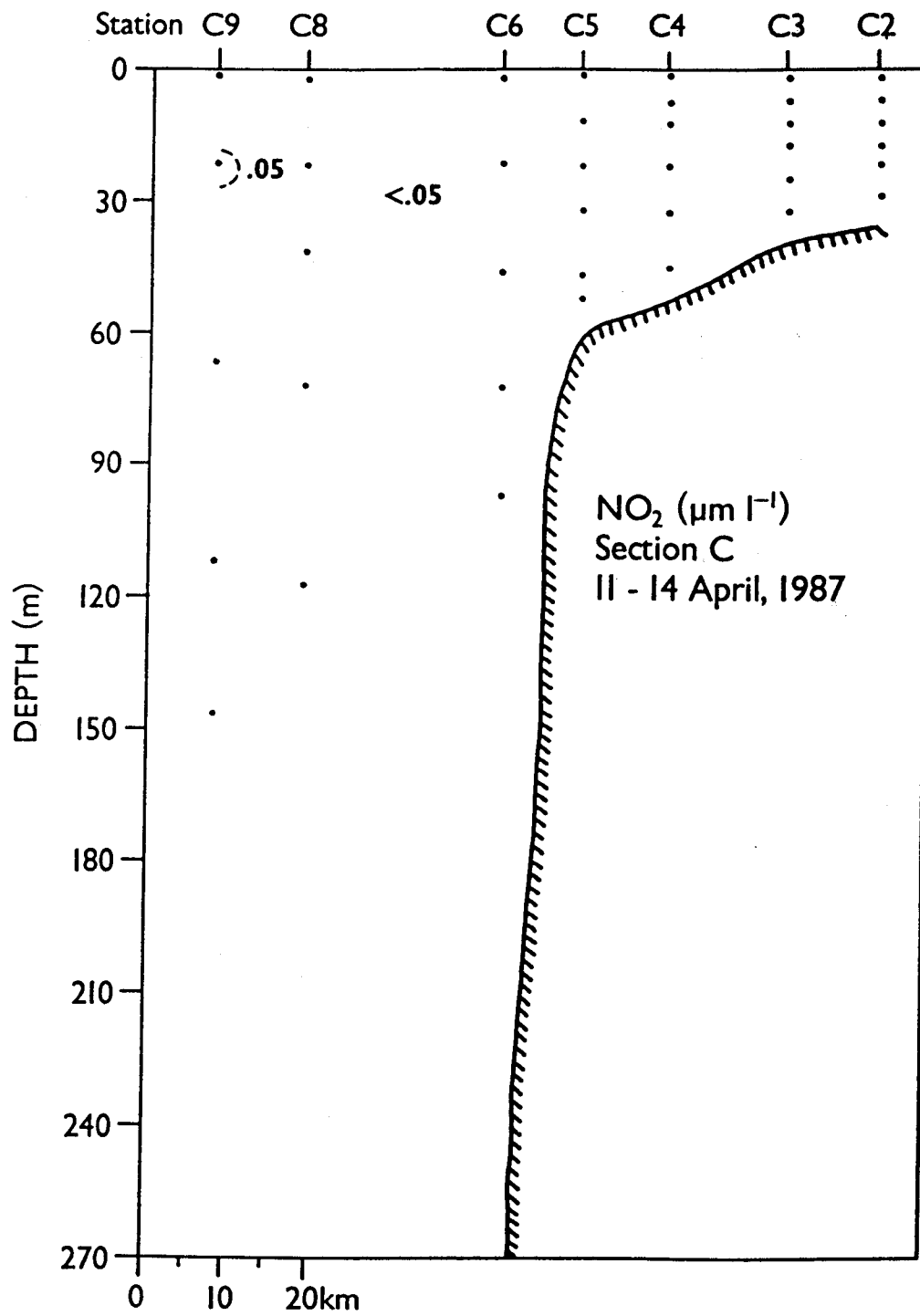


Figure 94. Nitrite at section C in April 1987.

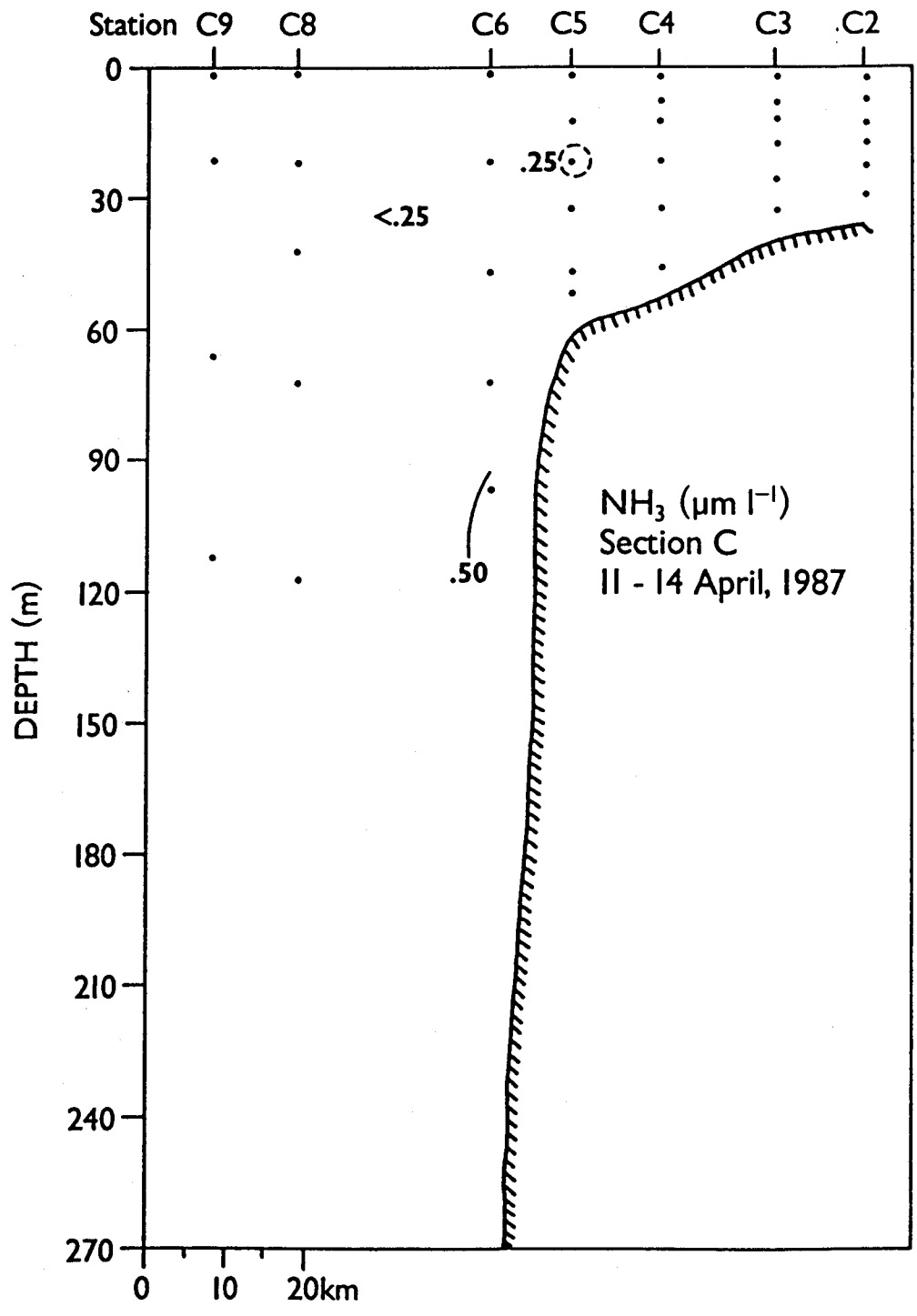


Figure 95. Ammonia at section C in April 1987.

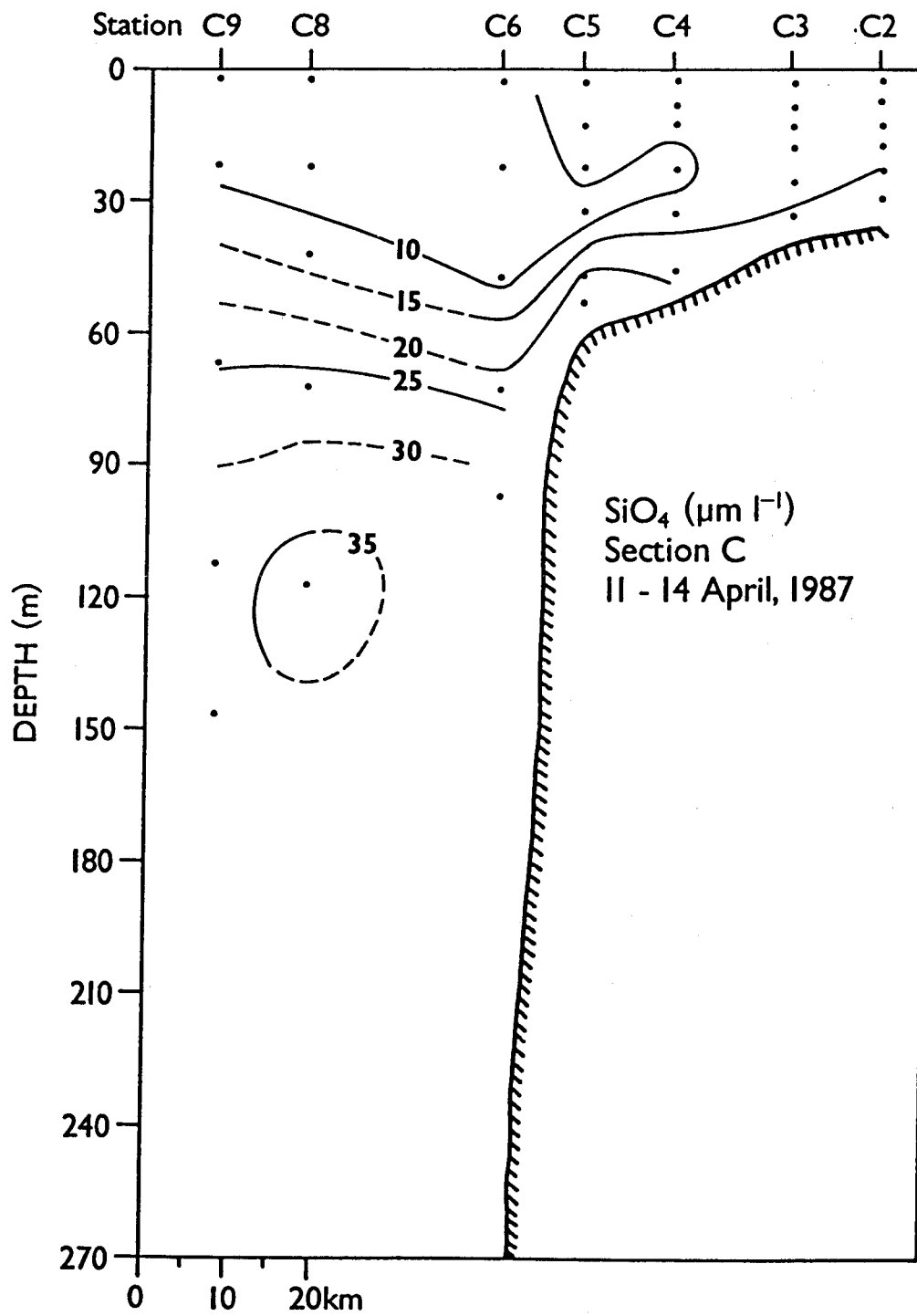
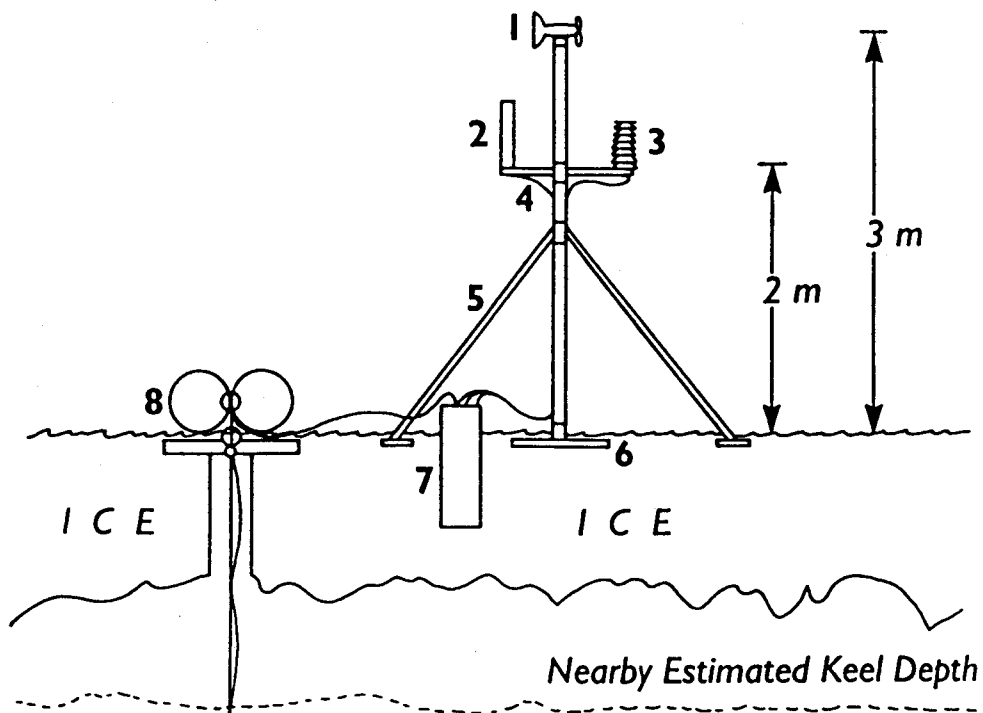


Figure 96. Silicate at section C in April 1987.



**Section View  
Beaufort Meteorological Station**

- 1 R.M. Young Wind Monitor (05103)
- 2 Synergetics ¼ Wave Antenna
- 3 YSI Thermistor Composite Set (44212)  
in R.M. Young Gill Multiplate Radiation Shield
- 4 Cross Arm with Barometer Port
- 5 Aluminum Mast with Wooden Legs
- 6 Wooden Base Plate with Al. Fittings
- 7 Coastal Climate Zeno Computer (ZE602)  
with Aanderaa Compass (I248) and  
with Telonics Argos Transmitter and  
with Paroscientific Barometer
- 8 2 Glass Floats plus 4x4 Brace over Core Hole
- 9 Wire Rope and Cabling
- 10 YSI Water Temperature Probe
- 11 Interocean S4 Current Meter
- 12 50# Chain Weight

Figure 97. Section view of an ARGOS station.

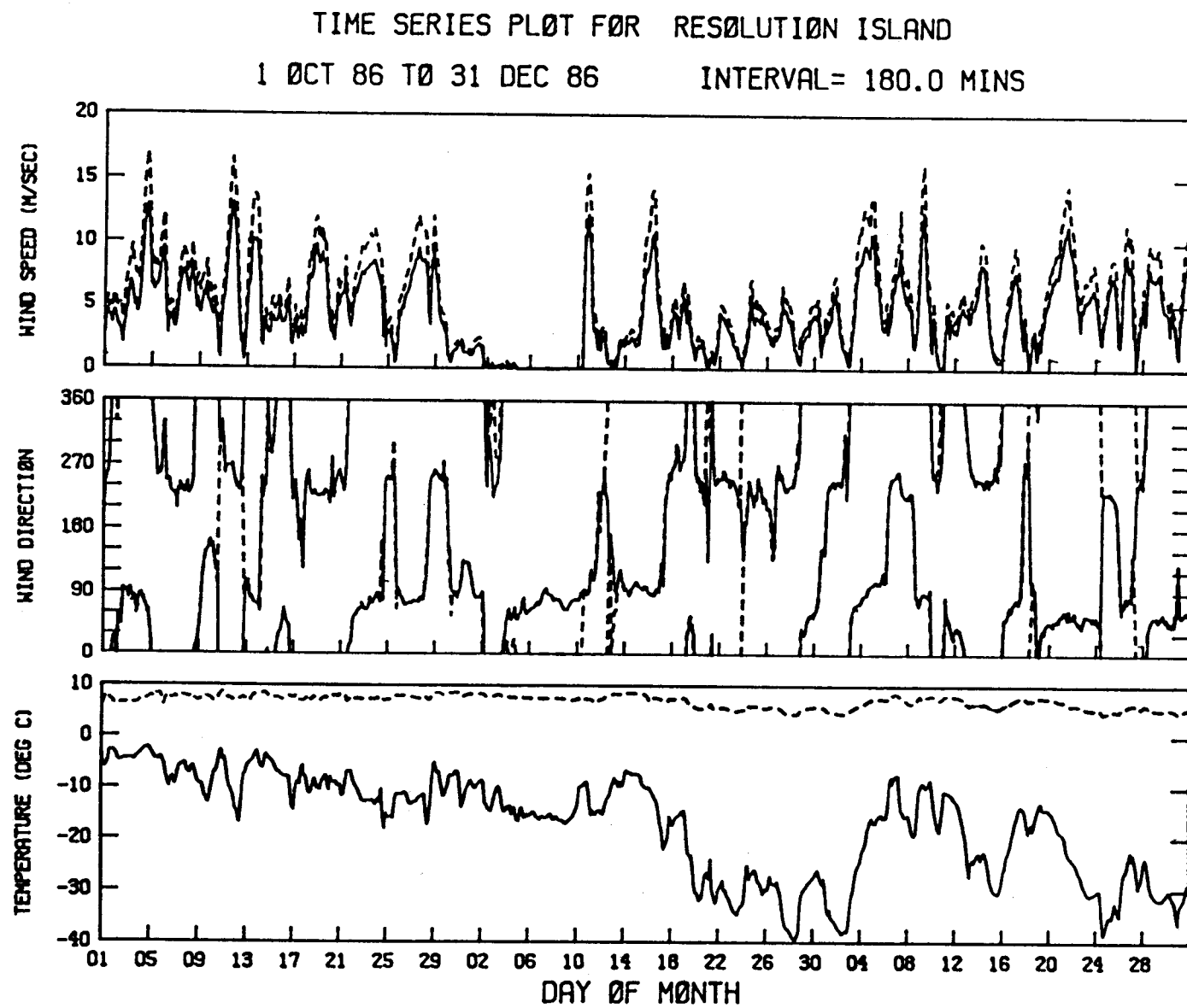


Figure 98. Air temperature and wind speed and direction from Resolution Island (Prudhoe Bay) for October-December 1986.

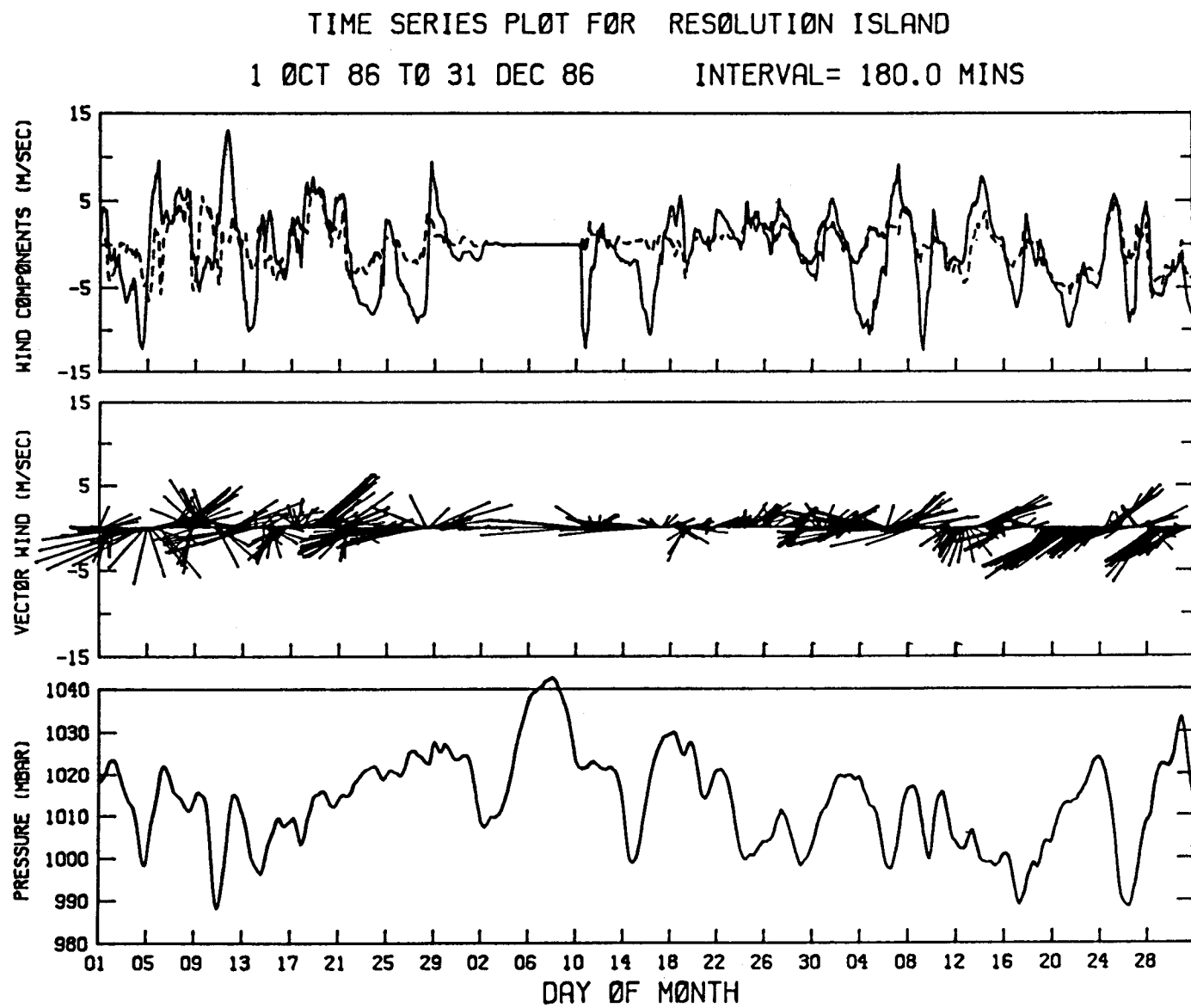


Figure 99. Sea-level pressure, wind components and vectors from Resolution Island (Prudhoe Bay) for October-December 1986.

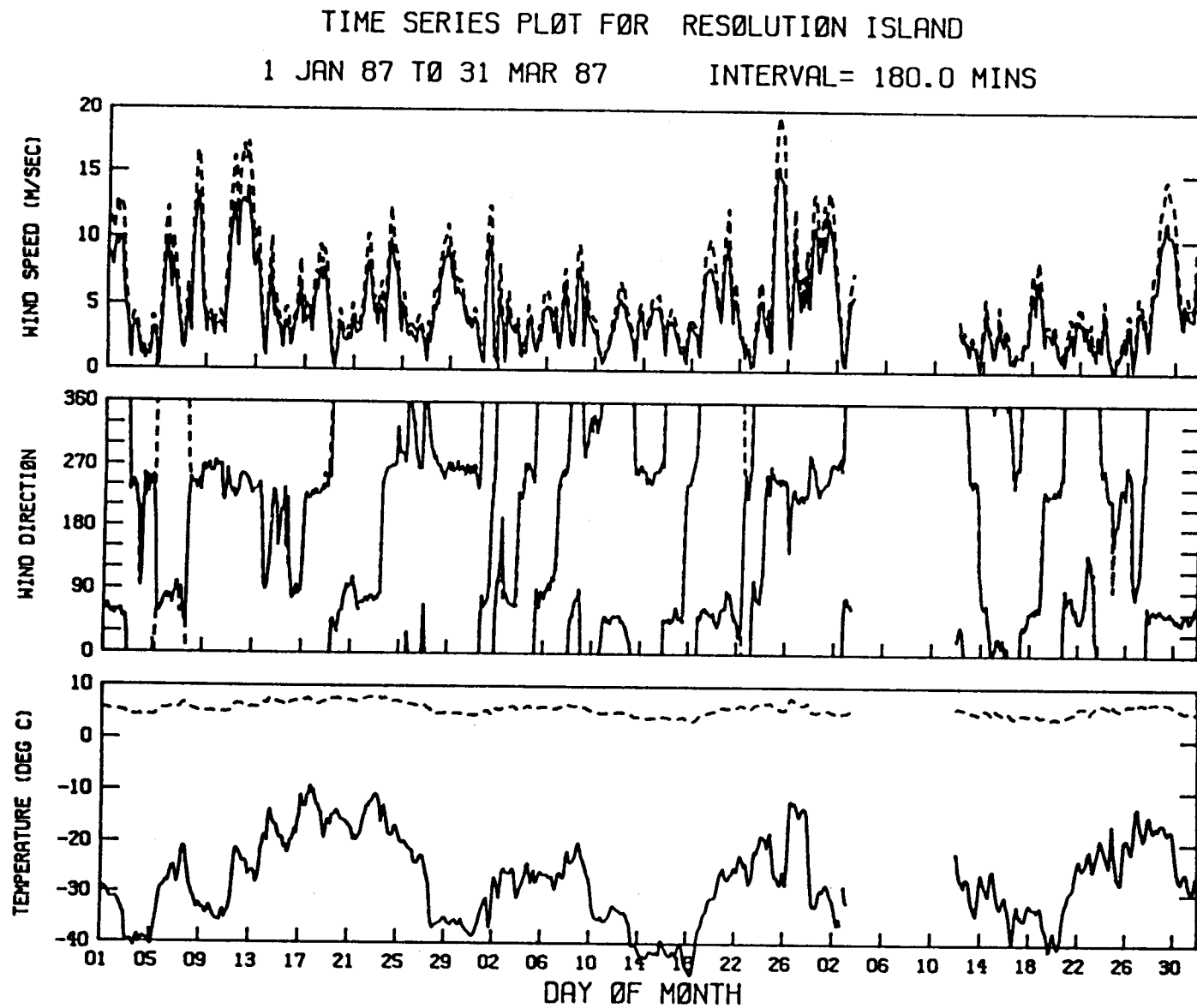


Figure 100. Air temperature and wind speed and direction from Resolution Island (Prudhoe Bay) for January-March 1987.

TIME SERIES PLOT FOR RESOLUTION ISLAND

1 JAN 87 TO 31 MAR 87

INTERVAL= 180.0 MINS

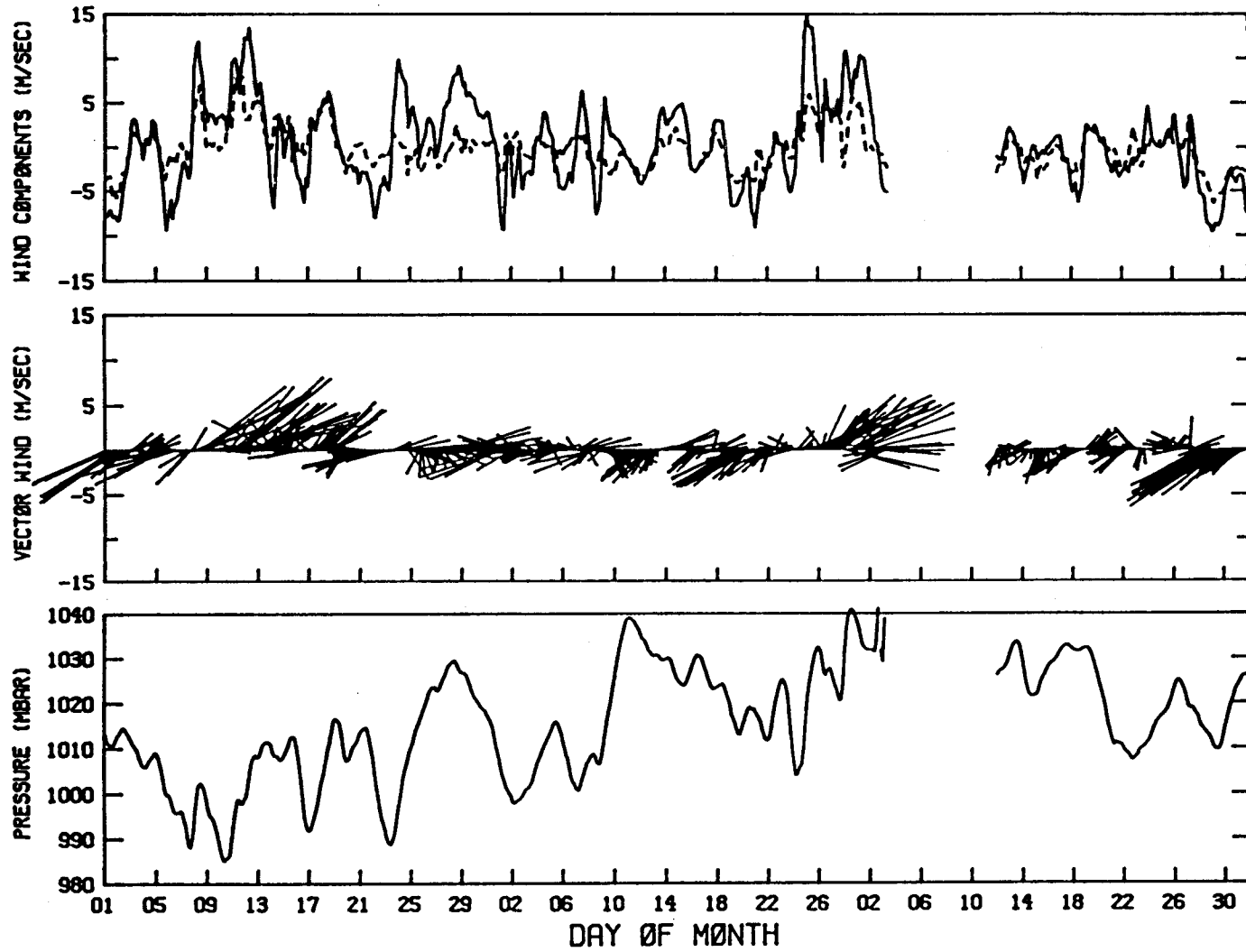


Figure 101. Sea-level pressure, wind components and vectors from Resolution Island (Prudhoe Bay) for January-March 1987.

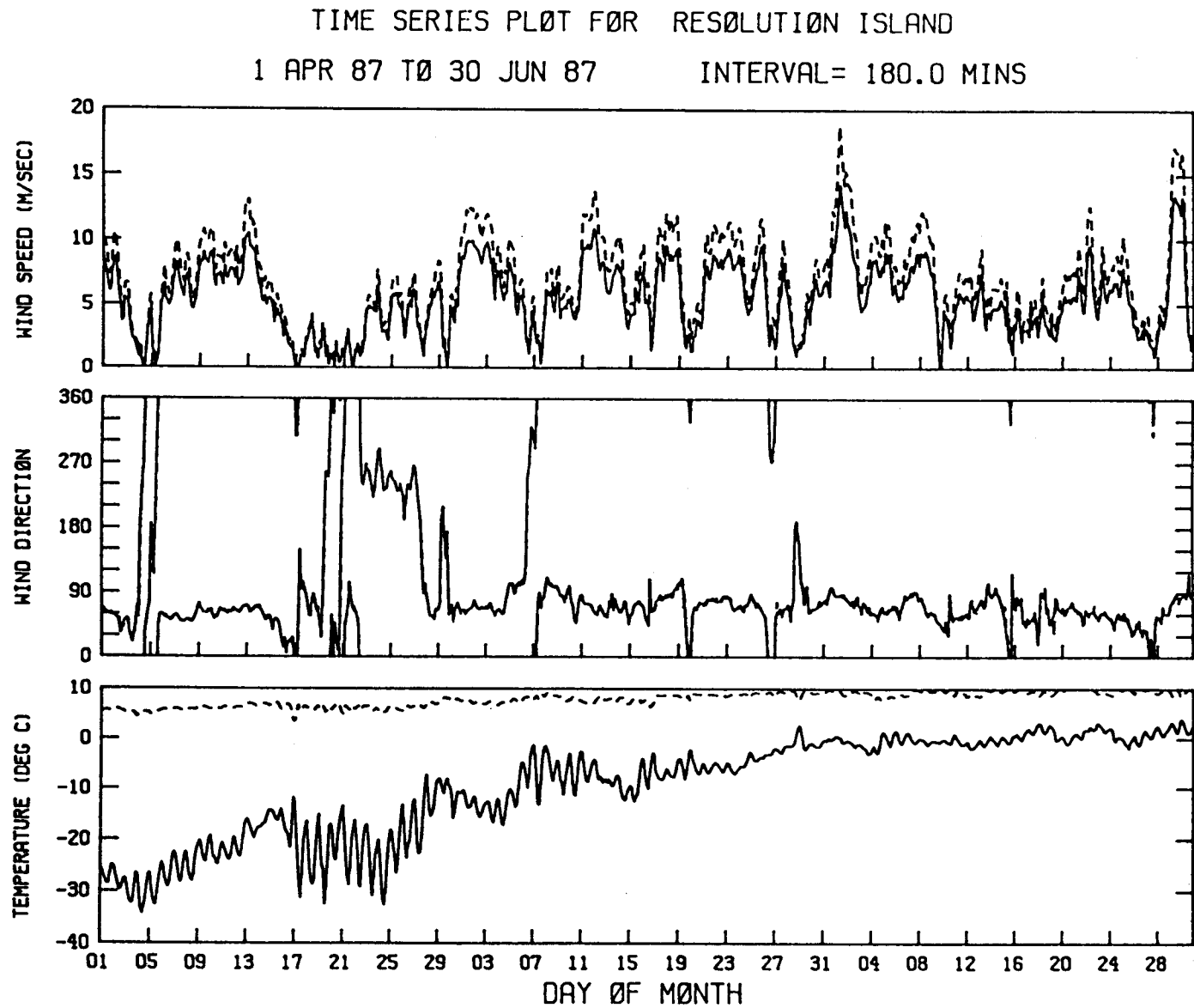


Figure 102. Air temperature and wind speed and direction from Resolution Island (Prudhoe Bay) for April-June 1987.

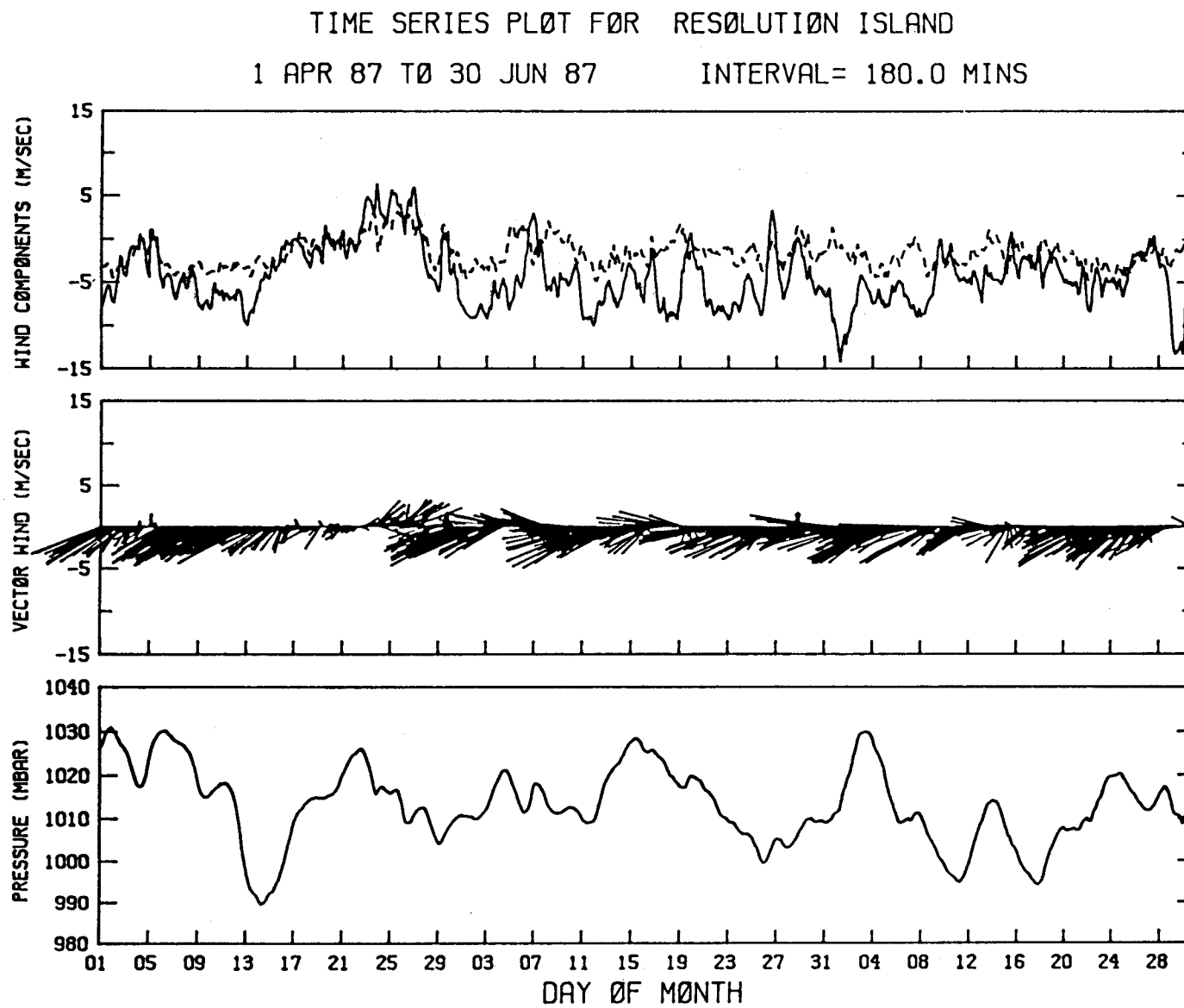


Figure 103. Sea-level pressure, wind components and vectors from Resolution Island (Prudhoe Bay) for April-June 1987.

TIME SERIES PLOT FOR RESOLUTION ISLAND

1 JUL 87 TO 30 SEP 87

INTERVAL= 180.0 MINS

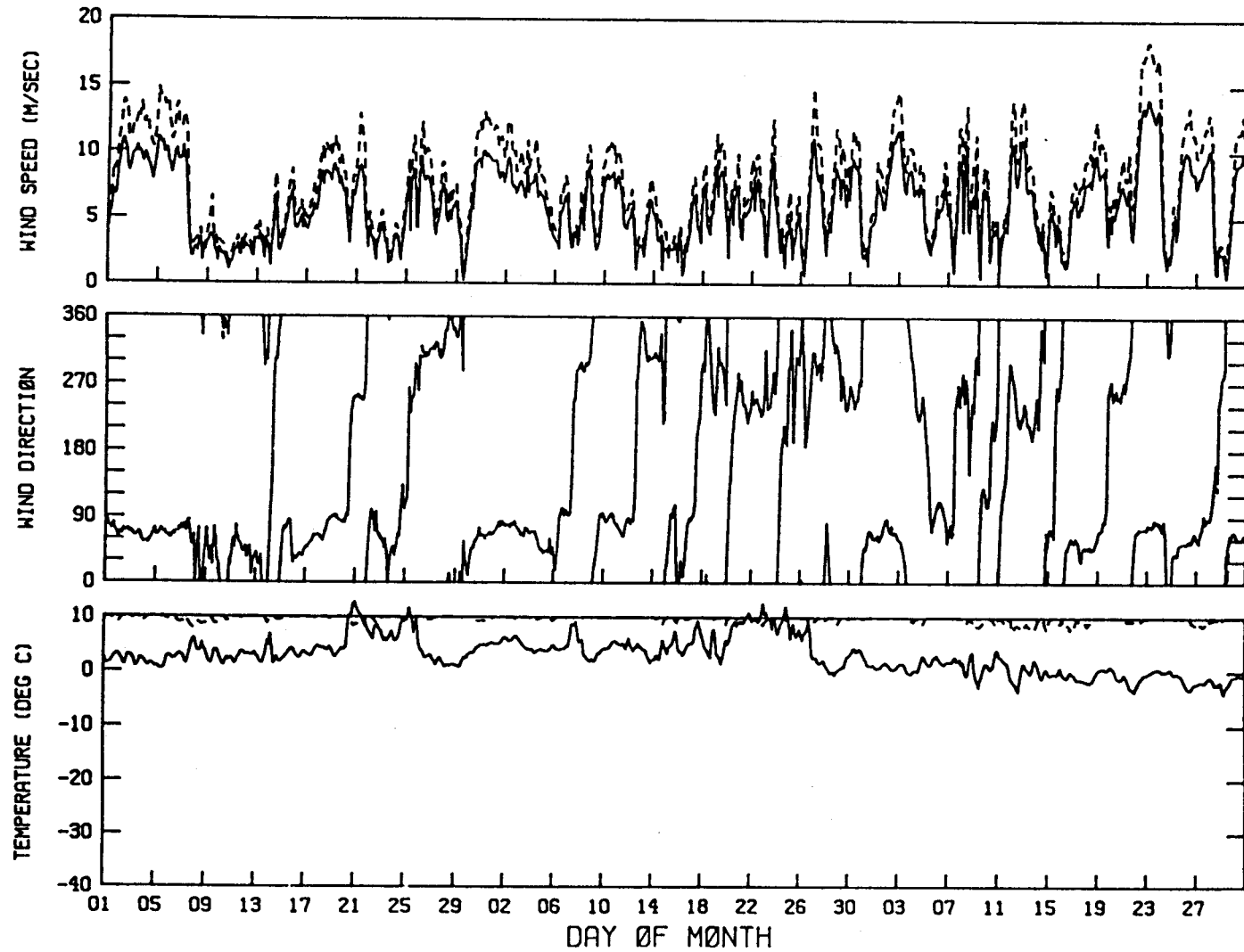


Figure 104. Air temperature and wind speed and direction from Resolution Island (Prudhoe Bay) for July-September 1987.

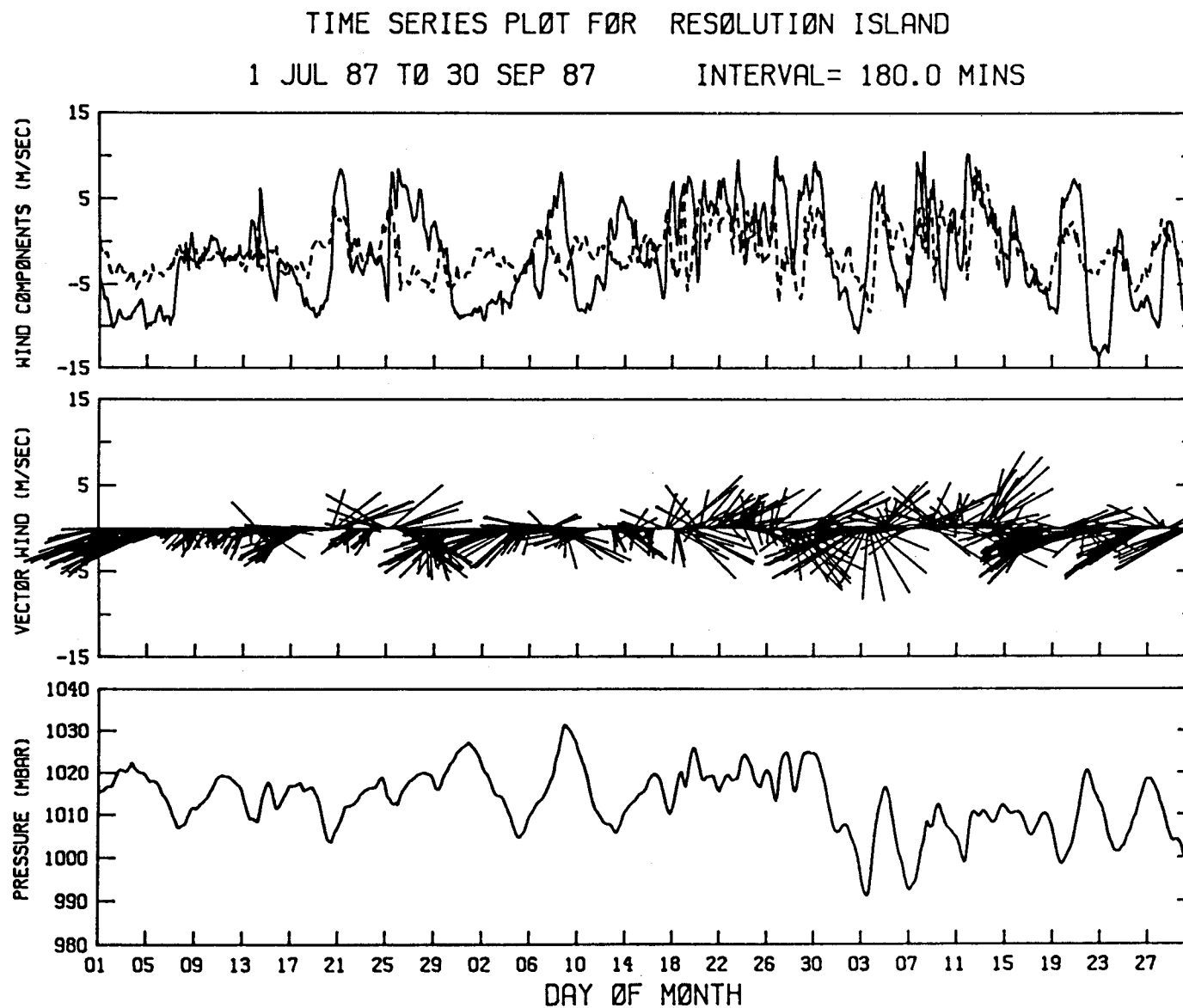


Figure 105. Sea-level pressure, wind components and vectors from Resolution Island (Prudhoe Bay) for July-September 1987.

TIME SERIES PLOT FOR RESOLUTION ISLAND

1 OCT 87 TO 31 DEC 87

INTERVAL= 180.0 MINS

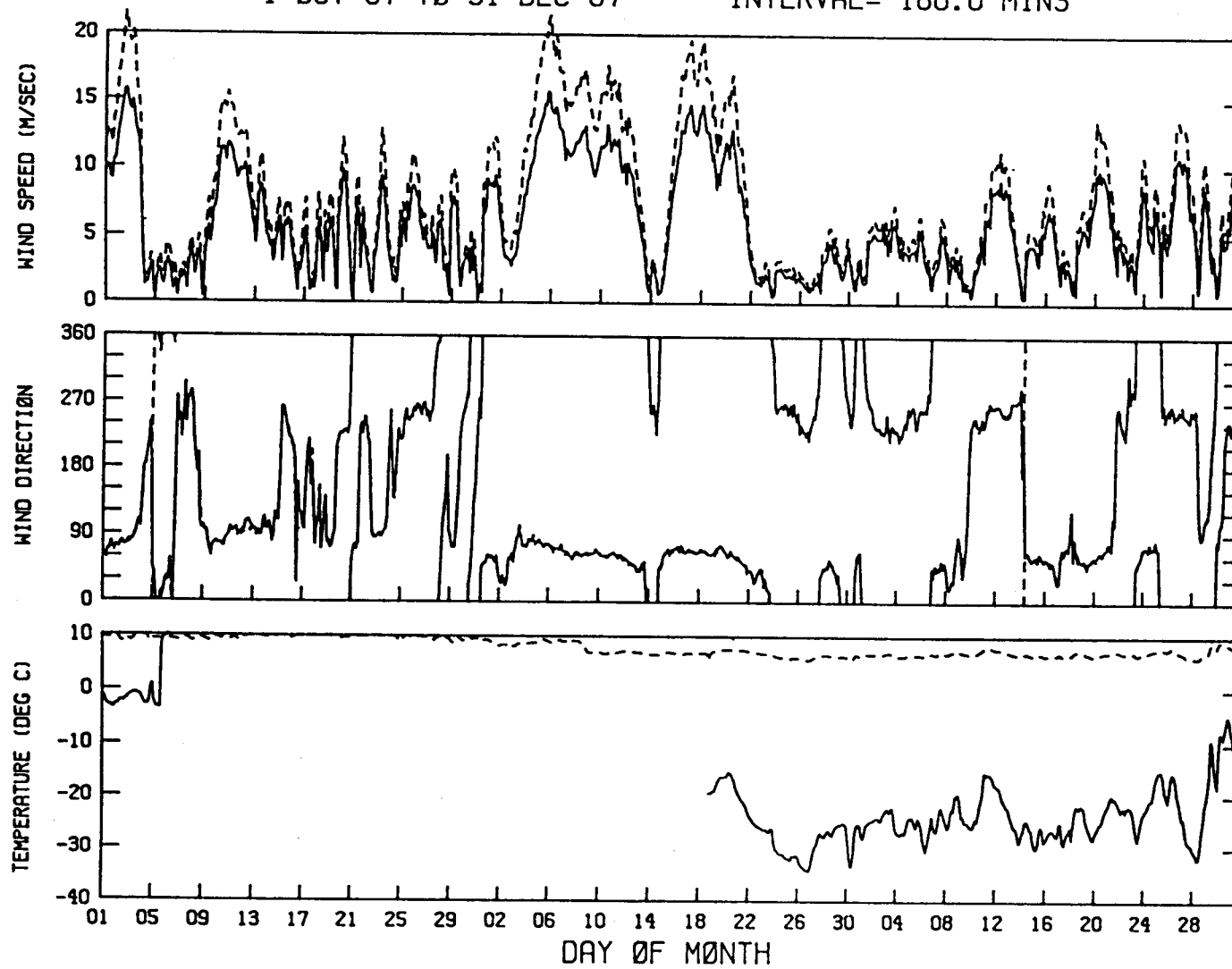


Figure 106. Air temperature and wind speed and direction from Resolution Island (Prudhoe Bay) for October-December 1987.

TIME SERIES PLOT FOR RESOLUTION ISLAND  
1 OCT 87 TO 31 DEC 87      INTERVAL= 180.0 MINS

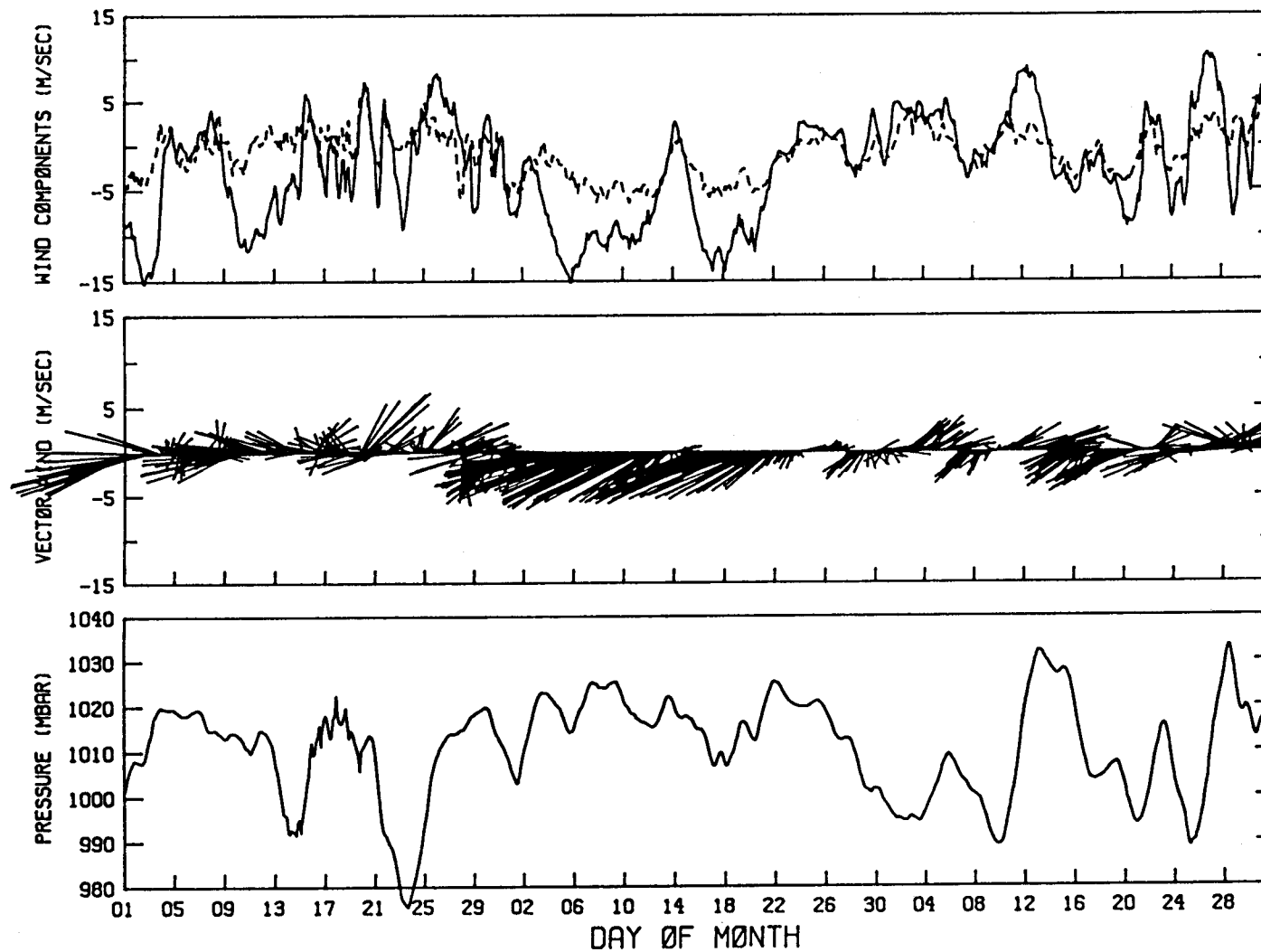


Figure 107. Sea-level pressure, wind components and vectors from Resolution Island (Prudhoe Bay) for October-December 1987.

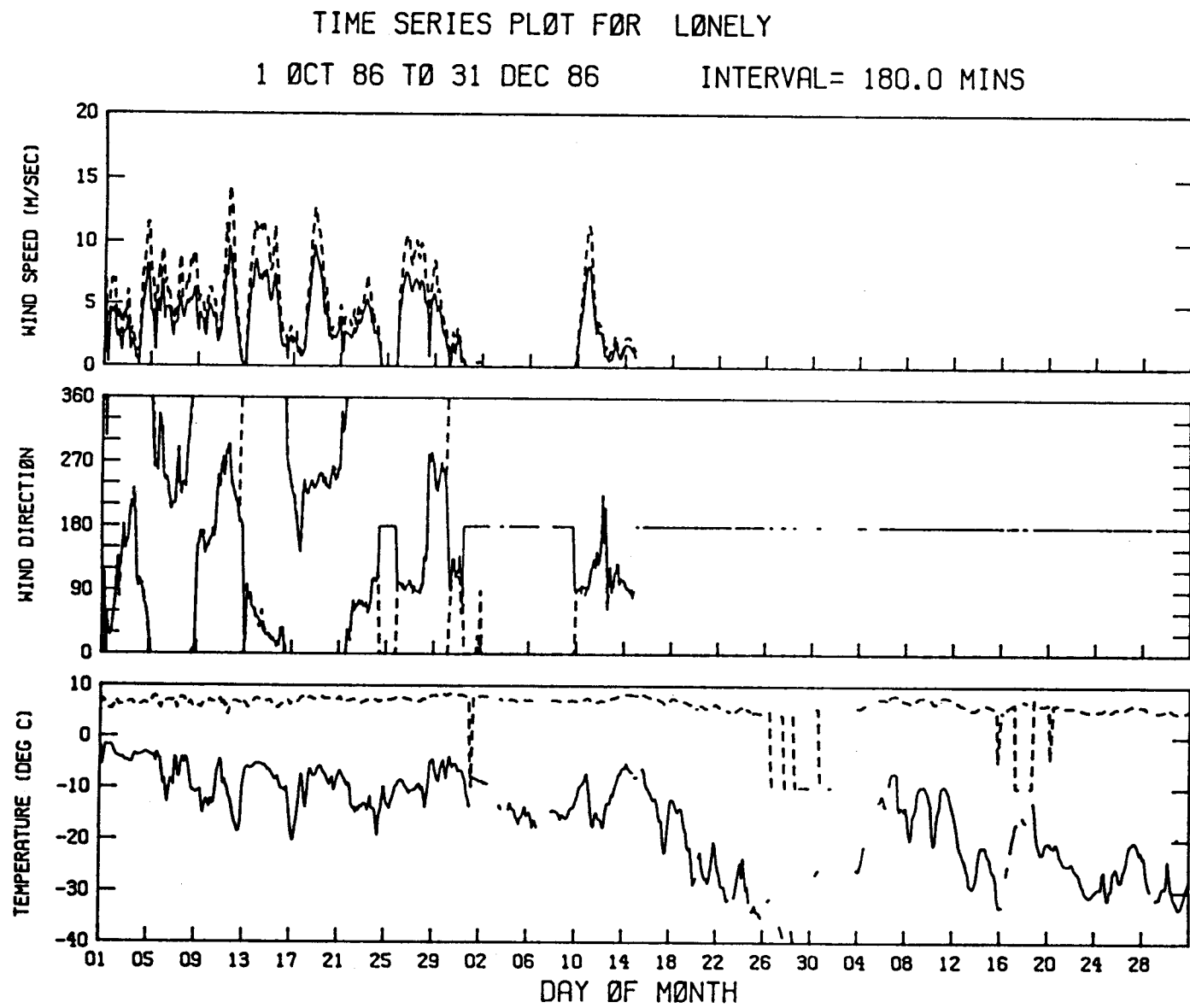


Figure 108. Air temperature and wind speed and direction from Lonely for October-December 1986.

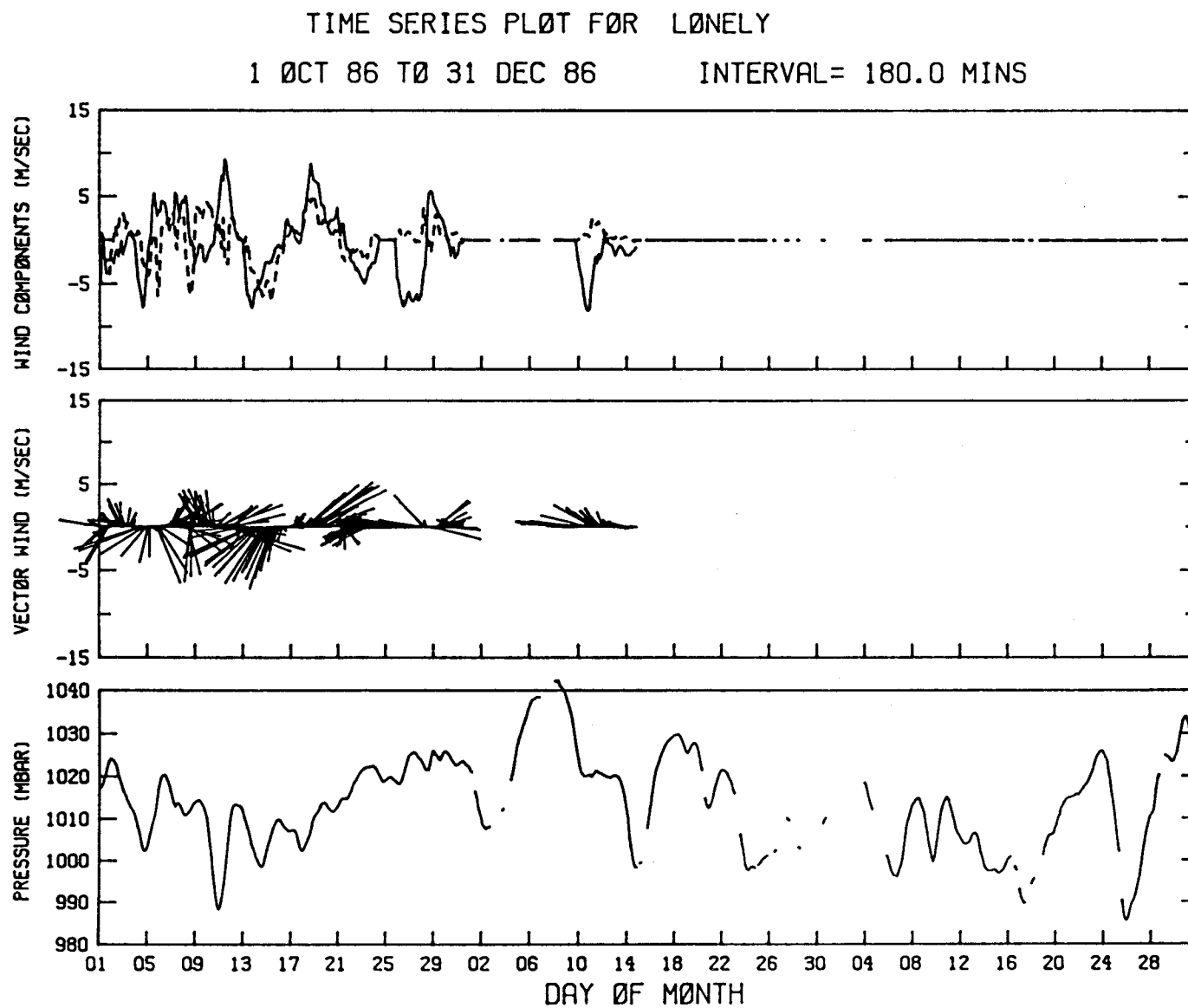


Figure 109. Sea-level pressure, wind components and vectors from Lonely for October-December 1986.

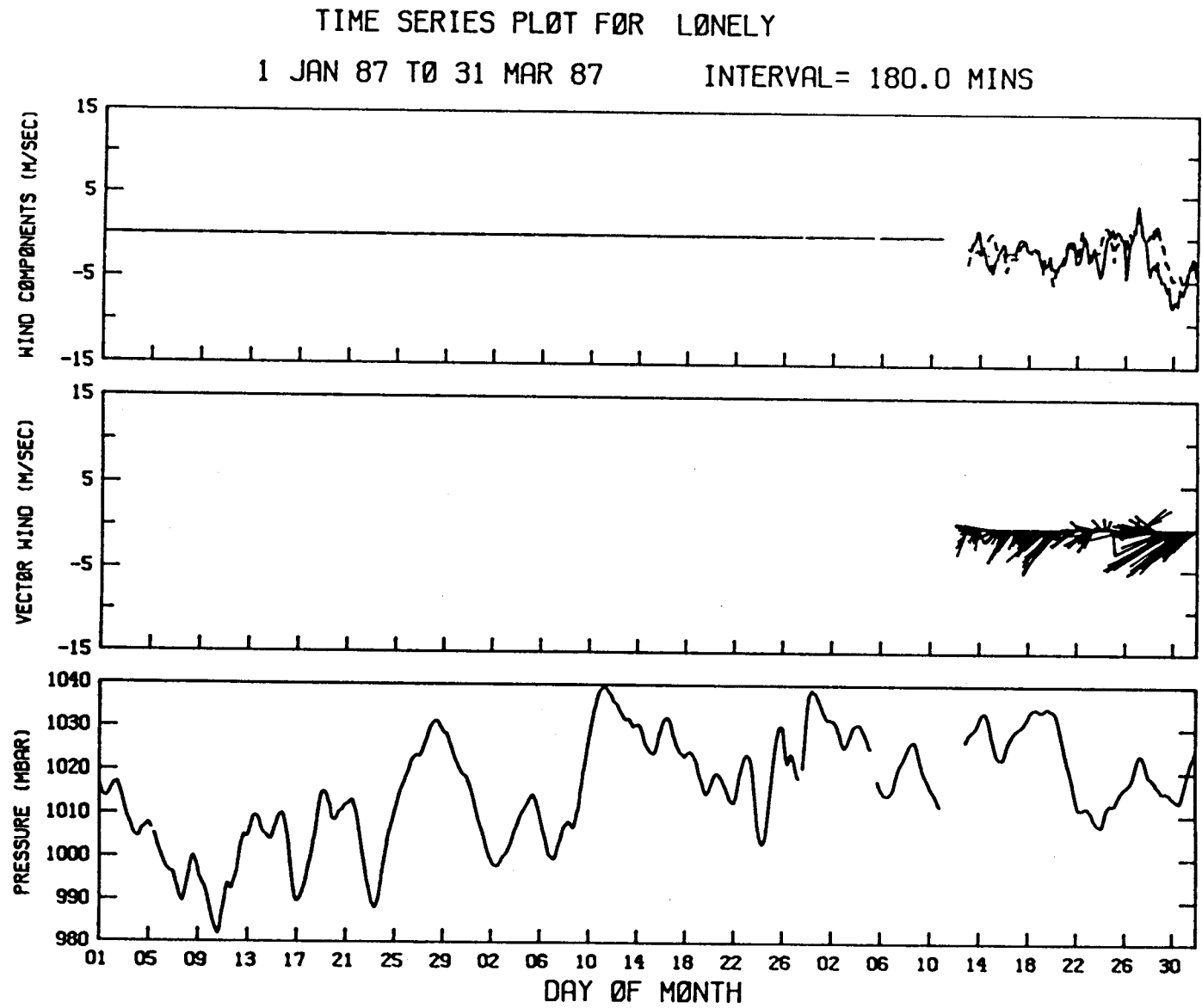


Figure 110. Air temperature and wind speed and direction from Lonely for January-March 1987.

TIME SERIES PLOT FOR LØNELY  
1 JAN 87 TO 31 MAR 87      INTERVAL= 180.0 MINS

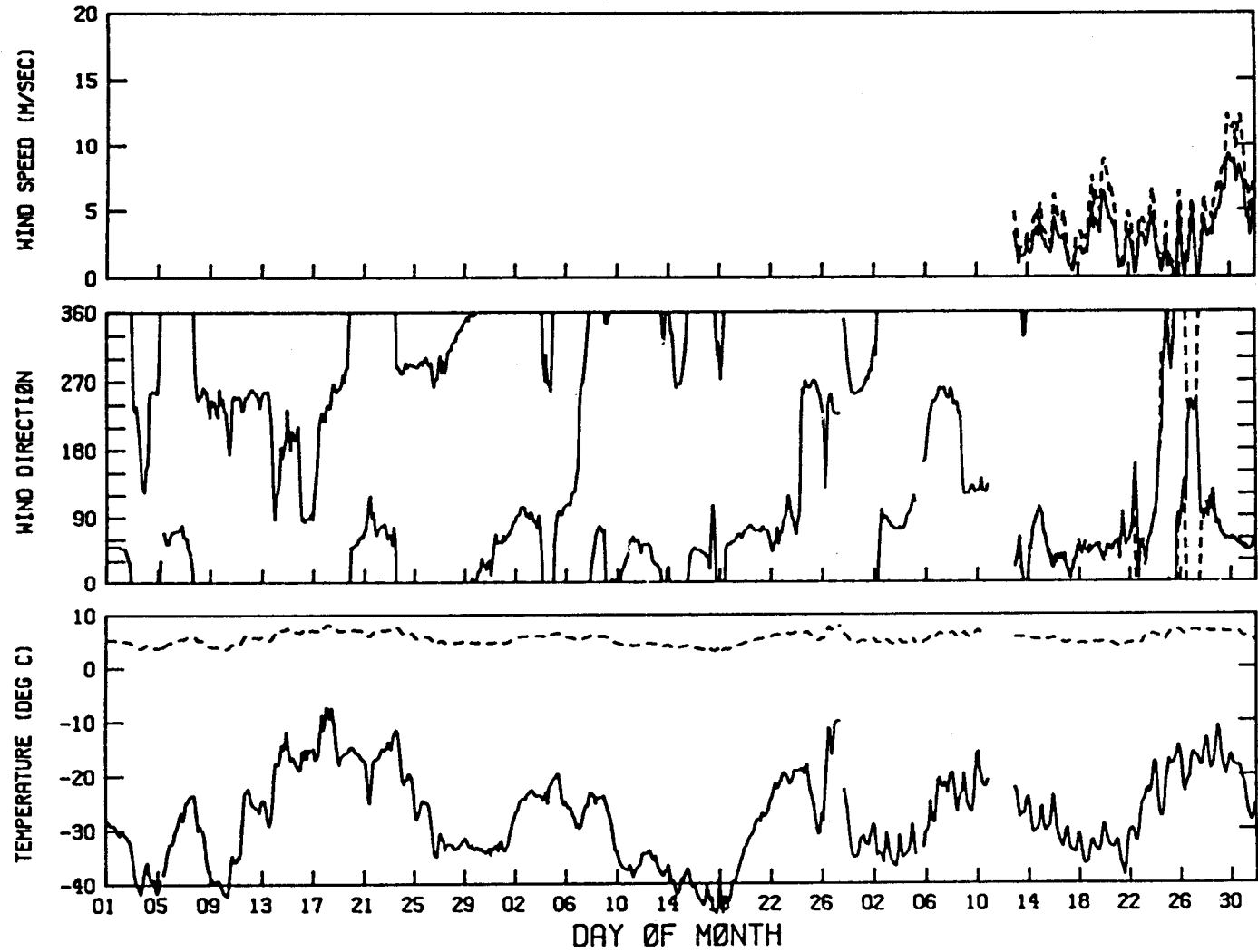


Figure 111. Sea-level pressure, wind components and vectors from Lonely for January-March 1987.

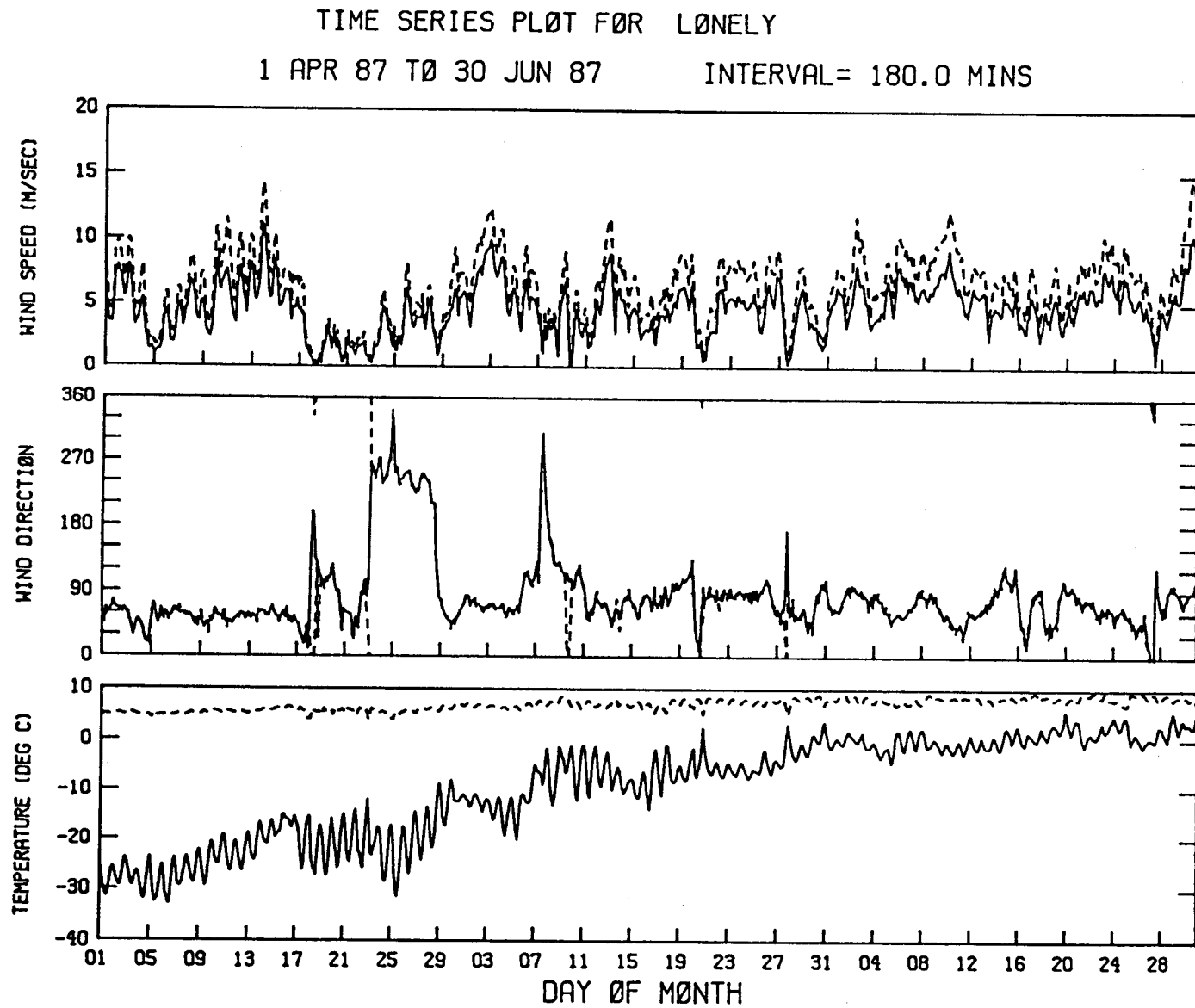


Figure 112. Air temperature and wind speed and direction from Lonely for April-June 1987.

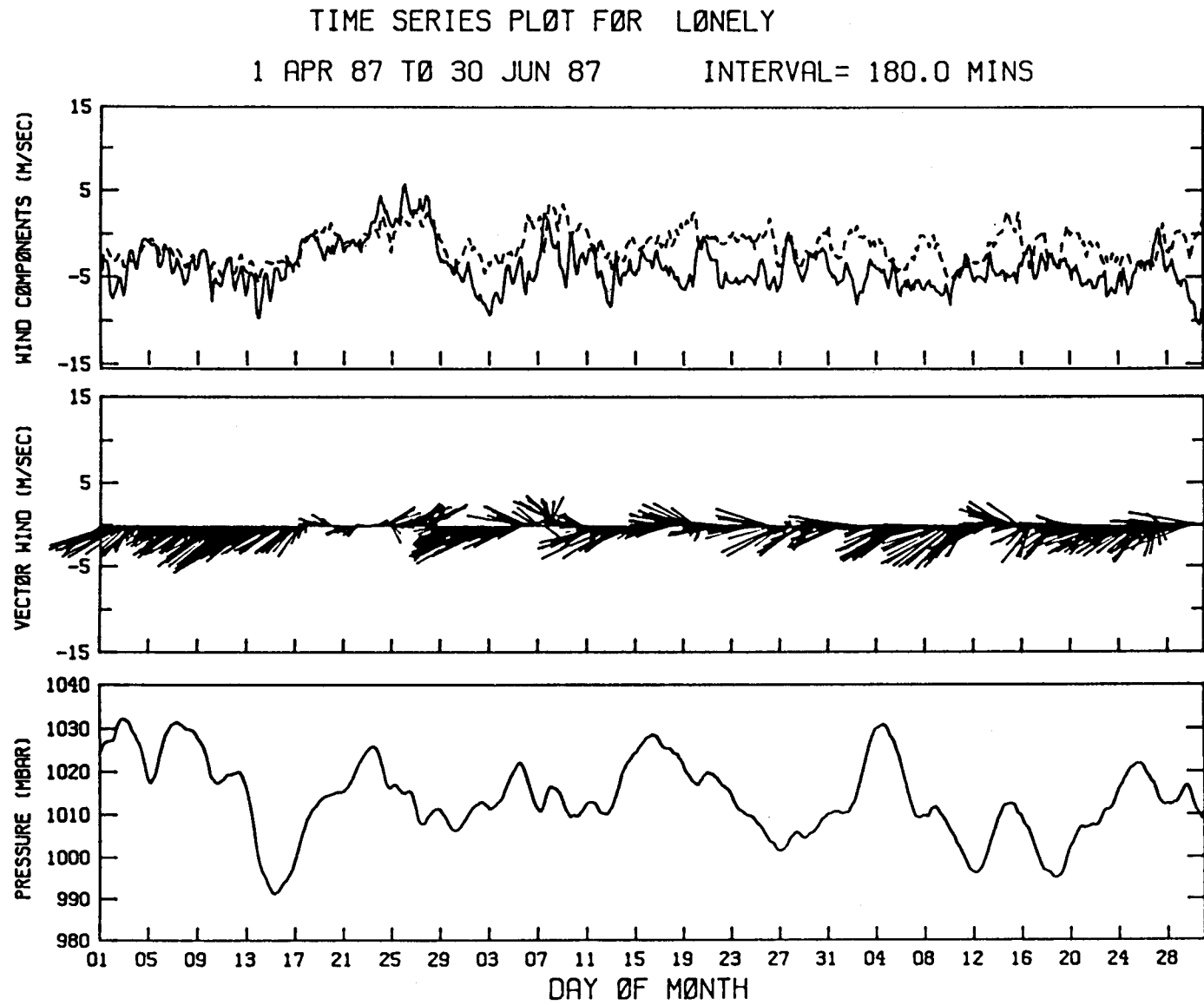


Figure 113. Sea-level pressure, wind components and vectors from Lonely for April-June 1987.

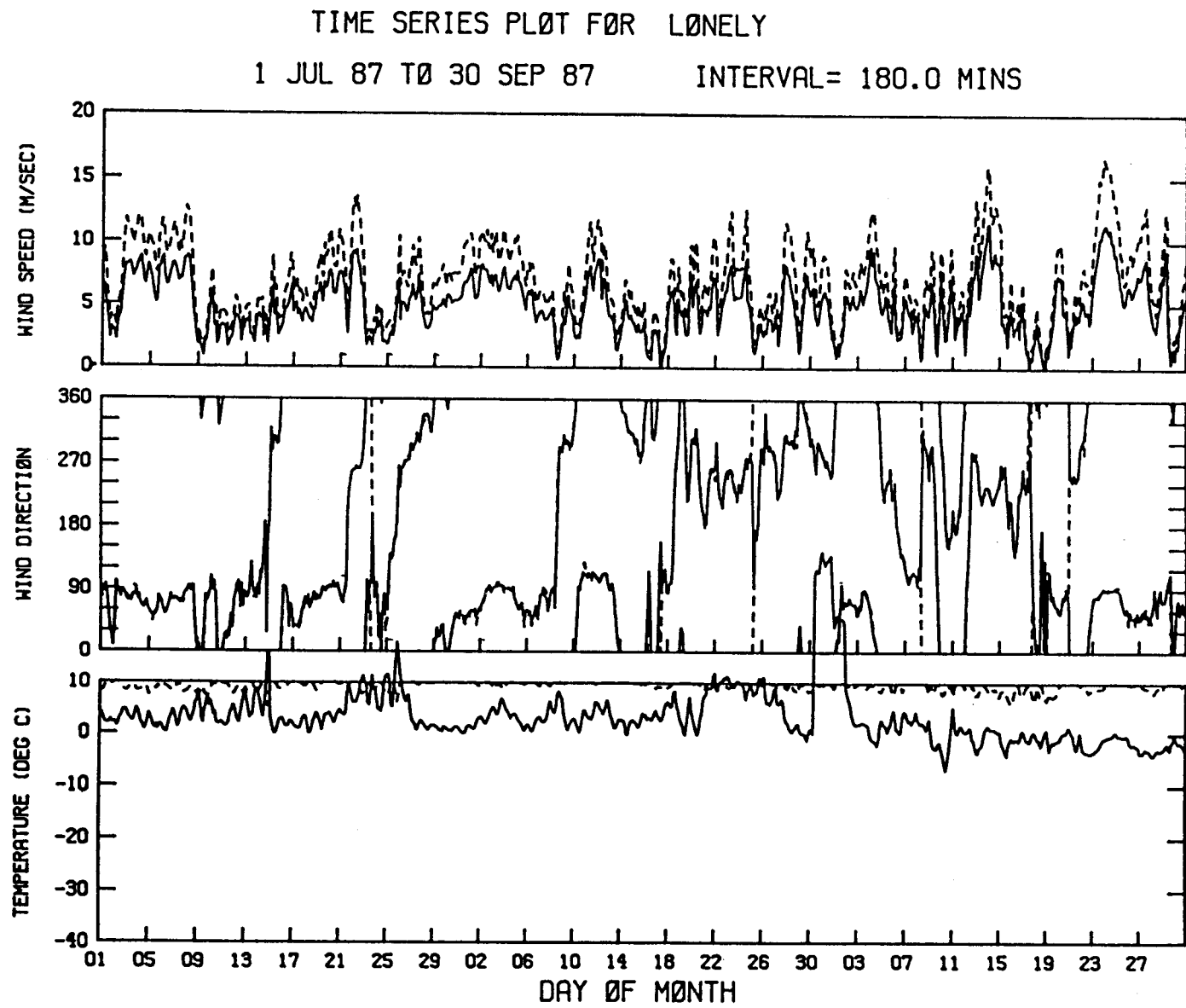


Figure 114. Air temperature and wind speed and direction from Lonely for July-September 1987.

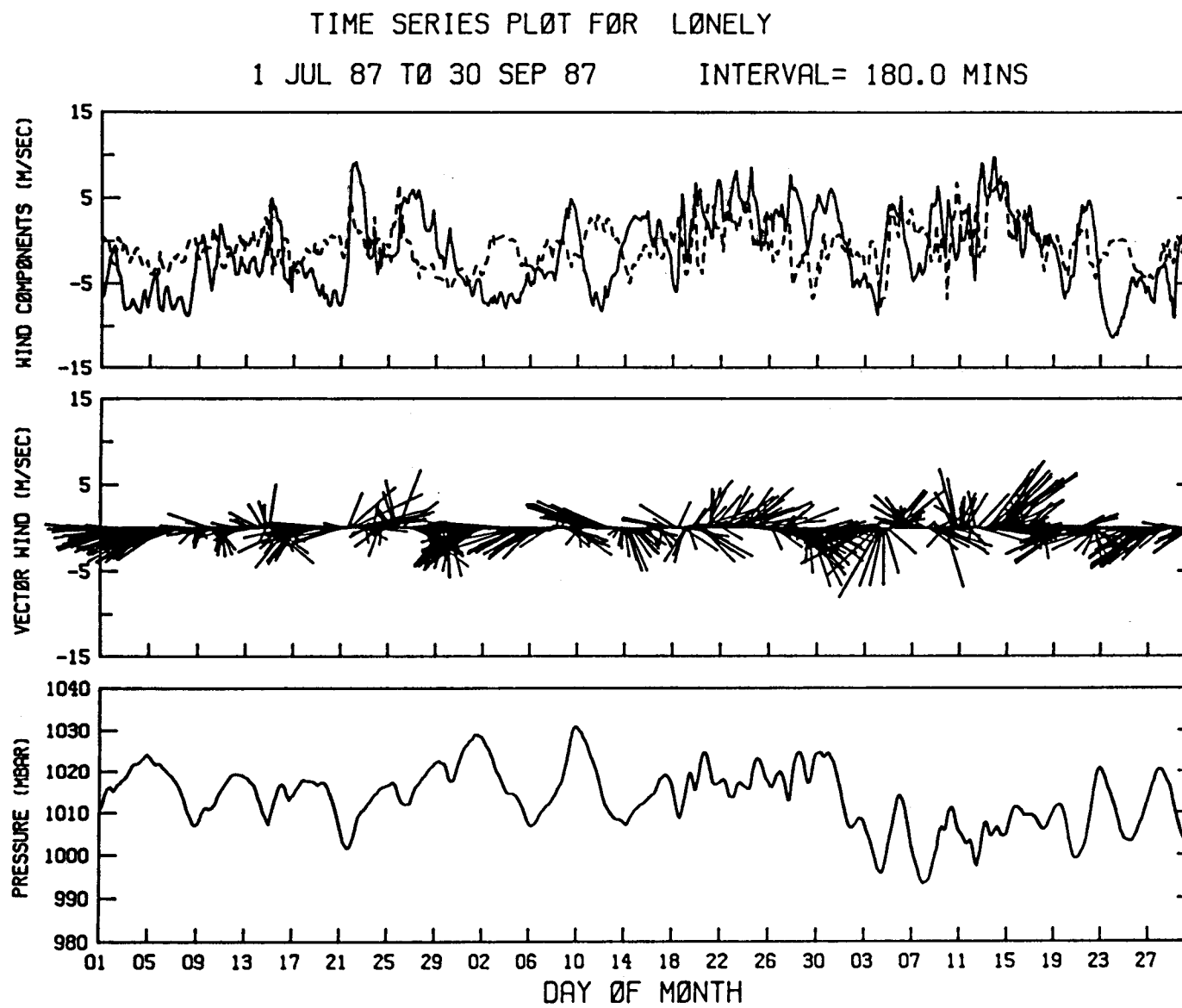


Figure 115. Sea-level pressure, wind components and vectors from Lonely for July-September 1987.

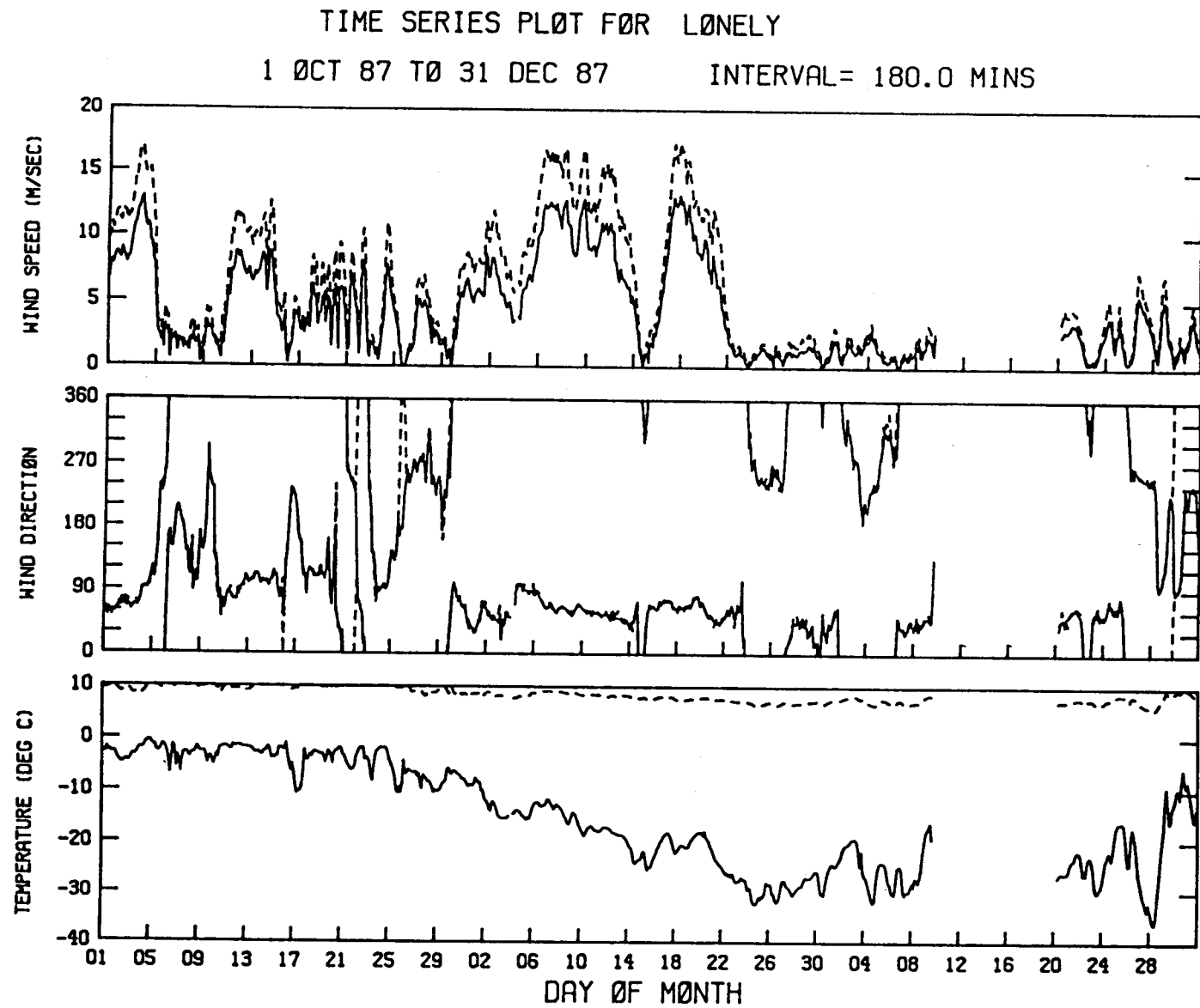


Figure 116. Air temperature and wind speed and direction from Lonely for October-December 1987.

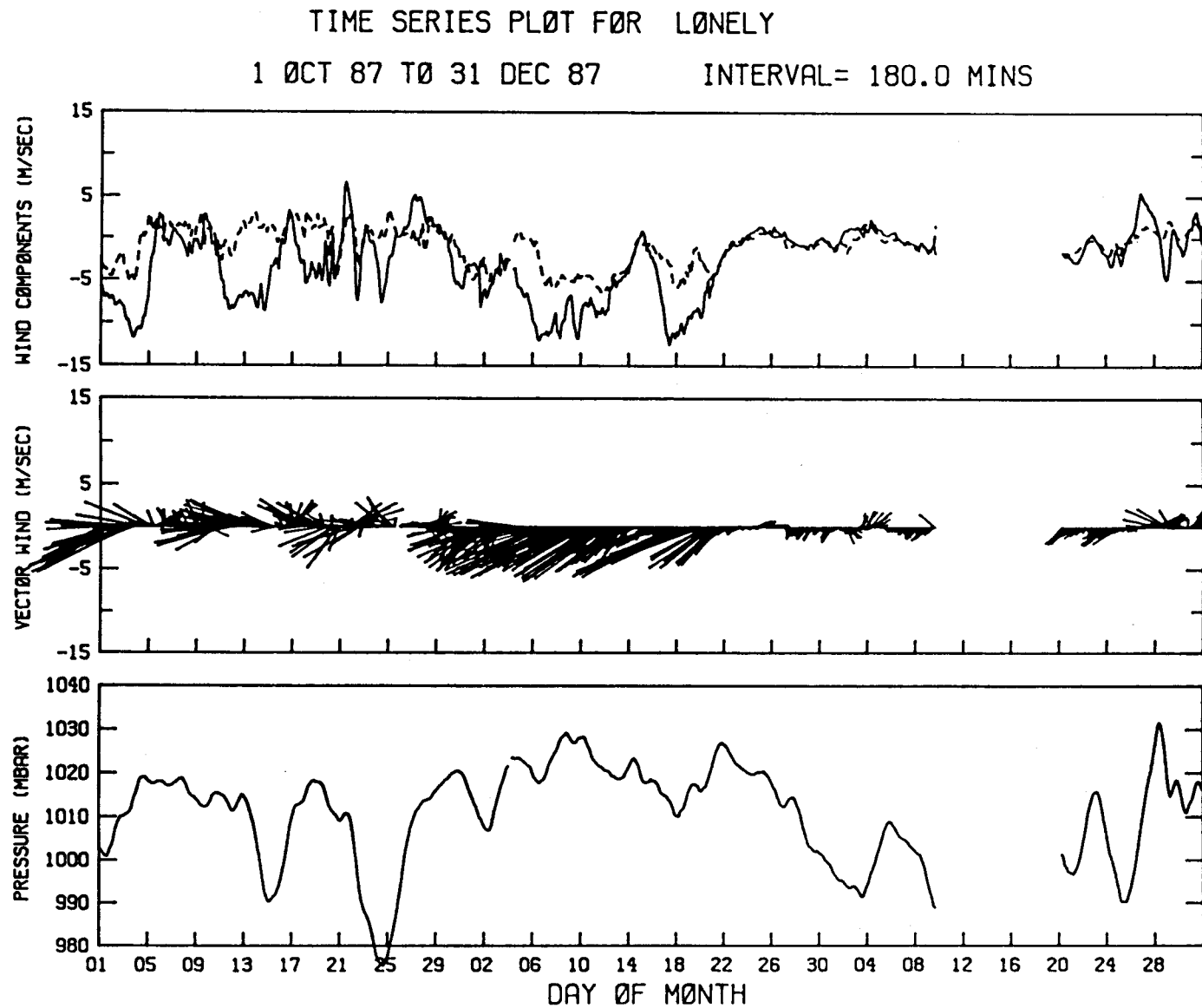


Figure 117. Sea-level pressure, wind components and vectors from Lonely for October-December 1987.

TIME SERIES PLOT FOR ICY CAPE  
1 APR 87 TO 30 JUN 87 INTERVAL= 180.0 MINS

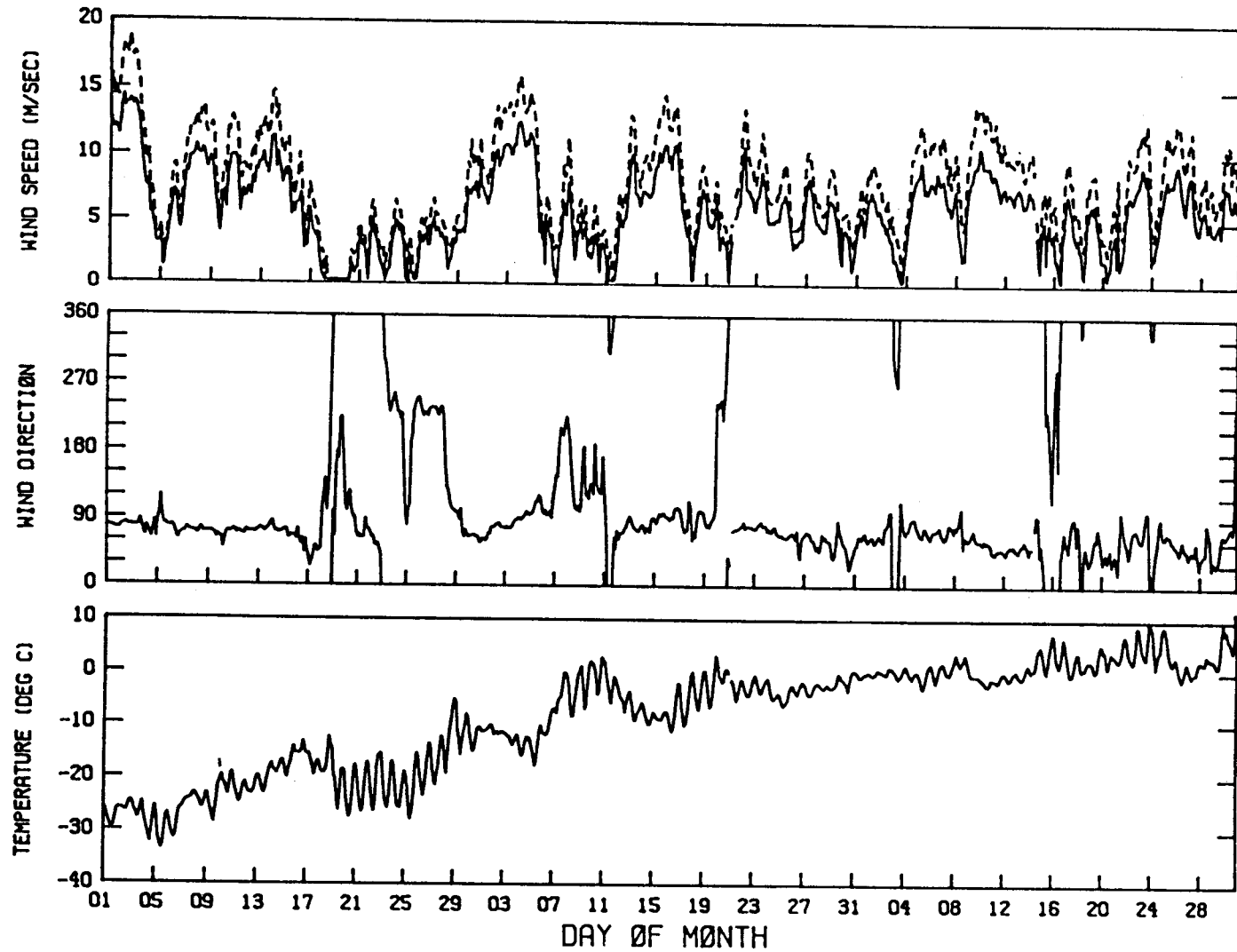


Figure 118. Air temperature and wind speed and direction from Icy Cape for April-June 1987.

TIME SERIES PLOT FOR ICY CAPE

1 APR 87 TO 30 JUN 87

INTERVAL= 180.0 MINS

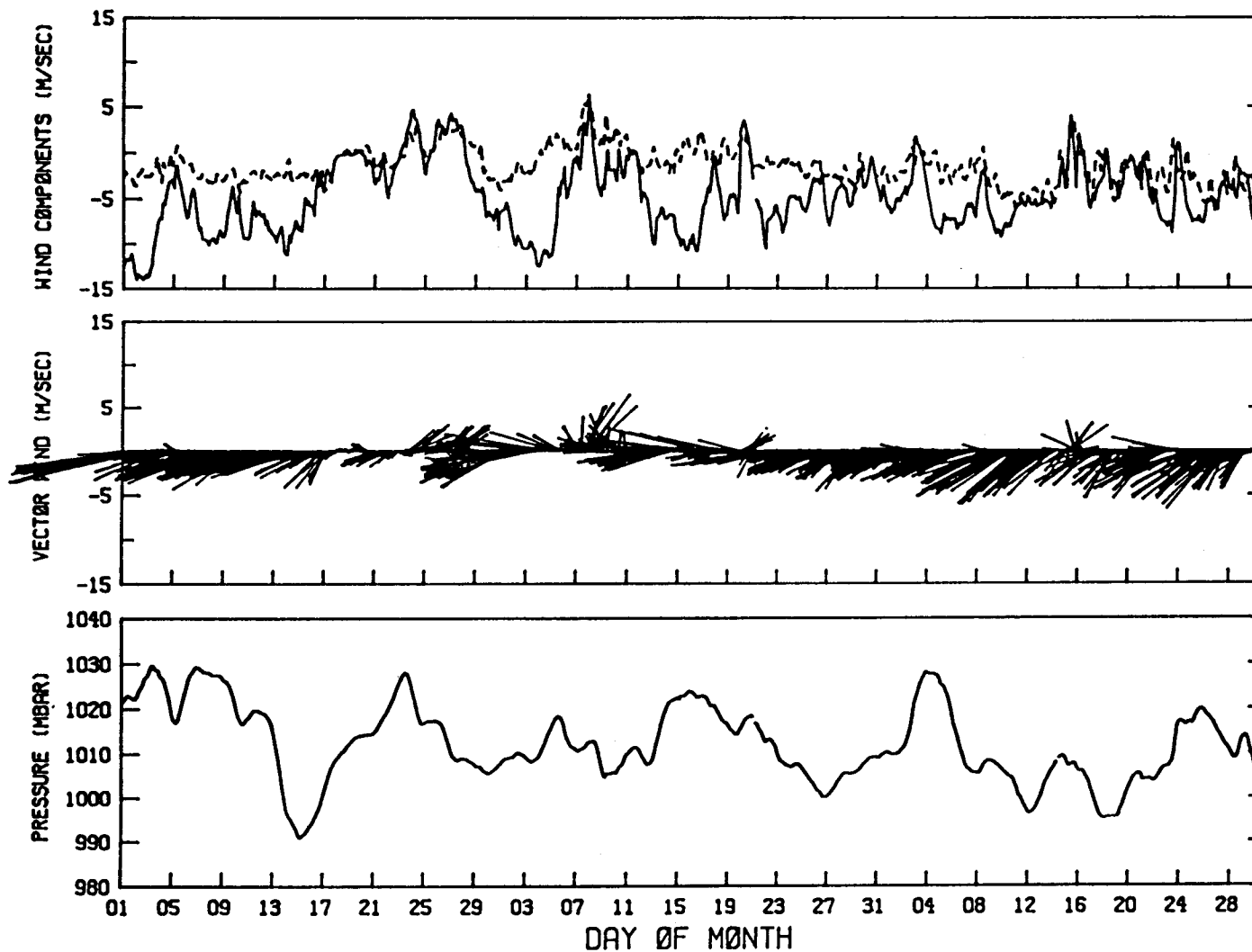


Figure 119. Sea-level pressure, wind components and vectors from Icy Cape for April-June 1987.

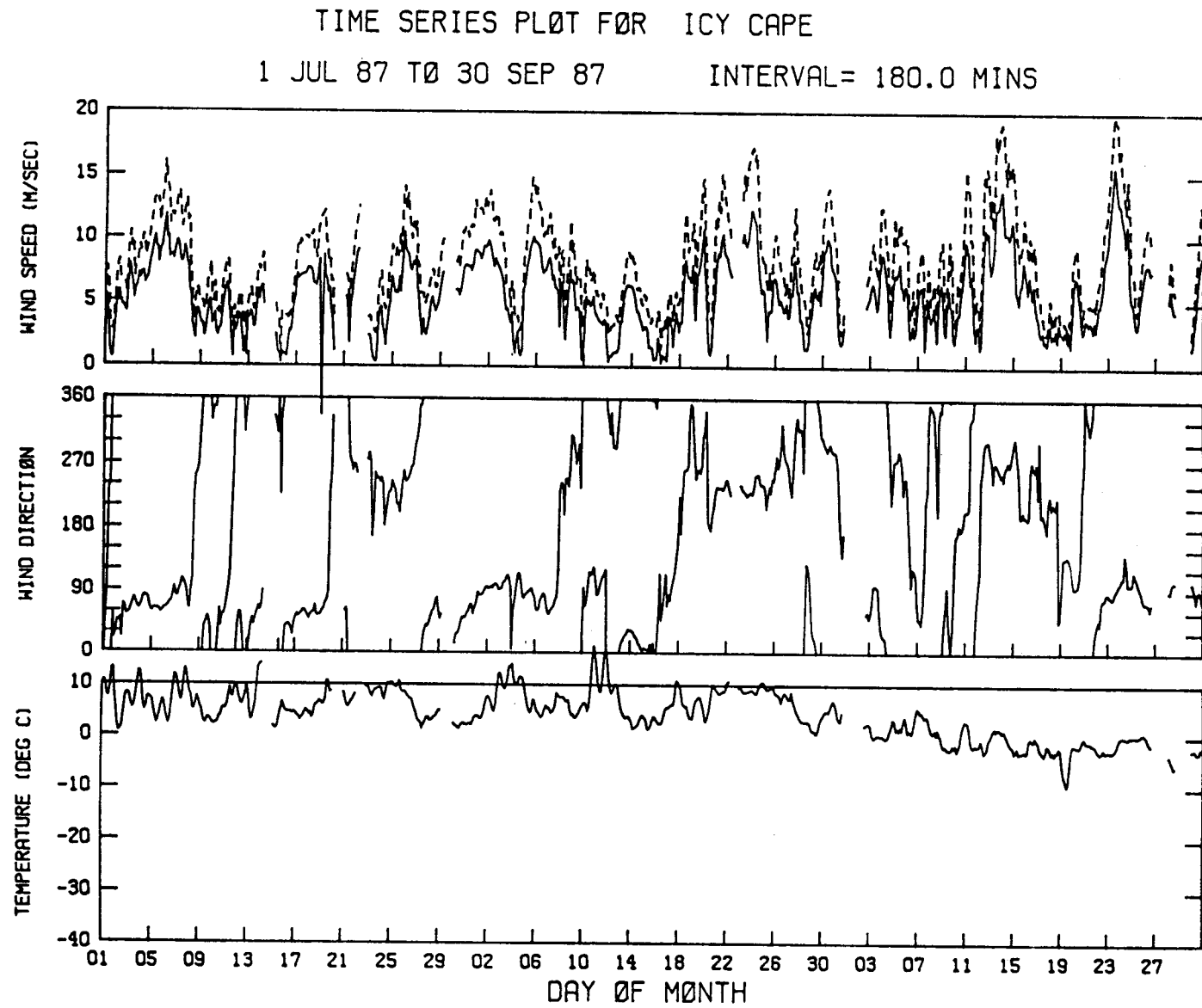


Figure 120. Air temperature and wind speed and direction from Icy Cape for July-September 1987.

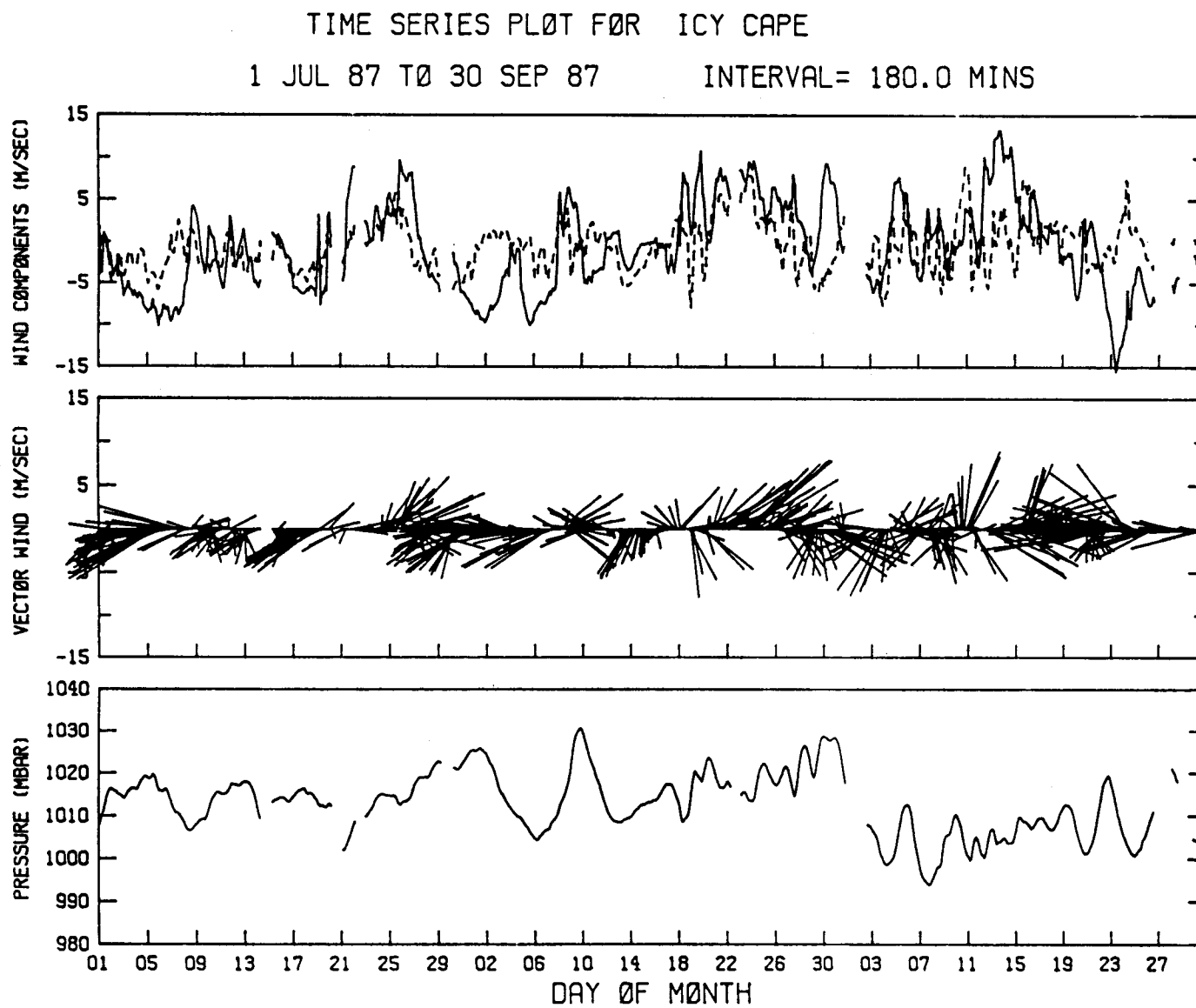


Figure 121. Sea-level pressure, wind components and vectors from Icy Cape for July-September 1987.

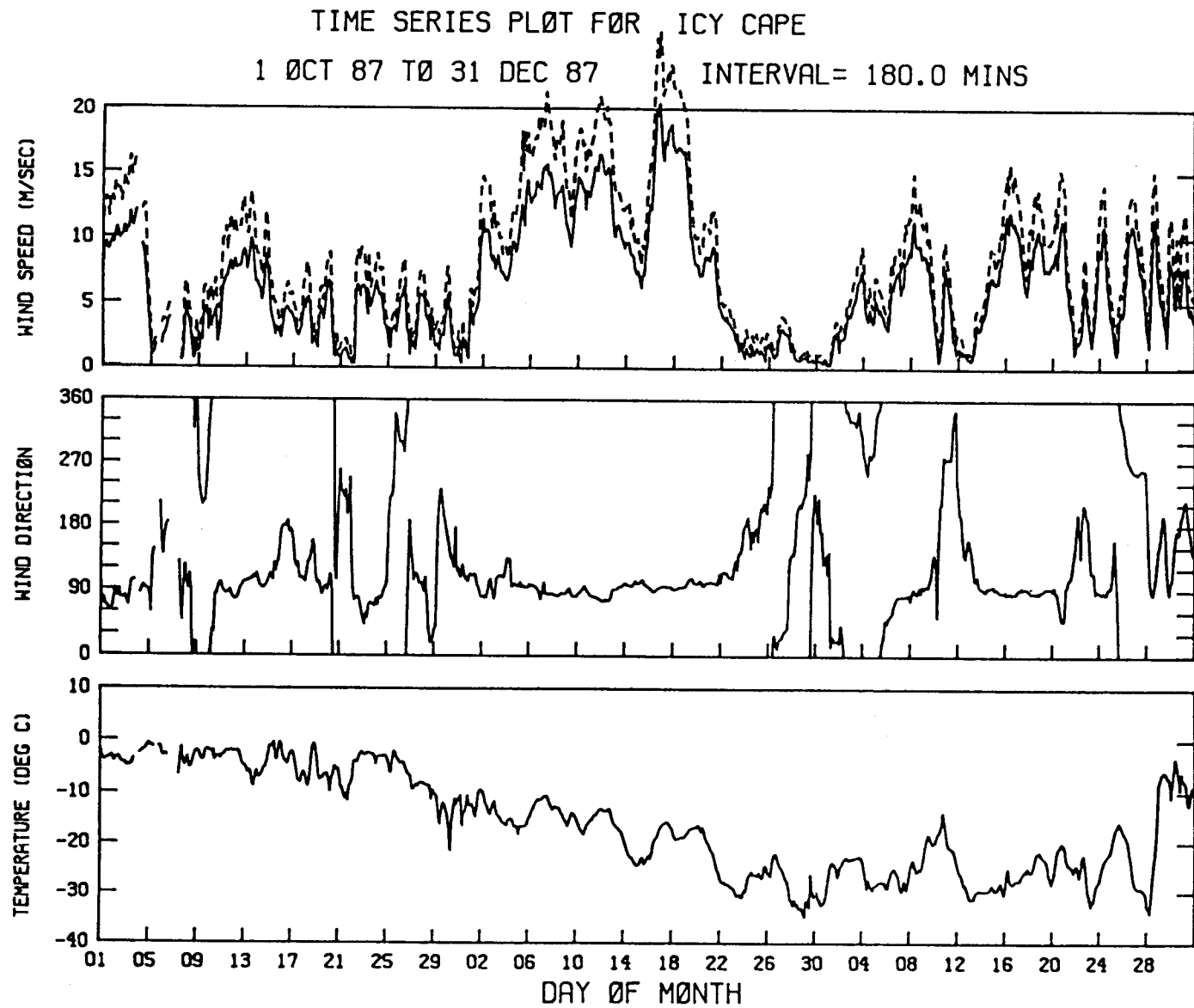


Figure 122. Air temperature and wind speed and direction from Icy Cape for October-December 1987.

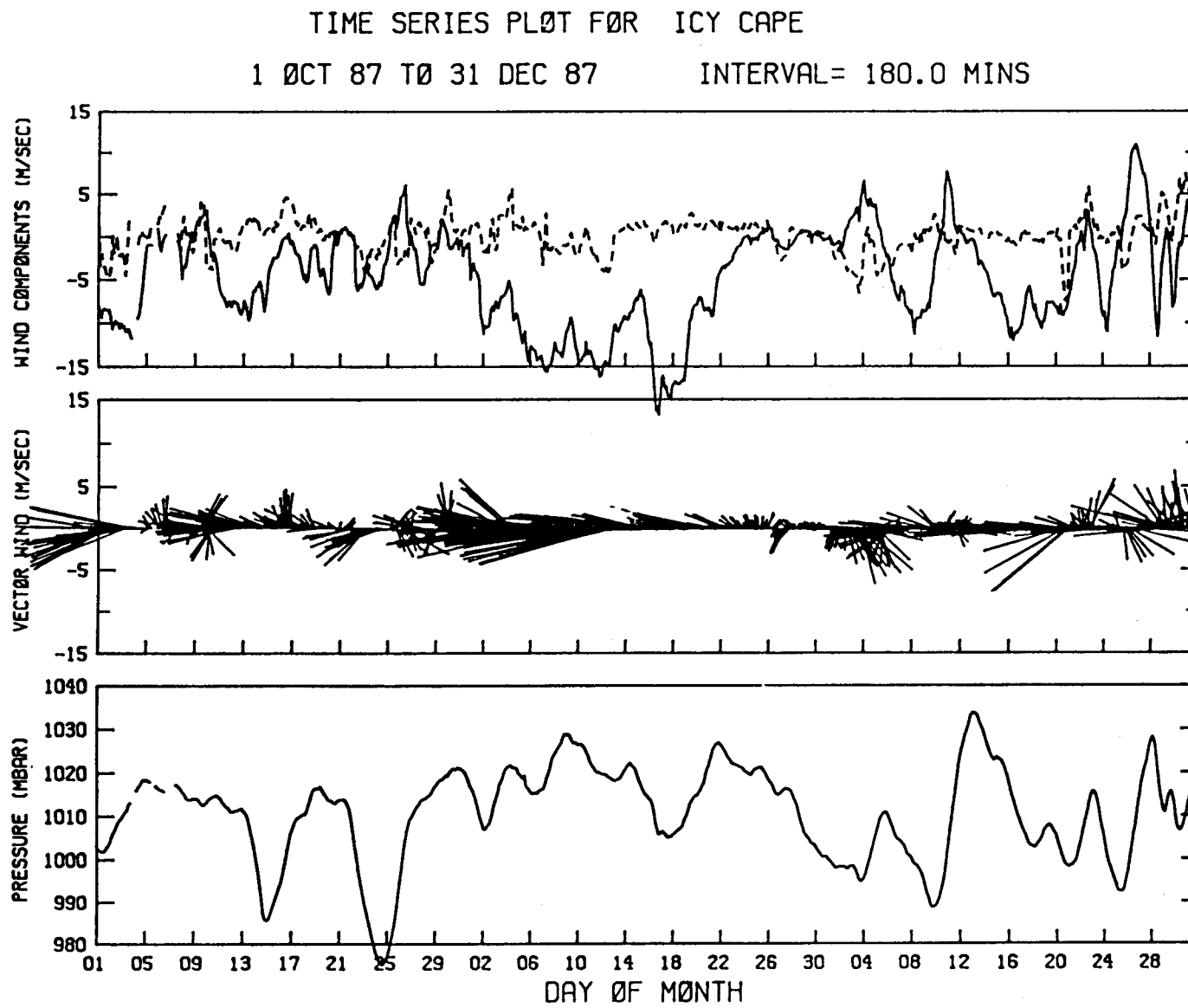


Figure 123. Sea-level pressure, wind components and vectors from Icy Cape for October-December 1987.

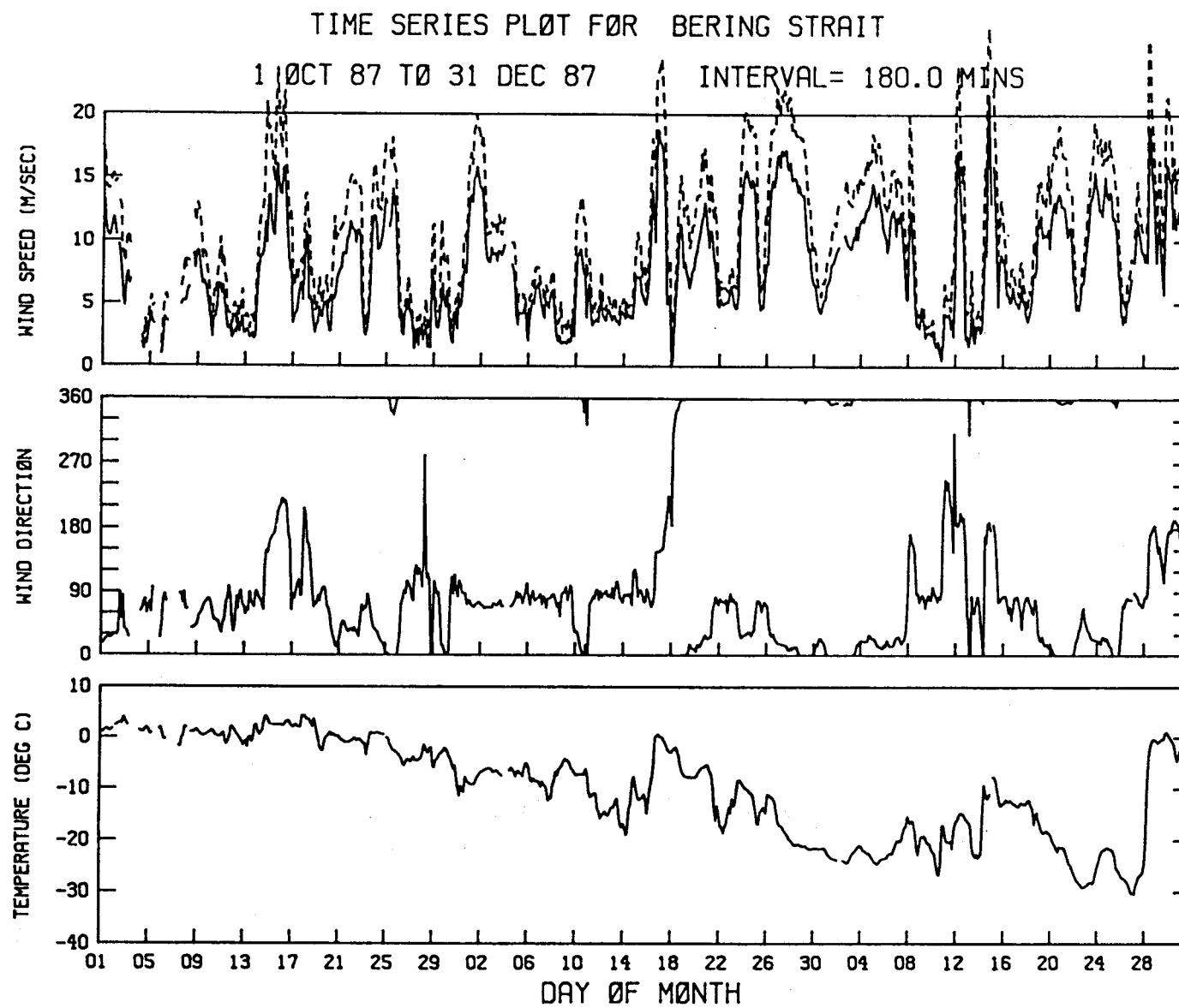


Figure 124. Air temperature and wind speed and direction from Bering Strait for October-December 1987.

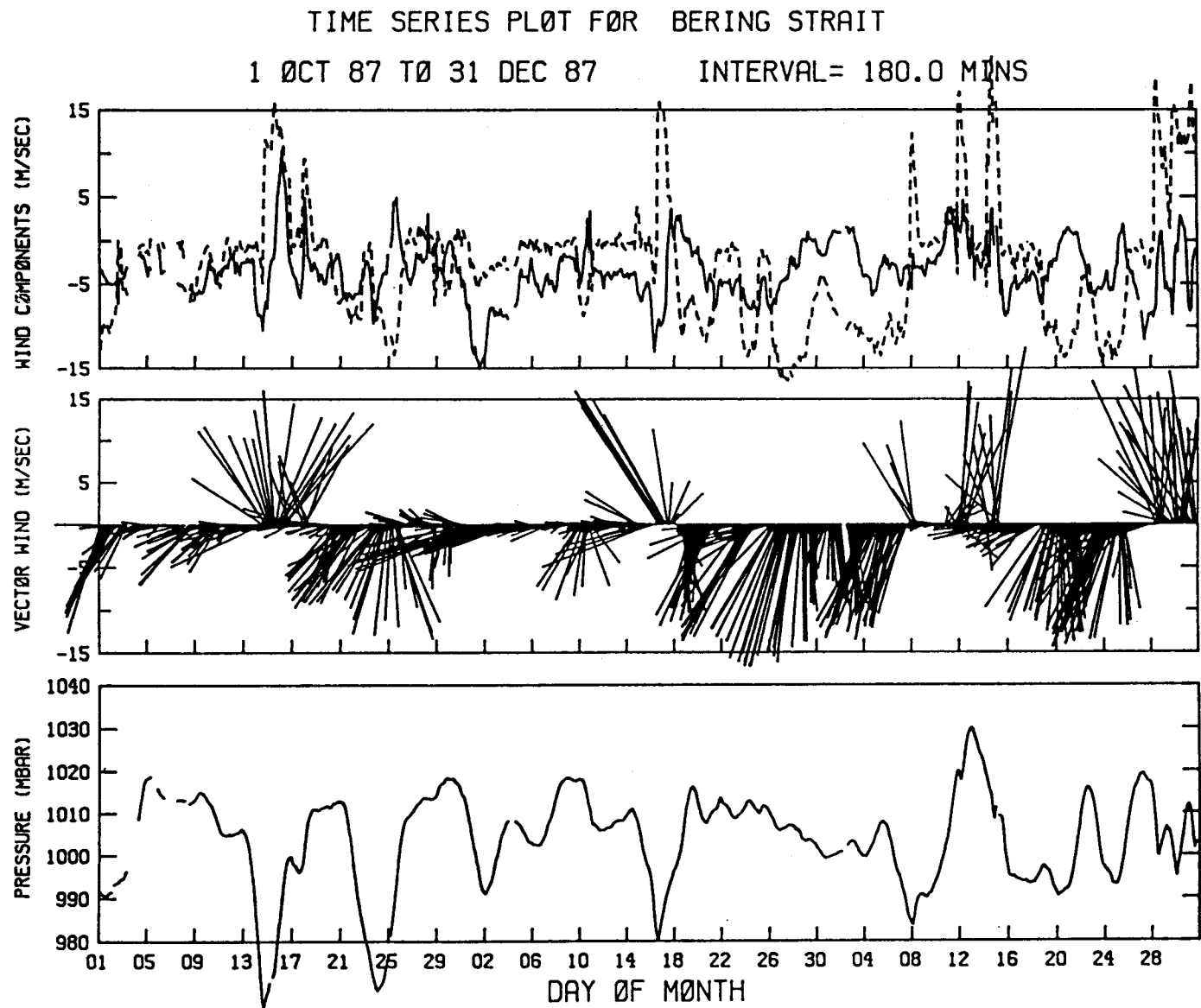


Figure 125. Sea-level pressure, wind components and vectors from Bering Strait for October-December 1987.

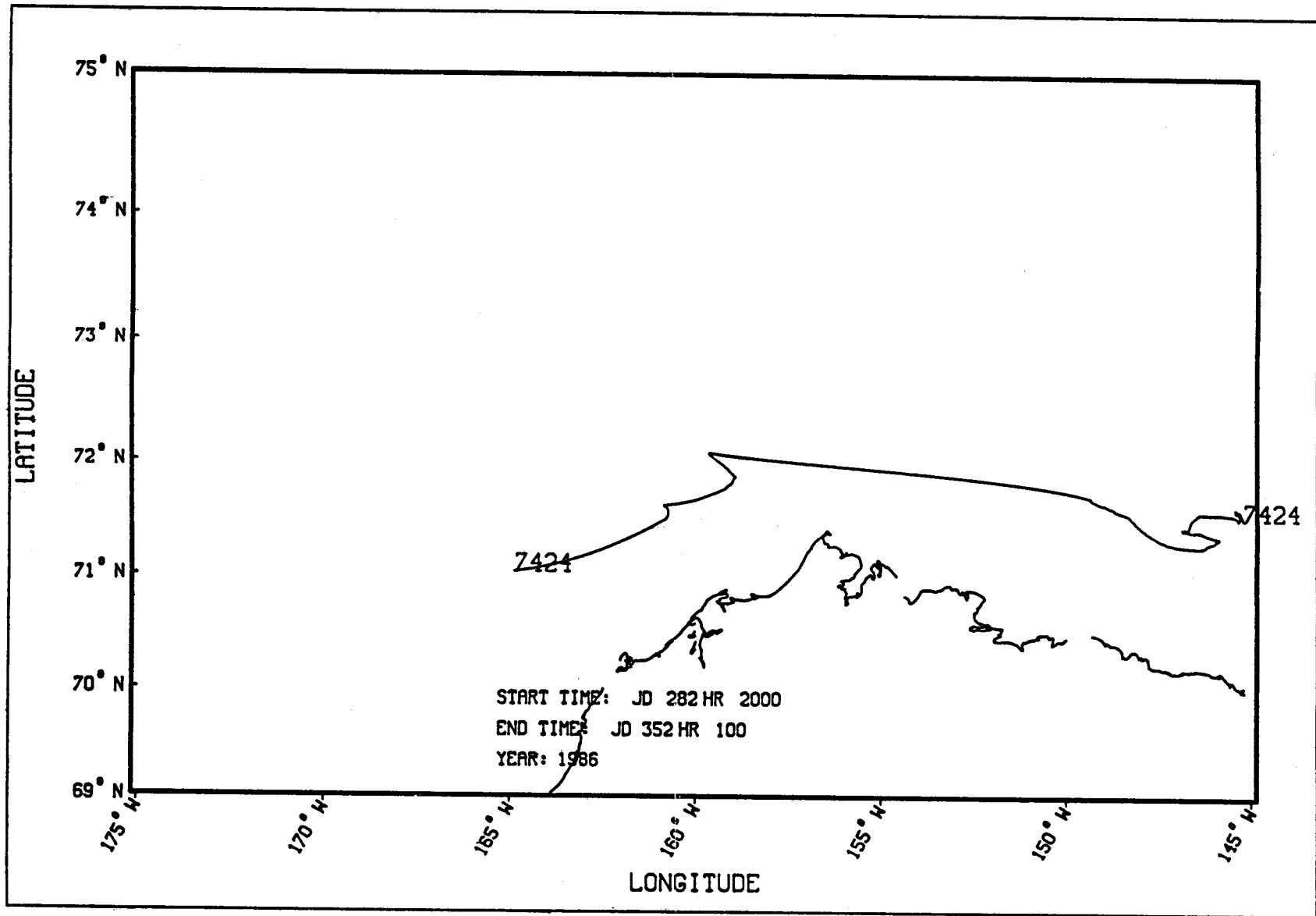


Figure 126. Drift tracks for ARGOS buoy 7424.

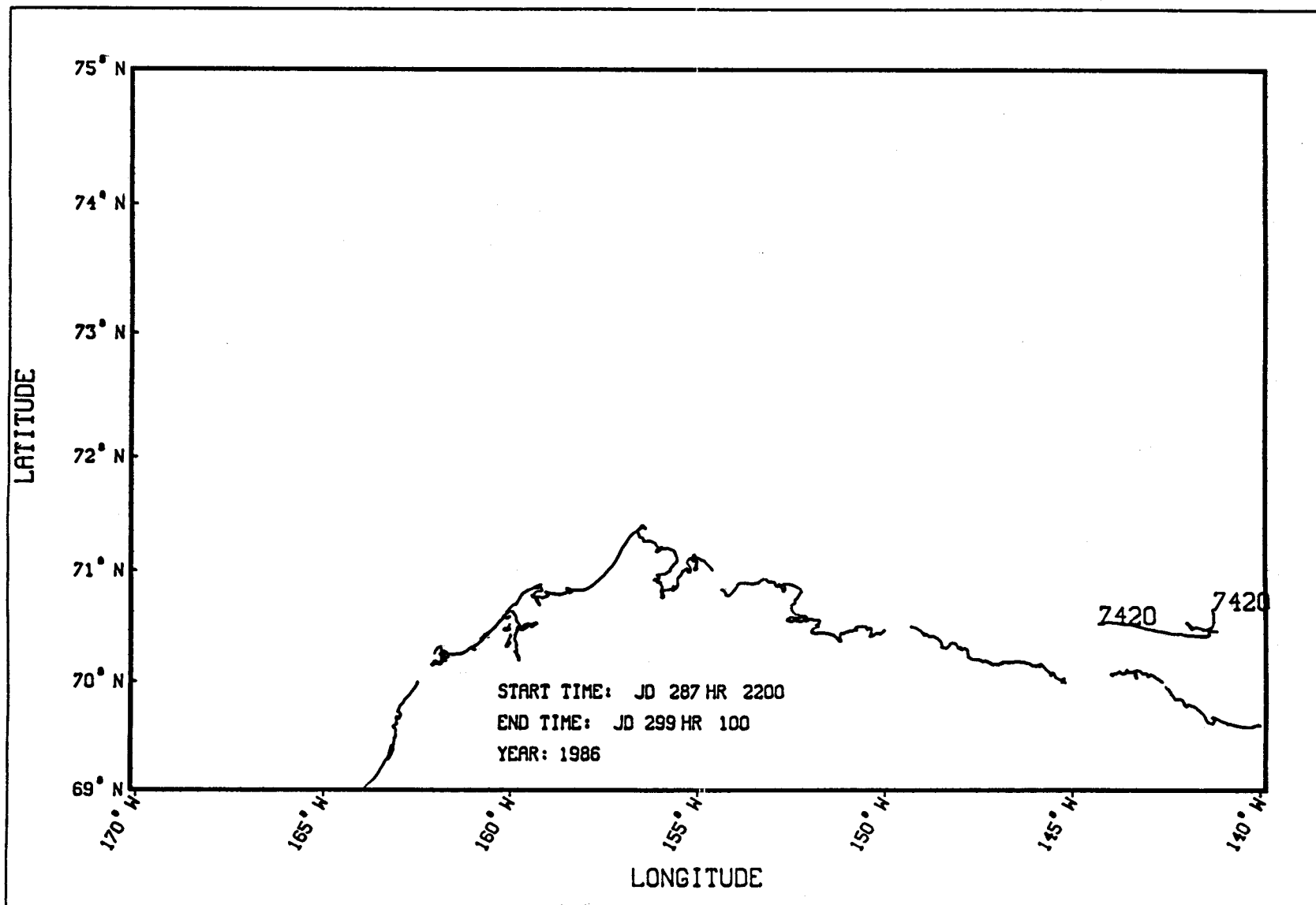


Figure 127. Drift tracks for ARGOS buoy 7420a.

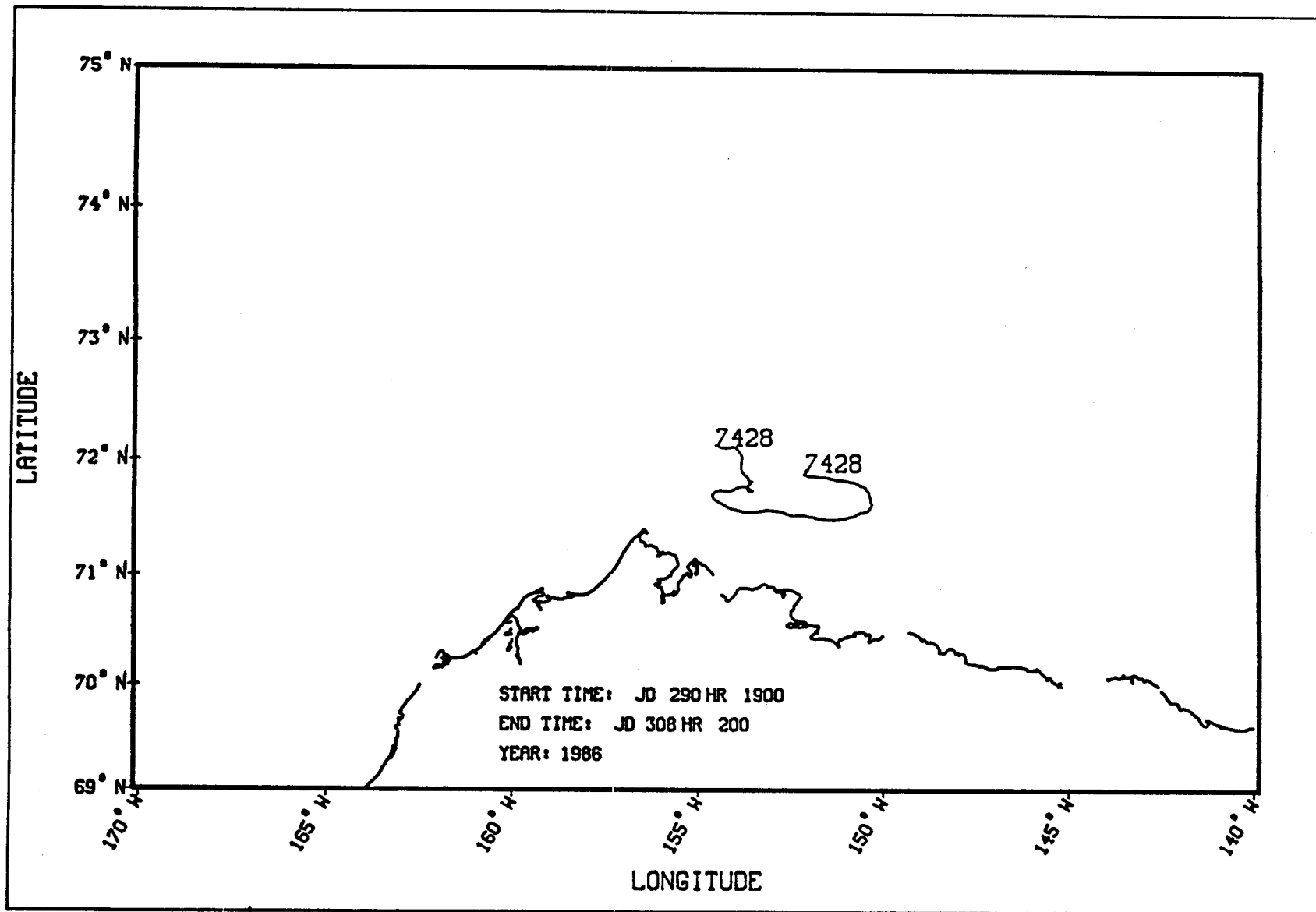


Figure 128. Drift tracks for ARGOS buoy 7428.

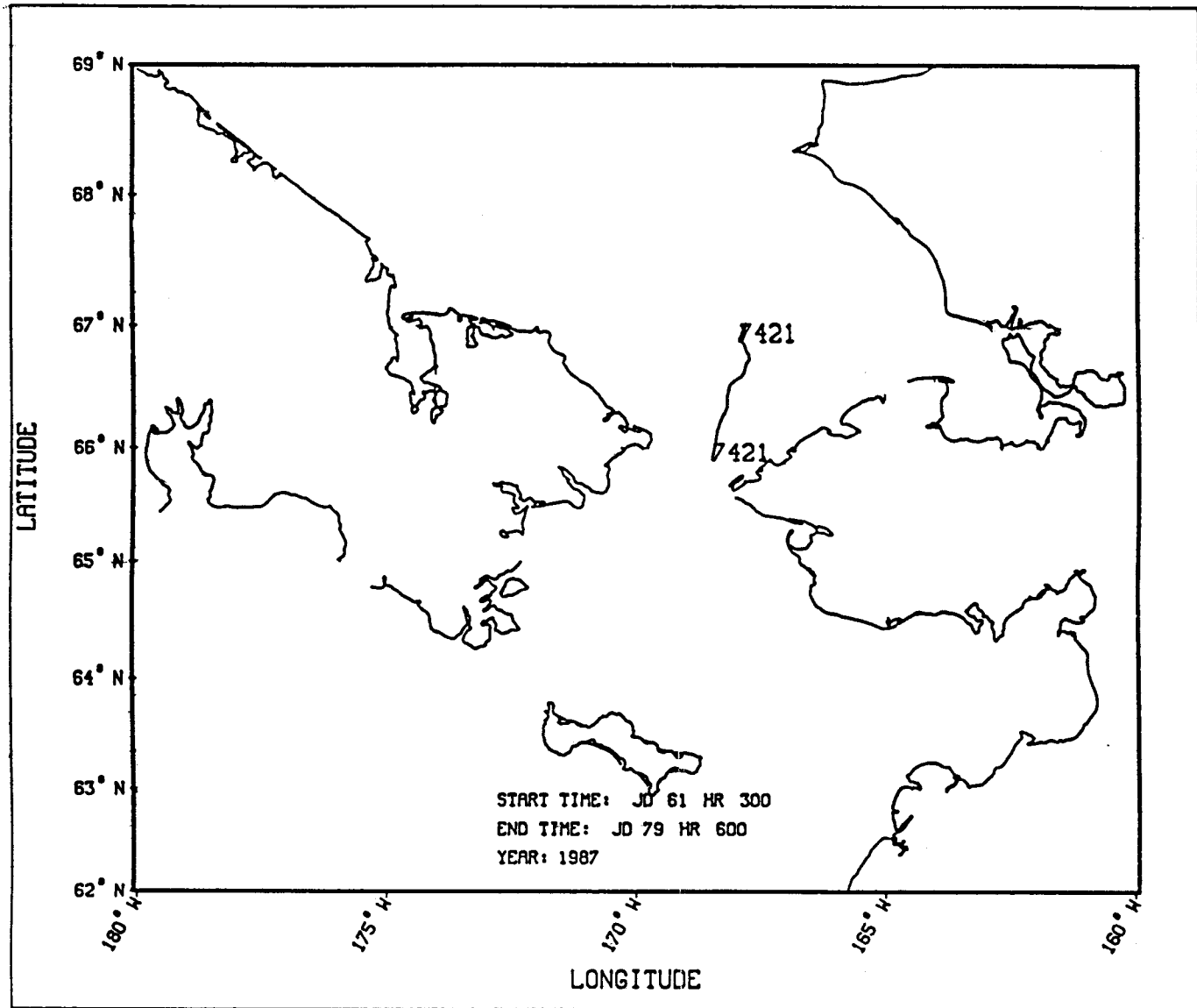


Figure 129. Drift tracks for ARGOS buoy 7421.

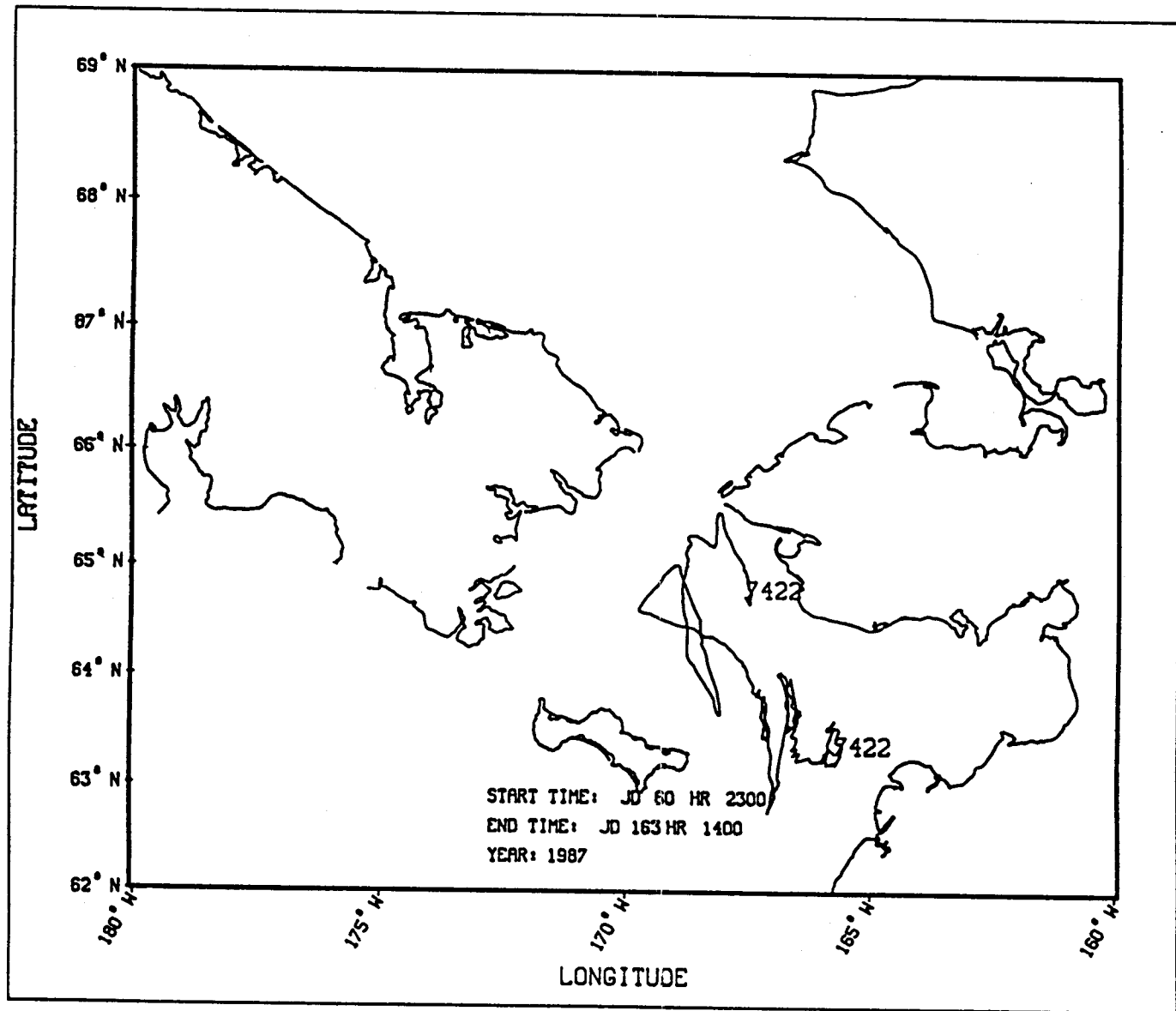


Figure 130. Drift tracks for ARGOS buoy 7422.

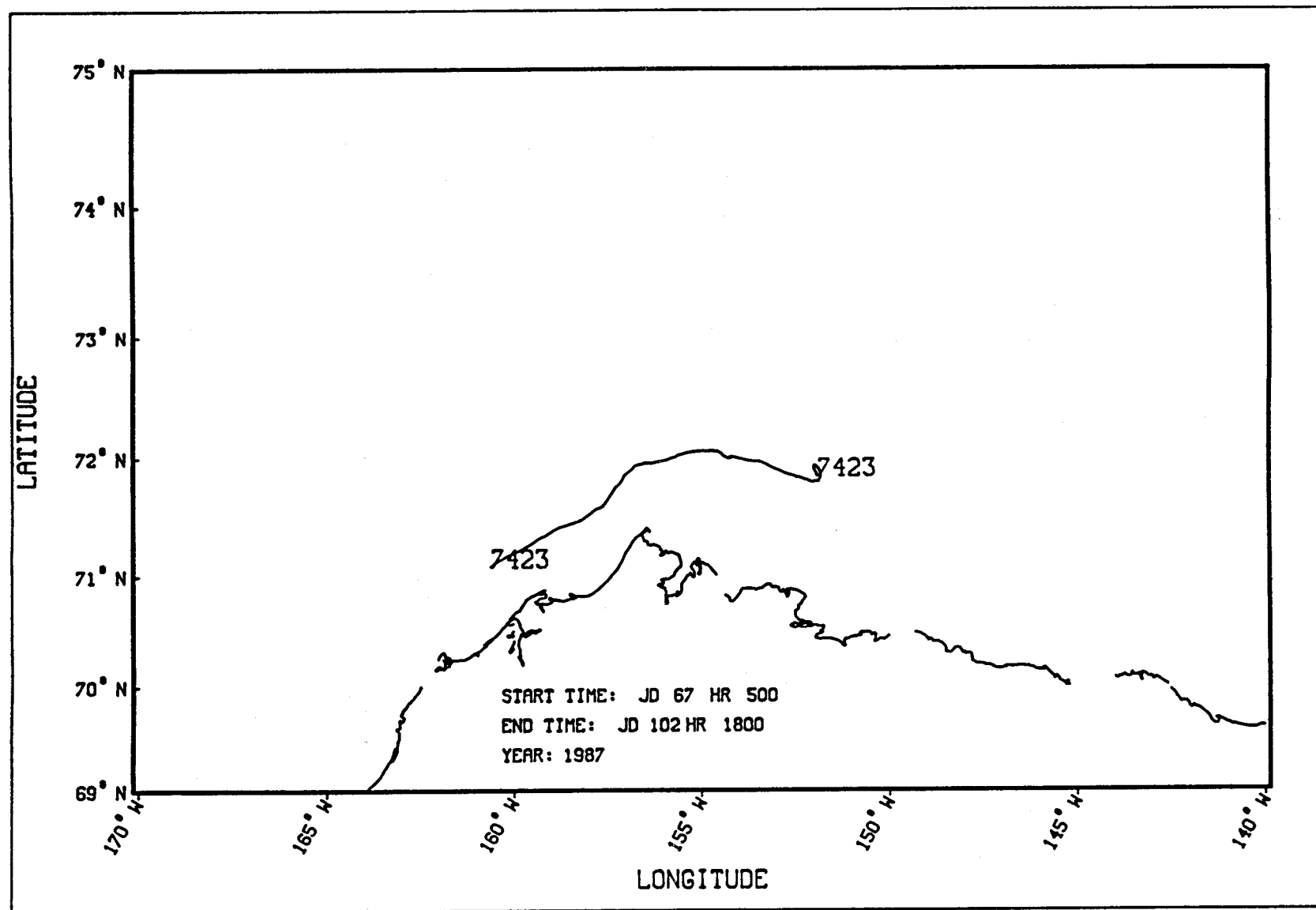


Figure 131. Drift tracks for ARGOS buoy 7423.

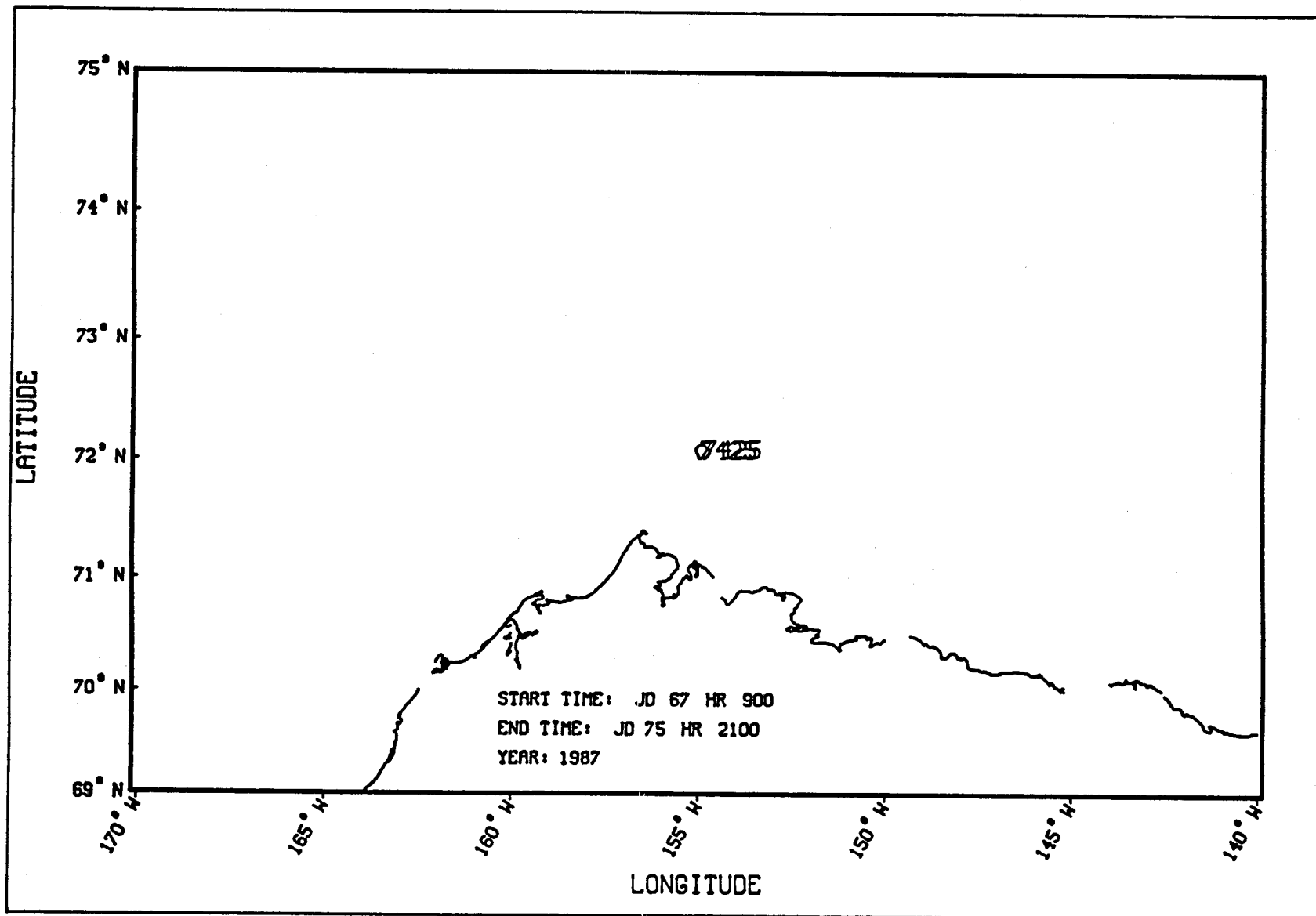


Figure 132. Drift tracks for ARGOS buoy 7425.

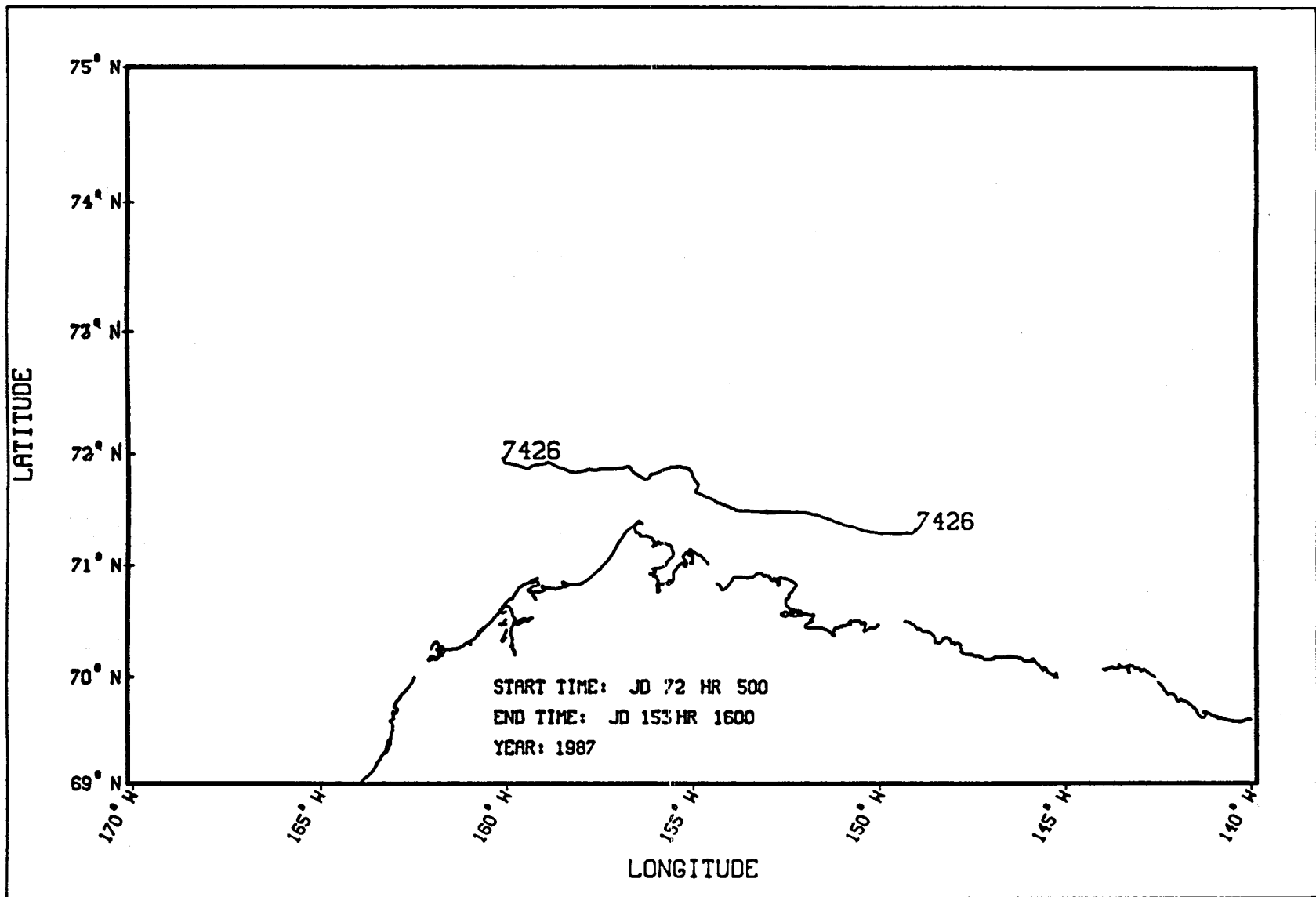


Figure 133. Drift tracks for ARGOS buoy 7426.

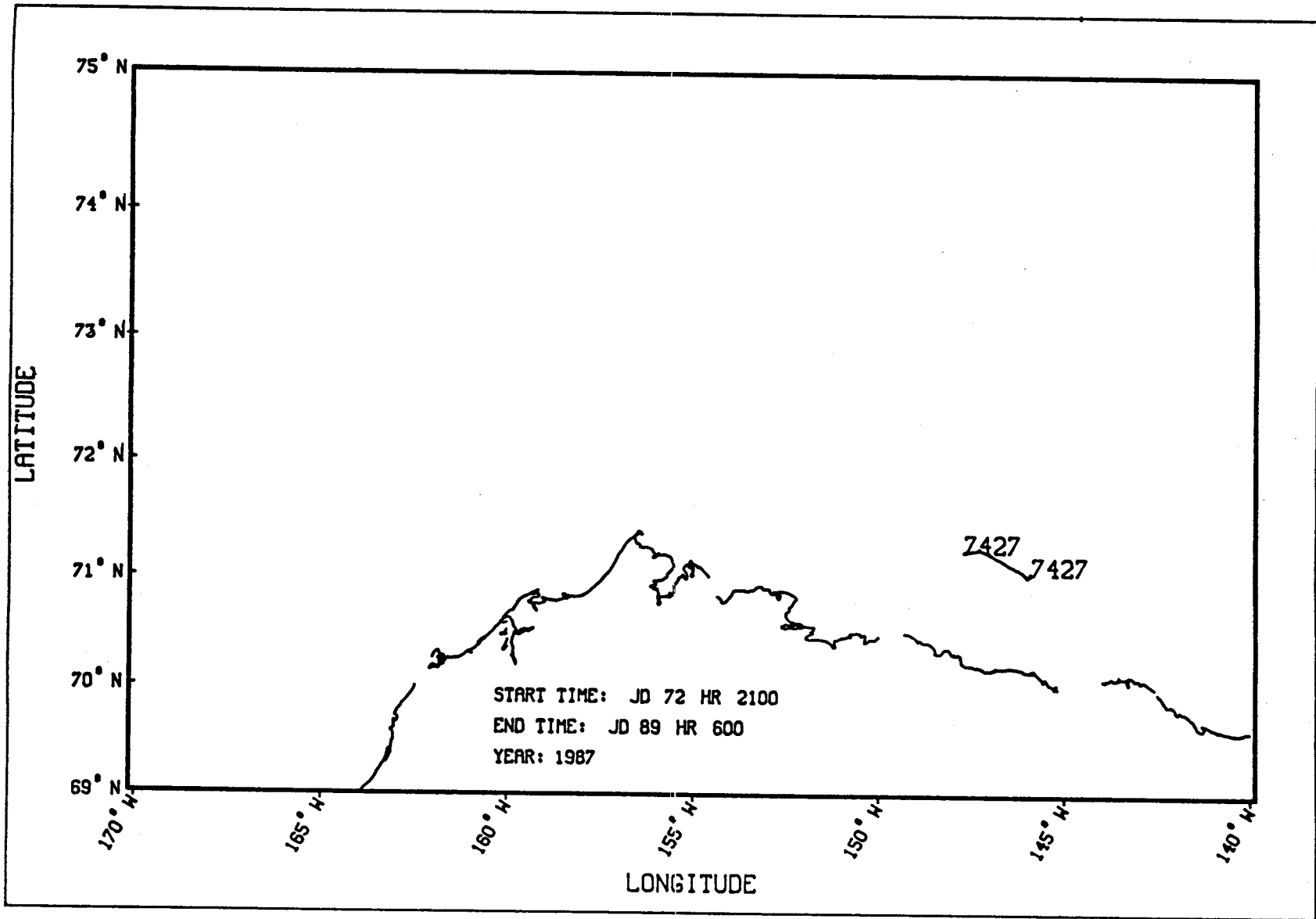


Figure 134. Drift tracks for ARGOS buoy 7427.

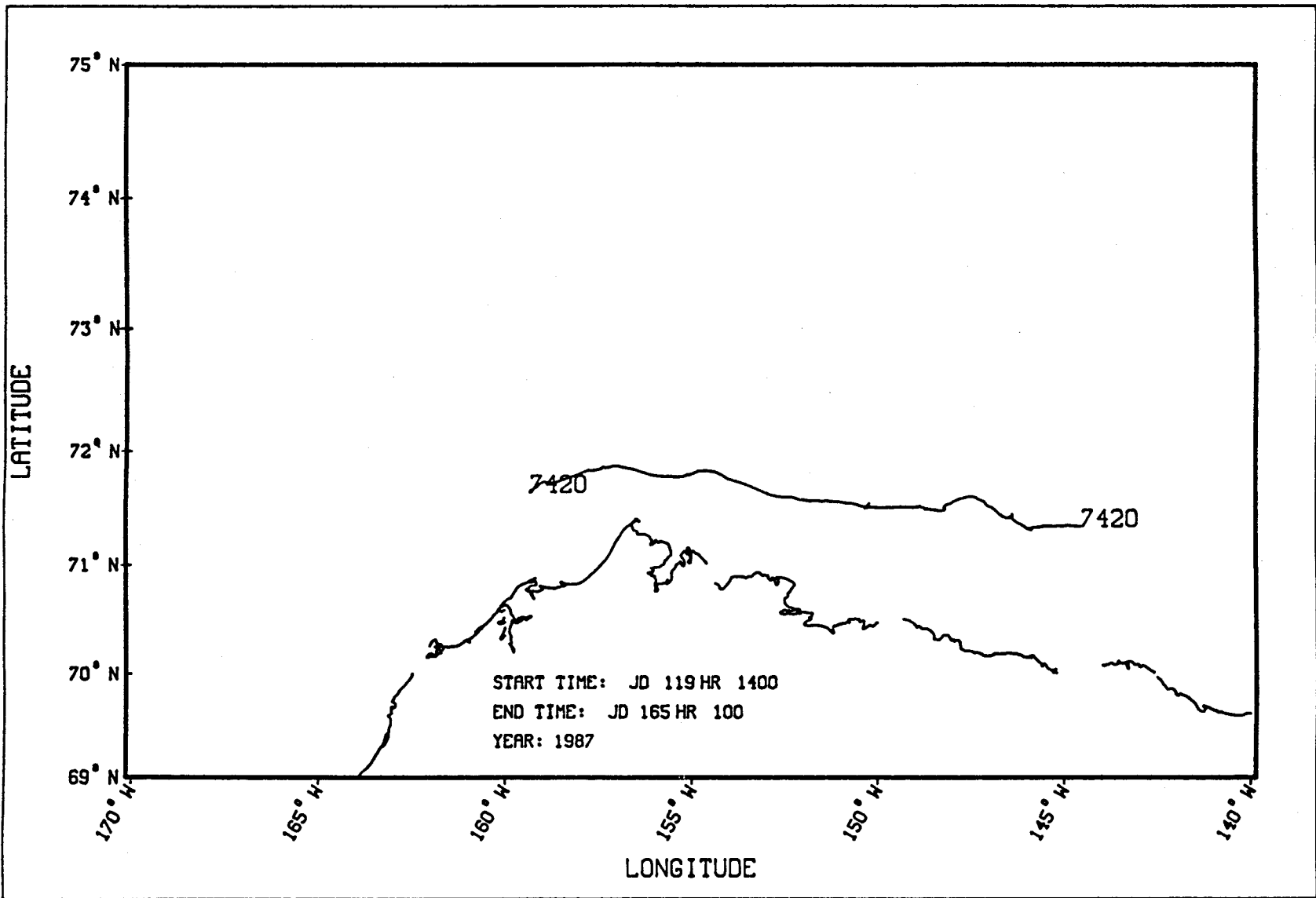


Figure 135. Drift tracks for ARGOS buoy 7420b.



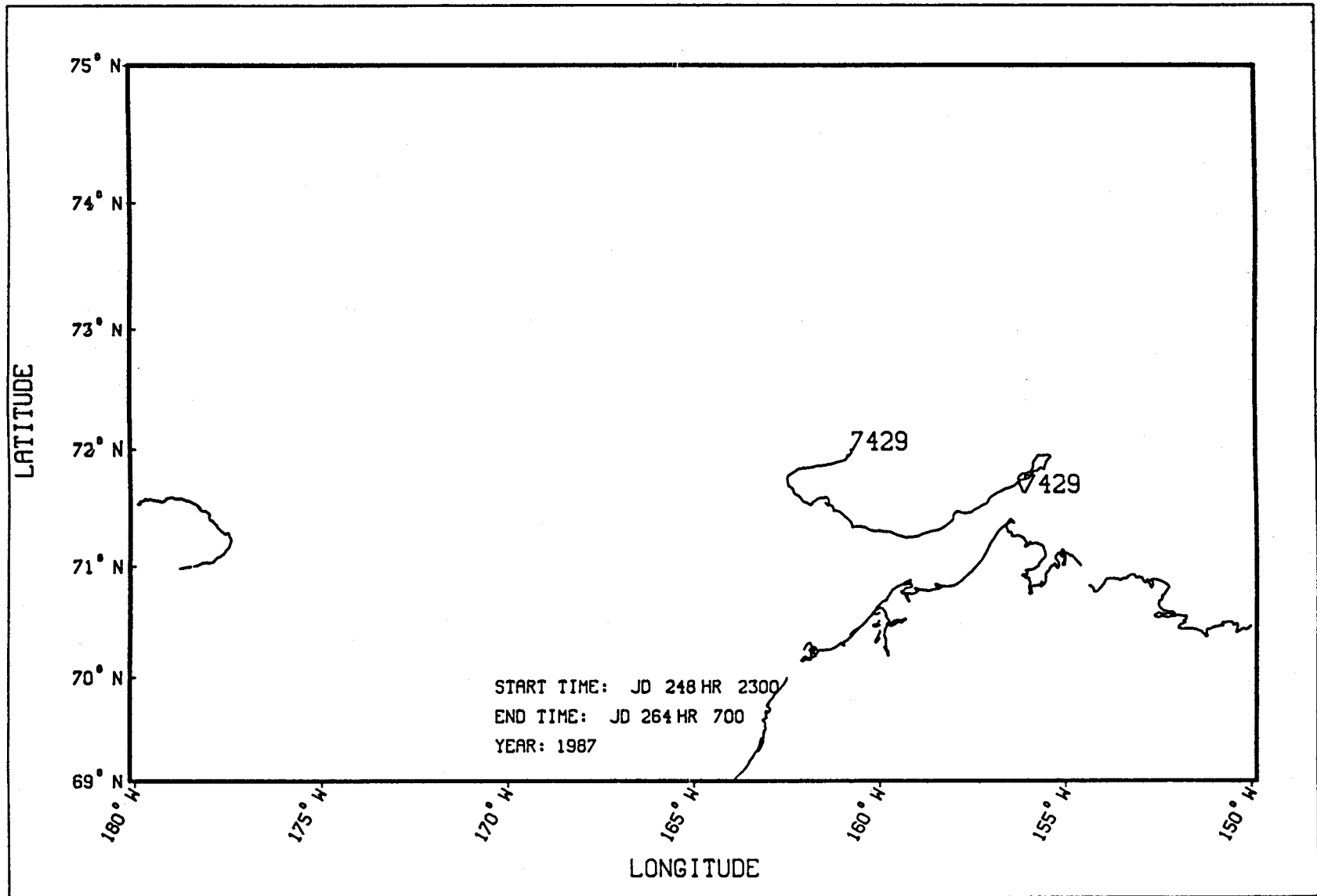


Figure 137. Drift tracks for ARGOS buoy 7429.

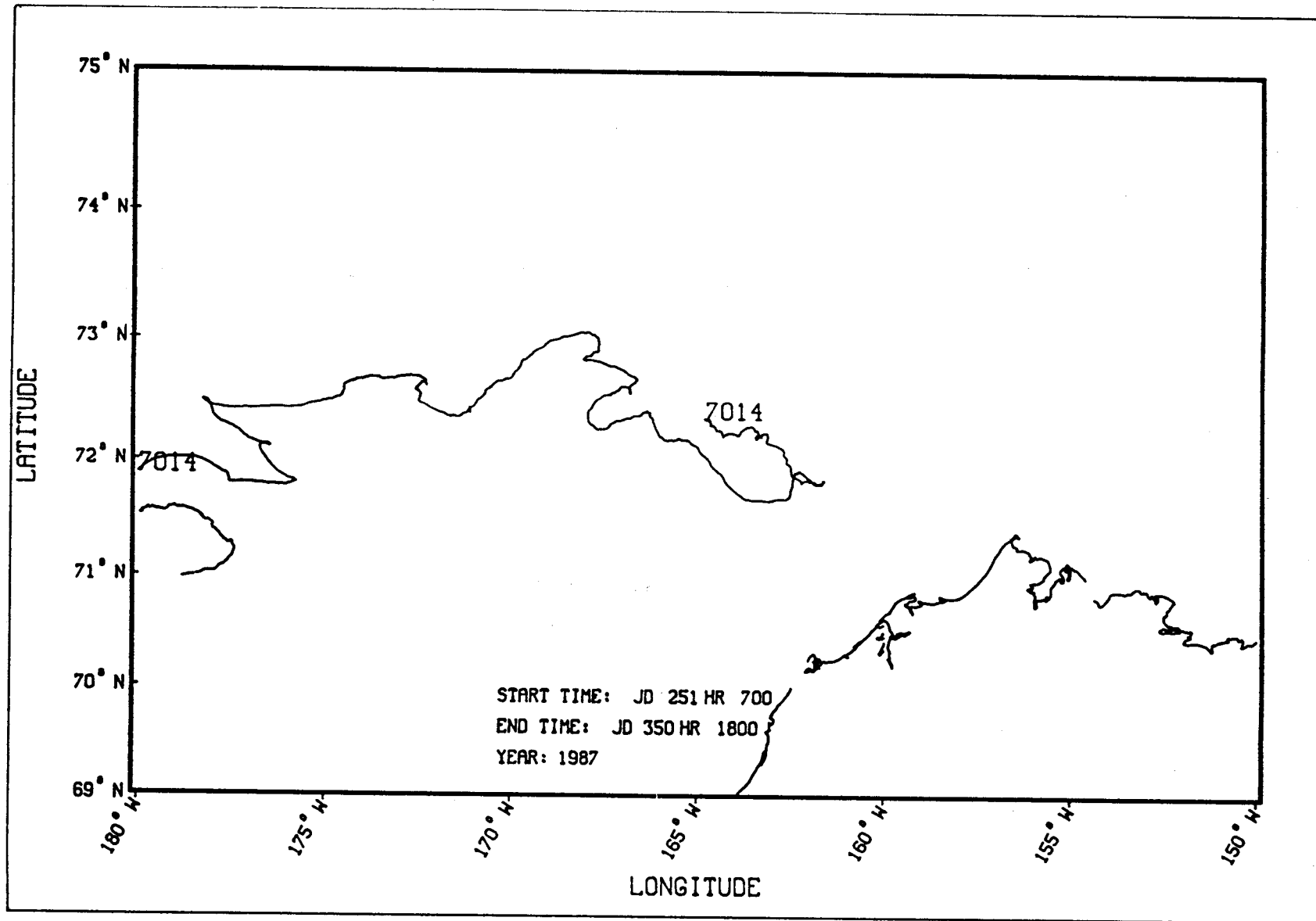


Figure 138. Drift tracks for ARGOS buoy 7014.

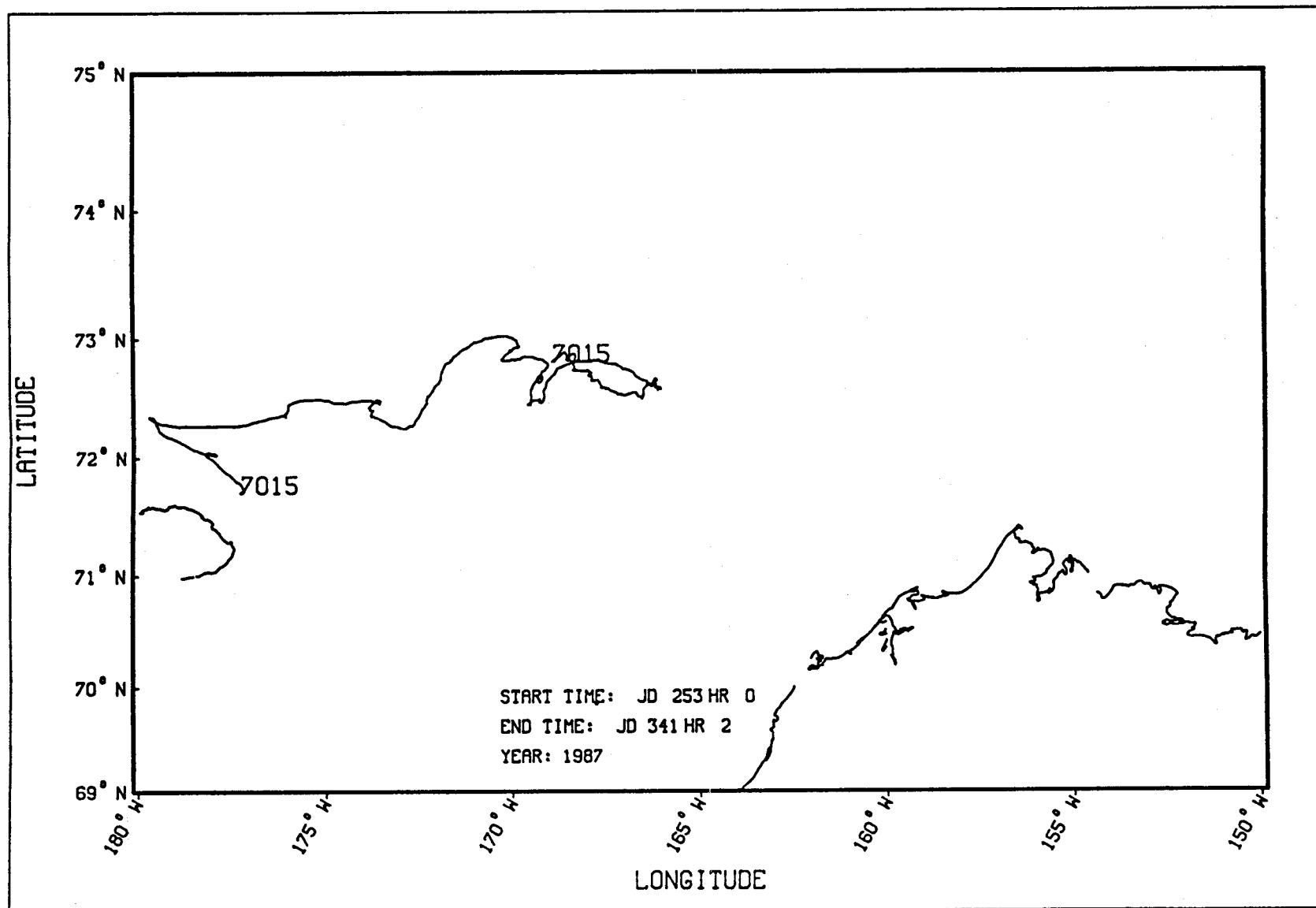


Figure 139. Drift tracks for ARGOS buoy 7015.

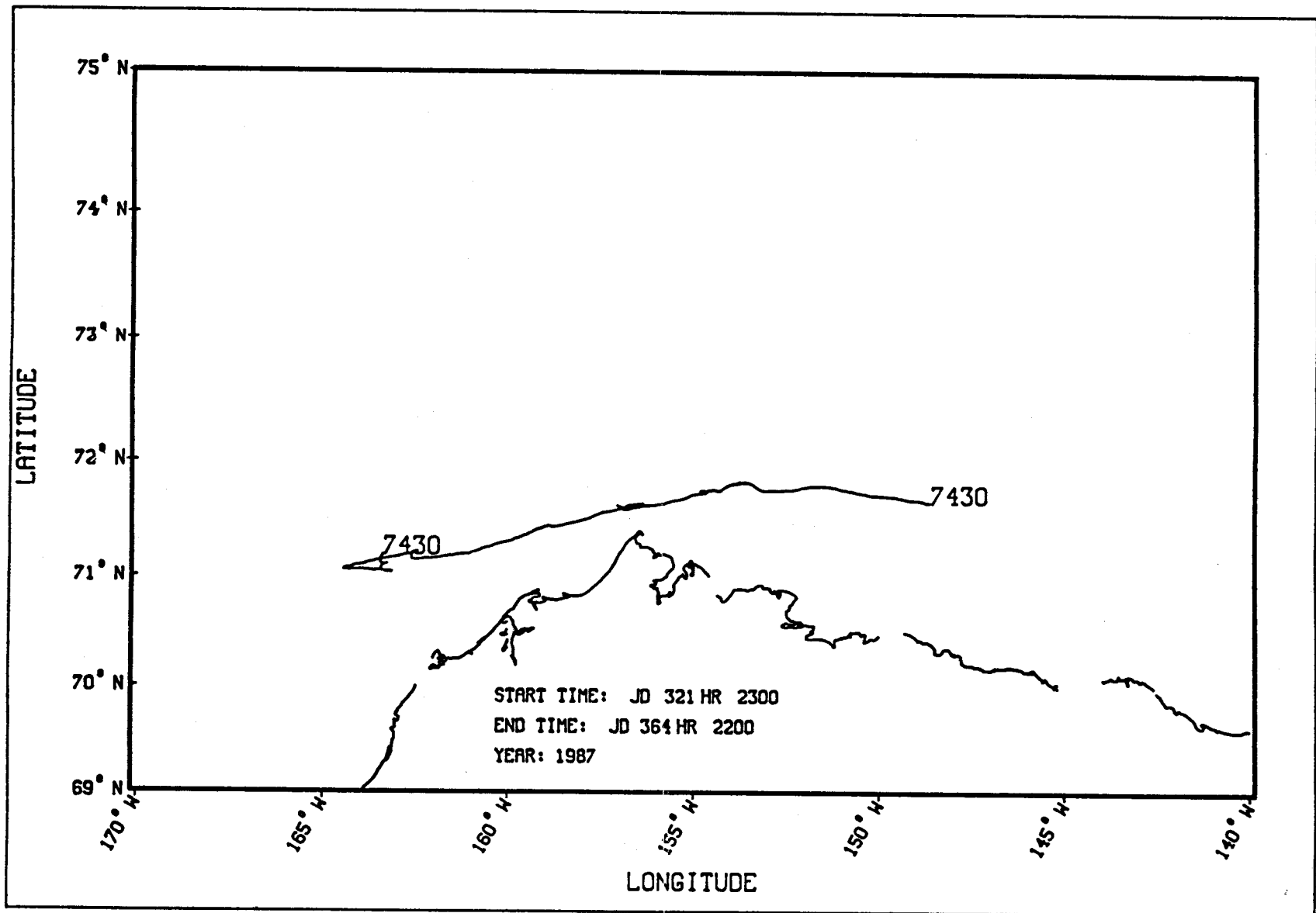


Figure 140. Drift tracks for ARGOS buoy 7430.

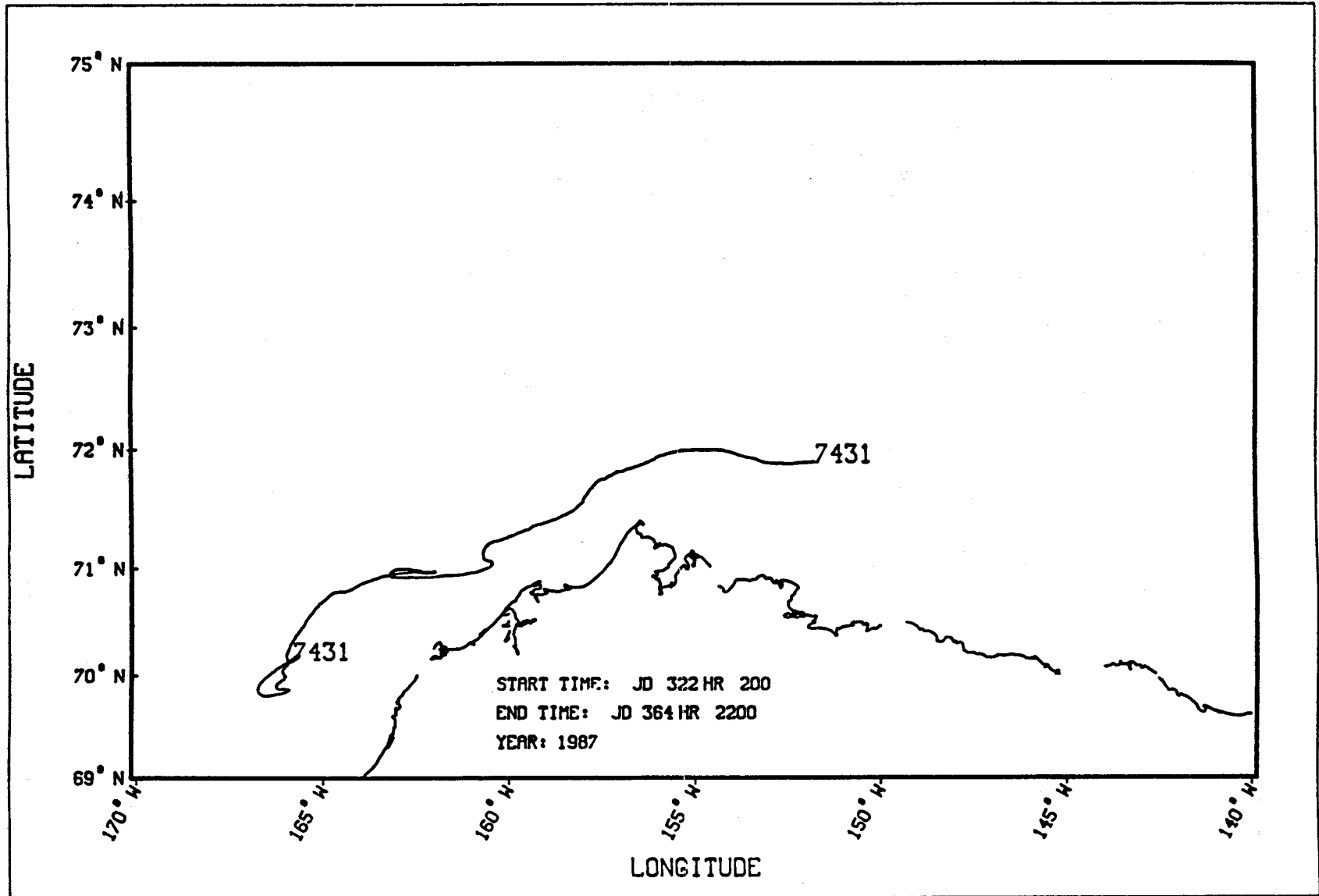


Figure 141. Drift tracks for ARGOS buoy 7431.

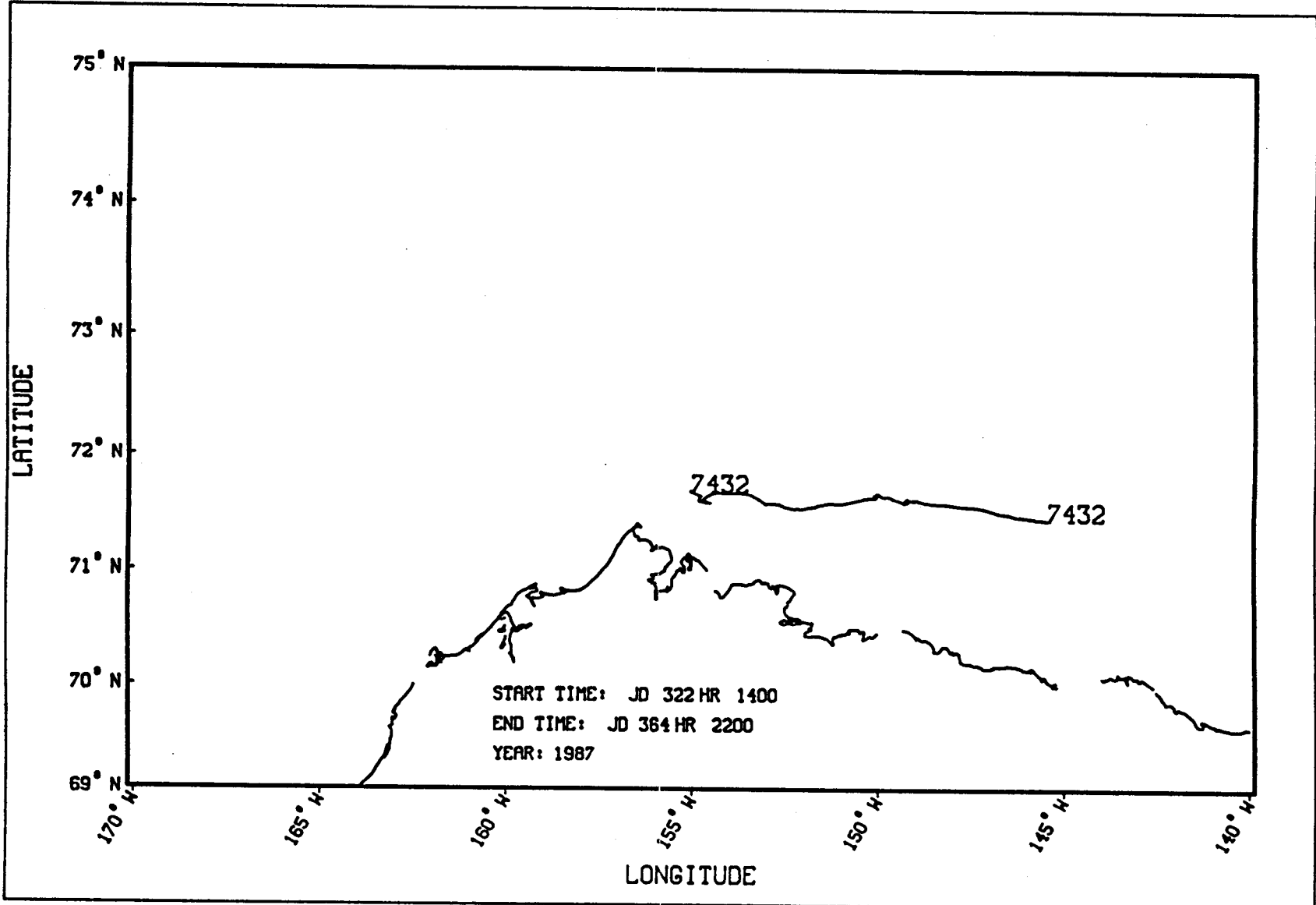


Figure 142. Drift tracks for ARGOS buoy 7432.

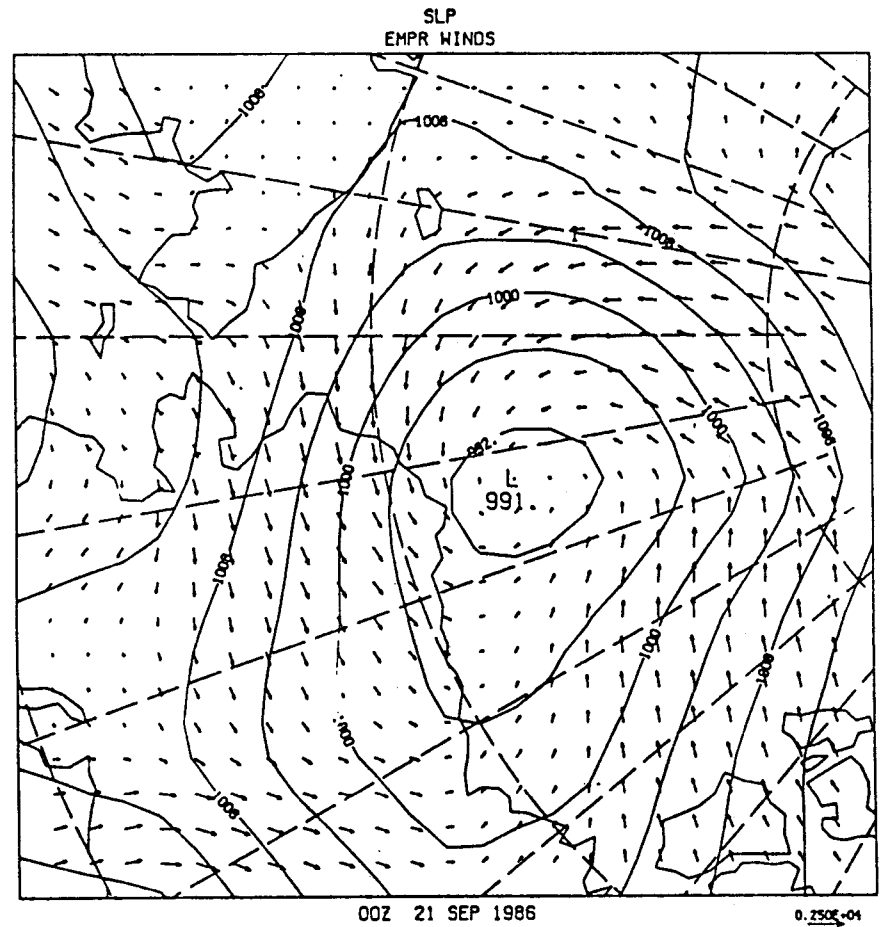
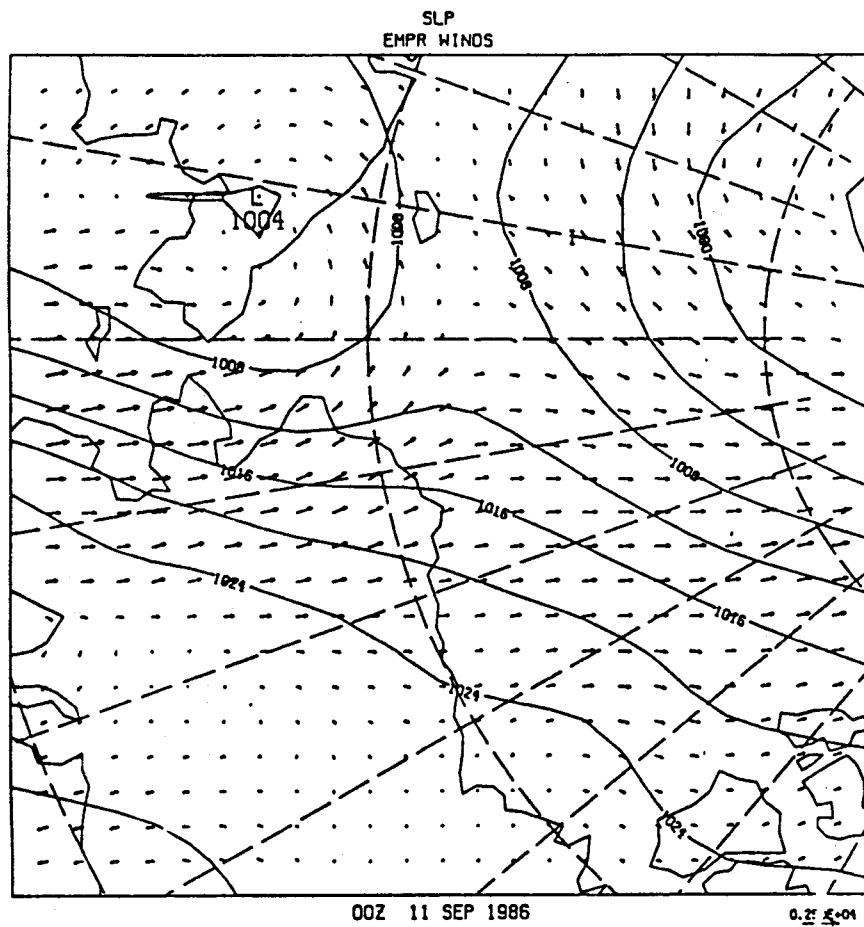


Figure 143. Sea-level pressure and gradient wind fields over the Beaufort and Chukchi Seas - 00 UTC 11 Sep 1986 and 00 UTC 21 Sep 1986.

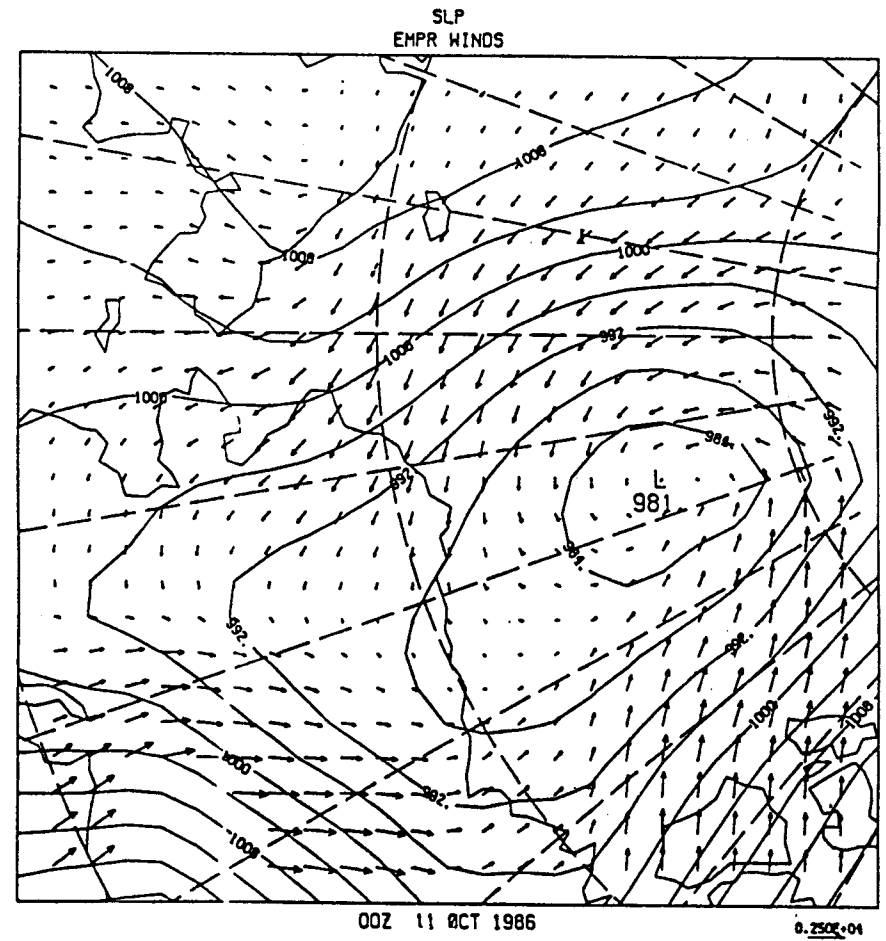
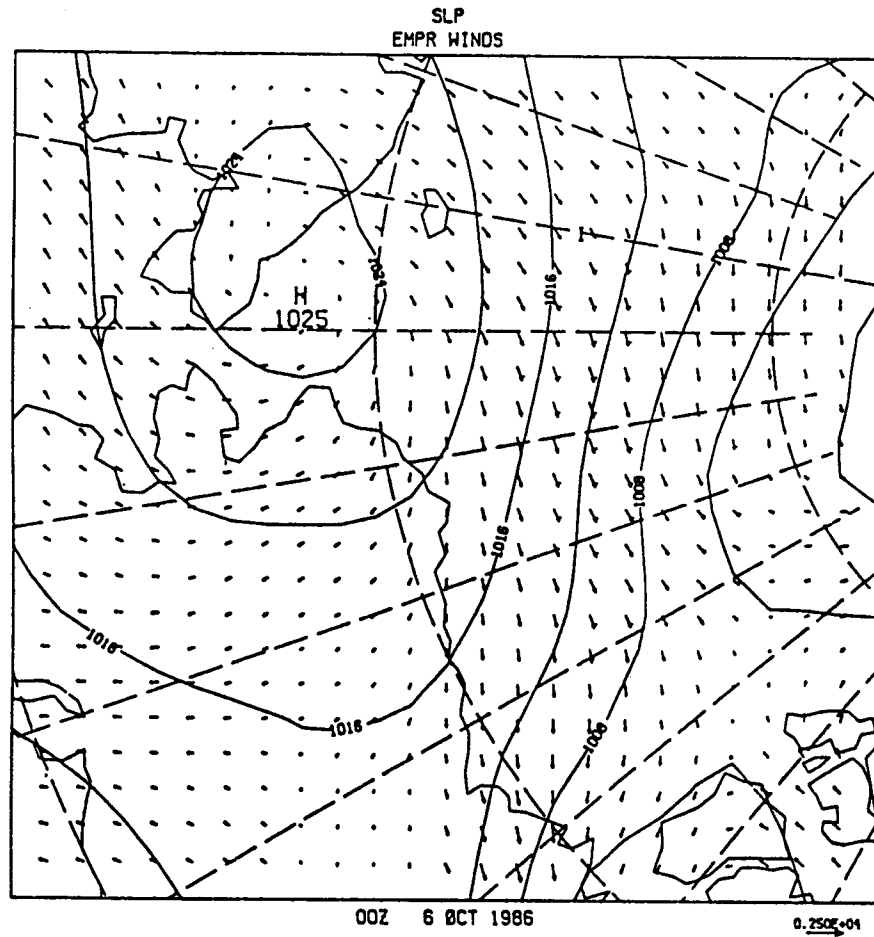


Figure 144. Sea-level pressure and gradient wind fields over the Beaufort and Chukchi Seas - 00 UTC 06 Oct 1986 and 00 UTC 11 Oct 1986.

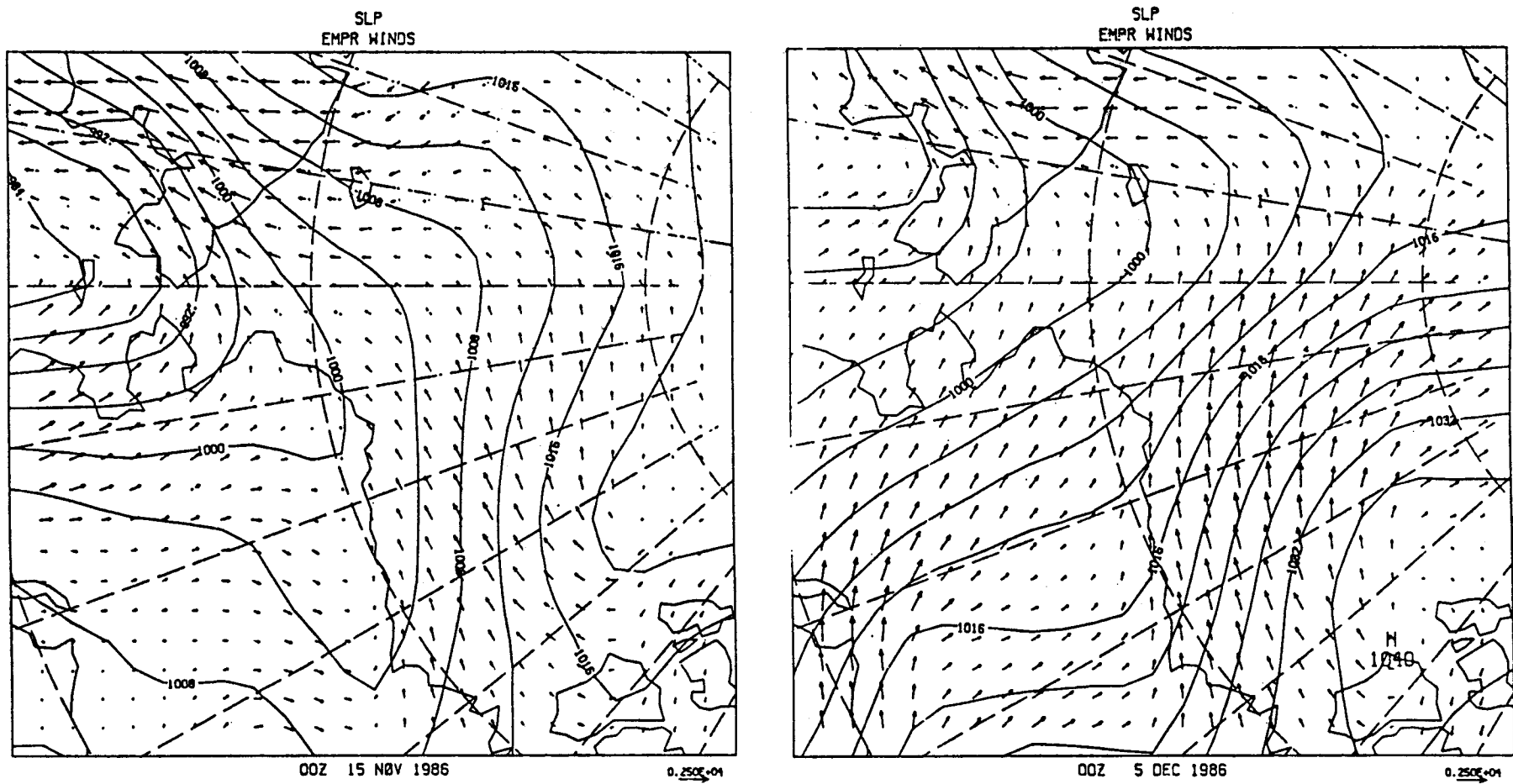


Figure 145. Sea-level pressure and gradient wind fields over the Beaufort and Chukchi Seas - 00 UTC 15 Nov 1986 and 00 UTC 05 Dec 1986.

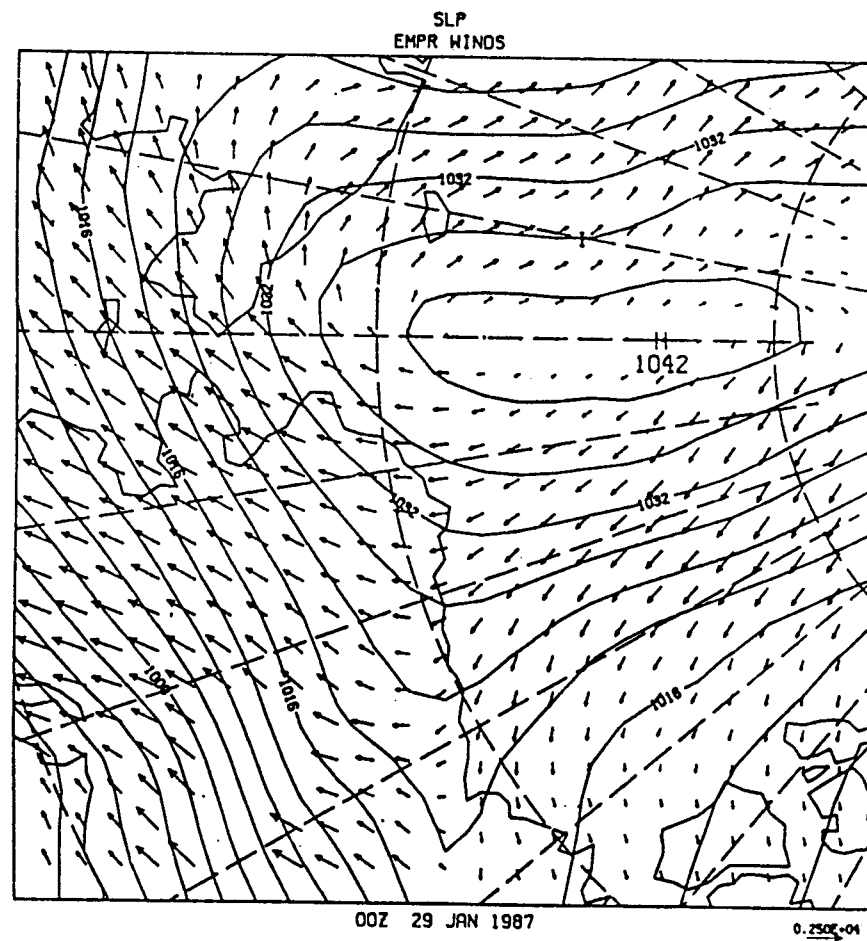
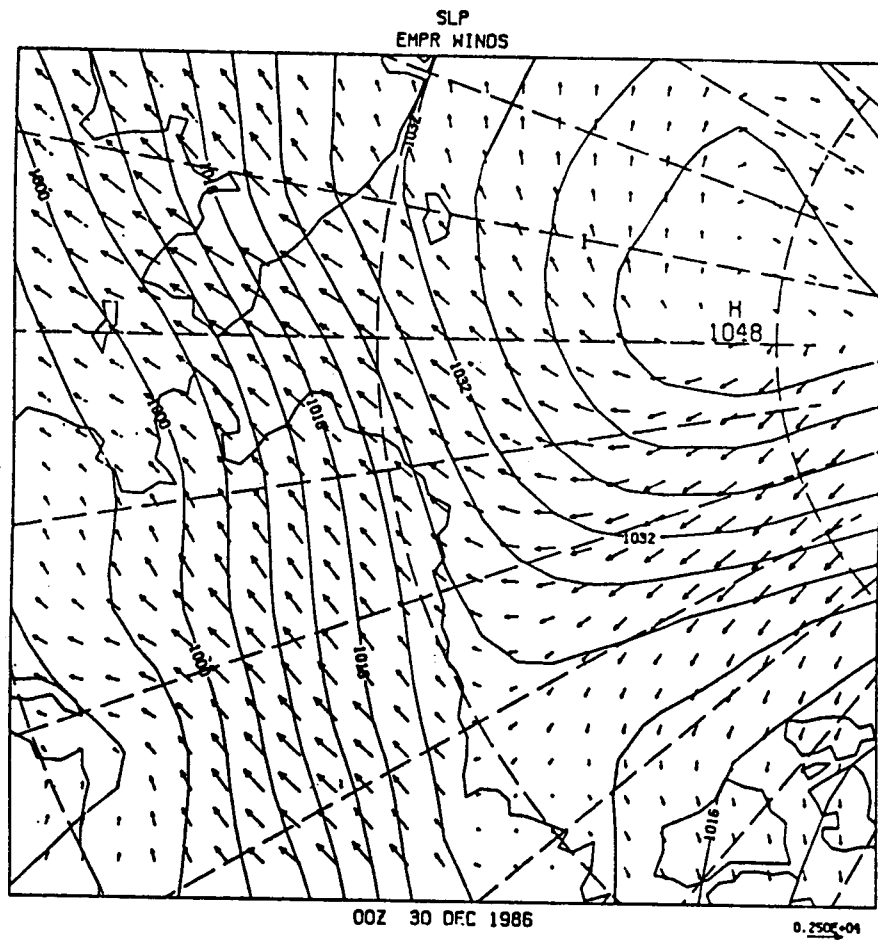
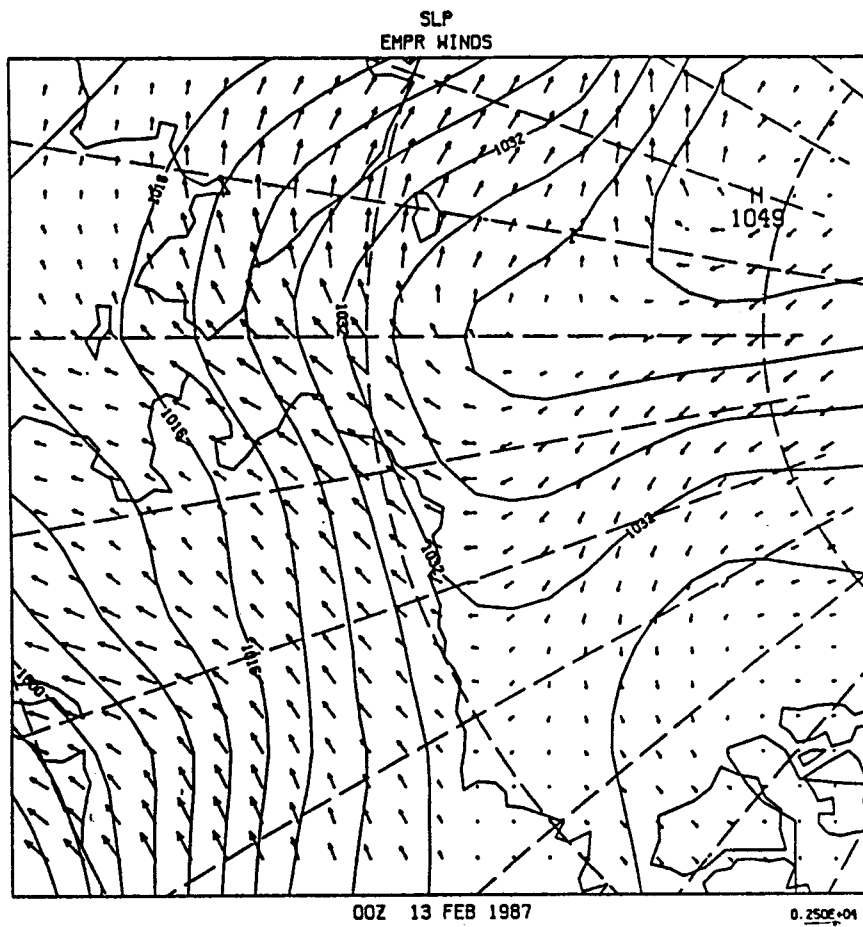


Figure 146. Sea-level pressure and gradient wind fields over the Beaufort and Chukchi Seas - 00 UTC 30 Dec 1986 and 00 UTC 29 Jan 1987.



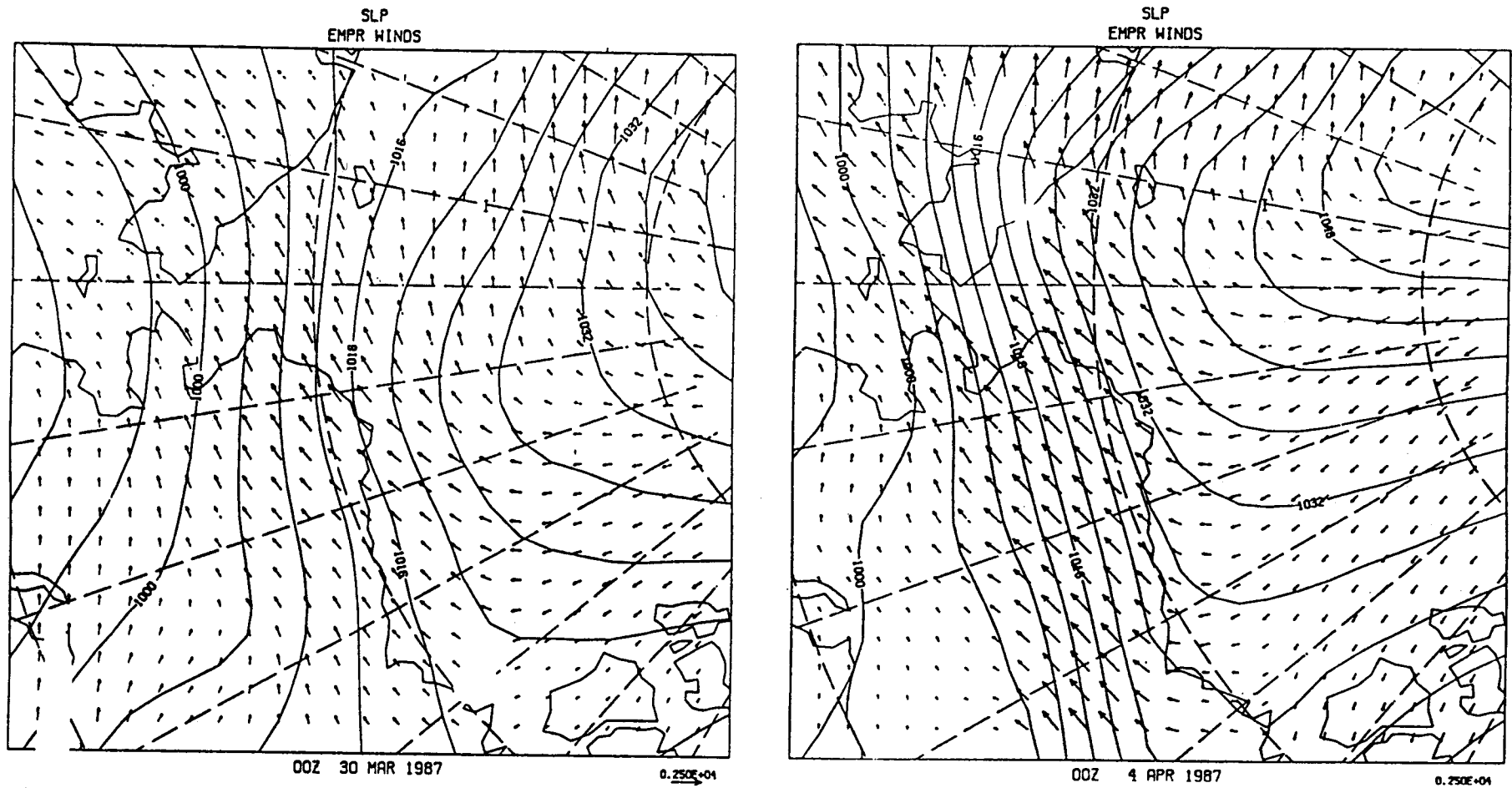


Figure 148. Sea-level pressure and gradient wind fields over the Beaufort and Chukchi Seas - 00 UTC 30 Mar 1987 and 00 UTC 04 Apr 1987.

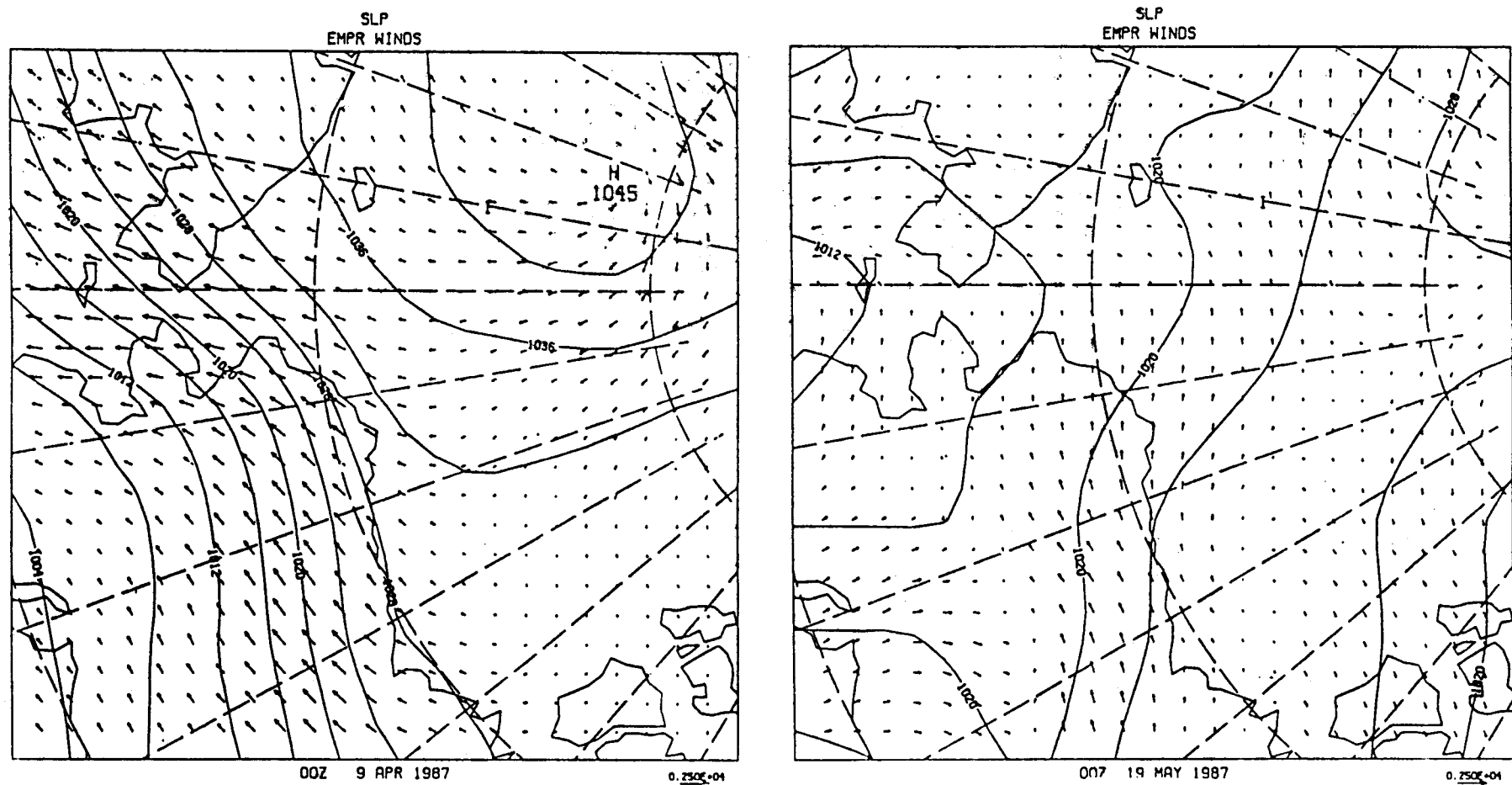


Figure 149. Sea-level pressure and gradient wind fields over the Beaufort and Chukchi Seas - 00 UTC 09 Apr 1987 and 00 UTC 19 May 1987.

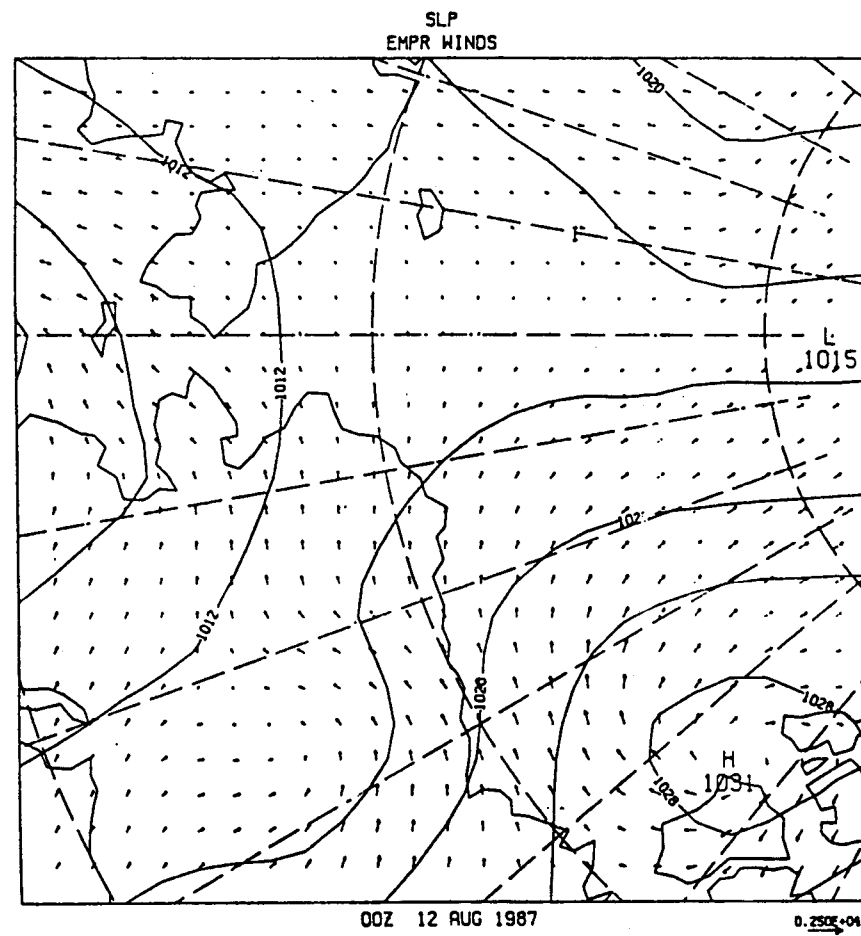
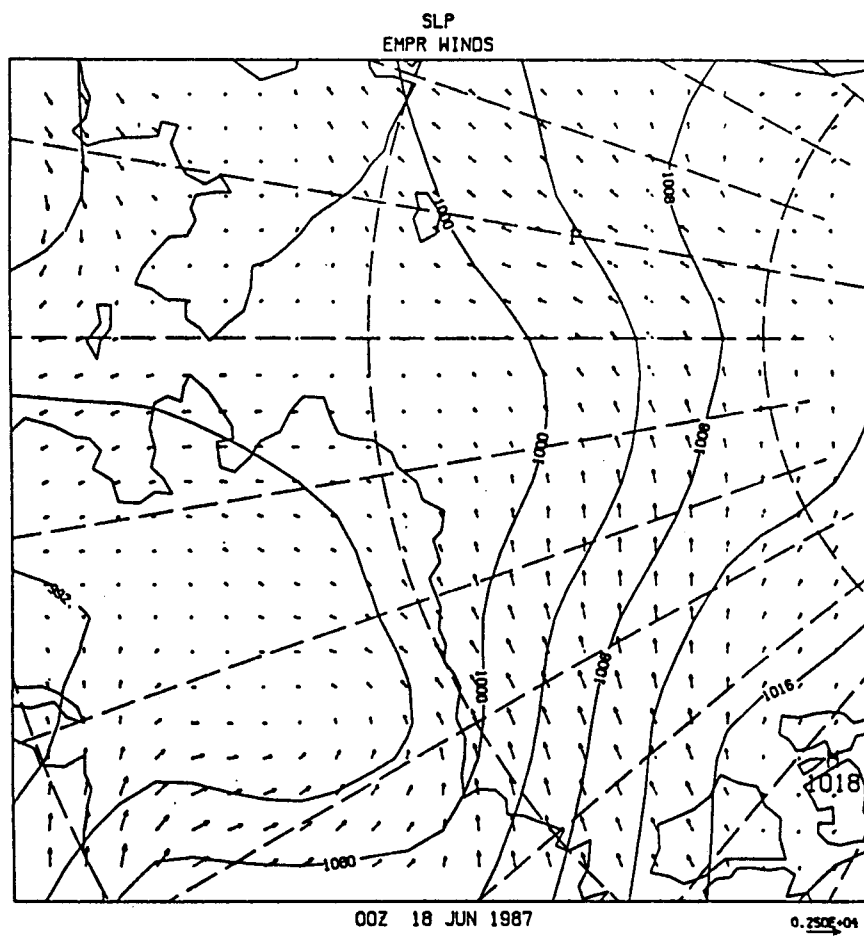


Figure 150. Sea-level pressure and gradient wind fields over the Beaufort and Chukchi Seas - 00 UTC 18 Jun 1987 and 00 UTC 12 Aug 1987.

[The page contains a large, faint watermark or bleed-through from the reverse side, which is illegible.]

**APPENDIX B.**  
**BEAUFORT SEA MESOSCALE CIRCULATION STUDY: HYDROGRAPHY**  
**USCGC POLAR STAR CRUISE, OCTOBER 1986**

**K. Aagaard, C. H. Pease, and K. Kroglund**

**U.S. Department of Commerce**  
**National Oceanic and Atmospheric Administration**  
**Environmental Research Laboratories**  
**Pacific Marine Environmental Laboratory**  
**Seattle, Washington**

**July 1987**

**Reprint of NOAA Data Report *ERL PMEL-19***

## NOTICE

Mention of a commercial company or product does not constitute an endorsement by NOAA/ERL. Use of information from this publication concerning proprietary products or the tests of such products for publicity or advertising purposes is not authorized.

Contribution No. 970 from NOAA/Pacific Marine Environmental Laboratory

---

For sale by the National Technical Information Service, 5285 Port Royal Road  
Springfield, VA 22161

## CONTENTS

INTRODUCTION.....	317
METHODOLOGIES.....	317
ACKNOWLEDGMENTS.....	318
REFERENCES .....	319
Figure 1 Location of CTD transects .....	320
Table 1 CTD chronology .....	321
Table 2 CTD sampling schedule .....	323
Table 3 Processed data .....	325

[The page contains extremely faint and illegible text, likely bleed-through from the reverse side of the document. No specific content can be transcribed.]

## INTRODUCTION

Data presented in this report were collected in October, 1986 from the USCGC Polar Star as part of the Beaufort Sea Mesoscale Circulation Study. The cruise took place on the Beaufort Sea continental shelf and continental slope, from Barrow Canyon to the Canadian border.

Sixty three CTD casts at 58 stations were made on the cruise (Table 1). The CTDs were taken along 6 transects, each roughly perpendicular to the coast (Fig. 1). Water samples were collected with each CTD cast, using 10 l and 30 l Niskin bottles. Samples were analyzed for oxygen, salinity, nutrients, suspended particulates, particulate carbon, chlorophyll, and phytoplankton (Table 2). The tabulation and plots of Table 3 show all these parameters, together with the density and light attenuation profiles. Samples were also taken for freons, tritium, and isotopes of cesium, radium, and strontium. These are being analyzed separately by other investigators.

## METHODOLOGIES

The CTD system used was a Neil Brown Mark III equipped with a SeaTech transmissometer. Since the ambient temperature was often very cold, the CTD was usually lowered to 30-40 m to warm it before starting the cast. It was then brought to the surface, and the cast was begun.

Processing of CTD data followed the method outlined in Giles and McDougall (1986) to correct for 1) the difference in the time constants of the salinity and temperature sensors (and of the platinum temperature sensor and the thermistor) and 2) the dependence of the time constants on the CTD lowering rate. Salinity and sigma-t were calculated using the algorithms of Fofonoff and Millard (1983).

Nutrients were determined using a 5 channel Technicon Auto Analyzer II system and the method outlined by Whitley *et al.* (1981). Oxygen concentration was measured by the Carpenter modification of the Winkler titration as described by Carpenter (1965). The method for the determination of the total suspended matter is standard method #208D of Standard Methods

for the Examination of Water and Wastewater (1975). Chlorophyll concentration was analyzed following the method of Parsons *et al.* (1984). Particulate carbon was analyzed with a Carlo Erba Elemental (CHN) Analyzer, model 1106.

#### ACKNOWLEDGMENTS

This work was supported by the Minerals Management Service through interagency agreement with the National Oceanic and Atmospheric Administration, as part of the Outer Continental Shelf Environmental Assessment Program. We appreciate the good efforts of Erdogan Ozturgut in bringing this project to fruition and in serving as chief scientist. Kimberly Kelly-Hansen spent many cold hours supervising water collection on the cruise and Susan Saupe of the University of Alaska volunteered her help continually and cheerfully. The ship's marine science technicians, Brian Branson, Jeff Newton and John Sullivan contributed considerably to the success and pleasure of the work. Lynn Long tabulated the data in Table 3.

## REFERENCES

- Carpenter, J.H., 1965. The Chesapeake Bay Institute technique for the Winkler dissolved oxygen method, *Limnology and Oceanography* 10: 141-143.
- Fofonoff, N.P. and R.C. Millard Jr., 1983. Algorithms for computation of fundamental properties of seawater, *Unesco Technical Papers in Marine Science* 44.
- Giles, A.B. and T.J. McDougall, 1986. Two methods for the reduction of salinity spiking of CTDs, *Deep-Sea Research* 33(9), 1253-1274.
- Parsons, T.R., Y. Maita, and C.M. Lalli, 1984. A manual of chemical and biological methods for Seawater Analysis, Pergamon Press, 173 pp.
- Standard Methods for the Examination of Water and Wastewater 14th Edition, 1975.
- Whitledge, T.E., S.C. Malloy, C.J. Patton, and C.D. Wirick, 1981. Automated nutrient analyses in seawater, *Report #BNL-51398*, Brookhaven National Laboratory, Upton, New York.

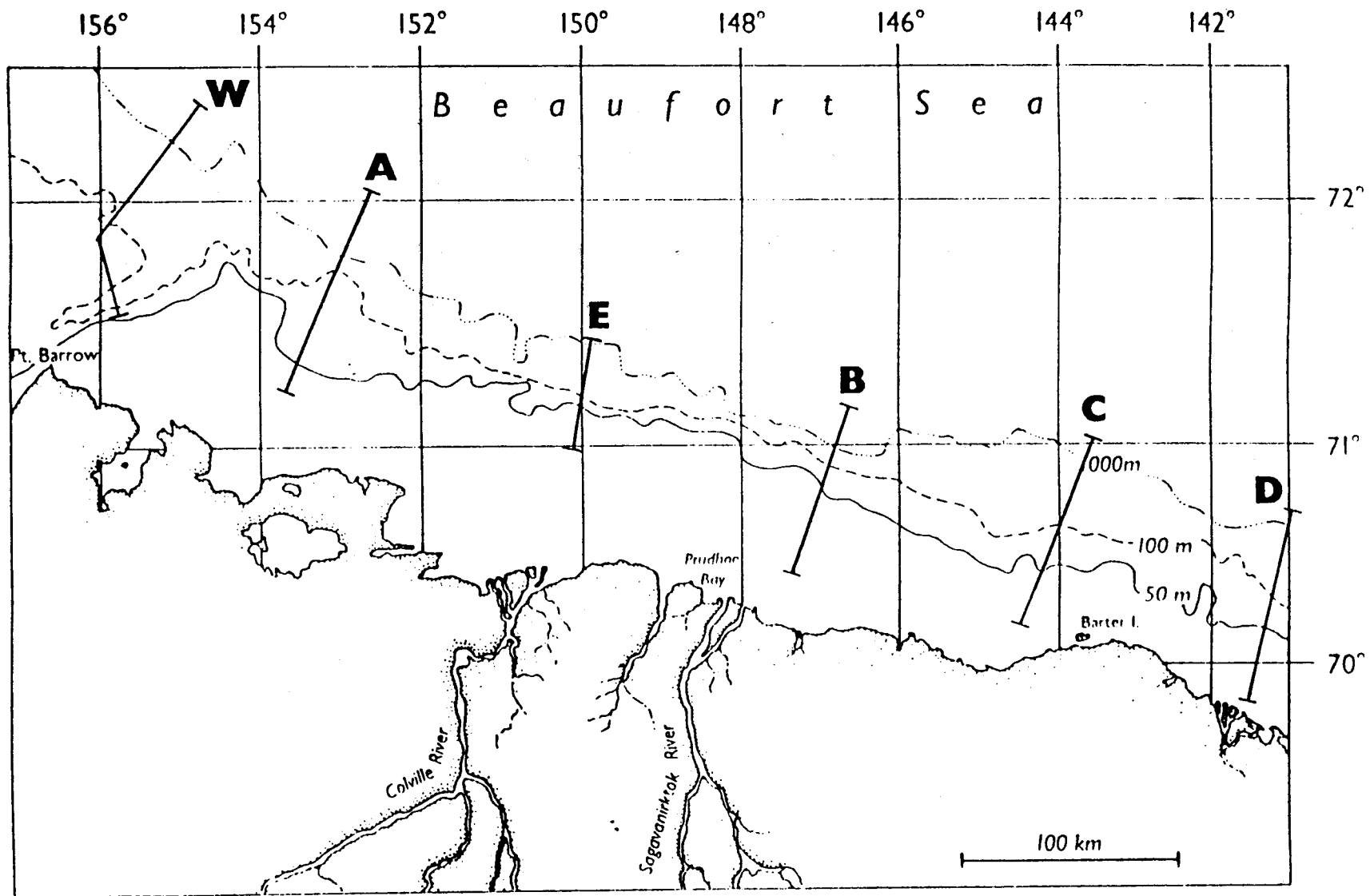


Figure 1.--Location of CTD transects.

Table 1. CTD chronology and positions. Stations A9 and A10 were accomplished in three steps because of the number of large-volume water samples required. Time is start of cast.

Sta. Name	Cast#	Time(UCT)	N. Lat.	W. Long.	Depth
W001	001	0823 03Oct	72 23.7	154 46.2	2315m
W002	002	1158 03Oct	72 16.4	154 58.8	1733m
W003	003	1450 03Oct	72 13.2	155 09.0	1086m
W004	004	1822 03Oct	72 08.0	155 17.9	401m
W005	005	2015 03Oct	72 04.6	155 29.0	263m
W006	006	2154 03Oct	72 00.0	155 39.2	177m
W007	007	2321 03Oct	71 55.6	155 49.7	121m
W008	008	0042 04Oct	71 50.7	156 01.0	80m
W009	009	0210 04Oct	71 45.0	155 57.4	106m
W010	010	0310 04Oct	71 40.4	155 52.9	123m
W011	011	0444 04Oct	71 34.6	155 47.2	172m
W012	012	0552 04Oct	71 32.0	155 45.6	101m
A002	013	0702 05Oct	71 13.2	153 40.0	27m
A003	014	0816 05Oct	71 19.4	153 33.9	47m
A004	015	0926 05Oct	71 24.4	153 25.9	46m
A005	016	1027 05Oct	71 29.8	153 18.1	62m
A006	017	1130 05Oct	71 35.5	153 10.1	57m
A007	018	1306 05Oct	71 43.6	152 55.2	208m
A008	019	1447 05Oct	71 46.5	152 53.5	221m
A009a	020	1750 05Oct	71 52.5	152 31.0	1609m
A009b	021	2019 05Oct	71 52.5	152 26.2	1576m
A009c	022	2145 05Oct	71 52.9	152 25.2	1608m
A010	023	Wire problems; cast redone			
A010a	024	2354 05Oct	71 58.5	152 40.4	2012m
A010b	025	0208 06Oct	72 00.5	152 42.8	2180m
A010c	026	0325 06Oct	72 02.9	152 39.3	2286m
B002	027	1703 08Oct	70 32.2	147 19.5	34m
B001	028	1838 08Oct	70 28.4	147 20.1	27m
B003	029	2012 08Oct	70 37.0	147 13.6	39m
B004	030	2111 08Oct	70 39.7	147 11.6	37m
B005	031	2230 08Oct	70 46.2	147 01.1	48m
B006	032	2343 08Oct	70 50.4	146 56.6	52m
B007	033	0100 09Oct	70 55.0	146 49.9	107m
B008	034	0228 09Oct	70 58.2	146 41.55	983m
B009	035	0521 09Oct	71 03.4	146 39.4	1693m
B010	036	0859 09Oct	71 08.9	146 36.4	2037m

Table 1. Continued

Sta. Name	Cast#	Time(UCT)	N. Lat.	W. Long.	Depth	
C005a	037	0743 11Oct	70 33.6	144 04.2	62m	
C006	038	0948 11Oct	70 39.0	143 55.5	305m	
C007	039	1222 11Oct	70 45.4	143 46.8	474m	
C008	040	1506 11Oct	70 50.8	143 40.7	860m	
C009	041	1803 11Oct	70 56.2	143 39.0	1479m	
C010	042	2223 11Oct	71 01.2	143 33.6	1608m	
C005b	043	0825 12Oct	70 33.8	144 05.0	61m	
C004	044	0950 12Oct	70 27.7	144 11.0	50m	
C003	045	1433 12Oct	70 21.4	144 17.2	45m	
C002	046	1606 12Oct	70 14.4	144 22.9	35m	
C001	047	1737 12Oct	70 10.2	144 30.4	24m	
D001	048	Rosette frozen; cast redone				
D001	049	0230 13Oct	69 50.8	141 32.1	26m	
D002	050	0347 13Oct	69 53.8	141 30.0	35m	
D003	051	0606 13Oct	70 00.2	141 25.8	44m	
D004	052	0725 13Oct	70 06.6	141 26.2	51m	
D005	053	0847 13Oct	70 13.0	141 23.3	52m	
D006	054	1039 13Oct	70 20.0	141 21.2	66m	
D007	055	1239 13Oct	70 25.6	141 20.0	359m	
D008	056	1612 13Oct	70 32.4	141 20.5	518m	
D009	057	2006 13Oct	70 39.0	141 19.0	1177m	
D010	058	2207 14Oct	70 43.0	140 59.3	1758m	
E001	059	1857 16Oct	71 00.0	150 06.6	27m	
E002	060	2008 16Oct	71 04.8	150 04.0	35m	
E003	061	2050 16Oct	71 06.6	150 02.6	41m	
E004	062	Rosette frozen; cast redone				
E004	063	2243 16Oct	71 12.0	149 59.6	62m	
E005	064	0026 17Oct	71 16.6	149 56.9	700m	
E006	065	0155 17Oct	71 21.1	149 54.6	1421m	
E007	066	0506 17Oct	71 24.9	149 55.1	1780m	

Table 2. Discrete samples taken at each CTD station.

Sta.	O <sub>2</sub>	Sal	Nut	Susp	Chl	Phyto
W1	7	2	7	-	-	-
W2	9	3	9	-	-	-
W3	10	3	10	4	4+	4
W4	7	2	7	-	-	-
W5	5	1	5	-	-	-
W6	5	2	5	4	-	-
W7	4	2	4	-	-	-
W8	7	2	7	3	6	6
W9	4	2	4	-	-	-
W10	7	2	7	3	4	4
W11	4	1	4	-	-	-
W12	6	2	6	4	6	6
A2	2	1	2	4	-	-
A3	6	1	6	4	6	6
A4	3	2	3	-	-	-
A5	6	2	6	4	6	6
A6	3	3	3	-	-	-
A7	7	2	7	4	6	6
A8	6	4	6	-	-	-
A9	11	16	11	4	5+	5
A10	12	18	12	-	-	-
B1	2	1	2	4	-	-
B2	6	6	6	-	-	-
B3	2	1	2	4	-	-
B4	3	1	3	-	-	-
B5	6	1	6	4	6+	6
B6	6	2	6	4	6	6
B7	7	2	7	4	6+	6
B8	7	4	7	-	-	-
B9	12	2	12	4	6	6
B10	12	3	12	-	-	-
C1	2	1	2	4	-	-
C2	3	1	3	4	-	-
C3	6	1	6	4	6+	6
C4	6	2	6	4	6	6
C5	4	2	4	-	-	-
C6	7	1	7	3	5+	5
C7	7	2	7	-	-	-
C8	9	2	9	-	-	-
C9	8#	2	12	4	6	6
C10	12	3	12	-	-	-

Table 2. Continued

Sta.	O <sub>2</sub>	Sal	Nut	Susp	Chl	Phyto
D1	2	1	2	-	-	-
D2	3	1	3	4	-	-
D3	3	1	3	3	-	-
D4	6	1	6	4	6	6
D5	7	2	7	4	6	6
D6	4	2	4	-	-	-
D7	8	2	8	4	6+	6
D8	9	2	9	-	-	-
D9	12	2	12	3	6	6
D10	12	4	12	-	-	-
E1	3	2	3	-	-	-
E2	5	2	5	4	5	5
E3	3	2	3	-	-	-
E4	7	2	7	6	6	6
E5	15	2	15	4	6+	5
E6	12	3	12	4	6	-
E7	12	3	12	-	-	-
Total	381	147	385	125	137	130

# Water was frozen in some of the Niskins at C9. Therefore, O<sub>2</sub> samples were not taken from the top 4 bottles.

+ At these stations one or more of the chlorophyll samples was damaged during shipping or processing.

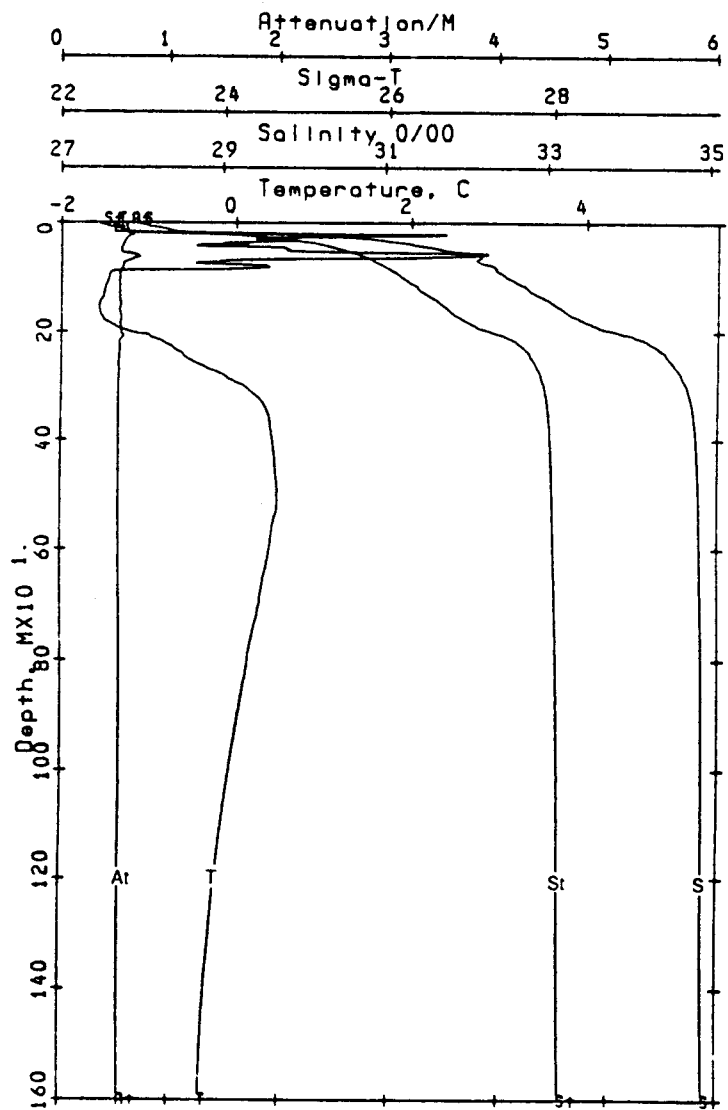
In Table 3 (pages 10-83), the symbol \* next to a salinity or temperature value indicates that on the downcast for the CTD station vertical salinity or temperature gradients were respectively greater than  $0.1 \text{ m}^{-1}$  or  $0.2^\circ\text{C m}^{-1}$  within one meter of the sample depth. Since the water samples were taken from bottles whose center was roughly 1.5 m above the CTD sensors, one should be cautious in associating precisely the given temperature or salinity value with the bottle data. Some casts also suggested large horizontal gradients in salinity and temperature: due to ship drift between the downcast and upcast, salinity or temperature values determined during the upcast were significantly different than those of the downcast. These values are not starred, since the numbers given indicate the conditions on the upcast, when the water samples were taken.

Replicate chlorophyll samples were taken; both values are presented in the table.

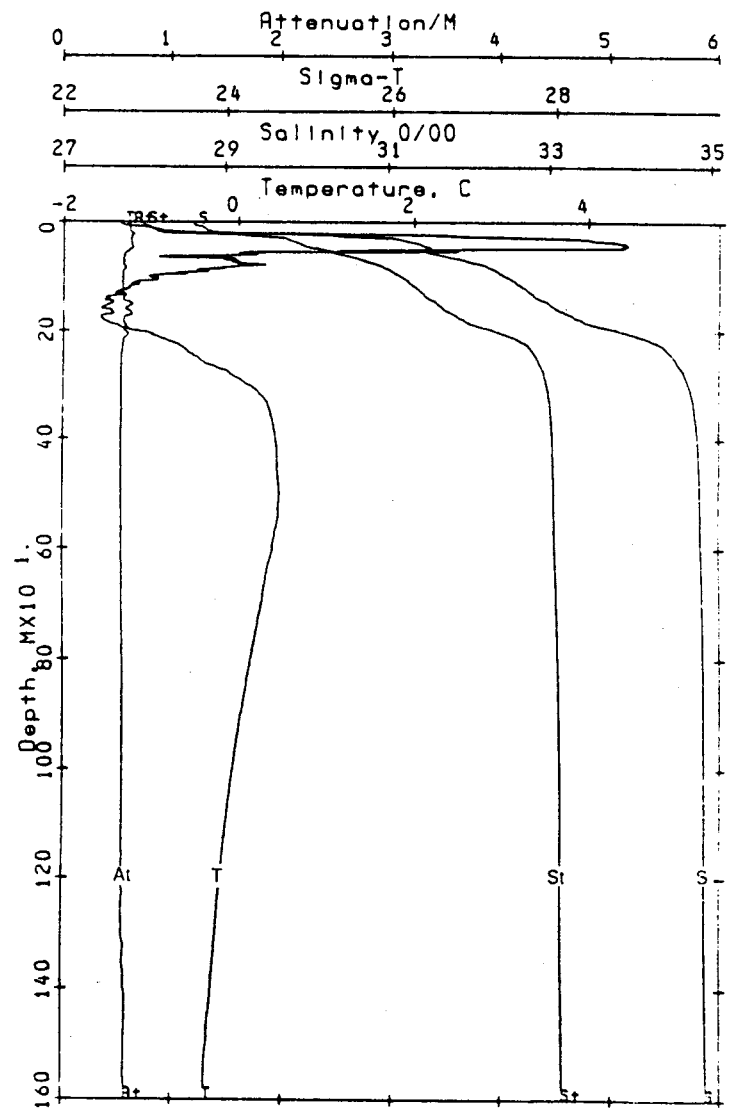
STATION W01		CAST 01	DATE 03 OCT 86	TIME 0823	LATITUDE 72 23.40N	LONGITUDE 154 46.40W	BOTTOM DEPTH 2315 M						
PRESS	TEMP	SAL	SIGMA-T	O <sub>2</sub>	SiO <sub>4</sub>	PO <sub>4</sub>	NO <sub>3</sub>	NO <sub>2</sub>	NH <sub>3</sub>	SPM	PC	LT.AT	CHLR-A
db	°C			ml l <sup>-1</sup>	µm l <sup>-1</sup>	µm l <sup>-1</sup>	µm l <sup>-1</sup>	µm l <sup>-1</sup>	µm l <sup>-1</sup>	mg l <sup>-1</sup>	µg l <sup>-1</sup>	m <sup>-1</sup>	µg l <sup>-1</sup>
8.6	-1.385	28.493	22.888	8.43		0.70	0.08	0.08	0.07			0.61	
154.4	-1.560	33.093	26.625	6.61	34.68	1.77	14.20	0.09				0.52	
305.3	0.162	34.729	27.879	6.31	11.03	0.94	12.50	0.09				0.52	
505.8	0.477	34.866	27.971	6.57	9.30	0.94	12.74	0.08	0.14			0.53	
705.3	0.256	34.886	28.000	6.44	8.68	0.97	12.70	0.06	0.29			0.53	
1004.8	-0.084	34.902	28.032	6.73	8.98	0.96	12.74	0.08	0.22			0.54	
1256.2	-0.250	34.913	28.049	5.96	9.46	0.98	12.98	0.08	0.22			0.54	

STATION W02		CAST 02	DATE 03 OCT 86	TIME 1159	LATITUDE 72 18.00N	LONGITUDE 154 58.10W	BOTTOM DEPTH 1733 M						
PRESS	TEMP	SAL	SIGMA-T	O <sub>2</sub>	SiO <sub>4</sub>	PO <sub>4</sub>	NO <sub>3</sub>	NO <sub>2</sub>	NH <sub>3</sub>	SPM	PC	LT.AT	CHLR-A
db	°C			ml l <sup>-1</sup>	µm l <sup>-1</sup>	µm l <sup>-1</sup>	µm l <sup>-1</sup>	µm l <sup>-1</sup>	µm l <sup>-1</sup>	mg l <sup>-1</sup>	µg l <sup>-1</sup>	m <sup>-1</sup>	µg l <sup>-1</sup>
4.2	-1.406	28.628	22.998	8.51	2.77	0.58	0.00	0.02	0.00			0.60	
47.7	-0.265	31.239	25.081	8.15	5.14	0.80	0.49	0.09	0.01			0.56	
149.3	-1.513	32.956	26.512	6.63	29.72	1.81	12.49	0.10	0.34			0.56	
198.4	-1.258	33.768	27.163	5.90	30.50	1.74	14.26	0.04	0.00			0.54	
497.9	0.472	34.863	27.969	6.55	7.33	0.84	12.40	0.03	0.00			0.53	
698.8	0.261	34.888	28.001	6.62	7.98	0.81	12.29	0.02	0.00			0.54	
999.0	-0.065	34.901	28.030	6.86	7.95	0.84	12.41	0.02	0.00			0.54	
1249.3	-0.213	34.914	28.048	6.89	9.26	0.91	12.75	0.02	0.00			0.56	
1578.8	-0.370	34.925	28.065	6.61	9.37	0.91	13.44	0.02	0.00			0.58	

327



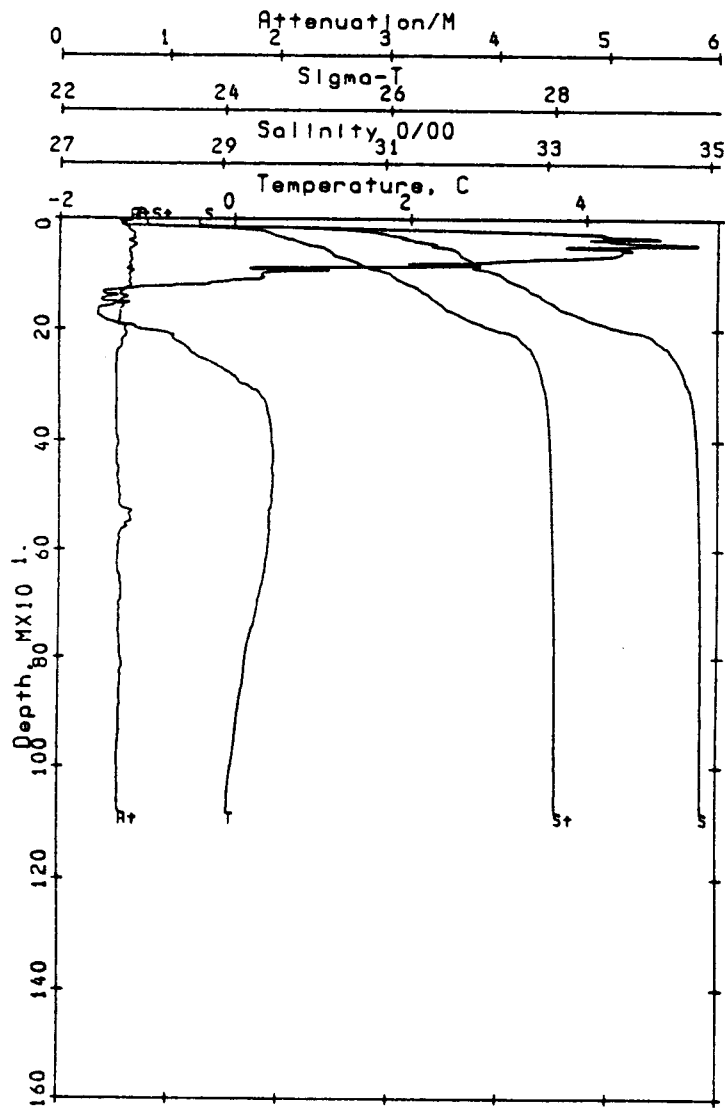
Ref. no. 1 Sta. w01 72.39 N  
 Time = 862760823 Beaufort 154.77 W



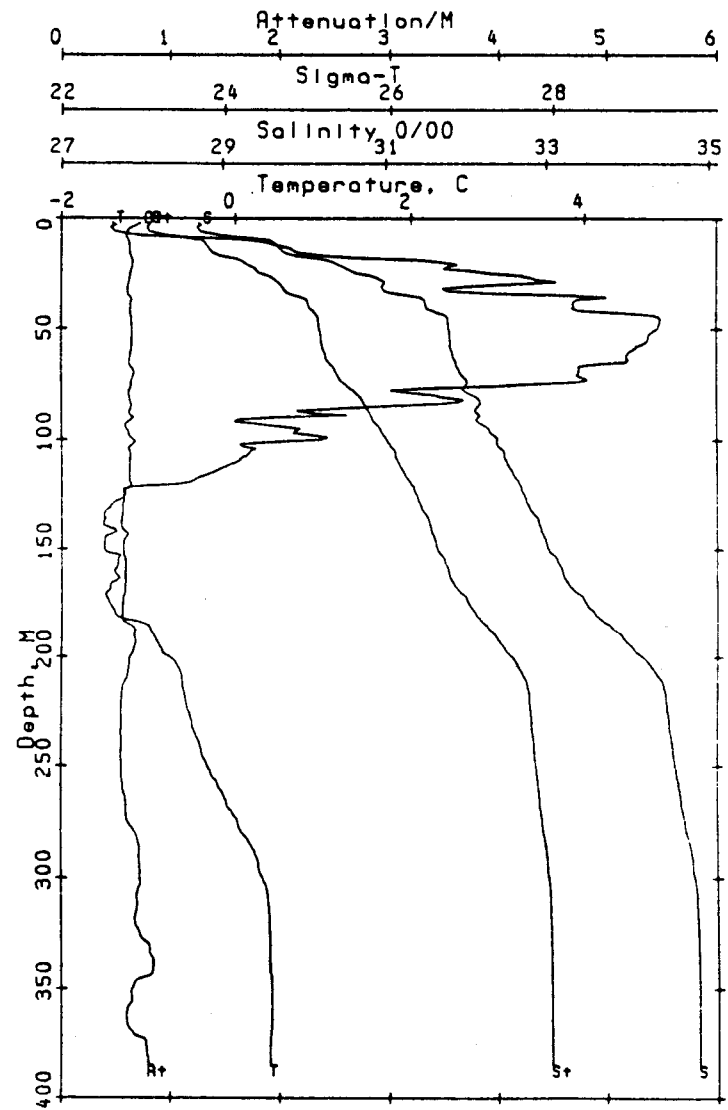
Ref. no. 2 Sta. w02 72.30 N  
 Time = 862761159 Beaufort 154.97 W

STATION W03		CAST 03	DATE 03 OCT 86		TIME 1456	LATITUDE 72 12.80N		LONGITUDE 155 09.00W		BOTTOM DEPTH 1086 M			
PRESS db	TEMP °C	SAL	SIGMA-T	O <sub>2</sub> ml l <sup>-1</sup>	SiO <sub>4</sub> µm l <sup>-1</sup>	PO <sub>4</sub> µm l <sup>-1</sup>	NO <sub>3</sub> µm l <sup>-1</sup>	NO <sub>2</sub> µm l <sup>-1</sup>	NH <sub>3</sub> µm l <sup>-1</sup>	SPM mg l <sup>-1</sup>	PC µg l <sup>-1</sup>	LT.AT m <sup>-1</sup>	CHLR-A µg l <sup>-1</sup>
0.4	-1.376	28.719	23.071										0.58
4.1	-1.373	28.701	23.056	8.50	2.14	0.64	0.03	0.02	0.00	0.6645	161	0.58	1.3
9.5	-1.354	28.731	23.081	8.44	4.25	0.64	0.03	0.02	0.00		292	0.59	.8
27.9	4.165*	31.133	24.695	6.95	5.55	0.65	0.02	0.03	1.26		191	0.69	
48.2	4.639*	31.708	25.104	6.97	6.46	0.67	0.02	0.04	1.67		231	0.69	
99.2	1.132	32.285	25.855	7.44	13.09	1.11	3.28	0.08	1.86	0.6605	201	0.66	
148.4	-1.252	32.976	26.521	6.97	26.37	1.65	10.02	0.17	1.57			0.59	
198.6	-1.098	33.865	27.237	6.35	10.38	0.82	12.33	0.02	0.00			0.58	
298.8	0.123	34.720	27.873	6.41	10.23	0.87	12.34	0.02	0.00			0.53	
599.3	0.379	34.878	27.987	6.74	7.01	0.79	12.17	0.02	0.00	0.8085		0.54	
1072.2	-0.064	34.904	28.032	6.78	7.65	0.81	12.40	0.02	0.00	1.0355		0.59	

STATION W04		CAST 04	DATE 03 OCT 86		TIME 1822	LATITUDE 72 07.90N		LONGITUDE 155 18.00W		BOTTOM DEPTH 0397 M			
PRESS db	TEMP °C	SAL	SIGMA-T	O <sub>2</sub> ml l <sup>-1</sup>	SiO <sub>4</sub> µm l <sup>-1</sup>	PO <sub>4</sub> µm l <sup>-1</sup>	NO <sub>3</sub> µm l <sup>-1</sup>	NO <sub>2</sub> µm l <sup>-1</sup>	NH <sub>3</sub> µm l <sup>-1</sup>	SPM mg l <sup>-1</sup>	PC µg l <sup>-1</sup>	LT.AT m <sup>-1</sup>	CHLR-A µg l <sup>-1</sup>
4.6	-1.380	28.647	23.013	7.73	1.89	0.64	0.07	0.01	0.00			0.59	
19.4	1.055*	30.136*	24.133	8.53	3.20	0.55	0.07	0.02	0.30			0.65	
49.6	4.775	31.791	25.156	6.72	3.57	0.56	0.00	0.03	0.46			0.64	
99.2	0.682*	32.278	25.875	7.57	6.21	0.61	0.00	0.03	1.68			0.61	
148.6	-1.508	33.017	26.561	6.67	30.79	1.80	12.43	0.08	0.40			0.55	
199.0	-0.814	34.139	27.449	6.10	25.58	1.33	13.40	0.13	0.00			0.61	
384.8	0.391	34.865	27.976	6.68	10.13	0.85	12.08	0.04	0.00			0.97	



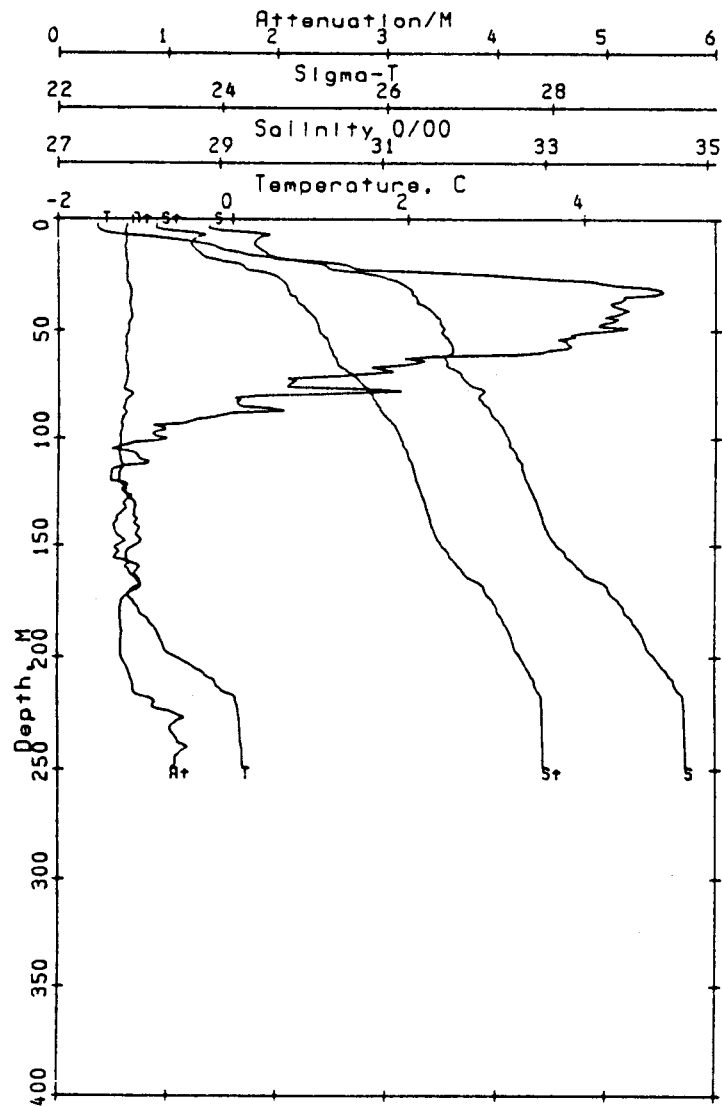
Ref. no. 3 Sta. w03 72.21 N  
 Time = 862761456 Beaufort 155.15 W



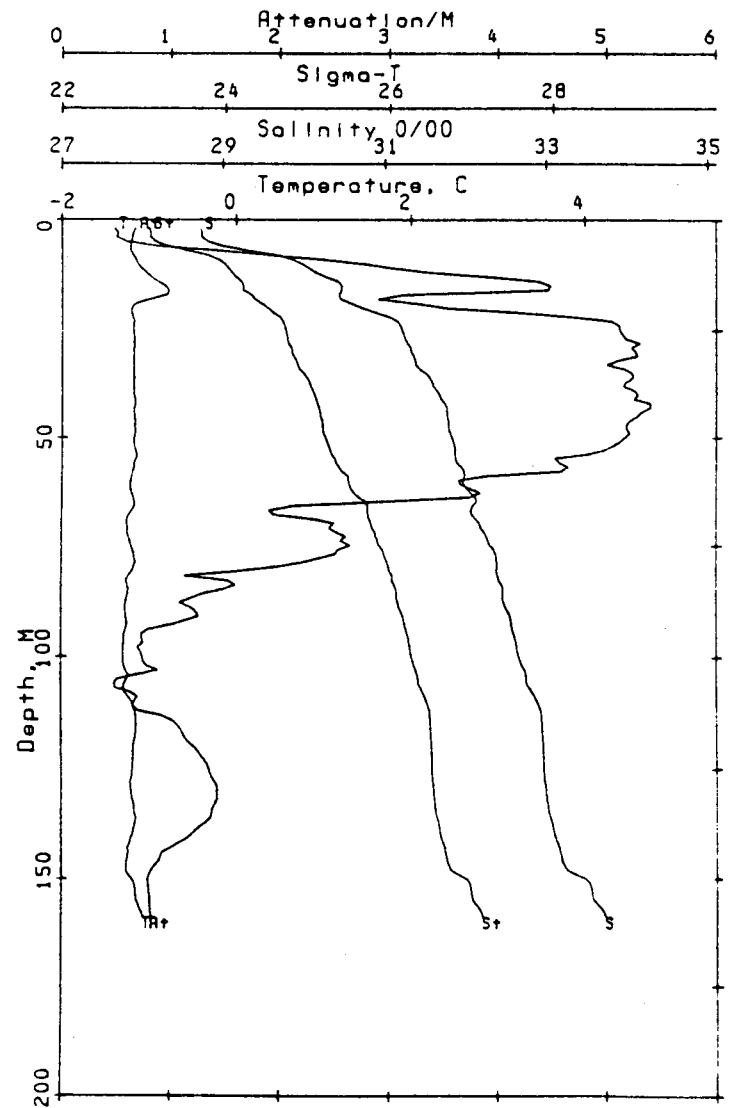
Ref. no. 4 Sta. w04 72.13 N  
 Time = 862761822 Beaufort 155.30 W

STATION W05		CAST 05	DATE 03-OCT 86	TIME 2015	LATITUDE 72 04.50N	LONGITUDE 155 29.00W	BOTTOM DEPTH 0263 M						
PRESS	TEMP	SAL	SIGMA-T	O <sub>2</sub>	SiO <sub>4</sub>	PO <sub>4</sub>	NO <sub>3</sub>	NO <sub>2</sub>	NH <sub>3</sub>	SPM	PC	LT.AT	CHLR-A
db	°C			ml l <sup>-1</sup>	µm l <sup>-1</sup>	µm l <sup>-1</sup>	µm l <sup>-1</sup>	µm l <sup>-1</sup>	µm l <sup>-1</sup>	mg l <sup>-1</sup>	µg l <sup>-1</sup>	m <sup>-1</sup>	µg l <sup>-1</sup>
19.2	0.991*	29.828*	23.889	8.26	2.40	0.52	0.24	0.03	0.00			0.63	
49.8	4.377*	31.756	25.170	7.17	5.05	0.65	0.50	0.04	1.22			0.63	
100.9	-1.166	32.558	26.180	7.23	22.04	1.51	9.78	0.08	0.31			0.56	
149.3	-1.286	33.112	26.633	6.78	29.04	1.79	12.30	0.15	0.92			0.70	
249.1	0.114	34.732	27.884	6.71	14.41	1.07	12.72	0.18	0.00			1.06	

STATION W06		CAST 06	DATE 03 OCT 86	TIME 2156	LATITUDE 72 00.00N	LONGITUDE 155 39.20W	BOTTOM DEPTH 0177 M						
PRESS	TEMP	SAL	SIGMA-T	O <sub>2</sub>	SiO <sub>4</sub>	PO <sub>4</sub>	NO <sub>3</sub>	NO <sub>2</sub>	NH <sub>3</sub>	SPM	PC	LT.AT	CHLR-A
db	°C			ml l <sup>-1</sup>	µm l <sup>-1</sup>	µm l <sup>-1</sup>	µm l <sup>-1</sup>	µm l <sup>-1</sup>	µm l <sup>-1</sup>	mg l <sup>-1</sup>	µg l <sup>-1</sup>	m <sup>-1</sup>	µg l <sup>-1</sup>
3.9	0.158*	29.477*	23.644	5.35	2.95	0.60	0.31	0.02	0.16	0.5150	220	0.63	
19.6	4.106*	31.125*	24.695	5.62	5.09	0.61	0.28	0.04	0.05			0.64	
49.5	4.469	31.845	25.230	5.50	5.05	0.60	0.29	0.07	0.00	0.9755	163	0.66	
98.6	-1.073	32.646	26.248	5.73	19.99	1.48	7.68	0.14	0.00	1.5770	78	0.56	
159.1	-1.061	33.746	27.139	6.33	28.02	1.71	13.25	0.18	0.20	1.9310	123	0.93	



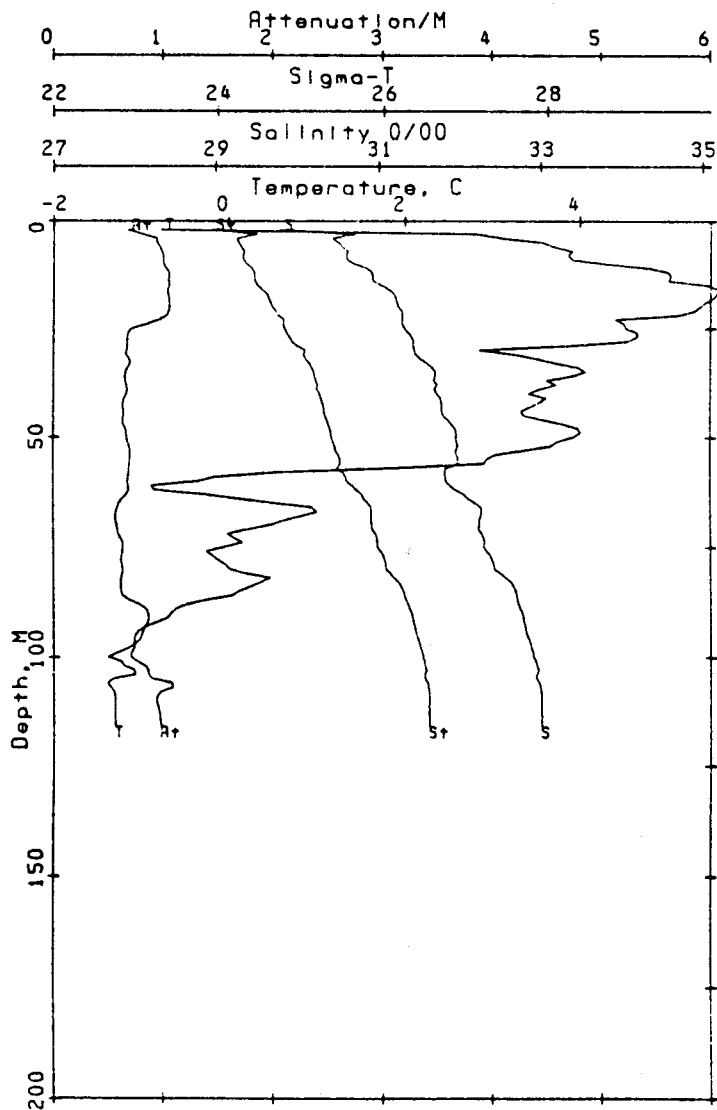
Ref. no. 5 Sta. w05 72.08 N  
 Time = 862762015 Beaufort 155.48 W



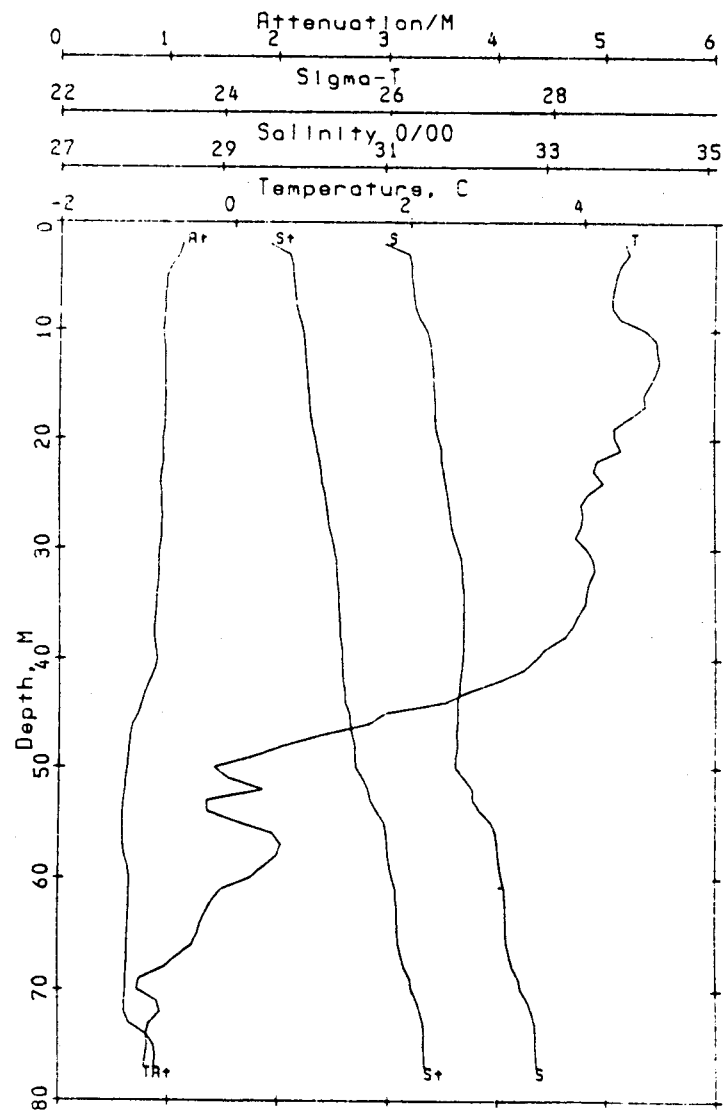
Ref. no. 6 Sta. w06 72.00 N  
 Time = 862762156 Beaufort 155.65 W

STATION W07		CAST 07	DATE 03 OCT 86	TIME 2321	LATITUDE 71 55.60N		LONGITUDE 155 49.70W		BOTTOM DEPTH 0121 M				
PRESS db	TEMP °C	SAL	SIGMA-T	O <sub>2</sub> ml l <sup>-1</sup>	SiO <sub>4</sub> µm l <sup>-1</sup>	PO <sub>4</sub> µm l <sup>-1</sup>	NO <sub>3</sub> µm l <sup>-1</sup>	NO <sub>2</sub> µm l <sup>-1</sup>	NH <sub>3</sub> µm l <sup>-1</sup>	SPM mg l <sup>-1</sup>	PC µg l <sup>-1</sup>	LT.AT m <sup>-1</sup>	CHLR-A µg l <sup>-1</sup>
3.5	2.314*	29.711*	23.716	6.50	8.11	0.92	0.44	0.07	0.30			0.85	
18.7	5.501	31.215	24.621	6.89	8.33	0.89	0.42	0.07	0.32			1.05	
48.5	3.952*	31.891	25.318	6.89	6.37	0.80	0.58	0.07	0.36			0.69	
111.2	-1.295	33.010	26.550	6.29	27.97	1.92	10.08	0.24	0.32			0.99	

STATION W08		CAST 08	DATE 04 OCT 86	TIME 0044	LATITUDE 71 50.80N		LONGITUDE 156 01.10W		BOTTOM DEPTH 0080 M				
PRESS db	TEMP °C	SAL	SIGMA-T	O <sub>2</sub> ml l <sup>-1</sup>	SiO <sub>4</sub> µm l <sup>-1</sup>	PO <sub>4</sub> µm l <sup>-1</sup>	NO <sub>3</sub> µm l <sup>-1</sup>	NO <sub>2</sub> µm l <sup>-1</sup>	NH <sub>3</sub> µm l <sup>-1</sup>	SPM mg l <sup>-1</sup>	PC µg l <sup>-1</sup>	LT.AT m <sup>-1</sup>	CHLR-A µg l <sup>-1</sup>
0.5	3.271	30.602	24.354	7.32	9.59	0.97	0.29	0.07	0.20		108	1.12	.4 .6
3.7	4.814	30.986*	24.514	7.19	10.71	1.02	0.38	0.08	0.27		86	1.02	.7 .4
8.8	4.369*	31.398	24.886	6.92	10.68	1.06	0.36	0.08	0.36		191	0.94	.3 .3
18.7	4.685	31.666	25.067	6.94	10.38	0.99	0.39	0.09	0.32		146	0.95	.0 .3
28.4	4.050	31.805	25.240	6.98	9.71	0.92	0.38	0.08	0.32	1.4270	492	0.91	.2
48.4	1.833	32.003	25.583	7.47	7.88	0.89	1.30	0.07	0.23	1.3590	98	0.63	.2
71.5	-0.862	32.545	26.159	7.23	21.18	1.66	7.85	0.17	0.27	0.8635	125	0.60	



Ref. no. 7 Sta. w07 71.93 N  
 Time = 862762322 Beaufort 155.83 W

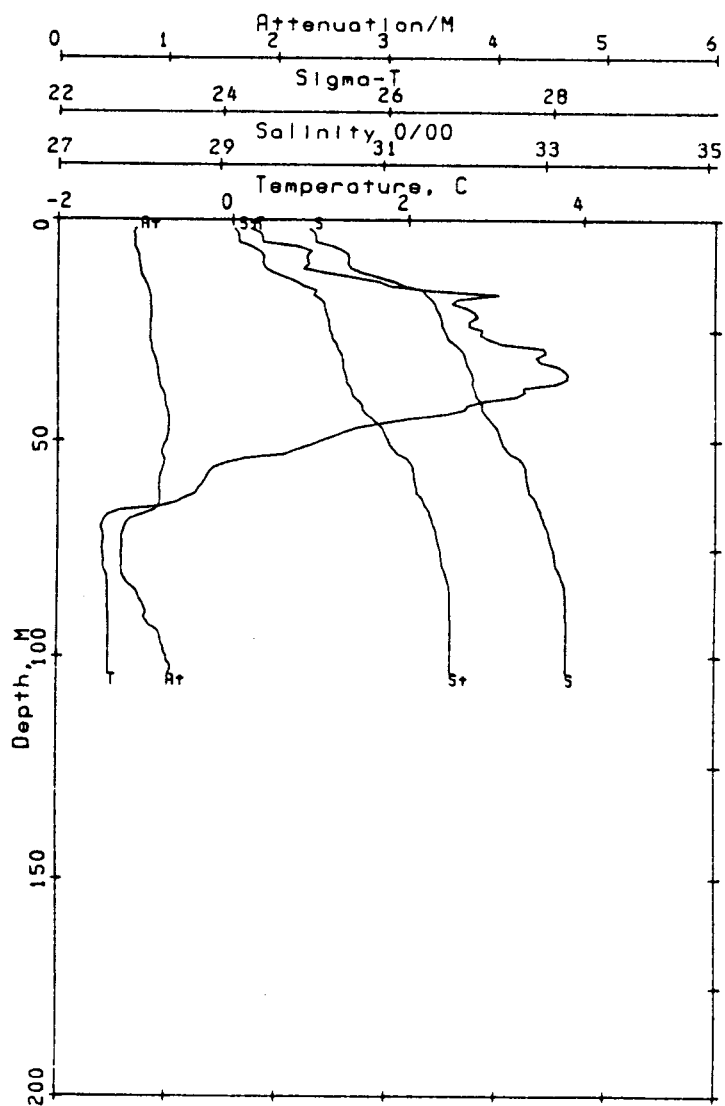


Ref. no. 8 Sta. w08 71.85 N  
 Time = 862770044 Beaufort 156.02 W

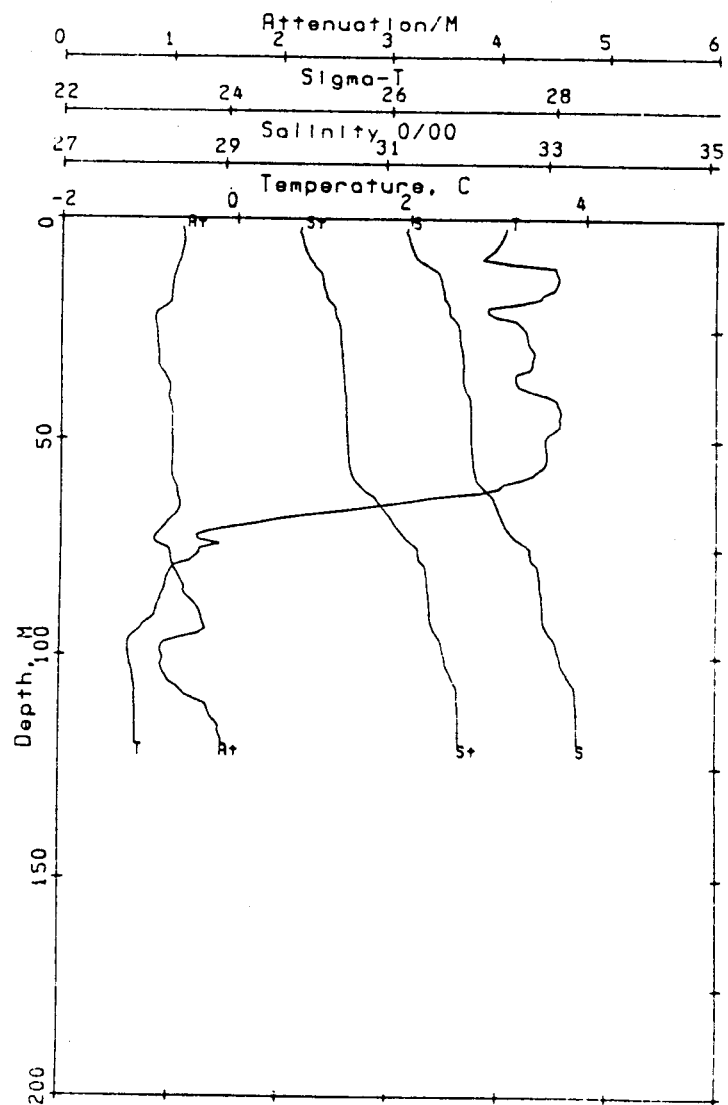
STATION W09		CAST 09	DATE 04 OCT 86		TIME 0211	LATITUDE 71 45.00N		LONGITUDE 155 56.30W		BOTTOM DEPTH 0106 M			
PRESS db	TEMP °C	SAL	SIGMA-T	O <sub>2</sub> ml l <sup>-1</sup>	SIO <sub>4</sub> µm l <sup>-1</sup>	PO <sub>4</sub> µm l <sup>-1</sup>	NO <sub>3</sub> µm l <sup>-1</sup>	NO <sub>2</sub> µm l <sup>-1</sup>	NH <sub>3</sub> µm l <sup>-1</sup>	SPM mg l <sup>-1</sup>	PC µg l <sup>-1</sup>	LT.AT m <sup>-1</sup>	CHLR-A µg l <sup>-1</sup>
3.7	0.705*	30.268*	24.257	8.09	2.57	0.53	0.00	0.03	0.02			0.72	
18.4	1.860*	31.430*	25.122	7.53	3.08	0.64	0.00	0.05	0.05			0.83	
48.7	1.400	32.414	25.941	7.50	9.49	1.16	2.30	0.11	0.00			0.99	
99.5	-1.413	33.270	26.764	6.75	29.33	1.88	12.11	0.11	0.05			0.94	

STATION W10		CAST 10	DATE 04 OCT 86		TIME 0310	LATITUDE 71 40.30N		LONGITUDE 155 52.80W		BOTTOM DEPTH 0123 M			
PRESS db	TEMP °C	SAL	SIGMA-T	O <sub>2</sub> ml l <sup>-1</sup>	SIO <sub>4</sub> µm l <sup>-1</sup>	PO <sub>4</sub> µm l <sup>-1</sup>	NO <sub>3</sub> µm l <sup>-1</sup>	NO <sub>2</sub> µm l <sup>-1</sup>	NH <sub>3</sub> µm l <sup>-1</sup>	SPM mg l <sup>-1</sup>	PC µg l <sup>-1</sup>	LT.AT m <sup>-1</sup>	CHLR-A µg l <sup>-1</sup>
0.7	0.998	30.563	24.479	7.49	6.81	0.90	0.06	0.08	0.00		284	0.76	.6
					7.33	0.91	0.05	0.08	0.00				.8
4.2	2.972	31.452	25.056									1.04	
19.0	2.844	31.772	25.322	7.32	3.50	0.64	0.07	0.05	0.00		198	0.84	.5
29.4	3.398	31.968	25.431	7.19	3.37	0.60	0.06	0.05	0.00	1.3275	171	0.92	.5
49.5	3.517	32.071	25.502	7.14	5.56	0.79	0.21	0.06	0.00		94	0.98	.3
99.3	-1.218	33.133	26.647	6.73	26.94	1.98	10.87	0.25	0.05	0.9170	147	0.89	.6
113.0	-1.136	33.386	26.850	6.55	28.35	1.92	11.48	0.21	0.07	2.0145	114	1.42	.3

335



Ref. no. 9 Sta. w09 71.75 N  
 Time = 86277021! Beaufort 155.94 W

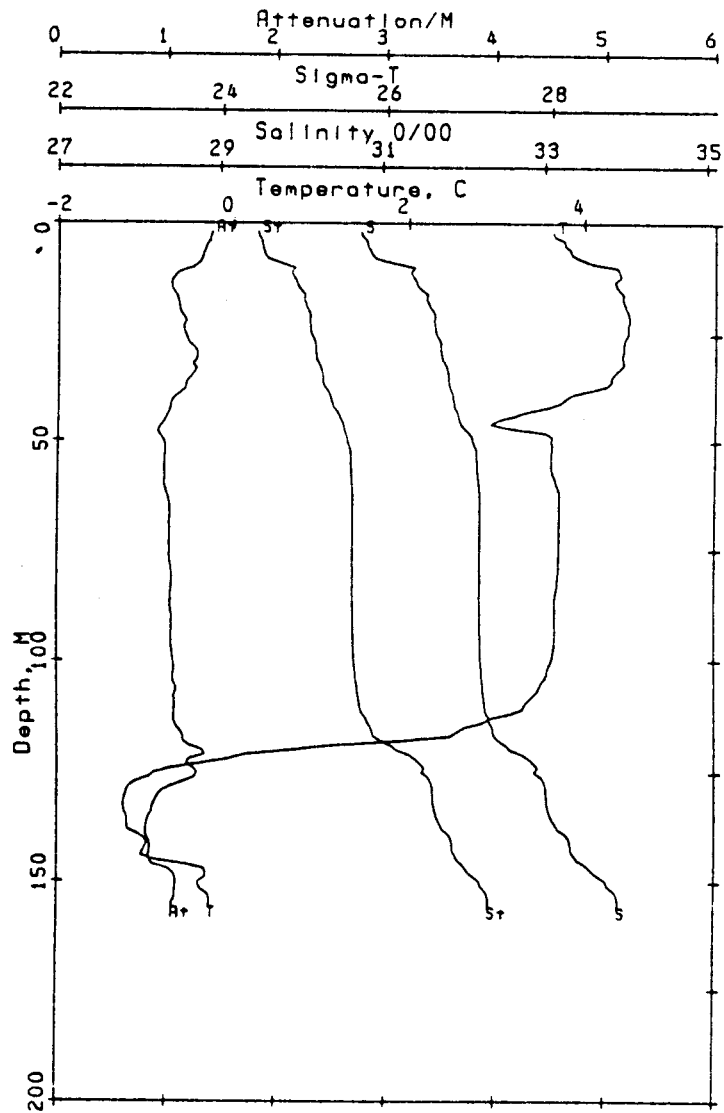


Ref. no. 10 Sta. w10 71.67 N  
 Time = 862770310 Beaufort 155.88 W

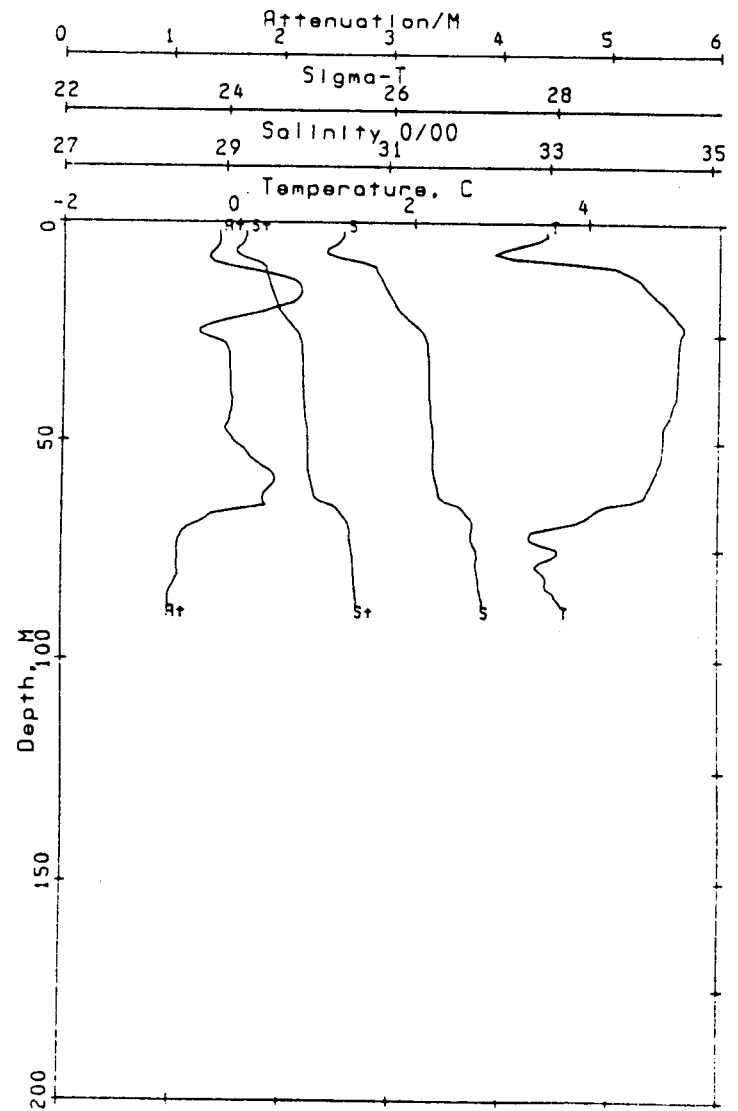
STATION W11		CAST 11	DATE 04 OCT 86	TIME 0444	LATITUDE 71 31.50N		LONGITUDE 155 47.60W		BOTTOM DEPTH 0172 M				
PRESS db	TEMP °C	SAL	SIGMA-T	O <sub>2</sub> ml l <sup>-1</sup>	SiO <sub>4</sub> µm l <sup>-1</sup>	PO <sub>4</sub> µm l <sup>-1</sup>	NO <sub>3</sub> µm l <sup>-1</sup>	NO <sub>2</sub> µm l <sup>-1</sup>	NH <sub>3</sub> µm l <sup>-1</sup>	SPM mg l <sup>-1</sup>	PC µg l <sup>-1</sup>	LT.AT m <sup>-1</sup>	CHLR-A µg l <sup>-1</sup>
19.4	4.523	31.627	25.053	7.24	9.67	1.04	0.10	0.09	0.07			1.08	
49.3	3.630*	32.102	25.516	7.10	7.63	0.83	0.11	0.07	0.14			0.95	
79.6	3.714	32.206	25.592	7.15	10.19	0.87	0.15	0.09	0.00			0.99	
155.7	-0.258	33.922	27.248	6.71	10.20	0.94	0.14	0.09	0.00			1.02	

STATION W12		CAST 12	DATE 04 OCT 86	TIME 0552	LATITUDE 71 32.10N		LONGITUDE 155 45.70W		BOTTOM DEPTH 0101 M				
PRESS db	TEMP °C	SAL	SIGMA-T	O <sub>2</sub> ml l <sup>-1</sup>	SiO <sub>4</sub> µm l <sup>-1</sup>	PO <sub>4</sub> µm l <sup>-1</sup>	NO <sub>3</sub> µm l <sup>-1</sup>	NO <sub>2</sub> µm l <sup>-1</sup>	NH <sub>3</sub> µm l <sup>-1</sup>	SPM mg l <sup>-1</sup>	PC µg l <sup>-1</sup>	LT.AT m <sup>-1</sup>	CHLR-A µg l <sup>-1</sup>
1.1	3.041	30.261	24.101	7.41	10.59	0.86	0.00	0.08	0.14		124	1.33	1.0 .8
4.4	2.887	30.211	24.073	7.42	10.34	0.86	0.00	0.09	0.14	1.9865	156	1.34	1.1 .8
9.5	4.100*	30.665*	24.330	7.28	11.63	0.94	0.05	0.09	0.14		499	1.43	.6 .9
19.5	4.854	31.072	24.578	7.09	12.02	1.00	0.22	0.09	0.23	2.5365	142	1.93	.8 .6
29.6	5.036	31.472	24.876	6.89	12.02	0.96	0.38	0.10	0.18	1.9370	140	1.46	.6 .6
87.5	3.713	32.178	25.569	7.17	7.93	0.76	0.28	0.07	0.23	1.6860	118	0.98	.4 .8

337



Ref. no. 11 Sta. w11 71.52 N  
 Time = 862770444 Beaufort 155.79 W

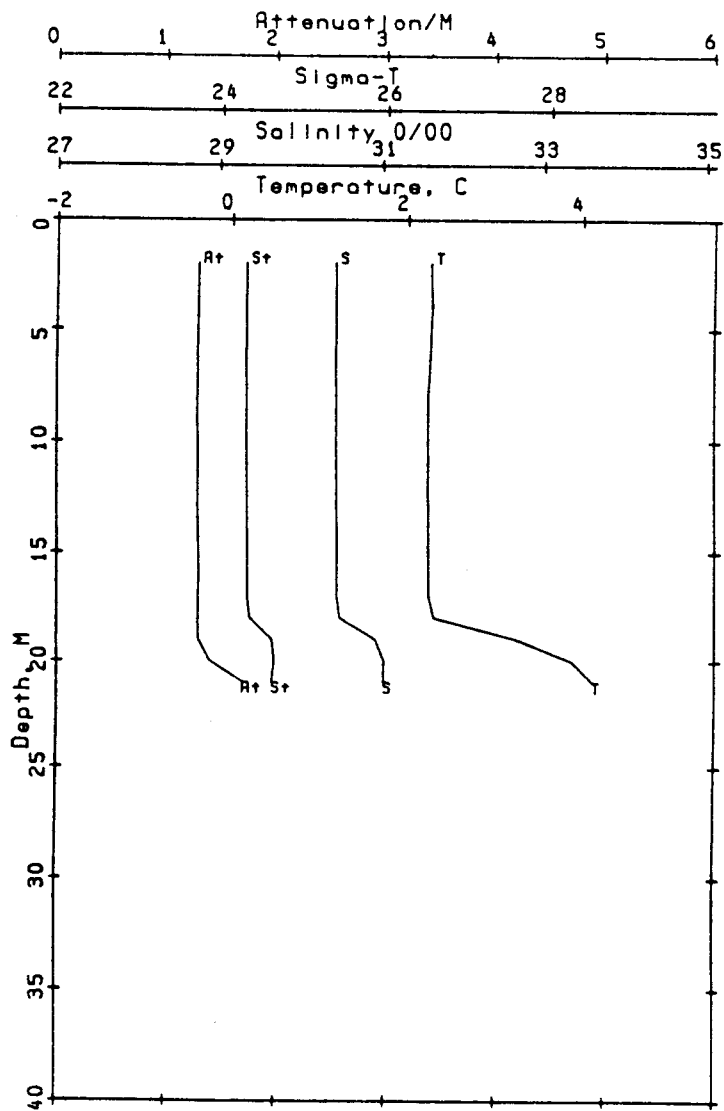


Ref. no. 12 Sta. w12 71.54 N  
 Time = 862770552 Beaufort 155.76 W

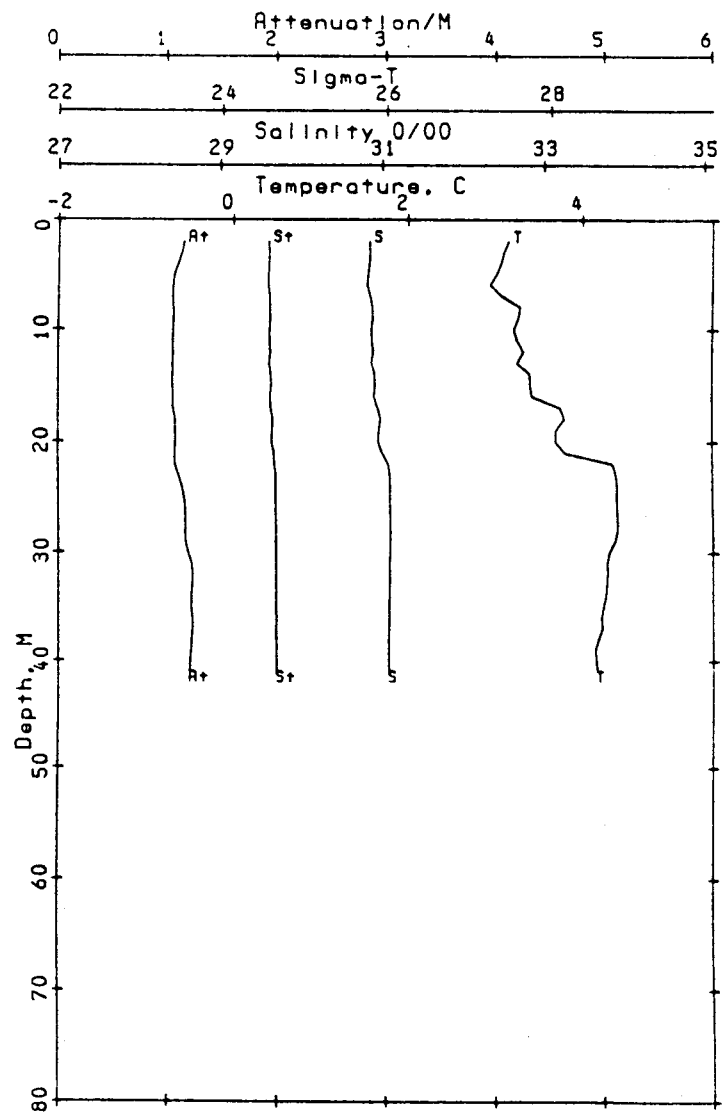
STATION A02		CAST 13	DATE 05 OCT 86		TIME 0702	LATITUDE 71 13.30N		LONGITUDE 153 40.00W		BOTTOM DEPTH 0027 M			
PRESS db	TEMP °C	SAL	SIGMA-T	O <sub>2</sub> ml l <sup>-1</sup>	SiO <sub>4</sub> µm l <sup>-1</sup>	PO <sub>4</sub> µm l <sup>-1</sup>	NO <sub>3</sub> µm l <sup>-1</sup>	NO <sub>2</sub> µm l <sup>-1</sup>	NH <sub>3</sub> µm l <sup>-1</sup>	SPM mg l <sup>-1</sup>	PC µg l <sup>-1</sup>	LT.AT m <sup>-1</sup>	CHLR-A µg l <sup>-1</sup>
3.8	2.256	30.460	24.318	7.52	6.74	1.02	0.14	0.03	0.63	1.9815		1.27	
7.3	2.245	30.460	24.319							1.9760		1.29	
10.2	2.263	30.461	24.319							2.0915		1.29	
21.3	4.115*	31.018*	24.609	7.21	8.12	0.99	0.22	0.03	1.26	2.6560		1.77	

STATION A03		CAST 14	DATE 05 OCT 86		TIME 0816	LATITUDE 71 19.40N		LONGITUDE 153 33.90W		BOTTOM DEPTH 0047 M			
PRESS db	TEMP °C	SAL	SIGMA-T	O <sub>2</sub> ml l <sup>-1</sup>	SiO <sub>4</sub> µm l <sup>-1</sup>	PO <sub>4</sub> µm l <sup>-1</sup>	NO <sub>3</sub> µm l <sup>-1</sup>	NO <sub>2</sub> µm l <sup>-1</sup>	NH <sub>3</sub> µm l <sup>-1</sup>	SPM mg l <sup>-1</sup>	PC µg l <sup>-1</sup>	LT.AT m <sup>-1</sup>	CHLR-A µg l <sup>-1</sup>
1.1	2.872	30.812	24.554	7.25	6.80	0.85	0.14	0.03	1.16	1.2855	380	0.98	.9 .8
4.5	2.806	30.788	24.539	7.34	6.91	0.94	0.15	0.03	1.29		239	0.98	1.0 .7
9.5	3.137*	30.893	24.597	7.31	7.59	1.00	0.16	0.03	1.34		178	0.99	.9 .6
19.1	4.373*	31.098	24.647	6.88	8.97	0.94	0.16	0.02	1.80	1.7060	228	1.05	.8 .8
29.1	4.314	31.108	24.661	6.98	8.80	0.94	0.21	0.02	1.99	2.1395	369	1.18	.8 .5
40.3	4.152	31.088	24.661	7.02	8.91	0.95	0.22	0.02	1.97	1.7915	255	1.21	.7 .6

339



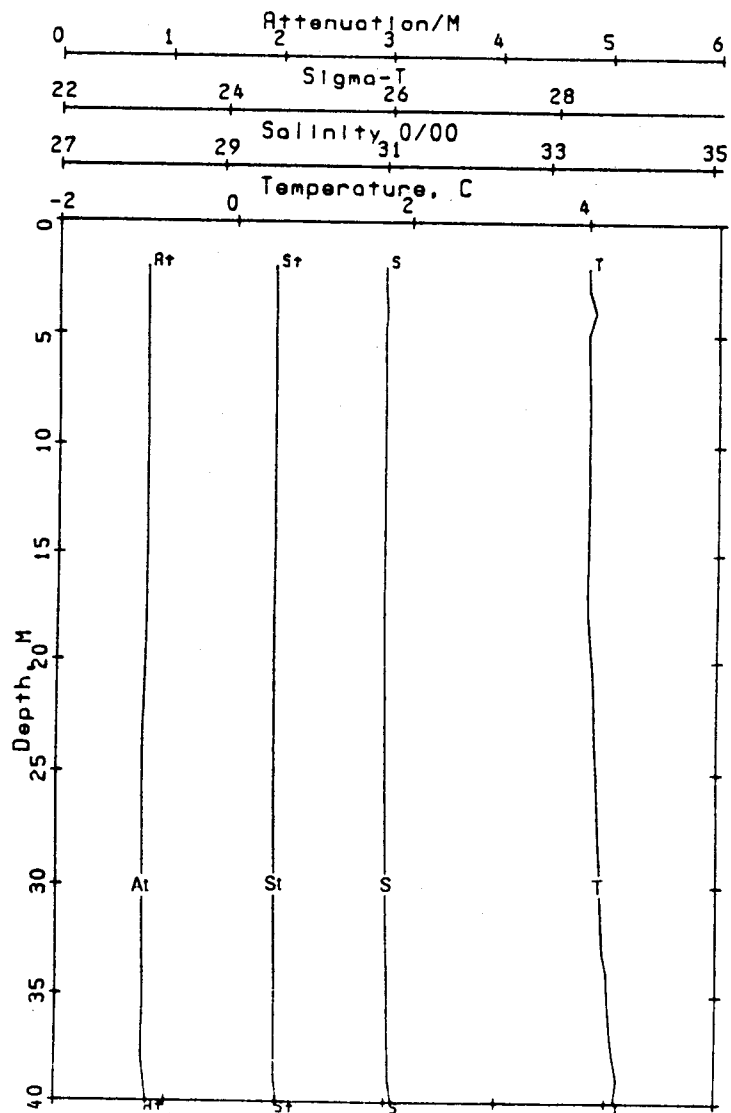
Ref. no. 13      Sta. 002      71.22 N  
 Time = 862780702      Beaufort      153.67 W



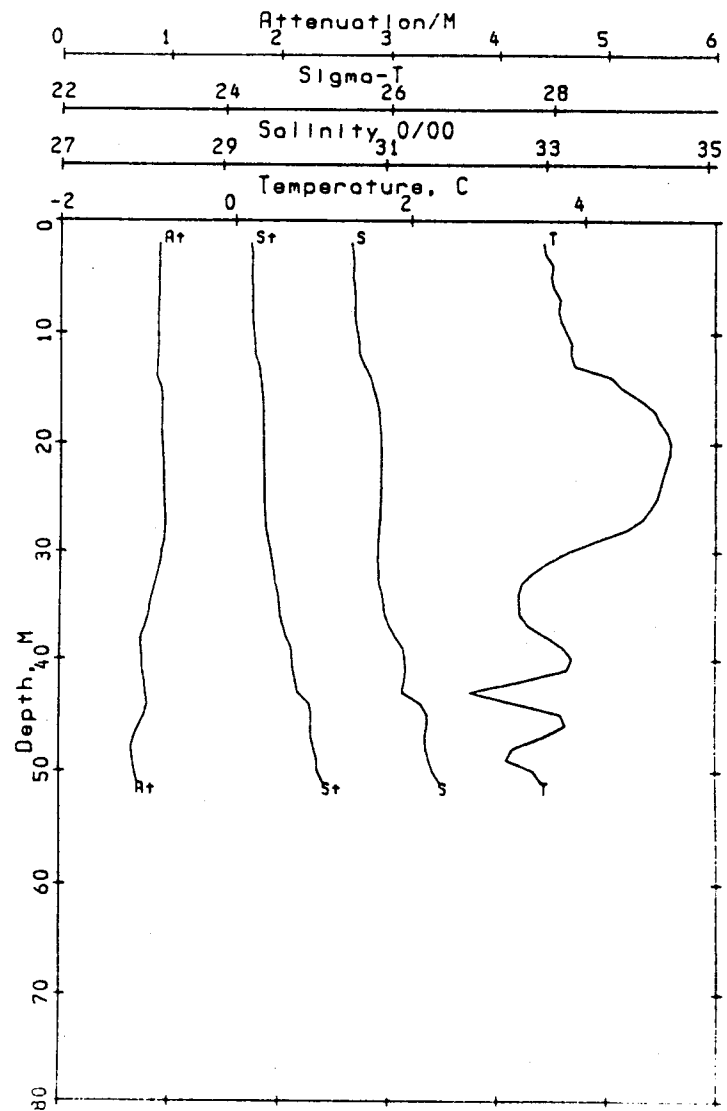
Ref. no. 14      Sta. 003      71.32 N  
 Time = 862780816      Beaufort      153.56 W

STATION A04		CAST 15	DATE 05 OCT 86		TIME 0926	LATITUDE 71 24.40N		LONGITUDE 153 25.90W		BOTTOM DEPTH 0046 M			
PRESS db	TEMP °C	SAL	SIGMA-T	O <sub>2</sub> ml l <sup>-1</sup>	SiO <sub>4</sub> µm l <sup>-1</sup>	PO <sub>4</sub> µm l <sup>-1</sup>	NO <sub>3</sub> µm l <sup>-1</sup>	NO <sub>2</sub> µm l <sup>-1</sup>	NH <sub>3</sub> µm l <sup>-1</sup>	SPM mg l <sup>-1</sup>	PC µg l <sup>-1</sup>	LT.AT m <sup>-1</sup>	CHLR-A µg l <sup>-1</sup>
4.6	4.005	30.996	24.602	7.06	8.57	1.02	0.11	0.01	1.94			0.79	
19.3	4.010	30.997	24.602	7.08	8.40	0.89	0.11	0.01	1.96			0.80	
40.4	4.407	31.098	24.644	7.01	8.38	0.93	0.12	0.00	2.05			0.84	

STATION A05		CAST 16	DATE 05 OCT 86		TIME 1027	LATITUDE 71 29.80N		LONGITUDE 153 18.10W		BOTTOM DEPTH 0062 M			
PRESS db	TEMP °C	SAL	SIGMA-T	O <sub>2</sub> ml l <sup>-1</sup>	SiO <sub>4</sub> µm l <sup>-1</sup>	PO <sub>4</sub> µm l <sup>-1</sup>	NO <sub>3</sub> µm l <sup>-1</sup>	NO <sub>2</sub> µm l <sup>-1</sup>	NH <sub>3</sub> µm l <sup>-1</sup>	SPM mg l <sup>-1</sup>	PC µg l <sup>-1</sup>	LT.AT m <sup>-1</sup>	CHLR-A µg l <sup>-1</sup>
1.0	3.564	30.598	24.326	7.28	9.31	1.10	0.16	0.01	1.62		185	0.88	.7 .6
4.5	3.603	30.598	24.322	6.64	9.14	1.05	0.20	0.02	1.71	1.0460	154	0.89	.5 .4
8.5	3.539	30.605	24.333	7.26	8.83	1.02	0.20	0.02	1.69		144	0.90	.6 .6
19.1	3.924	30.712	24.384	7.13	9.64	1.14	0.20	0.03	1.93	1.0410	118	0.88	.5 .3
28.5	4.337	31.101	24.654	7.10	8.77	1.18	0.16	0.03	2.01	1.1185	168	0.96	.1 .3
50.5	3.507*	31.688	25.198	7.15	5.64	0.93	0.30	0.01	1.79	1.0745	806	0.66	1.1 1.2



Ref. no. 15 Sta. 04 71.41 N  
 Time = 862780926 Beaufort 153.43 W



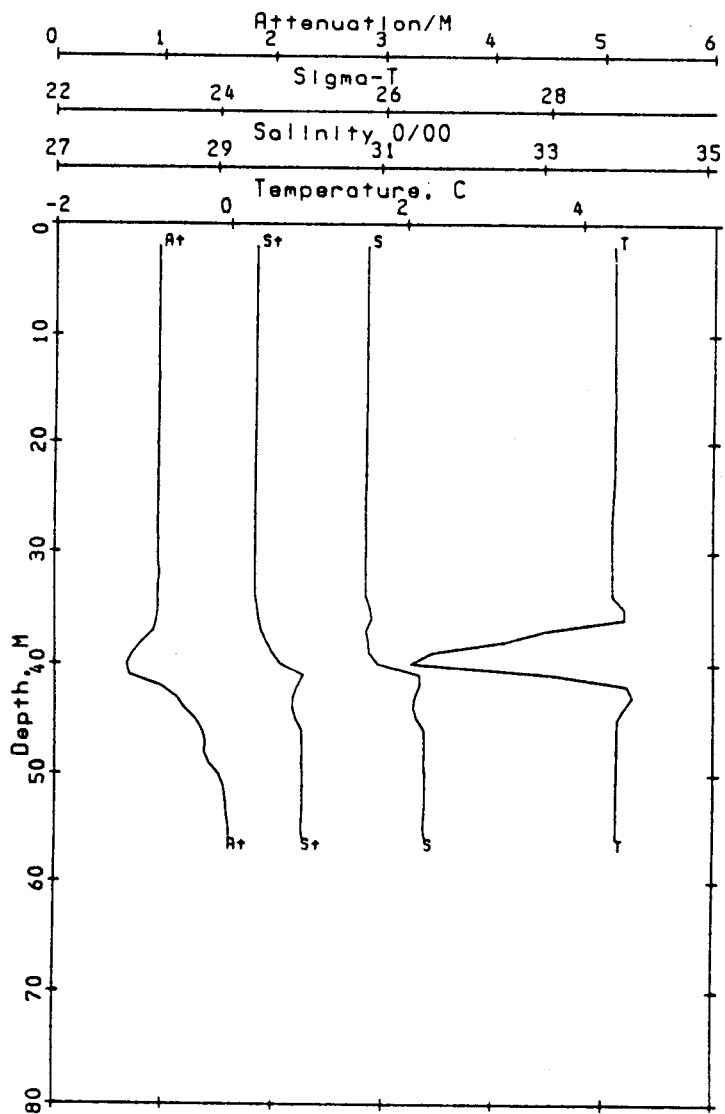
Ref. no. 16 Sta. 05 71.50 N  
 Time = 862781027 Beaufort 153.30 W

STATION A06		CAST 17	DATE 05 OCT 86		TIME 1130	LATITUDE 71 35.50N		LONGITUDE 153 10.10W		BOTTOM DEPTH 0057 M			
PRESS db	TEMP °C	SAL	SIGMA-T	O <sub>2</sub> ml l <sup>-1</sup>	SiO <sub>4</sub> µm l <sup>-1</sup>	PO <sub>4</sub> µm l <sup>-1</sup>	NO <sub>3</sub> µm l <sup>-1</sup>	NO <sub>2</sub> µm l <sup>-1</sup>	NH <sub>3</sub> µm l <sup>-1</sup>	SPM mg l <sup>-1</sup>	PC µg l <sup>-1</sup>	LT.AT m <sup>-1</sup>	CHLR-A µg l <sup>-1</sup>
50.2	4.387	31.568	25.019	6.70	11.87	1.26	0.70	0.04	2.91			1.59	

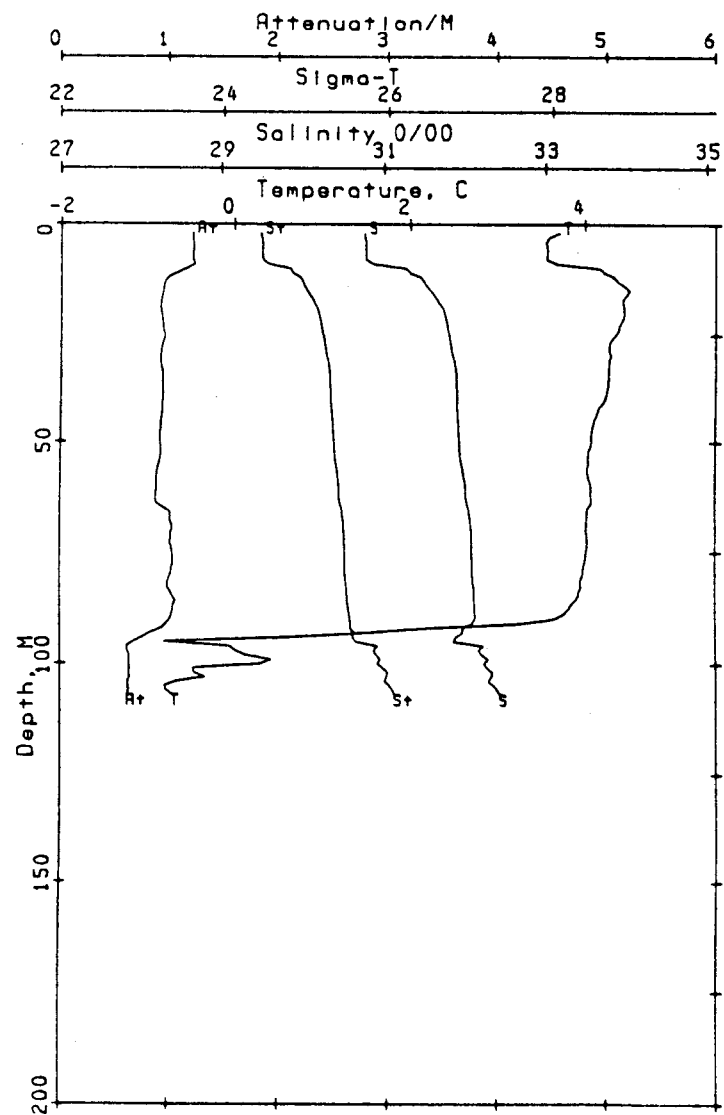
  

STATION A07		CAST 18	DATE 05 OCT 86		TIME 1306	LATITUDE 71 44.80N		LONGITUDE 152 46.80W		BOTTOM DEPTH 0108 M			
PRESS db	TEMP °C	SAL	SIGMA-T	O <sub>2</sub> ml l <sup>-1</sup>	SiO <sub>4</sub> µm l <sup>-1</sup>	PO <sub>4</sub> µm l <sup>-1</sup>	NO <sub>3</sub> µm l <sup>-1</sup>	NO <sub>2</sub> µm l <sup>-1</sup>	NH <sub>3</sub> µm l <sup>-1</sup>	SPM mg l <sup>-1</sup>	PC µg l <sup>-1</sup>	LT.AT m <sup>-1</sup>	CHLR-A µg l <sup>-1</sup>
0.9	3.451	30.763	24.467	7.18	11.49	1.27	0.23	0.01	1.97		145	1.21	2.2
4.4	3.526	30.772	24.468	7.17	11.83	1.42	0.23	0.01	2.26	1.6130	78	1.21	1.3
9.3	3.486*	30.772*	24.471	7.18	11.90	1.56	0.32	0.01	2.20		198	1.22	2.0
18.5	4.481	31.717	25.128	6.83	13.52	1.56	0.49	0.04	2.86		298	0.90	2.1
28.3	4.313	31.829	25.234	6.84	13.58	1.49	0.57	0.04	3.09	1.0565	205	0.90	1.2
49.4	4.076	31.926	25.335	6.94	12.52	1.46	0.49	0.04	2.88		243	0.89	1.5
80.2	3.961	32.101	25.484							1.6025	175	0.96	1.6
102.2	-0.540*	32.205	25.873	7.48	18.37	1.90	6.91	0.04	0.82	1.1403	131	0.61	1.4

343



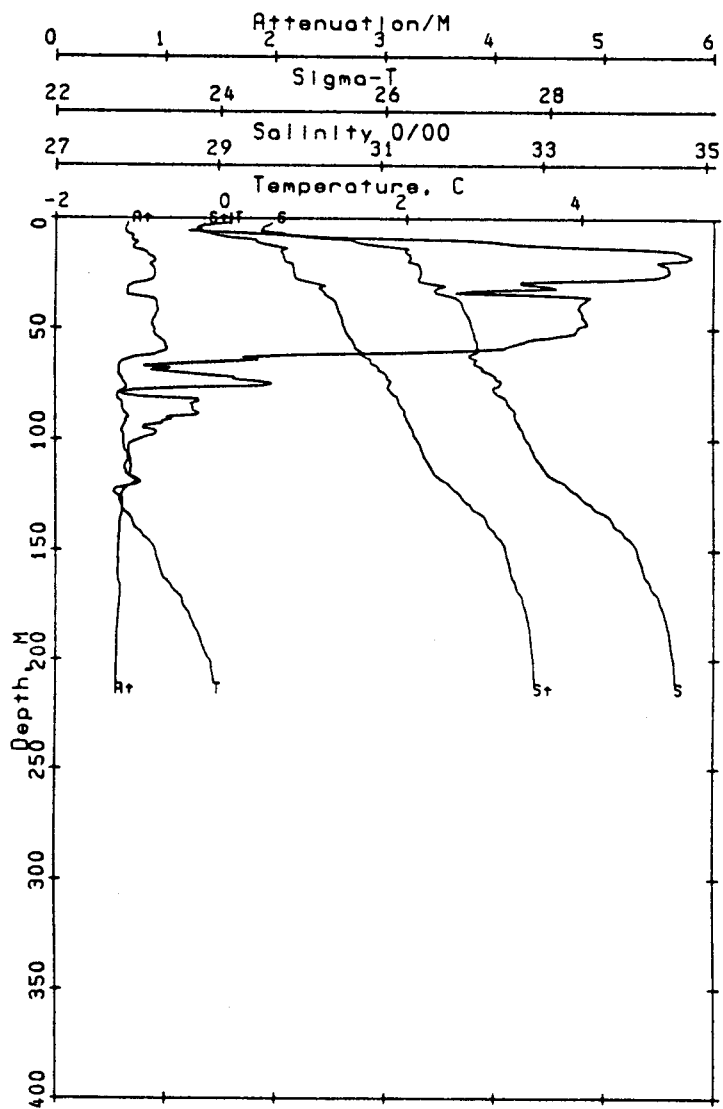
Ref. no. 17 Sta. a06 71.59 N  
 Time = 862781131 Beaufort 153.17 W



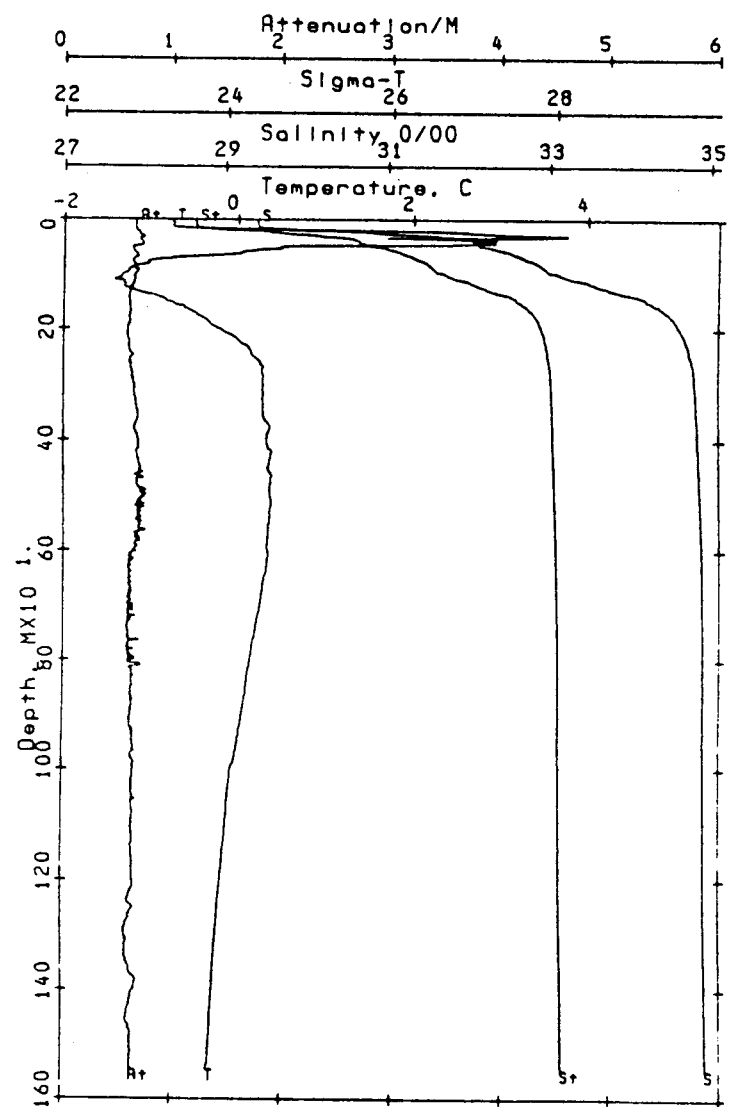
Ref. no. 18 Sta. a07 71.75 N  
 Time = 862781307 Beaufort 152.78 W

STATION A08		CAST 19	DATE 05 OCT 86	TIME 1447	LATITUDE 71 46.50N	LONGITUDE 152 53.00W	BOTTOM DEPTH 0221 M						
PRESS db	TEMP °C	SAL	SIGMA-T	O <sub>2</sub> ml l <sup>-1</sup>	SIO <sub>4</sub> µm l <sup>-1</sup>	PO <sub>4</sub> µm l <sup>-1</sup>	NO <sub>3</sub> µm l <sup>-1</sup>	NO <sub>2</sub> µm l <sup>-1</sup>	NH <sub>3</sub> µm l <sup>-1</sup>	SPM mg l <sup>-1</sup>	PC µg l <sup>-1</sup>	LT.AT m <sup>-1</sup>	CHLR-A µg l <sup>-1</sup>
4.0	-0.449	29.488	23.673	7.98	10.74	1.32	0.32	0.05	2.32			0.86	
19.0	5.243*	31.355*	24.760	6.82	4.32	0.99	0.12	0.00	0.53			3.83	
49.1	3.663	32.161	25.561	6.95	10.31	1.22	0.89	0.05	2.36			0.98	
124.6	-1.374	33.359	26.835	6.56	32.51	2.02	14.18	0.06	0.40			0.59	
149.2	-0.907	34.100	27.421	6.22	27.22	1.88	14.93	0.04	0.00			0.56	
204.6	-0.228	34.599	27.795	6.31	13.61	1.41	13.50	0.00	0.02			0.55	

STATION A09a		CAST 20	DATE 05 OCT 86	TIME 1750	LATITUDE 71 52.50N	LONGITUDE 152 33.20W	BOTTOM DEPTH 1609 M						
PRESS db	TEMP °C	SAL	SIGMA-T	O <sub>2</sub> ml l <sup>-1</sup>	SIO <sub>4</sub> µm l <sup>-1</sup>	PO <sub>4</sub> µm l <sup>-1</sup>	NO <sub>3</sub> µm l <sup>-1</sup>	NO <sub>2</sub> µm l <sup>-1</sup>	NH <sub>3</sub> µm l <sup>-1</sup>	SPM mg l <sup>-1</sup>	PC µg l <sup>-1</sup>	LT.AT m <sup>-1</sup>	CHLR-A µg l <sup>-1</sup>
701.5	0.252	34.888	28.002	6.84	7.75	0.67	12.60	0.00	0.02			0.56	
1000.7	-0.063	34.903	28.031	6.86	7.87	0.67	12.81	0.00	0.02			0.62	
1545.2	-0.337	34.926	28.064	6.81	10.54	0.79	13.56	0.01	0.07	0.9395		0.65	



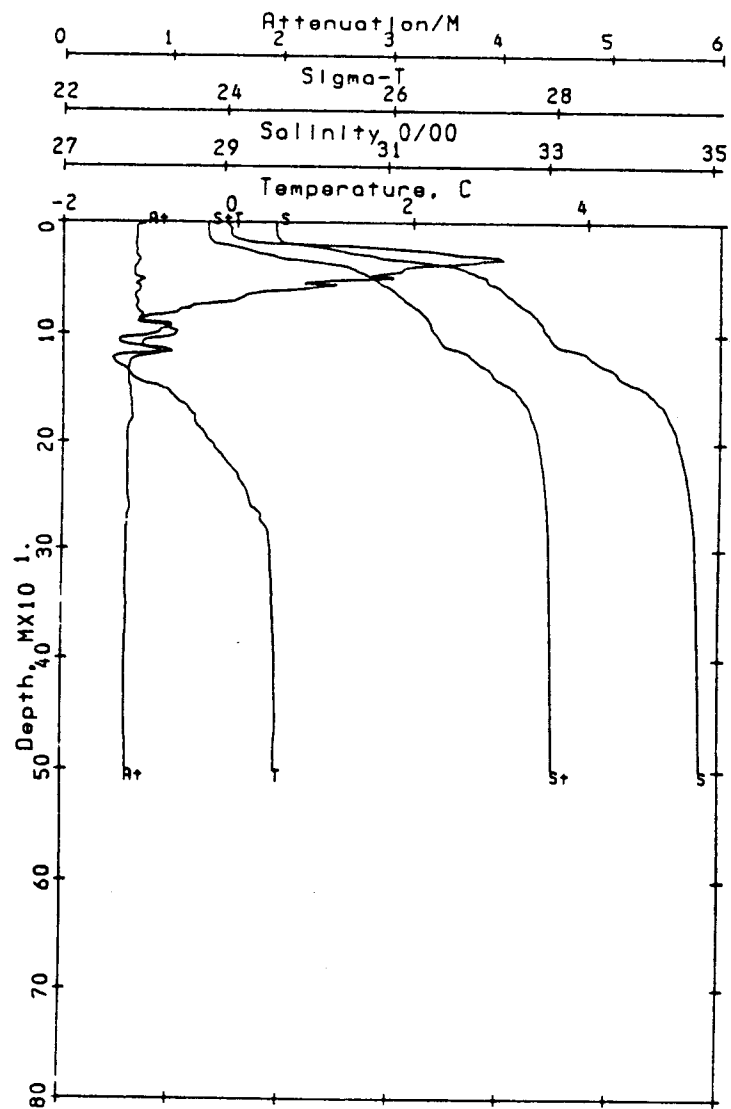
Ref. no. 19 Sta. 008 71.78 N  
 Time = 862781450 Beaufort 152.89 W



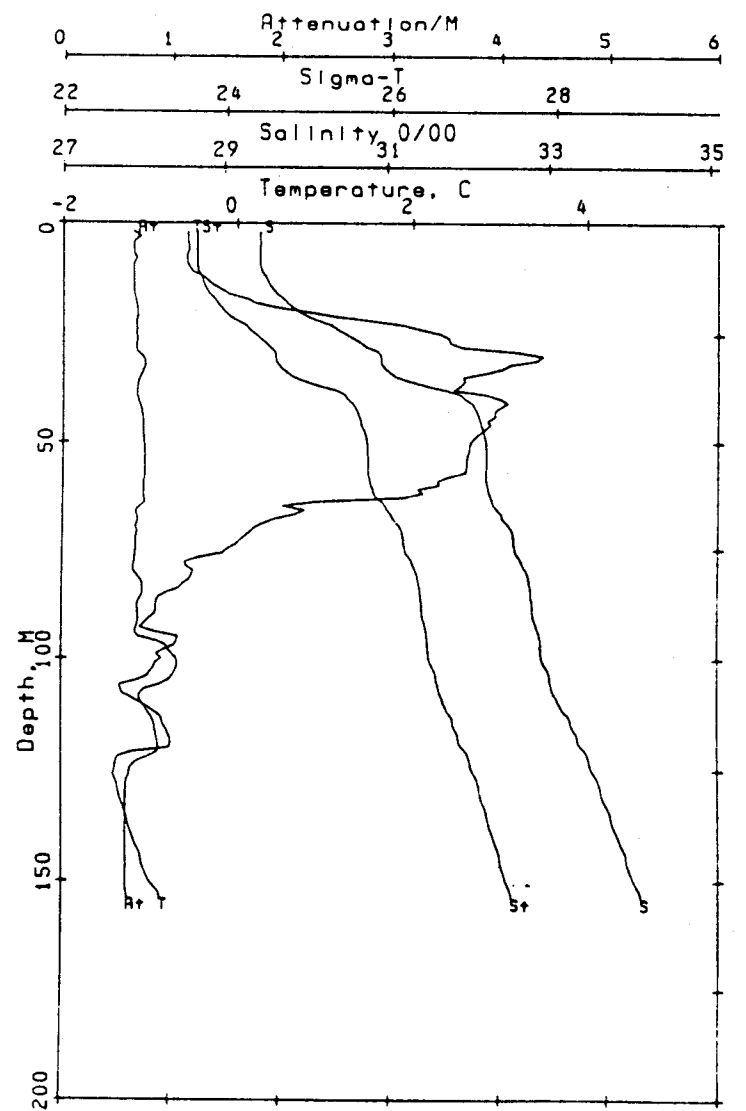
Ref. no. 20 Sta. 009 71.88 N  
 Time = 862781750 Beaufort 152.55 W

STATION A09b		CAST 21	DATE 05 OCT 86	TIME 2019	LATITUDE 71 52.40N	LONGITUDE 152 26.80W	BOTTOM DEPTH 1576 M						
PRESS db	TEMP °C	SAL	SIGMA-T	O <sub>2</sub> ml l <sup>-1</sup>	SiO <sub>4</sub> µm l <sup>-1</sup>	PO <sub>4</sub> µm l <sup>-1</sup>	NO <sub>3</sub> µm l <sup>-1</sup>	NO <sub>2</sub> µm l <sup>-1</sup>	NH <sub>3</sub> µm l <sup>-1</sup>	SPM mg l <sup>-1</sup>	PC µg l <sup>-1</sup>	LT.AT m <sup>-1</sup>	CHLR-A µg l <sup>-1</sup>
199.4	-0.287	34.589	27.789	6.26	12.95	0.76	12.93	0.02	-0.0			0.56	
299.8	0.361	34.800	27.925	6.71	9.02	0.70	12.47	0.01	-0.0	0.5970		0.58	
500.1	0.431	34.870	27.977	6.73	7.87	0.72	12.69	0.01	0.00			0.59	

STATION A09c		CAST 22	DATE 05 OCT 86	TIME 2145	LATITUDE 71 52.80N	LONGITUDE 152 25.10W	BOTTOM DEPTH 1608 M						
PRESS db	TEMP °C	SAL	SIGMA-T	O <sub>2</sub> ml l <sup>-1</sup>	SiO <sub>4</sub> µm l <sup>-1</sup>	PO <sub>4</sub> µm l <sup>-1</sup>	NO <sub>3</sub> µm l <sup>-1</sup>	NO <sub>2</sub> µm l <sup>-1</sup>	NH <sub>3</sub> µm l <sup>-1</sup>	SPM mg l <sup>-1</sup>	PC µg l <sup>-1</sup>	LT.AT m <sup>-1</sup>	CHLR-A µg l <sup>-1</sup>
3.8	-0.533	29.434	23.633	8.24	2.79	0.55	0.14	0.00	0.22	0.5880	159	0.64	
8.7	-0.480	29.382	23.588								233	0.65	
18.5	0.398*	29.812	23.904	7.82	2.79	0.60	0.12	0.00	0.48		256	0.68	
28.9	3.656*	30.885	24.546								503	0.78	1.0
49.2	2.735	32.217	25.686	7.02	7.87	0.85	1.29	0.05	2.26		172	0.75	1.8 1.6
109.4	-1.296	33.058	26.588	6.81	26.92	1.63	11.97	0.09	1.67	1.3183	106	0.71	
149.5	-1.004	34.055	27.387	6.42	26.54	1.40	14.56	0.03	0.08			0.59	



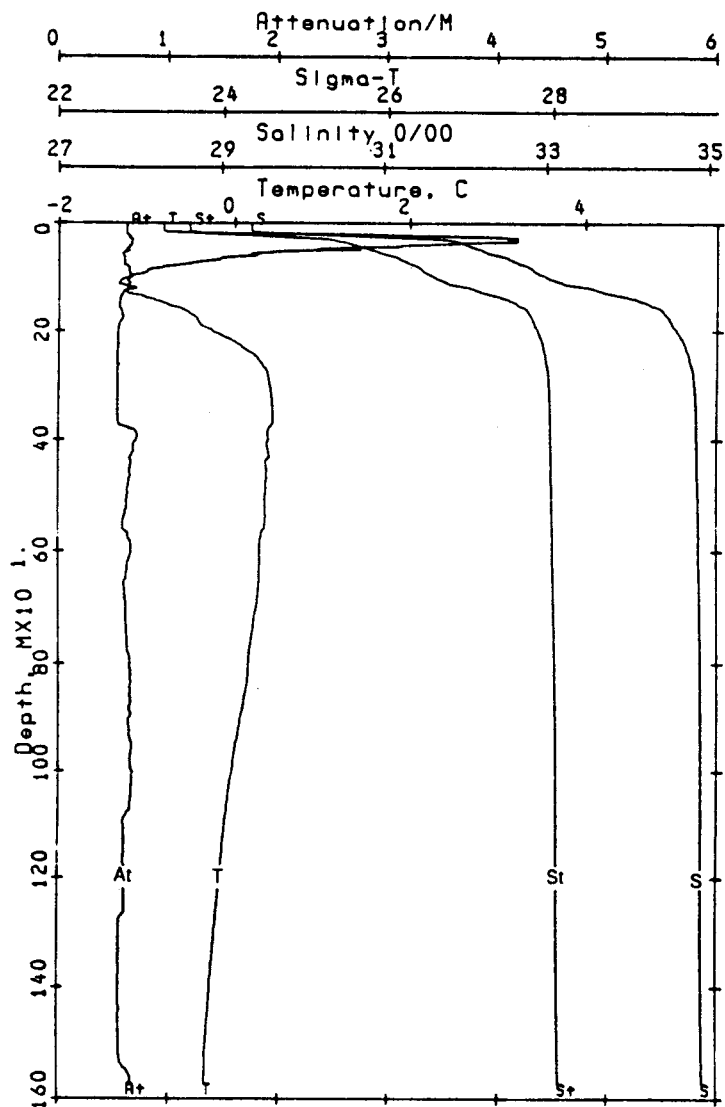
Ref. no. 21      Sta. a09      71.87 N  
 Time = 862782019      Beaufort      152.45 W



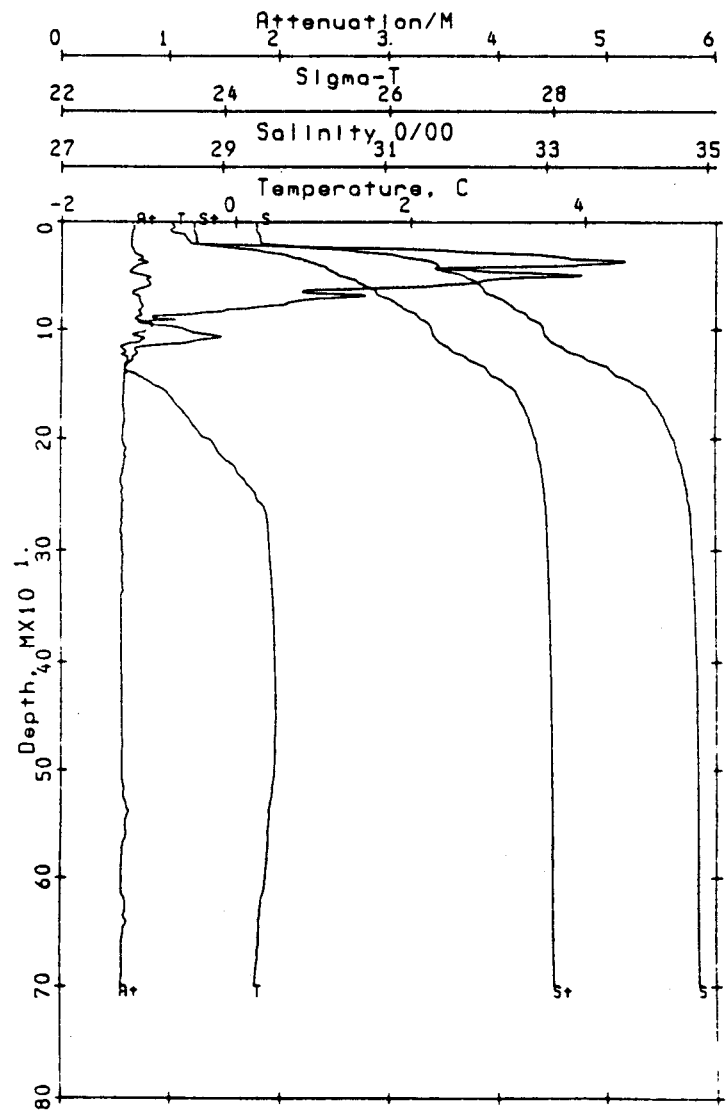
Ref. no. 22      Sta. a09      71.88 N  
 Time = 862782150      Beaufort      152.42 W

STATION A10a		CAST 24	DATE 05 OCT 86	TIME 2350	LATITUDE 71 58.00N	LONGITUDE 152 36.00W	BOTTOM DEPTH 2012 M						
PRESS db	TEMP °C	SAL	SIGMA-T	O <sub>2</sub> ml l <sup>-1</sup>	SIO <sub>4</sub> µm l <sup>-1</sup>	PO <sub>4</sub> µm l <sup>-1</sup>	NO <sub>3</sub> µm l <sup>-1</sup>	NO <sub>2</sub> µm l <sup>-1</sup>	NH <sub>3</sub> µm l <sup>-1</sup>	SPM mg l <sup>-1</sup>	PC µg l <sup>-1</sup>	LT.AT m <sup>-1</sup>	CHLR-A µg l <sup>-1</sup>
998.7	-0.024	34.900	28.027	6.88	6.54	0.67	13.01	0.00	0.00			0.67	
1249.2	-0.195	34.911	28.045	6.86	5.92	0.64	13.22	0.00	0.00			0.56	
1572.3	-0.335	34.925	28.063	6.82	6.95	0.64	13.81	0.02	0.20			0.67	

STATION A10b		CAST 25	DATE 06 OCT 86	TIME 0208	LATITUDE 71 59.60N	LONGITUDE 152 43.60W	BOTTOM DEPTH 2180 M						
PRESS db	TEMP °C	SAL	SIGMA-T	O <sub>2</sub> ml l <sup>-1</sup>	SIO <sub>4</sub> µm l <sup>-1</sup>	PO <sub>4</sub> µm l <sup>-1</sup>	NO <sub>3</sub> µm l <sup>-1</sup>	NO <sub>2</sub> µm l <sup>-1</sup>	NH <sub>3</sub> µm l <sup>-1</sup>	SPM mg l <sup>-1</sup>	PC µg l <sup>-1</sup>	LT.AT m <sup>-1</sup>	CHLR-A µg l <sup>-1</sup>
324.0	0.398	34.816	27.936	6.71	5.93	0.59	12.74	0.01	0.00			0.54	
501.0	0.431	34.873	27.979	6.77	5.58	0.63	12.82	0.00	0.00			0.54	
698.3	0.222	34.891	28.006	6.82	5.60	0.65	12.77	0.00	0.00			0.56	



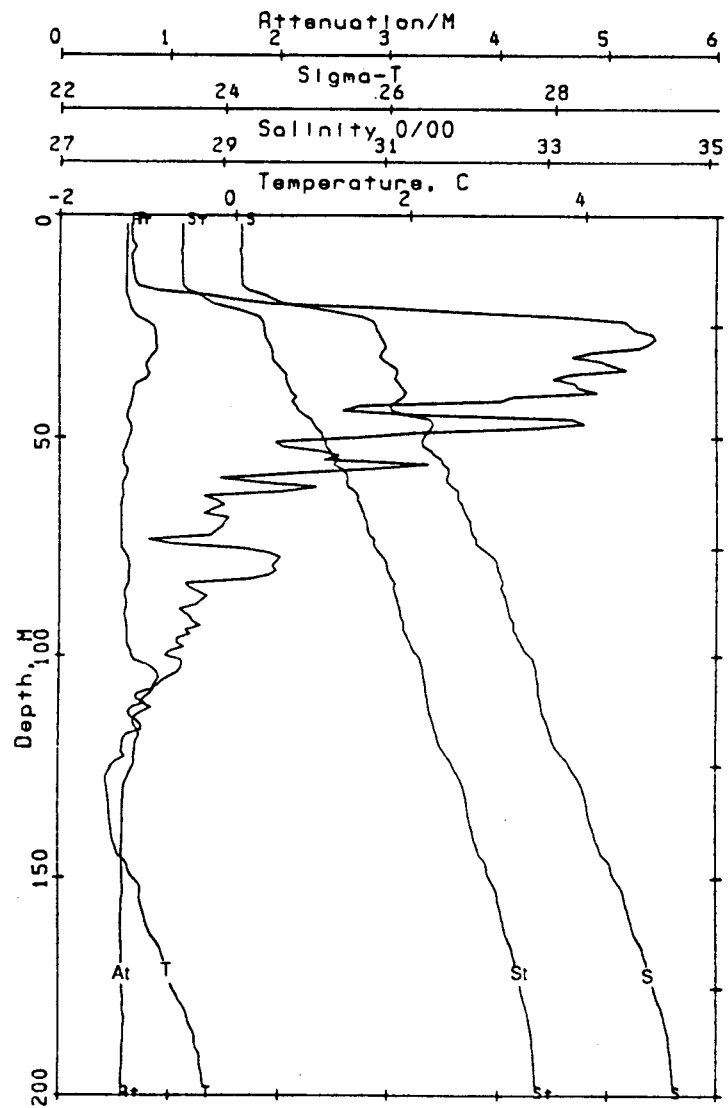
Ref. no. 24 Sta. a10 71.97 N  
 Time = 862782355 Beaufort 152.60 W



Ref. no. 25 Sta. a10 71.99 N  
 Time = 862790209 Beaufort 152.73 W

STATION A10c		CAST 26		DATE 06 OCT 86		TIME 0325		LATITUDE 72 02.70N		LONGITUDE 152 39.70W		BOTTOM DEPTH 2286 M	
PRESS	TEMP	SAL	SIGMA-T	O <sub>2</sub>	SiO <sub>4</sub>	PO <sub>4</sub>	NO <sub>3</sub>	NO <sub>2</sub>	NH <sub>3</sub>	SPM	PC	LT.AT	CHLR-A
db	°C			ml l <sup>-1</sup>	μm l <sup>-1</sup>	μm l <sup>-1</sup>	μm l <sup>-1</sup>	μm l <sup>-1</sup>	μm l <sup>-1</sup>	mg l <sup>-1</sup>	μg l <sup>-1</sup>	m <sup>-1</sup>	μg l <sup>-1</sup>
3.4	-1.260	29.228	23.482	8.30	2.50	0.61	0.00	0.00	-0.00				0.61
19.2	-0.192*	29.564*	23.727	7.95	2.33	0.60	0.00	0.00	0.31				0.63
48.7	2.695*	31.465*	25.089	7.66	4.37	0.79	0.26	0.05	0.92				0.64
129.9	-1.460	33.395	26.867	6.63	23.56	1.76	13.95	0.06	0.10				0.59
148.3	-1.246	33.780	27.173	6.43	22.66	1.56	14.75	0.04	0.00				0.57
198.5	-0.335	34.573	27.778	6.25	10.58	0.74	13.13	0.03	0.00				0.57

351

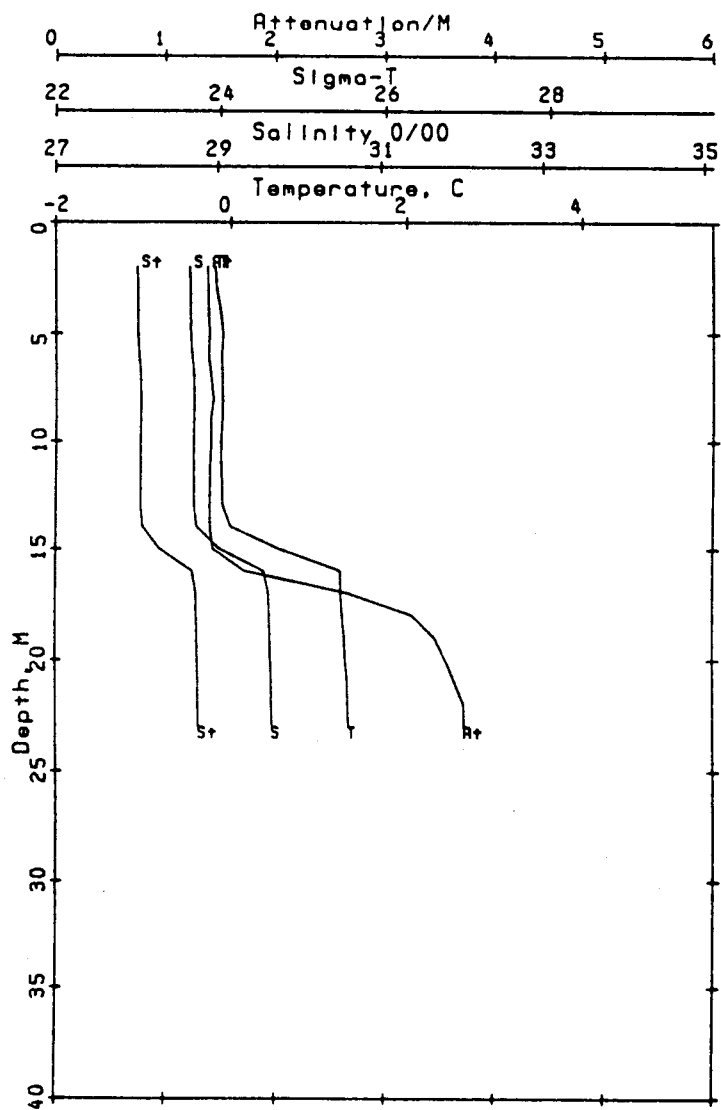


Ref. no. 26      Sta. 010      72.04 N  
Time = 862790325      Beaufort      152.66 W

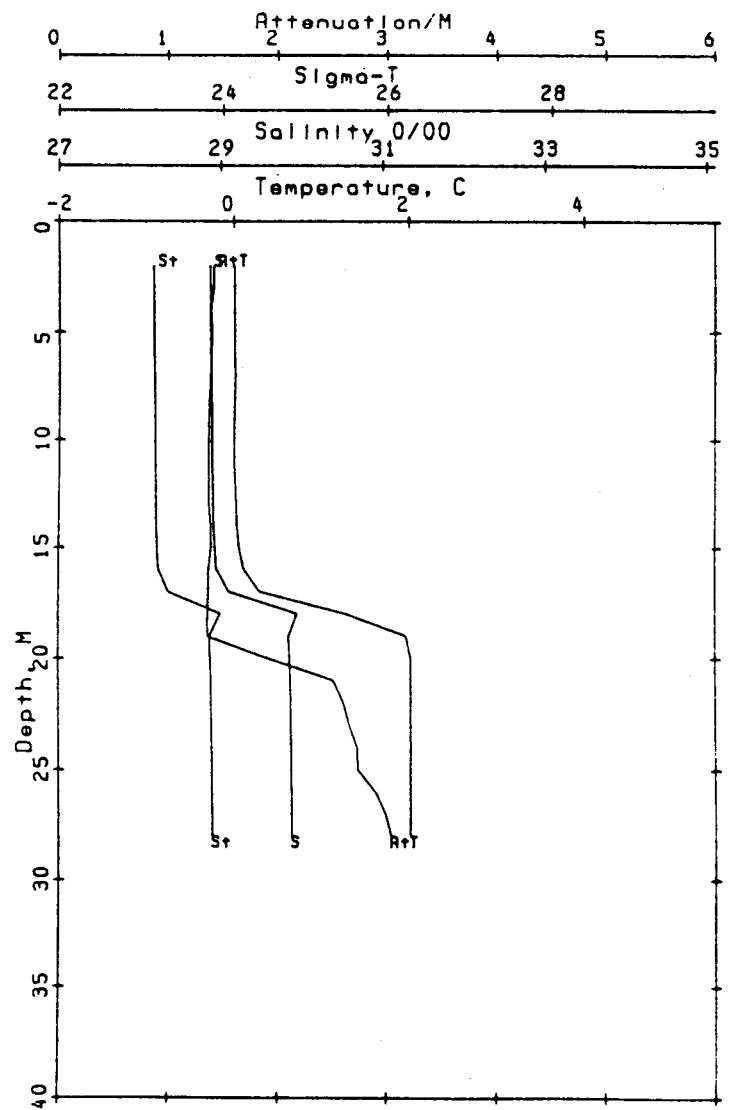
STATION B01		CAST 28	DATE 08 OCT 86		TIME 1838	LATITUDE 70 28.40N		LONGITUDE 147 20.30W		BOTTOM DEPTH 0027 M			
PRESS	TEMP	SAL	SIGMA-T	O <sub>2</sub>	SiO <sub>4</sub>	PO <sub>4</sub>	NO <sub>3</sub>	NO <sub>2</sub>	NH <sub>3</sub>	SPM	PC	LT.AT	CHLR-A
db	°C			ml l <sup>-1</sup>	µm l <sup>-1</sup>	µm l <sup>-1</sup>	µm l <sup>-1</sup>	µm l <sup>-1</sup>	µm l <sup>-1</sup>	mg l <sup>-1</sup>	µg l <sup>-1</sup>	m <sup>-1</sup>	µg l <sup>-1</sup>
4.5	-0.185	28.597	22.947	8.15	3.33	0.81	0.01	0.03	0.36	1.7615	434	1.36	
7.6	-0.232	28.559	22.917							2.5493	448	1.36	
10.4	-0.145	28.670	23.004							1.9210		1.38	
22.2	1.323	29.661	23.737	7.67	4.25	0.82	0.00	0.04	0.93	5.9880	814	3.54	

STATION B02		CAST 27	DATE 08 OCT 86		TIME 1703	LATITUDE 70 32.20N		LONGITUDE 147 19.50W		BOTTOM DEPTH 0034 M			
PRESS	TEMP	SAL	SIGMA-T	O <sub>2</sub>	SiO <sub>4</sub>	PO <sub>4</sub>	NO <sub>3</sub>	NO <sub>2</sub>	NH <sub>3</sub>	SPM	PC	LT.AT	CHLR-A
db	°C			ml l <sup>-1</sup>	µm l <sup>-1</sup>	µm l <sup>-1</sup>	µm l <sup>-1</sup>	µm l <sup>-1</sup>	µm l <sup>-1</sup>	mg l <sup>-1</sup>	µg l <sup>-1</sup>	m <sup>-1</sup>	µg l <sup>-1</sup>
4.7	0.015	28.902	23.186	8.09	4.46	0.73	0.00	0.04	0.34			1.34	
					4.42	0.80	0.00	0.04	0.36				
					4.37	0.81	0.00	0.04	0.36				
7.4	0.001	28.907	23.191	8.19								1.36	
10.4	0.009	28.913	23.194	8.09								1.36	
28.1	2.022	29.877	23.868	7.44	4.33	0.82	0.00	0.05	1.08			3.13	
				7.57	4.39	0.85	0.00	0.05	1.15				
				7.52	4.23	0.84	0.00	0.05	1.15				

353



Ref. no. 28      Sta. b01      70.47 N  
 Time = 862811838      Beaufort      147.34 W

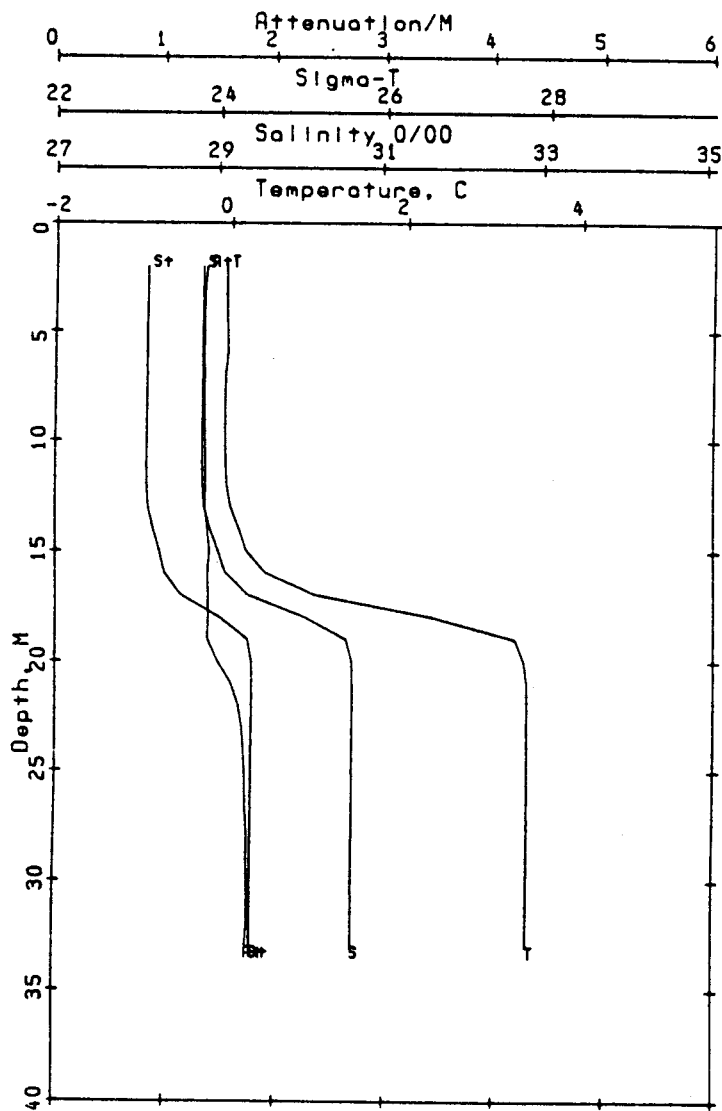


Ref. no. 27      Sta. b02      70.54 N  
 Time = 862811703      Beaufort      147.32 W

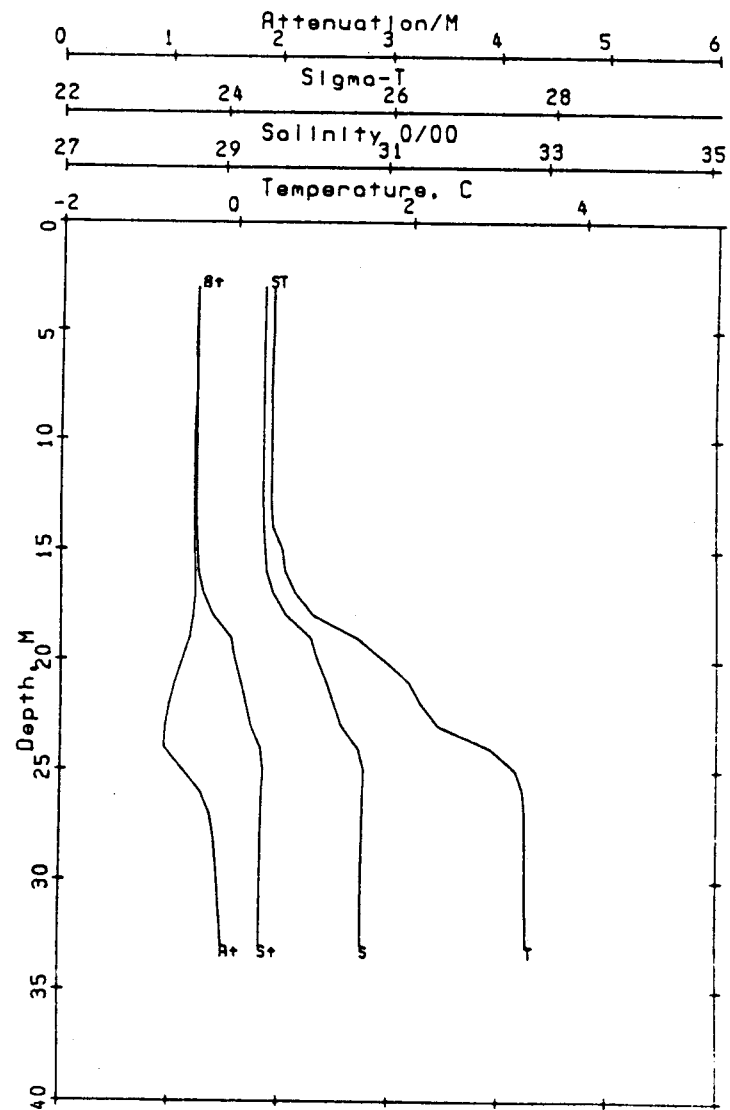
STATION B03		CAST 29	DATE 08 OCT 86		TIME 2012	LATITUDE 70 37.00N		LONGITUDE 147 13.80W		BOTTOM DEPTH 0039 M			
PRESS db	TEMP °C	SAL	SIGMA-T	O <sub>2</sub> ml l <sup>-1</sup>	SiO <sub>4</sub> µm l <sup>-1</sup>	PO <sub>4</sub> µm l <sup>-1</sup>	NO <sub>3</sub> µm l <sup>-1</sup>	NO <sub>2</sub> µm l <sup>-1</sup>	NH <sub>3</sub> µm l <sup>-1</sup>	SPM mg l <sup>-1</sup>	PC µg l <sup>-1</sup>	LT.AT m <sup>-1</sup>	CHLR-A µg l <sup>-1</sup>
4.3	-0.036	28.813	23.115	8.12	3.61	0.79	0.01	0.04	1.10	3.1313	188	1.36	
9.9	-0.037	28.813	23.116							2.7497	265	1.38	
18.6	2.608*	30.281*	24.150							2.0485	265	1.36	
32.8	3.396	30.654	24.384	7.18	3.90	0.80	0.01	0.03	0.34	1.8315		1.77	

STATION B04		CAST 30	DATE 08 OCT 86		TIME 2111	LATITUDE 70 39.80N		LONGITUDE 147 11.50W		BOTTOM DEPTH 0037 M			
PRESS db	TEMP °C	SAL	SIGMA-T	O <sub>2</sub> ml l <sup>-1</sup>	SiO <sub>4</sub> µm l <sup>-1</sup>	PO <sub>4</sub> µm l <sup>-1</sup>	NO <sub>3</sub> µm l <sup>-1</sup>	NO <sub>2</sub> µm l <sup>-1</sup>	NH <sub>3</sub> µm l <sup>-1</sup>	SPM mg l <sup>-1</sup>	PC µg l <sup>-1</sup>	LT.AT m <sup>-1</sup>	CHLR-A µg l <sup>-1</sup>
4.8	0.421	29.494	23.647	7.97	4.85	0.77	0.00	0.03	0.33			1.22	
19.7	1.617*	30.106*	24.077	7.65	4.03	0.77	0.00	0.03	0.65			1.06	
32.9	3.345	30.723	24.444	7.27	3.62	0.67	0.00	0.04	1.02			1.52	

355



Ref. no. 29 Sta. b03 70.62 N  
 Time = 862812012 Beaufort 147.23 W

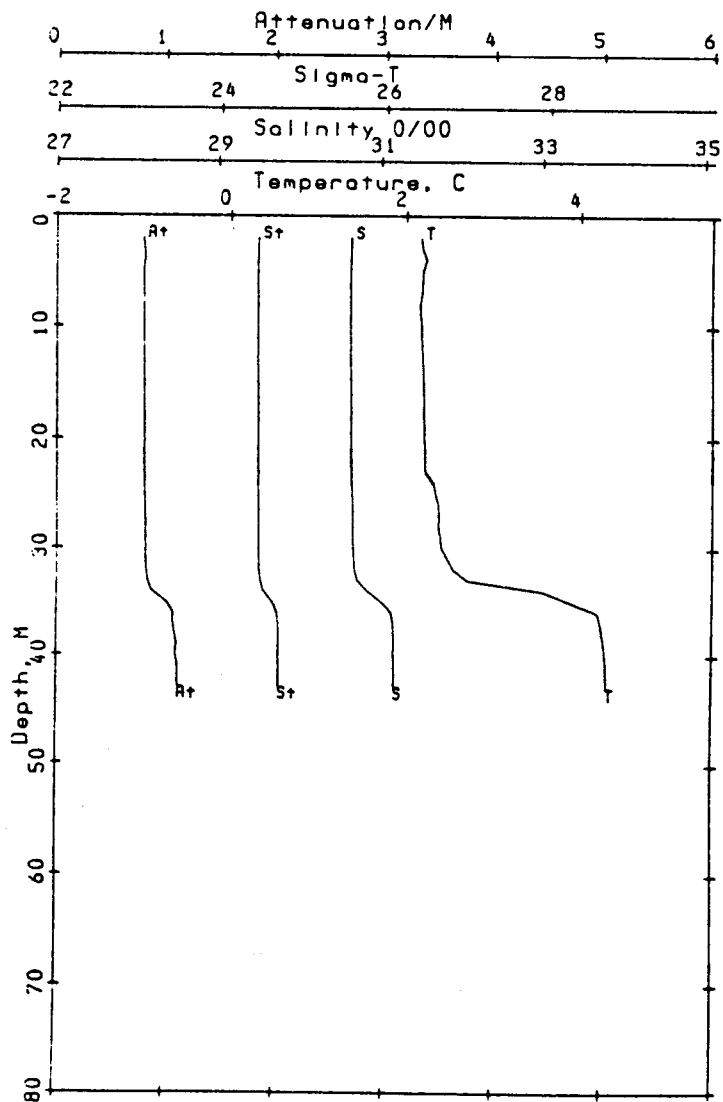


Ref. no. 30 Sta. b04 70.66 N  
 Time = 862812111 Beaufort 147.19 W

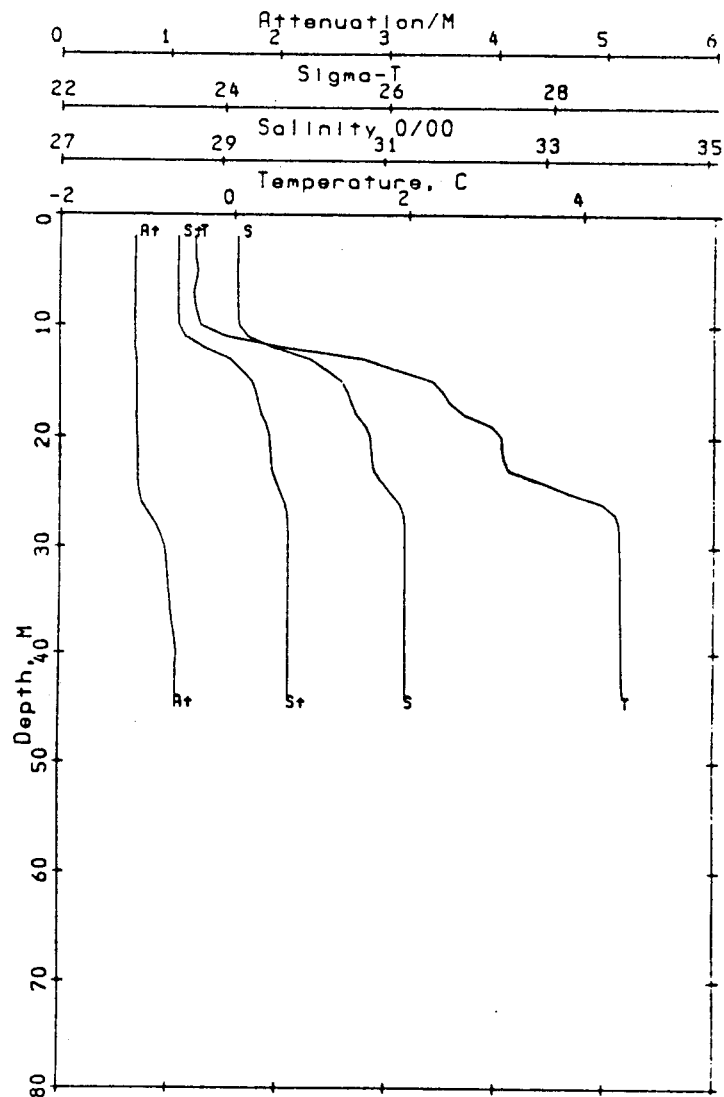
STATION B05		CAST 31	DATE 08 OCT 86	TIME 2231	LATITUDE 70 46.20N	LONGITUDE 147 01.10W	BOTTOM DEPTH 0048 M						
PRESS db	TEMP °C	SAL	SIGMA-T	O <sub>2</sub> ml l <sup>-1</sup>	SiO <sub>4</sub> µm l <sup>-1</sup>	PO <sub>4</sub> µm l <sup>-1</sup>	NO <sub>3</sub> µm l <sup>-1</sup>	NO <sub>2</sub> µm l <sup>-1</sup>	NH <sub>3</sub> µm l <sup>-1</sup>	SPM mg l <sup>-1</sup>	PC µg l <sup>-1</sup>	LT.AT m <sup>-1</sup>	CHLR-A µg l <sup>-1</sup>
1.2	2.197	30.637	24.464	7.52	3.84	0.76	0.00	0.04	0.78		195	0.81	2.7
3.8	2.233	30.625	24.452	7.54	3.74	0.77	0.00	0.04	0.95	0.9715	180	0.80	.7
8.9	2.182	30.667	24.490	7.49	3.64	0.69	0.00	0.03	0.95		204	0.84	1.2 .6
18.8	2.221	30.637	24.462	7.51	3.75	0.73	0.00	0.03	1.09	1.1175	185	0.82	.8 1.4
28.8	2.317	30.656	24.471	7.42	4.06	0.77	0.00	0.03	1.22	1.1525	403	0.84	.5 1.7
42.9	4.306	31.173	24.713	6.98	5.92	0.82	0.00	0.05	1.85	1.8675	115	1.17	1.0 .4

STATION B06		CAST 32	DATE 08 OCT 86	TIME 2341	LATITUDE 70 50.50N	LONGITUDE 146 56.70W	BOTTOM DEPTH 0052 M						
PRESS db	TEMP °C	SAL	SIGMA-T	O <sub>2</sub> ml l <sup>-1</sup>	SiO <sub>4</sub> µm l <sup>-1</sup>	PO <sub>4</sub> µm l <sup>-1</sup>	NO <sub>3</sub> µm l <sup>-1</sup>	NO <sub>2</sub> µm l <sup>-1</sup>	NH <sub>3</sub> µm l <sup>-1</sup>	SPM mg l <sup>-1</sup>	PC µg l <sup>-1</sup>	LT.AT m <sup>-1</sup>	CHLR-A µg l <sup>-1</sup>
0.8	-0.486	29.219	23.457	8.31	2.05	0.72	0.00	0.02	0.30		456	0.72	.6 1.4
3.7	-0.270	29.250	23.476	8.21	2.25	0.68	0.00	0.02	0.40	0.9270	181	0.70	.8 .6
9.0	-0.475*	29.214*	23.453	8.24	2.14	0.67	0.00	0.02	0.46		363	0.72	.7 .6
18.6	3.015*	30.818*	24.547	7.31	4.30	0.70	0.00	0.04	1.51	0.7870	135	0.74	1.1 .7
29.4	4.417	31.279	24.787	6.93	6.56	0.84	0.11	0.05	2.12	1.2170	202	0.98	1.2 1.2
44.2	4.461	31.290	24.791	6.89	6.45	0.84	0.11	0.05	1.91	1.7475	170	1.02	.4 .3

357



Ref. no. 31 Sta. b05 70.77 N  
 Time = 862812231 Beaufort 147.02 W

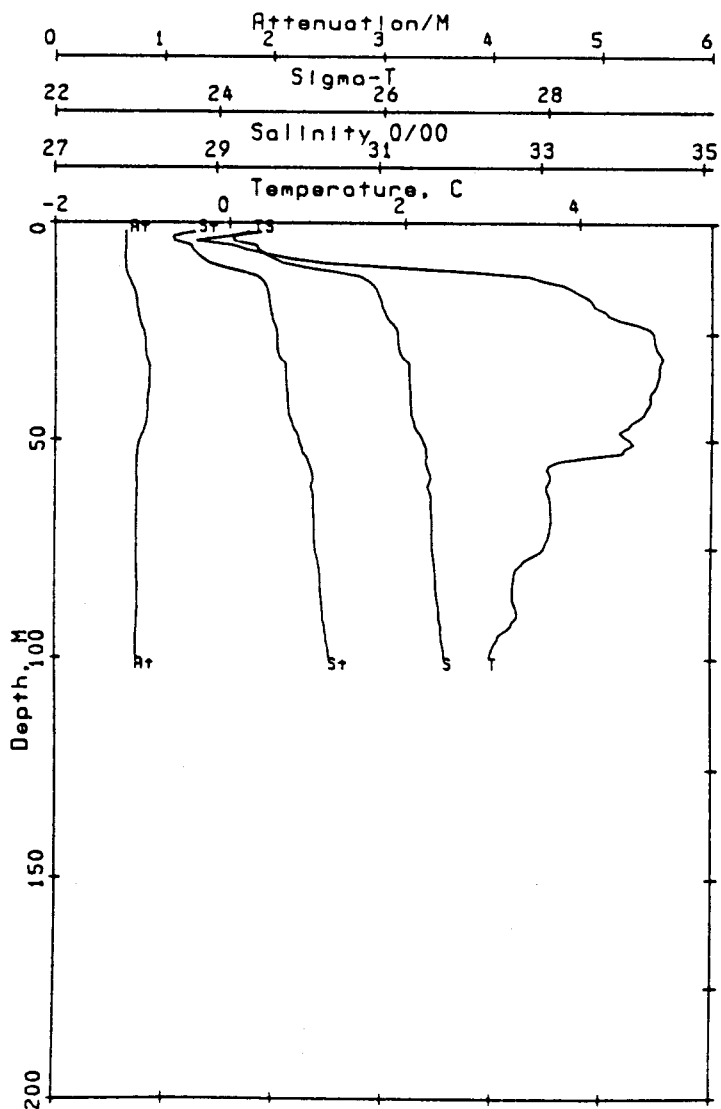


Ref. no. 32 Sta. b06 70.84 N  
 Time = 862812341 Beaufort 146.95 W

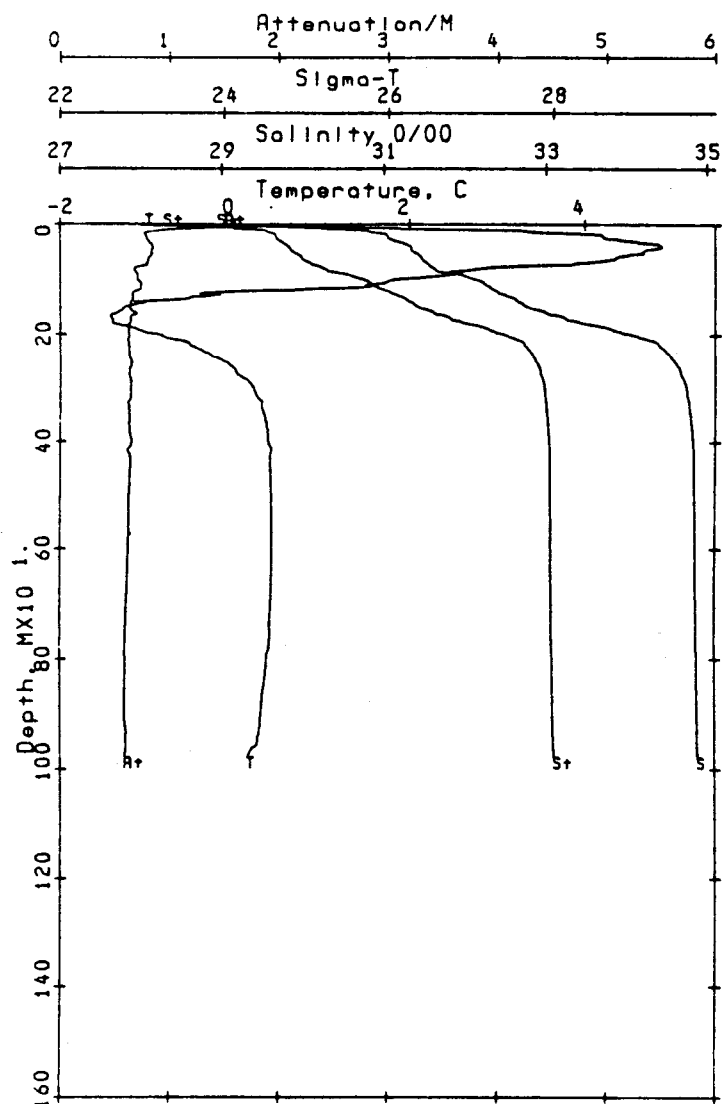
STATION B07		CAST 33	DATE 09 OCT 86		TIME 0100	LATITUDE 70 55.00N		LONGITUDE 146 50.10W		BOTTOM DEPTH 0107 M			
PRESS db	TEMP °C	SAL	SIGMA-T	O <sub>2</sub> ml l <sup>-1</sup>	SiO <sub>4</sub> µm l <sup>-1</sup>	PO <sub>4</sub> µm l <sup>-1</sup>	NO <sub>3</sub> µm l <sup>-1</sup>	NO <sub>2</sub> µm l <sup>-1</sup>	NH <sub>3</sub> µm l <sup>-1</sup>	SPM mg l <sup>-1</sup>	PC µg l <sup>-1</sup>	LT.AT m <sup>-1</sup>	CHLR-A µg l <sup>-1</sup>
1.2	0.028	29.371	23.563	8.06	2.05	0.66	0.00	0.00	0.29		334	0.62	.1
4.2	0.036*	29.184*	23.412	8.10	1.49	0.70	0.00	0.00	0.35	0.6285	241	0.65	.3
9.2	0.920*	29.788*	23.860	7.83	2.09	0.72	0.00	0.03	0.49		305	0.66	.4
18.8	4.201	31.015	24.598	7.00	7.15	0.90	0.00	0.05	1.72		179	0.78	.2
28.6	4.959	31.357	24.793	6.75	8.57	0.96	0.03	0.06	2.08	0.9715	197	0.87	.1
49.6	4.728	31.389	24.843	6.78	8.23	0.96	0.03	0.06	2.04	1.2250	234	0.86	.4
99.7	2.972	31.799	25.333	7.10	6.95	0.93	0.43	0.09	1.65	1.1413	194	0.74	.3
													.6

STATION B08		CAST 34	DATE 09 OCT 86		TIME 0228	LATITUDE 70 58.50N		LONGITUDE 146 44.50W		BOTTOM DEPTH 0983 M			
PRESS db	TEMP °C	SAL	SIGMA-T	O <sub>2</sub> ml l <sup>-1</sup>	SiO <sub>4</sub> µm l <sup>-1</sup>	PO <sub>4</sub> µm l <sup>-1</sup>	NO <sub>3</sub> µm l <sup>-1</sup>	NO <sub>2</sub> µm l <sup>-1</sup>	NH <sub>3</sub> µm l <sup>-1</sup>	SPM mg l <sup>-1</sup>	PC µg l <sup>-1</sup>	LT.AT m <sup>-1</sup>	CHLR-A µg l <sup>-1</sup>
4.3	-0.495*	28.848*	23.158	8.06	2.52	0.69	0.00	0.03	0.44			0.65	
48.6	4.812	31.385	24.830	6.83	7.99	0.92	0.06	0.05	2.02			0.79	
168.8	-1.399	33.285	26.776	6.69	30.84	1.90	12.93	0.09	0.38			0.58	
299.3	0.228	34.750	27.892	6.49	10.84	1.01	12.81	0.05	0.01			0.58	
498.7	0.407	34.843	27.956	6.68	8.63	0.96	12.64	0.05	-0.00			0.59	
748.5	0.402	34.870	27.979	6.67	7.86	0.88	12.70	0.03	-0.00			0.58	
978.7	0.133	35.010	28.107	6.84	7.83	0.90	12.46	0.03	0.06			0.62	

359



Ref. no. 33      Sta. b07      70.92 N  
 Time = 862820100      Beaufort      146.84 W

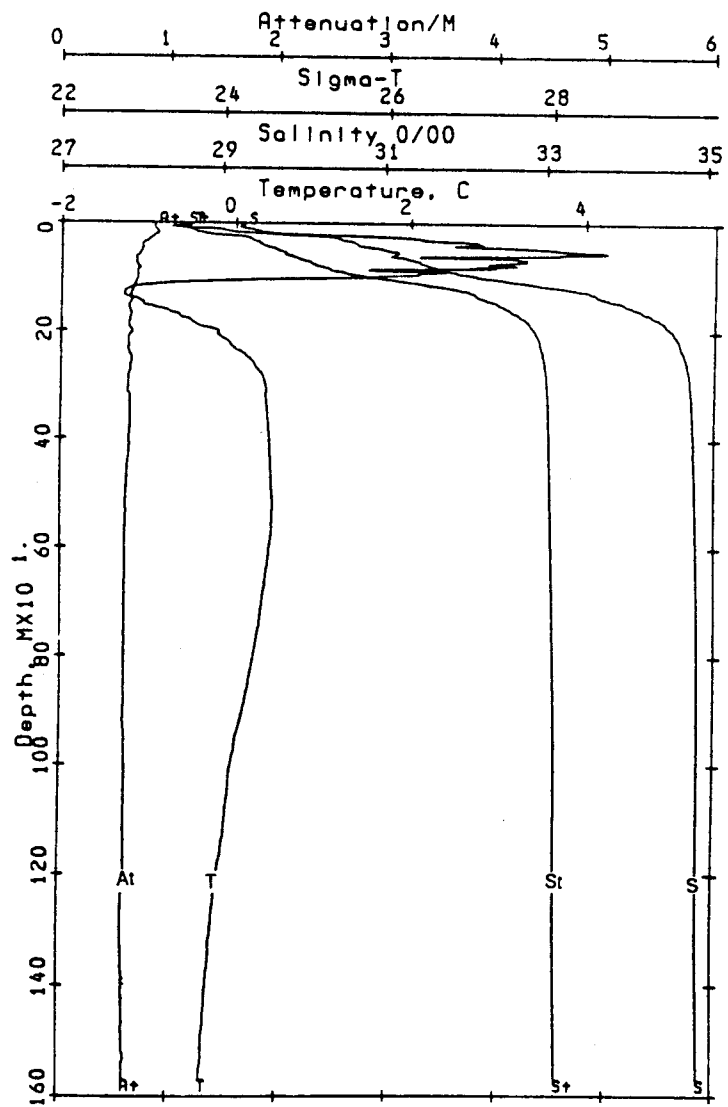


Ref. no. 34      Sta. b08      70.98 N  
 Time = 862820229      Beaufort      146.74 W

360

STATION B09		CAST 35	DATE 09 OCT 86	TIME 0521	LATITUDE 71 03.80N		LONGITUDE 146 39.40W		BOTTOM DEPTH 1693 M				
PRESS db	TEMP °C	SAL	SIGMA-T	O <sub>2</sub> ml l <sup>-1</sup>	SiO <sub>4</sub> µm l <sup>-1</sup>	PO <sub>4</sub> µm l <sup>-1</sup>	NO <sub>3</sub> µm l <sup>-1</sup>	NO <sub>2</sub> µm l <sup>-1</sup>	NH <sub>3</sub> µm l <sup>-1</sup>	SPM mg l <sup>-1</sup>	PC µg l <sup>-1</sup>	LT.AT m <sup>-1</sup>	CHLR-A µg l <sup>-1</sup>
1.4	-0.824	29.211	23.460	8.23	1.60	0.77	0.25	0.03	0.35		311	0.78	.5
4.0	-0.846	29.204	23.455	8.23	1.65	0.81	0.15	0.03	0.29	0.8625	287	0.77	.8
10.1	-0.730*	29.216	23.462	8.26	1.70	0.78	0.18	0.03	0.37		353	0.78	.6
19.9	0.189*	29.555	23.705	8.02	2.97	0.83	0.00	0.03	0.49		461	0.83	1.0
29.0	1.281	29.901	23.932	7.61	2.81	0.82	0.09	0.03	0.86		200	0.78	.9
49.1	3.072*	30.833	24.554	7.32	3.60	0.78	0.31	0.03	1.02		66	0.66	.6
134.1	-1.299	33.572	27.006	6.56	29.65	1.73	13.51	0.08	0.02	0.6960	249	0.56	1.3
149.1	-1.137	33.827	27.207	6.39	28.15	1.76	13.95	0.08	0.00			0.56	
199.6	-0.364	34.518	27.736	6.24	14.48	1.38	13.41	0.05	0.00			0.56	
309.9	0.371	34.795	27.920	6.64	14.43	1.41	13.38	0.05	0.00			0.54	
501.8	0.437	34.858	27.967	6.68	6.74	0.91	12.78	0.03	0.06	0.9610		0.56	
1570.2	-0.363	34.925	28.065	6.79	7.10	0.99	12.59	0.04	0.00	0.8755		0.61	

198  
361

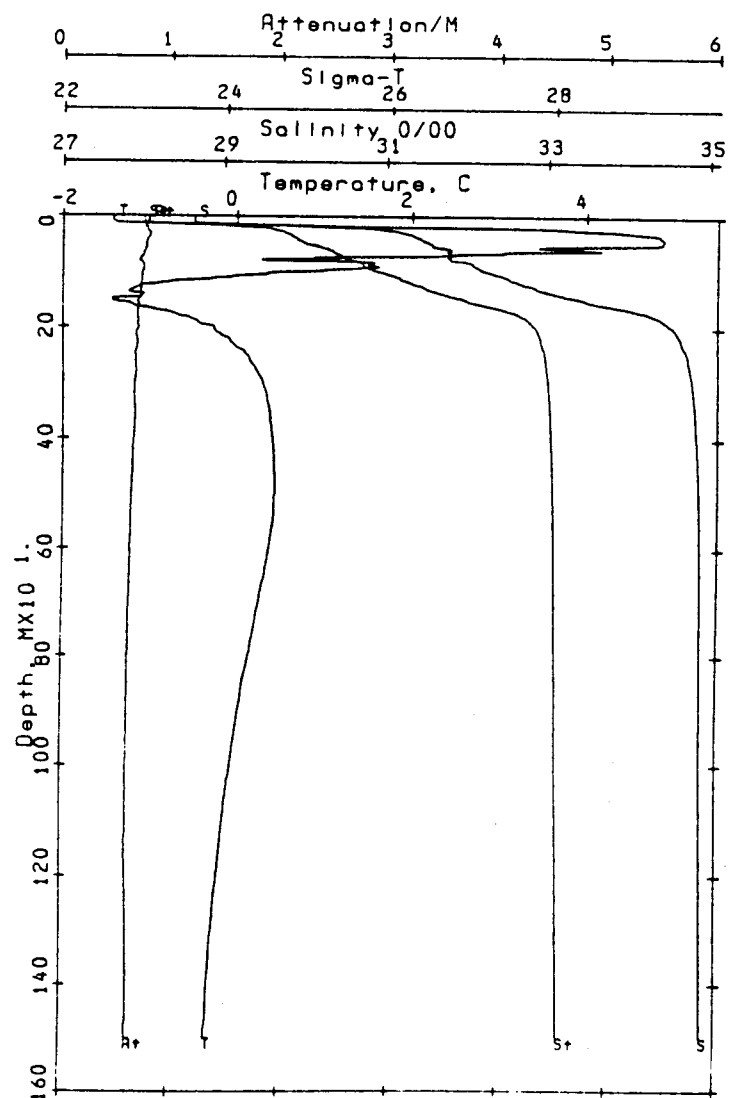


Ref. no. 35  
Time = 862820521

Sta. b09  
Beaufort

71.06 N  
146.66 W

STATION B10		CAST 36		DATE 09 OCT 86		TIME 0859		LATITUDE 71 08.90N		LONGITUDE 146 36.40W		BOTTOM DEPTH 2037 M	
PRESS	TEMP	SAL	SIGMA-T	O <sub>2</sub>	SiO <sub>4</sub>	PO <sub>4</sub>	NO <sub>3</sub>	NO <sub>2</sub>	NH <sub>3</sub>	SPM	PC	LT.AT	CHLR-A
db	°C			ml l <sup>-1</sup>	μm l <sup>-1</sup>	μm l <sup>-1</sup>	μm l <sup>-1</sup>	μm l <sup>-1</sup>	μm l <sup>-1</sup>	mg l <sup>-1</sup>	μg l <sup>-1</sup>	m <sup>-1</sup>	μg l <sup>-1</sup>
3.5	-1.543	28.569	22.951	8.79	3.22	0.73	0.09	0.00	0.21			0.60	
18.9	0.308*	29.450*	23.616	7.90	5.42	0.66	0.00	0.01	0.94			0.61	
48.8	4.801	31.551	24.963	6.92	6.46	0.76	0.22	0.08	2.00			0.63	
133.6	-1.213	32.950	26.498	7.00	31.66	1.69	11.65	0.17	1.10			0.59	
149.0	-1.377	33.529	26.974	6.66	35.00	1.54	13.42	0.08	0.23			0.58	
199.7	-0.312	34.513	27.728	6.31	17.65	0.95	13.44	0.08	0.02			0.58	
348.6	0.374	34.813	27.934	6.54	10.52	0.86	12.85	0.04	0.02			0.57	
498.7	0.429	34.861	27.970	6.70	9.61	0.87	12.87	0.04	0.03			0.56	
698.8	0.268	34.884	27.998	6.88	9.05	0.79	12.66	0.03	0.00			0.56	
998.6	-0.037	34.899	28.027	6.96	9.06	0.79	12.77	0.02	0.00			0.58	
1249.2	-0.230	34.910	28.045	6.88	10.10	0.86	13.03	0.02	0.06			0.60	
1050.4	-0.334	35.179	28.268	6.82	11.26	0.90	13.46	0.02	0.03			0.62	

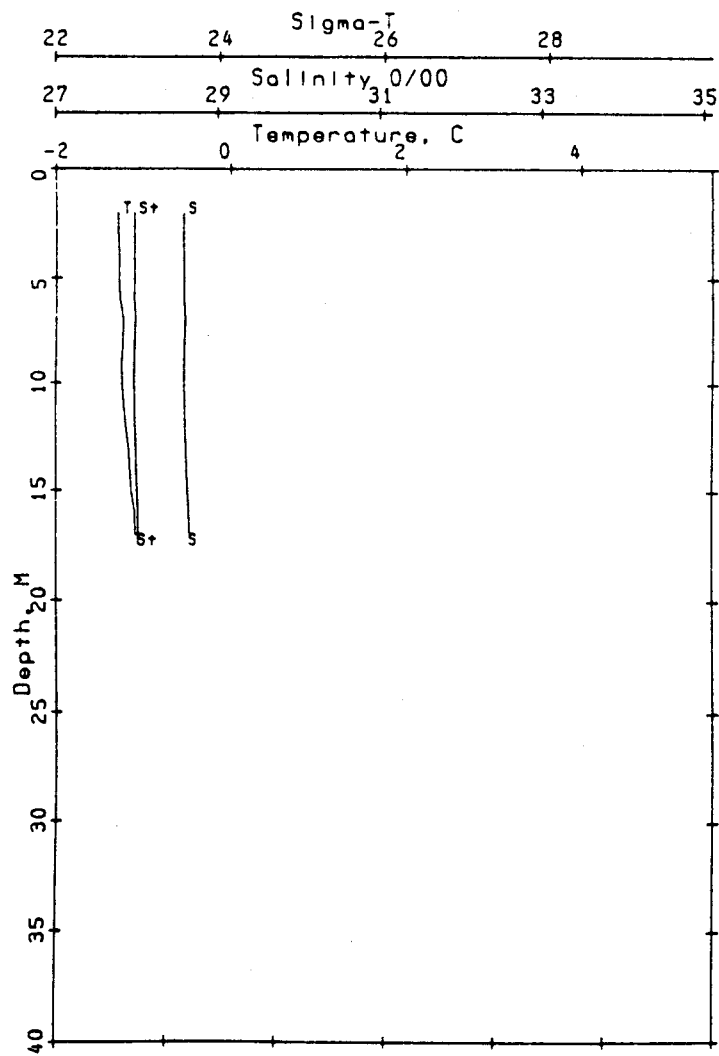


Ref. no. 36 Sta. b10 71.15 N  
 Time = 862820900 Beaufort 146.61 W

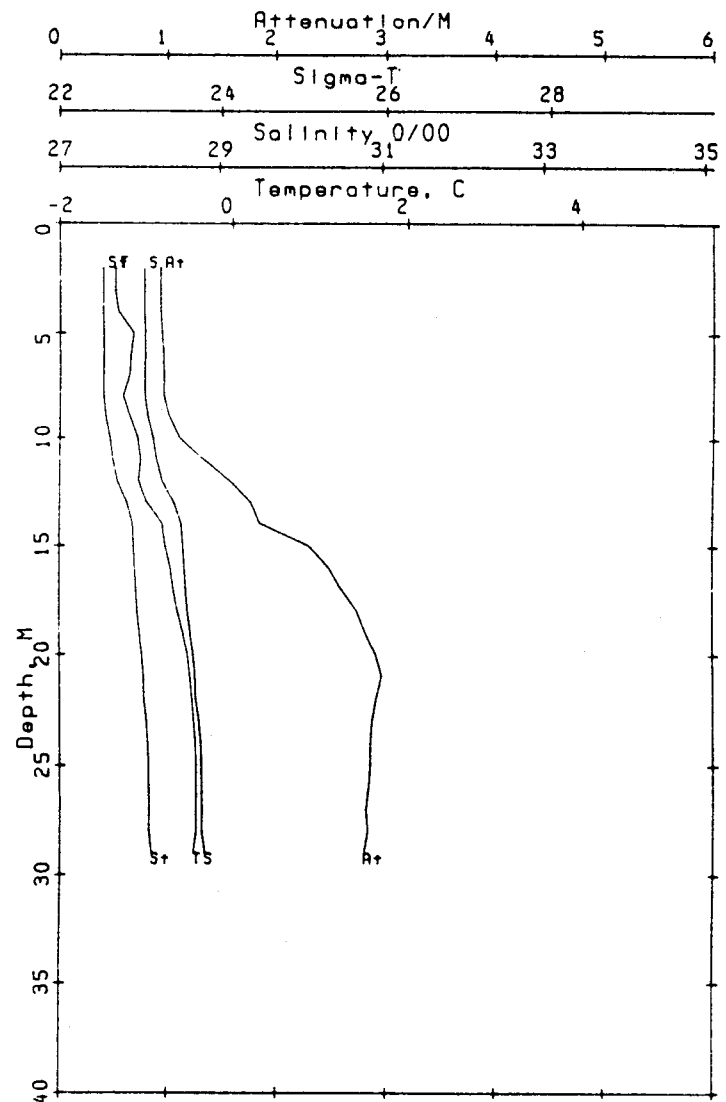
STATION C01		CAST 47	DATE 12 OCT 86		TIME 1737	LATITUDE 70 10.30N		LONGITUDE 144 30.10W		BOTTOM DEPTH 0024 M			
PRESS db	TEMP °C	SAL	SIGMA-T	O <sub>2</sub> ml l <sup>-1</sup>	SIO <sub>4</sub> µm l <sup>-1</sup>	PO <sub>4</sub> µm l <sup>-1</sup>	NO <sub>3</sub> µm l <sup>-1</sup>	NO <sub>2</sub> µm l <sup>-1</sup>	NH <sub>3</sub> µm l <sup>-1</sup>	SPM mg l <sup>-1</sup>	PC µg l <sup>-1</sup>	LT.AT m <sup>-1</sup>	CHLR-A µg l <sup>-1</sup>
4.4	-1.140	28.577	22.953	8.50	3.82	0.86	0.00	0.03	0.19	6.7260	216		
6.8	-1.267	28.561	22.942							5.8295	243		
10.3	-1.246	28.576	22.953							6.3717	145		
16.7	-1.076	28.646	23.007	8.56	3.80	0.86	0.00	0.03	0.15	5.4220	162		

STATION C02		CAST 46	DATE 12 OCT 86		TIME 1606	LATITUDE 70 14.50N		LONGITUDE 144 22.70W		BOTTOM DEPTH 0035 M			
PRESS db	TEMP °C	SAL	SIGMA-T	O <sub>2</sub> ml l <sup>-1</sup>	SIO <sub>4</sub> µm l <sup>-1</sup>	PO <sub>4</sub> µm l <sup>-1</sup>	NO <sub>3</sub> µm l <sup>-1</sup>	NO <sub>2</sub> µm l <sup>-1</sup>	NH <sub>3</sub> µm l <sup>-1</sup>	SPM mg l <sup>-1</sup>	PC µg l <sup>-1</sup>	LT.AT m <sup>-1</sup>	CHLR-A µg l <sup>-1</sup>
4.6	-1.212	28.028	22.509	8.56	3.24	0.69	0.17	0.01	0.15	1.8665	43	0.92	
9.4	-1.080	28.180	22.630							2.5237	135	1.30	
19.4	-0.537	28.650	22.999	8.42	3.77	0.76	0.06	0.03	0.21	5.1150	185	2.67	
28.7	-0.418	28.780	23.101	8.42	3.86	0.86	0.06	0.03	0.21	4.9200	78	2.63	

365



Ref. no. 47 Sta. c01 70.17 N  
 Time = 862851737 Beaufort 144.50 W



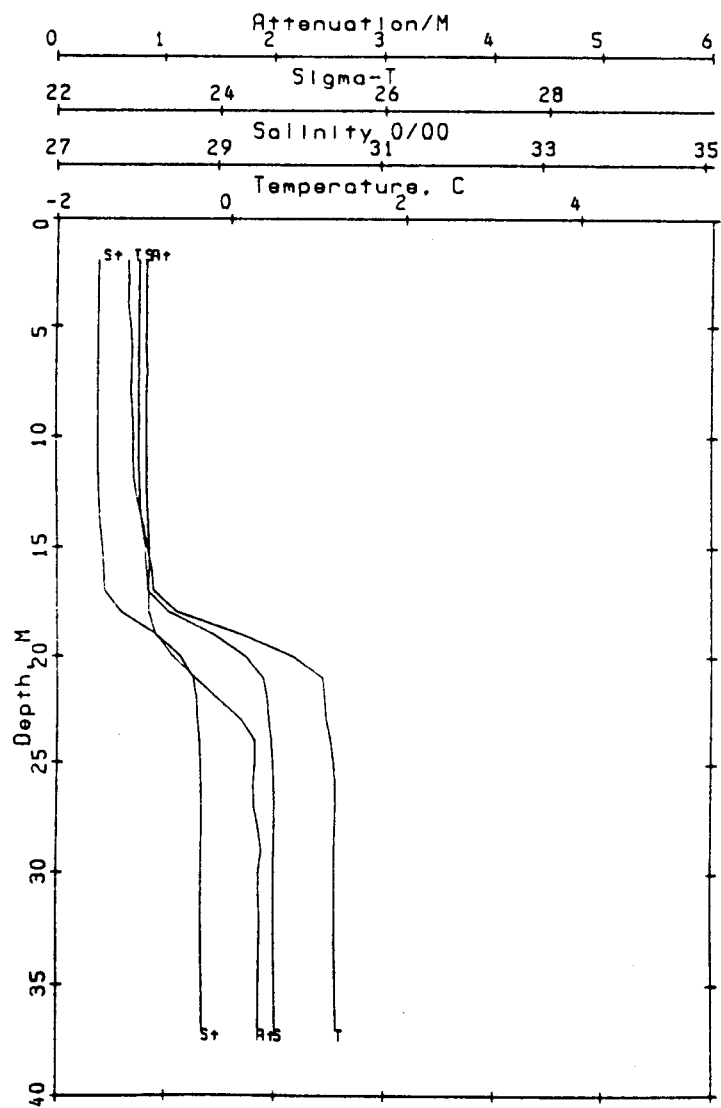
Ref. no. 46 Sta. c02 70.24 N  
 Time = 862851606 Beaufort 144.38 W

STATION C03		CAST 45	DATE 12 OCT 86		TIME 1433	LATITUDE 70 21.50N		LONGITUDE 144 17.00W		BOTTOM DEPTH 0045 M			
PRESS db	TEMP °C	SAL	SIGMA-T	O <sub>2</sub> ml l <sup>-1</sup>	SIO <sub>4</sub> µm l <sup>-1</sup>	PO <sub>4</sub> µm l <sup>-1</sup>	NO <sub>3</sub> µm l <sup>-1</sup>	NO <sub>2</sub> µm l <sup>-1</sup>	NH <sub>3</sub> µm l <sup>-1</sup>	SPM mg l <sup>-1</sup>	PC µg l <sup>-1</sup>	LT.AT m <sup>-1</sup>	CHLR-A µg l <sup>-1</sup>
0.9	-1.188	28.032	22.512	8.70	2.50	0.64	0.00	0.01	0.09		92	0.83	.2 .0
3.9	-1.192	28.031	22.512	8.56	2.48	0.66	0.00	0.01	0.11	0.9180	94	0.83	.2 .3
8.9	-1.090	28.000	22.485	8.55	2.45	0.62	0.00	0.02	0.12		44	0.84	.2 .2
19.1	0.410*	29.076*	23.311	8.21	3.21	0.61	0.00	0.02	0.19	1.7240	5	1.14	.3
29.0	1.202	29.704	23.778	7.99	3.63	0.68	0.00	0.03	0.26	3.1235	81	1.86	.3 .2
36.9	0.665	30.239	24.235	8.02	3.83	0.73	0.00	0.03	0.27	3.4615	12	1.92	.3

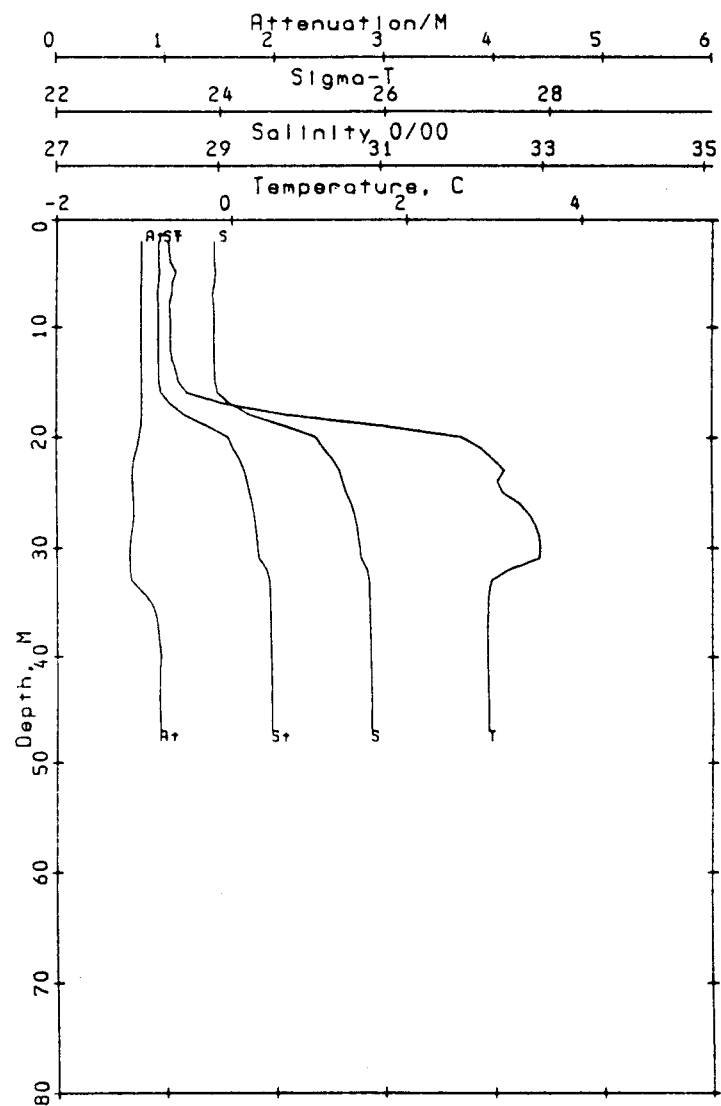
  

STATION C04		CAST 44	DATE 12 OCT 86		TIME 0950	LATITUDE 70 27.70N		LONGITUDE 144 11.00W		BOTTOM DEPTH 0050 M			
PRESS db	TEMP °C	SAL	SIGMA-T	O <sub>2</sub> ml l <sup>-1</sup>	SIO <sub>4</sub> µm l <sup>-1</sup>	PO <sub>4</sub> µm l <sup>-1</sup>	NO <sub>3</sub> µm l <sup>-1</sup>	NO <sub>2</sub> µm l <sup>-1</sup>	NH <sub>3</sub> µm l <sup>-1</sup>	SPM mg l <sup>-1</sup>	PC µg l <sup>-1</sup>	LT.AT m <sup>-1</sup>	CHLR-A µg l <sup>-1</sup>
1.4	-0.737	28.926	23.227	8.44	2.20	0.61	0.00	0.02	0.16		222	0.76	.2 .2
4.2	-0.699	28.928	23.228	8.37	2.18	0.62	0.00	0.01	0.16	0.7980	150	0.78	.3 .2
8.9	-0.692	28.946	23.242	8.42	2.27	0.66	0.00	0.01	0.15		173	0.79	.3 .3
18.9	2.840*	30.245*	24.104	8.02	2.14	0.61	0.00	0.01	0.27	1.4560	90	0.70	.2 .2
28.7	3.525	30.749	24.449	7.49	2.67	0.60	0.00	0.02	0.32	0.8000	166	0.67	.0 .4
46.5	2.930	30.884	24.607	7.47	5.65	0.69	0.01	0.03	0.35	1.2475		0.95	.1 .1

367



Ref. no. 45 Sta. c03 70.36 N  
 Time = 862851433 Beaufort 144.28 W

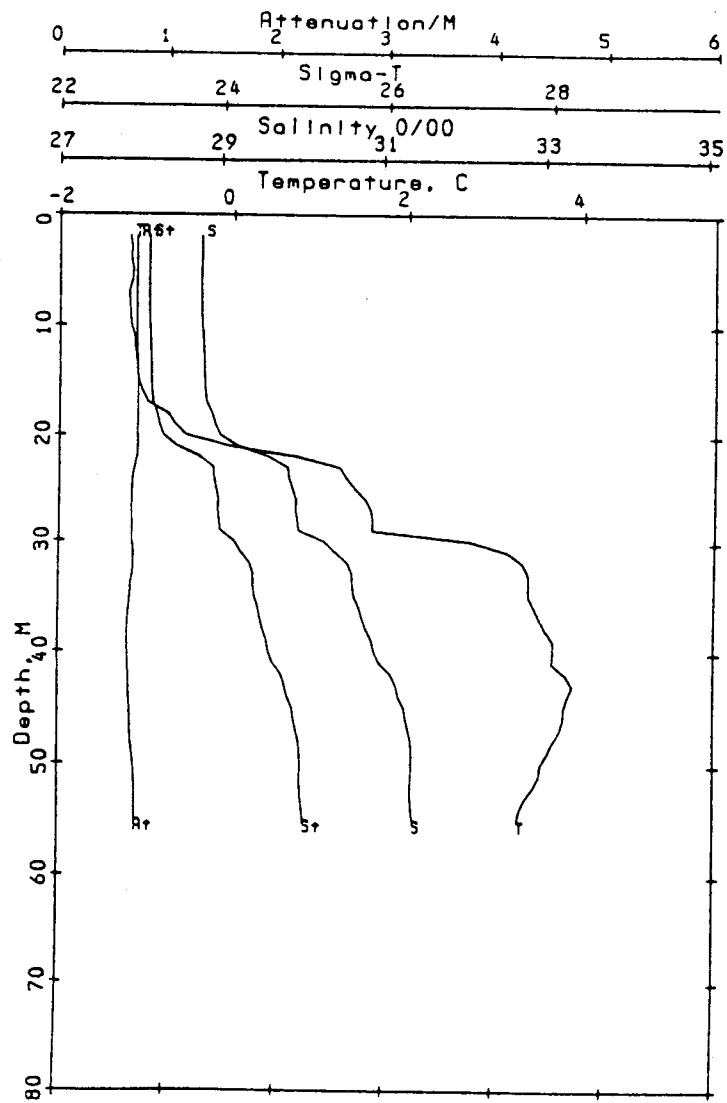


Ref. no. 44 Sta. c04 70.46 N  
 Time = 862850951 Beaufort 144.18 W

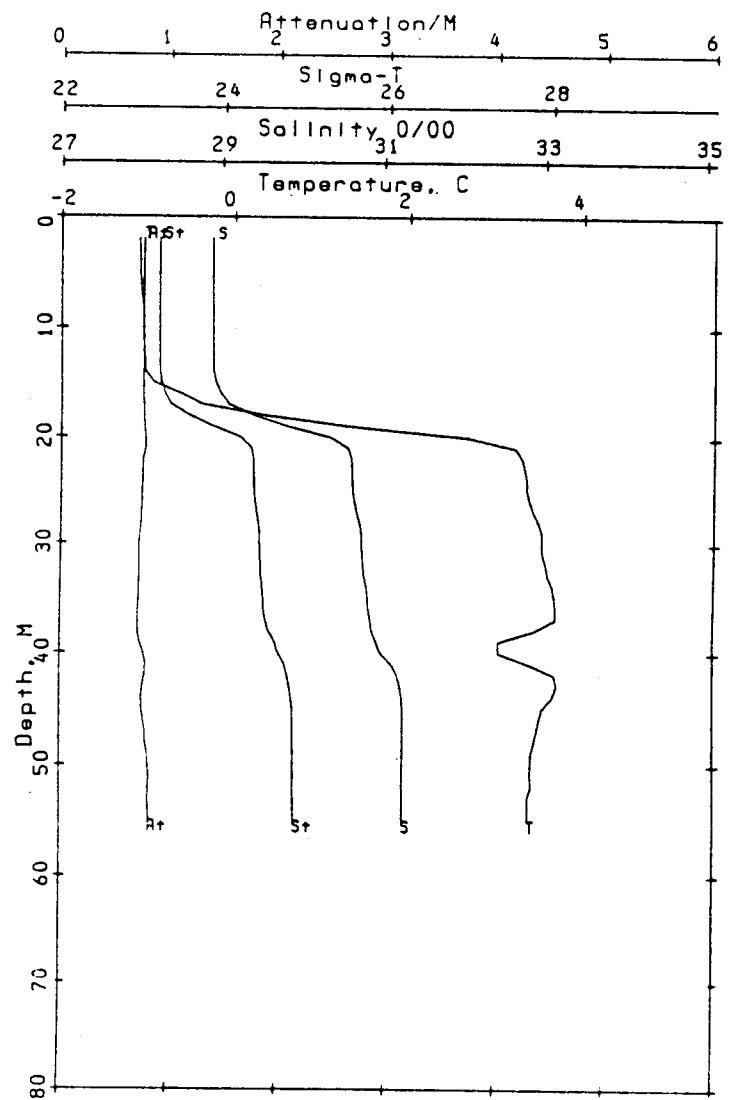
STATION C05a		CAST 37	DATE 11 OCT 86	TIME 0743	LATITUDE 70 33.60N		LONGITUDE 144 04.40W		BOTTOM DEPTH 0062 M				
PRESS db	TEMP °C	SAL	SIGMA-T	O <sub>2</sub> ml l <sup>-1</sup>	SIO <sub>4</sub> µm l <sup>-1</sup>	PO <sub>4</sub> µm l <sup>-1</sup>	NO <sub>3</sub> µm l <sup>-1</sup>	NO <sub>2</sub> µm l <sup>-1</sup>	NH <sub>3</sub> µm l <sup>-1</sup>	SPM mg l <sup>-1</sup>	PC µg l <sup>-1</sup>	LT.AT m <sup>-1</sup>	CHLR-A µg l <sup>-1</sup>
4.1	-1.059	28.880	23.196	8.45	2.22	0.68	0.00	0.00	0.17			0.76	
19.1	3.345*	30.610*	24.354	8.24	2.32	0.72	0.00	0.00	0.34			0.74	
46.4	3.479	31.262	24.861	7.31	6.02	0.93	0.36	0.04	1.50			0.81	
54.6	3.382	31.253	24.863	7.40	6.23	1.00	0.35	0.05	0.69			0.82	

STATION C05b		CAST 43	DATE 12 OCT 86	TIME 0825	LATITUDE 70 33.80N		LONGITUDE 144 05.00W		BOTTOM DEPTH 0061 M				
PRESS db	TEMP °C	SAL	SIGMA-T	O <sub>2</sub> ml l <sup>-1</sup>	SIO <sub>4</sub> µm l <sup>-1</sup>	PO <sub>4</sub> µm l <sup>-1</sup>	NO <sub>3</sub> µm l <sup>-1</sup>	NO <sub>2</sub> µm l <sup>-1</sup>	NH <sub>3</sub> µm l <sup>-1</sup>	SPM mg l <sup>-1</sup>	PC µg l <sup>-1</sup>	LT.AT m <sup>-1</sup>	CHLR-A µg l <sup>-1</sup>
4.5	-1.185	28.743	23.088	8.41	1.64	0.60	0.00	0.00	0.19			0.72	
19.4	-0.625*	28.944*	23.239	7.55	2.62	0.61	0.00	0.02	0.13			0.73	
49.9	3.535	31.385	24.954	7.27	6.26	0.71	0.31	0.04	0.43			0.72	
55.0	3.242	31.400	24.992	7.30	6.13	0.64	0.30	0.04	0.48			0.73	

698



Ref. no. 37 Sta. c05 70.56 N  
 Time = 862840743 Beaufort 144.07 W



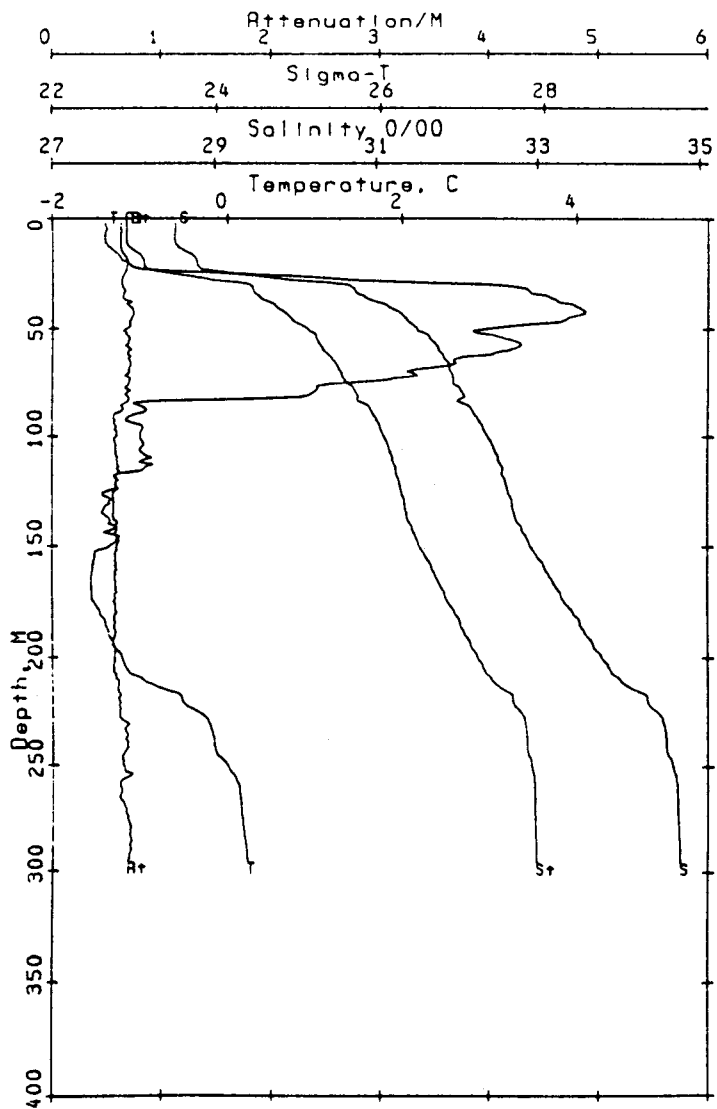
Ref. no. 43 Sta. c05 70.56 N  
 Time = 862850825 Beaufort 144.08 W

STATION C06		CAST 38	DATE 11 OCT 86	TIME 0948	LATITUDE 70 38.90N	LONGITUDE 143 57.30W	BOTTOM DEPTH 0305 M						
PRESS db	TEMP °C	SAL	SIGMA-T	O <sub>2</sub> ml l <sup>-1</sup>	SIO <sub>4</sub> µm l <sup>-1</sup>	PO <sub>4</sub> µm l <sup>-1</sup>	NO <sub>3</sub> µm l <sup>-1</sup>	NO <sub>2</sub> µm l <sup>-1</sup>	NH <sub>3</sub> µm l <sup>-1</sup>	SPM mg l <sup>-1</sup>	PC µg l <sup>-1</sup>	LT.AT m <sup>-1</sup>	CHLR-A µg l <sup>-1</sup>
1.8	-1.404	28.470	22.870	8.68	1.97	0.81	0.03	0.00	0.10		120	0.62	1.4 2.0
8.7	-1.430	28.470	22.870	8.67	1.97	1.84	0.03	0.00	0.08		279	0.63	2.1
19.3	-1.240	28.742	23.088	8.49	2.07	0.87	0.03	0.00	0.18		229	0.84	.2 .4
29.2	3.133*	30.588*	24.354	7.56	2.59	0.86	0.03	0.00	0.98		250	0.73	1.9 1.4
49.3	3.890	31.392	24.927	7.32	5.34	0.98	0.10	0.05	1.56	0.6940	177	0.80	.2
164.1	-1.546	33.141	26.664	6.80	31.83	2.09	12.72	0.03	0.08	0.8710	111	0.70	
296.2	0.227	34.757	27.898	6.50	11.79	1.25	12.11	0.04	0.13	1.3517		0.72	

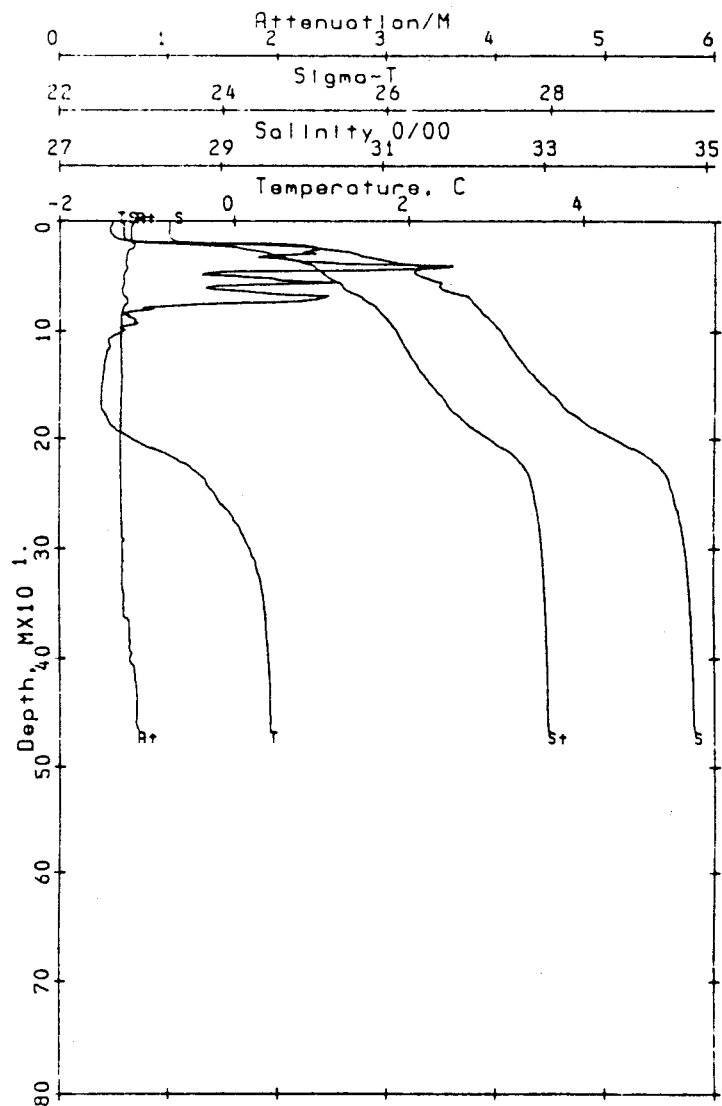
  

STATION C07		CAST 39	DATE 11 OCT 86	TIME 1222	LATITUDE 70 45.40N	LONGITUDE 143 46.80W	BOTTOM DEPTH 0474 M						
PRESS db	TEMP °C	SAL	SIGMA-T	O <sub>2</sub> ml l <sup>-1</sup>	SIO <sub>4</sub> µm l <sup>-1</sup>	PO <sub>4</sub> µm l <sup>-1</sup>	NO <sub>3</sub> µm l <sup>-1</sup>	NO <sub>2</sub> µm l <sup>-1</sup>	NH <sub>3</sub> µm l <sup>-1</sup>	SPM mg l <sup>-1</sup>	PC µg l <sup>-1</sup>	LT.AT m <sup>-1</sup>	CHLR-A µg l <sup>-1</sup>
4.2	-1.384	28.330	22.756	8.65	1.71	0.99	0.02	0.00	0.23			0.64	
48.5	-0.186*	31.450	25.249	8.78	6.15	1.34	0.56	0.26	0.53			0.57	
99.1	-1.242	32.429	26.077	7.62	22.36	2.13	7.77	0.13	0.84			0.55	
149.4	-1.522	32.978	26.530	6.72	32.21	2.38	13.50	0.00	0.05			0.55	
199.9	-1.143	33.873	27.245	6.49	28.71	2.14	13.94	0.00	0.04			0.55	
299.2	0.180	34.732	27.880	6.58	11.11	1.38	12.46	0.03	0.11			0.58	
467.5	0.412	34.855	27.966	6.74	10.04	1.38	12.37	0.01	0.06			0.67	

371



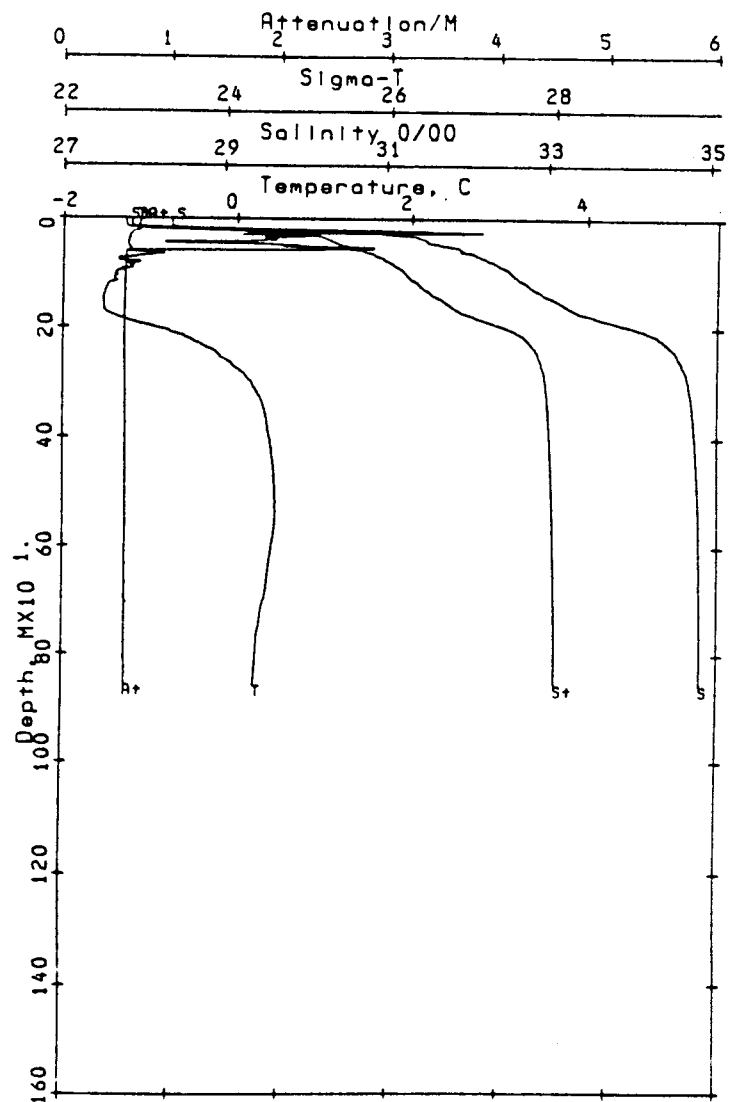
Ref. no. 38 Sta. c06 70.65 N  
 Time = 862840948 Beaufort 143.96 W



Ref. no. 39 Sta. c07 70.76 N  
 Time = 862841223 Beaufort 143.78 W

STATION C08		CAST 40		DATE 11 OCT 86		TIME 1506		LATITUDE 70 50.80N		LONGITUDE 143 42.40W		BOTTOM DEPTH 0860 M	
PRESS db	TEMP °C	SAL	SIGMA-T	O <sub>2</sub> ml l <sup>-1</sup>	SIO <sub>4</sub> μm l <sup>-1</sup>	PO <sub>4</sub> μm l <sup>-1</sup>	NO <sub>3</sub> μm l <sup>-1</sup>	NO <sub>2</sub> μm l <sup>-1</sup>	NH <sub>3</sub> μm l <sup>-1</sup>	SPM mg l <sup>-1</sup>	PC μg l <sup>-1</sup>	LT.AT m <sup>-1</sup>	CHLR-A μg l <sup>-1</sup>
3.6	-1.206	28.300	22.729	3.28	1.91	1.18	0.00	0.00	0.11			0.66	
18.7	-0.320*	28.946*	23.232	8.33	1.92	1.09	0.00	0.00	0.29			0.67	
49.1	0.733*	31.546	25.283	8.38	6.70	1.48	1.05	0.20	0.71			0.57	
99.0	-1.300	32.495	26.132	7.55	24.51	2.27	8.19	0.13	0.88			0.54	
149.2	-1.542	33.093	26.624	6.71	32.89	2.53	13.61	0.00	0.02			0.54	
198.7	-1.075	33.967	27.319	6.24	28.66	2.17	14.13	0.00	0.00			0.54	
300.9	0.166	34.731	27.880	6.51	10.65	1.30	12.17	0.00	0.00			0.55	
499.4	0.440	34.849	27.960	6.62	7.79	0.91	11.97	0.00	0.00			0.55	
855.0	0.253	34.832	27.957	6.94	7.69	1.28	12.13	0.00	0.00			0.58	

373

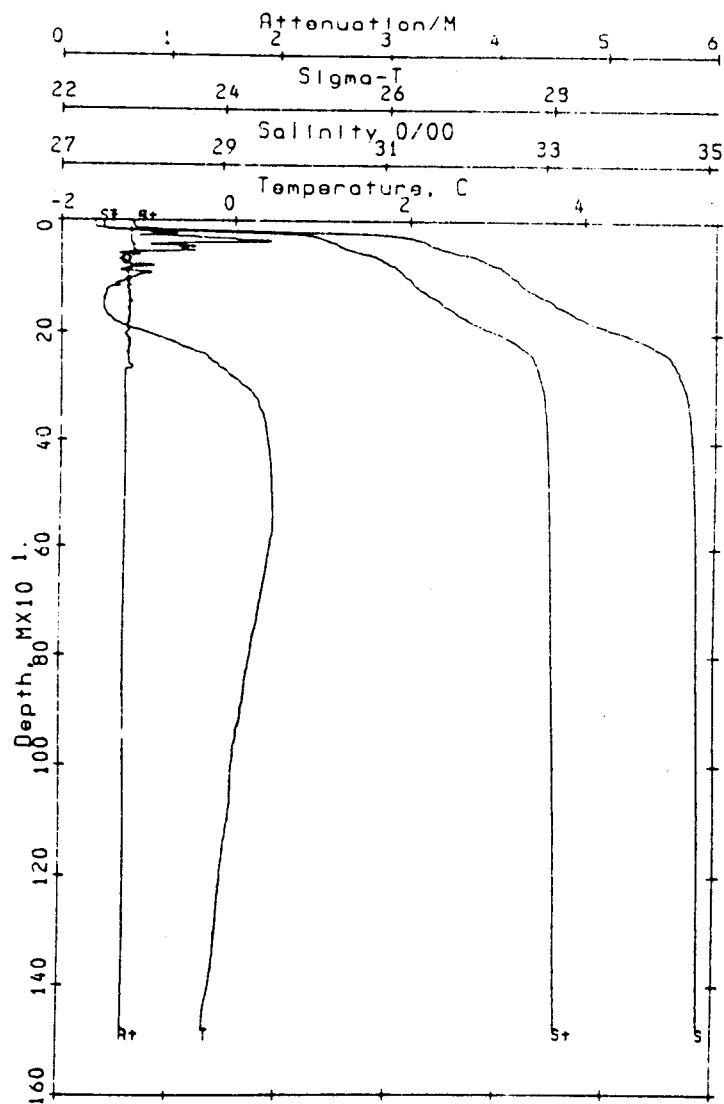


Ref. no. 40 Sta. c08 70.85 N  
Time = 862841507 Beaufort 143.71 W

374

STATION C09		CAST 41		DATE 11 OCT 86		TIME 1803		LATITUDE 70 56.80N		LONGITUDE 143 43.70W		BOTTOM DEPTH 1479 M	
PRESS db	TEMP °C	SAL	SIGMA-T	O <sub>2</sub> ml l <sup>-1</sup>	SiO <sub>4</sub> µm l <sup>-1</sup>	PO <sub>4</sub> µm l <sup>-1</sup>	NO <sub>3</sub> µm l <sup>-1</sup>	NO <sub>2</sub> µm l <sup>-1</sup>	NH <sub>3</sub> µm l <sup>-1</sup>	SPM mg l <sup>-1</sup>	PC µg l <sup>-1</sup>	LT.AT m <sup>-1</sup>	CHLR-A µg l <sup>-1</sup>
1.5	-1.510	27.920	22.424		3.78	0.85	0.12	0.00	0.00		102	0.59	.2
4.6	-1.509	27.917	22.422		3.75	0.86	0.11	0.00	0.00	0.8290	52	0.59	.2
9.7	-1.510	27.925	22.429		3.72	0.86	0.10	0.00	0.00		107	0.59	.2
19.0	-1.338	28.512*	22.903		3.48	0.86	0.09	0.00	0.00		151	0.60	.3
28.8	-0.259*	31.138	25.000	9.27	4.99	1.01	0.21	0.09	0.04		148	0.56	.2
49.0	-1.510	31.626	25.432	9.35	6.30	1.13	1.03	0.21	0.00		160	0.53	.1
99.7	-1.371	32.548	26.178	7.71	23.67	1.74	8.47	0.15	0.46	1.2017	193	0.54	.1
149.1	-1.516	33.120	26.646	6.49	34.46	2.14	15.47	0.00	0.00			0.54	
250.0	-0.302	34.544	27.754	6.60	15.99	1.14	13.69	0.00	0.00			0.54	
499.6	0.430	34.847	27.959	6.87	8.34	0.93	12.90	0.00	0.00	0.6500		0.56	
997.3	-0.016	34.894	28.022	6.97	7.99	0.90	12.89	0.00	0.00			0.58	
1478.5	-0.330	34.918	28.057	7.00	9.71	0.96	13.75	0.00	0.00	0.6865		0.59	

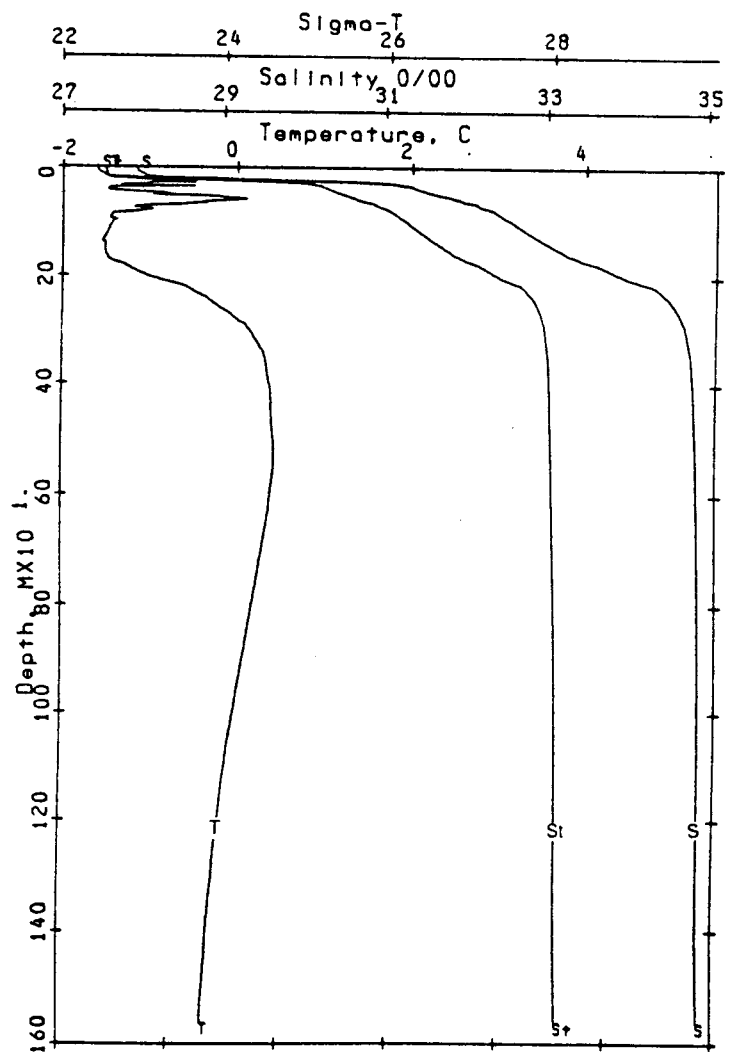
375



Ref. no. 41 Sta. 09 70.95 N  
Time = 862841803 Beaufort 143.73 W

STATION C10		CAST 42	DATE 11 OCT 86	TIME 2223	LATITUDE 71 01.20N	LONGITUDE 143 32.90W	BOTTOM DEPTH 1608 M						
PRESS db	TEMP °C	SAL	SIGMA-T	O <sub>2</sub> ml l <sup>-1</sup>	SiO <sub>4</sub> µm l <sup>-1</sup>	PO <sub>4</sub> µm l <sup>-1</sup>	NO <sub>3</sub> µm l <sup>-1</sup>	NO <sub>2</sub> µm l <sup>-1</sup>	NH <sub>3</sub> µm l <sup>-1</sup>	SPM mg l <sup>-1</sup>	PC µg l <sup>-1</sup>	LT.AT m <sup>-1</sup>	CHLR-A µg l <sup>-1</sup>
3.6	-1.499	27.915	22.421	9.19	4.24	0.92	0.03	0.00	0.07			0.58	
19.5	-1.410	29.620	23.803	9.41	5.08	1.08	0.22	0.05	0.13			0.58	
49.1	-1.453	31.629	25.433	9.06	7.15	1.26	1.49	0.19	0.16			0.54	
99.3	-1.351	32.520	26.154	7.73	27.56	2.01	9.76	0.12	0.63			0.54	
149.2	-1.525	33.100	26.629	6.72	34.69	2.22	15.23	0.00	0.04			0.55	
199.0	-0.972	34.015	27.354	6.13	30.48	1.83	15.83	0.00	0.08			0.54	
298.8	0.143	34.723	27.875	6.63	12.06	1.08	13.60	0.00	0.01			0.56	
499.0	0.429	34.850	27.961	6.82	8.57	1.02	13.37	0.00	0.10			0.56	
697.6	0.312	34.881	27.993	6.94	7.46	0.99	13.36	0.00	0.12			0.56	
998.8	-0.024	34.897	28.025	6.99	7.78	1.00	13.48	0.00	0.10			0.58	
1248.3	-0.213	34.909	28.044	6.97	8.31	1.06	13.72	0.00	0.05			0.59	
1562.9	-0.355	34.926	28.065	6.89	10.39	1.13	14.10	0.00	0.03			0.60	

377



Ref. no. 42  
Time = 862842223

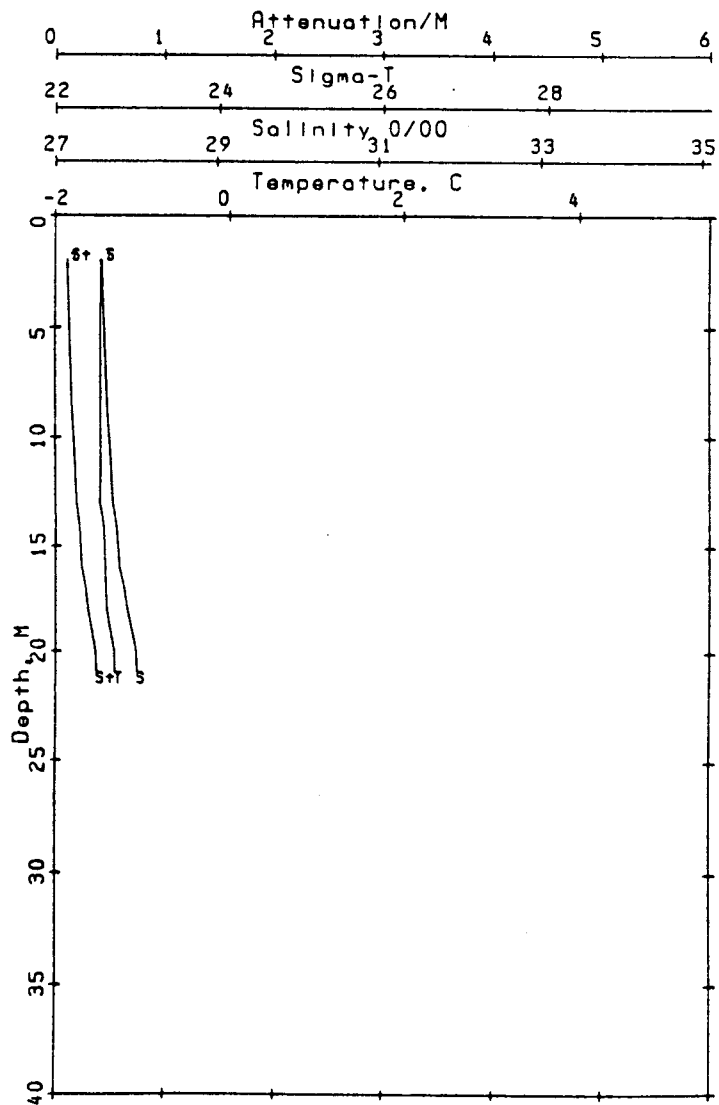
Sta. c10  
Beaufort

71.02 N  
143.55 W

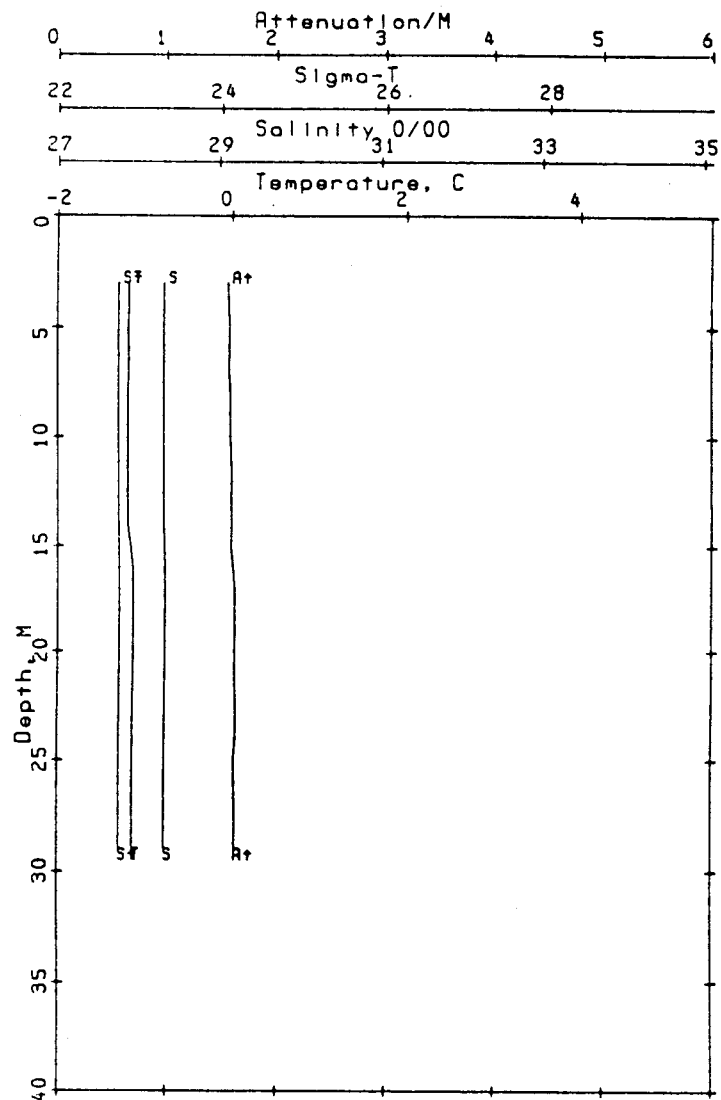
STATION D01		CAST 49	DATE 13 OCT 86	TIME 0230	LATITUDE 69 50.70N	LONGITUDE 141 30.80W	BOTTOM DEPTH 0026 M						
PRESS db	TEMP °C	SAL	SIGMA-T	O <sub>2</sub> ml l <sup>-1</sup>	SIO <sub>4</sub> µm l <sup>-1</sup>	PO <sub>4</sub> µm l <sup>-1</sup>	NO <sub>3</sub> µm l <sup>-1</sup>	NO <sub>2</sub> µm l <sup>-1</sup>	NH <sub>3</sub> µm l <sup>-1</sup>	SPM mg l <sup>-1</sup>	PC µg l <sup>-1</sup>	LT.AT m <sup>-1</sup>	CHLR-A µg l <sup>-1</sup>
3.7	-1.472	28.137	22.601	8.70	4.04	0.70	0.04	0.00	0.22				
20.7	-1.310	28.056	22.533	8.71	4.40	0.79	0.00	0.00	0.22				

STATION D02		CAST 50	DATE 13 OCT 86	TIME 0347	LATITUDE 69 53.50N	LONGITUDE 141 28.60W	BOTTOM DEPTH 0035 M						
PRESS db	TEMP °C	SAL	SIGMA-T	O <sub>2</sub> ml l <sup>-1</sup>	SIO <sub>4</sub> µm l <sup>-1</sup>	PO <sub>4</sub> µm l <sup>-1</sup>	NO <sub>3</sub> µm l <sup>-1</sup>	NO <sub>2</sub> µm l <sup>-1</sup>	NH <sub>3</sub> µm l <sup>-1</sup>	SPM mg l <sup>-1</sup>	PC µg l <sup>-1</sup>	LT.AT m <sup>-1</sup>	CHLR-A µg l <sup>-1</sup>
4.4	-1.191	28.326	22.750	8.40	3.12	0.69	0.00	0.00	0.19	2.7030	230	1.56	
9.5	-1.170	28.329	22.752							2.5737	220	1.58	
19.5	-1.134	28.340	22.761	8.41	3.22	0.69	0.00	0.00	0.21	2.2965	355	1.59	
28.8	-1.129	28.340	22.761	8.38	3.21	0.68	0.00	0.00	0.22	2.2210		1.62	

379

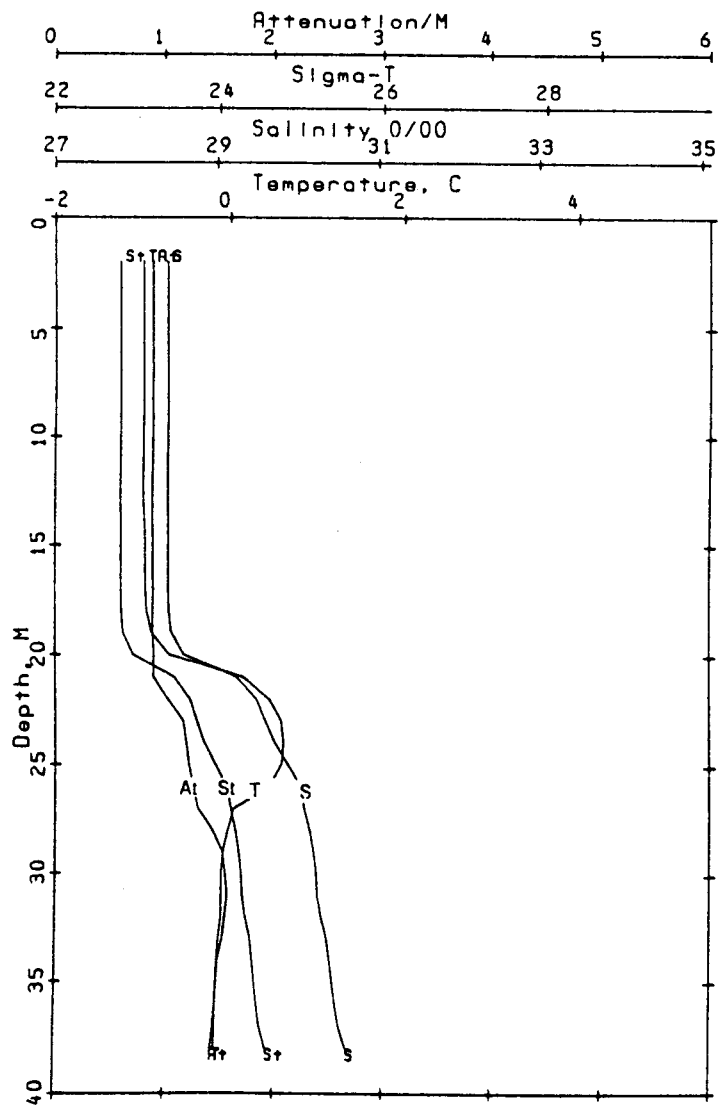


Ref. no. 49 Sta. d01 69.84 N  
 Time = 862860230 Beaufort 141.51 W

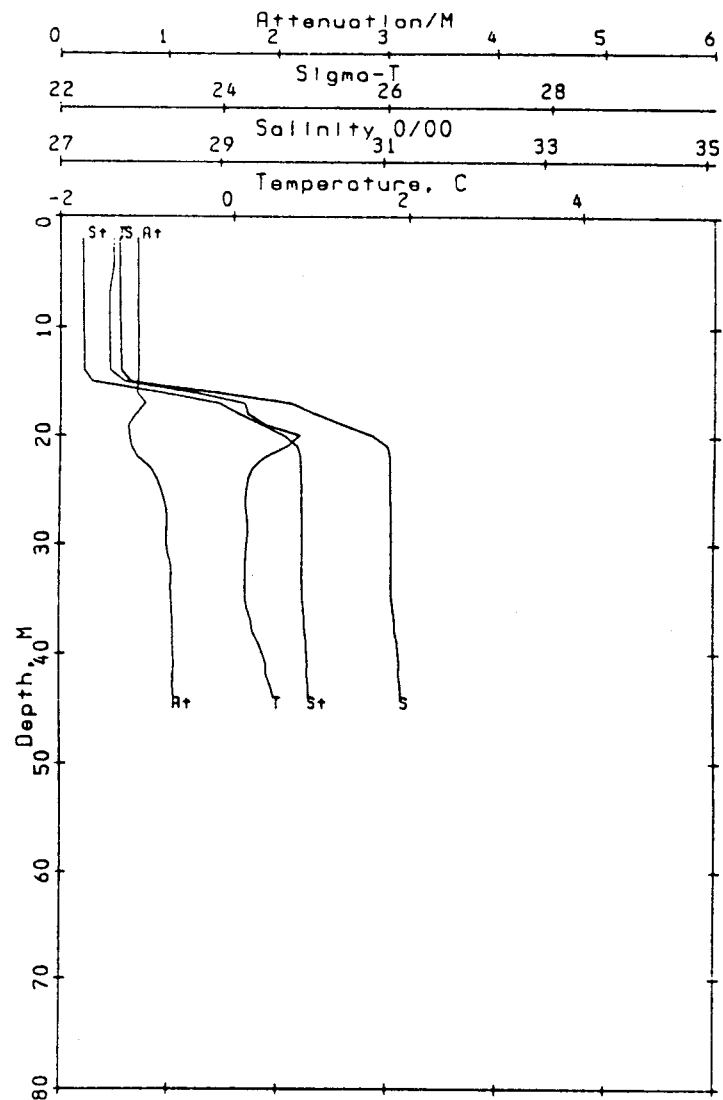


Ref. no. 50 Sta. d02 69.89 N  
 Time = 862860348 Beaufort 141.48 W





Ref. no. 51 Sta. d03 70.00 N  
 Time = 862860606 Beaufort 141.42 W

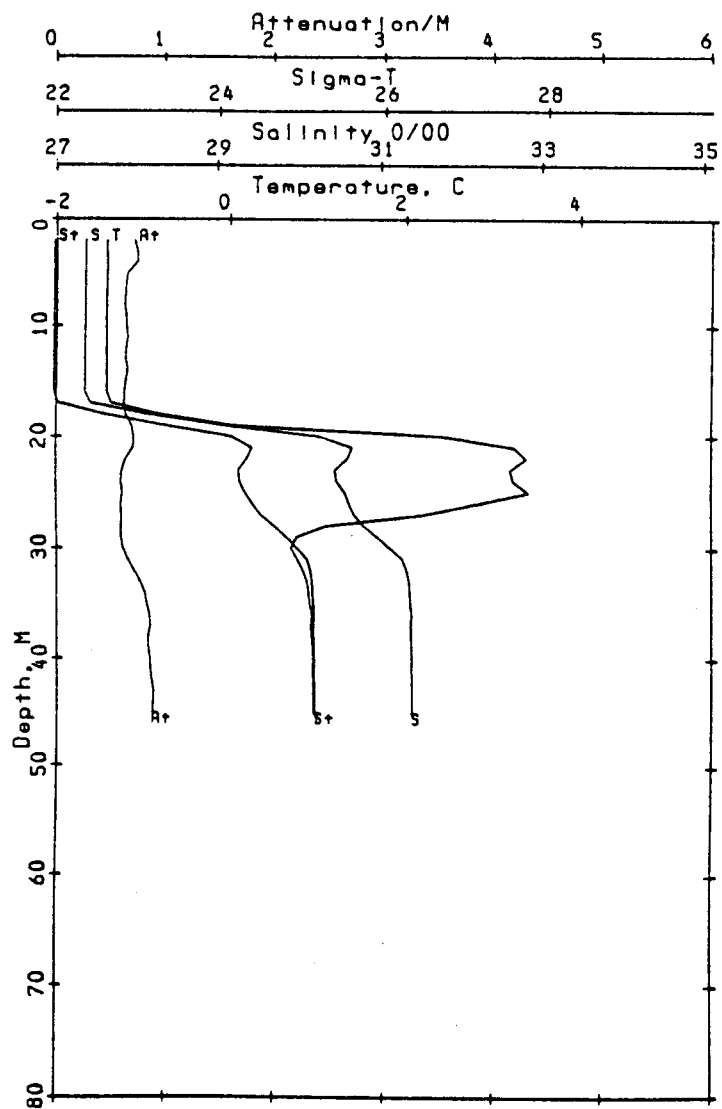


Ref. no. 52 Sta. d04 70.11 N  
 Time = 862860725 Beaufort 141.43 W

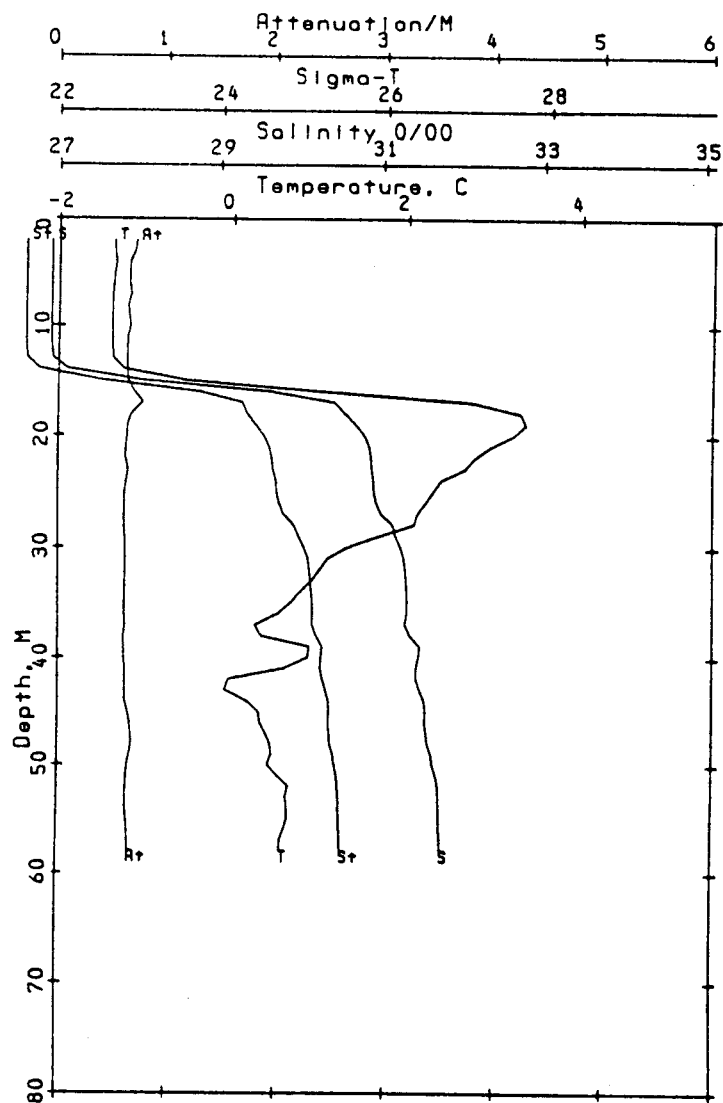
STATION D05		CAST 53	DATE 13 OCT 86		TIME 0847	LATITUDE 70 13.00N		LONGITUDE 141 23.30W		BOTTOM DEPTH 0052 M			
PRESS db	TEMP °C	SAL	SIGMA-T	O <sub>2</sub> ml l <sup>-1</sup>	SiO <sub>4</sub> µm l <sup>-1</sup>	PO <sub>4</sub> µm l <sup>-1</sup>	NO <sub>3</sub> µm l <sup>-1</sup>	NO <sub>2</sub> µm l <sup>-1</sup>	NH <sub>3</sub> µm l <sup>-1</sup>	SPM mg l <sup>-1</sup>	PC µg l <sup>-1</sup>	LT.AT m <sup>-1</sup>	CHLR-A µg l <sup>-1</sup>
0.4	-1.393	27.362	21.972	8.60	2.74	0.62	0.00	0.00	0.02		202	0.64	.0
4.3	-1.417	27.361	21.971	8.62	2.68	0.66	0.00	0.00	0.07	1.3090	248	0.63	.1
9.5	-1.413	27.360	21.970	8.50	2.72	0.71	0.00	0.00	0.60		123	0.63	.1
18.6	3.195*	30.633*	24.385	8.15	3.20	0.79	0.00	0.00	0.76		116	0.59	.2
29.2	0.645	31.139*	24.961	8.34	7.56	1.77	0.07	0.06	0.76	0.8700	69	0.69	.1
39.4	0.946	31.394	25.149	8.04	7.89	0.95	0.00	0.07	1.18	1.9880	330	0.91	
45.1	0.946	31.395	25.150	8.07	7.93	0.93	0.74	0.07	1.20	1.5575	170	0.90	

STATION D06		CAST 54	DATE 13 OCT 86		TIME 1039	LATITUDE 70 19.90N		LONGITUDE 141 21.20W		BOTTOM DEPTH 0066 M			
PRESS db	TEMP °C	SAL	SIGMA-T	O <sub>2</sub> ml l <sup>-1</sup>	SiO <sub>4</sub> µm l <sup>-1</sup>	PO <sub>4</sub> µm l <sup>-1</sup>	NO <sub>3</sub> µm l <sup>-1</sup>	NO <sub>2</sub> µm l <sup>-1</sup>	NH <sub>3</sub> µm l <sup>-1</sup>	SPM mg l <sup>-1</sup>	PC µg l <sup>-1</sup>	LT.AT m <sup>-1</sup>	CHLR-A µg l <sup>-1</sup>
3.6	-1.372	26.913	21.607	8.42	3.48	0.76	0.12	0.00	0.22			0.65	
19.3	3.268*	30.699*	24.432	7.73	3.63	0.76	0.11	0.01	0.97			0.63	
49.7	0.460	31.659	25.389	8.17	7.89	0.95	1.30	0.18	0.86			0.64	
58.1	0.317	32.005	25.674	8.01	9.23	1.03	1.79	0.18	0.89			0.63	

383



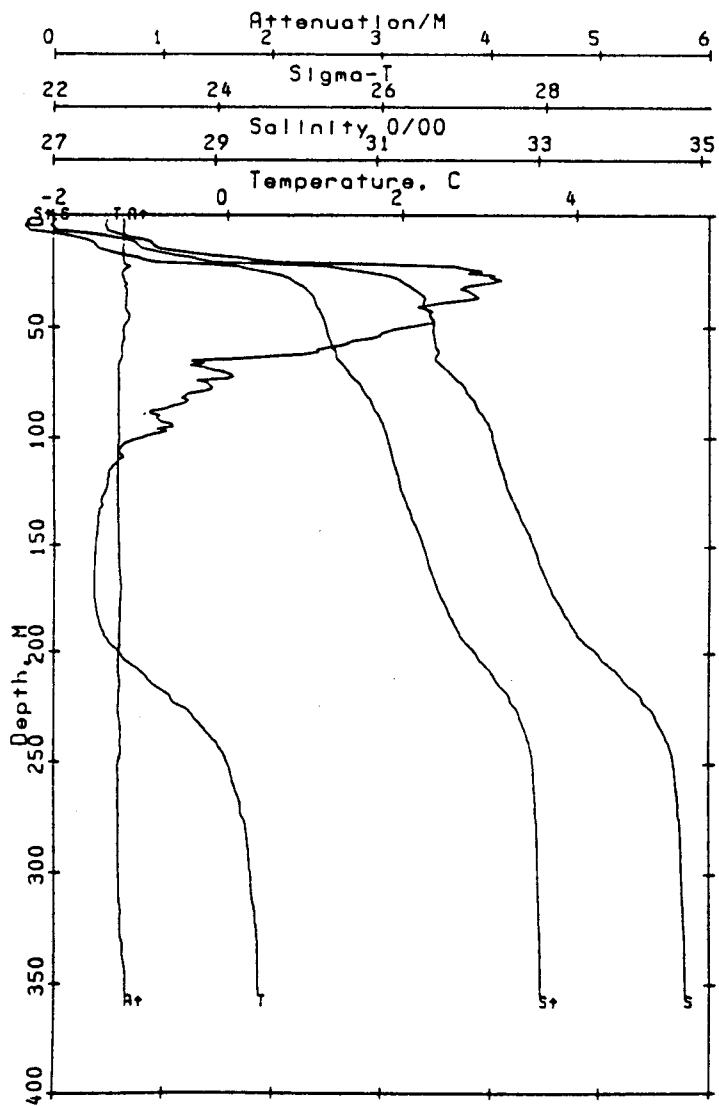
Ref. no. 53      Sta. d05      70.22 N  
 Time = 862860847      Beaufort      141.39 W



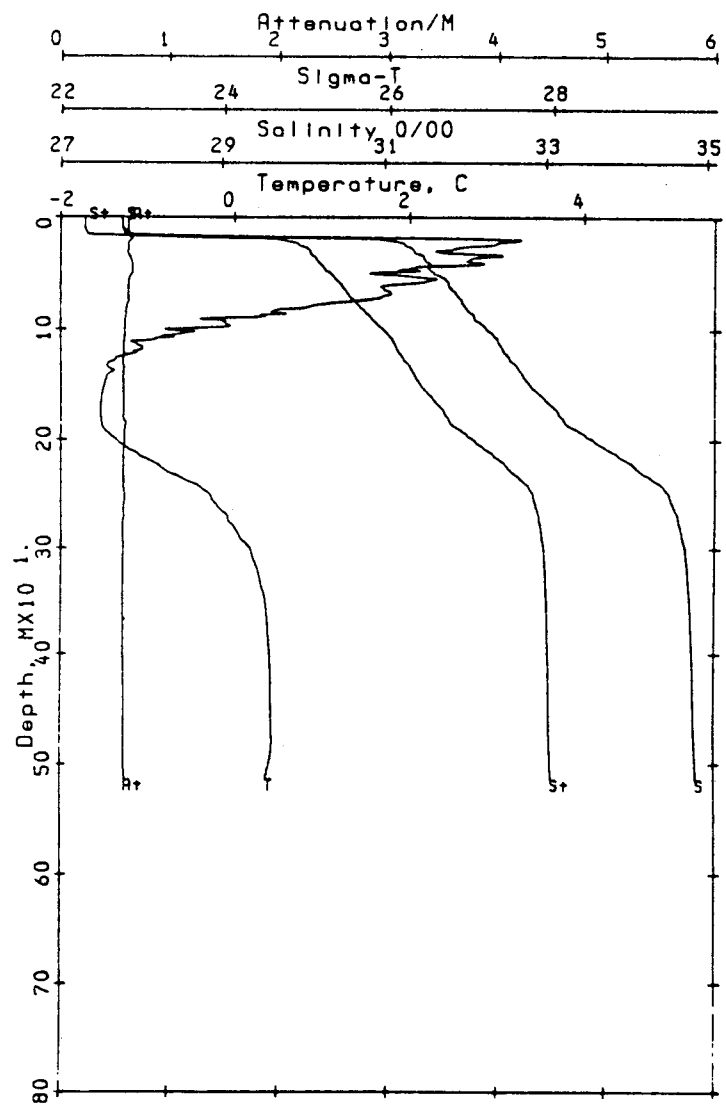
Ref. no. 54      Sta. d06      70.33 N  
 Time = 862861039      Beaufort      141.35 W

STATION D07		CAST 55	DATE 13 OCT 86	TIME 1239	LATITUDE 70 25.50N		LONGITUDE 141 19.70W		BOTTOM DEPTH 0359 M				
PRESS db	TEMP °C	SAL	SIGMA-T	O <sub>2</sub> ml l <sup>-1</sup>	SiO <sub>4</sub> µm l <sup>-1</sup>	PO <sub>4</sub> µm l <sup>-1</sup>	NO <sub>3</sub> µm l <sup>-1</sup>	NO <sub>2</sub> µm l <sup>-1</sup>	NH <sub>3</sub> µm l <sup>-1</sup>	SPM mg l <sup>-1</sup>	PC µg l <sup>-1</sup>	LT.AT m <sup>-1</sup>	CHLR-A µg l <sup>-1</sup>
1.4	-1.408	26.960	21.646	8.61	3.16	0.74	0.00	0.00	0.00		243	0.62	.1
4.3	-1.408	26.972	21.655	8.57	2.56	0.71	0.00	0.00	0.00	0.7555	245	0.63	.1 .1
8.9	-0.833	27.999*	22.479	8.49	2.17	0.71	0.00	0.00	0.00		120	0.63	.1 .2
18.7	-0.224*	28.715*	23.042	7.96	2.86	0.75	0.11	0.01	0.70		167	0.63	.2 .1
29.1	3.087*	31.257*	24.891	7.59	5.07	0.86	0.33	0.07	1.23		67	0.63	.1 .1
48.9	2.325	31.674	25.284	7.81	6.30	0.90	0.78	0.15	1.22	0.6230	95	0.67	.2
99.1	-0.878	32.398	26.041	7.65	20.27	1.41	6.66	0.17	0.69			0.58	
164.0	-1.544	33.055	26.594	6.61	32.20	1.67	13.38	0.01	0.08	1.1360		0.59	
354.6	0.340	34.808	27.932	6.44	10.64	0.93	12.61	0.01	0.15	0.9955		0.65	

STATION D08		CAST 56	DATE 13 OCT 86	TIME 1612	LATITUDE 70 32.20N		LONGITUDE 141 19.50W		BOTTOM DEPTH 0518 M				
PRESS db	TEMP °C	SAL	SIGMA-T	O <sub>2</sub> ml l <sup>-1</sup>	SiO <sub>4</sub> µm l <sup>-1</sup>	PO <sub>4</sub> µm l <sup>-1</sup>	NO <sub>3</sub> µm l <sup>-1</sup>	NO <sub>2</sub> µm l <sup>-1</sup>	NH <sub>3</sub> µm l <sup>-1</sup>	SPM mg l <sup>-1</sup>	PC µg l <sup>-1</sup>	LT.AT m <sup>-1</sup>	CHLR-A µg l <sup>-1</sup>
4.0	-1.271	27.753	22.287	8.41	3.71	0.72	0.00	0.00	0.22			0.62	
20.4	3.286*	31.152*	24.791	7.59	4.72	0.75	0.26	0.02	1.08			0.62	
49.2	1.858*	31.661	25.307	8.11	6.50	0.87	0.62	0.14	1.19			0.63	
99.7	-0.378	32.265	25.915	7.70	15.83	1.30	4.90	0.20	1.26			0.58	
148.1	-1.487	32.762	26.354	6.95	28.72	1.63	11.55	0.11	0.27			0.56	
200.0	-1.395	33.537	26.981	6.35	32.01	1.60	14.35	0.01	0.06			0.57	
300.1	0.146	34.728	27.879	6.33	11.96	0.95	12.86	0.01	0.08			0.56	
498.9	0.407	34.867	27.976	6.56	8.66	0.87	12.22	0.01	0.00			0.59	
513.4	0.363	34.876	27.986	6.61	8.70	0.88	12.66	0.01	0.00			0.61	



Ref. no. 55 Sta. d07 70.42 N  
 Time = 862861239 Beaufort 141.33 W

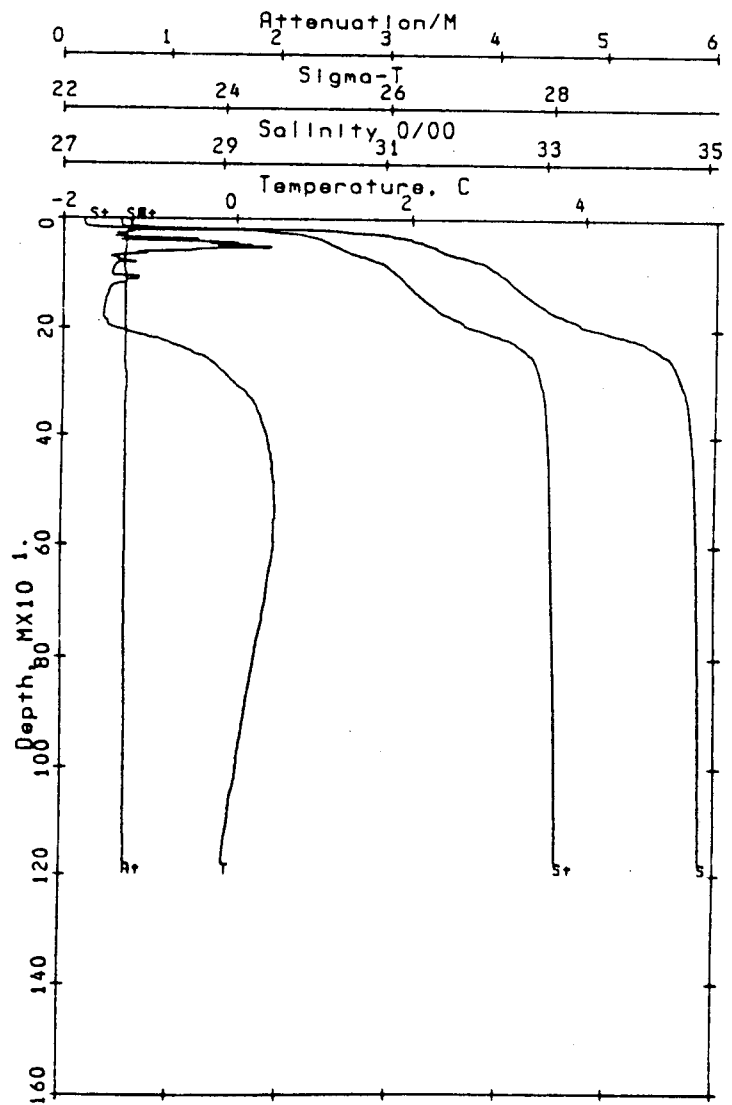


Ref. no. 56 Sta. d08 70.54 N  
 Time = 862861612 Beaufort 141.32 W

386

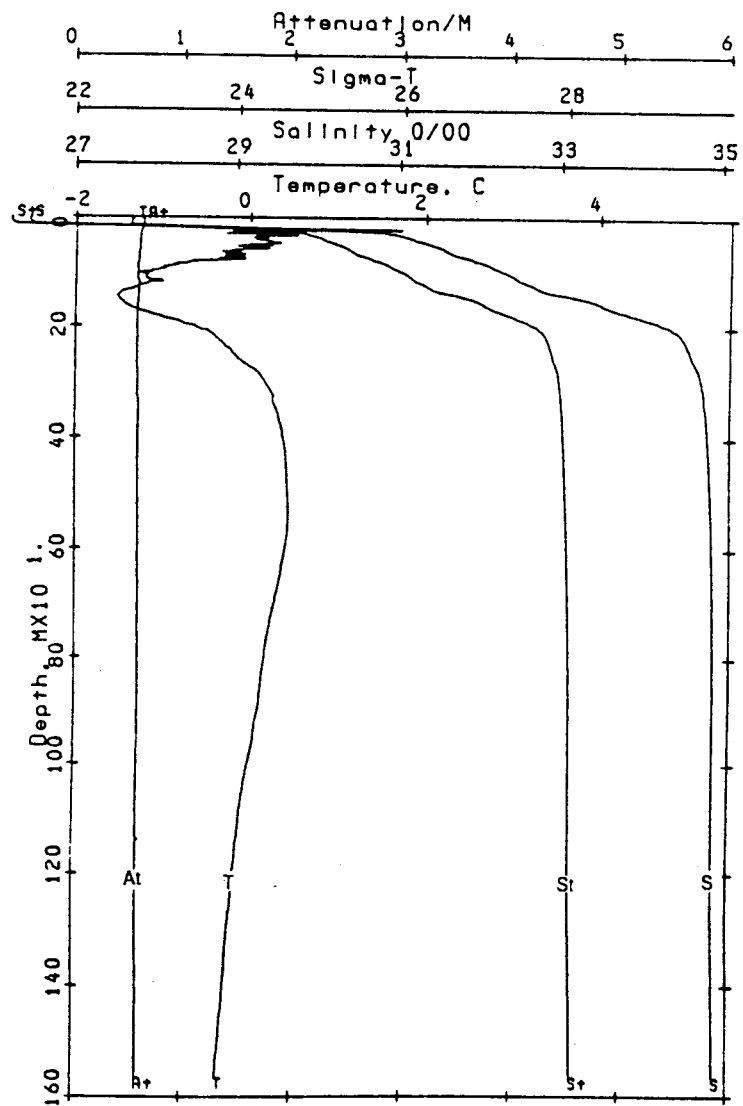
STATION D09		CAST 57		DATE 13 OCT 86		TIME 2006		LATITUDE 70 38.60N		LONGITUDE 141 18.00W		BOTTOM DEPTH 1177 M	
PRESS db	TEMP °C	SAL	SIGMA-T	O <sub>2</sub> ml l <sup>-1</sup>	SiO <sub>4</sub> µm l <sup>-1</sup>	PO <sub>4</sub> µm l <sup>-1</sup>	NO <sub>3</sub> µm l <sup>-1</sup>	NO <sub>2</sub> µm l <sup>-1</sup>	NH <sub>3</sub> µm l <sup>-1</sup>	SPM mg l <sup>-1</sup>	PC µg l <sup>-1</sup>	LT.AT m <sup>-1</sup>	CHLR-A µg l <sup>-1</sup>
1.6	-1.234	27.715	22.256	6.63	3.24	0.69	0.06	0.00	0.12		116	0.62	.3
4.6	-1.234	27.715	22.256	6.91	8.64	0.86	12.42	0.00	0.11		166	0.62	.3
9.6	-1.234	27.714	22.255	7.60	3.56	0.75	0.17	0.00	0.06		268	0.62	.4
18.5	-0.845*	27.961*	22.449	8.55	3.67	0.73	0.15	0.00	0.07		189	0.62	.1
28.6	0.389	31.096*	24.938	8.52	3.46	0.70	0.01	0.00	0.08		86	0.56	.3
49.3	-0.485*	31.482	25.286	8.65	3.13	0.75	0.00	0.00	0.23		51	0.56	.1
98.3	-1.199	32.369	26.027	8.76	4.32	0.88	0.24	0.05	0.43	0.4275		0.55	.0
149.2	-1.510	32.817	26.399	8.69	6.05	0.94	0.84	0.24	0.20			0.56	.1
198.5	-1.458	33.492	26.946	7.50	20.30	1.33	7.41	0.12	0.39			0.56	
299.0	-0.087	34.640	27.820	6.80	30.02	1.60	11.93	0.03	0.00			0.57	
499.3	0.445	34.851	27.961	6.32	29.16	1.55	13.39	0.00	0.00	1.0530		0.57	
1177.7	-0.125	34.911	28.041	6.28	12.96	0.97	12.89	0.00	0.00	0.4405		0.59	

387



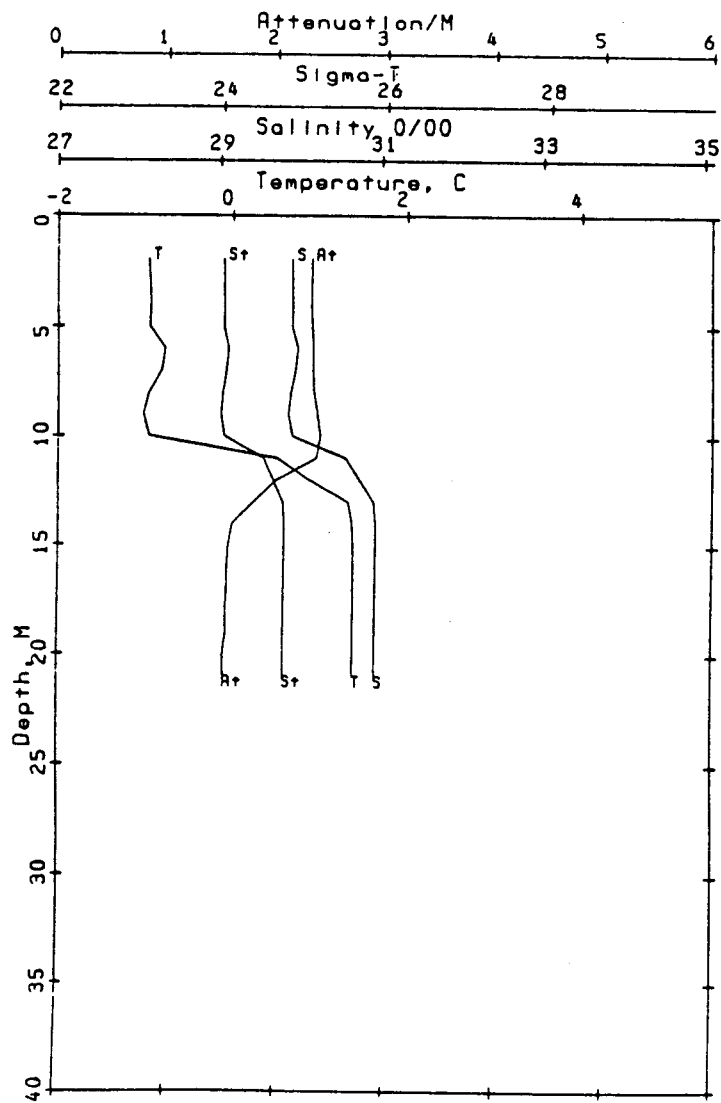
Ref. no. 57      Sta. d09      70.64 N  
Time = 862862006      Beaufort      141.30 W

STATION D10		CAST 58	DATE 14 OCT 86	TIME 0207	LATITUDE 70 43.10N		LONGITUDE 140 57.10W		BOTTOM DEPTH 1758 M				
PRESS db	TEMP °C	SAL	SIGMA-T	O <sub>2</sub> ml l <sup>-1</sup>	SiO <sub>4</sub> µm l <sup>-1</sup>	PO <sub>4</sub> µm l <sup>-1</sup>	NO <sub>3</sub> µm l <sup>-1</sup>	NO <sub>2</sub> µm l <sup>-1</sup>	NH <sub>3</sub> µm l <sup>-1</sup>	SPM mg l <sup>-1</sup>	PC µg l <sup>-1</sup>	LT.AT m <sup>-1</sup>	CHLR-A µg l <sup>-1</sup>
4.1	-1.360	26.196	21.026	8.78	5.31	0.76	0.03	0.00	0.00			0.61	
18.8	-0.802*	28.455*	22.848	8.95	4.14	0.80	0.03	0.00	0.00			0.59	
48.7	-0.122*	31.366	25.179	8.45	7.07	0.99	0.79	0.22	0.23			0.58	
98.5	-1.014	32.239	25.916	7.71	20.14	1.47	6.97	0.12	0.31			0.55	
148.4	-1.510	33.101	26.630	6.79	32.88	1.75	13.49	0.03	0.00			0.56	
198.9	-0.724	34.269	27.550	6.13	23.61	1.26	14.22	0.00	0.00			0.55	
298.6	0.158	34.734	27.883	6.44	12.06	0.92	13.18	0.00	0.00			0.56	
499.1	0.462	34.858	27.965	6.69	8.83	0.92	13.01	0.00	0.00			0.56	
698.7	0.277	34.889	28.001	6.82	8.57	0.91	13.05	0.00	0.00			0.57	
998.3	-0.005	34.903	28.028	6.86	8.54	0.85	12.96	0.00	0.00			0.58	
1248.6	-0.167	34.911	28.043	6.83	8.73	0.86	13.22	0.00	0.00			0.59	
1566.0	-0.343	34.928	28.066	6.77	10.52	0.94	13.98	0.00	0.00			0.59	

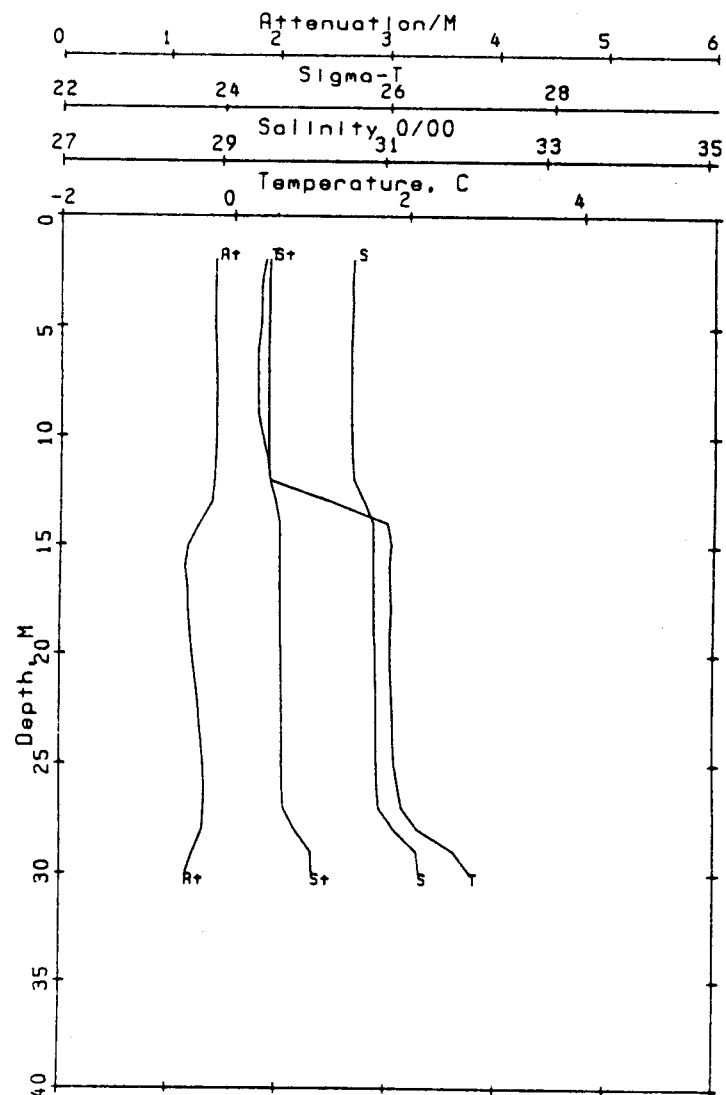


Ref. no. 58      Sta. d10      70.72 N  
 Time = 862870207      Beaufort      140.95 W





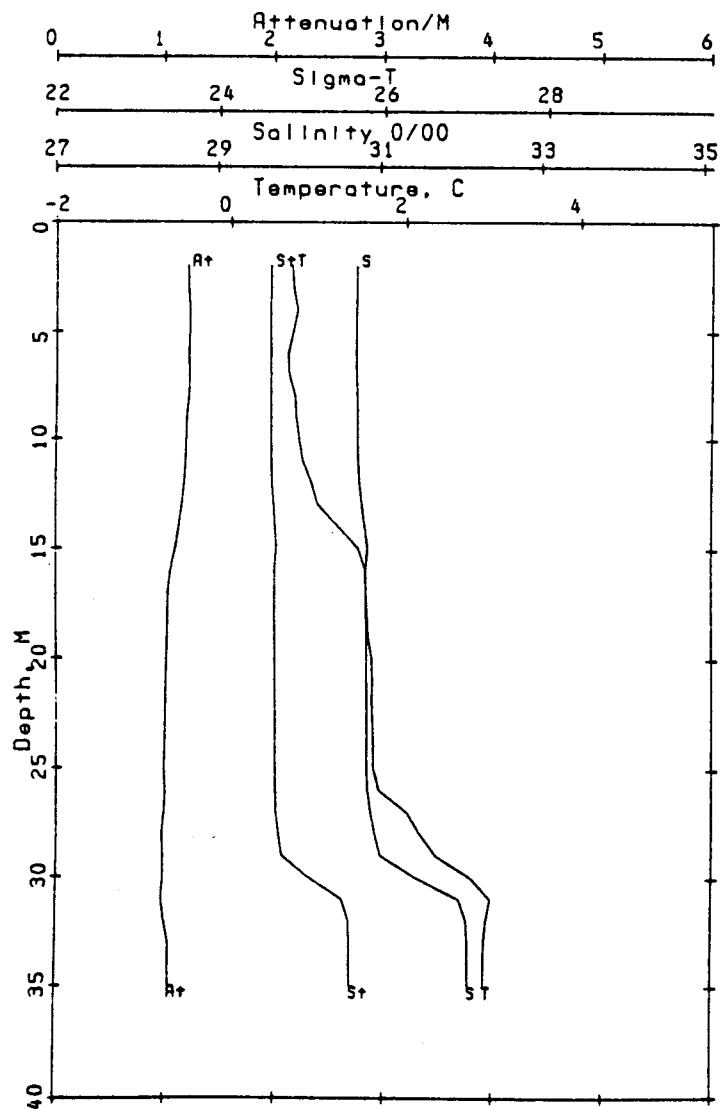
Ref. no. 59      Sta. e01      71.00 N  
 Time = 862891857      Beaufort      150.11 W



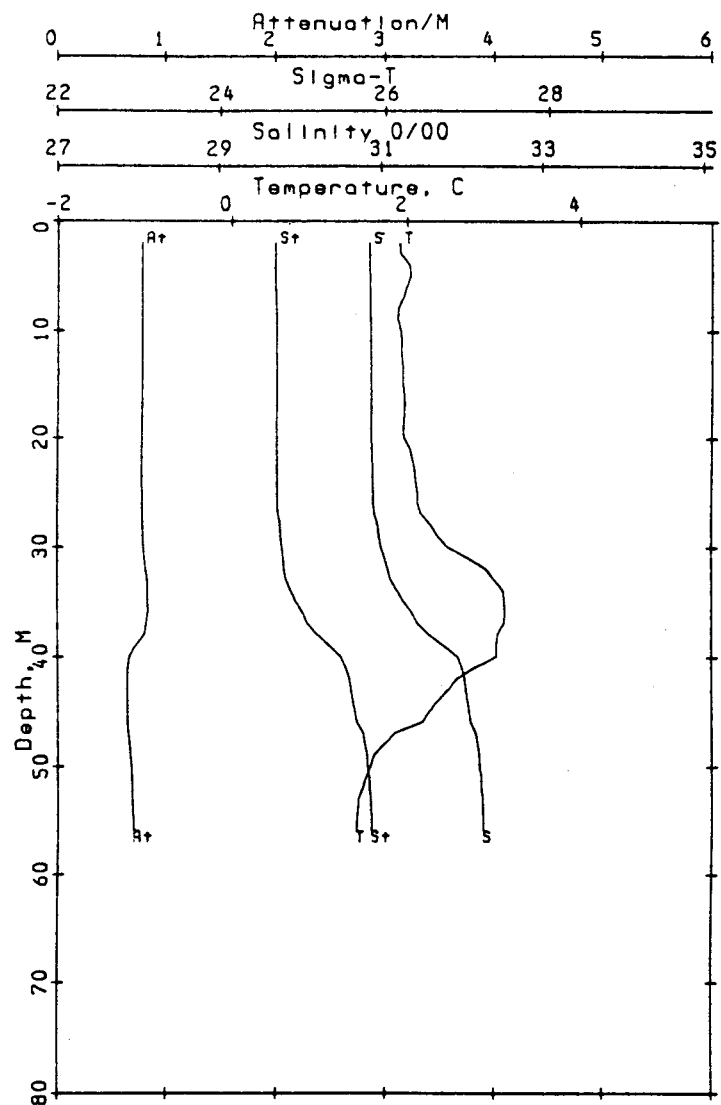
Ref. no. 60      Sta. e02      71.08 N  
 Time = 862892008      Beaufort      150.07 W

STATION E03		CAST 61	DATE 16 OCT 86	TIME 2050	LATITUDE 71 06.60N	LONGITUDE 150 02.60W	BOTTOM DEPTH 0041 M						
PRESS	TEMP	SAL	SIGMA-T	O <sub>2</sub>	SiO <sub>4</sub>	PO <sub>4</sub>	NO <sub>3</sub>	NO <sub>2</sub>	NH <sub>3</sub>	SPM	PC	LT.AT	CHLR-A
db	°C			ml l <sup>-1</sup>	µm l <sup>-1</sup>	µm l <sup>-1</sup>	µm l <sup>-1</sup>	µm l <sup>-1</sup>	µm l <sup>-1</sup>	mg l <sup>-1</sup>	µg l <sup>-1</sup>	m <sup>-1</sup>	µg l <sup>-1</sup>
4.4	0.775	30.715	24.613	7.70	5.64	0.62	0.00	0.04	1.06			1.19	
20.6	1.615	30.833	24.660	7.54	6.52	0.66	0.00	0.03	1.34			1.00	
35.2	2.899	32.109	25.587	7.00	9.19	0.80	0.00	0.07	2.20			1.10	

STATION E04		CAST 63	DATE 16 OCT 86	TIME 2243	LATITUDE 71 12.00N	LONGITUDE 149 59.40W	BOTTOM DEPTH 0062 M						
PRESS	TEMP	SAL	SIGMA-T	O <sub>2</sub>	SiO <sub>4</sub>	PO <sub>4</sub>	NO <sub>3</sub>	NO <sub>2</sub>	NH <sub>3</sub>	SPM	PC	LT.AT	CHLR-A
db	°C			ml l <sup>-1</sup>	µm l <sup>-1</sup>	µm l <sup>-1</sup>	µm l <sup>-1</sup>	µm l <sup>-1</sup>	µm l <sup>-1</sup>	mg l <sup>-1</sup>	µg l <sup>-1</sup>	m <sup>-1</sup>	µg l <sup>-1</sup>
0.9	1.922	30.891	24.686	7.57	7.74	0.70	0.30	0.05	1.56		503	0.78	.4
3.7	1.992	30.883	24.675	7.46	7.31	0.75	0.27	0.05	1.38	0.9140	000	0.79	.5
8.9	1.917	30.889	24.685	7.48	7.21	0.70	0.24	0.06	1.47	1.1690	049	0.79	.4
18.9	2.009	30.898	24.686	7.47	7.10	0.66	0.21	0.06	1.42	1.2715	228	0.79	.2
29.2	2.215*	30.946	24.710	7.39	7.42	0.74	0.23	0.06	1.33	1.4705	000	0.80	.3
49.0	1.517	32.245	25.798	7.42	10.18	0.93	2.20	0.11	1.66	0.7530	325	0.70	.3
56.0	1.423	32.271	25.825	7.43	10.18	0.98	2.21	0.12	1.68	1.5610	000	0.73	.1



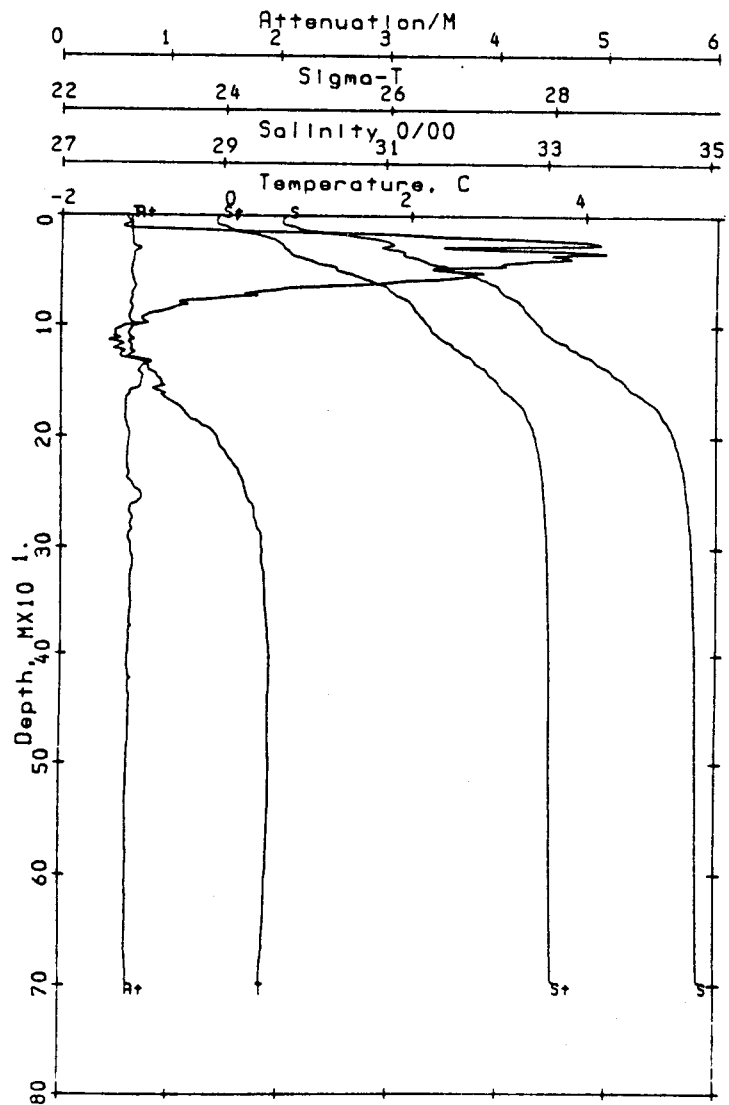
Ref. no. 61 Sta. e03 71.11 N  
 Time = 862892050 Beaufort 150.04 W



Ref. no. 63 Sta. e04 71.20 N  
 Time = 862892243 Beaufort 149.99 W

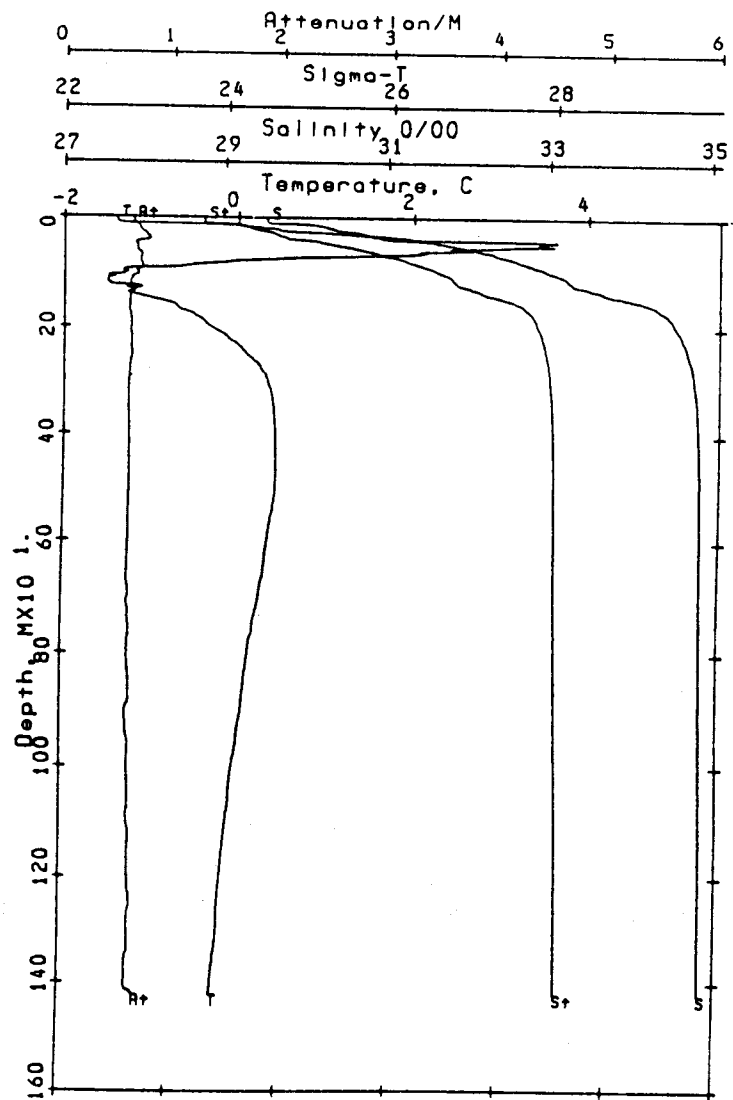
STATION E05		CAST 64	DATE 17 OCT 86	TIME 0026	LATITUDE 71 16.30N		LONGITUDE 149 57.90W		BOTTOM DEPTH 0700 M				
PRESS db	TEMP °C	SAL	SIGMA-T	O <sub>2</sub> ml l <sup>-1</sup>	SiO <sub>4</sub> μm l <sup>-1</sup>	PO <sub>4</sub> μm l <sup>-1</sup>	NO <sub>3</sub> μm l <sup>-1</sup>	NO <sub>2</sub> μm l <sup>-1</sup>	NH <sub>3</sub> μm l <sup>-1</sup>	SPM mg l <sup>-1</sup>	PC μg l <sup>-1</sup>	LT.AT m <sup>-1</sup>	CHLR-A μg l <sup>-1</sup>
1.1	-1.323	29.685	23.854	8.26	2.85	0.51	0.00	0.02	0.00		31	0.64	.4 .3
3.9	-1.332	29.694	23.861	8.16	3.48	0.55	0.00	0.02	0.36	0.4965	238	0.63	.4 .2
8.3	-1.239	29.815	23.958	8.06	3.89	0.61	0.00	0.03	0.50			0.64	.3 .4
19.3	1.819*	30.363*	24.270	7.50	5.57	0.70	0.00	0.03	0.95		19	0.63	.2 .2
28.6	3.490*	31.083	24.718	7.23	6.94	0.75	0.01	0.04	1.75		698	0.65	.2 .2
48.7	2.266	31.771*	25.366	7.48	7.46	0.77	0.68	0.08	1.39	0.7150	470	0.62	.5
113.6	-1.413	33.149	26.666	7.50 6.78	7.66 29.48	0.78 1.74	0.72 12.41	0.08 0.13	1.54 0.86	0.6550		0.65	
149.0	-0.859	33.910	27.264	6.44 6.40	25.22 25.00	1.37 1.35	13.36 13.35	0.14 0.14	0.65 0.71			0.72	
198.6	-0.308	34.530	27.742	6.29 6.29	15.34 15.23	0.96 0.97	13.07 13.02	0.08 0.08	0.06 0.03			0.61	
298.5	0.303	34.784	27.915	6.62	9.28	0.77	12.55	0.04	0.06			0.60	
697.4	0.300	34.881	27.994	6.76	8.00	0.71	12.55	0.08	0.03	1.1385		0.62	

395



Ref. no. 64      Sta. a05      71.27 N  
Time = 862900026      Beaufort      149.96 W

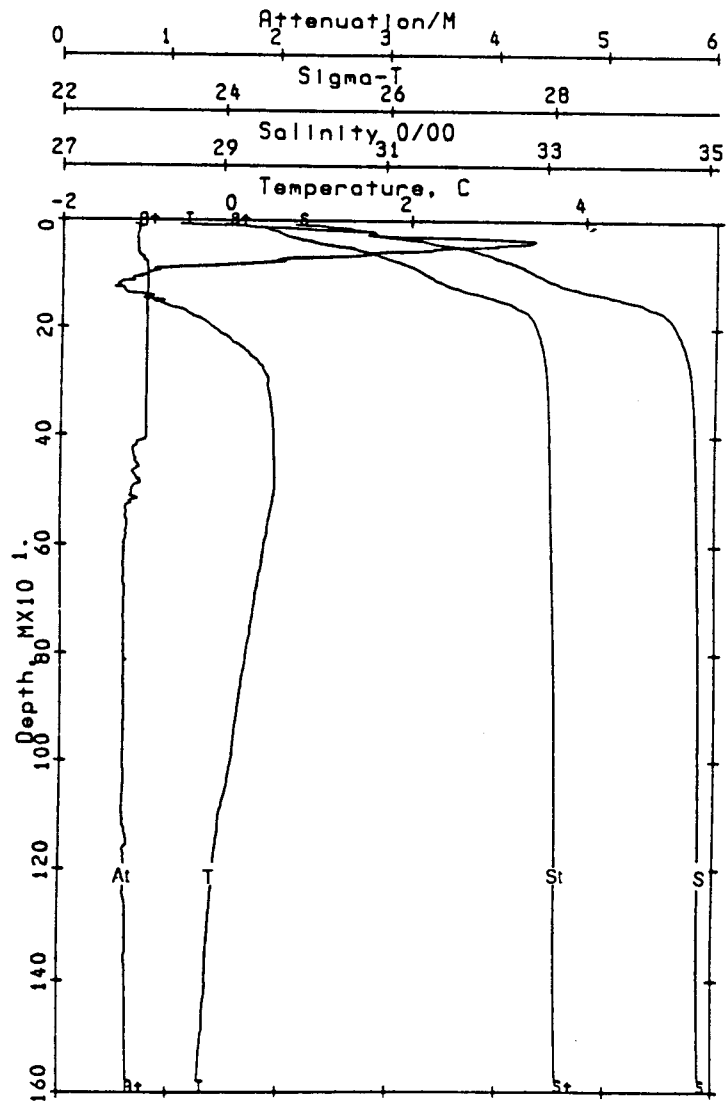
STATION E06		CAST 65	DATE 17 OCT 86	TIME 0155	LATITUDE 71 21.70N	LONGITUDE 149 56.20W	BOTTOM DEPTH 1421 M						
PRESS db	TEMP °C	SAL	SIGMA-T	O <sub>2</sub> ml l <sup>-1</sup>	SiO <sub>4</sub> μm l <sup>-1</sup>	PO <sub>4</sub> μm l <sup>-1</sup>	NO <sub>3</sub> μm l <sup>-1</sup>	NO <sub>2</sub> μm l <sup>-1</sup>	NH <sub>3</sub> μm l <sup>-1</sup>	SPM mg l <sup>-1</sup>	PC μg l <sup>-1</sup>	LT.AT m <sup>-1</sup>	CHLR-A μg l <sup>-1</sup>
1.2	-1.324	29.516	23.717	8.20	2.89	0.59	0.05	0.02	0.53		512	0.61	.8
3.6	-1.305	29.511	23.713	8.32	1.60	0.53	0.04	0.02	0.21	0.6995	300	0.61	.1 .0
8.7	-0.992	29.656	23.823	8.05	4.46	0.60	0.03	0.03	0.71		340	0.62	.0 .1
18.8	0.329	30.293	24.295	7.86	5.61	0.68	0.01	0.04	1.27		518	0.67	.2 .1
28.6	1.217*	30.699	24.576	7.69	6.77	0.78	0.00	0.04	1.51	0.6600	483	0.72	.1 .5
48.6	3.491	31.699	25.208	7.30	6.86	0.75	0.33	0.09	1.84		484	0.62	.5 .6
114.0	-1.458	33.244	26.744	6.65	31.23	1.55	13.47	0.08	0.47	0.6000		0.59	
498.6	0.391	34.858	27.970	6.80	8.22	0.75	12.43	0.06	0.00			0.61	
698.5	0.257	34.884	27.999	6.88	7.78	0.76	12.54	0.03	0.00			0.59	
999.0	-0.011	34.899	28.025	6.96	7.77	0.78	12.70	0.03	0.00			0.58	
1247.8	-0.174	34.909	28.042	6.96	8.71	0.81	12.87	0.03	0.18			0.63	
1423.3	-0.251	34.914	28.050	6.95	9.02	0.78	13.03	0.03	0.00	0.4545		0.69	



Ref. no.	65	Sta.	e06	71.36 N
Time =	862900155	Beaufort		149.94 W

STATION E07		CAST 66	DATE 17 OCT 86	TIME 0506	LATITUDE 71 25.30N	LONGITUDE 149 54.30W	BOTTOM DEPTH 1780 M						
PRESS	TEMP	SAL	SIGMA-T	O <sub>2</sub>	SiO <sub>4</sub>	PO <sub>4</sub>	NO <sub>3</sub>	NO <sub>2</sub>	NH <sub>3</sub>	SPM	PC	LT.AT	CHLR-A
db	°C			ml l <sup>-1</sup>	μm l <sup>-1</sup>	μm l <sup>-1</sup>	μm l <sup>-1</sup>	μm l <sup>-1</sup>	μm l <sup>-1</sup>	mg l <sup>-1</sup>	μg l <sup>-1</sup>	m <sup>-1</sup>	μg l <sup>-1</sup>
4.5	-1.429	29.373	23.602	8.45	2.44	0.59	0.05	0.01	0.16			0.61	
18.6	1.359*	30.609	24.496	7.50	5.09	0.75	0.13	0.04	0.95			0.67	
48.5	2.048	32.071	25.623	7.73	6.36	0.88	0.60	0.05	1.47			0.62	
123.3	-1.352	33.327	26.809	6.56	16.22	1.14	13.22	0.04	0.00			0.60	
148.6	-0.793	34.002	27.337	6.46	24.80	1.47	13.94	0.09	0.00			0.62	
199.1	-0.271	34.582	27.783	6.42	13.78	0.91	12.97	0.03	0.00			0.57	
298.0	0.367	34.792	27.918	6.84	8.48	0.80	12.79	0.02	0.00			0.55	
499.2	0.435	34.866	27.973	6.93	8.16	0.80	12.81	0.02	0.00			0.57	
698.8	0.242	34.887	28.001	6.99	7.74	0.87	12.77	0.03	0.00			0.57	
999.3	-0.047	34.900	28.028	6.98	8.48	0.80	12.92	0.03	0.00			0.61	
1246.0	-0.245	34.912	28.048	6.93	9.54	0.80	13.06	0.03	0.00			0.63	
1578.9	-0.387	34.931	28.070	6.91	11.55	0.90	14.01	0.03	0.00			0.63	

399



Ref. no. 66 Sta. e07 71.42 N  
Time = 862900506 Beaufort 149.91 W



**APPENDIX C.**  
**BEAUFORT SEA MESOSCALE CIRCULATION STUDY: HYDROGRAPHY**  
**HELICOPTER OPERATIONS, APRIL, 1987**

**K. Aagaard, C. H. Pease, and K. Kroglund**

**U.S. Department of Commerce**  
**National Oceanic and Atmospheric Administration**  
**Environmental Research Laboratories**  
**Pacific Marine Environmental Laboratory**  
**Seattle, Washington**

**March 1988**

**Reprint of NOAA Data Report ERL PMEL-22**

## NOTICE

Mention of a commercial company or product does not constitute an endorsement by NOAA/ERL. Use of information from this publication concerning proprietary products or the tests of such products for publicity or advertising purposes is not authorized.

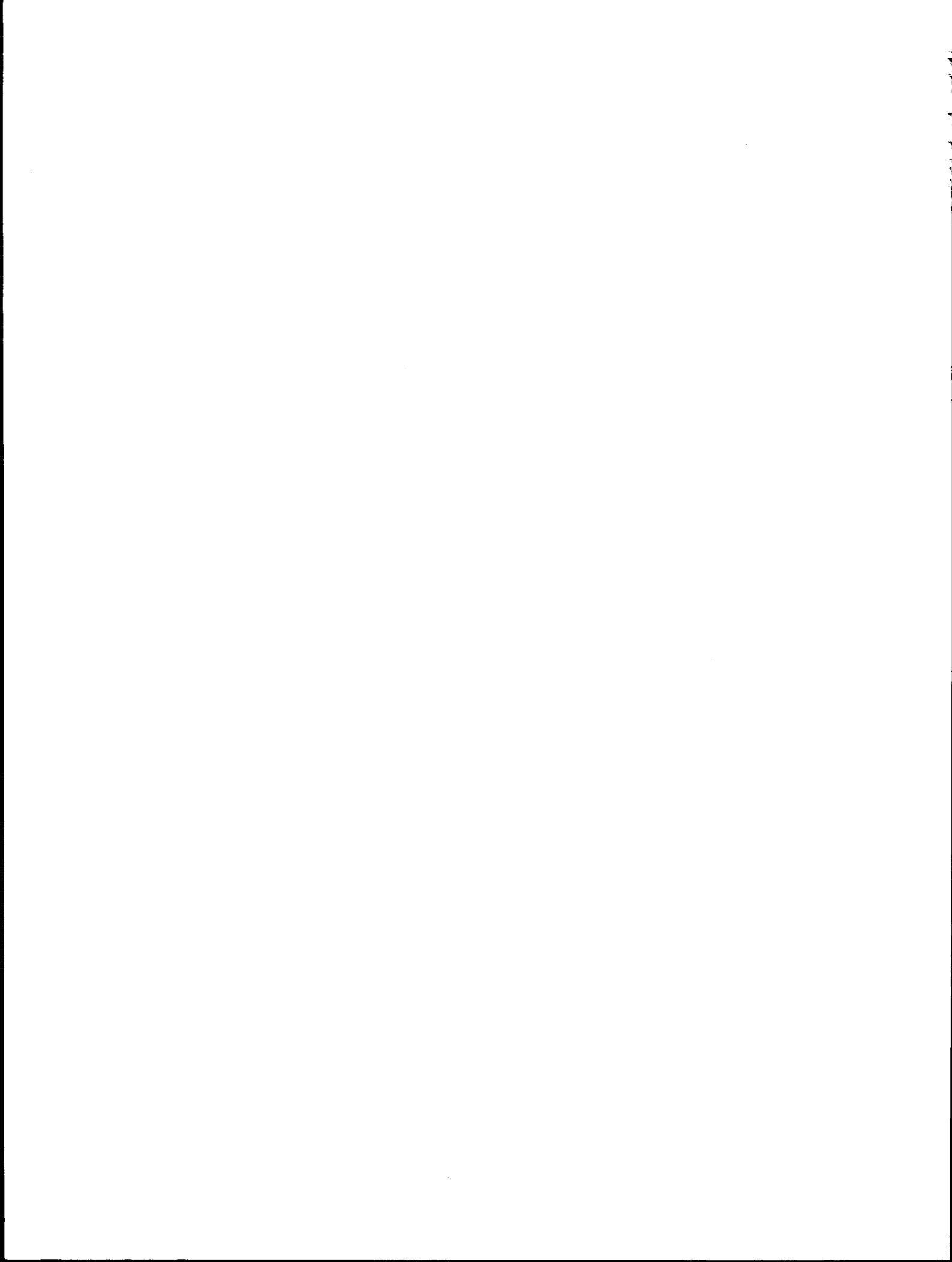
Contribution No. 1029 from NOAA/Pacific Marine Environmental Laboratory

---

For sale by the National Technical Information Service, 5285 Port Royal Road  
Springfield, VA 22161

## CONTENTS

1. INTRODUCTION .....	405
2. METHODOLOGIES .....	405
3. ACKNOWLEDGMENTS .....	406
4. REFERENCES .....	406



BEAUFORT SEA MESOSCALE CIRCULATION STUDY:  
HYDROGRAPHY HELICOPTER OPERATIONS, APRIL, 1987

K. Aagaard<sup>1</sup>, S. Salo<sup>1</sup>, and K. Kroglund<sup>2</sup>

1. INTRODUCTION

This report presents data from 28 hydrographic stations occupied in April, 1987 over the Beaufort Sea continental shelf and slope, as part of the Beaufort Sea Mesoscale Circulation Study (Table 1). The casts (Figure 1), which were made along 4 transects, each roughly perpendicular to the coast, repeat most of the stations sampled in October, 1986 from the USCGC Polar Star (Aagaard *et al.*, 1987).

2. METHODOLOGIES

Personnel and equipment were transported to each hydrographic station site by NOAA helicopters. A hole was augered in the ice, a tent was erected over the hole, and the cast was made from the tent. A Neil Brown Mark III CTD system, modified for Arctic work, was used during this experiment. Each cast was done in two parts, as follows. The profile was recorded, then the CTD fish was brought back to the surface. As it was lowered the second time, five or six 5 l Niskin bottles were clamped to the wire. They were tripped when the fish was again at depth.

CTD data were analyzed as outlined in Giles and McDougall (1986) and Aagaard *et al.* (1987). Salinity and sigma-t were calculated using the algorithms of Fofonoff and Millard (1983).

All water samples were analyzed for dissolved oxygen and nutrients in Deadhorse (Prudhoe Bay), Alaska. Nutrients were determined with a 5-channel Technicon Auto Analyzer II system and the method outlined by Whitledge *et al.* (1981). Oxygen concentration was measured by the Carpenter modification of the Winkler titration (Carpenter, 1965). Samples were also taken for freons and tritium. These are being analyzed separately by other investigators.

The discrete sample values are listed in Table 2. Salinity/nutrient correlation diagrams suggest that the five nitrate and six reactive silicate values marked in Table 2 by asterisks are anomalously high. However, a review of the sampling and analytical procedures suggests no systematic source of error.

---

<sup>1</sup> Pacific Marine Environmental Laboratory, 7600 Sand Point Way NE, Seattle, WA 98115-0070

<sup>2</sup> School of Oceanography, University of Washington, Seattle, WA 98195

### 3. ACKNOWLEDGMENTS

This work was supported by the Minerals Management Service through an interagency agreement with the National Oceanic and Atmospheric Administration, as part of the Outer Continental Shelf Environmental Assessment Program. Clark Darnall and Peter Proctor carried through each day's work with diligence and good humor. We also appreciate the efforts of the NOAA helicopter crews. This data report is a contribution to the Marine Services project at PMEL.

### 4. REFERENCES

Carpenter, J.H. 1965: The Chesapeake Bay Institute technique for the Winkler dissolved oxygen method. *Limnology and Oceanography* 10, 141-143.

Fofonoff, N.P. and R.C. Millard Jr., 1983: Algorithms for computation of fundamental properties of seawater. *Unesco Technical Papers in Marine Science*, 44.

Giles, A.B. and T.J. McDougall, 1986: Two methods for the reduction of salinity spiking of CTD's. *Deep-Sea Research* 33(9), 1253-1274.

Whitledge, T.E., S.C. Malloy, C.J. Patton, and C.D. Wirick, 1981: Automated nutrient analyses in seawater. Report #BNL-51398, Brookhaven National Laboratory, Upton, New York.

## **DATA**

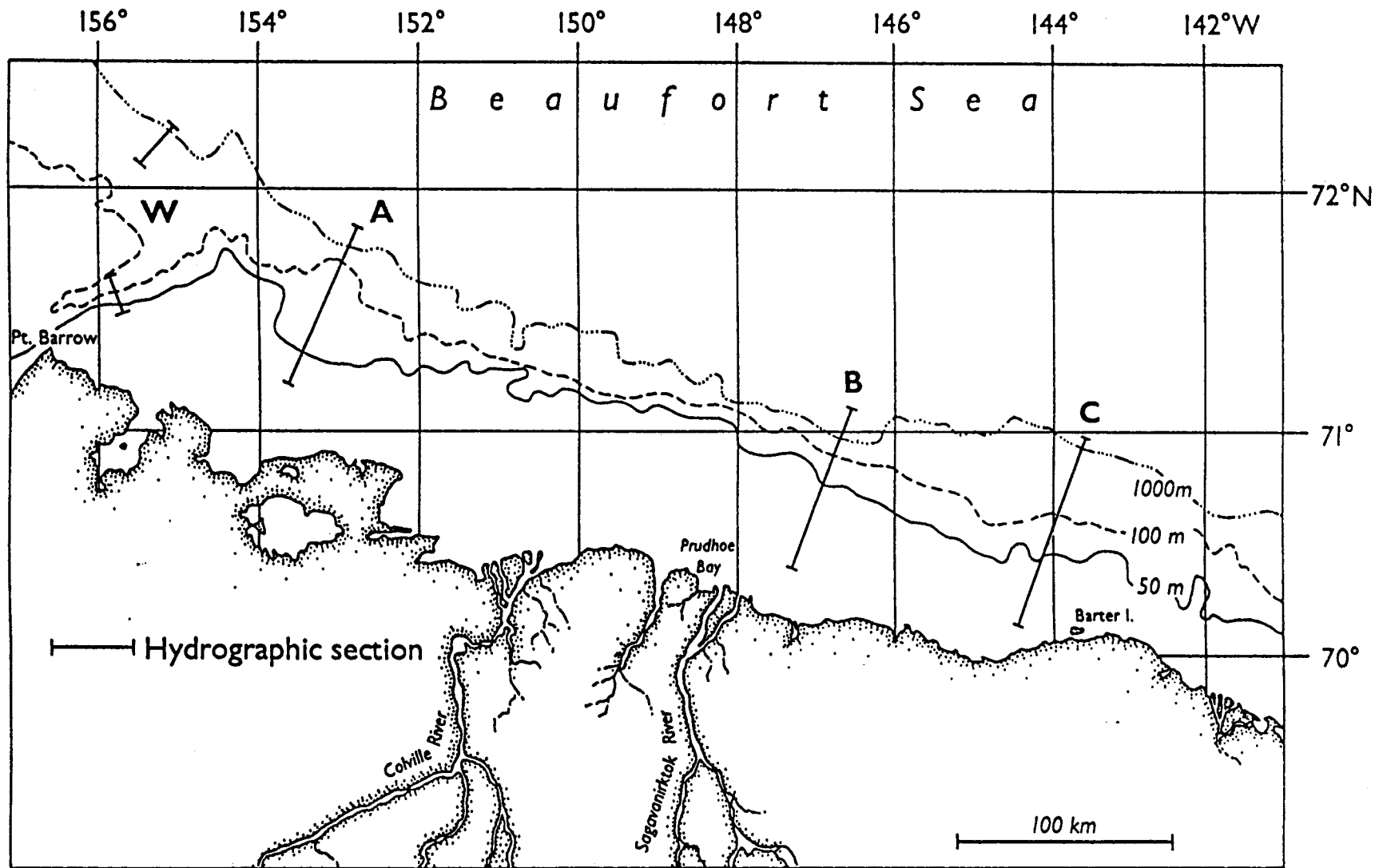


Figure 1.--Location of CTD transects

Table 1. CTD Chronology and Positions

Station	Cast#	Time (UTC)	N. Lat.	W. Long.	Depth (m)
C 09	1	2109 11 April	70° 56.3'	143° 33.3'	>1000
C 08	2	1944 12 April	70° 51.0'	143° 41.0'	>1000
C 06	3	2241 12 April	70° 38.9'	143° 55.9'	304
C 04	4	0057 13 April	70° 28.8'	144° 11.2'	52
C 02	5	1831 13 April	70° 15.5'	144° 23.8'	36
C 03	6	2108 13 April	70° 21.0'	144° 16.4'	39
C 05	7	0025 14 April	70° 34.0'	144° 03.6'	60
A 09	8	2015 18 April	71° 52.4'	152° 41.3'	>1000
A 08	9	0040 19 April	71° 46.9'	152° 54.4'	808
A 07	10	2020 20 April	71° 41.8'	153° 00.1'	156
A 06	11	2210 20 April	71° 36.2'	153° 09.9'	56
A 05	12	2342 20 April	71° 29.9'	153° 18.1'	57
A 04	13	0106 21 April	71° 23.7'	153° 26.8'	56
A 03	14	1927 21 April	71° 18.8'	153° 33.8'	46
A 02	15	2159 21 April	71° 13.0'	153° 39.9'	26
W 12	16	2315 21 April	71° 31.7'	155° 46.0'	124
W 11	17	1802 22 April	71° 35.0'	155° 46.8'	200
W 03	18	2055 22 April	72° 13.7'	155° 07.4'	>1000
W 04	19	0004 23 April	72° 08.2'	155° 18.9'	498
B 09	20	1839 26 April	71° 03.3'	146° 38.3'	>1000
B 08	21	2240 26 April	70° 57.7'	146° 44.5'	859
B 07	22	1808 27 April	70° 53.1'	146° 49.3'	68
B 06	23	1957 27 April	70° 49.9'	146° 53.8'	60
B 05	24	2129 27 April	70° 45.1'	147° 00.6'	48
B 04	25	2252 27 April	70° 42.1'	147° 04.6'	44
B 03	26	1720 28 April	70° 37.7'	147° 07.7'	38
B 02	27	1855 28 April	70° 32.0'	147° 15.0'	32
B 01	28	2016 28 April	70° 27.8'	147° 20.0'	23

<u>Station</u>	<u>Cast</u>	<u>Time (UCT)</u>	<u>Latitude (°N)</u>	<u>Longitude (°W)</u>	<u>Bottom Depth (m)</u>
C09	1	2109 11 Apr 1987	70° 56.3	143° 33.3	>1000

<u>Depth</u>	<u>S (PSU)</u>	<u>T (°C)</u>	<u>Sigma-t</u>	<u>O<sub>2</sub> (ml/l)</u>	<u>PO<sub>4</sub> (μm/l)</u>	<u>SiO<sub>4</sub> (μm/l)</u>	<u>NO<sub>3</sub> (μm/l)</u>	<u>NO<sub>2</sub> (μm/l)</u>	<u>NH<sub>3</sub> (μm/l)</u>
2.3	29.623	-1.606	23.808	9.05	0.79	8.74	2.24	0.04	0.07
22.3	30.958	-1.405	24.888	9.14	0.91	8.04	2.29	0.05	0.25
67.3	32.470	-1.314	26.112		1.50	24.77*	7.81	0.03	0.08
112.3	32.944	-1.490	26.502	6.60	1.76	34.38*	12.94	0.03	0.10
147.3	33.457	-1.344	26.914		1.66	32.87*	12.44	0.03	
497.3	34.831	0.427	27.946	6.93	0.87	9.02	7.57	0.02	0.00

<u>Station</u>	<u>Cast</u>	<u>Time (UCT)</u>	<u>Latitude (°N)</u>	<u>Longitude (°W)</u>	<u>Bottom Depth (m)</u>
C08	2	1944 12 Apr 1987	70° 51.0	143° 41.0	>1000

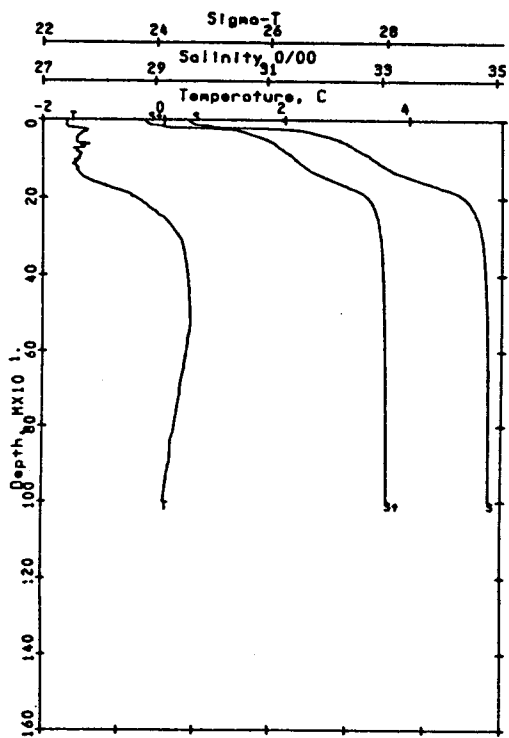
  

<u>Depth</u>	<u>S (PSU)</u>	<u>T (°C)</u>	<u>Sigma-t</u>	<u>O<sub>2</sub> (ml/l)</u>	<u>PO<sub>4</sub> (μm/l)</u>	<u>SiO<sub>4</sub> (μm/l)</u>	<u>NO<sub>3</sub> (μm/l)</u>	<u>NO<sub>2</sub> (μm/l)</u>	<u>NH<sub>3</sub> (μm/l)</u>
2.3	29.808	-1.637	23.954	9.23	0.79	8.47	2.38	0.03	0.01
22.3	30.185	-1.578	24.264	9.19	0.81	7.86	2.38	0.03	0.02
42.3	31.953	-1.360	25.694		1.12	12.47	4.90	0.02	0.02
72.3	32.566	-1.405	26.192		1.61	27.80*	14.07*	0.02	0.10
117.3	33.106	-1.474	26.632	6.39	1.88	37.61*	17.64*	0.02	0.00
497.3	34.838	0.424	27.952	6.82	0.88	8.95	11.99	0.02	0.01

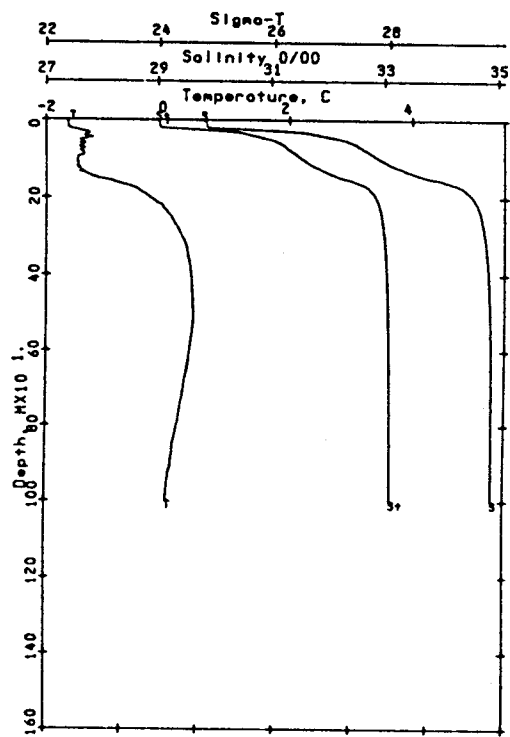
<u>Station</u>	<u>Cast</u>	<u>Time (UCT)</u>	<u>Latitude (°N)</u>	<u>Longitude (°W)</u>	<u>Bottom Depth (m)</u>
C06	3	2241 12 Apr 1987	70° 38.9	143° 55.9	304

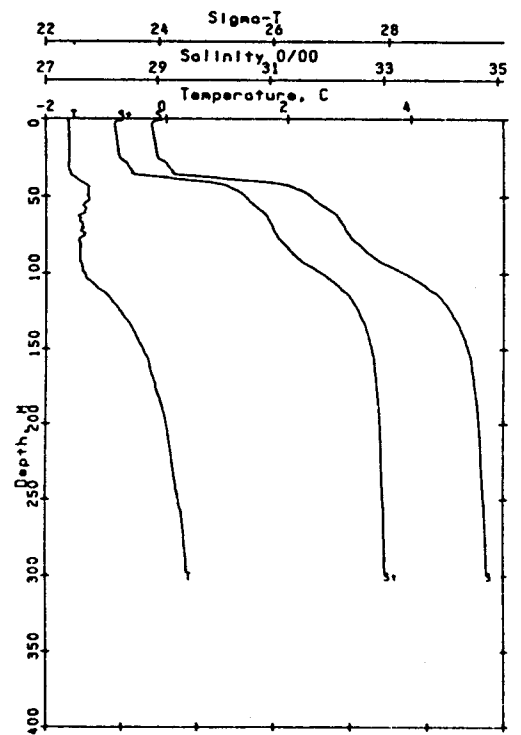
<u>Depth</u>	<u>S (PSU)</u>	<u>T (°C)</u>	<u>Sigma-t</u>	<u>O<sub>2</sub> (ml/l)</u>	<u>PO<sub>4</sub> (μm/l)</u>	<u>SiO<sub>4</sub> (μm/l)</u>	<u>NO<sub>3</sub> (μm/l)</u>	<u>NO<sub>2</sub> (μm/l)</u>	<u>NH<sub>3</sub> (μm/l)</u>
2.3	28.922	-1.616	23.239	9.07	0.77	9.50	1.72	0.03	0.06
22.3	28.990	-1.615	23.294	9.09	0.77	9.50	1.80	0.03	0.02
47.3	31.584	-1.290	25.393		1.03	9.19	3.31	0.02	0.06
72.3	32.313	-1.423	25.988	7.53	1.42	22.11	10.69*	0.03	0.06
97.3	33.181	-1.397	26.692	6.67	1.72	33.83*	17.24*	0.03	0.14
287.3	34.778	0.316	27.909	6.74	0.89	10.38	15.26*	0.03	0.04



Ref. no. 1      Stn. C09      70.94 N  
 Time = 871012109      Beaufort      143.56 W



Ref. no. 2      Stn. C08      70.85 N  
 Time = 871021944      Beaufort      143.68 W



Ref. no. 3      Stn. C06      70.65 N  
 Time = 871022241      Beaufort      143.93 W

<u>Station</u>	<u>Cast</u>	<u>Time (UCT)</u>	<u>Latitude (°N)</u>	<u>Longitude (°W)</u>	<u>Bottom Depth (m)</u>
C04	4	0057 13 Apr 1987	70° 28.8	144° 11.2	52

<u>Depth</u>	<u>S (PSU)</u>	<u>T (°C)</u>	<u>Sigma-t</u>	<u>O<sub>2</sub> (ml/l)</u>	<u>PO<sub>4</sub> (μm/l)</u>	<u>SiO<sub>4</sub> (μm/l)</u>	<u>NO<sub>3</sub> (μm/l)</u>	<u>NO<sub>2</sub> (μm/l)</u>	<u>NH<sub>3</sub> (μm/l)</u>
2.3	29.397	-1.613	23.624	9.20	0.75	10.16	1.81	0.02	0.06
7.3	29.402	-1.615	23.629	9.17	0.75	10.16	1.80	0.02	0.06
12.3	29.404	-1.615	23.630	9.26	0.75	10.15	1.79	0.02	0.05
22.3	30.171	-1.644	24.253	8.84	0.88	9.24	2.20	0.02	0.06
32.3	31.739	-1.225	25.517	8.12	1.12	13.35	5.08	0.02	0.05
45.3	32.294	-1.313	25.970	7.59	1.22	19.96	7.04	0.02	0.05

<u>Station</u>	<u>Cast</u>	<u>Time (UCT)</u>	<u>Latitude (°N)</u>	<u>Longitude (°W)</u>	<u>Bottom Depth (m)</u>
C02	5	1831 13 Apr 1987	70° 15.5	144° 23.8	36

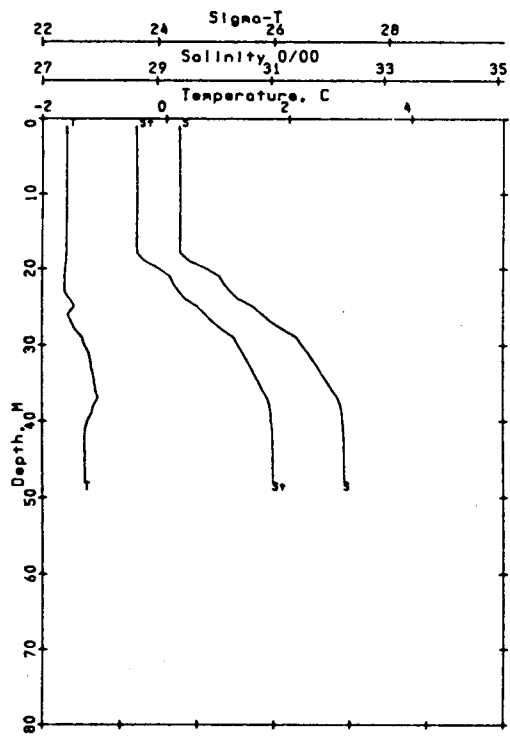
  

<u>Depth</u>	<u>S (PSU)</u>	<u>T (°C)</u>	<u>Sigma-t</u>	<u>O<sub>2</sub> (ml/l)</u>	<u>PO<sub>4</sub> (μm/l)</u>	<u>SiO<sub>4</sub> (μm/l)</u>	<u>NO<sub>3</sub> (μm/l)</u>	<u>NO<sub>2</sub> (μm/l)</u>	<u>NH<sub>3</sub> (μm/l)</u>
2.3	30.805	-1.681	24.769	9.08	0.88	10.22	2.04	0.01	0.03
7.3	30.816	-1.687	24.777	9.10	0.90	10.21	2.07	0.03	0.03
12.3	30.835	-1.692	24.794	9.05	0.91	10.21	2.06	0.03	0.00
17.3	31.038	-1.709	24.959	8.86	0.96	12.21	2.98	0.01	0.03
22.3	31.790	-1.743	25.570	8.48	1.04	15.01	4.07	0.01	0.02
29.3	32.159	-1.752	25.870	8.37	1.07	16.31	4.51	0.02	0.11

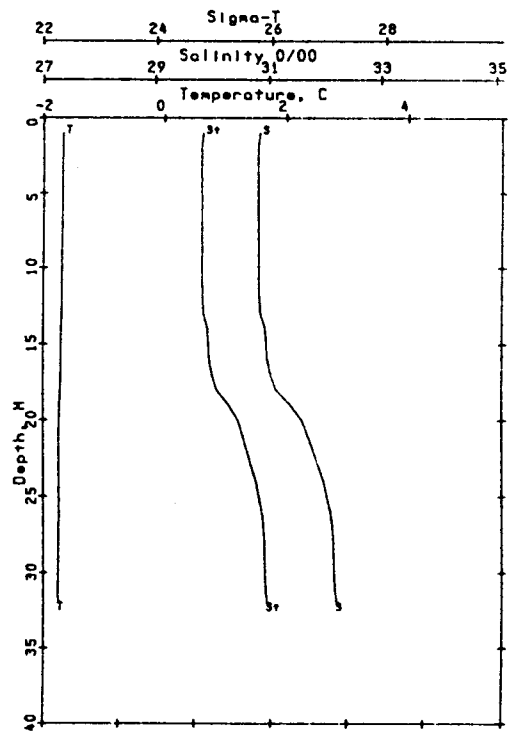
<u>Station</u>	<u>Cast</u>	<u>Time (UCT)</u>	<u>Latitude (°N)</u>	<u>Longitude (°W)</u>	<u>Bottom Depth (m)</u>
C03	6	2108 13 Apr 1987	70° 21.0	144° 16.4	39

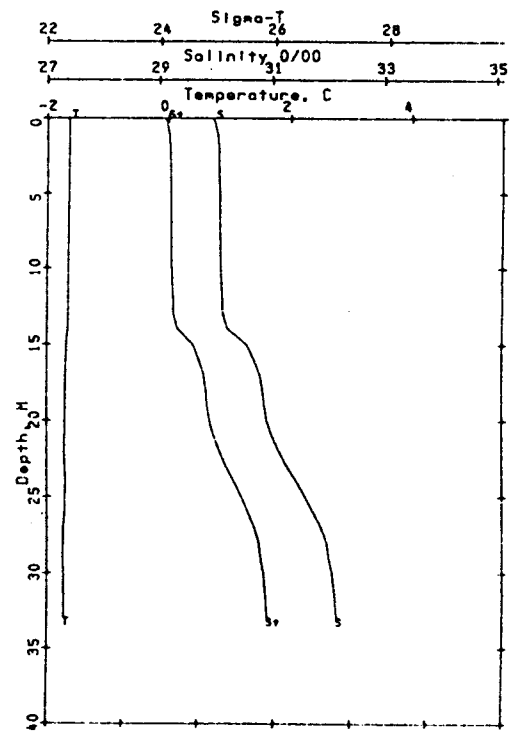
<u>Depth</u>	<u>S (PSU)</u>	<u>T (°C)</u>	<u>Sigma-t</u>	<u>O<sub>2</sub> (ml/l)</u>	<u>PO<sub>4</sub> (μm/l)</u>	<u>SiO<sub>4</sub> (μm/l)</u>	<u>NO<sub>3</sub> (μm/l)</u>	<u>NO<sub>2</sub> (μm/l)</u>	<u>NH<sub>3</sub> (μm/l)</u>
2.3	30.051	-1.648	24.156	9.13	0.80	11.19	2.15	0.02	0.10
7.3	30.079	-1.655	24.179	9.11	0.84	11.18	2.19	0.02	0.21
12.3	30.130	-1.660	24.220	9.08	0.83	11.18	2.18	0.02	0.08
17.3	30.793	-1.698	24.759	8.97	0.90	11.68	2.82	0.01	0.07
25.3	31.584	-1.706	25.402	8.60	1.02	13.68	4.23	0.02	0.06
32.3	31.118	-1.727	25.836	8.27	1.08	16.18	4.96	0.02	0.05



Ref. no. 4 Sta. C04 70.48 N  
 Time = 871030057 Beaufort 144.19 W



Ref. no. 5 Sta. C02 70.26 N  
 Time = 871031831 Beaufort 144.40 W



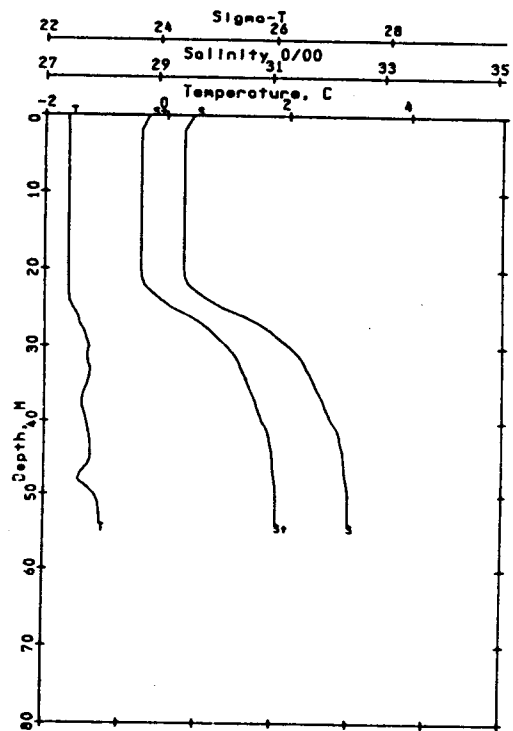
Ref. no. 6 Sta. C03 70.35 N  
 Time = 871032108 Beaufort 144.27 W

<u>Station</u>	<u>Cast</u>	<u>Time (UCT)</u>	<u>Latitude (°N)</u>	<u>Longitude (°W)</u>	<u>Bottom Depth (m)</u>				
C05	7	0025 14 Apr 1987	70° 34.0	144° 03.6	60				
<u>Depth</u>	<u>S (PSU)</u>	<u>T (°C)</u>	<u>Sigma-t</u>	<u>O<sub>2</sub> (ml/l)</u>	<u>PO<sub>4</sub> (μm/l)</u>	<u>SiO<sub>4</sub> (μm/l)</u>	<u>NO<sub>3</sub> (μm/l)</u>	<u>NO<sub>2</sub> (μm/l)</u>	<u>NH<sub>3</sub> (μm/l)</u>
2.3	29.484	-1.618	23.695	9.11	0.76	10.63	1.98	0.02	0.07
12.3	29.486	-1.618	23.697	9.04	0.77	10.53	2.06	0.02	0.03
22.3	29.555	-1.615	23.753	9.06	0.82	10.52	2.23	0.02	0.26
32.3	31.571	-1.292	25.383	8.82	0.99	9.12	2.87	0.02	0.04
47.3	32.310	-1.405	25.985	7.68	1.29	20.13	8.23	0.02	0.05
52.3	32.380	-1.101	26.033	7.49	1.32	21.93	8.96	0.02	0.08

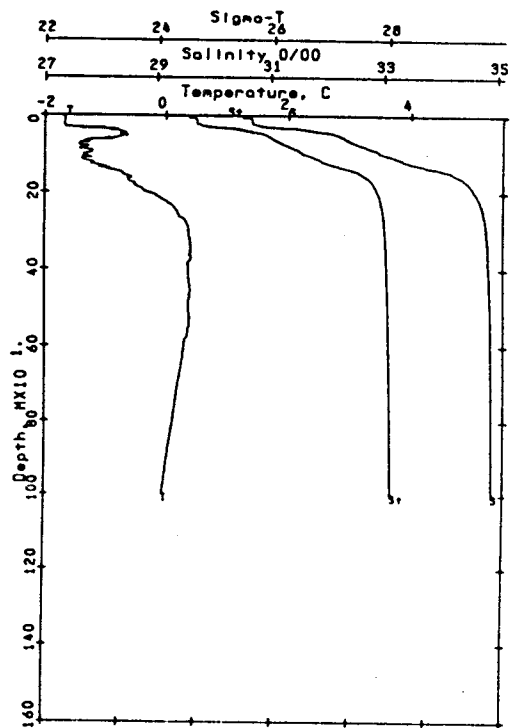
<u>Station</u>	<u>Cast</u>	<u>Time (UCT)</u>	<u>Latitude (°N)</u>	<u>Longitude (°W)</u>	<u>Bottom Depth (m)</u>				
A09	8	2015 18 Apr 1987	71° 52.4	152° 41.3	>1000				
<u>Depth</u>	<u>S (PSU)</u>	<u>T (°C)</u>	<u>Sigma-t</u>	<u>O<sub>2</sub> (ml/l)</u>	<u>PO<sub>4</sub> (μm/l)</u>	<u>SiO<sub>4</sub> (μm/l)</u>	<u>NO<sub>3</sub> (μm/l)</u>	<u>NO<sub>2</sub> (μm/l)</u>	<u>NH<sub>3</sub> (μm/l)</u>
2.3	30.515	-1.674	24.533	8.46	2.46	0.82	1.04	0.23	0.14
42.3	31.880	-0.749	25.617	7.79	1.01	6.14	3.33	0.23	0.15
112.3	33.220	-1.394	26.723	6.53	1.91	24.71	12.29	0.22	0.34
347.3	34.820	0.416	27.937	6.79	1.82	1.16	10.66	0.22	1.12
452.3	34.850	0.412	27.962	6.69	0.78	1.08	10.81	0.22	0.04
997.3	34.890	-0.052	28.020	6.94	0.80	1.49	10.99	0.20	0.07

<u>Station</u>	<u>Cast</u>	<u>Time (UCT)</u>	<u>Latitude (°N)</u>	<u>Longitude (°W)</u>	<u>Bottom Depth (m)</u>				
A08	9	0040 19 Apr 1987	71° 46.9	152° 54.4	808				

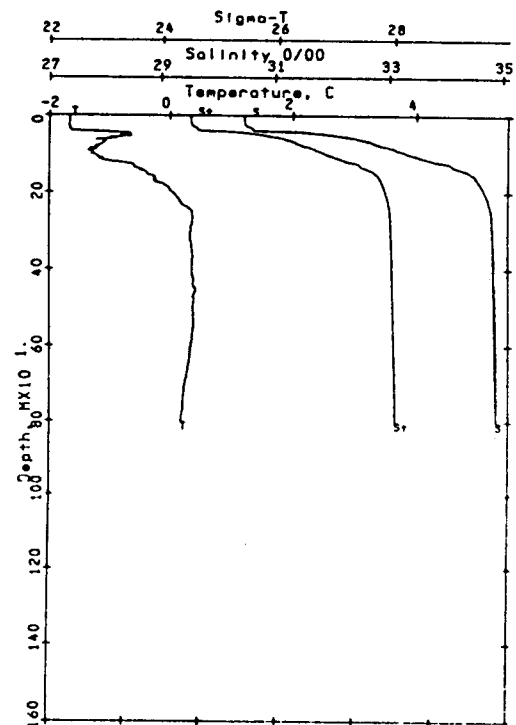
NO SAMPLES TAKEN



Ref. no. 7 Sta. C05 70.57 N  
 Time = 871040025 Beaufort 144.06 W



Ref. no. 8 Sta. A09 71.87 N  
 Time = 871082015 Beaufort 152.69 W

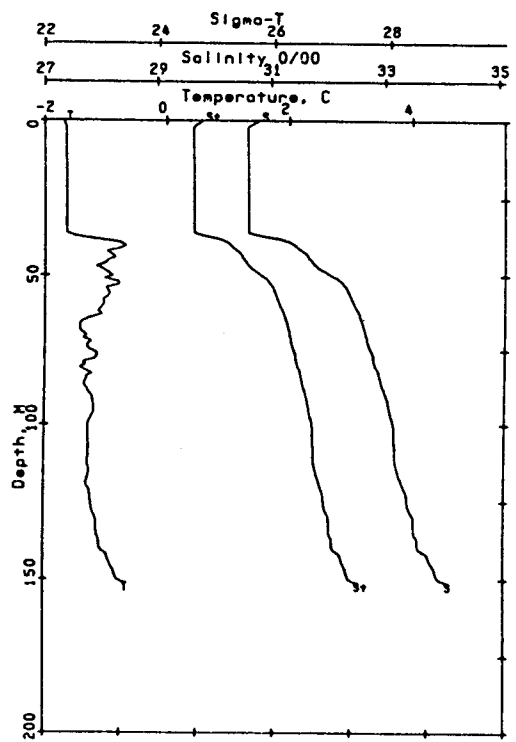


Ref. no. 9 Sta. A08 71.78 N  
 Time = 871090040 Beaufort 152.91 W

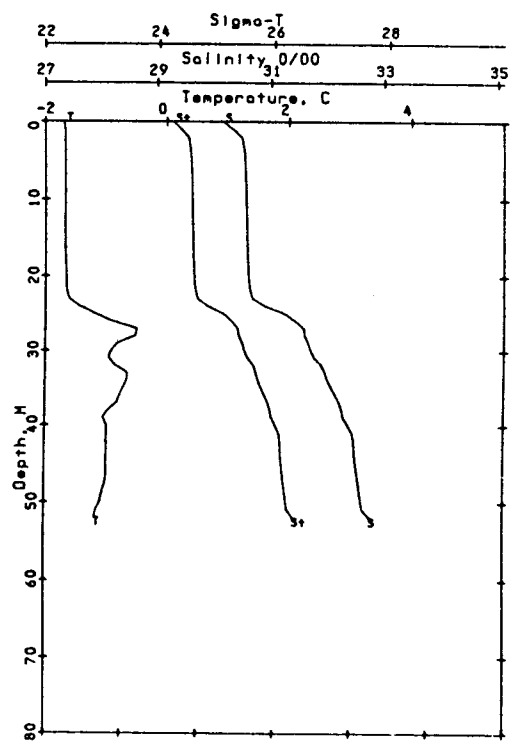
<u>Station</u>	<u>Cast</u>	<u>Time (UCT)</u>	<u>Latitude (°N)</u>	<u>Longitude (°W)</u>	<u>Bottom Depth (m)</u>				
A07	10	2020 20 Apr 1987	71° 41.8	153° 00.1	156				
<u>Depth</u>	<u>S (PSU)</u>	<u>T (°C)</u>	<u>Sigma-t</u>	<u>O<sub>2</sub> (ml/l)</u>	<u>PO<sub>4</sub> (μm/l)</u>	<u>SiO<sub>4</sub> (μm/l)</u>	<u>NO<sub>3</sub> (μm/l)</u>	<u>NO<sub>2</sub> (μm/l)</u>	<u>NH<sub>3</sub> (μm/l)</u>
2.3	30.591	-1.658	24.595	8.52	0.73	0.00	0.86	0.17	0.03
22.3	30.594	-1.658	24.597	8.51	1.01	0.00	0.86	0.18	0.09
37.3	30.801	-1.515	24.763	8.36	0.84	1.58	1.52	0.18	0.35
92.3	33.034	-1.219	26.567	6.70	1.46	19.66	11.80	0.18	0.02
117.3	33.245	-1.284	26.740	6.52	1.45	20.77	11.11	0.17	0.00
147.3	33.882	-0.851	27.242	6.46	1.20	16.44	11.14	0.18	0.00

<u>Station</u>	<u>Cast</u>	<u>Time (UCT)</u>	<u>Latitude (°N)</u>	<u>Longitude (°W)</u>	<u>Bottom Depth (m)</u>				
A06	11	2210 20 Apr 1987	71° 36.2	153° 09.9	56				
<u>Depth</u>	<u>S (PSU)</u>	<u>T (°C)</u>	<u>Sigma-t</u>	<u>O<sub>2</sub> (ml/l)</u>	<u>PO<sub>4</sub> (μm/l)</u>	<u>SiO<sub>4</sub> (μm/l)</u>	<u>NO<sub>3</sub> (μm/l)</u>	<u>NO<sub>2</sub> (μm/l)</u>	<u>NH<sub>3</sub> (μm/l)</u>
2.3	30.482	-1.672	24.506	8.55	0.70	0.00	0.86	0.18	0.00
7.3	30.550	-1.672	24.561	8.56	0.74	0.00	0.79	0.18	0.00
12.3	30.564	-1.672	24.573	8.58	0.72	0.00	0.76	0.18	0.00
22.3	30.629	-1.642	24.626	8.44	0.79	0.00	0.95	0.18	0.00
32.3	31.888	-0.853	25.627	7.65	1.11	5.62	4.07	0.18	0.02
47.3	32.540	-0.986	26.159	7.15	1.40	6.27	8.45	0.18	0.00

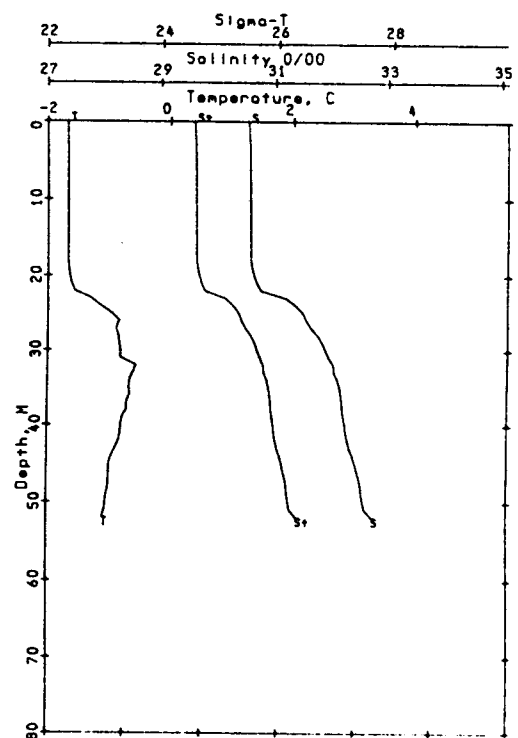
<u>Station</u>	<u>Cast</u>	<u>Time (UCT)</u>	<u>Latitude (°N)</u>	<u>Longitude (°W)</u>	<u>Bottom Depth (m)</u>				
A05	12	2342 20 Apr 1987	71° 29.9	153° 18.1	57				
<u>Depth</u>	<u>S (PSU)</u>	<u>T (°C)</u>	<u>Sigma-t</u>	<u>O<sub>2</sub> (ml/l)</u>	<u>PO<sub>4</sub> (μm/l)</u>	<u>SiO<sub>4</sub> (μm/l)</u>	<u>NO<sub>3</sub> (μm/l)</u>	<u>NO<sub>2</sub> (μm/l)</u>	<u>NH<sub>3</sub> (μm/l)</u>
7.3	30.553	-1.671	24.564	8.54	0.77	0.00	0.87	0.18	0.00
17.3	30.562	-1.670	24.571	8.52	0.66	0.00	0.93	0.16	0.00
32.3	32.018	-0.558	25.722	7.64	1.08	6.12	4.34	0.16	0.00
42.3	32.285	-0.824	25.947	7.15	1.12	10.87	6.36	0.17	0.00
47.3	32.502	-0.984	26.128	7.01	1.29	14.22	7.41	0.17	0.00



Ref. no. 10 Sta. A07 71.70 N  
 Time = 871102020 Beaufort 153.00 W



Ref. no. 11 Sta. A06 71.60 N  
 Time = 871102210 Beaufort 153.16 W



Ref. no. 12 Sta. A05 71.50 N  
 Time = 871102342 Beaufort 153.30 W

<u>Station</u>	<u>Cast</u>	<u>Time (UCT)</u>	<u>Latitude (°N)</u>	<u>Longitude (°W)</u>	<u>Bottom Depth (m)</u>
A04	13	0106 21 Apr 1987	71° 23.7	153° 26.8	50

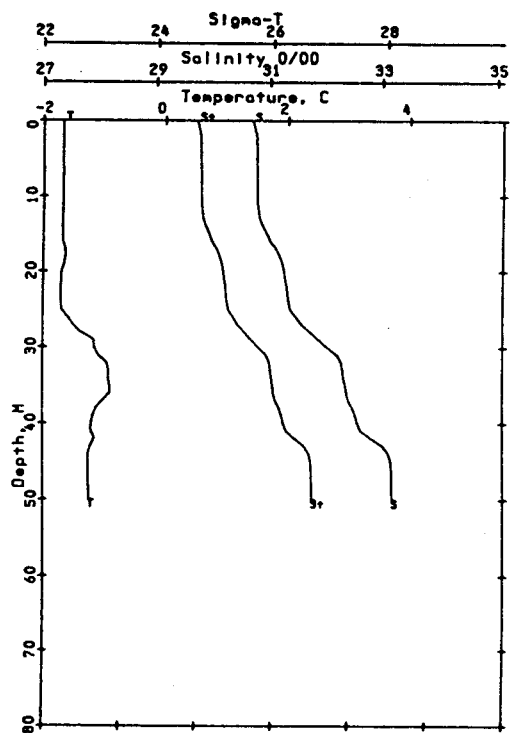
<u>Depth</u>	<u>S (PSU)</u>	<u>T (°C)</u>	<u>Sigma-t</u>	<u>O<sub>2</sub> (ml/l)</u>	<u>PO<sub>4</sub> (µm/l)</u>	<u>SiO<sub>4</sub> (µm/l)</u>	<u>NO<sub>3</sub> (µm/l)</u>	<u>NO<sub>2</sub> (µm/l)</u>	<u>NH<sub>3</sub> (µm/l)</u>
7.3	30.777	-1.681	24.746	8.54	0.98	6.25	1.15	0.01	0.02
17.3	31.116	-1.640	25.021	8.24	0.94	7.82	1.72	0.00	0.00
32.3	32.280	-0.958	25.947	7.42	1.30	19.08	6.12	0.00	0.00
37.3	32.404	-1.020	26.050	7.08	1.33	19.20	6.48	0.00	0.00
47.3	33.165	-1.253	26.674	6.55	1.92	27.87	11.61	0.07	0.00

<u>Station</u>	<u>Cast</u>	<u>Time (UCT)</u>	<u>Latitude (°N)</u>	<u>Longitude (°W)</u>	<u>Bottom Depth (m)</u>
A03	14	1927 21 Apr 1987	71° 18.8	153° 33.8	46

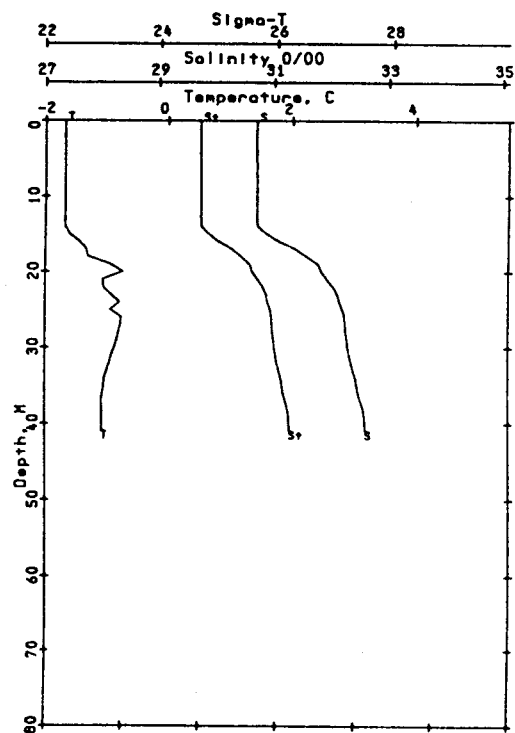
<u>Depth</u>	<u>S (PSU)</u>	<u>T (°C)</u>	<u>Sigma-t</u>	<u>O<sub>2</sub> (ml/l)</u>	<u>PO<sub>4</sub> (µm/l)</u>	<u>SiO<sub>4</sub> (µm/l)</u>	<u>NO<sub>3</sub> (µm/l)</u>	<u>NO<sub>2</sub> (µm/l)</u>	<u>NH<sub>3</sub> (µm/l)</u>
2.3	30.695	-1.680	24.680	8.70	1.14	6.40	1.08	0.01	0.00
12.3	30.706	-1.680	24.689	8.74	0.97	5.95	1.06	0.01	0.00
17.3	31.362	-1.332	25.214	7.95	1.05	9.94	2.84	0.00	0.00
22.3	32.031	-1.050	25.749	7.47	1.26	15.06	5.03	0.00	0.00
27.3	32.238	-0.770	25.907	7.25	1.36	18.00	6.50	0.00	0.00
37.3	32.511	-1.073	26.138	7.02	1.40	21.68	7.97	0.00	0.00

<u>Station</u>	<u>Cast</u>	<u>Time (UCT)</u>	<u>Latitude (°N)</u>	<u>Longitude (°W)</u>	<u>Bottom Depth (m)</u>
A02	15	2159 21 Apr 1987	71° 13.0	153° 39.9	26

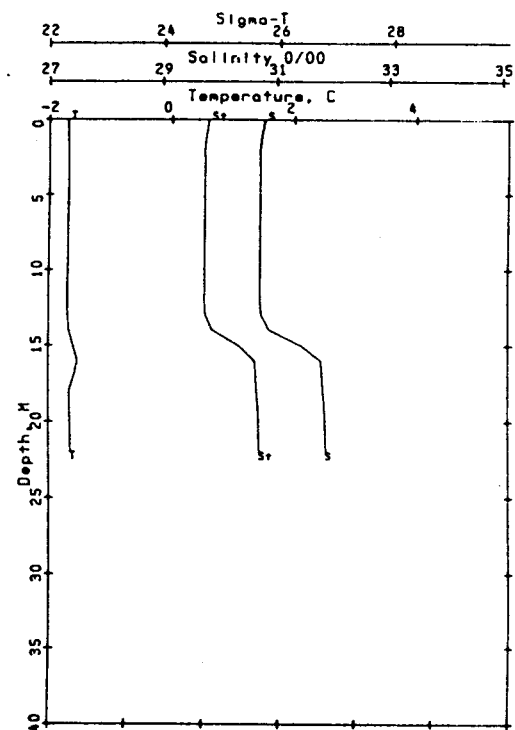
<u>Depth</u>	<u>S (PSU)</u>	<u>T (°C)</u>	<u>Sigma-t</u>	<u>O<sub>2</sub> (ml/l)</u>	<u>PO<sub>4</sub> (µm/l)</u>	<u>SiO<sub>4</sub> (µm/l)</u>	<u>NO<sub>3</sub> (µm/l)</u>	<u>NO<sub>2</sub> (µm/l)</u>	<u>NH<sub>3</sub> (µm/l)</u>
2.3	30.696	-1.687	24.680	8.00	0.78	5.64	1.05	0.01	0.00
6.3	30.703	-1.688	24.686	8.00	0.83	5.68	1.13	0.02	0.00
9.3	30.708	-1.690	24.690	8.49	1.06	5.96	1.24	0.01	0.00
13.3	30.729	-1.688	24.707	8.49	1.00	6.98	1.29	0.01	0.00
17.3	31.816	-1.577	25.588	8.62	1.04	10.65	2.39	0.00	0.00
20.3	31.868	-1.649	25.631	8.64	0.99	10.77	2.48	0.01	0.00



Ref. no. 13      Sta. R04      71.40 N  
 Time = 871110106      Beaufort      153.45 W



Ref. no. 14      Sta. R03      71.31 N  
 Time = 871111927      Beaufort      153.56 W



Ref. no. 15      Sta. R02      71.22 N  
 Time = 871112159      Beaufort 316      153.66 W

<u>Station</u>	<u>Cast</u>	<u>Time (UCT)</u>	<u>Latitude (°N)</u>	<u>Longitude (°W)</u>	<u>Bottom Depth (m)</u>
W04	19	0004 23 Apr 1987	72° 08.2	155° 18.9	498

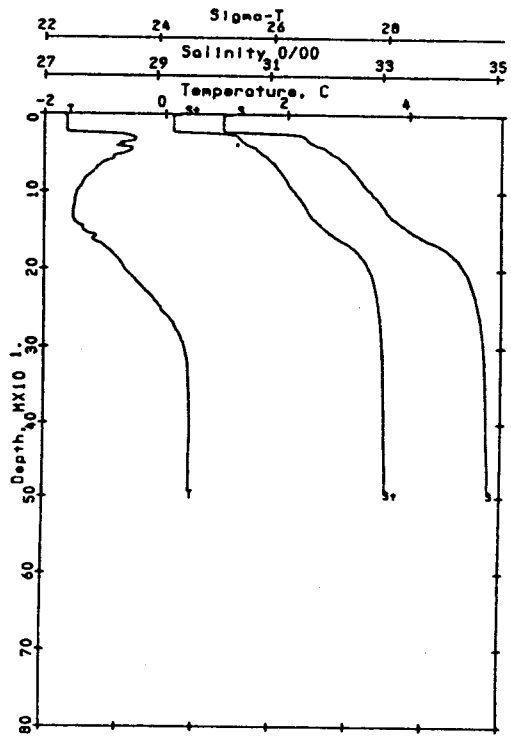
NO SAMPLES TAKEN

<u>Station</u>	<u>Cast</u>	<u>Time (UCT)</u>	<u>Latitude (°N)</u>	<u>Longitude (°W)</u>	<u>Bottom Depth (m)</u>
B09	20	1839 26 Apr 1987	71° 03.3	146° 38.3	>1000

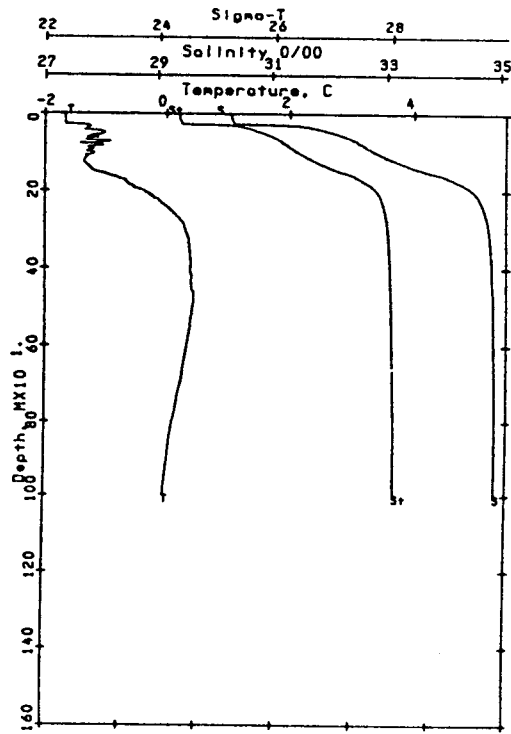
<u>Depth</u>	<u>S (PSU)</u>	<u>T (°C)</u>	<u>Sigma-t</u>	<u>O<sub>2</sub> (ml/l)</u>	<u>PO<sub>4</sub> (µm/l)</u>	<u>SiO<sub>4</sub> (µm/l)</u>	<u>NO<sub>3</sub> (µm/l)</u>	<u>NO<sub>2</sub> (µm/l)</u>	<u>NH<sub>3</sub> (µm/l)</u>
7.3	30.302	-1.669	24.360	9.21	0.74	4.42	0.02	0.79	0.00
47.3	32.007	-1.058	25.730	8.07	1.10	11.33	3.34	0.66	0.00
82.3	32.583	-1.057	26.196	7.27	1.40	21.70	7.44	0.66	0.00
122.3	33.124	-1.344	26.644	6.69	1.60	28.97	10.84	0.65	0.00
467.3	34.855	0.435	27.964	6.81	0.80	5.21	10.44	0.65	0.00
997.3	34.896	-0.040	28.024	6.93	0.81	5.27	9.68	0.64	0.00

<u>Station</u>	<u>Cast</u>	<u>Time (UCT)</u>	<u>Latitude (°N)</u>	<u>Longitude (°W)</u>	<u>Bottom Depth (m)</u>
B08	21	2240 26 Apr 1987	70° 57.7	146° 44.5	859

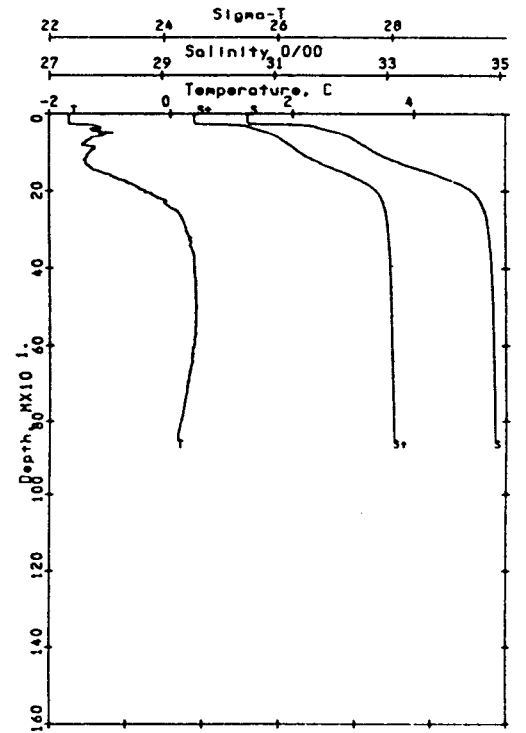
<u>Depth</u>	<u>S (PSU)</u>	<u>T (°C)</u>	<u>Sigma-t</u>	<u>O<sub>2</sub> (ml/l)</u>	<u>PO<sub>4</sub> (µm/l)</u>	<u>SiO<sub>4</sub> (µm/l)</u>	<u>NO<sub>3</sub> (µm/l)</u>	<u>NO<sub>2</sub> (µm/l)</u>	<u>NH<sub>3</sub> (µm/l)</u>
7.3	30.530	-1.673	24.545	9.12	0.55	4.60	0.38	0.42	0.00
17.3	30.536	-1.672	24.550	9.12	0.56	4.57	0.46	0.43	0.00
87.3	32.631	-1.239	26.241	7.18	1.42	22.59	7.68	0.44	0.00
167.3	34.002	-0.894	27.340	6.42	1.32	23.19	10.75	0.49	0.00
467.3	34.848	0.405	27.961	6.78	0.80	5.56	9.52	0.53	0.00
837.3	34.891	0.111	28.013	6.95	0.80	4.92	8.97	0.53	0.00



Ref. no. 19 Sta. W04 72.14 N  
 Time = 871130004 Beaufort 155.32 W



Ref. no. 20 Sta. B09 71.06 N  
 Time = 871161839 Beaufort 146.64 W



Ref. no. 21 Sta. B08 70.96 N  
 Time = 871162240 Beaufort 146.74 W

<u>Station</u>	<u>Cast</u>	<u>Time (UCT)</u>	<u>Latitude (°N)</u>	<u>Longitude (°W)</u>	<u>Bottom Depth (m)</u>
B07	22	1808 27 Apr 1987	70° 53.1	146° 49.3	68

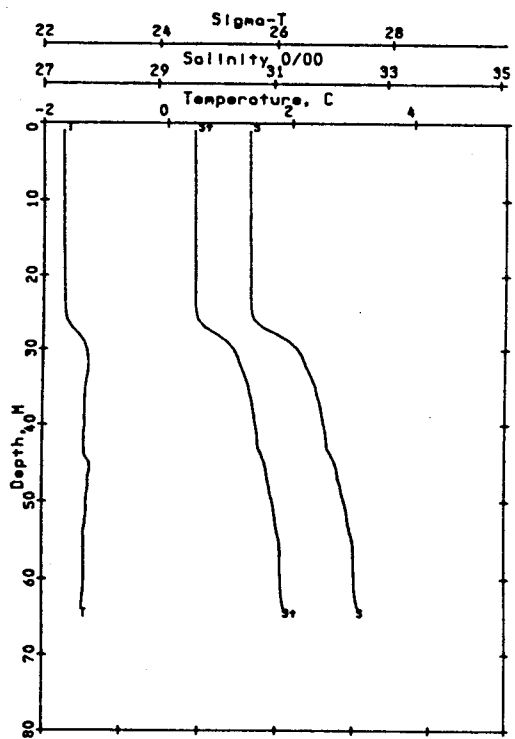
<u>Depth</u>	<u>S (PSU)</u>	<u>T (°C)</u>	<u>Sigma-t</u>	<u>O<sub>2</sub> (ml/l)</u>	<u>PO<sub>4</sub> (μm/l)</u>	<u>SiO<sub>4</sub> (μm/l)</u>	<u>NO<sub>3</sub> (μm/l)</u>	<u>NO<sub>2</sub> (μm/l)</u>	<u>NH<sub>3</sub> (μm/l)</u>
7.3	30.593	-1.673	24.596	9.00	0.80	8.01	1.60	0.03	0.00
17.3	30.604	-1.662	24.605	9.04	0.82	8.09	1.67	0.02	0.00
27.3	30.807	-1.541	24.768	8.82	0.90	8.16	2.10	0.02	0.00
37.3	31.816	-1.318	25.582	8.67	1.03	9.66	3.01	0.02	0.29
47.3	32.151	-1.261	25.852	7.74	1.23	17.50	6.92	0.02	0.01
57.3	32.424	-1.326	26.075	7.41	1.38	22.26	9.03	0.03	0.00

<u>Station</u>	<u>Cast</u>	<u>Time (UCT)</u>	<u>Latitude (°N)</u>	<u>Longitude (°W)</u>	<u>Bottom Depth (m)</u>
B06	23	1957 27 Apr 1987	70° 49.9	146° 53.8	60

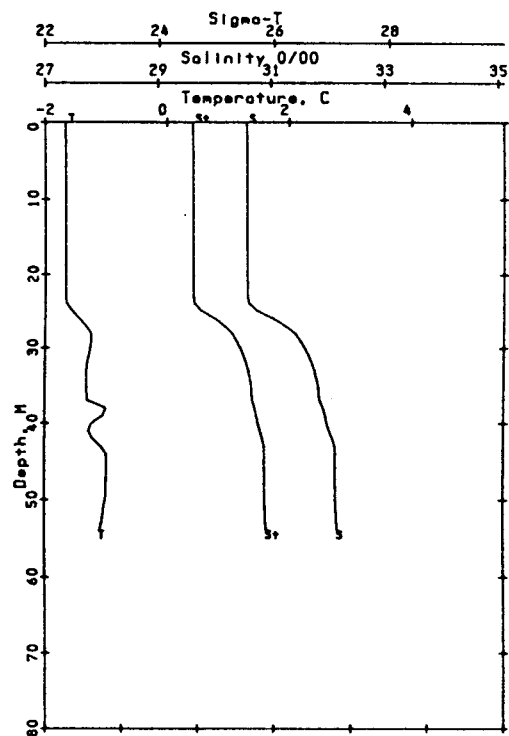
<u>Depth</u>	<u>S (PSU)</u>	<u>T (°C)</u>	<u>Sigma-t</u>	<u>O<sub>2</sub> (ml/l)</u>	<u>PO<sub>4</sub> (μm/l)</u>	<u>SiO<sub>4</sub> (μm/l)</u>	<u>NO<sub>3</sub> (μm/l)</u>	<u>NO<sub>2</sub> (μm/l)</u>	<u>NH<sub>3</sub> (μm/l)</u>
7.3	30.575	-1.672	24.582	9.03	0.83	8.05	1.73	0.03	0.00
17.3	30.576	-1.672	24.582	9.03	0.83	8.05	1.66	0.03	0.00
27.3	31.245	-1.340	25.119	8.77	0.93	8.71	2.38	0.04	0.00
37.3	31.865	-1.307	25.622	8.15	1.11	13.04	4.85	0.04	0.00
42.3	32.086	-1.220	25.798	7.66	1.20	18.05	6.26	0.04	0.00
47.3	32.143	-0.988	25.838	7.70	1.22	18.12	6.48	0.04	0.00

<u>Station</u>	<u>Cast</u>	<u>Time (UCT)</u>	<u>Latitude (°N)</u>	<u>Longitude (°W)</u>	<u>Bottom Depth (m)</u>
B05	24	2129 27 Apr 1987	70° 45.1	147° 00.6	48

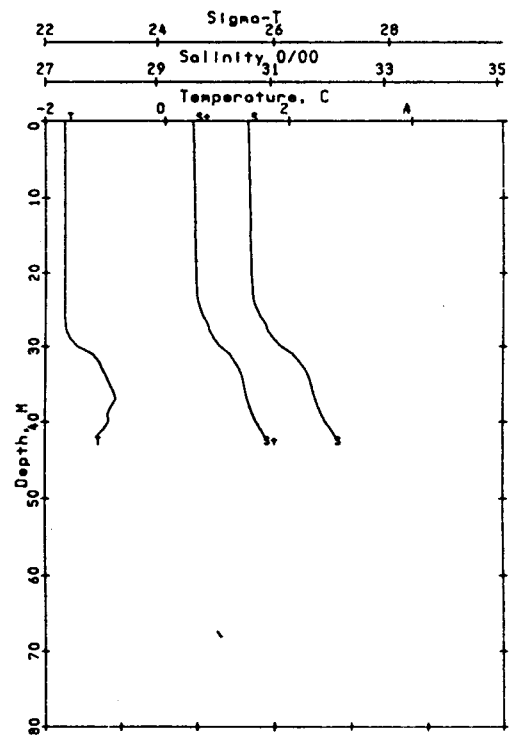
<u>Depth</u>	<u>S (PSU)</u>	<u>T (°C)</u>	<u>Sigma-t</u>	<u>O<sub>2</sub> (ml/l)</u>	<u>PO<sub>4</sub> (μm/l)</u>	<u>SiO<sub>4</sub> (μm/l)</u>	<u>NO<sub>3</sub> (μm/l)</u>	<u>NO<sub>2</sub> (μm/l)</u>	<u>NH<sub>3</sub> (μm/l)</u>
7.3	30.627	-1.677	24.624	9.08	0.83	8.26	1.82	0.04	0.06
17.3	30.651	-1.679	24.644	9.02	0.85	8.34	1.82	0.04	0.00
22.3	30.679	-1.680	24.667	9.04	0.86	8.58	1.91	0.04	0.00
27.3	30.908	-1.672	24.852	8.87	0.90	9.24	2.47	0.04	0.00
32.3	31.486	-1.110	25.309	8.52	0.97	9.66	3.06	0.04	0.00
37.3	31.764	-0.828	25.526	8.27	1.03	10.99	3.84	0.04	0.00



Ref. no. 22      Sta. 807      70.88 N  
 Time = 871171808      Beaufort      146.82 W



Ref. no. 23      Sta. 806      70.83 N  
 Time = 871171957      Beaufort      146.90 W



Ref. no. 24      Sta. 805      70.75 N  
 Time = 871172129      Beaufort      147.01 W

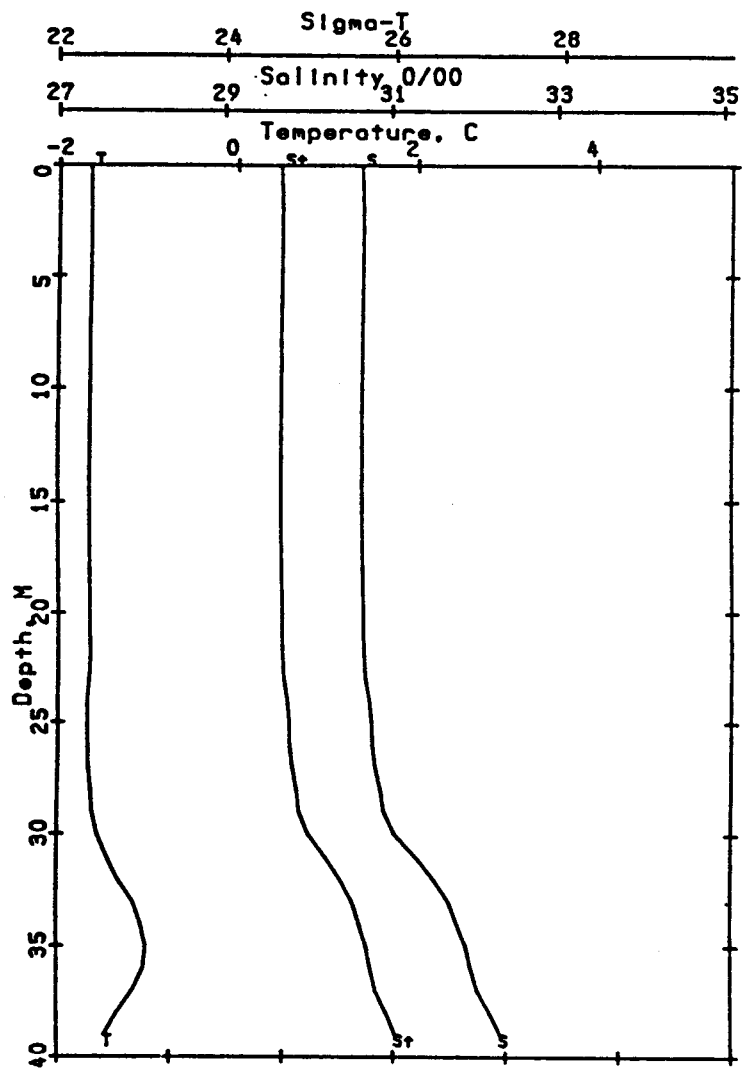
<u>Station</u>	<u>Cast</u>	<u>Time (UCT)</u>	<u>Latitude (°N)</u>	<u>Longitude (°W)</u>	<u>Bottom Depth (m)</u>
B04	25	2252 27 Apr 1987	70° 42.1	147° 04.6	44

<u>Depth</u>	<u>S (PSU)</u>	<u>T (°C)</u>	<u>Sigma-t</u>	<u>O<sub>2</sub> (ml/l)</u>	<u>PO<sub>4</sub> (μm/l)</u>	<u>SiO<sub>4</sub> (μm/l)</u>	<u>NO<sub>3</sub> (μm/l)</u>	<u>NO<sub>2</sub> (μm/l)</u>	<u>NH<sub>3</sub> (μm/l)</u>
7.3	30.665	-1.648	24.654	9.06	0.84	8.30	1.82	0.04	0.00
17.3	30.667	-1.652	24.656	9.06	0.84	8.38	1.88	0.04	0.00
22.3	30.684	-1.647	24.670	9.01	0.86	8.71	1.91	0.05	0.00
27.3	30.827	-1.668	24.787	8.85	0.88	9.29	2.36	0.05	0.01
32.3	31.534	-1.328	25.353	8.33	1.01	11.62	3.70	0.05	0.00
37.3	32.063	-1.160	25.778	7.85	1.07	15.87	4.97	0.05	0.04

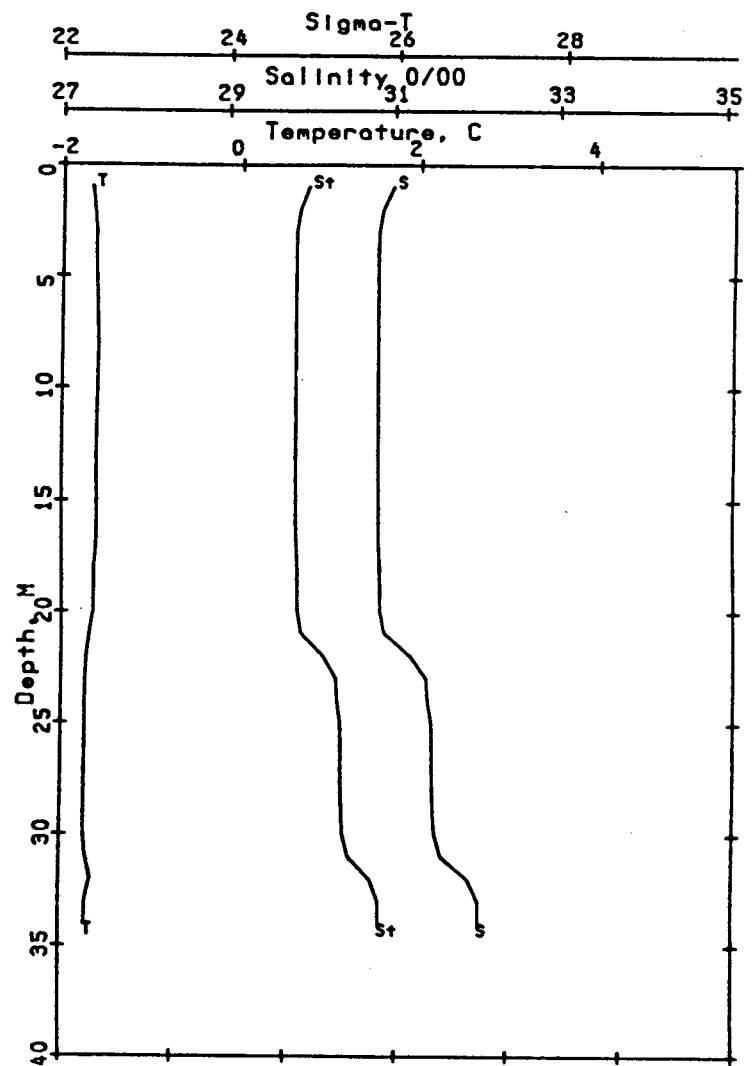
<u>Station</u>	<u>Cast</u>	<u>Time (UCT)</u>	<u>Latitude (°N)</u>	<u>Longitude (°W)</u>	<u>Bottom Depth (m)</u>
B03	26	1720 28 Apr 1987	70° 37.7	147° 07.7	38

<u>Depth</u>	<u>S (PSU)</u>	<u>T (°C)</u>	<u>Sigma-t</u>	<u>O<sub>2</sub> (ml/l)</u>	<u>PO<sub>4</sub> (μm/l)</u>	<u>SiO<sub>4</sub> (μm/l)</u>	<u>NO<sub>3</sub> (μm/l)</u>	<u>NO<sub>2</sub> (μm/l)</u>	<u>NH<sub>3</sub> (μm/l)</u>
7.3	30.811	-1.600	24.772	9.03	0.85	8.97	1.90	0.05	0.01
12.3	30.820	-1.607	24.780	9.05	0.87	8.87	1.97	0.05	0.03
17.3	30.828	-1.611	24.787	9.03	0.88	9.67	1.97	0.05	0.00
22.3	31.218	-1.718	25.105	9.07	0.91	10.46	2.42	0.08	0.00
27.3	31.494	-1.734	25.329	8.97	0.92	10.45	2.48	0.08	0.00
31.3	31.615	-1.707	25.427	8.39	1.00	12.95	3.72	0.08	0.00

425



Ref. no. 25      Sta. B04      70.70 N  
 Time = 871172252      Beaufort      147.08 W



Ref. no. 26      Sta. B03      70.63 N  
 Time = 871181720      Beaufort      147.13 W

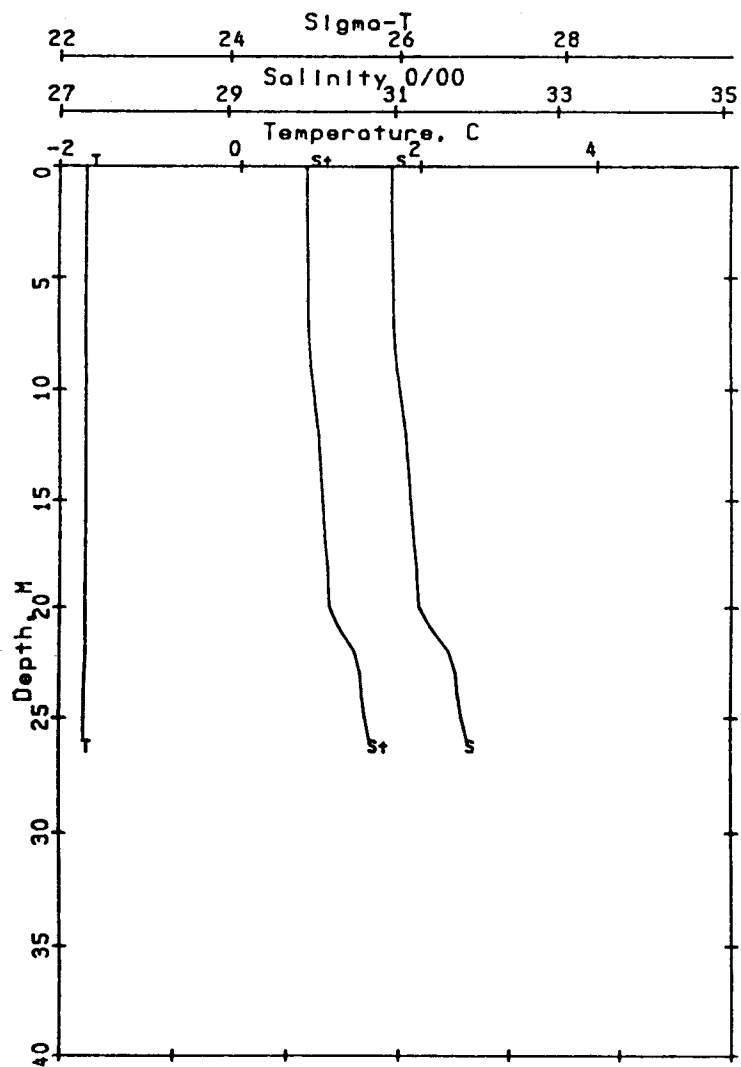
<u>Station</u>	<u>Cast</u>	<u>Time (UCT)</u>	<u>Latitude (°N)</u>	<u>Longitude (°W)</u>	<u>Bottom Depth (m)</u>
B02	27	1855 28 Apr 1987	70° 32.0	147° 15.0	32

<u>Depth</u>	<u>S (PSU)</u>	<u>T (°C)</u>	<u>Sigma-t</u>	<u>O<sub>2</sub> (ml/l)</u>	<u>PO<sub>4</sub> (µm/l)</u>	<u>SiO<sub>4</sub> (µm/l)</u>	<u>NO<sub>3</sub> (µm/l)</u>	<u>NO<sub>2</sub> (µm/l)</u>	<u>NH<sub>3</sub> (µm/l)</u>
2.3	30.974	-1.705	24.907	8.93	0.88	9.52	2.18	0.06	0.00
7.3	31.006	-1.706	24.932	8.97	0.90	8.70	2.22	0.06	0.00
12.3	31.142	-1.714	25.043	8.97	0.91	9.34	2.27	0.06	0.03
17.3	31.237	-1.719	25.121	9.00	0.88	9.40	2.14	0.07	0.00
22.3	31.660	-1.714	25.464	8.69	0.94	10.60	2.89	0.06	0.00
24.3	31.775	-1.733	25.558	8.67	0.94	11.40	2.91	0.07	0.00

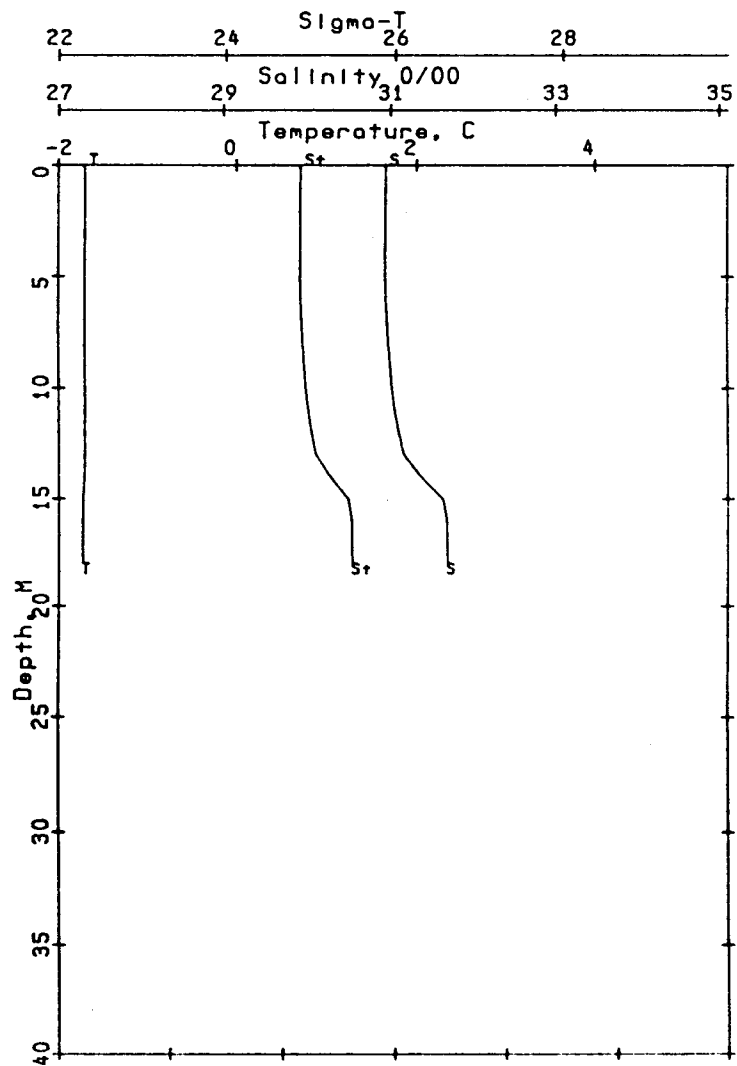
<u>Station</u>	<u>Cast</u>	<u>Time (UCT)</u>	<u>Latitude (°N)</u>	<u>Longitude (°W)</u>	<u>Bottom Depth (m)</u>
B01	28	2016 28 Apr 1987	70° 27.8	147° 20.0	23

<u>Depth</u>	<u>S (PSU)</u>	<u>T (°C)</u>	<u>Sigma-t</u>	<u>O<sub>2</sub> (ml/l)</u>	<u>PO<sub>4</sub> (µm/l)</u>	<u>SiO<sub>4</sub> (µm/l)</u>	<u>NO<sub>3</sub> (µm/l)</u>	<u>NO<sub>2</sub> (µm/l)</u>	<u>NH<sub>3</sub> (µm/l)</u>
2.3	30.945	-1.703	24.882	9.01	0.88	8.87	2.09	0.04	0.00
5.3	30.947	-1.702	24.884	8.99	0.88	8.85	2.12	0.04	0.00
8.3	30.982	-1.703	24.913	8.95	0.90	9.33	2.19	0.04	0.00
11.3	31.055	-1.704	24.972	8.92	0.91	10.04	2.28	0.04	0.04
14.3	31.368	-1.711	25.227	8.77	0.91	10.03	2.53	0.05	0.00
17.3	31.680	-1.734	25.480	8.74	0.94	10.82	2.73	0.08	0.00

427



Ref. no. 27      Sta. B02      70.53 N  
 Time = 871181855      Beaufort      147.25 W



Ref. no. 28      Sta. B01      70.46 N  
 Time = 871182016      Beaufort      147.33 W

**U.S. DEPARTMENT OF COMMERCE**  
NATIONAL OCEANIC AND ATMOSPHERIC ADMINISTRATION  
NATIONAL OCEAN SERVICE

Alaska Office  
Federal Bldg., U.S. Courthouse, Room A13  
222 W. Eighth Ave., #56  
Anchorage, Alaska 99513-7543

OFFICIAL BUSINESS  
PENALTY FOR PRIVATE USE \$300

FOURTH-CLASS MAIL  
POSTAGE AND FEES PAID  
U.S. Department of Commerce  
Permit Number G-19

**SPECIAL FOURTH CLASS**  
CLASS OF POSTAL SERVICE

---

UNIV OF ALASKA/INFO SERVICES  
ARCTIC ENV INFO AND DATA CTR  
707 A STREET  
ANCHORAGE, AK 99501